

DOUTORAMENTO

CIÊNCIAS BIOMÉDICAS

# Bioactive effects of selected marine-derived compounds on breast cancer cell lines

Fernanda Malhão

D

2022

Fernanda Malhão. Bioactive effects of selected marine-derived compounds on breast cancer cell lines



**Bioactive effects of selected marine-derived compounds on breast cancer cell lines**

Fernanda Cristina Rodrigues Malhão Pereira



FERNANDA CRISTINA RODRIGUES MALHÃO PEREIRA

**Bioactive effects of selected marine-derived compounds on breast cancer cell lines**

Tese de candidatura ao grau de Doutor em  
Ciências Biomédicas, submetida ao Instituto  
de Ciências Biomédicas Abel Salazar  
(ICBAS) da Universidade do Porto (U.Porto)

Orientador – Eduardo Jorge Sousa Rocha

Categoria – Professor Catedrático

Afiliação – ICBAS, U.Porto

Coorientador – Alice Fernanda Abreu Ramos

Categoria – Professora Auxiliar Convidada

Afiliação – ICBAS, U.Porto





Type your text

### Financial support

This research was supported by the strategic funding UIDB/04423/2020 and UIDP/04423/2020 through national funds provided by FCT – Fundação para a Ciência e a Tecnologia. The Doctoral Program in Biomedical Sciences of the ICBAS - University of Porto, provided additional funds.





## **Agradecimentos**

Chegar ao fim de um doutoramento, significa que percorremos um longo caminho cheio de altos e baixos, de imprevistos, onde muitas vezes tivemos de mudar o rumo, encontrar soluções, buscar forças para seguir em frente no meio do cansaço e da desmotivação que muitas vezes se instalam. É um caminho cheio de sacrifícios: profissionais e sobretudo pessoais. Um caminho que exige resiliência, persistência e muita força interior. Mas sem sombra de dúvidas, não teria chegado à meta sem a preciosa ajuda daqueles que estiveram ao meu lado, que me deram a mão (ou uns empurrões) para me fazerem seguir em frente quando as pernas quiseram fraquejar. Por isso deixo aqui registada a minha gratidão.

Ao meu orientador e chefe, Professor Doutor Eduardo Rocha, estou muito agradecida por ter sempre apoiado o meu desenvolvimento científico desde que trabalho no ICBAS. Eu tenho a certeza de que mais ninguém teria dado o mesmo incentivo para as duas técnicas do laboratório fazerem o doutoramento em simultâneo. Obrigada por ter proporcionado condições para que isso acontecesse. Eu admiro profundamente a sua capacidade de trabalho, grande conhecimento científico e o enorme entusiasmo que tem na Ciência e que transmite aos seus alunos. Obrigada pela orientação, paciência, excelentes partilhas de conhecimento e pela compreensão em momentos pessoais mais difíceis. Tudo isso contribuiu para o meu crescimento científico e profissional, e para que não tenha medo de encarar desafios futuros.

À minha coorientadora Doutora Alice Ramos, obrigada por ter aceitado me guiar durante o caminho, por todo o conhecimento transmitido, pelas horas a tirar dúvidas, a discutir resultados, a planear ensaios e conferir cálculos sempre com a serenidade e sorriso que te caracterizam. Mas sobretudo, obrigada pela valiosa amizade, por me lembrar muitas vezes que cada passo dado significava estar mais perto da meta, por me fazer ter clareza nos meus objetivos e me ajudar a superar todas as dificuldades, tornando o caminho mais leve.

Ao Professor Anake Kijjoa, um grande incentivador deste doutoramento, obrigada por ter disponibilizado a preussina para o desenvolvimento deste trabalho. Mas o seu contributo vai muito para além disto, obrigada pela revisão rápida e cuidada do artigo, pelos ensinamentos de química, pelo desenho dos compostos, pela imensa disponibilidade, simpatia e apoio nas horas que mais precisei.

A colega Ana Catarina Macedo, que tive o prazer de ensinar e acompanhar diariamente durante a sua tese de Mestrado, muito obrigada por teres contribuído tanto nas diferentes fases dos artigos desta tese. A nossa “Triologia” como referiste tantas vezes, ficou completa e eu não teria conseguido sem a tua contribuição. Obrigada também por teres usado o teu talento no design estético, para embelezar a triologia. Alguns períodos foram duros, mas com as nossas mudanças de turnos, bom humor e amizade tudo foi possível. Fizemos uma excelente equipa! Foi um prazer trabalhar contigo!

Agradeço também ao Departamento de Saúde Ambiental do Instituto Nacional de Saúde Dr. Ricardo Jorge (INSA), ao seu diretor Professor Doutor João Paulo Teixeira e principalmente à Doutora Carla Costa, por nos terem recebido e permitido realizar a análise dos ensaios do Cometa

Grata a vários amigos que me ajudaram em momentos chave em que eu precisei de ajuda extra para revisão e submissão de artigos e para formatação da tese. Rui Henriques, nunca vou me esquecer da tua generosidade e paciência em me ajudar em tempo recorde a rever o inglês do primeiro artigo. Paula Medeiros, que leu os meus artigos sem entender nada do que estava a ler, mas que encontrava os lapsos de inglês. Rui Fernandes do I3S, foste a minha salvação com a ajuda impagável que deste na observação das amostras quando o microscópio eletrónico do ICBAS não estava a funcionar, sem ti não teria terminado o artigo. Obrigada pela tua amizade aos longo de tantos anos, espero também celebrar contigo o teu doutoramento.

Na fase final de formatação da tese, agradeço a disponibilidade, paciência e amizade da Filipa Vieira, que é e sempre foi um exemplo de uma pessoa de muitas capacidades, profissionalismo e humildade, e que despretenciosamente, pôs-se ao dispor para me ajudar. Ainda, um obrigada especial a minha amiga de longa data Raquel Carvalho, que já me acompanhou em tantas etapas e desafios da vida, e que arranjou tempo no meio da sua vida supercomplicada para me ajudar nestas lides de formatação! Mais uma vez estiveste lá! Uma amizade sem igual que eu tenho o privilégio de ter.

À minha amiga Elisabeth Vieira, pelas horas que passou comigo a fazer-me entender um pouco melhor o mundo da estatística, foram horas regadas a chá quentinho em boa companhia.

À minha querida amiga Célinha, minha co-chefe e companheira de jornada profissional, e não só, há vinte tal anos, sou mesmo muito grata por ter uma verdadeira companheira

de laboratório, com quem posso sempre contar, dividir tarefas, conhecimentos, momentos bons e menos bons. Surpreendes-me sempre com os teus rasgos de inteligência, admiro a tua dedicação e rigor no trabalho. Obrigada por todo o apoio de sempre e também durante esta tese, por teres segurado as pontas tantas vezes, por teres assumido mais tarefas para que eu pudesse estar mais livre, por todo apoio moral, científico e também pelos ralhetes que as vezes foram bem precisos! Espero daqui em diante termos mais tempo para nos lançarmos em novos desafios e também usufruirmos de momentos mais descontraídos.

À colega Rosária Seabra, que acompanho desde a sua formação académica, e que muito me orgulho do crescimento científico que teve, agradeço a sua disponibilidade e ajuda em tantos momentos, a partilha de conhecimentos sobre a preussina. És muito trabalhadora e organizada, mostras sempre humildade e serás sempre uma mais-valia em qualquer laboratório.

À minha amiga Daniela Gargiulo, que esteve sempre comigo (ainda que distante fisicamente), que me ajudou a pôr em prática todos os passos deste caminho, desde quando ele era apenas um sonho, que me acendeu tantas vezes uma lanterna quando o caminho estava escuro, que comemorou comigo cada avanço, obrigada de coração.

Aos muitos amigos contribuíram de diversas maneiras para que eu continuasse no caminho, espero não me esquecer de ninguém, mas atrevo-me a dizer alguns nomes que foram importantes em diferentes fases: Madalena Santos, Ana Maria Silva, Madalena Rodrigues e Raquel Bernardino.

A dream team que é a equipa técnica do Departamento de Microscopia as colegas Célia Lopes (outra vez, mas não poderias ficar de fora do dream team), Elsa Oliveira, Ângela Alves, Cláudia Oliveira e Paula Teixeira, (Nádia, chegaste depois, mas ainda vais para o dream team). Vocês são incríveis! Obrigada pelo companheirismo e ambiente ímpar que proporcionam sempre. É muito mais fácil e prazeroso trabalharmos quando temos colegas assim. O vosso apoio esteve presente em todas as ocasiões, comemoramos juntas cada artigo publicado. Esta tese também é um bocadinho vossa!

Agradeço também o apoio e compreensão dos restantes docentes do Laboratório de Histologia e Embriologia, com quem já trabalho há tantos anos, e com os quais desenvolvemos relações para além do trabalho profissional, Marta Santos, Ricardo Marcos, Tânia Madureira, Paula Silva e Maria João Rocha.

Aos restantes membros do Departamento de Microscopia, especialmente ao nosso atual diretor Professor Alexandre Lobo-da Cunha que me estava sempre a perguntar quando acabava o doutoramento (parece que é desta vez), obrigada pelas palavras de incentivo.

E por fim devo muito, muito mesmo a toda minha família, principalmente as quase intermináveis horas privadas da minha companhia e atenção para que eu pudesse me dedicar a esta tese em todas as suas fases.

Aos meus pais que sempre me incentivaram a estudar e me proporcionaram todas as condições para que isso acontecesse da melhor forma, que me apoiaram e foram os grandes pilares em todos os sentidos nesta caminhada quer em termos logísticos quer em termos de apoio emocional. Minha madrinha Rita, que desde que me lembro como pessoa, me apoiou em tudo o que estava ao seu alcance, mesmo distante, está sempre presente. In memoriam aos meus avós maternos que teriam nesta fase muito orgulho de onde consegui chegar. À minha irmã, que ia pondo pozinhos de incentivo pelo caminho e que partilha comigo os meus desejos e angústias. Os meus sogros que muitas vezes foram cuidadores e ajudantes de tarefas domésticas, pois o tempo era pouco para tudo.

Ao meu marido Vítor que aguentou firme e me apoiou durante estes anos em que direcionei esforços, tempo e recursos financeiros para este doutoramento. Sei reconhecer que não foram períodos fáceis e foi preciso muita gestão familiar, obrigada por cada detalhe.

Aos meus amados filhos Francisco e Alexandre, a quem tantos momentos não pude dedicar a devida atenção, principalmente a ti Alexandre que tanto pedias para brincar mais com a mãe, que vocês possam um dia mais tarde se inspirarem no meu exemplo, que com dedicação e esforço conseguimos concretizar os nossos objetivos. Espero poder desfrutar muitos e muitos momentos de qualidade convosco. Vocês são os meus maiores tesouros!

## **Declaração de Honra**

Declaro que a presente tese é de minha autoria e não foi utilizada previamente noutro curso ou unidade curricular desta, ou de outra instituição. As referências a outros autores (afirmações, ideias, pensamentos) respeitam escrupulosamente as regras da atribuição e encontram-se devidamente indicadas no texto e nas referências bibliográficas, de acordo com as normas de referência. Tenho consciência de que a prática de plágio e auto-plágio constitui um ilícito académico.

*Fernanda Cristina Rodrigues Malhão Pereira*





## List of publications

The author declares that this thesis includes 4 published articles in peer-reviewed international journals, in chapters 2, 3, 4, and 5. All journals are open access. Therefore, there is inherent permission to reproduce the articles in this thesis.

The doctoral candidate participated in the conception, execution of the experimental work, and data analysis and wrote the original drafts of all articles included in the thesis.

### Publications included in this thesis:

- 1- Malhão, F.,** Ramos, A. A., Buttachon, S., Dethoup, T., Kijjoa, A. and Rocha, E. (2019). "Cytotoxic and antiproliferative effects of preussin, a hydroxypyrrolidine derivative from the marine sponge-associated fungus *Aspergillus candidus* KUFA 0062, in a panel of breast cancer cell lines and using 2D and 3D cultures." *Mar. Drugs* 17(8): 448. Doi: 10.3390/md17080448 (Chapter 3). Scimago: Q1 (Pharmaceutical Science). IF: 6.085.
- 2- Malhão, F.,** Ramos, A. A., Macedo, A. C. and Rocha, E. (2021). "Cytotoxicity of seaweed compounds, alone or combined to reference drugs, against breast cell lines cultured in 2D and 3D." *Toxics* 9(2): 24. Doi: 10.3390/toxics9020024 (Chapter 4). Scimago: Q1 (Toxicology). IF: 4.472.
- 3- Malhão, F.,** Macedo, A. C., Costa, C., Rocha, E. and Ramos, A. A. (2021). "Fucoxanthin holds potential to become a drug adjuvant in breast cancer treatment: Evidence from 2D and 3D cell cultures." *Molecules* 26(14): 4288 Doi:10.3390/molecules26144288 (Chapter 5). Scimago: Q1 (Pharmaceutical Science). IF: 4.927.
- 4- Malhão, F.,** Macedo, A. C., Costa, C., Rocha, E. and Ramos, A. A. (2022). "Morphometrical, morphological and immunocytochemical characterization of a tool for cytotoxicity research: 3D cultures of breast cell lines grown in ultra-low attachment plates." *Toxics* 24; 10(8):415. Doi: 10.3390/toxics10080415 (Chapter 2). Scimago: Q1 (Toxicology). IF: 4.472.



## **Abstract**

Breast cancer (BC) is a very heterogeneous disease in terms of histological, molecular subtypes, and clinical outcomes, namely having different patterns of positivity for estrogen and progesterone receptors (ER and PR), as well as for expression of the oncogene human epidermal growth factor receptor 2 (HER-2). Besides the existence of target therapies for the ER and HER-2 receptors, chemotherapy is still a very used approach, especially in tumors without the expression of these receptors (triple-negative breast cancer – TNBC). Because drug resistance is a major concern in BC treatment, the scientific community and the pharmaceutical industry struggle to find new drugs or drug adjuvants that can help in BC treatment. In this vein, several studies reported using natural products in combinatorial therapy with drugs to potentiate the drug effects, act synergistically, lower the drug's doses or alleviate drug side effects. Marine-derived compounds have demonstrated unique chemical structures with many pharmacological activities, including anticancer ones. Studies related to combining marine-derived compounds with conventional anticancer drugs are not abundant yet, and the existing ones are on monolayer cell culture.

This study used a panel of four cell lines: three BC cell lines representative of the main BC subtypes: MCF7- luminal A; SKBR3 - HER-2 overexpression, MDA-MB-231-TNBC and one non-tumoral cell line - MCF12A.

Our first objective was to obtain and characterize three-dimensional (3D) cell cultures from the four cell lines, here called multicellular aggregates (MCAs) (Chapter 2). We used a scaffold-free stationary technique for obtaining the MCAs: the ultra-low attachment (ULA) plates. The MCAs were then characterized using stereomicroscopic morphometry, descriptive cytology (at light and electron microscopy), and qualitative and quantitative immunocytochemistry (ICC). Moreover, we provided a detailed methodology with technical tips for successfully obtaining and analyzing the MCAs. With this technique, MCF7 and MDA-MB-231 MCAs were compact with smaller areas and presented an oblate ellipsoid/discoid shape, while MCF12A and SKBR3 MCAs formed loose, more flattened MCAs with consequent bigger areas. MCF7 MCAs showed tissue recapitulation features with acini-like formation, cell polarization with microvilli display, and accumulation of secretory vesicles towards the lumen. ICC revealed a random distribution of the proliferating and apoptotic cells throughout the MCAs. All the presented characteristics do not fit well in the traditional spheroid model. The other used ICC markers (cytokeratin, vimentin, E-cadherin, ER, PR, and HER-2) presented different results according to the cell lines. This characterization of the MCAs in non-exposed

conditions provided a good baseline for interpreting experimental results related to screening potential anticancer compounds.

After the characterization of the 3D model, we moved to the second objective, testing the cytotoxic and antiproliferative effects of preussin derived from a marine sponge-associated fungus *Aspergillus candidus* (Chapter 3). The following assays were carried out to evaluate the effects of the compound on cell viability: 3-(4,5-dimethylthiazol-2-yl)-2,5-diphenyl tetrazolium bromide (MTT), resazurin, and lactate dehydrogenase (LDH). For measuring cell proliferation, we used the 5'-bromo-2'-deoxyuridine (BrdU) assay. Preussin at 50  $\mu$ M decreased cell viability and proliferation in 2D and 3D cultures in all cell lines. However, in 3D culture, cells were less responsive. The cytotoxic effects and anti-proliferative were confirmed by caspase-3 and ki67 ICC and histological evaluation.

Concerning the third and fourth objectives, on monolayer culture, first, we assessed the cytotoxic effects of six brown seaweed-derived compounds belonging to different chemical classes: carotenoids - astaxanthin (Asta) and fucoxanthin (Fx); polysaccharides - fucoidan (Fc) and laminarin (Lm); sterols - fucosterol (Fct) and phlorotannins - phloroglucinol (Phg). Then two selected concentrations of each compound were tested in combination with two drugs used in BC treatment: cisplatin (Cis) and doxorubicin (Dox) (Chapters 4 and 5).

In some situations, the combinations inhibited the drugs' effects but in others potentiated without a specific pattern, varying with the doses and the cell lines. The most promising combinations were the ones whose effects differed simultaneously from the control and the compounds alone. The two best combinations were observed in the MDA-MB-231 cell line, with fucosterol (Fct) and fucoxanthin (Fx) combined with Dox. Fct alone, at 10  $\mu$ M affected the cell viability in all BC cell lines without affecting the non-tumoral cell line. Fct in combination with Dox, using both at non-cytotoxic concentrations (Fct 5  $\mu$ M +Dox 0.1  $\mu$ M), potentiated Dox cytotoxicity reducing cell viability and inhibiting cell proliferation. As for Fx, at 10  $\mu$ M, it was cytotoxic in all cell lines. Combined with Dox 1  $\mu$ M, it enhanced Dox's already existing effects in terms of cytotoxicity and inhibition of cell proliferation.

To achieve our fifth objective, the most promising combinations were tested using a comparative approach, with monolayer versus 3D culture, applying a multi-end approach for assessing the effects on cell viability and proliferation, morphology, and immunocytochemistry targets. At least two viability assays were performed for each of the selected conditions, as well as proliferation assays, morphometry, ICC for caspase-3 and ki67, morphological analysis and, in the case of Fx, the effects on the cellular

ultrastructure were also studied (Chapters 4 and 5). In 3D cell culture, the cytotoxic and antiproliferative effects of Fct and its combination with Dox were not observed, revealing greater resistance to treatments. In contrast, the combination of Fx and Dox continued showing higher cytotoxic effects on 3D cultures compared to the isolated compounds. The histological analysis and ICC results corroborated the cell-based assays. In the case of the combination of Dox with Fx, ICC showed an increase in the number of cells in apoptosis, a decrease in cell proliferation, structural cell damage and ultrastructural changes. The overall findings suggest Fx has the potential to become an adjuvant for Dox chemotherapy regimens in BC treatment, especially in TNBC. Even not reproducing the effects in 3D, the mixture of Dox of Fct needs further investigation, from increasing the concentration of Fct to recurring to other technologies for delivering both types of chemicals.

Besides the promising findings, further *in vitro* and *in vivo* studies are necessary to fully understand and explore the underlying mechanisms of action of preussin and the most promising seaweed compounds, as well as the enhancement of Dox effects unveiled in the combinations.



## Resumo

O cancro da mama (BC) é uma doença muito heterogénea em termos histológicos, subtipos moleculares e comportamentos clínicos, apresentando diferentes padrões de positividade para os recetores de estrogénio e progesterona (ER e PR), bem como para a expressão do oncogene recetor tipo 2 do fator de crescimento epidérmico humano (HER-2). Apesar da existência de terapias-alvo para os ER e HER-2, a quimioterapia ainda é uma abordagem muito utilizada, principalmente em tumores sem expressão desses recetores (cancro de mama triplo negativo – TNBC). A resistência aos fármacos é uma grande preocupação no tratamento do BC, por isso, a comunidade científica e a indústria farmacêutica lutam para encontrar novos fármacos ou adjuvantes de fármacos que possam ajudar no tratamento da doença. Nesse sentido, diversos estudos reportaram a utilização de produtos naturais, em terapia combinada com fármacos pré-existentes, para potenciar os efeitos desses fármacos, atuando sinergicamente, baixando as suas doses e/ou diminuindo os seus efeitos secundários. Os compostos de origem marinha revelaram ter estruturas químicas únicas com diversas propriedades farmacológicas, incluindo efeitos antitumorais. Os estudos relacionados com a combinação de compostos de origem marinha com drogas antitumorais convencionais ainda são pouco abundantes, e os existentes foram realizados maioritariamente em cultura de células em monocamada (cultura celular 2D).

Neste estudo, foi utilizado um painel de linhas celulares constituído por três linhas celulares representativas dos principais subtipos de BC: MCF7- luminal A; SKBR3 – sobreexpressão de HER-2, MDA-MB-231-TNBC e uma linha celular não tumoral - MCF12A.

O nosso primeiro objetivo foi obter e caracterizar culturas celulares tridimensionais (3D) – aqui denominadas de agregados multicelulares (MCAs), das quatro linhas celulares (Capítulo 2). Para a obtenção dos MCAs, foi utilizada uma técnica estática sem matriz tridimensional (scaffold): as placas de adesão ultrabaixa (ULA). Os MCAs foram então caracterizados recorrendo a estereomicroscopia, citologia descritiva (microscopia ótica e eletrónica) e imunocitoquímica (ICC) com análise quantitativa. Além disso, toda a metodologia foi detalhadamente descrita e foram fornecidas dicas técnicas essenciais para o sucesso na obtenção e análise dos referidos MCAs. Utilizando esta metodologia, as linhas MCF7 e MDA-MB-231 formaram MCAs compactos, com áreas menores e formato oblato elipsoide/discoide, enquanto as linhas MCF12A e SKBR3 formaram MCAs laxos, mais achatados, e conseqüentemente com maiores áreas. Os MCAs da linha MCF7 apresentaram ainda características de recapitulação tecidual, com a



formação de estruturas semelhantes a ácinos, polarização celular com presença de microvilosidades e acumulação de vesículas secretoras na direção do lúmen. A ICC mostrou que as células em apoptose e proliferação estavam distribuídas de forma aleatória pelos MCAs. Todas as características apresentadas não se encaixam bem no modelo tradicional de esferoide, onde as células em proliferação se encontram na periferia e as células em apoptose num núcleo central. Os restantes marcadores de ICC (citoqueratina, vimentina, E-caderina, ER, PR e HER-2) apresentaram resultados diferentes de acordo com as linhas celulares. A caracterização dos MCAs, em condições de não-exposição, constituiu uma boa base para a interpretação dos resultados experimentais relacionados com a triagem de potenciais compostos antitumorais.

Após a caracterização do modelo 3D, passamos para o segundo objetivo, que foi testar os efeitos citotóxicos e anti proliferativos da preussina, composto derivado do fungo associado esponjas marinhas *Aspergillus candidus* (Capítulo 3), em culturas 2D e 3D. Para avaliar os efeitos na viabilidade celular foram realizados diferentes ensaios (brometo de 3-(4,5-dimetiltiazol-2il) -2,5-difenil tetrazólio (MTT), resazurina e lactato desidrogenase (LDH). A avaliação dos efeitos na proliferação foi feita com o ensaio de 5'-bromo-2'-desoxiuridina (BrdU). A preussina a 50 µM diminuiu a viabilidade e proliferação celular em culturas 2D e 3D de todas as linhas celulares, porém, na cultura 3D as células foram menos responsivas. Os efeitos foram observados em diferentes concentrações de preussina, dependendo da linha celular e do ensaio realizado. Os efeitos citotóxicos e anti proliferativos foram confirmados por ICC para caspase-3 e ki67 e pela avaliação histológica.

Relativamente aos terceiro e quarto objetivos, primeiro em cultura em monocamada, avaliamos, usando o ensaio MTT, os efeitos citotóxicos de seis compostos derivados de algas castanhas pertencentes a diferentes classes químicas: carotenóides - astaxantina (Asta) e fucoxantina (Fx); polissacarídeos - fucoïdan (Fc) e laminarina (Lm); esteróis - fucosterol (Fct) e florotaninos - floriglucinol (Phg). Em seguida, foram selecionadas duas concentrações de cada composto para serem testadas em combinação com duas concentrações de duas drogas usadas em tratamento de BC: cisplatina (Cis) e doxorubicina (Dox) (Capítulos 4 e 5).

As combinações consideradas como mais promissoras foram aquelas cujos efeitos citotóxicos diferiam significativamente simultaneamente do controlo e dos compostos isolados. As duas combinações melhores foram observadas na linha MDA-MB-231, com o Fct e a Fx, combinados com Dox. Em cultura de monocamada, o Fct isolado, a 10 µM, diminuiu a viabilidade celular em todas as linhas celulares de BC, sem afetar a linha

celular não tumoral. O Fct em combinação com Dox, ambos em concentrações não citotóxicas (Fct 5  $\mu$ M + Dox 0,1  $\mu$ M), potencializou a citotoxicidade da Dox, reduzindo a viabilidade e a proliferação celular. A Fx, a 10  $\mu$ M, foi citotóxica em todas as linhas celulares e, em combinação com Dox 1  $\mu$ M, potencializou os efeitos da Dox já existentes, em termos de citotoxicidade e inibição da proliferação celular. Quanto às demais condições experimentais, algumas combinações inibiram o efeito das drogas e outras potencializaram-no, sem nenhum padrão específico, variando de acordo com as doses e com as linhas celulares.

Para atingir o quinto objetivo, as combinações mais promissoras foram testadas usando uma abordagem comparativa, monocamada versus cultura 3D, aplicando uma abordagem com diferentes ensaios para avaliar os efeitos na viabilidade e proliferação celular. Foram feitos pelo menos dois ensaios de viabilidade para cada uma das condições selecionadas, ensaios de proliferação, morfometria, ICC para caspase-3 e ki67, análise morfológica e no caso da Fx ainda foram ainda estudados os efeitos na ultraestrutura celular (Capítulos 4 e 5). Em cultura celular 3D, os efeitos citotóxicos e antiproliferativos do Fct e da sua combinação com Dox não foram observados, revelando estas uma maior resistência aos tratamentos. Pelo contrário, a combinação de Fx e Dox continuou a apresentar maiores efeitos citotóxicos em relação aos compostos isolados. A análise histológica e os resultados de ICC corroboraram os ensaios celulares. No caso da combinação da Dox com Fx, a ICC mostrou um aumento do número de células em apoptose, diminuição da proliferação celular, danos celulares estruturais e alterações ultraestruturais. Os resultados globais sugerem que Fx tem potencial para se tornar um adjuvante em regimes de quimioterapia com Dox no tratamento de BC em TNBC. Mesmo não reproduzindo os efeitos em 3D, a combinação da Dox com o Fct merece mais investigação, como aumentar a concentração de Fct e/ou testar outras tecnologias para entrega nas células destes compostos.

Apesar dos resultados promissores, mais estudos *in vitro* e *in vivo* são necessários para um maior entendimento e investigação dos mecanismos subjacentes à ação da preussina, e dos compostos de algas marinhas mais promissores Fct e Fx, e o aumento dos efeitos da Dox nas combinações.



## **List of Abbreviations and Acronyms**

ABC - ATP- binding cassettes  
ADCs - Antigen-drug conjugates  
AIs - Aromatase inhibitors  
Akt - Protein kinase B  
ALDH1 - Aldehyde dehydrogenase 1  
ASCO - American Society of Clinical Oncology  
Asta - Astaxanthin  
ATP - Adenosine triphosphate  
Bax - Bcl-2 associated X protein  
BC - Breast cancer  
BCs - Breast cancers  
Bcl-2 - B-cell lymphoma-2  
BCSCs - Breast cancer stem cells  
BRCA1 - Breast cancer 1  
BRCA2 - Breast cancer 2  
BrdU - 5'-bromo-2'-deoxyuridine  
CAM - Complementary and Alternative Medicine  
CAP - College of American Pathologists  
CK - Cytokeratin  
CSC - Cancer stem cells  
CYP - Cytochrome P450  
DCIS - Ductal carcinoma in situ  
ECM - Extracellular matrix  
EGFR - Epidermal growth factor receptor  
EMA - European Medicines Agency  
EMT - Epithelial-mesenchymal transition  
ER - Estrogen receptor  
ERK - Extracellular-signal-regulated kinase  
FDA - Food and Drug Administration  
FBS - Fetal bovine serum  
FGFb - Fibroblast growth factor-basic

FCS - Fetal calf serum  
Fc - Fucoidan  
Fcol - Fucosterol  
Fx - Fucoxanthin  
Fxl - Fucoxanthinol  
GFP - Green fluorescent protein  
GRAS - Generally recognized as safe  
GTS - Glutathione S-transferase  
IC<sub>50</sub> - Half-maximal inhibitory concentration  
HER-2 - Human epidermal growth factor-2  
HMECs - Human mammary epithelial cells  
IARC - International Agency for Research on Cancer  
IDC - Invasive ductal carcinoma  
ILC - Invasive lobular carcinoma  
ICC - Immunocytochemistry  
IHC - Immunohistochemistry  
ISH - In situ hybridization  
KUFA - Kasetsart University Fungal Collection  
LCIS - Lobular carcinoma in situ  
LDH - Lactate dehydrogenase  
Lm - Laminarin  
MAPK - Mitogen-activated protein kinase  
MDR - Multidrug resistance  
MEK - Mitogen-activated protein kinase  
MHT - Menopausal hormonal therapy  
MMP - Metalloproteinase  
MTT - 3 - (4,5-dimethylthiazol-2yl)-2,5-diphenyl tetrazolium bromide  
NADPH - Nicotinamide adenine dinucleotide phosphate  
NCI - National Cancer Institute  
NDI - New dietary ingredient  
NF-κB - Nuclear factor-kappa B  
NSG - NOD-scid gamma

p-ERK1/2 - phosphorylated extracellular signal-regulated kinase1/2  
PARP - Poly-(ADP-ribose) polymerase protein  
PCR - Polymerase chain reaction  
PDT - Population doubling time  
PEG - Polyethylene glycol  
Pen/Strep - Penicillin/streptomycin  
Phg - Phouroglucinol  
PI3K - Phosphoinositide 3-kinase  
PR - Progesterone receptor  
qRT-PCR - Quantitative real-time polymerase chain reaction  
rBM - Reconstituted basal membrane  
ROS - Reactive oxygen species  
RTK - Receptor tyrosine kinase  
SERMs - Selective estrogen receptor modulators  
SERDs - Selective estrogen receptor degraders  
SMP-30 - Senescence marker protein-30  
SOD - Superoxide dismutase  
TIMP-1 - Tissue inhibitor metalloproteinase-1  
TKIs - Tyrosine kinase inhibitors  
TME - Tissue microenvironment  
TNBC - Triple-negative breast cancer  
TRAIL - Tumor necrosis factor-related apoptosis-inducing ligand  
VGFE - Vascular endothelium growth factor  
WB - Western Blot  
WHO - World Health Organization  
5-FU - 5-Fluorouracil



Index	
Agradecimentos.....	v
Declaração de Honra.....	ix
List of publications .....	xi
Abstract .....	xiii
Resumo .....	xvii
List of Abbreviations and Acronyms .....	xxi
<b>Chapter 1 - General Introduction .....</b>	<b>1</b>
1. Introduction to Breast Cancer and its Biological Subtypes .....	3
1.1. Breast Histology and Dynamic Tissue Remodeling .....	3
1.2. Breast Cancer .....	5
1.3. Breast Cancer Etiology.....	5
1.4. Breast Cancer Pathogenesis.....	6
1.5. Breast Cancer Diagnostic and Grading .....	7
1.6. Breast Cancer Classification .....	8
1.6.1. Histological Classification .....	8
1.6.2. Molecular Classification – Breast Cancer Subtypes .....	8
1.6.2.1. Luminal .....	10
1.6.2.2. HER-2.....	10
1.6.2.3. Triple-negative vs Basal-like .....	11
2. Breast Cancer Treatment.....	12
2.1. Treatment Options .....	12
2.1.1. Surgery.....	12
2.1.2. Radiotherapy .....	12
2.1.3. Chemotherapy .....	13
2.1.3.1. Cyclophosphamide.....	14
2.1.3.2. Anthracyclines.....	15
2.1.3.3. Taxanes .....	15
2.1.3.4. 5-Fluorouracil .....	15
2.1.3.5. Capecitabine.....	16
2.1.3.6. Platinum compounds.....	16
2.1.4. Target Therapies .....	16
2.1.4.1. Endocrine Therapy.....	17
2.1.4.2. HER-2 Target Therapy.....	18
2.1.5. Combination Therapy .....	18



2.1.6. Complementary Therapies.....	19
3. Breast Cancer Caveats and Needs.....	21
3.1. Drug Resistance.....	21
4. Natural and Nature-Inspired Compounds for Cancer Prevention and Treatment..	23
4.1. Marine-derived Compounds in Cancer Prevention .....	24
4.2. Marine-derived Compounds in Cancer Treatment .....	25
5. An Overview of Marine-derived Anticancer Bioactive Compounds.....	26
5.1. Marine Fungi-derived Bioactive Compounds - Sources, Molecules, Uses, and Mechanisms of Action.....	27
5.1.1. Preussin .....	28
5.2. Seaweeds-derived Compounds - Sources, Molecules, Uses, and Anticancer Effects .....	30
5.2.1. Seaweed Consumption and Breast Cancer .....	32
5.3. Brown Seaweed Bioactive Compounds.....	32
5.3.1. Carotenoids .....	33
5.3.1.1. Astaxanthin (Asta).....	34
5.3.1.2. Fucoxanthin (Fx).....	36
5.3.2. Polysaccharides .....	40
5.3.2.1. Laminarin (Lm).....	41
5.3.2.2. Fucoidan (Fc).....	43
5.3.3. Sterols .....	47
5.3.3.1. Fucosterol (Fct).....	47
5.3.4. Phlorotannins.....	49
5.3.4.1. Phloroglucinol (Phg).....	50
6. Role of <i>In Vitro</i> Models for Drug Screening and Mechanistic Insights .....	52
6.1. 2D Cell Culture.....	53
6.2. 3D Cell Culture.....	56
6.2.1. Scaffold-based Methods .....	60
6.2.2. Scaffold-free Methods.....	61
6.2.2.1. Stationary Methods .....	61
6.2.2.2. Agitation-based Systems.....	63
6.3. Breast Cancer 3D <i>In Vitro</i> Models .....	64
6.4. Breast Cell Lines Used in This Study .....	65
6.4.1. MCF7.....	65
6.4.2. SKBR3.....	66
6.4.3. MDA-MB-231.....	67
6.4.4. MCF12A .....	67
6.4.5. Cell Lines Characterization .....	68

6.5. Outputs in 3D Cell Culture.....	71
7. Thesis Aims and Objectives.....	73
7.1. Aims.....	73
7.2. Objectives .....	73
Supplementary Tables.....	75
References .....	100

**Chapter 2** - Morphometrical, Morphological and Immunocytochemical Characterization of a Tool for Cytotoxicity Research: 3D Cultures of Breast Cell Lines Grown in Ultra-low Attachment Plates.....173

**Chapter 3** - Cytotoxic and Antiproliferative Effects of Preussin, a Hydroxypyrrolidine Derivative from the Marine Sponge-Associated Fungus *Aspergillus candidus* KUFA 0062, in a Panel of Breast Cancer Cell Lines and Using 2D and 3D Culture.....205

**Chapter 4** - Cytotoxicity of Seaweed Compounds, Alone or Combined to Reference Drugs, against Breast Cell Lines Cultured in 2D and 3D.....235

**Chapter 5** - Fucoxanthin Holds Potential to Become a Drug Adjuvant in Breast Cancer Treatment: Evidence from 2D and 3D Cell Cultures.....269

**Chapter 6** - General Discussion.....299

6.1. What is this thesis about?.....299

6.2. What were the new aspects tested in this thesis?.....299

6.3. How were obtained the 3D cell cultures? What were the advantages and disadvantages of the method used?.....300

6.4. What were the main characteristics of the formed MCAs?.....301

6.5. What were the effects of the preussin on the panel of BC cell lines cultivated in 2D and 3D cell cultures? Are they worth exploring further?.....304

6.6. What were the effects of the seaweed compounds (alone or combined with Cis and Dox) on the panel of BC cell lines cultivated in 2D cell culture?.....304

6.7. Which were the most promising combinations of seaweed compounds plus drugs to be studied in 3D cell culture?.....306

6.8. Screening compounds in 3D – the importance of a multi-end point assay.....308

6.9. What is the importance of using a panel of BC cell lines? Is it worth including a non-tumoral breast cell line?.....309

6.10. Why is it important to study the interactions of seaweed compounds with chemotherapy drugs?.....310

References.....313

**Chapter 7** - Concluding Remarks.....321

**Chapter 8** - Future Perspectives.....325



# **Chapter 1** - General Introduction





## 1. Introduction to Breast Cancer and its Biological Subtypes

### 1.1. Breast Histology and Dynamic Tissue Remodeling

The female mammary gland has a primary function in the production of milk to feed newborn children. To fulfill this function, it consists of 15 to 25 secretory lobes of the tubular acinar glands. Each lobe has its secretory (lactiferous) duct that is individualized from the next one by dense connective and adipose tissues (Figures 1a, b) and is constituted by many lobules, sometimes called terminal duct lobular units. This duct lobular unit, by its turn, consists of several branched ducts that end in secretory alveoli (acini) (Mescher, 2018). Lobular units are constituted by two types of cells: the cuboidal, or low columnar epithelial cells that encircle the lumen, named luminal cells, and the myoepithelial cells that surround the epithelial cells and are so-called basal cells (Figure 1c). In the region of the nipple, the ducts are surrounded by smooth muscle bundles responsible for nipple contraction (Mescher, 2018, Biswas et al., 2022).

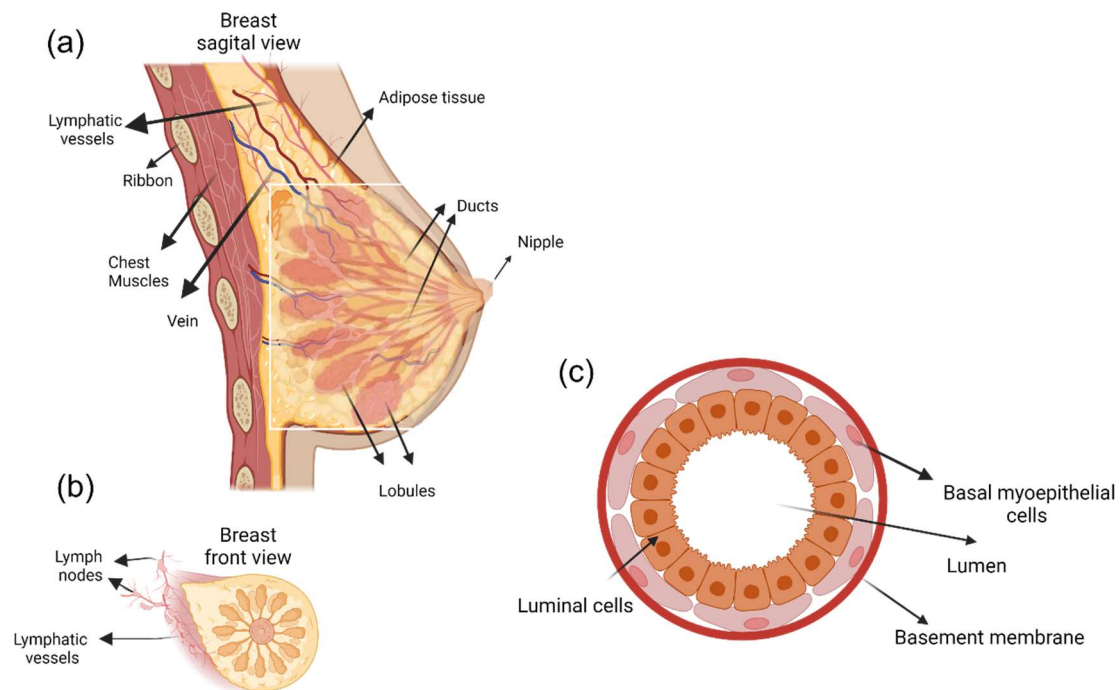


**Figure 1** - Mammory gland in schematic diagram (a) sagittal view and (b) front view showing the lobules and ducts ending in the nipple, and (c) cross-section of acini structures constituted by luminal cells surrounded by myoepithelial cells laying on the basement membrane. Image created with BioRender.com and paint.net.

The mammary gland is very dynamic, especially in females, and its histological structure undergoes tissue remodeling according to age and physiological status. There are three major stages of breast development - embryonic, pubertal, and reproductive (pregnancy

and lactation) (Macias and Hinck, 2012). At birth, the mammary gland is rudimentary, corresponding to some ducts around the nipple. Until puberty, these ducts have no alveoli. Then, with the estrogen augmentation of puberty, breast budding occurs, which corresponds to the development of the ducts forming lobular units with alveoli. This process shares many molecular similarities to the epithelial-mesenchymal transition (EMT) that occurs during embryological development as epithelial cells infiltrate the mammary stroma (Mazzarella and Pelicci, 2017). During the reproductive period, with hormonal fluctuations, breast tissue undergoes slight transformations, which include cyclic apoptosis and epithelium regeneration (Navarrete et al., 2005). In the follicular phase, the development of the follicles raises estrogen levels, inducing cell proliferation within the breast epithelial cells. In the luteal phase, the increase of progesterone causes dilatation of mammary ducts and the differentiation of secretory vesicles, accompanied by an increment in cell proliferation (Slepicka et al., 2021). If no fertilization occurs, there is a sudden drop in estrogen and progesterone levels, and menstruation occurs with regression of the secretory activity accompanied by a decrease in breast volume (Bistoni and Farhadi, 2015).

Accordingly, during pregnancy, massive breast development achieves morphological and functional maturity. In the first weeks, under estrogen influence, there is ductal sprouting, lobular proliferation, and secreting alveoli appear. In the second trimester, progesterone leads to lobular formation to exceed the ductal sprouting with concomitant augmentation of prolactin levels. The third trimester is characterized by lobules hypertrophy and secretion of colostrum that is substituted by milk after birth (Macias and Hinck, 2012, Bistoni and Farhadi, 2015). This epithelium expansion is accompanied by other alterations, like the loss of lipidic content in the adipose tissue and a great increment in the vasculature to supply nutrients for milk production. After the lactation period, breast tissue returns to its resting state (Oakes et al., 2006). The involution processes in the mammary gland are closely associated with apoptosis (Watson, 2006).

Finally, when women reach menopause, with diminished ovary function and consequent low estrogen and progesterone levels, there is a loss of glandular tissue, which is replaced by adipose tissue (Bistoni and Farhadi, 2015).

The male breast is very similar to the female breast before puberty since hormone regulation does not stimulate the development of specialized lobules (Blau et al., 2016).

## 1.2. Breast Cancer

According to Globocan 2020, female Breast Cancer (BC) is the most common cancer. However, in terms of death by the disease female BC occupies the fifth place after lung, colorectal, liver, and stomach (Figure 2). BC is the deadliest cancer when solely considering females (IARC, 2021, Sung et al., 2021). Among women, BC accounts for 1 in 4 cancer cases and 1 in 6 cancer deaths, being the most incident in 159 of 185 countries and the one with the highest mortality in 110 countries (Sung et al., 2021).

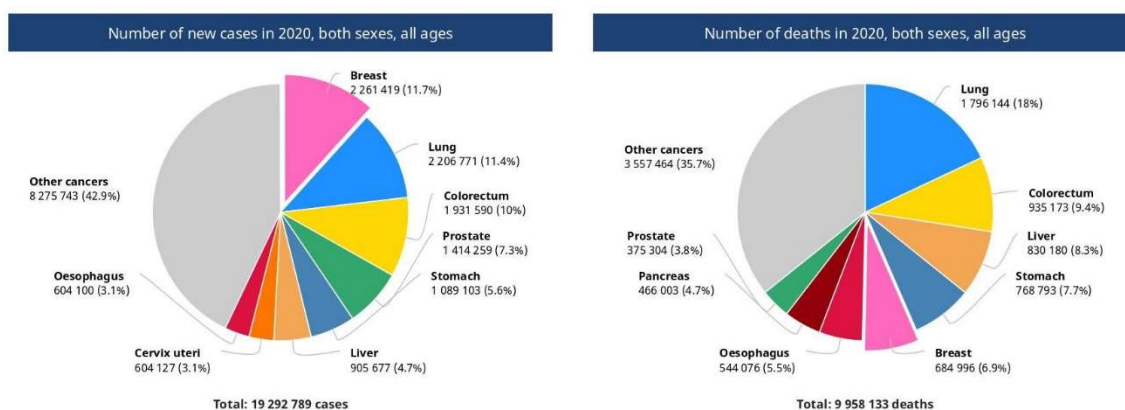


**Figure 2** - Estimated number of new cancer cases and deaths by cancer in both sexes, all ages worldwide, in 2020. Source: GLOBOCAN 2020. Graph Production: Global Cancer Observatory 2020.

Transitioned countries present 88% higher incidence rates than transitioning countries in which the mortality rates are 17% higher. Higher incidence in high-income countries is related to a higher prevalence of reproductive and lifestyle risk factors, and increased detection through organized mammographic screening (Sung et al., 2021). In most high-income countries mortality rates are decreasing. This trend is associated with early detection and improvements in BC treatments. The opposite is true in low-income countries, where rising incidence does not meet good access to specialized oncology healthcare and treatment resources, which are few due to the high cost of cancer drugs and radiotherapy units (DeSantis et al., 2015).

Male BC is very rare, representing less than 1% of BCs and less than 1% of men's cancers (Yalaza et al., 2016, Gucalp et al., 2019). The worldwide ratio of female-to-male BC is 122 :1 (Ly et al., 2013).

## 1.3. Breast Cancer Etiology

The etiology of BC is multifactorial and involves age, lifestyle, obesity, hormonal exposure to endogenous estrogen and progesterone, reproductive factors, and family



history (Sun et al., 2017). The main risk of BC is age. Young women with BC generally have poorer survival and tend to have larger tumors and lymph node-positive (Weiss et al., 2003).

Lifestyle risks are a vast group of items such as smoking, alcohol consumption, lack of physical exercise, diets with high fat intake, and stress. Smoking and alcohol consumptions are strongly related to the increase in BC risk (Dieterich et al., 2014, Hashemi et al., 2014). Obesity is strongly associated with higher BC risk, but this association varies with menopausal status. Physical activity has been pointed out as protective for BC (Maisonneuve, 2017).

Breast cancer risk, especially estrogen receptor (ER)-positive BC, is related to reproductive risk factors that are higher among women who have early menarche and/or late menopause, remain nulliparous, or have few children at a late age, with less breastfeeding (Dall and Britt, 2017). Contraceptives and menopausal hormonal therapy (MHT), are also associated with increased BC risk (Jiang et al., 2021). Concerning MHT, recent epidemiological studies evidenced that this risk is associated with the type and timing of the MHT (Collaborative Group on Hormonal Factors in Breast Cancer, 2019).

Only 5-10% of female BC are associated with autosomal inheritance in susceptibility genes as the most known BC genes (BCRA). BRCA1 and BRCA2, are responsible for 60-90% of inherited BC and the early onset of this type of tumor (Mahdavi et al., 2019, Lee et al., 2020a). Both BRCA1 and 2 encode tumor suppressor proteins. Their mutations are inherited in an autosomal dominant gene even if the second allele is normal (Lee et al., 2020a). Male BC is commonly associated with mutations in BRCA 2 gene (Fentiman et al., 2006).

### **1.4. Breast Cancer Pathogenesis**

Most breast tumors start from ductal hyperproliferation. There are two main theories for cancer initiation and progression: the cancer stem cell theory and the stochastic theory (Rich, 2016, Butti et al., 2019). The cancer stem cell theory defends that all tumor subtypes are derived from the same stem cells: the breast cancer stem cells (BCSCs). The BCSCs population, present within BC tumors, is thought to be derived from breast stem cells and possess self-renewal capacities and tumorigenic potential. They also have been associated with tumor initiation, and recurrence and are resistant to chemo and radiotherapy (Butti et al., 2019). In the stochastic theory, each tumor subtype derives from a single cell type (stem, progenitor, or differentiated cell) (Sun et al., 2017). Recently another model was proposed — “the plasticity model” —, in which it is claimed that

differentiation can be bidirectional so that differentiated nontumorigenic cancer cells may revert to cancer stem cells (CSC) (Rich, 2016). Several data support all these theories, but the origin of BC is not fully understood yet. Recent reviews such as Kong et al. (2020), Song and Farzaneh (2021) can be consulted for more detailed information.

### **1.5. Breast Cancer Diagnostic and Grading**

Breast Cancer early detection is of utmost importance; thus, if detected in an early phase and correctly treated, BC has a chance of cure in 70-80%, contrary to advanced metastatic disease that is not curable. In this case, the goal of therapy is to prolong survival and control the secondary effects of cancer treatment with quality-of-life improvements (Harbeck et al., 2019).

In this vein, the World Health Organization (WHO) has defined 2 distinct but related strategies: a) early diagnosis, which identifies the symptoms of BC at early stages normally by a physical exam to detect any lump or other unusual breast aspects, and b) screening, which allows detection of asymptomatic disease in a target population. The latter usually use mammography as a screening exam (Ginsburg et al., 2020). Imaging is a determinant weapon for BC's detection, diagnosis, and clinical management (Bhushan et al., 2021). Generally, the suspicious breast lesions require further anatomopathological diagnosis confirmation by fine needle aspiration, or core histological biopsies (Pesapane et al., 2020).

After the BC diagnostic, patients are evaluated to establish more appropriate treatment options. This evaluation considers several aspects, such as tumor grade, stage, and molecular subtype.

The tumor grade compares the neoplastic with normal cells, where it is attributed the scores 1, 2, or 3 taking into consideration three main characteristics: the amount of gland formation, nuclear pleomorphisms, and mitotic activity. The sum of these scores leads to three tumor grades: Grade I (low grade), Grade II (intermediate grade), and Grade III (high grade) corresponding to well-differentiated, moderately differentiated, and poorly differentiated tumors (John Hopkins Medicine Pathology, 2021).

The tumor stage measures how advanced the disease is considering the TNM classification. The TNM is an acronym where T stands for tumor, N is for node, and M is for metastasis. Thus, there are evaluated aspects such as tumor size and other relations with surrounding structures, affected lymph nodes (number and localization, and

extracapsular extension), and the presence or absence of multiple metastases (Cserni et al., 2018). The joint information allows the classification into four stages (Stage 0-IV), where Stage 0 corresponds to non-invasive disease and Stage IV to metastatic disease (Rosen and Sapra, 2021).

BC commonly metastasizes to distant organs such as bone, liver, lung, and brain, which adds to the difficulty of controlling the disease and decreases the survival probability after treatment (Sun et al., 2017). Generally, the 5-year BC survival rate is considerably high reaching 90%. However, when referring just to metastatic BC this rate drops to 29% and is even lower (12%) in metastatic triple-negative breast cancer (TNBC) (American Cancer Society, 2021). This data draws our attention to the need to investigate new treatment options for metastatic BC, especially TNBC.

### **1.6. Breast Cancer Classification**

#### **1.6.1. Histological Classification**

Breast cancer (BCqa), like other types of cancer, is not one disease. It represents various diseases corresponding to different histological and molecular types with distinct clinical outcomes (Dai et al., 2017).

Breast carcinomas represent the vast majority of BC, accounting for nearly 95% of BC, although other malignant lesions such as sarcomas and lymphomas can occur (Makki, 2015). The histological classification of carcinomas is based on the origin of the tumor (from the epithelium of the ducts or the lobules) and the characteristics of the tumor itself. Most breast carcinomas (around 55%) derive from duct cells and are divided into ductal carcinoma in situ (DCIS) when cells from the tumor do not invade the basement membrane, and invasive ductal carcinoma (IDC) when there is the invasiveness of the tumor into the stroma. This classification of in situ/invasive also applies to lobular carcinomas: lobular carcinoma in situ (LCIS) and invasive lobular carcinoma (ILC) (Makki, 2015). Each type of in situ or invasive carcinoma has several subclassifications according to its architectural features and the amount, type, and localization of the secretions. The WHO Classification of Breast Tumors, World Health Organization (2019) is recommended for further reading and information.

#### **1.6.2. Molecular Classification – Breast Cancer Subtypes**

There has been a great effort to stratify breast tumors based on the morphological architecture and molecular characteristics that can be better predictors of tumors' behavior and direct the therapeutic approach. One approach is to look at the presence

or absence of estrogen (ER) or progesterone receptors (PR) and human epidermal growth factor 2 (HER-2). Accordingly, BC is commonly classified into three main subtypes: Luminal, HER-2 overexpression and triple-negative BC (TNBC) (Waks and Winer, 2019). Figure 3 resumes the main molecular subtypes of BC with their main characteristics.

These subtypes are usually defined by immunohistochemistry (IHC) or genetic techniques (Grimaldi et al., 2020). Genetic techniques provide more information than IHC but are much more expensive. Therefore, IHC is the most used to determine these molecular subtypes, and patients within a particular subtype are directed to a subtype-specific therapeutic approach (Zaha, 2014, Bonacho et al., 2020).

Based on genetic techniques and their respective gene expression profiles, BC tumors were classified into five subtypes: Luminal A, luminal B, HER-2-enriched, basal-like, and normal-like (Perou et al., 2000, Sorlie et al., 2003). Later another group was described in human and mouse tumors: the claudin-low subtype (Herschkwitz et al., 2007).

	Luminal A	Luminal B	HER-2	TNBC
ER/PR	+	+	-	-
HER-2	-	-	+	-
Ki67	Low	Low	Any	High
Frequency *	50-60%	20-30%	10-20%	10-20%
5 years survival	94.3%	90.5%	84%	76.9%
Grade	Low (Grade I)			High (Grade III)
Histological differentiation	Well-differentiated			Poorly-differentiated
Prognostic	Good			Intermediate
Treatment	Endocrine Therapy		Target HER-2 Therapy	Chemotherapy

**Figure 3** - Molecular classification of breast cancer subtypes with their main characteristics using immunocytochemistry markers. Adapted from do Nascimento and Otoni (2020), Burguin et al. (2021). \* Range described <sup>o</sup>+ in the referenced literature.

### **1.6.2.1. Luminal**

The luminal subtype is the most common BC tumor. Luminal tumors are subdivided into luminal A (ER+, PR+, low ki67) and luminal B (ER+, PR+, high ki67, and sometimes HER-2+). In both subtypes, there is a high expression of low molecular weight cytokeratins and expression of hormone receptors (ER and PR), similar to the epithelium of origin in the normal breast. However, in luminal A tumors, there is a high expression of ER and PR, while in luminal B the expression of these hormone receptors is moderate to weak (Makki, 2015). Although most luminal tumors co-express ER and PR, some cases are ER+/PR– and less frequently, ER–/PR+ (Godoy-Ortiz et al., 2019).

The main difference between luminal A and B is related to the expression of the proliferative gene ki67 (Sorlie et al., 2003, Waks and Winer, 2019). Ki67 is a very important marker reflecting the tumor's proliferative status and has been extensively assessed as a prognostic and predictive marker in invasive BC (Chen et al., 2017, Muftah et al., 2017). Ki67 is absent in quiescent cells and expressed in all proliferating cells, being low during G1 and early S-phase and progressively increasing in S and G2 phases, reaching the maximum during mitosis and then rapidly decreasing during anaphase and telophase (Urruticoechea et al., 2005). Overall, ki67 is a marker of poor prognosis because it indicates highly proliferative tumors (Min et al., 2016, Wu et al., 2019). Notwithstanding, a good chemotherapy response is related to higher ki67 levels (Kim et al., 2014, Bahaddin, 2020).

For this subclassification into luminal A and B, a cut-off > 20% of ki67-positive cells is applied to classify the tumor as luminal B (Lombardi et al., 2021). More recently, the criteria of > 20% of PR-positive cells were included in this classification (Fragomeni et al., 2018).

Luminal A is the most prevalent, accounting for 50% of invasive BCs (Makki, 2015), and tends to have a better prognosis and lower tumor grade. Luminal B generally is more aggressive with a worse prognosis, possesses higher tumor grades, and variable responses to endocrine therapy and chemotherapy (Poloz et al., 2017).

### **1.6.2.2. HER-2**

This subtype accounts for 10-20% of all invasive BC (do Nascimento and Otoni, 2020, Burguin et al., 2021). It is characterized by the overexpression of HER-2, a member of the ERBB family of RTKs (Receptor tyrosine kinases) (Makki, 2015, Maadi et al., 2021). These kinases regulate key biological processes such as apoptosis, cell cycle,

cytoskeletal rearrangement, and cell differentiation, thus, their dysregulation is related to several diseases, including BC (Roskoski, 2014). Indeed, in rare conditions, it can also express ER and PR receptors. BC with HER-2 amplification can have up to 25-50 copies of the HER-2 gene, corresponding to a 40-100-fold increase in HER-2 protein (Kallioniemi et al., 1992).

For HER-2, the assessment is commonly performed by the IHC and/or ISH (in situ hybridization). The ASCO/CAP (American Society of Clinical Oncology/College of American Pathologists) guidelines divide the positivity for HER-2 in IHC into 4 scores (Score 3+, 2+, 1+, and 0) according to the percentage of positively stained cells, the complete circumferential membrane staining and the intensity of this immunostaining. (Ahn et al., 2020a).

HER-2 subtype usually occurs at a young age with poor tumor grade and lymph node involvement and normally expresses high levels of ki67. Thus, it is characterized by aggressive behavior and poor response to conventional therapy (Godoy-Ortiz et al., 2019, Wang and Xu, 2019).

### **1.6.2.3. Triple-negative vs Basal-like**

As the name indicates, triple-negative breast cancer (TNBC) lacks the expression of the ER, PR, and HER-2 and thus does not respond to targeted therapies. TNBC accounts for 10-20% of sporadic invasive BC (do Nascimento and Otoni, 2020, Burguin et al., 2021) and is considerably higher in BRCA1 hereditary cancers varying from 66-100% according to different studies (Peshkin et al., 2010, Lee et al., 2020a).

TNBC is a broad and heterogeneous group, and most TNBC (about 75%) are basal-like, but they cannot be considered synonyms (Wahba and El-Hadaad, 2015). Generally, TNBC is applied when IHQ is applied, whereas the basal-like subtype is more related to subtype determination by gene expression microarray analysis (Yersal and Barutca, 2014). Basal-like cancers typically exhibit basal markers such as cytokeratin (CK) 5, 6, or 17, as do normal basal and myoepithelial cells, and strongly express ki67 (Alluri and Newman, 2014, Makki, 2015).

In addition to basal-like tumors, other authors describe that TNBC can include claudin-low, luminal androgen receptor, mesenchymal, mesenchymal stem-like, immunomodulatory, mesenchymal, basal-like immune-activated, basal-like immunosuppressed tumors (Lee et al., 2020b). TNBC is associated with a poor

prognosis, higher early recurrence (metastatic and local), and drug resistance rates, which is a problem as chemotherapy is the only therapeutic option (Landry et al., 2022).

## **2. Breast Cancer Treatment**

### **2.1. Treatment Options**

The decision on adequate therapies is often taken by a multidisciplinary group, including the oncologist, surgeon, radiation therapist, and other health professionals, taking into account the patient's characteristics and the type and stage of the tumor (Murawa et al., 2014). Breast cancer treatment is a complex process in which surgery, radio, and chemotherapy are complementary weapons. However, according to the BC subtype, they can better respond to target therapies (Yersal and Barutca, 2014), acting directly into ER or HER-2 (Masoud and Pagès, 2017).

#### **2.1.1. Surgery**

The treatment options for BC have changed a lot in recent years. A few decades ago, women with BC diagnostics were submitted to radical mastectomy, including the dissection of the axillary lymph node chain (Keelan et al., 2021). This treatment approach is still valid, but the surgical procedure has become more conservative for both the breast and the axillary lymph nodes, providing women with a better quality of life and self-esteem. Instead of radical mastectomy, breast-conserving surgery frequently followed by radiotherapy is adopted whenever possible. In conservative breast surgery, the tumor is removed with margins of normal breast tissue. The sentinel node technique, implemented in the early 1990s, prevented total axillary resection in many BC patients, reducing the morbidities of lymphedema and arm pain connected with the axillary lymph node chain. These lymph nodes can be quickly analyzed during surgery, but it is always necessary to perform other laboratory techniques including ICQ techniques to reassure the results and identify macro and micrometastasis (Bouquet de Jolinière et al., 2018). If there is no metastasis involvement in the sentinel lymph node(s), the patient can be spared from axillary lymph node dissection, which commonly does not happen if the sentinel node(s) is/are positive, meaning metastatic spread (Malter et al., 2018).

#### **2.1.2. Radiotherapy**

Radiotherapy consists of the use of ionizing radiation to kill cancer cells (Senkus, 2018). The use of radiotherapy has been widely used in BC treatment for years in a wide range of applications, as part of the treatment of early and advanced BC, also including palliative treatments. It can be applied in neoadjuvant, preoperative, intraoperative, or

adjuvant therapy, especially after conservative breast surgery (Yang and Ho, 2013). Neoadjuvant radiotherapy is mainly used for tumor downstaging in some inoperable BC, allowing a more conservative surgery (Sousa et al., 2020). In some BC treatment centers, intraoperative is applied in a set of specific medical indications (Murawa et al., 2014). As for adjuvant therapy, several variants are applied according to the patient's age and specific disease conditions; for instance, partial breast irradiation is widely used, especially after breast-conserving surgery in selected patients with early-stage BC. Also, nodal radiation therapy may benefit when lymph nodes are positive for metastasis (Castaneda and Strasser, 2017). Radiotherapy can be administered simultaneously with other treatments, such as target therapies (Li et al., 2016, Castaneda and Strasser, 2017) and under certain conditions with chemotherapy (Fernando et al., 2020). However, to prevent excessive toxicity, the use of chemotherapy and radiotherapy in sequence may be preferred (Pinnarò et al., 2011, Hickey et al., 2013).

### **2.1.3. Chemotherapy**

Chemotherapy is a systemic drug-based treatment that interferes with tumor cells' growth and cell division to kill them (Jimenez et al., 2018). It is one major weapon against cancer in general, including in BC (Vasir and Labhasetwar, 2005). Chemotherapy can be administered before (neoadjuvant) or after surgery (adjuvant) depending on several factors such as the condition of the patient, size, and location of the tumor, degree of lymph node involvement, expression of the ER, and PR, and expression of the HER-2 (Masood, 2016, Asaoka et al., 2020).

Neoadjuvant therapy was initially applied to prevent the progression of the disease by killing disseminated tumor cells. Then, after many trials and clinical studies, neoadjuvant therapy was associated with other advantages, such as improved surgical outcomes (allowing more conservative surgeries) and assessing the response to the treatment of cancer candidates for adjuvant chemotherapy (Rezai and Kraemer, 2017). Adjuvant therapy is commonly used in metastatic BC tumors and can also be followed by target therapies (Burguin et al., 2021).

One of the major drawbacks of chemotherapy is its side effects. These include fatigue, alopecia, cytopenia, muscle pain, neurocognitive dysfunction, and chemo-induced peripheral neuropathy. The chronic or late side effects (after 6 months of treatment) include cardiomyopathy, second cancers, early menopause, sterility, and psychosocial impacts (Tao et al., 2015).



For chemotherapy in BC, several approved drugs belonging to different classes with distinct mechanisms of action to prevent and treat the disease. The main classes are antimetabolites, alkylating agents, antimetotic drugs, and hormonal and immunological target therapies (Abotaleb et al., 2018). Among the most used drugs approved for treating BC are cyclophosphamide, anthracyclines (e.g. doxorubicin), taxanes (e.g. paclitaxel), and 5-Fluorouracil (5-FU), capecitabine, platinum compounds (e.g. cisplatin) (Al-Mahayri et al., 2020) (Figure 4).

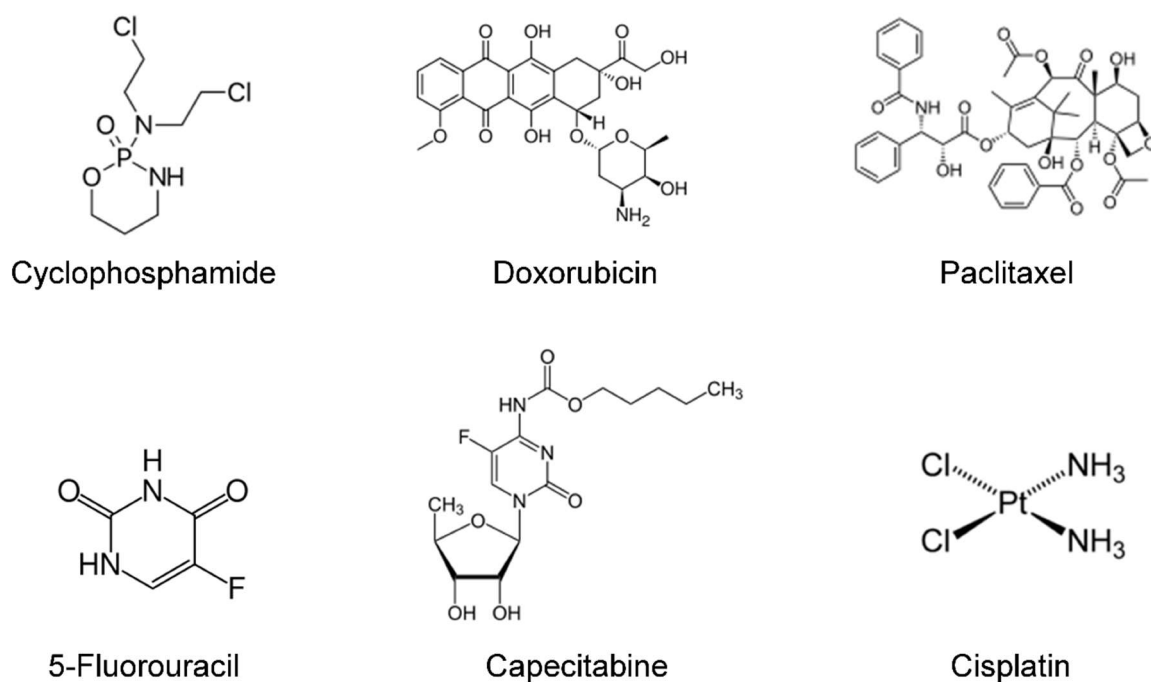


**Figure 4** - Chemical structure of the current main drugs used in breast cancer chemotherapy.

### 2.1.3.1. Cyclophosphamide

Cyclophosphamide belongs to the group of alkylating nitrogen mustard compounds. It is used to treat various cancer types, including BC, and is an essential component of many effective drug combinations. Cyclophosphamide requires metabolic activation by liver cytochrome P450 enzymes into reactive alkylating agents (Wang et al., 2007). These alkylating agents bind covalently irreversibly to DNA forming adducts that lead to DNA breaks and consequently cause apoptosis (More et al., 2019). It is used in high doses for effective chemotherapy, driving to immunosuppression. That is why this drug is also used, for example, to prevent graft-versus-host disease in transplantation (Lien and Scott, 2000).

### 2.1.3.2. Anthracyclines

Anthracyclines are a class of natural antibiotics that are extensively used as antineoplastic agents due to their efficiency in a broad spectrum of cancers, including both solid (also in BC) and liquid tumors (Shah and Gradishar, 2018). The first anthracycline to be identified was daunorubicin, originally isolated from the soil actinobacterium *Streptomyces peucetius* (Arcamone et al., 1969), as well as its derivate adriamycin, also known as doxorubicin (Dox). Dox anticancer effects are based on two main mechanisms (i) intercalation into DNA which inhibits DNA transcription and replication and disruption of topoisomerase-II-mediated DNA repair, and (ii) generation of reactive oxygen species and respective oxidative damages (Thorn et al., 2011). Like any other chemotherapy drug, Dox induces several systemic side effects, including hepatotoxicity, neuropathy, neurotoxicity, and the most relevant, cardiotoxicity (Carvalho et al., 2009, Ajaykumar, 2020). The causal mechanisms underlying Dox-induced cardiotoxicity are still not completely elucidated. However, owing to its acute and chronic cardiac toxicity, Dox has dose-limiting effects. Another limitation of using Dox as the main treatment is the emergence of multidrug resistance (MDR) (Al-Malky et al., 2019).

### 2.1.3.3. Taxanes

Taxanes emerged as a powerful group of compounds in the 1990s. Taxanes can be used in monotherapy or combination therapy (Abal et al., 2003) or associated with anthracyclines (anthracycline followed by taxane) (Zaheed et al., 2019). The taxanes used in BC treatment are paclitaxel, docetaxel, and cabazitaxel; however, they have many differences in efficacy–toxicity ratio and pharmacokinetic interactions with anthracyclines (Nabholtz and Gligorov, 2005). Taxanes stabilize microtubules through centrosomal impairment, induction of abnormal spindles, and suppression of spindle microtubule dynamics (Maloney et al., 2020). As microtubule dynamics are essential for cell division, taxanes inhibit spindle formation, thus blocking mitosis and inducing apoptosis (Jordan and Wilson, 2004).

### 2.1.3.4. 5-Fluorouracil

5-Fluorouracil is a pyrimidine analog that belongs to antimetabolite drugs. 5-FU anticancer effects are caused by inhibiting thymidylate synthase and incorporating its metabolites into RNA and DNA (Longley et al., 2003). 5-Fluorouracil is commonly used in combination with anti-HER-2-targeting therapies (Yi et al., 2020).

### **2.1.3.5. Capecitabine**

Capecitabine is an antimetabolite prodrug, which means it is not cytotoxic per se. It needs enzymatic conversion by cancer cells to be converted into 5-FU (Parsons and Burstein, 2021). It is used in the neoadjuvant and adjuvant chemotherapy setting of TNBC as neoadjuvant and adjuvant chemotherapy (Huo et al., 2021). Food and Drug Administration (FDA) approved this compound for a single agent in metastatic BC patients who are resistant to anthracycline- and paclitaxel-based regimens or situations where anthracycline treatment is contraindicated and in combination with docetaxel followed by failure of anthracycline therapy (Walko and Lindley, 2005).

### **2.1.3.6. Platinum compounds**

Platinum compounds have been extensively used in cancer treatment. In BC, they may be used in treating TNBC (Gerratana et al., 2016, Poggio et al., 2018) and advanced metastatic disease (Petrelli et al., 2016). Platinum compounds have a high affinity to DNA and establish cross-link DNA strands, distorting the double helix of DNA and causing single and double-strand breaks. This action causes inhibition of DNA synthesis, induces cell cycle arrest, and if the damage is permanent, it leads to cell death (Siddik, 2003). The platinum compounds used in BC treatment are commonly cisplatin and carboplatin. They have never been used as a drug of choice due to their high toxicity and complexity in their administration compared to other medications (Martín, 2001).

### **2.1.4. Target Therapies**

Unlike chemotherapy drugs that act broadly in cancer-dividing cells, target therapy drugs act preferentially in cells harboring specific proteins or molecular targets involved in the tumorigenesis process to block or eliminate altered pathways in such cells (Baudino, 2015). Among the approved target therapy for cancer treatment are signal transduction inhibitors, hormone therapies, gene expression modulators, apoptosis inducers, angiogenesis inhibitors, immunotherapies, and toxin delivery molecules. Target therapies have been contributing to increasing the treatment efficacy, reducing the therapeutic side effects, and improving the quality of patients' lives (Widmer et al., 2014). The most common target therapies in BC are hormone or endocrine therapy for positive hormone tumors and signal transduction inhibitors for HER-2 (Mohamed et al., 2013, Meisel et al., 2018).

### 2.1.4.1. Endocrine Therapy

In ER-positive tumors, the therapeutic management of endocrine estrogen levels and their interaction is vital. For this reason, an accurate assessment of ER status is essential, as it directs patients to different treatment approaches. IHC is the main methodology used for this assessment (Noordhoek et al., 2019). The established ASCO/CAP guidelines for directing patients to target ER therapy recommend the cut-off of more than 10% of ER-positive cells, tumors with 1-10% of positive cells are classified as low positive, and when less than 1% of cells are positive they are considered negative (Allison et al., 2020). Another important marker in this classification is proliferation marker ki67, referred to for the subclassification of Luminal A and B tumors (Davey et al., 2021).

Anti-estrogen drugs can interfere with ER signaling by acting as (i) ER modulators as the selective estrogen receptor modulators (SERMs) (e.g., tamoxifen); (ii) promoting ER degrading — selective modulators estrogen receptor degraders (SERDs) (e.g., fulvestrant), or (iii) blocking the production of estrogens as aromatase inhibitors (AIs) (e.g., anastrozole, letrozole) (Sleightholm et al., 2021).

The most used drugs in BC are SERMs, which compete with estrogens by binding to the ER, changing its configuration, so that when it is translocated to the nucleus it blocks the transcription of genes related to cell proliferation and migration; both processes related to the cancer growth (Patel and Bihani, 2018, Burguin et al., 2021). The most famous drug in this class is tamoxifen, which is used in all stages of ER-positive BC (Swaby et al., 2007).

The other class of anti-estrogens, the SERDs, completely block the ER pathway. SERDs inhibit ER dimerization, blocking translocation to the nucleus and causing ER degradation (Patel and Bihani, 2018, Burguin et al., 2021). Initially, the SERD fulvestrant was approved by FDA for the treatment of metastatic luminal BC in postmenopausal women, nowadays SERDs are considered an effective therapeutic approach to treat luminal BC in both early stages, as first-line treatment or in advanced BC that is AI or tamoxifen drug-resistant (Hernando et al., 2021).

AIs have been used mainly in post-menopause BC, as they reduce the plasma levels of estrogen, as its name indicates, inhibiting the activity of the enzyme aromatase, responsible for the biosynthesis of estrogen from androgens (Caciolla et al., 2020).

### **2.1.4.2. HER-2 Target Therapy**

The HER-2 targeting therapies relay basically into two approaches. One is the class of antibodies and their conjugates that use the HER-2 overexpression as a tumor cell identifier. Another category includes drugs that inhibit the signaling of HER-2 - tyrosine kinase inhibitors (TKIs) (Escriva-de-Romani et al., 2018).

The most common antibodies are trastuzumab and pertuzumab, being trastuzumab the standard of care in the HER-2 BC subtype. Trastuzumab is a monoclonal antibody directed to the sub-domain IV, a juxtamembrane region of the HER-2 extracellular domain. Although the mechanisms of action of trastuzumab are not fully understood, it is thought to involve the inhibition of HER-2 dimerization and suppression of HER-2-mediated downstream signaling pathways involved in the mechanisms of tumor growth (Maximiano et al., 2016). Pertuzumab is another approved drug for use in combination with trastuzumab and docetaxel in patients with HER-2-positive metastatic BC and as neoadjuvant treatment for patients with HER-2-positive early BC (Kirschbrown et al., 2019).

Antigen-drug conjugates (ADCs) consist of the combination of a monoclonal antibody with a cytotoxic drug that is released in antigen-expressing cells (Diamantis and Banerji, 2016). This technology improves the efficacy of the treatment and minimizes the exposure of non-target cells. The Ado-trastuzumab emtansine (T-DM1, Kadcyla) is already approved for HER-2 metastatic BC in patients previously treated with trastuzumab and taxane (Trail et al., 2018).

This anti-HER-2 therapy has a significant impact on HER-2-positive patients, but additional options such as TKI (e.g., lapatinib, neratinib, or pyrotinib) have been developed due to antibody resistance. They are small molecules that compete for the adenosine triphosphate binding domain within the cytoplasmic portion of HER-2, which prevents the phosphorylation and consequent signaling transduction pathways (Escriva-de-Romani et al., 2018).

### **2.1.5. Combination Therapy**

Combination therapy is a treatment modality that combines two or more therapeutic agents (Bayat Mokhtari et al., 2017). The combination of drugs evolved over many centuries as in traditional Chinese medicines it was common to use a combination of herbs to treat diseases (Chou, 2006). The use of adjuvant combined chemotherapy using two different drugs with distinct mechanisms of action is a common practice in the

oncology field as it may offer benefits: lower drug dosage with consequent less toxicity without compromising the level of efficacy of the treatment, and lower possibility of drug resistance as different pathways are targeted (Foucquier and Guedj, 2015). The use of one single drug (monotherapy) is more prone to drug resistance because the constant treatment with that compound can make cancer cells recruit alternative pathways to escape from cell death. Thus, the use of drugs with different mechanisms for killing the tumor cells is more appropriate to face the multi-factorial process of drug resistance (Khdair et al., 2010), as cancer cells have more difficulty of escaping from different cytotoxic effects caused by the use of more than one drug (Zimmermann et al., 2007). However, it is important to mention that the drug combination can also be harmful as synergistic toxicity can occur (Yilancioglu et al., 2014).

Initially, the combination therapy for BC used a combination of an alkylating agent (e. g. cyclophosphamide) and an antimetabolite (5-FU). Then, over the years, various combinations of different classes of agents have been under investigation. In BC, there are some drug combinations approved by FDA, combining two or three drugs. In these combinations, Dox is a common drug, e.g. Dox with cyclophosphamide, Dox with cyclophosphamide followed by paclitaxel (taxol), Dox with cyclophosphamide, and 5-fluorouracil (Correia et al., 2021). However, there are other approved drug combinations and others under investigation (Hatem et al., 2018, Ahmad et al., 2020, Domchek et al., 2020, Kang and Syed, 2020), especially for metastatic BC, including the combination of immunotherapy and targeted therapy (Esteva et al., 2019).

#### **2.1.6. Complementary Therapies**

The term “complementary therapies” embraces a wide range of treatments that are not considered traditional in Western countries (Crocetti et al., 1998). It is widespread to find in the literature the acronym CAM which stands for Complementary and Alternative Medicine. Complementary therapies are adjunctive procedures that can be applied alongside mainstream treatment to control symptoms and/or provide well-being. On the other side, alternative therapies are often promoted as surrogates for mainstream treatment (Cassileth et al., 2009). The use of complementary therapies has gained more relevance in the past decades, especially in the oncology field (Abrahão et al., 2019).

Some patients believe they can benefit from complementary techniques such as homeopathy, yoga, acupuncture, medicinal plant intake, and manual healing methods. The use of complementary therapies is commonly applied to alleviate side effects of treatment-related symptoms, reduce the toxicity of the treatments (Abrahão et al., 2019),

stimulate immunity (Chandwani et al., 2012), or relieve physical distress (Crocetti et al., 1998).

Although most patients do not refer these complementary medicines to their oncologists, many studies that investigated the proportion of patients that use those therapies showed that their use ranged from 10-60% of patients (Crocetti et al., 1998). This range is related to many factors, such as the socio-demographic characteristics of the patients and cultural differences relative to the use of these therapies (Irmak et al., 2019). About BC, the percentage of survivors that used some CAM also reached 62% (Buettner et al., 2006). The most problematic question about this type of therapy is whether patients use it in a desperate attempt to secure a cure together or after the failure of conventional medicine.

Unfortunately, there is a cultural fallacy: “Anything natural is good”, and the ingestion of natural products has no secondary effects. In the context of this thesis, the intake of herbs and dietary supplements is the only complementary therapy that will be considered as some of the seaweed compounds tested here are sold free on the internet or by herbalists without needing any medical prescription. Doctors need to be aware of the intake of herbs and herbal-derived compounds, as they can interact with cytochrome P450 (Zhou et al., 2003, Russo et al., 2014, Cho and Yoon, 2015, Zhang et al., 2020b) and P-Glycoprotein (Cho and Yoon, 2015), which can compromise the efficacy of medications, including chemotherapeutic agents or have unpredictable effects (Cassileth et al., 2009, Lin et al., 2020a). Indeed, many botanical extracts and herbal products do not possess a well-defined composition and often contain unidentified compounds (Deng and Cassileth, 2014). Moreover, they are sold without strict governmental regulations or verification by competent authorities. Therefore, the possibility of interference in the intake of herbal compounds with conventional therapies should not be undervalued and certainly requires further investigation. As a precaution, doctors should include questions about this kind of consumption in medical history taking.

Paradoxically, the general public does not know that many anticancer medications are made from natural substances found in plants, fungi, or marine sources. Examples are the cases of plant-derived drugs: taxanes (paclitaxel and docetaxel), camptothecin analogs, vinca alkaloids (vinblastine, vincristine, and vindesine), epipodophyllotoxins (etoposide and teniposide) (Mann, 2002, Amin et al., 2009). Some of these are directly extracted, and other serves as a base to produce semi-synthetic or synthetic analogs.

Given the above scenario, either from a perspective of prevention of misuse or medical use, it is vital to investigate the combination of natural compounds with anticancer drugs, as they can potentially augment or interfere with the efficacy of the anticancer drugs.

### **3. Breast Cancer Caveats and Needs**

#### **3.1. Drug Resistance**

In advanced healthy systems, 80-85% of BC patients will be cured after treatment, although a systemic failure of these initially cured patients can occur over the next 5-10 years (Becker, 2015). The remaining 15% die from the disease, generally associated with complications of metastasis or due to the appearance of drug resistance and recurrence. Despite significant advances in cancer treatments, the development of drug resistance and, in some cases, multidrug resistance (MDR) continues to be a great challenge in fighting against the disease. Apart from metastasis, MDR is the leading cause of tumor relapse and failure of the therapy (Mansoori et al., 2017). Drug resistance can be classified as intrinsic (*de novo*) or acquired. *De novo* resistance occurs before drug exposure, while acquired resistance occurs after initially sensitive tumors (Hazlehurst and Dalton, 2006).

There are several mechanisms and factors that can influence drug resistance in BC, such as: 1) efflux pumps that reduce the concentration of the drugs inside the cells; 2) alterations in the membrane structure that alters the cellular uptake; 3) increased and altered drug targets; 4) metabolic alterations of the drugs; 5) inhibition apoptosis; 6) repair of DNA damage (Núñez et al., 2016); 7) cancer resistance genes and micro RNAs; 8) tumor heterogeneity; 9) tumor microenvironment conditions; and 10) cancer stem cells (Ji et al., 2019).

The efflux pumps have a major contribution to MDR. They are mediated by ATP-binding cassette (ABC) transporters, like the most well-described P-glycoprotein (P-gp), overexpressed in 40-50% of BC patients. The P-gp efflux transporters need ATP from the mitochondria to pump the chemotherapy drugs out of cells. Thus, mitochondrial metabolism has been investigated for future cancer therapies (Weinberg and Chandel, 2015).

Alterations in the membranes and other drug targets, due to either a secondary mutation in the target protein or changes in epigenetics, also interfere with the efficacy of drugs, contributing to drug resistance. The drug's action can also be dependent on its interaction with other proteins that can alter these drugs, consequently interfering with



their efficacy. One example is the glutathione S-transferase (GST) which has a major role in the detoxification of drugs. These enzymes increase drug resistance through the detoxification of anti-cancer drugs or indirectly by the mitogen-activated protein kinase (MAPK) pathway inhibition (Mansoori et al., 2017).

Another relevant mechanism that plays an essential role in drug resistance is enhanced DNA damage repair, especially in drugs that cause DNA damage by cisplatin (Wang et al., 2019b).

Moreover, several genetic and epigenetic changes can occur within the tumor, leading to tumor heterogeneity. Other extrinsic factors, including pH, hypoxia, and paracrine signaling interactions with stromal and other tumor cells, can also interfere with the genes and their respective products associated with drug resistance (Mansoori et al., 2017). There is a complex crosstalk between the neoplastic cells and the microenvironment. This crosstalk influences tumor development and the resistance to anticancer therapies. Among the molecules involved in this process are the microRNAs, which help induce pro-tumoral traits and fuel tumor aggressiveness (Cosentino et al., 2021). Along this line, some genes, such as Twist and MRD1 have been associated with drug resistance in BC. Twist one is a regulator of EMT and MRD1 encodes proteins such as P-gp, GTS, and p53, all related to drug resistance mechanisms (Ji et al., 2019).

The presence of breast cancer stem cells (BCSCs) has been pointed out as an important cause of drug resistance, as they are described to be more resistant to chemotherapeutic agents and radiotherapy (Pavlopoulou et al., 2016). BCSCs possess stem cell characteristics as the self-renewal capacity and are characterized by the expression of surface marker CD44 and a low or complete absence of surface marker CD24 (CD44+/CD24-/low) (Butti et al., 2019). BCSCs with high aldehyde dehydrogenase 1 (ALDH1) activity have also been associated with an increased tumorigenic potential (Gote et al., 2021).

It is important to mention that drug resistance can occur in any treatment with chemotherapy, endocrine, and target therapies. For instance, 20-30% of hormone-positive tumors develop resistance to SERMs (Viedma-Rodríguez et al., 2014, Ali et al., 2016). Therefore, the search for more new drugs and more selective compounds with fewer side effects or compounds that can contribute to lowering cancer therapy resistance is of paramount importance. In this scenario, several scientists and the pharmacology industries have been exploring natural and natural-inspired compounds to fulfill this need.

#### 4. Natural and Nature-Inspired Compounds for Cancer Prevention and Treatment

“Natural products” include a large and diverse group of substances from various sources. They are produced by marine organisms, bacteria, fungi, and plants. The term encompasses complex extracts from these producers and the isolated compounds derived from those extracts. It also includes vitamins, minerals, and probiotics” (Milshteyn et al., 2014).

In folk medicine, natural products have historically been part of treating human ailments (Cragg and Pezzuto, 2016). Thus, plants and other natural products have been a source of interest for investigation for drug discovery, including in the cancer field. Currently, over 50% of anticancer drugs are derived from natural products or are synthetic analogs of natural products (Newman and Cragg, 2020). A good example of this translational medicine from folk to modern medicine was the first plant-derived anticancer drug, vinca alkaloids, derived from the Madagascar periwinkle, *Catharanthus roseus* (Apocynaceae). Because several populations traditionally used this plant to treat diabetes (Al-Shaqha et al., 2015), there was an investigation into its application as an oral hypoglycemic drug in rats. Surprisingly, its extracts also reduced white blood cell counts and caused bone marrow depression, so it was tested for the treatment of lymphocytic leukemia in mice and later in humans and approved as an anti-leukemia drug (Cragg and Pezzuto, 2016).

Natural products are one of the main starting points for drug discovery and have demonstrated considerable potential in the biomedical area (Ruiz-Torres et al., 2017). Therefore, in oncology, natural derived products are used as first-line treatments for different cancers, like vinblastine, vincristine, and their analogs, paclitaxel, and the analogs, docetaxel, and cabazitaxel, podophyllotoxin and analogs, etoposide, camptothecin and analogs, topotecan and irinotecan (Jimenez et al., 2018).

Another "front of attack" for natural compounds is their use in combination therapy with anticancer drugs; in certain situations, these combinations have been highlighted as a rising research focus with potentially successful outcomes (Kapadia et al., 2013, Lichota and Gwozdzinski, 2018, Rejhová et al., 2018, Mosca et al., 2020, Sauter, 2020). A revision by Lin et al. (2020a) is recommended for a thorough analysis of the pre-clinical data of natural compounds as potential adjuvants to cancer therapy.

Similarly, recent attention has been given to the role of natural products in the chemoprevention setting. The concept of chemoprevention was introduced in the mid-

seventies (Sporn et al., 1976). It refers to the use of natural or synthetic pharmacologically active substances to prevent, postpone, or reverse the carcinogenesis process (before the invasion step) (Sporn and Suh, 2000, Cragg and Pezzuto, 2016, Melo et al., 2018). A plethora of natural-derived compounds from plants, fruits, vegetables (Melo et al., 2018), seaweeds (Namvar et al., 2013a, Park and Pezzuto, 2013b, Moussavou et al., 2014), fungi-derived compounds (Petrova et al., 2008, Park and Pezzuto, 2013b, Pięć et al., 2021) have been indicated as possible chemopreventive agents.

Most studies of putative chemopreventive agents came from *in vitro* or *in vivo* studies with animal models. The results show that some nutrients and bioactive foods regulate different epigenetic mechanisms. Other agents have been associated with anti-inflammatory effects by triggering reactive oxygen species (ROS) scavenging, inducing apoptosis, inhibiting EMT, and epigenetic regulation (Melo et al., 2018). However, the mechanisms behind these chemopreventive effects are generally not fully understood.

#### **4.1. Marine-derived Compounds in Cancer Prevention**

There are on the global market a great variety of food supplements that correspond to extracts and semi-purified fractions of edible marine organisms such as seaweeds that are publicized as antioxidant, immunostimulatory, and cancer-preventive (Suleria et al., 2015). This commercial trend agrees with the fact that some marine-derived products have long been used in the folk medicine of many Asian countries to treat different pathological conditions, including cancer (Bandaranayake, 1998, Ntie-Kang and Svozil, 2020).

Some evidence of chemopreventive effects is based on observation of low incidence of a certain type of tumors in a population, which is commonly associated with eating habits such as the low incidence of BC in Asian countries associated with seaweeds intake (Yang et al., 2010, Teas et al., 2013). Consistent with the epidemiological association, seaweed's compounds have exhibited several *in vitro* chemopreventive effects (Gamal-Eldeen et al., 2009, Lee et al., 2013, Park and Pezzuto, 2013a, Vishchuk et al., 2016), including in BC cell lines (Funahashi et al., 2001). There are available revisions on the topic for more detailed information about the chemopreventive action of marine-derived compounds, such as Stonik and Fedorov (2014), Dyshlovoy (2021).

## 4.2. Marine-derived Compounds in Cancer Treatment

The search for new compounds with pharmacological activity has been largely extended to the oceans as they harbor enormous biodiversity in fauna and flora that live in different conditions, such as a wide range of temperatures, light exposure, oxygen levels, pH, pressure, nutrients availability, salinity, and predators attacks. Due to this huge diversity of environments, marine organisms such as fishes, microalgae and seaweeds, mollusks, sponges, other invertebrates and microorganisms, mainly bacteria and fungi, developed adaptive mechanisms and symbiotic interactions, that are, in part, responsible for the production of compounds with bioactive activity, mostly corresponding to secondary metabolites (Wang et al., 2020).

Secondary metabolites mean that these compounds are not part of or are not generated by the main metabolic basic pathways (Cappello and Nieri, 2021) and have no primary function in the development, growth, or reproduction (Martins et al., 2014). Still, they are part of organisms' homeostasis and natural defense against extreme environmental stress (Kaur et al., 2018). Among the biological activities of the secondary metabolites, there have been reported many with health benefits, such as antimicrobial, antioxidant, antidiabetic, anti-obesity, anticoagulant, anti-inflammatory, and anticancer effects (Jha and Zi-rong, 2004, Yatiwella et al., 2018, El-Demerdash et al., 2019, Cotas et al., 2021, Wibowo et al., 2022).

Undoubtedly, the marine milieu is a reservoir of bioactive compounds with uncommon and unique chemical features that can be used as scaffolds in drug discovery and development (Ercolano et al., 2019). A preclinical cytotoxicity screening from the USA National Cancer Institute demonstrated that marine samples had a ten times higher incidence of antitumor properties than terrestrial ones (Munro et al., 1999).

In the last decades, the number of scientific publications about the anticancer properties of marine compounds has been showing an upward trend (Ruiz-Torres et al., 2017), and several compounds entered the drug discovery pipeline. The first marine-derived approved drug was cytarabine, a synthetic pyrimidine nucleoside derived from spongothymidine, isolated from a Caribbean sponge species *Tethya crypta* (Lindequist, 2016). Until 2021, more than ten compounds have already been approved for cancer treatment (Table S1) by FDA and EMA (European Medicines Agency) (Cappello and Nieri, 2021), and one more by the Australian authorities (Gomes et al., 2020). There are three marine-derived drugs under phase III while at least six are in Phase II clinical trials (Table S2), and many others are under preclinical experiments. However, some marine-

derived compounds failed to be effective against cancer cells in phase I and II clinical trials, such as the folastatin-10 and 15, derived from the shell-less mollusk *Dolabella auricularia* (Edwards et al., 2012), and the PM02734 of kahalalide F derived from other marine mollusk, *Elysia rufescens* (Petty et al., 2016). A recent work presents more detailed information on the high number of marine-derived compounds in the earlier phases of clinical trials (Jimenez et al., 2020).

The approved drugs or those under clinical trials belong to different drug classes, such as terpenes and terpenoids, peptides, macrolides, alkaloids, and ADCs with diverse mechanisms of action (Malve, 2016). It is relevant to mention that most of these drugs are synthetic analogs of the initially isolated natural products. As with other drugs, these marine-derived drugs can have side effects such as gastrointestinal toxicity, diarrhea, intestinal ulceration, oral mucositis, hematologic side effects, hepatotoxicity, and septicemia that varies according to the different drugs (Nigam et al., 2019). Also, they are commonly used in second-line chemotherapy in advanced tumors, such as eribulin mesylate, which is used in metastatic or locally advanced BC previously treated with an anthracycline and a taxane (Dybdal-Hargreaves et al., 2015). Another example is the trabectedin that is applied in the treatment of unresectable or metastatic liposarcoma or leiomyosarcoma that has failed a prior anthracycline regimen (Gordon et al., 2016). These drugs have been under several cohort studies in combination therapy with other drugs like cytarabine and daunorubicin for the treatment of acute myeloid leukemia (Murphy and Yee, 2017) or brentuximab-vedotin in combination with doxorubicin, vinblastine, and dacarbazine in patients with newly diagnosed early-stage, unfavorable-risk Hodgkin lymphoma (Kumar et al., 2021).

## **5. An Overview of Marine-derived Anticancer Bioactive Compounds**

From a broad perspective, “bioactive compounds can be defined as nutrients and non-nutrients present in the food matrix (vegetal and animal sources) that can produce physiological effects beyond their classical nutritional properties” (Cazarin et al., 2022). Still quoting verbatim other authors’ opinions, “bioactive compounds are capable of modulating metabolic processes and demonstrate positive properties such as antioxidant effect, inhibition of receptor activities, inhibition or induction of enzymes, and induction and inhibition of gene expression” (Carbonell-Capella et al., 2014).

Marine bioactive compounds display diverse biological activities with nutraceutical and pharmacological potential. From the vast number of marine species, in this thesis, we

dedicated efforts to one marine fungus and seaweed, more specifically brown seaweeds, derived compounds.

### **5.1. Marine Fungi-derived Bioactive Compounds - Sources, Molecules, Uses, and Mechanisms of Action**

Fungi are heterotrophic eukaryotes involved in the decomposition of dead plant tissues and animal tissues to a lesser extent (Bugni and Ireland, 2004). Fungi species produce multiple secondary metabolites, and a significant part of their genomes is responsible for encoding and regulating these metabolites (Bills and Gloer, 2016). The main metabolites from fungi include flavonoids, amines and amides, steroids, indole derivatives, quinones, phenylpropanoids, aliphatic compounds, and phenylpropanoids (Kornienko et al., 2015). Marine-derived fungi have also been described as a source of new metabolites with promising pharmacological activities (Bugni and Ireland, 2004, Rateb and Ebel, 2011), including anticancer effects (Rateb and Ebel, 2011, Deshmukh et al., 2018, Uzma et al., 2018). Fungi-derived drugs have played a crucial role in the treatment of various diseases. Examples of this are the already mentioned  $\beta$ -lactam antibiotics, including penicillin and cephalosporins (Bills and Gloer, 2016), and the “blockbuster” drugs known as statins used to lower cholesterol (Parihar et al., 2019). Also, it is worth mentioning that paclitaxel, one of the most used drugs to treat BC, was discovered in an endophytic fungus *Taxomyces andreanae*, from the yew plant *Taxus brevifolia* (Ji et al., 2006).

Marine fungi are a chemically and biologically diverse group of microorganisms (Bugni and Ireland, 2004) that can be found free in water or sediments or, more commonly, associated with other marine organisms, mostly sessile invertebrates (sponges, mollusks, and crustaceans), and also as endophytes (fungi internally living in plants) in micro and macroalgae. These fungal-host interactions have physiological and ecological relevance as they comprise nutritional enhancement, stabilization of the host skeleton, and secondary metabolite production, representing a great potential for drug discovery (Debbab et al., 2012). Marine fungi produce cytotoxic metabolites to survive in the harsh conditions of the oceans, which is also useful for protecting the associated organisms (Wahl et al., 2012).

Among the fungi-associated organisms, sponges harbor the greatest microbiota diversity (mainly fungi and bacteria), also corresponding to the source of the largest number (33%) of bioactive compounds in the literature (Bugni and Ireland, 2004). Marine sponges are multicellular, sessile, filter-feeding animals. While they feed, many microorganisms are inhaled from the seawater and start residing in the sponge or are phagocytized. As

sessile organisms, their mechanisms of protection against predators rely mostly on chemical protection that is partially obtained due to their interactions with microorganisms such as marine fungi. In the same way, these microorganisms benefit from the sponge nutrient supply (Taylor et al., 2007). Microbial associates comprise as much as 40% of sponge volume (Ji et al., 2006). Sponges and their symbionts' evolution are closely linked, favoring the production of new metabolites (Moitinho-Silva et al., 2017). Furthermore, sponges live in harsh conditions, including low temperatures, elevated hydrostatic pressure, absence of light, high concentrations of metals, and hypoxic conditions, which may be responsible for producing secondary metabolites with promising activities (Jin et al., 2016). There have described several bioactive compounds isolated from sponge-associated fungi with cytotoxicity against different cell lines, being effective from low to high micromolar concentrations (< 1 to nearly 100  $\mu$ M) (Deshmukh et al., 2018). *Aspergillus* and *Penicillium* are the most common marine genera, probably due to their salt tolerance and rapid growth (Jin et al., 2016).

#### 5.1.1. Preussin

In this thesis, we studied just a secondary metabolite isolated from one of these interactions between sponges and marine fungi: preussin. This naturally occurring compound was originally isolated from the fermentation of *Aspergillus ochraceus* (Schwartz et al., 1988) and *Preussia* sp. (Johnson et al., 1989). Since then, several methodologies for the synthesis of preussin and its analogs have been reported (Armas et al., 1998, Okue et al., 2001, Zhou et al., 2014), altogether over thirty synthetic approaches using novel reactions and strategies (Huang et al., 2015).

Preussin demonstrated broad-spectrum effects in microorganisms: antifungal activity (Schwartz et al., 1988, Kasahara et al., 1997), antibiotic (Buttachon et al., 2018), and antiviral activities (Goss Kinzy et al., 2002). Interestingly, preussin is structurally related to anisomycin (Johnson et al., 1989), which is also used as an antibiotic. In turn, anisomycin targeted leukemia cell lines and CD34 stem/progenitor cells and had little effect on normal bone marrow cells (Li et al., 2018b).

Additionally, preussin also revealed *in vitro* anticancer effects, showing inhibition of cell growth and induction of apoptosis with nuclei fragmentation in normal rat fibroblasts (Kasahara et al., 1997). Other authors reported that preussin inhibited cell growth in human cell lines, including a BC one (MCF7) (Achenbach et al., 2000, Buttachon et al., 2018, Abd El-Hack et al., 2019). Achenbach et al. (2000) associated the inhibition of cell growth with the inhibition of the cyclin E kinase, causing a consequent block of cell cycle

progression in the G1 phase. Preussin also induced apoptosis through the release of cytochrome c and the activation of caspases 3 and 8. The same authors reported that the induction of cell death by preussin was p53-dependent and simultaneously was not responsive to Bcl-2 blocking, suggesting that preussin could be a lead structure for the design of novel antitumor drugs (Achenbach et al., 2000).

Buttachon et al. (2018) have chemically characterized several bis-indolyl benzenoids from the ethyl acetate extract of the marine fungus *Aspergillus candidus* KUFA 0062 (Kasetsart University Fungal Collection 0062) isolated from the marine sponge *Epipolasis* sp., collected from the coral reef at the Similan Islands National Park in Phang-Nga province, Southern Thailand. Among these compounds, there were two hydroxypyrrolidine derivatives, preussin (Figure 5a) and preussin C (Figure 5b). Although preussin has been previously isolated from other fungi species, this was the first report of the isolation of hydroxypyrrolidine alkaloids from marine *Aspergillus candidus*. Besides the importance of terrestrial filamentous fungi *Aspergillus candidus* in medical and industrial applications and their role in food spoilage (de Vries et al., 2017), its marine counterpart is poorly chemically investigated.

Preussin and preussin C (Figures 5a and b) demonstrated cytotoxic effects on eight human cell lines from different cell types, including the BC cell line MCF7. The effects of preussin were more effective than preussin C, which was attributed to the presence of the N-methyl group on the pyrrolidine ring in preussin (Buttachon et al., 2018). The  $IC_{50}$  for preussin varied among cell lines from 2.3  $\mu\text{M}$  (in HT29) to 74.1  $\mu\text{M}$  (in U251), while in the case of preussin C, the  $IC_{50}$  values ranged from 57.2  $\mu\text{M}$  (in HT29) to 215.7  $\mu\text{M}$  (in A549). Concerning the BC cell line MCF7, the  $IC_{50}$  for preussin and preussin C were 56.3 and 128.8  $\mu\text{M}$ , respectively.

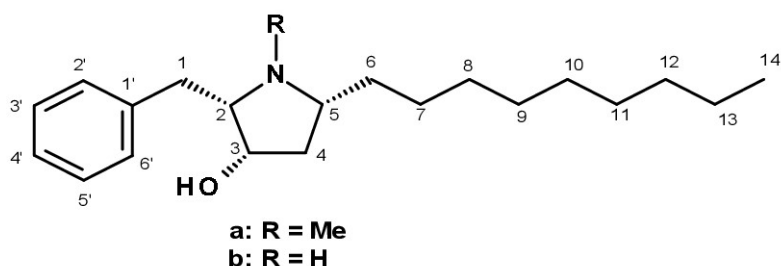


**Figure 5** - Chemical structure of preussin (a) and preussin C (5b).

In the following Table S3 we summarized the main *in vitro* anticancer effects of preussin. In this case, we did not focus only on impacts on BC cell lines because studies are still very scarce.



Other preussins have been reported, like preussin B isolated from *Simplicillium lanosoniveum* (Huang et al., 2015). Preussin B has already been synthetically produced; however, its biological activities have not been explored.

A more recent work reports the synthesis of other preussin such as preussin C-I, and preussins J and K were isolated from the sponge-derived fungus *Aspergillus flocculosus* (KM605191) isolated from the marine sponge *Phakellia fusca*. These preussins revealed moderate to strong inhibition of IL-6 expression on THP-1, A549, and HepG2 cell lines (Gu et al., 2018). L-6 is a pleiotropic cytokine that plays an essential role in the host immune defense mechanism and the modulation of tumor growth and antitumor immunity (Gu et al., 2018).

## **5.2. Seaweeds-derived Compounds - Sources, Molecules, Uses, and Anticancer Effects**

Seaweeds or macroalgae are multicellular photosynthetic organisms found in all oceans, rivers, and other water bodies. According to their natural pigmentation, seaweeds are classified into three main groups: Chlorophyta (green algae); Rhodophyta (red algae), and Phaeophyta (brown algae), with more than 25,000 species (Costa et al., 2021). Seaweeds historically have been used as food, folk medicine, dyes, and fertilizers (Shannon and Abu-Ghannam, 2019). In the last decades, new applications have appeared in the food, cosmetic, pharmaceutical, and biotechnological industries (Rhein-Knudsen et al., 2015, Jesumani et al., 2019, Aslam et al., 2021). This multiplicity of the current uses of macroalgae has raised their economic interest, and their production more than duplicated in the last decade (Costa et al., 2021). Moreover, they present some advantages in production because they can be aquacultured and have high-growth rates, fast processing, and a short harvesting cycle (Ercolano et al., 2019).

Seaweed consumption has been a common practice in many East Asian coastal populations. Additionally, the global human consumption of seaweeds is increasing, and according to the Seafood Source report, the global seaweed market is expected to grow to USD 22.1 billion by 2024 (Blank, 2018). This trend is in line with increasing consumers' awareness of the benefits of consuming healthier and more sustainable products.

Seaweeds possess an excellent nutritional profile presenting a high level of essential minerals (sodium, calcium, iron, iodine, magnesium, phosphorus, potassium, zinc, copper, manganese, selenium, and fluoride), vitamins (A, B1, B2, B9, B12, C, D, E, and K), dietary fibers, proteins and polysaccharides (Shannon and Abu-Ghannam, 2019).

However, this nutritional content can vary according to many factors, such as species, maturity, and environmental conditions, including season, temperature, salinity, oceanic currents, waves, or even depth of immersion, as well as post-harvesting storage and processing conditions of the seaweeds (Afonso et al., 2021).

Because seaweeds have low lipid and polyunsaturated fatty acid content and human intestinal enzymes cannot completely digest their carbohydrates, such algae are low-caloric and appealing to healthy diets (Ganesan et al., 2019). Aside from their nutritional relevance, in seaweed-consuming populations, there has been observed a lower incidence of some chronic diseases, such as hyperlipidemia, coronary heart disease, diabetes, and cancer, compared to Western countries (Bocanegra et al., 2009, Brown et al., 2014, Peñalver et al., 2020).

Seaweeds have been demonstrated as functional foods, having several health benefits such as anticancer (Lichota and Gwozdziński, 2018, Al-Muqbal et al., 2019, Khan et al., 2019), anti-obesity (Gammone and D'Orazio, 2015, Hu et al., 2016, Ojulari et al., 2020), anti-diabetic (Beppu et al., 2012, Maeda, 2015, Lin et al., 2017), anti-oxidative (Lee et al., 2013, Park et al., 2019) and cardiovascular protective effect (Mayakrishnan et al., 2013, Shannon and Abu-Ghannam, 2019). In this line, seaweed and seaweed-derived compounds have been incorporated as functional food ingredients in meat products, allowing consumers to continue eating while reducing their risk of adverse health effects (Shannon and Abu-Ghannam, 2019).

Despite all the potential health benefits of seaweed consumption and its bioactive compounds, caution should be taken as to the excessive intake, as some worrying incidents have been reported. An example is that seaweeds may contain heavy metals such as arsenic in the form of arsenosugars and other metals such as cadmium, plumb, and mercury (Lee et al., 2022). Also, the intake of brown seaweeds such as *Laminaria* spp. (kombu) is many times considered healthy due to its high content of iodine. Although the latter is essential for the normal functioning of the thyroid, excess iodine as high as 1000 mg can eventually lead to deranged thyroid levels (Zava and Zava, 2011). Some individuals are also sensitive to iodine and should be careful about the amount of seaweed intake to prevent symptoms of hyperthyroidism, such as nervousness, insomnia, and increased heart rate (Kumar and Sharma, 2021). Additionally, its high sodium can increase blood pressure and cause heart disease (Kumar and Sharma, 2021).

It is also noteworthy to mention that it can occur interactions of seaweed supplements, such as the kelp ones, with drugs like digoxin, potassium supplements, spironolactone, amiloride, and thyroid supplements. Kelp can also increase the effects of antihypertensive and anticoagulant agents. Thus, much care should be taken when ingesting herbal supplements in general (Tachjian et al., 2010). Kelps are known as large brown seaweed with high nutritional value within the orders Laminariales ('true kelps') and Fucales (forest-forming 'fucoids') (Vergés and Campbell, 2020), and their supplement is used as fat burner (Jeukendrup and Randell, 2011). High potassium levels in Laminaria may also lead to kidney damage and thus are contraindicated with anti-hypertensive agents. Seaweeds may also decrease the pharmacological effect of anticoagulants (aspirin, warfarin) (Holbrook et al., 2005). These examples raise concern, as there is a general lack of knowledge about herb-drug interactions among patients and health care providers (Tachjian et al., 2010).

### **5.2.1. Seaweed Consumption and Breast Cancer**

In Traditional Chinese Medicine, seaweeds and other edible natural products were used in an attempt to treat BC (Namvar et al., 2013b). Even in modern times, some people use natural products or derived formulations alone or as adjuvants to existing chemotherapy regimens to improve efficacy, reduce drug-induced toxicity, and alleviate drug side effects (Liao et al., 2013). The early intake of seaweed has been associated with a lower risk of BC in a case-control study in South Korea (Yang et al., 2010) and other studies reported that dietary seaweed may help explain lower BC incidence and mortality among postmenopausal women in Japan (Teas et al., 2013). Accordingly, the mekabu solution, an extract of the wakame seaweed (*Undaria pinnatifida*), showed a potent suppressive effect on rat mammary carcinogenesis and induced apoptosis in human BC cell lines MCF7, MDA-MB-231, and TD47, without toxicity to the normal breast cell line MCF10A (Funahashi et al., 2001).

### **5.3. Brown Seaweed Bioactive Compounds**

Brown algae are the most consumed species (66.5%), followed by red (33%) and green (5%) algae, generally part of the diet in Asian countries such as Japan, China, and Korea (Afonso et al., 2019). This type of seaweed is usually large and ranges from giant kelp to smaller species. The typical brown color of these seaweeds is due to the abundant presence of a pigment called fucoxanthin (Lourenço-Lopes et al., 2021). They have many health claims as they are rich in nutrients and bioactive compounds.

The most common brown seaweeds used in human consumption are *Fucus vesiculosus*, *Fucus serratus*, *Himanthalia elongata*, *Undaria pinnatifida*, *Ascophyllum nodosum*, *Laminaria digitata*, *Laminaria saccharina*, *Laminaria japonica* and *Alaria esculenta* (Afonso et al., 2019). As many brown seaweeds live in harsh environmental conditions, they possess a great variety of bioactive compounds (Lomartire et al., 2021).

This section is dedicated to the main bioactive compounds of brown seaweeds, highlighting their chemical structure and relevant bioactivities, with a special focus on their anticancer effects in BC cells. The bioactive compounds included in this thesis belong to the group of carotenoids (astaxanthin and fucoxanthin), polysaccharides (laminarin and fucoidan), sterols (fucosterol) and phlorotannins (phloroglucinol).

### 5.3.1. Carotenoids

Carotenoids are the most widely distributed natural pigments that can exhibit yellow, orange, red, and purple colors. They are present in photosynthetic organisms like bacteria, fungi, seaweeds and plants. Most carotenoids consist of eight isoprene units with a 40-carbon backbone (Maoka, 2020). Still, they can present different double bond distributions in the polyene chain and other cyclic end groups at both ends, making them lipophilic (Takaichi, 2011, Maoka, 2020).

Carotenoids include two main groups: carotenes and xanthophylls. Xanthophylls are oxygenated derivatives of carotenes. The presence of oxygen makes them more polar than carotenes, but they still are non-polar compounds (Pereira et al., 2021a).

Carotenes include, among others,  $\alpha$  and  $\beta$  carotenes, lycopene, and phytoene. Xanthophylls contain fucoxanthin (the most abundant carotenoid), astaxanthin, zeaxanthin, neoxanthin, lutein, and violaxanthin (Pereira et al., 2021a). Animals cannot synthesize carotenoids, so the only way to access these compounds is through ingestion of diet, dietary supplements, or food additives (Galasso et al., 2017).

In the last decades, many works have highlighted several health-beneficial properties of carotenoids including their antioxidants properties that are described to prevent the damage caused by oxidative stress and chronic diseases (Agarwal and Rao, 2000, Cooper, 2004), anti-inflammatory (Pereira et al., 2021b), antimicrobial (Karpiński and Adamczak, 2019), and anticancer effects (Kozuki et al., 2000, Eid et al., 2012, Almeida et al., 2020).

The intake of antioxidants of natural origin has been suggested as cancer chemopreventive (Nishino et al., 2002, Tanaka et al., 2012) and anticancer effects (Linnewiel-Hermoni et al., 2015). However, the intake of antioxidants during cancer treatments is highly controversial (Mut-Salud et al., 2016, Akanji et al., 2020). The most common relevant questions are: (i) do antioxidants increase or decrease the efficacy of anticancer agents?; (ii) do antioxidants protect normal tissue and ameliorate toxicity or protect cancer cells from chemotherapy? (Singh et al., 2018).

The studies about these relevant questions differ in conclusions. In relation to BC, using vitamins C and E in the period following BC diagnosis was associated with a decreased likelihood of recurrence. In contrast, frequent use of a combination of carotenoids was associated with increased mortality, pointing out that the effects of antioxidant supplements after BC diagnosis can differ by type of antioxidant (Greenlee et al., 2012). Others showed that administering vitamins C, D, and E supplements in the first six months after BC diagnosis, could reduce the risk of mortality and tumor recurrence (Nechuta et al., 2011).

Contrarily, some studies advised against the intake of antioxidants during BC treatment proposing that antioxidant use during cancer treatment was associated with worsened BC prognosis in postmenopausal women (Jung et al., 2019). Currently, there is insufficient data from clinical studies, so clinicians should advise their patients against using antioxidant dietary supplements during chemotherapy or radiotherapy (D'Andrea, 2005, Khurana et al., 2018). The inconsistency of the results suggests they can depend on the dose intake (Pan et al., 2011). A recent study calls attention to the importance of patient stratification based on “redoxidomics” to define the dosage for future personalized treatment of patients with antioxidants (Griñan-Lison et al., 2021). Moreover, many antioxidants can often exert both anti-oxidant and pro-oxidant properties, depending on the type of antioxidants and the used concentration (Greenlee et al., 2012), cell type, exposure time, and environmental conditions (Sznarkowska et al., 2017).

### **5.3.1.1. Astaxanthin (Asta)**

Astaxanthin is a xanthophyll carotenoid found in various marine organisms, including seaweeds (Ambati et al., 2014). It is a yellow to red pigment, considered a super-antioxidant, as it has more antioxidant activity than other carotenoids. For instance, Asta's antioxidant capacity is 10 times stronger than  $\beta$  carotenes and 65 times more potent than acid ascorbic (Pereira et al., 2021a). The explanation for its enhanced

antioxidant activity is related to its chemical structure with two hydroxyl and keto groups on each ring (Tanaka et al., 2012), as shown in Figure 6.

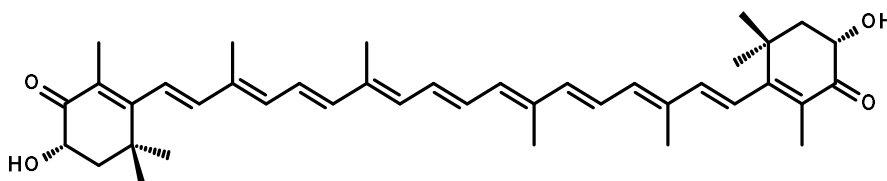


**Figure 6** - Chemical structure of astaxanthin.

This particular configuration also makes this compound polar-nonpolar-polar. The polar parts turn it fat-soluble and thus easily incorporated into cell membranes. This special chemical structure allows Asta to scavenge and quench ROS in the inner and outer layers of cellular membranes, differing from most antioxidants that can only act on the side of the membrane (Sztretye et al., 2019). Its antioxidant properties repressed ROS production and displayed anti-inflammatory effects *in vitro* and *in vivo* (Yasui et al., 2011, Dose et al., 2016, Bi et al., 2017, Farruggia et al., 2018), as well as presented a protective effect against aging (Davinelli et al., 2018), neuroprotective (Grimmig et al., 2017), hepatic and cardiovascular protective effects (Yang et al., 2013b). Its efficacy in counteracting all categories of photodamages, *in vitro* and *in vivo* is one area of much interest, especially in dermatology (Davinelli et al., 2018, Catanzaro et al., 2020).

*In vitro* studies showed that Asta has anticancer activities. The induction of apoptosis was a very common effect in several cell lines (Palozza et al., 2009, Song et al., 2011, Li et al., 2015), including BC ones (Sowmya et al., 2017, Vijay et al., 2018, Kim et al., 2020b). Asta also exerted cell cycle arrest and inhibition of growth in cells lines from different origins (Kotake-Nara et al., 2001, Palozza et al., 2009, Sun et al., 2020) and including BC cells (McCall et al., 2018), and inhibition of cell migration in MCF7 and MDA-MB-231 cells (McCall et al., 2018). One study reported that Asta induced cell death in the BC cell lines T47D and MDA-MB-231 without cell cytotoxicity for non-cancerous cells of the MCF10A cell line (Karimian et al., 2022).

In 3D culture, the effects of Asta are still poorly explored. However, its effects have been tested in the BC cell lines T47D and BT20 in which Asta inhibited cancer stem cell (CSC) stemness genes; being proposed that Asta could be used in combination with other anti-cancer therapies against BC cells (Ahn et al., 2020b). When combined with antineoplastic drugs, Asta demonstrated some interesting synergistic effects, e.g., in combination with Dox, it potentiated drug effect in MDA-MB-231 (Vijay et al., 2018) and

MCF7 cell lines (Fouad et al., 2021). Also, it enhanced the antiproliferative effect of carbendazim, while alleviating the carbendazim treatment-associated ROS production in MCF7 cells (Atalay et al., 2019). A summary of the main findings of Asta's effects on human breast cell lines is presented in Table S4.

Asta displayed *in vivo* anticancer effects. An Asta-supplemented diet reduced the severity of *Helicobacter pylori* infection in mice, which is marked by an increase in myeloperoxidase activity, lipid peroxide expression, pro-inflammatory cytokine IFN- $\gamma$ , c-myc oncogene, cyclin D1, and ROS generation (Han et al., 2020). The same study also proposed that Asta could also protect gastric mucosa from inflammatory and oncogenic responses and from the oxidative damage resulting from gastric *Helicobacter pylori* infection. Indeed, Asta's antioxidant activity can protect normal tissues against the oxidative stress of some antineoplastic drugs (Akca et al., 2018). Moreover, the anticancer activities of Asta in rodent models include the diminished development of the urinary bladder (Tanaka et al., 1994), colon carcinogen-induced tumors (Tanaka et al., 1995a), and oral cancer (Tanaka et al., 1995b).

In humans, oral ingestion of Asta suppressed the transplantable methylcholanthrene-induced fibrosarcoma tumor (Meth-A-tumor) growth and stimulated host immunity against Meth-A tumor antigen (Jyonouchi et al., 2000). In accordance, dietary Asta increased in a dose-dependent manner the stimulation of the immune system and decreased oxidative stress and DNA damage biomarkers (Park et al., 2010).

Asta is a lipid-soluble molecule with low oral bioavailability compared to other potential therapeutic agents (Hussein et al., 2006, Madhavi et al., 2018). Still, it is considered the carotenoid with the highest bioavailability (Sy et al., 2012), and its absorption seems influenced by the type of oil consumed (Yang et al., 2013b). Asta is marketed in various forms, including oils, tablets, capsules, syrups, soft creams, biomass, or ground (Ambati et al., 2014). The daily intake of Asta was established by 0.2 mg/kg body weight by European Food Safety Authority (Ambati et al., 2014) and FDA (2010) recognized Asta as GRAS "Generally recognized as safe". Asta from *Haematococcus pluvialis* is approved for human consumption at 12 mg per day and up 24 mg per day for no more than 30 days (Visioli and Artaria, 2017).

#### **5.3.1.2. Fucoxanthin (Fx)**

Fucoxanthin is a xanthophyll carotenoid whose color is orange to brown and is the most abundant carotenoid of brown algae (accounting for around 10% of the total carotenoids) (Peng et al., 2011). It is produced by many algae as a secondary metabolite and is

localized in the chloroplasts, where it is involved in photosynthesis (Pereira et al., 2021a). The content of Fx is highly variable amongst different species and dependent on extrinsic environmental factors (Afonso et al., 2019). Fx has a unique molecular structure consisting of an oxygenated carotene backbone with an unusual allenic bond (with a C8 ketone and an epoxide), and different functional groups such as epoxy, hydroxyl, carbonyl, and carbonyl moieties (Peng et al., 2011) (Figure 7). The presence of the allenic bond is linked to Fx's greater ability to scavenge free radicals than other carotenoids (Sachindra et al., 2007).

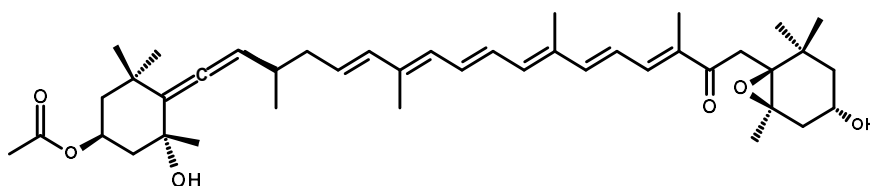


**Figure 7** - Chemical structure of fucoxanthin.

The biological activities of Fx *in vitro* and *in vivo* are very vast, including antidiabetic (Maeda, 2015, Oliyaei et al., 2021), anti-inflammatory (Kim et al., 2010b, Tan and Hou, 2014, Liu et al., 2020), anti-obesity (Gammone and D'Orazio, 2015, Maeda, 2015, Gille et al., 2019), anti-malarial (Afolayan et al., 2008) and antioxidant activities (Xia et al., 2013, Lourenço-Lopes et al., 2021). Several protective effects have been reported: hepatic (Woo et al., 2010, Chang et al., 2018, Zheng et al., 2019), cardiovascular (Martin, 2015, Satomi, 2017, Chang et al., 2019), ocular (Shiratori et al., 2005) and skin protective activities (Heo and Jeon, 2009).

The *in vitro* anticancer effects of Fx included different mechanisms. The most studied is the induction of apoptosis in cell lines from different origins like prostate, colon, bladder, lymphoid, and others (Hosokawa et al., 2004, Kotake-Nara et al., 2005, Yamamoto et al., 2011, Kumar et al., 2013, Wang et al., 2014). Generally, the apoptosis triggering was related to caspase pathways and other proteins like Bax/Bcl-2, MAPK, nuclear factor kappa B families (NF- $\kappa$ B) (Kotake-Nara et al., 2001, Hosokawa et al., 2004, Kotake-Nara et al., 2005, Tafuku et al., 2012, Kumar et al., 2013, Wang et al., 2014, Martin, 2015). For example, in colon cancer cells, Fx induced apoptosis via caspase-3 and suppressed the expression of Bcl-2 proteins (Hosokawa et al., 2004). Interestingly, one study described less Fx cytotoxicity in non-transformed cells compared to several cancer cell lines and that subtoxic doses of Fx (up to 5  $\mu$ M) caused a significant delay in cell migration (Garg et al., 2019).



Antiproliferative effects (Hosokawa et al., 2004) and cell cycle arrest (Kumar et al., 2013, Satomi, 2017) were also commonly described mechanisms. For instance, Fx arrested the cell cycle in G0/G1 in a dose-dependent manner in liver cell lines (Das et al., 2005, Das et al., 2008, Satomi, 2012). In the human gastric MGC-803 cell line induced cell cycle arrest in G2/M with down-regulation of surviving and cyclin B1 (Yu et al., 2011).

Fx was also reported to exert anti-metastasis effects in lung cancer cells (Ming et al., 2021) and a highly metastatic melanoma cell line B6-F10 by downregulation of metalloproteinase-9 (MMP-9); which plays a vital role in the cell migration as it degrades collagen IV, a major constituent of basement membranes. Additionally, Fx also inhibited angiogenesis (Sugawara et al., 2006, Jang et al., 2021).

There is some evidence showing that the use of Fx in combination therapy with other drugs can bring some benefits in different scenarios. Liu et al. (2013) observed that Fx potentiated the chemotherapeutic efficacy of cisplatin by enhancing cisplatin-induced apoptosis in HepG2 cells via NF- $\kappa$ B-mediated pathway and downregulation of DNA repair gene expression. Fx sensitized lung cancer cells to Gefitinib, an EGFR inhibitor (Ming et al., 2021), and presented synergistic effects with Dox in multidrug-resistant cell lines, including BC ones (Eid et al., 2020). Another example of Fx sensitization is their combination with TRAIL (Tumor necrosis factor-related apoptosis-inducing ligand), a promising anti-cancer drug in cervical cancer (Ye et al., 2020). Drug resistance was also reverted in Caco-2 cells using a carotenoid mixture, including Fx, by interfering with ABC-transporters, with the conclusion that these carotenoids were competitive inhibitors of ABC-transporters (Eid et al., 2012). Similarly, Fx enhanced several drug effects, such as 5-Fu effects in colon cancer cells (Lopes-Costa et al., 2017, Manmuan and Manmuan, 2019), Cis effects via NF- $\kappa$ B-mediated pathway on Hep-G2 cell line (Liu et al., 2013). In the combinations of Fx plus Dox and Imatinib, Fx inhibited cell proliferation in human leukemia cell lines K562 and TK6, but it did not differ from Fx alone (Almeida et al., 2018). On the other side, Fx also attenuated Dox-induced cardiotoxicity in mouse cardiomyocytes (Zhao et al., 2019).

Fx was claimed as a chemopreventive agent by inhibiting the enzyme activity of CYP1A2 (cytochrome P450-1A2) and CYP3A4, xenobiotic metabolizing enzymes responsible for the activation of pro-carcinogens (Satomi and Nishino, 2013). Over the years, other authors also reported the cytotoxicity of Fx against BC cell lines, for instance, in MCF7 and MDA-MB-231 cell lines (Konishi et al., 2006, Ayyad et al., 2011, de la Mare et al., 2013, Vijay et al., 2018) but with a lower extent in the non-transformed BC cell line

MCF12A (de la Mare et al., 2013). Besides cytotoxic effects, Fx inhibited cell migration and invasion in MDA-MB-231 cells at 25  $\mu$ M (Wang et al., 2019a).

All the above-mentioned studies are relative to monolayer-2D cultures, as the literature on the effects of Fx in 3D culture is very scarce. As far as we know, it is limited to three studies (just one with BC cells). In one of each, Fx inhibited the maturation of melanosomes and the synthesis of melanin in human-melanocytes spheroids (Zurina et al., 2020). The other study consisted of the injection of HT-29 colon spheres in BALB/c nu/nu mice administered with Fx for 4 weeks and reported that in these mice there was a significative reduction of tumor formation in comparison to the control ones with concomitant suppression of cyclin D1 expression in tumors cells (Terasaki et al., 2019b). To the best of our knowledge, in BC cell lines only Rwigemera et al. (2014) described, in 3D, the cytotoxic effect of Fx and Fxol in MCF7 and MDA-MB-231 cell lines. The decrease in cell viability was associated mainly with the modulation of the NF- $\kappa$ B pathway. Further, the same authors concluded that Fxol had a more rapid effect on the nuclear translocation of NF- $\kappa$ B (Rwigemera et al., 2015). The only study that evaluated the effect of Fx in the inhibition of mammospheres concluded that it did not affect the formation of the mammospheres (de la Mare et al., 2013).

As for the combination of Fx with anticancer drugs, only Vijay et al. (2018) evaluated the effects of Fx in combination therapy, in this case with Dox in MCF7 and MDA-MB-231 cell lines, where the effects of inhibition of cell growth were more effective in the combination than in the compounds alone. Table S5 summarizes the main findings of Fx effects on human breast cell lines.

Regarding *in vivo* studies, Fx presents similar anticancer effects to those reported *in vitro* studies. For example, Fx reduced cancer growth in the intestinal and liver when orally administrated to mice (Kumar et al., 2013, Satomi, 2017). In S180 xenografts-bearing mice, Fx induced apoptosis and significantly inhibited lung metastasis when the melanoma cell line B6-F10 was injected into a mice model (Chung et al., 2013). Terasaki et al. demonstrated that Fx caused anoikis as a cancer-preventive activity in a model of AOM/DSS-induced colon carcinogenesis (Terasaki et al., 2019a). Recent studies described the chemopreventive effects of Fx in colorectal carcinogenesis in azoxymethane/dextran sodium sulfate murine model by administration of Fx-containing biscuits (Terasaki et al., 2022) and in pancreatic cancer in C57BL/6J transplanted mice (Murase et al., 2021). In an MDA-MB-231 BC xenograft model using BALB/c nude mouse, Fx also decreased the micro-lymphatic vascular density (Wang et al., 2019a).

In humans, dietary Fx is absorbed in the small intestine similarly to other lipids, where it is metabolized by the intestinal esterases undergoing deacetylation resulting in fucoxanthinol (Fxol) (Terasaki et al., 2017). Then, the circulating Fxol is further converted into amarouciaxanthin A in the liver (Asai et al., 2004). Both metabolites, Fxol and amarouciaxanthin, also displayed several biological activities, namely anticancer activities (Asai et al., 2004, Konishi et al., 2006, Ishikawa et al., 2008, Beppu et al., 2009, Terasaki et al., 2017, Tamura et al., 2019). Indeed, Fxol displays more potent effects on the viability of human cell lines (Rwigemera et al., 2015).

The bioavailability of Fx is relatively high, and its metabolites are detected, according to the animal model, in plasma, liver, or adipose tissue (Lourenço-Lopes et al., 2021).

However, its pharmacokinetics and metabolism can differ among species. In humans, its bioavailability and metabolism are higher than in mice (Matsumoto et al., 2010, Hashimoto et al., 2012). In a human trial where Fx from *Undaria pinnatifida* was ingested as supplementation of an extract for one week, Fx was not detected in the blood, and the metabolite Fxol was found at a very low concentration, which indicated a limited intestinal absorption (Asai et al., 2008). Mechanisms to improve Fx absorption have been investigated, such as its encapsulation in micelles or liposomes (Wang et al., 2017b) or dietary combination with edible oil or lipids (Peng et al., 2011).

The toxicity of Fx has not been observed in animal studies (Beppu et al., 2009, Iio et al., 2011). In humans, there are insufficient clinical trials for assessing Fx safety. However, FDA approved the ingestion of Fx extracted from the algae *Phaeodactylum tricornutum*, 3 mg daily with no time limit or 5 mg daily up to 90 days (NDI 1048 – Fucoxanthin). There is one clinical trial in phase II on Fx intake to test its effects on metabolic syndrome (ClinicalTrials.gov Identifier: NCT03613740). Even with limited human trials studies, Fx has raised increasing interest in the scientific community, which quickly grew in recent years, as reported by a recent bibliometric review (Khaw et al., 2021). Meanwhile, it is possible to buy Fx as food supplements with the commercial name ThinOgen® and Fucovital® (Pereira et al., 2021a).

### **5.3.2. Polysaccharides**

Polysaccharides constitute the main component of the algae cell wall (Deniaud-Bouët et al., 2017). Brown-algal polysaccharides are present in large amounts in algal biomass. More precisely, depending on the seaweed species and other factors such as season and environmental conditions, they can vary from 40% to 70% of dry weight (Zvyagintseva et al., 2003). Brown algae's principal polysaccharides include alginates,

fucoidans, and laminarin, which form the cell wall and the core carbohydrate reserve (Li et al., 2021b). Polysaccharides are easily isolated, with numerous biological activities allowing their widespread use in food, cosmetic, pharmaceutical, and technological industries (Abbott and Kaplan, 2015, Fitton et al., 2015, Sanjeewa et al., 2018). They have been investigated, for instance, for wound dressings (Andryukov et al., 2020), drug-delivered systems (Cardoso et al., 2016, Bilal and Iqbal, 2019), tissue engineering scaffolds for different tissue formation (Bilal and Iqbal, 2019). This thesis investigated the cytotoxic effects of laminarin (Lm) and fucoidan (Fc).

### 5.3.2.1. Laminarin (Lm)

Laminarins, also known as laminarans, are relatively underexploited polysaccharides. Laminarins are low-molecular-weight, branched polysaccharides made of a linear  $\beta$ -(1 $\rightarrow$ 3)-linked glucose-based chain ( $\beta$ -glucans) (Becker et al., 2020) (Figure 8). Glucans are FDA-approved compounds to lower cholesterol levels (Park et al., 2012).

Their structure and percentages in dry weight, similar to fucoidan the other studied polysaccharide, can vary among species (Kadam et al., 2015b). Moreover, other environmental conditions such as water temperature, salinity, depth of immersion in the harvest period, and extraction methodology can also influence the biological activity of the laminarins.

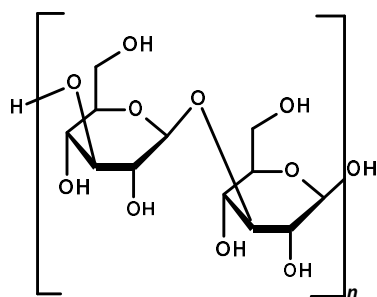


**Figure 8** - Chemical structure of laminarin.

The primary function of Lm in brown algae is related to reserve metabolites and is located in cells' vacuoles (Kadam et al., 2015b). Similar to fucoidans the other studied polysaccharides, the structure of these compounds and percentages in seaweeds dry weight can vary among species (Kadam et al., 2015b).

Due to its high solubility in an aqueous medium and the biodegradable nature of Lm, sustained release in the physiological condition has attracted attention for several biomedical applications (Zargarzadeh et al., 2020) such as microparticles, biocompatible polymeric carriers for a sustained/controlled drug-delivery and Lm has revealed to be an efficient, biocompatible and biodegradable system (Castanheira et al., 2020).

Laminarin has exhibited some biological activities similar to other glucans such as immuno-stimulating (Kim et al., 2006, Song et al., 2017a), antibacterial (Kadam et al., 2015a, Ercolano et al., 2019), hypoglycemic (Kim et al., 2020a), antioxidant (Choi et al., 2011, Kadam et al., 2015a), anti-inflammatory (Neyrinck et al., 2007), anticoagulant (Miao et al., 1995) and anticancer activities (Kim et al., 2006, Ercolano et al., 2019).

Regarding its anticancer activity *in vitro*, Lm inhibited cell growth in human colon cancer HT-29 by decreasing cell proliferation and inducing apoptosis (Park et al., 2012). Lm has also shown a dose-dependent sub-G1 and G2-M phase cell cycle arrest, followed by apoptosis in the highly proliferative HT-29 colon cancer cell (Park et al., 2013). Lm also demonstrated antiproliferative effects, inhibiting the proliferation in the human hepatic cell lines (Bel-7404 and HepG2) by upregulating the senescence marker protein-30 (SMP-30) (Tian et al., 2020b). In ovarian cancer cell lines, Lm decreased cell growth by cell cycle arrest regulating PI3K/MAP intracellular signaling and increased cell death through different mechanisms, including DNA damage, ROS generation, endoplasmic stress regulation of calcium levels interfering with the axis endoplasmic reticulum-mitochondria (Bae et al., 2020b).

Modifications of the backbone of Lm have improved its physicochemical and mechanical properties leading to increased biological activity. In this vein, sulfated Lm induced apoptosis in colon cancer LoVo cells, via a death receptor pathway (Ji and Ji, 2014). Moreover, sulfated Lm had higher antitumor activity than conventional Lm at the same concentration (Ji et al., 2013), showing anti-angiogenic effects by suppressing tubule formation by endothelial cells cultured on Matrigel and inhibiting vascularization of the chick chorioallantoic membrane assay (Hoffman et al., 1996).

Another study reported the inhibition of cell proliferation, colony formation, and migration in human cell lines from colorectal, melanoma, and breast adenocarcinomas (Malyarenko et al., 2016). *In vitro* inhibition of colony forming was demonstrated in melanoma SK-MEL-28 and colon cancer DLD-1 cell lines (Menshova et al., 2014). Concerning Lm effects in 3D cell cultures, the studies are still scarce. Lm from brown

alga *Alaria angusta* inhibited viability, colony growth, and the invasion of the colon HCT 116 spheroids (Malyarenko et al., 2021b).

Specifically in BC, laminarins and their sulfated derivatives from *Saccharina japonica* and *Fucus evanescens*, strongly inhibited cell proliferation, colony formation, and migration by suppressing the activity of the MMP-2 and 9. Interestingly, the same effect was not observed with the laminarins from *Saccharina cichorioides* (Malyarenko et al., 2016). However, Malyarenko et al. (2020) described that when this Lm was chemically changed to aminated laminarin, it decreased survival and colony formation in the MDA-MB-231 cell line and had a synergistic impact with X-ray radiation, resulting in fewer cell colonies. This radiosensitizing effect was accompanied by induction of apoptosis induction with the involvement of caspases 3 and 9 and poly [ADP (ribose)] polymerase 1 (PARP) enzyme, which prevents the repair of DNA damage in irradiated cells. The main findings and mechanisms of Lm reported in human breast cell lines are summarized in Table S6.

Regarding combination therapy, Lm has also been applied in combination with cisplatin, showing protective effects on cisplatin-induced ototoxicity in HEIOC1 auditory cells (Han and Shi, 2016).

The available studies with Lm *in vivo* models are more related to its the immune - stimulatory effects (Song et al., 2017a, Zhu et al., 2019, Tian et al., 2020a). Additionally, in a zebrafish embryo xenograft model, Lm inhibited the growth of ovarian cancer cells without demonstrating cytotoxicity to the animals until the dose of 2 mg/mL (Bae et al., 2020b).

### **5.3.2.2. Fucoidan (Fc)**

The designation fucoidan is commonly applied to complex polysaccharides. Fc is isolated from marine algae, mainly consisting of polymer of  $\alpha$ -(1→3) linked fucose, but also can have many other monosaccharides, with sulfate and/or acetyl groups (Bilan et al., 2002) (Figure 9). However, it is common to find in the literature other denominations, such as fucan or fucosan (Cunha and Grenha, 2016). Fc is the main component of the brown algae cell wall, and its function is mainly related to preventing dehydration. However, its structure can also vary according to the species, habitat, harvesting time, and maturity stage of seaweeds (Sanjeewa and Jeon, 2021). Thus, the term “fucoidan” does not refer to one specific structure but corresponds to a heterogenous group with different basic chemical structures, including the type of sugar and sulfate content,

obviously having different molecular weights. Because of such heterogeneity, some authors name this group fucoidans (Malyarenko and Ermakova, 2017).

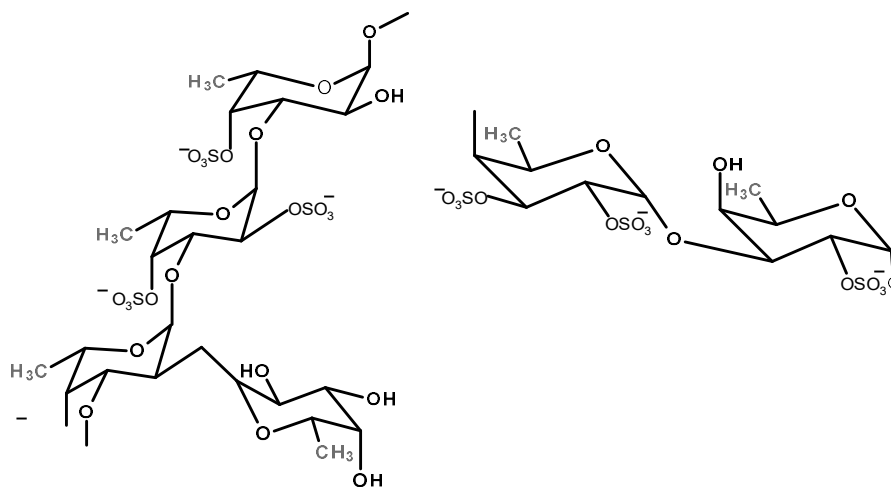


**Figure 9** - Chemical structure of fucoidan.

Accordingly, different chemical structures correspond to diverse physicochemical and biological properties (Ale et al., 2011). For instance, the molecular weight of Fc was considered a critical factor for its anticancer activity. Low-molecular-weight fucoidans were more effective against the proliferation of BC cells than the high molecular weights of Fc (Lu et al., 2018). Another example of the influence of the molecular weight was that low molecular weight Fc was generally considered to be pro-angiogenic. In contrast, Fc with high-molecular-weight demonstrated the opposite effect displaying antiangiogenic activity. Another study reported that the inhibition of cell proliferation by Fc was related to its degree of sulfation (Koyanagi et al., 2003, Ermakova et al., 2011). Moreover, the methods used for extraction and purification can interfere with the biological activity of this compound, for instance, destroying its sulfation pattern (Cunha and Grenha, 2016). Furthermore, low-molecular-weight Fc presented a higher absorption rate and bioavailability than medium-molecular-weight Fc (Matsubara et al., 2005). Additionally, Fc can be easily modified by chemical or enzymatic procedures, making them a good candidate for therapeutic applications, alone or adjuvant to another chemotherapeutic (Reyes et al., 2020).

In seaweeds, Fc isolated from *Fucus vesiculosus* and *Undaria pinnatifida* are the most studied for their chemical and biological properties (Ercolano et al., 2019), and both were approved by FDA as “Generally Recognized As Safe” category as food ingredients at levels up to 250 mg/day (Citkowska et al., 2019).

Fc exhibit several biological activities, including antibacterial (Ahmadi et al., 2015, Ayrapetyan et al., 2021), antiviral (Lee et al., 2004a, Ahmadi et al., 2015, Apostolova et al., 2020), anti-inflammatory (Phull and Kim, 2017, Takahashi et al., 2017, Apostolova et al., 2020), immunomodulatory (Apostolova et al., 2020), immune system activation (Jin et al., 2014, Vetvicka and Vetvickova, 2017), anticoagulant (Cumashi et al., 2007, Qi et al., 2022) and hypolipidemic (Huang et al., 2010). Moreover, fucoidans have been associated with the prevention of some illnesses, such as Parkinson's (Zhang et al., 2018, Silva et al., 2019), and Alzheimer's diseases (Subaraja et al., 2020), AIDS (Thuy et al., 2015, Sanniyasi et al., 2019), and diabetes (Mabate et al., 2021, Wen et al., 2021). In the cancer field, Fc also has demonstrated several anticancer effects as revised by the following authors Senthilkumar and Kim (2014), Malyarenko and Ermakova (2017), Lin et al. (2020b).

Studies conducted *in vitro* have identified potential mechanisms for the anticancer effects of Fc: induction of apoptosis in several cell lines (Aisa et al., 2005, Kim et al., 2010a, Banafa et al., 2013), cell cycle arrest (Chantree et al., 2021), inhibition of cell growth (Vishchuk et al., 2016), epithelial-mesenchymal transition (Wu et al., 2016, He et al., 2019) and migration (Han et al., 2015) and anti-angiogenic effects (Koyanagi et al., 2003, Hsu et al., 2020). Some authors associated ROS generation as the cause of apoptosis triggering (Yang et al., 2013a, Han et al., 2017). In 3D culture, one study described that Fc from *Fucus evanescens* inhibited the viability of SK-MEL-28 spheroids (Malyarenko et al., 2021a).

Relatively to BC cells, Fc induced apoptosis (Yamasaki-Miyamoto et al., 2009, Jin et al., 2010, Zhang et al., 2011, Zhang et al., 2013a), inhibited cell proliferation (Yamasaki-Miyamoto et al., 2009, Zhang et al., 2011, Banafa et al., 2013), adhesion and invasiveness (Haroun-Bouhedja et al., 2002), while displaying antimetastatic effects (Cumashi et al., 2007, Hsu et al., 2013, Wu et al., 2016) and anti-estrogenic effects (Zhang et al., 2016). Fucoidan has also been tested in combination with other drugs in BC cells. Co-exposure of Fc with cisplatin, tamoxifen, or paclitaxel potentiated the effect of the drug in the MCF7 and MDA-MB-231 cell lines (Zhang et al., 2013b).

Table S7 overviews the main *in vitro* findings and proposed mechanisms of Fc effects on human breast cell lines.

Concerning *in vivo* anticancer effects, oral administration of Fc in a mouse xenograft model suppressed HCT 116 colon tumor growth (Vishchuk et al., 2016). Sulfated Fc demonstrated antiangiogenic effects by suppressing the neovascularization induced by



Sarcoma 180 cells implanted in mice (Koyanagi et al., 2003) and antiangiogenic and anti-micrometastatic activities in an *in vivo* zebrafish model (Hsu et al., 2020).

*In vivo*, Fc has also been tested in combination therapy. Fc enhanced (also *in vitro*) the action of arsenic trioxide and all-trans retinoic acid in acute promyelocytic leukemia, (Atashrazm et al., 2016). Fc synergized with lapatinib, exhibiting more inhibition of tumor growth in combination than the drug alone in melanoma cell lines, also reducing the morbidity associated with prolonged lapatinib treatment in mice (Thakur et al., 2017). Additionally, Fc increased the sensitivity to gefitinib in lung cancer cells (Qiu et al., 2020). In mouse models, sulfated Fc demonstrated antimetastatic effects in C57Bl/6 mice with transplanted lung adenocarcinoma and potentiated the toxic effect of cyclophosphamide (Alekseyenko et al., 2007). Similarly, Fc in another lung model association with cisplatin promoted greater inhibition of tumor volume (Hsu et al., 2018). Still, in a mouse model inoculated with MCF7 and ZR-75D BC cells, Fc demonstrated improved activity compared to tamoxifen. While in combination with paclitaxel, it had an antagonistic effect (Burney et al., 2017). Another finding of using Fc in combination with drugs is alleviating the drug's side effects. In rats, Fc attenuated doxorubicin-induced acute cardiotoxicity (Zhang et al., 2020a).

In humans, Fc as a complementary cancer therapy, enhanced the activation of NK cells in male cancer survivors (Nagamine et al., 2020), and demonstrated anti-inflammatory effects in advanced cancer (Takahashi et al., 2017).

Otherwise, some clinical trials concerning the intake of Fc, mainly as low molecular weight fucoidan, with chemotherapy drugs have been performed in colorectal cancer, where the combination with Fc significantly improved the disease control rate (Tsai et al., 2017). The effects of Fc in combination with platinum-based chemotherapy in advanced non-small cell lung carcinoma patients have been subjected to clinical trials. However, it was withdrawn due to an insufficient target population (ClinicalTrials.gov. identifier NCT 03130829). Another ongoing phase II study (NCT04066660) evaluates the antitumoral effect of Fc dietary ingestion in advanced hepatocellular cancer.

Besides the lack of sufficient scientific evidence of the benefits of the intake of Fc with chemotherapy in cancer patients, it has been prescribed as a food supplement to reduce chemotherapy-related side effects, such as fatigue (Ikeguchi et al., 2011, Hsu et al., 2018). The digestive product of fucoidan from *Sargassum fusiforme* showed a potential to alleviate hematopoietic damage caused by cyclophosphamide (Ma et al., 2022).

In BC, the objective of one study was to evaluate the interaction of Fc with letrozole or tamoxifen, and the results suggested that Fc could be taken concomitantly with either drugs without the risk of clinically significant interactions (Tocaciu et al., 2016).

Fucoidan cytotoxic effects lead to the investigation of fucoidan-based nanoparticles or for coating nanoparticles of other compounds in drug delivery (Tengdelius et al., 2015). Its negative ionic nature favors the formation of complexes with other, oppositely charged molecules. Fc has been used as a nanocarrier for several medications, including anticancer treatments, which is an attractive approach since Fc not only functions as a drug excipient and nanocarrier but also has therapeutic properties (Citkowska et al., 2019). An example of this was a study in BC cells using immunotherapeutic nanoparticles where Dox was prepared with Fc (Pawar et al., 2019). The results revealed *in vitro* and *in vivo*, the improvement of cytotoxicity, cell cycle arrest in the G1-S phase, and apoptosis in tumor cells compared to free Dox.

Despite all the above evidence, insufficient research analyzed the adverse consequences of fucoidan, which should be investigated further.

### **5.3.3. Sterols**

#### **5.3.3.1. Fucosterol (Fct)**

Fucosterol (Fct) is a sterol that belongs to the class of cholesterol-like molecules. Sterols are an integral part of the cellular membranes of plants and algae, having a role in the organization of the fluid bilayer of the membranes, thus related to their permeability and signal transduction (Mouritsen et al., 2017). They also act as plant hormones and hormonal precursors (Milovanovic et al., 2009). Brown algae possess a greater amount of Fct than green and red algae, and their amounts can also vary among species (Meinita et al., 2021). The chemical structure of Fct resembles the molecule of cholesterol in vertebrates, and it consists of four rings, a hydroxyl group at C-3, and a side chain with an alkyl group at C-24 (Lopes et al., 2014) (Figure 10).

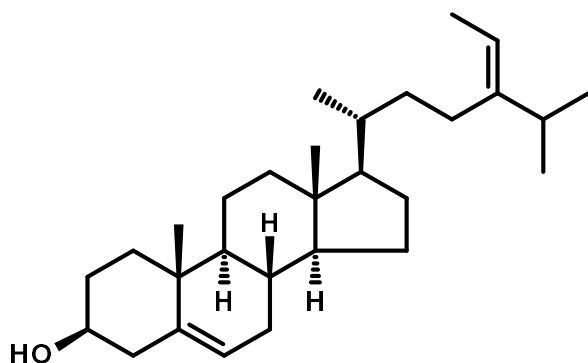


**Figure 10** - Chemical structure of fucosterol.

Previous studies have reported several bioactivities of Fct: antioxidant (Lee et al., 2003, Jayawardena et al., 2020), antidiabetic (Lee et al., 2004b), anti-inflammatory (Jung et al., 2013, Fernando et al., 2019, Jayawardena et al., 2020), anti-obesity with suppression of lipogenesis (Lee et al., 2017, Song et al., 2017b), antimicrobial (Kumar et al., 2010), osteoprotective (Bang et al., 2011, Lee et al., 2014), neuroprotective (Hannan et al., 2019), hepatoprotective (Choi et al., 2015) and antiphotaging (Kim et al., 2013).

Fct also displayed *in vitro* anticancer effects in several cell lines acting by several mechanisms of action as cytotoxicity as induction of apoptosis (Ji et al., 2014, Jiang et al., 2018, Mao et al., 2019), cell cycle arrest (Jiang et al., 2018, Mao et al., 2019, Bae et al., 2020a), inhibition of cell migration (Jiang et al., 2018), ROS production and mitochondrial dysfunction (Bae et al., 2020a). Interestingly, some studies reported that Fct cytotoxicity was more pronounced in cancer cell lines than in non-tumoral cell lines (where the cytotoxic effects were not detected or were minimal). As examples of this, Ramos et al. (2019) reported that Fct at 10  $\mu\text{M}$  only displayed cytotoxicity to colon cancer cells without affecting the non-tumoral cells. Mao et al. (2019) reported an  $\text{IC}_{50}$  of 15  $\mu\text{M}$  in lung cancer cells with minimal cytotoxic effects in non-tumoral lung cell lines ( $\text{IC}_{50}$  over 100  $\mu\text{M}$ ).

The pointed pathways involved in the anticancer activities were mitochondrial-mediated apoptosis, the downregulation of key proteins of the mTOR/PI3K/Akt signaling pathway in HeLa cells (Jiang et al., 2018), and PI3K and MAPK signal pathways in the ovarian cancer cell lines ES2 and OV9 and activation of Raf/mitogen-activated protein kinase/extracellular-signal-regulated kinase (MEK/ERK) pathway in non-small cell lung cancer cells (Li et al., 2021a). In addition, Fct increased the expression of Bax and cleaved caspase-3 in lung cells while decreasing the expression of Bcl-2 (Mao et al., 2019). In the latter study, the cell cycle arrest was related to a decrease in the expression

of Cdc2, Cyclin A, Cyclin B1, and upregulation of the negative regulators of cell cycle progression (p21Cip1, and p27Kip1).

According to all the above information, there has been a rising trend in the number of publications with Fct in the last twenty years (Meinita et al., 2021), however, concerning its effects on BC cell lines, the information is very scarce, and the mechanisms of action are not explored. Table S8 summarizes the remaining limited evidence on the effects of Fct in BC cells derived from *in vitro* studies.

As far as we know, until October of 2022, there is only one study reporting the effect of Fct in 3D cultures. In this study Ramos et al. (2019), compared the effects of Fct alone and combined with 5-Fu in colon cancer cells in 2D and 3D, reporting that the concentrations used in 2D had no effects in 3D culture.

Fct was already tested in combination therapy with 5-Fu in cancer colon cells, showing higher antiproliferative effects than the Fct and drug alone (Ramos et al., 2019). Also, in combination with Cis and paclitaxel in ovarian cancer cells, revealed a synergistic effect with both drugs showing higher caspase cleavage and cytochrome C release and decreased expressions of different VGFE (Bae et al., 2020a).

*In vivo*, Fct decreased ovarian tumor formation in a zebrafish xenograft model and suppressed angiogenesis, without cytotoxicity to the animals (Bae et al., 2020a). In a zebrafish embryo assay, Fct at a low concentration of 0.1-3 µg/mL reduced the embryos' pigmentation without embryo cytotoxicity until the concentration of 100 µg/mL. In mice, Fct inhibited the growth of xenografted lung tumors (Mao et al., 2019).

Despite all the studies reporting Fct biological activities, there is still little knowledge about its toxicity and bioavailability in animals and humans. In mice, one study showed that Fct from *Sargassum fusiforme* had poor absorption and slow elimination, mainly through fecal excretion (Wang et al., 2022). Until the present data, there seems to be no clinical trial with Fct. Further studies are necessary to elucidate the Fct effects and clarify its potential as a new compound for different therapeutical uses, including anticancer purposes.

#### **5.3.4. Phlorotannins**

Seaweeds are rich in polyphenolic compounds such as phlorotannins, bromophenols, flavonoids, phenolic terpenoids, and mycosporine-like amino acids (Cotas et al., 2020).

However, phlorotannins are exclusively found in brown seaweeds, accounting for about 5–12% of the brown seaweed's dry mass (Venkatesan et al., 2019).

Phlorotannins are formed by polymerizing phloroglucinol (Phg) units through diaryl ether or C–C bonds (Kumar et al., 2022). Phlorotannins can have different molecular weights according to the oligomerization of the Phg units, and their presence and activity vary depending on the seaweed species and environmental conditions (Heffernan et al., 2015).

#### 5.3.4.1. Phloroglucinol (Phg)

Phloroglucinol (1,3,5-trihydroxybenzene) is a phenolic compound constituted by one aromatic ring with 3 hydroxyl groups (Figure 11). This forms a unique structure as other phenolic compounds have only one hydroxyl bound to the benzene ring (Crozier et al., 2009). Phg has several functions ranging from structural cell wall components contributing to cell wall resistance, protection of seaweeds against UV radiations, and stress (Kang et al., 2006), and defense against herbivores acting as herbivore deterrents (Catarino et al., 2017). Phg extracted from natural sources is commercially used in medicine, cosmetics, pesticides, cement, and dyes (Singh et al., 2010).

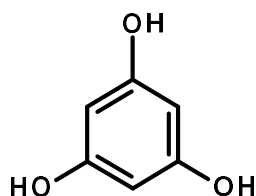


**Figure 11** - Chemical structure of Phloroglucinol.

Data from *in vitro* and *in vivo* studies revealed several biological activities of Phg and Phg-based compounds. Among them, the most representative activities are antioxidant (Kang et al., 2006, Zou et al., 2008, Queguineur et al., 2012), anti-inflammatory (Kim and Kim, 2010, Li et al., 2018a), antimicrobial (Khan et al., 2022), antidiabetic (Lee and Jeon, 2013, Yoon et al., 2017), antiadipogenic (Jung et al., 2014a, Karadeniz et al., 2015) hepatoprotective (Kang et al., 2012a, Jung et al., 2014b), cardioprotective (Ahn et al., 2017) and neuroprotective (Kang et al., 2012b). The antioxidant activity of Phg-based compounds also seems to act in a chemopreventive way against the carcinogenesis process (Kang et al., 2006, Kim and Kim, 2010).

Phg-based compounds have also demonstrated several *in vitro* anticancer properties against different types of cell lines (Kang et al., 2014, Almeida et al., 2020, Catarino et al., 2021a), including in BC ones (Kong et al., 2009, Kim et al., 2015a, Kim et al., 2015b). Catarino et al. (2021a) reported cytotoxicity of *Fucus vesiculosus*-derived phlorotannins on gastric and colon tumor cell lines, without affecting normal cells. Similarly, the absence of cytotoxicity on normal cells was also observed in another study with colon cell lines (Lopes-Costa et al., 2017).

The anticancer effects on BC cell lines included induction of apoptosis, cell proliferation, migration inhibition, and invasion capacity (Kong et al., 2009, Kim et al., 2015a, Kim et al., 2015b, Young-Ju, 2020). Phg has also been tested in BC cell lines in the form of biopolymer, encapsulated with starch (Kumar et al., 2014) and as Phg engineered silver nanoparticles (Kumar et al., 2018), revealing cytotoxic effects against the tested BC cell lines. In 3D cell culture, Phg suppressed the sphere formation in MCF7 (Kim et al., 2015b). Table S9 summarizes the main effects and mechanisms of Phg and its derivatives in BC cell lines.

After verifying that, *in vitro*, Phg inhibited the invasiveness of BC cells, Kim et al. (2015a) tested the metastatic suppression potential of Phg *in vivo*. This activity was tested in NOD-scid gamma (NSG) mice, in which GFP-labeled metastatic MDA-MB-231 cells were transplanted into mammary fat pads. Primary tumor formation was attenuated in the group treated with Phg, and less lung metastasis was detected compared to vehicle-treated mice. Another part of this study involved injecting the same cells in athymic nude mice; similarly, Phg-treated mice presented less lung metastasis.

The effects of the combination of Phg-derived compounds have also been tested *in vivo*, using a BALB/c nude mice model (Yang et al., 2015). It was shown that phlorotannin-rich extract from *Ecklonia cava* improved the efficacy of cisplatin in ovarian cancer by enhancing cancer cell apoptosis via the ROS/Akt/NF- $\kappa$ B pathway and reduced nephrotoxicity by protecting against normal kidney cell damage.

In general, phlorotannins from brown seaweeds displayed low toxicity in microalgae, seaweeds, plants, invertebrates, and vertebrates (fish, mice, rats, dogs, and humans) (Negara et al., 2021).

In humans, a few studies are dedicated to the bioavailability and toxicity of phlorotannins. From these studies, the consumption of 250 mg/capsule/day, especially dieckol, is safe with extremely mild adverse effects, including mild fatigue, dizziness, nausea, and

abdominal distension (Okeke et al., 2021). Recent studies on the bioavailability of phlorotannins in humans demonstrated that they are degraded throughout the gastrointestinal tract, remaining just a small amount accessible for further absorption (Catarino et al., 2021b).

## **6. Role of *In Vitro* Models for Drug Screening and Mechanistic Insights**

In the current scenario of cancer burden, with the number of new cases in a continuously increasing trend (Sung et al., 2021), the run for new anticancer drugs is in the spotlight of the pharmaceutical industry. This constant search is dedicated to finding new drugs or adjuvants of prescription drugs that can be more effective, safe, with fewer secondary effects, and economically viable (Kitaeva et al., 2020). Associated with this is the major concern of drug resistance which is one of the leading causes of unsuccessful cancer treatment (Rezayatmand et al., 2022). These issues canalize the drug screening process, which includes several preclinical steps using *in vitro* and *in vivo* studies, by which potential drugs are identified, optimized, and validated (Hughes et al., 2011).

In a very simplistic way, the classical drug development process consists of three steps: *in vitro* study, *in vivo* study, and clinical trials (Liu et al., 2015). It starts with basic research, and many widely used drugs have their origins in academia (Frearson and Wyatt, 2010). Most *in vitro* screening studies start in a 2D monolayer culture of human-immortalized cell lines from different origins (Allen et al., 2005). Within this type of culture, some approaches tried to increase the complexity of these models, that was the case of co-cultures, e.g., growing epithelial cancer cells with stromal cells and the called 2.5 D cultures, which consist of cells growing on top of a thick layer of ECM proteins (Langhans, 2018).

A 2D culture is a straightforward methodology with many advantages. It is also possible to cultivate in 2D primary cultures cells directly derived from living tissue that, in theory, are more likely to reflect the properties of native cells *in vivo*. However, primary cell cultures have limited applications due to the difficulties in assessing primary human cells compared to the cell lines and because their lifespan is very short, normally with a small number of divisions achievable *in vitro*, which hampers long-term studies (Vidi et al., 2013). However, due to several limitations associated with this type of culture, 2D cell culture has been recognized as inadequate for predicting drug responses.

Regarding the cell and tissue-based systems, other models such as three-dimension (3D) culture, 3D co-culture, tissue slices, patient-derived explant, matrix embedded

cultures (Sant and Johnston, 2017), Boyden's chamber, microfluid systems, 3D bioprinting organoids (Kitaeva et al., 2020) and organ-on-a-chip models (Azimi et al., 2020) have been developed.

In recent decades there has been a special interest in optimizing 3D culture generation. This change of paradigm from 2D to 3D cell cultures aims to narrow the gap between *in vitro* and *in vivo* studies (Froehlich et al., 2016), especially in the field of drug screening, constituting a more predictive model of the *in vivo* response to anticancer drugs (Antoni et al., 2015, Fang and Eglen, 2017, Langhans, 2018).

According to current regulatory requirements, before a novel drug moves to clinical trial, it must be tested *in vivo* in at least two species of animal models (rodent and non-rodent) (Prior et al., 2018). This effort represents several issues of costs, feasibility in terms of facilities and time, and ethical concerns, as most experiments cause pain or reduce the quality of life of these animals (Antoni et al., 2015). Additionally, the politics of the 3Rs (replacement, reduction, and refinement) applied to animal studies has led scientists to more appropriate *in vitro* models (Martinez-Pacheco and O'Driscoll, 2021). Moreover, other animal models such as the invertebrates, e.g., *Caenorhabditis elegans* (nematode) and *Drosophila melanogaster* (fruit fly), have gained relevance because they imply lower costs, have genetic amenability and easy high-throughput screening (Singh and Seed, 2021).

*In vivo* testing in animals has the advantage of the complexity of a whole living organism. However, it has some handicaps as the different animal physiology, drug metabolism, and tissue microenvironment can be very different from humans. For instance, the immune system of xenograft models is compromised, and xenograft tumor growth is faster than in primary human tumors (Sant and Johnston, 2017). Besides all the efforts to find potential new drugs, the most promising compounds selected by *in vitro* and *in vivo* trials fail during the different phases of clinical trials. It is estimated that only 7% of potential anticancer drugs gained clinical (Hay et al., 2014).

Here we describe the main *in vitro* tools used in drug screening, giving a broad view of their applications and drawbacks.

### 6.1. 2D Cell Culture

The simplest *in vitro* screening tools are established cell lines cultured in monolayer - two-dimensional (2D) cultures, in which cells normally are cultivated attached to plastic surfaces (Baker and Chen, 2012), in an artificial environment consisting of a culture



medium with the essential nutrients (amino acids, carbohydrates, vitamins, minerals), growth factors, hormones, oxygen and carbon dioxide, and regulated the physicochemical environment (pH, osmotic pressure, temperature) (Antoni et al., 2015). The large use of this methodology is closely related to its easy handling, cost-effectiveness, good reproducibility, and the possibility to apply to a vast diversity of cell types (Breslin and O'Driscoll, 2013). An exception is the hematopoietic cells that grow on cell suspensions (Ribeiro-Filho et al., 2019).

Two-dimensional cell cultures have largely contributed to a better knowledge of many processes related to carcinogenesis, such as migration (Baker and Chen, 2012), invasion, and drug screening (Kitaeva et al., 2020). The screening on 2D is considered the baseline in the pipeline of preclinical tests in drug discovery, as at this level is easy to perform high-throughput screening in a fast low-cost way (Capula et al., 2019). By the end of the 1980s, National Cancer Institute (NCI) developed for *in vitro* drug screening a panel consisting of 60 different human cell lines originating from tumors (leukemia, melanoma, tumors of the central nervous system, cancer of the lungs, colon, ovaries, breast, kidney, and prostate), which was called NCI60 (Shoemaker, 2006). Since then, many studies have reported drug screening in the referred panel and other smaller cell line panels (Close et al., 2019, Krushkal et al., 2021). *In vitro* screening, especially in monolayer cultures, has some limitations as the lack of tissue microenvironment (TME) and extracellular matrix (ECM) (Kitaeva et al., 2020). The TME includes the interactions with cells like cancer-associated fibroblasts, mesenchymal cells, adipocytes, different types of immune-inflammatory cells, and the blood and lymphatic vascular networks (Wang et al., 2017a) included in an ECM. ECM is constituted by a complex mixture of proteins, glycoproteins, polysaccharides, proteoglycans, and glycosaminoglycans that provides physical support for the interactions of the TME cells (Insua-Rodríguez and Oskarsson, 2016). These drawbacks make this model inaccurate or insufficient for the assessment of the effects of the screened compounds (Costa et al., 2016). The main advantages and disadvantages of 2D cell culture are presented in Table 1.

**Table 1** - Advantages and disadvantages of 2D cultures compared to 3D cultures.

<b>Advantages</b>	<b>References</b>
Simple and low-cost effective screening of multiple compounds or libraries	(Breslin and O'Driscoll, 2013, Kapalczynska et al., 2018)
Easy cell observation and measurement of viability, image capture	(Freshney, 2010)
Very reproducible	(Breslin and O'Driscoll, 2013, Antoni et al., 2015)
Fast cellular growth	(Antoni et al., 2015, Verjans et al., 2018)
Easy to high-throughput screening	(Barbosa et al., 2022)
<b>Disadvantages</b>	<b>References</b>
Lacks ECM interactions	(Breslin and O'Driscoll, 2013, Kitaeva et al., 2020)
Altered morphology and polarity for growing in 2D, also influence the cell's secretion and signaling	(Kapalczynska et al., 2018)
Lack of 3D tissue architecture, with hypoxic conditions and other effects of barrier to oxygen and nutrients present in tumors	(Kapalczynska et al., 2018, Barbosa et al., 2022)
Lack of communication between tumor cells and the tumor microenvironment	(Barbosa et al., 2022)
Lower gene expression and biosynthesis of drug-metabolizing enzymes	(Wang et al., 2021)
Poor correlation between preclinical <i>in vitro</i> and <i>in vivo</i> data	(Kitaeva et al., 2020)
Cell lines undergo genetic drift over time	(Kimlin et al., 2013)

## 6.2. 3D Cell Culture

The 3D cell culture models consist of systems where cells are grown in more complex cell arrangements that offer more cell-to-cell interactions comprising a more physiological and functional environment (Friedrich et al., 2009, Antoni et al., 2015, Imamura et al., 2015), with the gene expression profiles more similar to the *in vivo* (Souza et al., 2018, Melissaridou et al., 2019, Jensen and Teng, 2020).

Classical 3D structures are described as a spherical or nearly spherical shape cultures, with a decreasing gradient of nutrients, growth factors, oxygen, and pH value (Sutherland et al., 1986, Friedrich et al., 2007). Heterogeneous cell populations constitute these 3D cell arrangements within a 3-layer configuration: 1) an outer proliferative zone (where cells have direct access to the oxygen and nutrients); 2) an intermediate zone with quiescent cells; and 3) an inner core with dying cells due to the lack of nutrients and oxygen (Mehta et al., 2012, Costa et al., 2016, Reynolds et al., 2017, Sant and Johnston, 2017) (Figure 12).

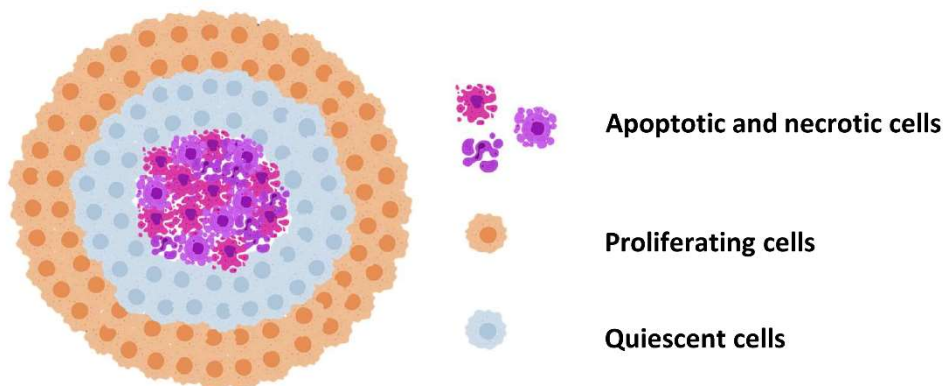


**Figure 12** - Schematic figure of the structure of spheroids with three layers, consisting of an outer layer with proliferating cells, an intermediate layer with quiescent cells and a central core containing cells in dying processes.

Relatively to this central core with dying cells, it is named differently according to different authors, with some calling it necrotic core (Mehta et al., 2012, Costa et al., 2016), and, in a contradictory way, using apoptosis markers for assessing cell death (Costa et al., 2016). Other studies use a mixture of nomenclatures, indiscriminately called necrotic or apoptotic cores (Reynolds et al., 2017). Nonetheless, it is imperative to note that necrosis and apoptosis are not synonymous, notwithstanding the hypoxia in the central core can induce both apoptosis and necrosis; thus, the nomenclature apoptotic/necrotic core can be applied (Daster et al., 2017). Similarly, both types of cell death can be simultaneously

detected in tissues and cell cultures (Dursun et al., 2006, Hirschhaeuser et al., 2010, Yoon et al., 2014).

In 3D cell cultures, cells interact and adhere with each other through the formation of desmosomes, membrane adhesion specializations and by secretion of ECM proteins (collagen, fibronectin, tenascin, laminin, etc.) (Chan et al., 2013). These close interactions, plus the barrier formed by multilayers of cells, enhance spheroid density, increasing the interstitial fluid pressure (Minchinton and Tannock, 2006), constituting a barrier to compounds' penetration, not only for nutrients and oxygen but also to drugs (Sant and Johnston, 2017). Moreover, this close cell arrangement allows tissue recapitulation, showing a more differentiated morphology (Sant and Johnston, 2017).

This type of cell culture model is particularly useful for studying metabolic and proliferative gradients as well as the responsiveness of hypoxic cells (Friedrich et al., 2007). The presence of a hypoxic environment is related to a decrease in some drugs' effects, as in the case of Dox, which needs oxygen to induce an effective anticancer effect through the formation of reactive oxygen species (ROS) (Daster et al., 2017, Nunes et al., 2019). It is known that under anaerobic conditions cells undergo a metabolic switch from oxidative phosphorylation to glycolysis called the Warburg effect, where pyruvate is converted into lactate. Lactate accumulation acidifies the microenvironment, which is related to the emergence of chemoresistance (de la Cruz-López et al., 2019). Moreover, the low pH in the central core can alter some drugs, such as melphalan, preventing its effective action (Wojtkowiak et al., 2011).

Related to drug resistance, 3D models also can better mimic *in vivo* response because stem cell markers are upregulated in 3D cell cultures (Chaicharoenaudomrung et al., 2019, Zhang et al., 2020), including the ones of BC cell lines such as MCF7 (Yilmazer, 2018). Additionally, spheroids have a lower proliferation rate (Verjans et al., 2018) and the inner cells of the 3D arrangements are less proliferative, being cells less susceptible to drugs that interfere with cell division (Jensen and Teng, 2020).

Having into consideration all the above-mentioned characteristics, the 3D cell cultures resemble avascular tumor nodules or can mimic micro-metastases (Sant and Johnston, 2017). Despite the cited advantages of 3D cell culture, there are also several drawbacks. Table 2 presents the main advantages and disadvantages of using 3D cell culture

**Table 2** - Advantages and disadvantages of 3D cultures.

<b>Advantages</b>	<b>References</b>
Complex architecture where cell-cell interactions predominate over cell-substrate interactions	(Sant and Johnston, 2017)
Paracrine and direct intercellular interaction	(Bogdanowicz and Lu, 2014)
Expression of genes and biochemistry of cells more similar <i>in vivo</i>	(Kapalczynska et al., 2018, Verjans et al., 2018)
Gradient diffusion of oxygen and nutrients, hypoxic conditions in the center of the spheroid, mimicking how drug delivery might occur <i>in vivo</i>	(Mehta et al., 2012, Langhans, 2018)
Adhesion and tight junction barriers	(Mehta et al., 2012)
Heterogeneous tumor cell populations of proliferating cells, senescent cells, and dying cells	(Costa et al., 2016)
Greater stability and longer life span	(Antoni et al., 2015)
Simple measurements of spheroids size by phase-contrast microscopy and computer image analysis	(Friedrich et al., 2007)
<b>Disadvantages</b>	<b>References</b>
More complex, time-consuming, and expensive	(Jensen and Teng, 2020, Barbosa et al., 2022)
More difficult to standardize and analyze	(Kapalczynska et al., 2018)
Do not completely reproduce the interaction between ECM and cells	(Yamada et al., 2022)
Individual cell analysis, such as flow cytometry, requires techniques of cell dissociation like the use of enzymes	(Demuynck et al., 2020)
Worse performance and reproducibility, difficult to interpret, cultures more difficult to carry out	(Hickman et al., 2014)
More difficult to compare with other studies due to the large variabilities between 3D models	(Barbosa et al., 2022)
Lack of standard methodologies and efficient assays for evaluation of cell viability on 3D	(Barbosa et al., 2022)
More difficult for high-throughput screening	(Antoni et al., 2015)
Difficulty in obtaining spheres for some cell lines	(Froehlich et al., 2016, Ahn et al., 2020)

Importantly, there are several methodologies described for the generation of 3D cell cultures, but according to the used technique and the internal cell lines characteristics, the outcomes can be very distinct, varying in size, shape, density, and surface features (Harma et al., 2014, Froehlich et al., 2016, Zanoni et al., 2016, Gencoglu et al., 2018). A good example of this is the study of Froehlich et al. (2016) in which 42 different experimental setups were tested using the BC cell lines MCF7, SKBR3, and MDA-MB-231, and within the same cell line, e.g., MDA-MB-231 different types of 3D structures were formed according to the methodology used, with outcomes varying from multiple small spheroids, loose aggregates to single cell suspensions. Indeed, other studies described the formation of 3D aggregates of different morphologies rather than the spheroid, e.g., grape-like, stellate, mass (Thakuri et al., 2018), compact vs loose aggregates (Vinci et al., 2012, Froehlich et al., 2016). These types of morphologies are not in accordance with the definition of spheroids, which considers spheroids as typically round or elliptic, globe-like, compact structures (similar to *in vivo* tumors) that allow manipulation without causing mechanical damage (Nagelkerke et al., 2013). Despite these incongruences, most studies use spheroids for all the morphologies of multicellular aggregates forming a 3D cell culture.

In the same vein, there is no consensus on the nomenclature of the 3D cell cultures. The most common name is spheroid (Ivascu and Kubbies, 2007, Zanoni et al., 2016). However, as detailed reviewed by Weiswald et al. (2015), there is a wide range of terms, e.g., microtumors (Benton et al., 2015), microtissues (Vantangoli et al., 2015), or multicellular cancer aggregates (MCAs) (Azadi et al., 2019). In the case of breast cells, sometimes they are referred to as mammospheres (Cioce et al., 2014, Lombardo et al., 2015).

A further consideration related to the differences in the 3D cell cultures is that the morphology directly affects drug delivery and the consequent outcome (Verjans et al., 2018). Based on this, many researchers call attention to the need for more studies dedicated to the morphological and physiological characterization of 3D cell cultures to understand better the results, reduce the variability between different experimental setups, and properly compare results (Froehlich et al., 2016, Katt et al., 2016, Verjans et al., 2018, Huang et al., 2020).

There are several methodologies to form 3D cell cultures, but there are two main big groups: scaffold-based and scaffold-free techniques (Langhans, 2018, Nunes et al., 2019, Barbosa et al., 2022). Most common 3D cell culture systems use monocultures, i.e., only one cell type. At the same time, others introduced heterotypic cultures, i.e.,

using two or more cell types, normally co-culture epithelial cells with fibroblasts, immune cells such as macrophages, endothelial cells, and adipocytes (Weigelt et al., 2014).

### **6.2.1. Scaffold-based Methods**

In scaffold-based systems, cells can grow on matrices that attempt to mimic the natural microenvironment of the cells, giving physical support and biochemical components to cell growth (Valdoz et al., 2021). Thus, better mimicking the interactions between stromal cells and ECM, and allowing cell proliferation, migration, and growth (Zanoni et al., 2019). Over the past years, considerable progress has been made in finding different matrices serving as scaffolds for 3D cell culture. The scaffolds can be made from a great variety of materials. A popular option for 3D culture is the use of hydrogels that can be of natural origin (e.g., collagen, alginate, Matrigel™) or synthetic matrices (e.g., polyethylene glycol (PEG), poly(vinyl alcohol) (PVA), polyglycolic acid (PGA) and polylactic acid (PLA)) and hybrid scaffold-based models (Ferreira et al., 2018). The matrices also can have different porosities, pore sizes, permeabilities, and mechanical characteristics. These various attributes of the matrices determine not only the size and shape of the scaffold but also is important to the nutrient supply and functional effects (Antoni et al., 2015).

Scaffolds of natural origin are largely used in research due to their abundance and facility in isolation from plants and animals and their high biocompatibility, as they share many biochemical similarities with natural ECM (Zanoni et al., 2019). Synthetic scaffolds are relatively cheap and inert; however, they do not provide a good tumor microenvironment as they do not have critical biochemical molecules such as growth factors and hormones (Zanoni et al., 2019).

In these culture systems, the main difficulties are the variability between batches of scaffolds, and it is more difficult to extract all cells for analysis of cellular responses to drug interactions, such as dose-dependent cell viability (Antoni et al., 2015). Also, some matrices require gelation, which can be challenging to automate. Moreover, the great variability in the form and sizes of the 3D cultures and the opacity of gels or matrices can be very challenging for cell morphological analysis (Sant and Johnston, 2017).

A more sophisticated approach called microfluid devices consists of a chip composed of microchambers and microchannels, where cells typically are involved in hydrogels are under a continuous flow of medium/exposure drug exposure (inlet/outlet) due to the use of external pumps (Young and Beebe, 2010), enabling improved supply of nutrients and oxygen, and efficient removal of metabolic waste (Järvinen et al., 2020). Also, the development of automatic 3D bioprinting is a promising technology that allows the

dispensing of both low and high-viscosity polymer solutions with high levels of reproducibility, and the manipulation and control of selected features of complex scaffolds that can better mimic a tissue model (Dankó et al., 2022).

### **6.2.2. Scaffold-free Methods**

In scaffold-free, cells are usually obtained from a single cell suspension derived from a cell line or primary cell cultures, formed by self-assembling in stationary or agitation-based systems 3D cell cultures (Zanoni et al., 2019).

#### **6.2.2.1. Stationary Methods**

The most common stationary systems are the hanging drop and forced floating with low attachment surfaces. In these systems, normally, cells cannot adhere by being in a drop (Hanging drop method) or by the presence of a coated surface (Forced floated method). Magnetic levitation is less commonly used because it involves pre-loading metallic nanoparticles to the cells under an external magnetic field, like a magnet placed on the top of the plate lid, forcing cells to be aggregated to form multicellular aggregates (Lewis et al., 2017).

In the hanging drop technique, cells aggregate at the bottom of a drop formed by the inversion of a plate lid. The drops remain in place due to surface tension, and the cells aggregate, forming a spheroid at the air-liquid interface (Kelm et al., 2003). However, after the formation, spheroids have to be transferred to a new plate for the desired exposure (Amaral et al., 2017). Another disadvantage of this technique is that the spheroid shape is not homogenous (Kelm et al., 2003).

The forced floating (Breslin and O'Driscoll, 2013), also called liquid overlay (Froehlich et al., 2016, Verjans et al., 2018), is a method in which cells are seeded in non-adhesive coated surfaces. This coat can be agarose (Ho et al., 2012, Abe-Fukasawa et al., 2018, Gao et al., 2018), poly-Hema (Ivascu and Kubbies, 2006, Froehlich et al., 2016), or a hydrophilic neutrally charged coating that covalently bound to the polystyrene well surface, as in the commercially available ultra-low attachment (ULA) plates (Selby et al., 2017, Melissaridou et al., 2019). The plates have most commonly U-shaped bottomed wells. As cells cannot adhere, they are forced to stay suspended, forming one spheroid per well (Friedrich et al., 2007, Vinci et al., 2012). A centrifugation step is commonly included to help cells aggregate and form spheroids (one per well) (Zanoni et al., 2016, Malhão et al., 2019). The formation of the spheroids comprises an initial phase in which



cells aggregate and the spheroids' volume increases (the period of spheroidization), and then the volume tends to decrease until it stabilizes (Zanoni et al., 2016).

Additionally, ULA plates allow easy plating, observing, photographing, accessing, and manipulating of the spheroid before, during, and after drug exposure, and just a small amount of volume is needed for the drug exposure (Friedrich et al., 2007). Furthermore, it is possible to adjust the spheroid size by increasing or decreasing cell density (Baru et al., 2022). Also, it is possible to culture spheroids of just one cell type (homotypic spheroids) or with two or more cell types (heterotypic spheroids) (Zanoni et al., 2019). Likewise, some assays can be performed directly on ULA plates (Bresciani et al., 2019).

ULA plates are described as an easy technique, able to generate reproducible and uniform size-controlled spheroids, suitable for throughput drug screening (Breslin and O'Driscoll, 2013, Sant and Johnston, 2017), high content analysis, automation systems, and some viability measurements (Piccinini, 2015, Zanoni et al., 2016, Mittler et al., 2017).

As with any other methodology, ULA plates also have some disadvantages. First, due to their wells' curvature, it is necessary to transfer the MCAs to flat-bottom plates when performing techniques that require absorbance or immunofluorescence measurements. Besides being time-consuming, this step can also disrupt the MCAs, especially if the spheroids are not very compact. Furthermore, if exposure medium change is considered, this method can be a low throughput strategy due to the difficulty of implementing automation to medium change without aspirating the MCAs (Katt et al., 2016).

3D cultures of different cell lines, including BC ones, have been obtained using ULA 96-well plates (de la Mare et al., 2013, Howes et al., 2014, Froehlich et al., 2016, Raghavan et al., 2016), either alone or as co-cultures with human fibroblasts or HUVECs (Howes et al., 2014). This methodology has already been used for drug screening (Rotem et al., 2015, Mittler et al., 2017, Kochanek et al., 2020, Roper and Coyle, 2022).

In both hanging drop and ULA techniques, some studies have reported the unsuccessful formation of spheroids from different cell lines (Piggott et al., 2011, Froehlich et al., 2016, Gencoglu et al., 2018). Another possibility commonly reported in the literature is the addition of Matrigel™, a commercially used ECM gel, or other ECM constituents such as collagen and fibronectin as an attempt to serve as a more biologically relevant model system (Lee et al., 2007, Badea et al., 2019, Ruud et al., 2020). Also, the adding other compounds that work as viscosity raisers, e.g., methylcellulose, improves spheroid

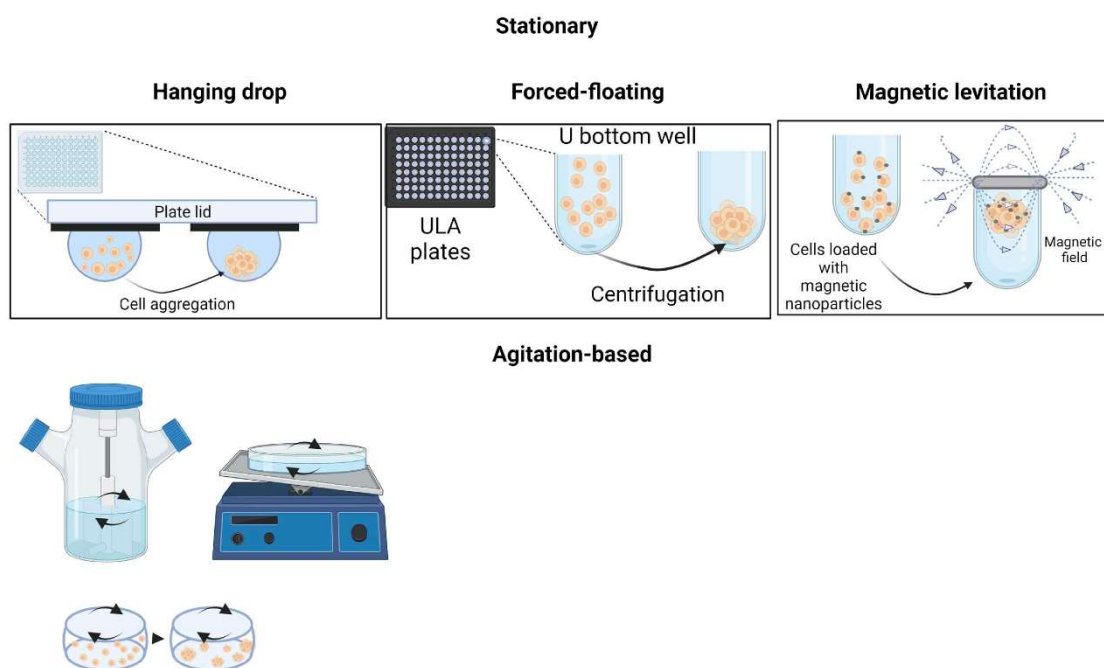
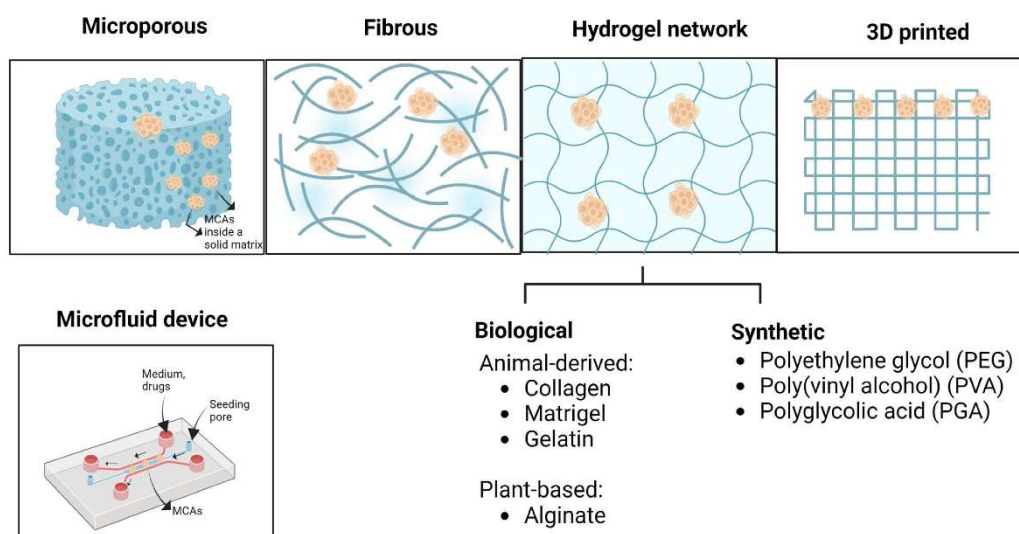
assembly (Casey et al., 2001, Ivascu and Kubbies, 2006, Maritan et al., 2017, Badea et al., 2019).

### **6.2.2.2. Agitation-based Systems**

In this system, cells are suspended under continuous spinning in flasks or culture plates with a treated surface that prevents them from settling down. Examples of these systems are spinner flasks and rotary vessels that produce spheroids via continuous spinning of the cell suspension to keep cells from settling down. These systems have the advantage of forming a great number of spheroids and long-term culture; however, they are very heterogenous in size (Mehta et al., 2012). Moreover, the spheroidization time can take up to 15 days; after that, they can be transferred to ULA plates (Zanoni et al., 2016).

Also, agitation-based systems are not a good choice for drug testing as they need high quantities of the medium, which is impractical for testing new drug candidates that generally are available in small amounts (Friedrich et al., 2007). Some sophisticated devices, such as bioreactors, can grow an immense number of 3D MCAs under controlled temperature, pH, medium flow rate, oxygen, nutrient supply, and waste metabolite removal (Antoni et al., 2015).

The main techniques used for generation of 3D cell cultures are schematically represented in Figure 13.

**(a) Scaffold-free methods****(b) Scaffold-based methods**

**Figure 13** - Schematic representation of the different 3D cell culture techniques. (a) scaffold-free methods and (b) scaffold-based methods (Figure created with BioRender.com and paint.net).

**6.3. Breast Cancer 3D *In Vitro* Models**

Several studies reported the formation of 3D cell cultures from breast human cell lines using different methodologies, e.g., Ivascu and Kubbies (2007), do Amaral et al. (2011), Nagelkerke et al. (2013), Froehlich et al. (2016), Brancato et al. (2018), Swaminathan et al. (2019).

The 3D BC models have been used to study the effects of chemotherapeutic agents (Halfter et al., 2016, Fong et al., 2017, Lanz et al., 2017, Augustine et al., 2021, Boyer et al., 2021), the process of invasion and metastasis (Li et al., 2011, Roarty and Echeverria, 2021, Nanou et al., 2022) and radiotherapy (Yakavets et al., 2020, Ravichandran et al., 2021), but also for screening new anticancer drugs (Imamura et al., 2015, Stock et al., 2016, Fitzpatrick et al., 2017). Generally, these models are poorly characterized. Few studies in the literature are dedicated to the characterization of 3D cell BC models (Bowers et al., 2020, Huang et al., 2020, Dankó et al., 2022).

There is a great level of inconsistency concerning the formation of these structures in terms of successful obtention, times for spheroidization, and time viable in culture, as well as morphologies and degree of compactness. The inconsistencies can be due to several factors: the technique used to obtain the 3D aggregates, different medium supplementations, different cell lines, and time.

To illustrate these different results among studies, we made three supplementary Tables (Tables S10, S11, and S12) comparing various works that used the same cell lines used in our studies, focusing only on the ones that applied similar methodologies as the one applied to this thesis: stationary scaffold-free models only in homotypic cultures. In the literature survey, the encountered information relative to the culture conditions for the generation of the 3D cell culture is very diverse and sometimes incomplete or even omitted. For instance, some studies report that the cell density for plating do not refer to the volume plated per well. Thus, it was impossible to use the same units among studies directly. In the presented Tables, it is possible to observe the great diversity not only in methodologies used but also in culture mediums and respective supplementations, also reflecting different outcomes in the 3D cell culture.

### **6.4. Breast Cell Lines Used in This Study**

#### **6.4.1. MCF7**

MCF7 is probably the most used BC cell line. It was isolated from a pleural effusion of metastatic adenocarcinoma in 1973 by the Michigan Cancer Foundation, being named MCF as an acronym for its foundation of origin (Comsa et al., 2015). MCF7 has been described to express epithelial markers such as E-cad,  $\beta$ -catenin, and cytokeratin 8/18 and the absence of mesenchymal markers such as vimentin. These cells in culture condition with egg white, exhibited features of differentiation such as polarized MCF7 forming acini and mammary duct-like structures with secretory vesicles in the apical part, toward the lumen, corresponding to high levels of  $\beta$ -casein (D'Anselmi et al., 2013). This

cell line is considered a poorly aggressive, noninvasive cell line (Gest et al., 2013) and poorly angiogenic (Aonuma et al., 1999).

MCF7 cells are ER and PR positive representing the Luminal A, the BC subtype with high levels of  $Er\alpha$  and  $Er\beta$  (Papoutsi et al., 2009). Thus, it is widely used for studying hormone resistance, anti-hormone compounds, or compounds that interfere with hormonal receptors (Leung et al., 2014, Lee et al., 2015).

MCF7 generally formed multicellular 3D aggregates using different methodologies. However, some studies like Ivascu and Kubbies (2007) obtained compact spheroid without the need to add 2.5 % of the reconstituted basal membrane (rBM) to the medium. Similarly, do Amaral et al. (2011) showed that the addition of Matrigel was not necessary to obtain the MCF7 cell line spheroids. In contrast, others report the need for additives like methylcellulose or Matrigel to successfully obtain 3D structures (Ivascu and Kubbies, 2006, Nagelkerke et al., 2013). Table S10 resumes the main scaffold-free techniques used for generating 3D cell cultures of MCF7.

Lumen-like structures were also observed (Krause et al., 2010, do Amaral et al., 2011) and justify their existence because this cell line was derived from an invasive ductal carcinoma metastasis (do Amaral et al., 2011). The immunomarking for E-cad was maintained in 3D culture (Krause et al., 2010). Indeed E-cad is described as a mediator in the formation of the MCF7 spheroids (Ivascu and Kubbies, 2007).

### **6.4.2. SKBR3**

SKBR3 is a human BC cell line isolated from pleural effusion cells of a female breast adenocarcinoma (ATCC, SKBR3 HTB 30™). SKBR3 overexpresses the HER-2, thus, it is commonly used in cancer research to represent the HER-2 BC subtype and the context of HER-2 targeting (ATCC, 2022). It is considered highly proliferative and responsive to trastuzumab and chemotherapy (Holliday and Speirs, 2011).

Most studies reported difficulties obtaining a compact 3D culture of the SKBR3 cell line. Only in very specific conditions does SKBR3 form a compact spheroid. Froehlich et al. (2016) have tested 42 different conditions, and only in one best condition (Cell star cell-repellent surface with 3.5% of Matrigel) was it possible to obtain compact spheroids; the others generated loose aggregates, multiple small spheroids, or cell suspensions. Ivascu and Kubbies (2007) only obtained compact spheroid when 2.5% rBM was added to the medium, describing that the formation of the 3D aggregates is not involved with E-cad,

but is mediated by the collagen I/integrin  $\beta 1$  interaction, which is considered related to a more aggressive phenotype. One study reported that SKBR3 formed compact spheroids in ULA plates (Balalaeva et al., 2017). Contrarily, other study concluded that it does not form spheroids (Ahn et al., 2020). Interestingly, there were increased HER-2 levels when SKBR3 cells were grown in 3D (Azimi et al., 2020). Table S11 resumes the main scaffold-free techniques used for generating 3D cell cultures of SKBR3.

#### **6.4.3. MDA-MB-231**

The MDA-MB-231 was established in the 1970s at M. D. Anderson Cancer Center. It is one of the most used BC cell lines in cancer research, especially when representing the TNBC cells in *in vitro* studies due to its plasticity, invasive phenotype, and high metastatic potential. Some authors consider it a basal-like subtype (Chavez et al., 2010). It possesses a spindle-shaped cell morphology and mesenchymal phenotype with cells expressing vimentin and over 90% of cells expressing CD44+/CD24 low (Hero et al., 2019). According to genetic profiling, it was classified into the Basal B subtype (Kao et al., 2009). However, it has also been mentioned as the claudin-low subtype (Rädler et al., 2021).

Concerning MDA-MB-231 3D cell cultures, the obtained results show a great disparity. Some authors reported the formation of loose aggregates without medium additives, like Ivascu and Kubbies (2007), describing that the formation of MDA-MB-231 spheroids was related to the collagen I/integrin  $\beta 1$  interaction. The formation of loose spheroids without medium additives was also reported by other authors (Piggott et al., 2011, Nagelkerke et al., 2013), while others were unable to form MDA-MB-231 spheroids (Iglesias et al., 2013, Imamura et al., 2015). In practical terms, compact MDA-MB-231 spheroids were only obtained when medium additives, mostly different basal membrane commercial reagents, were incorporated into the culture (Ivascu and Kubbies, 2006, Nagelkerke et al., 2013). Table S12 resumes the main scaffold-free techniques used for generating 3D cell cultures of MDA-MB-231.

#### **6.4.4. MCF12A**

MCF12A cell line is a non-tumorigenic epithelial cell line from tissue taken at reduction mammoplasty from a nulliparous patient with fibrocystic breast disease with focal areas of intraductal hyperplasia, according to the product data sheet of ATCC (MCF-12A, ATCC CRL-10782™). Like MCF7, this cell line is also deposited by Michigan Cancer Foundation (Sweeney et al., 2018) and is described as forming round polarized acini-like

structures similar to those seen in normal human breast tissue (Holliday and Speirs, 2011).

Just a few studies performed 3D cultures of this cell line. The literature we identified uses Matrigel (Marchese and Silva, 2012, Weber-Ouellette et al., 2018, Engel et al., 2019). All the cited studies referred to the formation of well-differentiated acinus-like structures in the 3D cell culture of this cell line after 14-20 days in culture.

#### **6.4.5. Cell Lines Characterization**

Diverse groups that employed these cell lines in scientific studies performed some cell line characterization for different purposes and used various techniques such as polymerase chain reaction (PCR), Western blot (WB), and immunocytochemistry (ICC), reaching some conflicting results that are highlighted in gray in Table 3. Most studies refer to monolayer cell culture, whenever information was available in 3D cell cultures, it was discriminated in the table.

**Table 3** - Characterization of the cell lines used in this study highlighting in gray the information that is not in agreement with the literature.

Marker	MCF7	SKBR3	MDA-MB-231	MCF12A
<b>CK</b>	<p><b>+</b></p> <p>(Sommers et al., 1989, Holliday and Speirs, 2011, Bock et al., 2012)</p> <p><b>CK19 +</b></p> <p>(Alix-Panabières et al., 2009, Keyvani et al., 2016)</p> <p><b>CK 8/18 +</b></p> <p>(Taylor et al., 2010)</p>	<p><b>+</b></p> <p>(Sommers et al., 1989, Bock et al., 2012)</p> <p><b>CK19 +</b></p> <p>(Keyvani et al., 2016, Uawisetwathana et al., 2016)</p> <p><b>Weak CK19</b></p> <p>(Zhang et al., 2010)</p>	<p><b>-</b></p> <p>(Sommers et al., 1989, Keyvani et al., 2016)</p> <p><b>+</b></p> <p>(Keyvani et al., 2016)</p> <p><b>CK19 +</b></p> <p>(Taylor et al., 2010)</p>	<p><b>+</b></p> <p>(Sweeney et al., 2018)</p>
<b>Vim</b>	<p><b>-</b></p> <p>(Sommers et al., 1989, Taylor et al., 2010, Comsa et al., 2015)</p> <p><b>Low expression</b></p> <p>(Tanaka et al., 2016)</p>	<p><b>-</b></p> <p>(Sommers et al., 1989, Serrano et al., 2014)</p> <p><b>Low expression</b></p> <p>(Tanaka et al., 2016)</p>	<p><b>+</b></p> <p>(Sommers et al., 1989, Taylor et al., 2010)</p>	<p><b>+</b></p> <p>(Gelfand et al., 2016, Sweeney et al., 2018)</p>
<b>E-cad</b>	<p><b>+</b></p> <p>(Lombaerts et al., 2006, Kenny et al., 2007, Vamvakidou et al., 2007, D'Anselmi et al., 2013)</p> <p><b>in 3D:</b></p> <p><b>+</b></p> <p>(Dittmer et al., 2009, Iglesias et al., 2013, Amaral et al., 2017)</p>	<p><b>-</b></p> <p>(Kenny et al., 2007, Iglesias et al., 2013, Tanaka et al., 2016)</p> <p><b>in 3D:</b></p> <p><b>-</b></p> <p>(Iglesias et al., 2013)</p>	<p><b>-</b></p> <p>(Lombaerts et al., 2006, Kenny et al., 2007, Vamvakidou et al., 2007)</p> <p><b>Weakly express</b></p> <p>(D'Anselmi et al., 2013)</p>	<p><b>-</b></p> <p>(Lombaerts et al., 2006)</p> <p><b>+</b></p> <p>(Kenny et al., 2007, Sweeney et al., 2018, Weber-Ouellette et al., 2018)</p>



Marker	MCF7	SKBR3	MDA-MB-231	MCF12A
<b>ER</b>	<p><b>+</b></p> <p>(Sommers et al., 1989, Neve et al., 2006, Bock et al., 2012)</p> <p><b>in 3D:</b></p> <p><b>+</b></p> <p>(Iglesias et al., 2013)</p>	<p><b>-</b></p> <p>(Sommers et al., 1989, Neve et al., 2006, Holliday and Speirs, 2011)</p> <p><b>in 3D:</b></p> <p><b>-</b></p> <p>(Iglesias et al., 2013)</p>	<p><b>-</b></p> <p>(Sommers et al., 1989, Neve et al., 2006, Kenny et al., 2007, Bock et al., 2012)</p> <p><b>in 3D:</b></p> <p><b>-</b></p> <p>(Iglesias et al., 2013)</p>	<p><b>-</b></p> <p>(Zeillinger et al., 1996, Neve et al., 2006, Kenny et al., 2007, Subik et al., 2010, Sweeney et al., 2018)</p> <p><b>+</b></p> <p>(Dai et al., 2008, Marchese and Silva, 2012, Schröder et al., 2017, Engel et al., 2019)</p>
<b>PR</b>	<p><b>+</b></p> <p>(Neve et al., 2006, Dai et al., 2008, Holliday and Speirs, 2011)</p> <p><b>in 3D:</b></p> <p><b>+</b></p> <p>(Iglesias et al., 2013)</p>	<p><b>-</b></p> <p>(Neve et al., 2006, Holliday and Speirs, 2011)</p> <p><b>in 3D</b></p> <p><b>-</b></p> <p>(Iglesias et al., 2013)</p>	<p><b>-</b></p> <p>(Neve et al., 2006, Kenny et al., 2007, Dai et al., 2008, Holliday and Speirs, 2011)</p> <p><b>in 3D:</b></p> <p><b>-</b></p> <p>(Iglesias et al., 2013)</p>	<p><b>-</b></p> <p>(Neve et al., 2006, Kenny et al., 2007, Subik et al., 2010)</p> <p><b>+</b></p> <p>(Dai et al., 2008)</p>
<b>HER-2</b>	<p><b>-</b></p> <p>(Neve et al., 2006, Bock et al., 2012, Gelfand et al., 2016)</p> <p><b>in 3D:</b></p> <p><b>-</b></p> <p>(Iglesias et al., 2013)</p> <p><b>+</b></p> <p>(Comsa et al., 2015)</p>	<p><b>+</b></p> <p>(Neve et al., 2006, Kenny et al., 2007, Holliday and Speirs, 2011, Bock et al., 2012)</p> <p><b>in 3D:</b></p> <p><b>+</b></p> <p>(Iglesias et al., 2013)</p>	<p><b>-</b></p> <p>(Neve et al., 2006, Kenny et al., 2007, Holliday and Speirs, 2011, Bock et al., 2012)</p> <p><b>in 3D:</b></p> <p><b>-</b></p> <p>(Iglesias et al., 2013)</p>	<p><b>-</b></p> <p>(Neve et al., 2006, Kenny et al., 2007)</p>

**+** stands for positive presence according to the different techniques used (ICC, WB, and PCR)

**-** stands for the absence of according to the different used techniques (ICC, WB, and PCR)

## 6.5. Outputs in 3D Cell Culture

Besides all the efforts in constructing 3D cell culture models, there is a vast number of studies concerning drug testing that relies only on 2D cell cultures (Cox et al., 2015, Langhans, 2018), probably due to the already referred advantages related to low costs, easy performance and reproducible results (Jensen and Teng, 2020).

There has been a great effort to improve 3D culture to obtain more appropriate preclinical models for testing new anticancer drugs and drug leads and, consequently, meliorate the success rate of drug candidates in the screening pipeline. In this vein, a complete characterization of these 3D cultures is of extreme importance, using different readout techniques for model validation in preclinical assays (Zanoni et al., 2019).

Many different readouts are used to interfere with the state of health of the cells after exposure to a drug or tested compound. The main studied readouts are colorimetric, fluorometric, and luminescent techniques for studying the effects of a compound, generally by evaluating the activity of specific enzymes. Examples of this type of assay are the 3-(4,5-dimethylthiazol-2-yl)-2,5-diphenyltetrazolium bromide (MTT) (Ho et al., 2012, Guzmán et al., 2021), Alamar Blue (Walzl et al., 2014, Eilenberger et al., 2018), lactate dehydrogenase (LDH) (Perche and Torchilin, 2012, El Hassouni et al., 2020) and CellTiterGlo® (Zanoni et al., 2016, Murali et al., 2019).

Another technique used for evaluating multiparametric outputs, for instance, cell death and the effects on cell cycle, is flow cytometry, however in this technique, a cell suspension is required; thus it is necessary to disaggregate the 3D cell cultures using enzyme (e.g. trypsin or Accutase®) and mechanical dissociation (Patra et al., 2016). The 5'-Bromo-2'-deoxyuridine (BrdU) assay is also frequently used to evaluate cell proliferation (Ivascu and Kubbies, 2006, Khaitan et al., 2006). Techniques that assess the protein and gene expressions, such as Western Blot (Xu et al., 2016, Kopp et al., 2018a) and quantitative real-time polymerase chain reaction (qRT-PCR) (Kopp et al., 2018b, Li et al., 2021), respectively are commonly used. Other alternatives, like immunocytochemistry using fluorochromes or enzyme-substrate visualization, allow the evaluation of the expression of specific antigens, such as proteins and localizing them into the 3D structure (Costa et al., 2016, Bresciani et al., 2019).

Additionally, the 3D cell culture morphology evaluation can give some useful information about their response to different exposure conditions. The morphology can be assessed

by a phase-contrast microscope or other optical microscopes, usually equipped with digital cameras that allow image capture for further software-assisted image analysis.

Similarly, alterations in the inner structure of the 3D models can be investigated by optical and electron microscopes after adequate cell processing (Costa et al., 2016) . Moreover, there are other techniques to investigate the invasive and metastatic potential of cancer cells in a 3D context (Vinci et al., 2015, Hira et al., 2020).

Besides the great number of assays that can be performed to discover new drugs or drug leads and their mechanisms of action, their application in 3D cultures still requires optimization and validation.

## **7. Thesis Aims and Objectives**

### **7.1. Aims**

This thesis aimed to obtain new information in the research fields of bioactivity of natural compounds derived from selected seaweed and marine fungi compounds and their drug interactions, and contribute to new fundamental insights that, in the long run, may help to support better BC treatment in the future.

### **7.2. Objectives**

1. Generate and characterize 3D cell cultures using one non-tumoral breast cell line and three human breast cancer (BC) cell lines representing the three main BC subtypes.
2. Analyse in the four breast cell lines the cytotoxic and antiproliferative effects of preussin, a bioactive compound isolated from a marine-sourced fungus.
3. Likewise, in all breast cell lines, examine the cytotoxic and antiproliferative effects of bioactive compounds found in brown seaweeds — astaxanthin, fucoidan, fucosterol, fucoxanthin, laminarin, and phloroglucinol.
4. Investigate the modeling effects of the tested seaweed compounds on the cytotoxicity of anticancer drugs (cisplatin and doxorubicin) in the same cell lines.
5. Compare the data obtained in monolayers with those acquired in 3D cultures to determine the degree of consistency of effects between the two procedures and improve the screening to identify the most promising compounds.
6. In some of the most impactful situations, start uncovering the processes underlying the modeling effects of the tested bioactive compounds.



# Supplementary Tables



**Table S1** - Marketed marine-derived drugs approved by the EMA and/or the FDA for cancer treatment.

<b>Drug (Generic name)</b>	<b>Commercial name</b>	<b>Species of origin</b>	<b>Chemical Class</b>	<b>Approved for</b>	<b>Approved by FDA or EMA</b>	<b>References</b>
Cytarabine	Cytosar-U® Ara-C	Marine sponge <i>Tethya crypta</i>	Antimetabolite DNA polymerase inhibitor	Lymphocytic and acute myeloid leukemias non- Hodgkins lymphoma, and myelodysplastic syndrome	1969 (FDA)	(Mayer et al., 2010, Ercolano et al., 2019)
Fludarabine	Fludara®	Marine sponge	Antimetabolite	Chronic lymphocytic leukemia	1994 (EMA) 2004 (FDA)	(Ricci et al., 2009)
Nelarabine	Arranon® (US) Atriance® (EU)	Marine sponge	Antimetabolite	Relapsed or refractory T-cell acute lymphoblastic leukemia and T-cell lymphoblastic lymphoma	2005 (FDA) 2007 (EMA)	(Cooper, 2007)
Trabectedin	Yondelis®	Tunicate <i>Ecteinascidia turbinata</i>	Alkylating agents	Advanced ovarian cancer and tumor soft tissue sarcoma	2007 (EMA) 2015 (FDA)	(Gordon et al., 2016)



Table S1 (Cont.).

Drug (Generic name)	Commercial name	Species of origin	Chemical Class	Approved for	Approved by FDA or EMA	References
Eribulin mesylate	Halaven®	Sponge <i>Halichondria okadai</i> and <i>Lyssodendoryx</i> <i>sp</i>	Macrolide inhibitor of microtubule function	Metastatic BC	2010 (FDA) 2011 (EMA)	(Dybdal- Hargreaves et al., 2015, Swami et al., 2015)
Brentuximab vedotin	Adcetris®	Mollusk/ Cyanobacterium <i>Dolabella</i> <i>auricularia/</i> Genus <i>Symploca</i>	ADC  Mitotic arrest and apoptosis	Advanced Hodgkin lymphoma	2011 (FDA) 2012 (EMA)	(Scott, 2017)
Lurbinectedin	Zepzelca®	Tunicate Mollusk/ <i>Ecteinascidia</i> <i>turbinata</i>	Alkylating agents	Ovarian cancer Small cell lung cancer	2020 (FDA) 2019 (FDA)	(Gaillard et al., 2021) (Kepp et al., 2020)
Polatuzumab vedotin	Polivy®	Mollusk/ cyanobacterium	ADC	Relapsed/refractor diffuse large B-cell lymphoma patients who have received at least two prior therapies	2019 (FDA) 2020 (EMA)	(Deeks, 2019)

Table S1 (Cont.)

Drug (Generic name)	Commercial name	Species of origin	Chemical Class	Approved for	Approved by FDA or EMA	References
Enfortumab vedotin	Padcev®	Mollusk/ cyanobacterium	ADC	Metastatic urothelial cancer	2019 (FDA) 2021 (EMA)	(Powles et al., 2021)
Belantamab mafodotin	Blenrep®	Mollusk/ cyanobacterium	ADC	Relapsed or refractory multiple myeloma	2020 (FDA) 2020 (EMA)	(Lassiter et al., 2021)
Plitidepsin		Tunicate <i>Aplidium</i> <i>albicans</i>	Depsipeptides Induces apoptosis and cell cycle arrest	Multiple myeloma	Approved only in Australia	Muñoz-Alonso et al., 2009, Leisch et al., 2019)

Adapted from (Nigam et al., 2019, Cappello and Nieri, 2021)

**Table S2** - Marine-derived drugs under phases II and III of clinical trials for cancer treatment.

<b>Drug</b>	<b>Species of origin</b>	<b>Clinical Trial Phase</b>	<b>Chemical Class</b>	<b>Type of cancer</b>	<b>References</b>
Plinabulin	Fungus <i>Aspergillus</i> sp.	III	Diketopiperazine Interacts with microtubule dynamic	Non-small lung cancer carcinoma	(Hardin et al., 2017)
Gemcitabine	Sponge	III	Nucleoside	Advanced Urothelial Carcinoma	(Rosenberg et al., 2021)
Marizomib (salinosporamide A)	Fungus Actinomycetes	III	$\gamma$ -lactam- $\beta$ -lactone	Glioma, ependymoma, other solid cancers	(Bota et al., 2021)
Glembatumumab vedotin	Mollusk/ cyanobacterium	IIb	ADC	TNBC	(Vahdat et al., 2021)
		II		Advanced melanoma	(Ott et al., 2019)
		II		Metastatic Uveal Melanoma	(Hasanov et al., 2020)
Elisidepsin	Mollusk	II	Depsipetide	Metastatic or advanced gastroesophageal cancer	(Petty et al., 2016)
Plocabulin (PM060184)	Sponge	II	Polyketide	Advanced colorectal cancer	(Cappello and Nieri, 2021)

**Table S2 (Cont.).**

<b>Drug</b>	<b>Species of origin</b>	<b>Clinical Trial Phase</b>	<b>Chemical Class</b>	<b>Type of cancer</b>	<b>References</b>
Tisotumab vedotin	Mollusk/cyanobacterium	II	ADC	Recurrent or metastatic cervical cancer	(Coleman et al., 2021)
Ladiratumumab vedotin (SGN-LIV1A)	Mollusk/cyanobacterium	II	ADC	Prostate cancer	(Sher et al., 2021)
Telisotuzumab vedotin	Mollusk/cyanobacterium	II	ADC	Recurrent squamous cell lung cancer and patients with c-MET-positive	(Waqar et al., 2021)
CAB-ROR2 (BA-3021)	Mollusk/cyanobacterium	II	ADC	Non-small cell lung cancer TNBC Melanoma Head and Neck Cancer	(Cappello and Nieri, 2021)

**Table S3** - Sources, main effects, and mechanisms of preussin in *in vitro* studies.

Cell type	Preussin source	Main effects	Mechanisms of action	Tested concentrations	References
Normal rat fibroblast 3Y1	<i>Aspergillus</i> sp., strain 693 (Extract)	Inhibition of cell growth Induction of apoptosis	Inhibits G1 phase cell progression Nuclei fragmentation	1 -100 µg/mL	(Kasahara et al., 1997)
HeLa A549 PC-3 MeWO Du-145 LNCap MCF7*	Sintetic	Inhibition of cell growth  Induction of apoptosis	↓ cyclin E kinase, block of cell cycle progression in the G1 phase ↑ caspases 3 and 8	5 - 20 µM	(Achenbach et al., 2000)
Hep G2 HT29 HCT116 A549 A375 U251 T98G MCF7 *	<i>Aspergillus candidus</i> (Extract)	Cytotoxic effects	Not studied	100 µM	(Buttachon et al., 2018)

\*The only breast cell line

**Table S4** - Sources, main effects, and mechanisms of Asta on breast cell lines.

<b>Cell Type</b>	<b>Asta Source</b>	<b>Main effects</b>	<b>Mechanisms of action</b>	<b>Tested Concentrations</b>	<b>References</b>
MCF7	Commercial	Induction of apoptosis and inhibition of cell proliferation	↓ Cyclin D1 ↓ Bcl-2 ↑ p53 ↑ Bax Cell cycle arrest at G0/G1	10 - 50 µM (IC <sub>50</sub> 20 µM)	(Sowmya et al., 2017)
MCF7 MDA-MB-231 MCF10A	Commercial	Induction of apoptosis Inhibition of cell proliferation Synergistic with Dox No effects on the non-tumoral cell line	Not studied for Asta, for other carotenoids: ↑ caspases 3, 8 and 9; ↓ Cyclin D1; Cell cycle arrest at G0/ G1	2 -10 µM	(Vijay et al., 2018)
MCF7 MDA-MB-231 MCF10A	Commercial	Antiproliferative and inhibition of cell migration No effects on the non-tumoral cell line	Modulation of Bax and Bcl-2	10 - 50 µM	(McCall et al., 2018)
MCF7	<i>Blakeslea trispora</i> (Extract)	Inhibition of cell proliferation; Enhanced carbendazim antiproliferative effect	Cell cycle arrest at G2/M ↓ ROS levels caused by carbendazim	5 - 30 µg/mL	(Atalay et al., 2019)

Table S4 (Cont.)

Cell Type	Asta Source	Main effects	Mechanisms of action	Tested Concentrations	References
SKBR3 T47D BT20	Not mentioned	Cytotoxic effects Repression of stemness markers	↓ Pontin ↓ mutp53, ↓ Oct4 ↓ Nanog	20 -100 µM	(Ahn et al., 2020)
SKBR3	Commercial	Induction of apoptosis	↓ mutp53 ↓ PARP-1 ↓ Bcl-2 ↓ intracellular ROS ↓ SOD and Pontin; ↑ Bax ↑ caspases 3, 9 ↑ phosphorylation of ERK1/2, JNK, and p38 ↑ MAPKs	20 - 80 µM	(Kim et al., 2020)
MCF7	Commercial	Enhanced Dox cytotoxic effects	↑ Caspase 8 ↑ Bax/Bcl-2 ratio ↑ Epigenetic histones acetylation ↓ EGFR	20 - 80 µM	(Fouad et al., 2021)
T47D MDA-MB-231 MCF10A	Commercial	Induction of apoptosis and DNA damage with less damage to the normal cell line	Modulation of Bcl-2	100 µM	(Karimian et al., 2022)

**Table S5** - Sources, main effects, and mechanisms of Fx and Fucoxanthinol (Fxol) on breast cell lines.

<b>Cell Type</b>	<b>Fx and Fxol Source</b>	<b>Main Effects</b>	<b>Mechanisms of action</b>	<b>Tested concentrations</b>	<b>References</b>
MCF7	<i>Fx, U. pinnatifida</i> (Extract)	Induction of apoptosis	Not studied	12.5 - 50 $\mu$ M	(Konishi et al., 2006)
MCF7	Fx <i>Sargassum</i> sp. (Extract)	Induction of cytotoxicity	Not studied	11.5 $\mu$ g/mL (IC 50)	(Ayyad et al., 2011)
MCF7 MDA-MB-231 MCF12A	Fx (Commercial)	Induction of cytotoxicity lesser extent in MCF12A	Not studied	5 -15 $\mu$ M	(de la Mare et al., 2013)
MCF7 MDA-MB-231	Fx and Fxol (Commercial)	Induction of apoptosis	↓ NF-kB pathway ↑ Cleavage of pro- caspase-3 and PARP ↓ Nuclear Sox 9 in MDA-MB-231	20 - 40 $\mu$ M	(Rwigemera et al., 2014)
MCF7 MDA-MB-231	Fx (Commercial)	Induction of cytotoxicity ↑ Dox effects	↑ Lipid peroxides ↑ ROS levels	2 - 10 $\mu$ M	(Vijay et al., 2018)
MCF7 MDA-MB-231	Fx (Commercial)	Decreased cell viability Inhibited cell migration	Not studied	1 - 30 $\mu$ M	(Garg et al., 2019)



**Table S5 (Cont.)**

MDA-MB-231	<i>Fx</i> , <i>U. pinnatifida</i> (Extract)	Decreased cell viability, migration, invasion and lymphagenesis	↓ VEGF-C, MMP-2, MMP-9, NF-κB, p-Akt and p-PI3K	25 - 100 μM	(Wang et al., 2019)
------------	---	---	---	-------------	---------------------

**Table S6** - Sources, main effects, and mechanisms of Lm on breast cell lines.

<b>Cell Type</b>	<b>Lm Source</b>	<b>Main effects</b>	<b>Mechanisms of action</b>	<b>Tested concentrations</b>	<b>References</b>
MDA-MB-231	<i>Saccharina japonica</i> <i>Fucus evanescens</i> (Extract)	Inhibition of cell proliferation, colony-forming, and migration	↓ MMP2 and 9	200 µg/mL	(Malyarenko et al., 2016)
MDA-MB-231 T-47D	<i>Saccharina cichorioides</i> (Extract) * <i>Aminated laminarin</i>	Apoptosis induction	↑ caspases 9 and 3 ↓ PARP enzyme	100 - 800 µg/mL	(Malyarenko et al., 2020)

**Table S7** - Sources, main effects, and mechanisms of Fc on breast cell lines.

Cell Type	Fc Source	Main Effects	Mechanisms of action	Tested concentrations	References
MDA-MB-231	<i>Ascophyllum nodosum</i> (Extract)	Inhibition of cell adhesion and invasiveness	No specific mechanism was explored	1 - 1,000 µg/mL	(Haroun-Bouhedja et al., 2002)
MDA-MB-231	<i>Laminaria saccharina</i> , <i>Laminaria digitata</i> , <i>Fucus serratus</i> , <i>Fucus distichus</i> , and <i>Fucus vesiculosus</i> (Extracts)	Antimetastatic	Blocking of cell adhesion to platelets	100 µg/mL	(Cumashi et al., 2007)
MCF7 HMECs (Human mammary epithelial cells)	<i>Cladosiphon okamuranus</i> (Commercial)	Antiproliferative and cytotoxic without any effect on the viability of normal HMECs	↑ Caspase 7, 8 and 9 ↑ DNA fragmentation	1 - 1,000 µg/mL	(Yamasaki-Miyamoto et al., 2009)
MCF7	<i>Cladosiphon novae-caledoniae</i> (Extract)	Antiproliferative and cytotoxic	↑Caspase-independent apoptotic pathway ↑ROS-mediated MAP kinases Regulation of the Bcl-2	82 - 820 µg/mL	(Zhang et al., 2011)
T47D	<i>Saccharina japonica</i> and <i>Undaria pinnatifida</i> (Extracts)	Antiproliferative; Colony formation inhibition	No specific mechanism was explored	100 - 800 µg/mL	(Vishchuk et al., 2011)

Table S7 (Cont.)

Cell Type	Fc Source	Main Effects	Mechanisms of action	Tested concentrations	References
MCF7	<i>Fucus vesiculosus</i> (Commercial)	Antiproliferative and cytotoxic	↓ Cyclin D1, CDK-4 ↑ ROS ↑ Cytochrome C ↑ Caspase-8 ↑ Bax ↓ Bcl-2	200 - 1,000 µg/mL	(Banafa et al., 2013)
MDA-MB-231	<i>Fucus vesiculosus</i> (Commercial)	Antimetastatic	↑ Epithelial markers ↓ Mesenchymal marker	60 - 120 µg/mL	(Hsu et al., 2013)
MDA-MB-231	<i>Cladosiphon navae-caledoniae</i> (Extract)	Cytotoxic, antimetastatic, and anti-angiogenic	↑ Caspases ↓ Bcl-2	1,640 µg/mL	(Zhang et al., 2013a)
MCF7 MDA-MB-231	<i>Cladosiphon navae-caledoniae</i> (Extract)	Enhanced the cytotoxic effects of cisplatin, tamoxifen, or paclitaxel	↓ Bcl-xL and Mcl-1 ↓ ERK and Akt in MDA-MB-231 ↑ ERK in MCF7 ↑ intracellular ROS levels and reduced glutathione	200 - 400 µg/mL	(Zhang et al., 2013b)
MDA-MB-231	<i>Fucus vesiculosus</i> (Commercial)	Induction of apoptosis and antiproliferative effects	↓ Glucose regulated protein 78 ↑ ER stress cascades ↑ p-CAMKII/Bax and caspase 12	10-100 µg/mL	(Chen et al., 2014)

Table S7 (Cont.)

Cell Type	Fc Source	Main Effects	Mechanisms of action	Tested concentrations	References
MDA-MB-231 MCF7	<i>Fucus vesiculosus</i> (Extract)	Cytotoxic anti-estrogenic	↓ Aromatase activity ↓ Phosphorylation of Ak ↑ Caspases -3,7	Expressed as % of the stock solution	(Zhang et al., 2016)
MCF7 MCF12A	<i>Fucus vesiculosus</i> (Commercial)	Cytotoxic and antiproliferative in MCF7	↑ Caspases -3, 7 and 9	400 - 1,200 µg/mL	(Abudabbus et al., 2017)
MCF7 MDA-MB-231	<i>Undaria pinnatifida</i> (Extract)	Antiproliferative and cytotoxic effects	Apoptosis is triggered via both intrinsic and extrinsic pathways	5 - 300 µg/mL	(Lu et al., 2018)
MCF7	<i>Fucus vesiculosus</i> (Conditioned serum from Fc-treated rats) (Commercial)	Induction of apoptosis and antimetastatic	↑ E-cadherin ↓ MMP-9	1,000 – 2,500 pg/mL	(He et al., 2019)
MDA-MB-231	<i>Fucus vesiculosus</i> (Commercial)	Antimetastatic	↓ N-Cadherin ↓ Vim ↓ Nuclear translocation of HIF-1α ↓ TWIST-1, SNAIL, CAIX and GLUT-1 ↑ ZO-1, ↑ E-Cadherin	6.25 - 25 mg/mL	(Li et al., 2019)
MDA-MB-231	<i>Laminaria japonica</i> (Commercial)	Antiproliferative Inhibition of migration and invasion	↓ MAPK and PI3K ↓ AP-1 and NF-κB signaling	1,250 - 2,000 µg/mL	(Hsu et al., 2020)

Table S7 (Cont.)

<b>Cell Type</b>	<b>Fc Source</b>	<b>Main Effects</b>	<b>Mechanisms of action</b>	<b>Tested concentrations</b>	<b>References</b>
MCF7 MDA-MB-231	(Commercial)	Induction of autophagy Inhibition of tumor enhanced sensitivity to Dox and Cis	↓ mTOR/ p70S6K/TFEB pathway	50 -1,600 µg/mL	(Zhang et al., 2021)

**Table S8** - Sources, main effects, and mechanisms of Fct on breast cell lines.

<b>Cell Type</b>	<b>Fct Source</b>	<b>Main effects</b>	<b>Mechanisms of action</b>	<b>Tested concentrations</b>	<b>References</b>
MCF7	Fx from <i>Sargassum sp.</i> (Extract)	Cytotoxic	Not studied	79.2 µg/mL (IC <sub>50</sub> )	(Ayyad et al., 2011)
T47D	<i>Sargassum angustifolium</i> (Extract)	Cytotoxic (IC <sub>50</sub> 86-166 mg/mL depending on the fraction)	No specific mechanism was explored	Not mentioned	(Khanavi et al., 2012)
MCF7	<i>Dictyota ciliolata</i> , <i>Padina sanctae-crucis</i> and <i>Turbinaria tricostrata</i> (Extract, hexane fractions)	Cytotoxicity (IC <sub>50</sub> 43.3 mg/mL)	No specific mechanism was explored	Not mentioned	(Caamal-Fuentes et al., 2014)
MCF7	Commercial	Cytotoxicity (IC <sub>50</sub> 125 µM)	Not studied	160 µM	(Jiang et al., 2018)
MCF7 MDA-MB-231	<i>Adenocystis utricularis</i> (Extract)	Inhibition of cell growth	Not studied	200 µg/mL	(Pacheco et al., 2018)

**Table S9** - Sources, main effects, and mechanisms of Phg and Phg-derived compounds on breast cell lines.

<b>Cell Type</b>	<b>Phg Source</b>	<b>Main effects</b>	<b>Mechanisms of action</b>	<b>Tested concentrations</b>	<b>References</b>
MCF7 MDA-MB-231	Phg derived Dioxinodehydroeckol from <i>Ecklonia cava</i>	Inhibition of cell proliferation Induction of apoptosis	↓NF-kB ↑caspase-3 and 9 ↑DNA fragmentation ↓ BCL-2 ↑ Bax	1 - 100 µM	(Kong et al., 2009)
MDA-MB-231	Starch encapsulated (Commercial)	Induction of apoptosis	↑ Nuclei condensation loss of mitochondrial membrane potential ↑ caspase 3, 8 and 9	50 - 250 µg/mL	(Kumar et al., 2014)
BT549 MDA-MB-231	(Commercial)	Suppression of metastatic ability	↓ SLUG ↓ SNAIL-related zinc- finger transcription factors ↓ PI3K/Akt and Ras/Raf-1/ERK Without cytotoxic effects on cells	100 µM	(Kim et al., 2015a)



Table S9 (Cont.)

Cell Type	Phg Source	Main effects	Mechanisms of action	Tested concentrations	References
MCF7 SKBR3 BT549	(Commercial)	Suppression of sphere formation, anchorage-independent colony formation	↓ CD44+ cancer cell population ↓ CSC regulators such as Sox2, CD44, Oct4, Notch2, and β-catenin ↓ PI3K/Akt and Ras/Raf-1/ERK Sensitized BC cells to cisplatin, taxol, etoposide, and radiation	100 μM	(Kim et al., 2015b)
MCF7	Phg engineered silver (Ag) nanoparticles	Cytotoxic effects	Not studied	50 - 250 μg/mL	(Kumar et al., 2018)
MCF7 MDA-MB-231	Dieckol or phlorofuocufuroeckol from <i>Ecklonia cava</i> (Phg-derived compounds) (Extracts)	Inhibition of invasiveness and migration	↓NF-kB ↓MMP2 and MMP9	50 μM	(Young-Ju, 2020)

**Table S10** - Examples of different scaffold-free techniques used for 3D cell culture of MCF7 cell line.

<b>Techniques used for 3D cell culture</b>	<b>Cells/ spheroid or cell density Culture medium Spheroidization time or time in culture</b>	<b>Formation of the spheroid</b>	<b>References</b>
<ul style="list-style-type: none"> <li>- Round bottom 96-well plated coated with 0.5% of poly-Hema</li> <li>- Culture medium + 2.5% rBM</li> <li>- Centrifugation of the plates at 1000 g for 10 min in a swinging bucket centrifuge</li> <li>- 200 µL/well</li> </ul>	<ul style="list-style-type: none"> <li>- 5,000 cells/spheroid</li> <li>- RPMI 1640 with 10% FCS and 2 mM L-glutamine</li> <li>- Spheroidization time: 24 h</li> </ul>	<ul style="list-style-type: none"> <li>- Formed compact spheroids generated without rBM</li> </ul>	(Ivascu and Kubbies, 2006)
<ul style="list-style-type: none"> <li>- Hydrofobic Petri dishes</li> <li>- 5 mL/petri dish</li> </ul>	<ul style="list-style-type: none"> <li>- 400,000 cells/plate</li> <li>- DMEM with 10% FBS</li> <li>- Days in culture 7-50 days</li> </ul>	<ul style="list-style-type: none"> <li>- Formed compact spheroids</li> </ul>	(do Amaral et al., 2011)
<ul style="list-style-type: none"> <li>- ULA plates</li> <li>- 100 µL/well</li> </ul>	<ul style="list-style-type: none"> <li>- 4,000 cells/spheroid</li> <li>- Serum-free epithelial growth medium supplemented with B27 20 ng/mL EGF Insulin, b-mercaptoethanol, and hydrocortisone</li> <li>- Spheroidization time: 7 days</li> </ul>	<ul style="list-style-type: none"> <li>- Formed compact large spheroids</li> </ul>	(Piggott et al., 2011)
<ul style="list-style-type: none"> <li>- 96-well plate was pre-coated with 1% agar</li> <li>- 200 µL/ well</li> <li>- Centrifugation of the plates at 1000 g 5 min</li> </ul>	<ul style="list-style-type: none"> <li>- 50,000 cells/spheroid</li> <li>- DMEM with 10% of heat-inactivated FBS</li> <li>- Spheroidization time: 3 days</li> </ul>	<ul style="list-style-type: none"> <li>- Formed compact spheroids</li> </ul>	(Ho et al., 2012)

Table S10 (Cont.)

Techniques used for 3D cell culture	Cells/ spheroid or cell density Culture medium Spheroidization time or time in culture	Formation of the spheroid	References
- V-shaped 96-wells plates coated with 0.5% poly-Hema - Culture medium + 2.5% Matrigel - Centrifugation, 1000 g, 10 min	- 10,000 cells/spheroid - Culture medium not referred - Spheroidization time: 3 days	- Formed compact spheroids	(Nagelkerke et al., 2013)
- 96 well, flat-bottom ultra-low adhesion plates coated with 50 µL of BME at 4°C - Culture medium + 2% ECM - Centrifugation 300 g, 4°C, 10 min	- 2,000 cells/spheroid - RPMI with 10% FBS	- Formed compact spheroids	(Benton et al., 2015)
- 3D plates NanoCluture 96-well Plate® - 100 µL/well	- 10,000 cells/spheroid - RPMI-164 with 10% FBS - Time in culture: 3 days	- Unsuccessful spheroid formation	(Imamura et al., 2015)
- Different types of 96-well plates, coated with 2% poly-Hema - Culture medium - 25% methocel, 25% methocel plus 1% Matrigel or 3.5% Matrigel - 100 µL/well	- 10,000 cells/ spheroid - DMEM high glucose with 10% FCS - Spheroidization time: 3 days	- Only formed compact spheroids in Cellstar® round bottom cell-repellent surface plates with 3.5% of Matrigel and CellStar® suspension plated with 25 % Methocel	(Froehlich et al., 2016)
- ULA U-bottom plates	- 500 cells/spheroid - RPMI 1640 with 10% FBS - Time in culture: 7 days	- Formed compact spheroids	(Raghavan et al., 2016)
- ULA plates U-bottom	- 5,000/spheroid	- Formed compact spheroids	(Selby et al., 2017)

## Chapter 1

---

- 190 $\mu$ L/well	- RPMI with 10% FBS - Spheroidization time: 2-3 days		
- 6-well flat ULA plates	- $1.05 \times (10^4; 10^3, \text{ or } 10^2)$ cells/cm <sup>2</sup> - DMEM high glucose with 10% FBS and 1% Pen/strep - Spheroidization time: 3 days	Formed a grape-like spheroid	(Gencoglu et al., 2018)

---

**Table S11** - Examples of different scaffold-free techniques used for 3D cell culture of SKBR3 cell line.

<b>Techniques used for 3D cell culture</b>	<b>Cells/ spheroid or cell density Culture medium Spheroidization time or time in culture</b>	<b>Formation of the spheroid</b>	<b>References</b>
<ul style="list-style-type: none"> <li>- Round bottom 96-well plated coated with 0.5% of poly-Hema</li> <li>- Culture medium + 2.5% rBM</li> <li>- Centrifugation of the plates at 1000 g for 10 min in a swinging bucket centrifuge</li> <li>- 200 µL/well</li> </ul>	<ul style="list-style-type: none"> <li>- 5,000 cells/spheroid</li> <li>- McCoy's 5A with 10% FCS and 2 mM L-glutamine</li> <li>- Spheroidization time: 24 h</li> </ul>	<ul style="list-style-type: none"> <li>- SKBR3 formed loose aggregates without medium additives.</li> <li>- Compacts spheroids were formed with 2.5% rBM</li> </ul>	(Ivascu and Kubbies, 2006)
<ul style="list-style-type: none"> <li>- ULA plates</li> <li>- 100 µL/well</li> </ul>	<ul style="list-style-type: none"> <li>- 20,000 cel/mL</li> <li>- Serum-free epithelial growth medium supplemented with B27 20 ng/mL EGF Insulin, b-mercaptoethanol, and hydrocortisone</li> <li>- Spheroidization time: 7 days</li> </ul>	<ul style="list-style-type: none"> <li>- Formed loose and irregular spheroids</li> </ul>	(Piggott et al., 2011)

Table S11 (Cont.)

Techniques used for 3D cell culture	Cells/ spheroid or cell density Culture medium Spheroidization time or time in culture	Formation of the spheroid	References
<ul style="list-style-type: none"> <li>- 6-well plates covered with poly-2-hydroxyethylmethacrylate</li> <li>- Culture medium + 0.5% Methylcellulose</li> <li>- mL per well not referred</li> </ul>	<ul style="list-style-type: none"> <li>- 1,000 cells/mL</li> <li>- Serum-free DMEM supplemented with 1% L-glutamine, 1% Pen/Strep, 30% F12, 2% B27, 20 ng/mL EGF and 20 ng/mL FGFb</li> <li>- Time in culture: 7 days</li> </ul>	<ul style="list-style-type: none"> <li>- Unsuccessful spheroid formation</li> </ul>	(Iglesias et al., 2013)
<ul style="list-style-type: none"> <li>- Different types of 96-well plates, coated with 2% poly-Hema</li> <li>- Culture medium + 25% methocel, 25% methocel plus 1% Matrigel, or 3.5% Matrigel</li> <li>- 100 µL/well</li> </ul>	<ul style="list-style-type: none"> <li>- 10,000 cells/spheroid</li> <li>- DMEM high glucose with 10% FCS</li> <li>- Spheroidization time: 3 days</li> </ul>	<ul style="list-style-type: none"> <li>- SKBR3 only formed compact spheroids in Cellstar® cell-repellent surface with 3.5% of Matrigel</li> </ul>	(Froehlich et al., 2016)
<ul style="list-style-type: none"> <li>- 96-well plates pre-coated with 1% agarose and 96-well ULA plates with flat or round bottom</li> <li>- Volume/ well not referred</li> </ul>	<ul style="list-style-type: none"> <li>- 200-2,000/ spheroid</li> <li>- McCoy's 5A with 10% FCS and 1.5 mM L-glutamine</li> <li>- Spheroidization time: 24 h</li> </ul>	<ul style="list-style-type: none"> <li>- SKBR3 formed compact spheroids only in ULA plates with round bottom</li> </ul>	(Balalaeva et al., 2017)
<ul style="list-style-type: none"> <li>- 6-well flat ULA plates</li> </ul>	<ul style="list-style-type: none"> <li>- <math>1.05 \times (10^4; 10^3, \text{ or } 10^2)</math> cells/cm<sup>2</sup></li> <li>- DMEM high glucose with 10% FBS and 1% Pen/strep</li> <li>- Spheroidization time: 3 days</li> </ul>	<ul style="list-style-type: none"> <li>- SKBR3 did not form spheroids</li> </ul>	(Gencoglu et al., 2018)

## References

- Abal, M., Andreu, J. M. and Barasoain, I. (2003). "Taxanes: microtubule and centrosome targets, and cell cycle dependent mechanisms of action." *Curr. Cancer Drug Targets* 3(3): 193-203. 10.2174/1568009033481967.
- Abbott, R. D. and Kaplan, D. L. (2015). "Strategies for improving the physiological relevance of human engineered tissues." *Trends Biotechnol.* 33(7): 401-407. 10.1016/j.tibtech.2015.04.003.
- Abd El-Hack, M. E., Abdelnour, S., Alagawany, M., Abdo, M., Sakr, M. A., Khafaga, A. F., Mahgoub, S. A., Elnesr, S. S., et al. (2019). "Microalgae in modern cancer therapy: Current knowledge." *Biomed. Pharmacother.* 111: 42-50. 10.1016/j.biopha.2018.12.069.
- Abe-Fukasawa, N., Otsuka, K., Aihara, A., Itasaki, N. and Nishino, T. (2018). "Novel 3D liquid cell culture method for anchorage-independent cell growth, cell imaging and automated drug screening." *Sci. Rep.* 8(1): 3627. 10.1038/s41598-018-21950-5.
- Abotaleb, M., Kubatka, P., Caprnda, M., Varghese, E., Zolakova, B., Zubor, P., Opatrilova, R., Kruzliak, P., et al. (2018). "Chemotherapeutic agents for the treatment of metastatic breast cancer: An update." *Biomed. Pharmacother.* 101: 458-477. 10.1016/j.biopha.2018.02.108.
- Abrahão, C. A., Bomfim, E., Lopes-Júnior, L. C. and Pereira-da-Silva, G. (2019). "Complementary therapies as a strategy to reduce stress and stimulate immunity of women with breast cancer." *J. Evid. Based Integr. Med.* 24: 2515690x19834169. 10.1177/2515690x19834169.
- Abudabbus, A., Badmus, J. A., Shalaweh, S., Bauer, R. and Hiss, D. (2017). "Effects of fucoidan and chemotherapeutic agent combinations on malignant and non-malignant breast cell lines." *Curr. Pharm. Biotechnol.* 18(9): 748-757. 10.2174/1389201018666171115115112.
- Achenbach, T. V., Slater, E. P., Brummerhop, H., Bach, T. and Müller, R. (2000). "Inhibition of cyclin-dependent kinase activity and induction of apoptosis by preussin in human tumor cells." *Antimicrob. Agents Chemother.* 44(10): 2794-2801. 10.1128/AAC.44.10.2794-2801.2000.
- Afolayan, A. F., Bolton, J. J., Lategan, C. A., Smith, P. J. and Beukes, D. R. (2008). "Fucoxanthin, tetraprenylated toluquinone and toluhydroquinone metabolites from *Sargassum heterophyllum* inhibit the in vitro growth of the malaria parasite *Plasmodium falciparum*." *Z. Naturforsch. C. J. Biosci.* 63(11-12): 848-852. 10.1515/znc-2008-11-1211.

- Afonso, C., Correia, A. P., Freitas, M. V., Baptista, T., Neves, M. and Mouga, T. (2021). "Seasonal changes in the nutritional composition of *Agarophyton vermiculophyllum* (Rhodophyta, Gracilariales) from the center of Portugal." *Foods* 10(5): 1145. 10.3390/foods10051145.
- Afonso, N. C., Catarino, M. D., Silva, A. M. S. and Cardoso, S. M. (2019). "Brown macroalgae as valuable food ingredients." *Antioxidants* 8(9): 365. 10.3390/antiox8090365.
- Agarwal, S. and Rao, A. V. (2000). "Carotenoids and chronic diseases." *Drug Metabol. Drug Interact.* 17(1-4): 189-210. 10.1515/dmdi.2000.17.1-4.189.
- Ahmad, S., He, Q., Williams, K. P. and Scott, J. E. (2020). "Identification of a triple drug combination that is synergistically cytotoxic for triple-negative breast cancer cells using a novel combination discovery approach." *SLAS Discov.* 25(8): 923-938. 10.1177/2472555220924478.
- Ahmadi, A., Zorofchian Moghadamtousi, S., Abubakar, S. and Zandi, K. (2015). "Antiviral potential of algae polysaccharides isolated from marine sources: A review." *BioMed Research International* 2015: 825203. 10.1155/2015/825203.
- Ahn, H. S., Lee, D. H., Kim, T. J., Shin, H. C. and Jeon, H. K. (2017). "Cardioprotective effects of a phlorotannin extract against doxorubicin-induced cardiotoxicity in a rat model." *J. Med. Food* 20(10): 944-950. 10.1089/jmf.2017.3919.
- Ahn, S., Woo, J. W., Lee, K. and Park, S. Y. (2020a). "HER2 status in breast cancer: changes in guidelines and complicating factors for interpretation." *J. Pathol. Transl. Med.* 54(1): 34-44. 10.4132/jptm.2019.11.03.
- Ahn, Y. T., Kim, M. S., Kim, Y. S. and An, W. G. (2020b). "Astaxanthin reduces stemness markers in BT20 and T47D breast cancer stem cells by inhibiting expression of p53 and mutant p53." *Mar. Drugs* 18(11): 577. 10.3390/md18110577.
- Aisa, Y., Miyakawa, Y., Nakazato, T., Shibata, H., Saito, K., Ikeda, Y. and Kizaki, M. (2005). "Fucoïdan induces apoptosis of human HS-sultan cells accompanied by activation of caspase-3 and down-regulation of ERK pathways." *Am. J. Hematol.* 78(1): 7-14. 10.1002/ajh.20182.
- Ajaykumar, C. (2020). Overview on the side effects of doxorubicin. In H. Arnouk, & B. A. R. Hassan (Eds.), *Advances in Precision Medicine Oncology*. IntechOpen. 10.5772/intechopen.94896.
- Akanji, M. A., Fatinukun, H. D., Rotimi, D. E., Afolabi, B. L. and Adeyemi, O. S. (2020). The two sides of dietary antioxidants in cancer therapy. In (Ed.), *Antioxidants - Benefits, Sources, Mechanisms of Action*. IntechOpen. 10.5772/intechopen.94988.
- Akca, G., Eren, H., Tumkaya, L., Mercantepe, T., Horsanali, M. O., Deveci, E., Dil, E. and Yilmaz, A. (2018). "The protective effect of astaxanthin against cisplatin-induced



- nephrotoxicity in rats." *Biomed. Pharmacother.* 100: 575-582. 10.1016/j.biopha.2018.02.042.
- Al-Mahayri, Z. N., Patrinos, G. P. and Ali, B. R. (2020). "Toxicity and pharmacogenomic biomarkers in breast cancer chemotherapy." *Front. Pharmacol.* (11):445. 10.3389/fphar.2020.00445.
- Al-Malky, H. S., Al Harthi, S. E. and Osman, A.-M. M. (2019). "Major obstacles to doxorubicin therapy: Cardiotoxicity and drug resistance." *J. Oncol. Pharm.* 26(2): 434-444. 10.1177/1078155219877931.
- Al-Muqbali, M. H. S., Al-Alawi, A., Waly, M. I. and Shafiur Rahman, M. (2019). "Anticancer properties of fucoidans extracted from brown seaweed (*Sargassum ilicifolium*) in a rat model of gastric cancer." *Can. J. Clin. Nutr.* 7(2): 43-61. 10.14206/canad.j.clin.nutr.2019.02.04.
- Ale, M. T., Mikkelsen, J. D. and Meyer, A. S. (2011). "Important determinants for fucoidan bioactivity: A critical review of structure-function relations and extraction methods for fucose-containing sulfated polysaccharides from brown seaweeds." *Mar. Drugs* 9(10): 2106-2130 .10.3390/md9102106.
- Alekseyenko, T. V., Zhanayeva, S. Y., Venediktova, A. A., Zvyagintseva, T. N., Kuznetsova, T. A., Besednova, N. N. and Korolenko, T. A. (2007). "Antitumor and antimetastatic activity of fucoidan, a sulfated polysaccharide isolated from the Okhotsk Sea *Fucus evanescens* brown alga." *Bull Exp. Biol. Med.* 143(6): 730-732. 10.1007/s10517-007-0226-4.
- Ali, S., Rasool, M., Chaoudhry, H., N Pushparaj, P., Jha, P., Hafiz, A., Mahfooz, M., Abdus Sami, G., et al. (2016). "Molecular mechanisms and mode of tamoxifen resistance in breast cancer." *Bioinformation* 12(3): 135-139. 10.6026/97320630012135.
- Alix-Panabières, C., Vendrell, J. P., Slijper, M., Pellé, O., Barbotte, E., Mercier, G., Jacot, W., Fabbro, M., et al. (2009). "Full-length cytokeratin-19 is released by human tumor cells: a potential role in metastatic progression of breast cancer." *Breast Cancer Res.* 11(3): R39. 10.1186/bcr2326.
- Allen, D. D., Caviedes, R., Cárdenas, A. M., Shimahara, T., Segura-Aguilar, J. and Caviedes, P. A. (2005). "Cell lines as in vitro models for drug screening and toxicity studies." *Drug Dev. Ind. Pharm.* 31(8): 757-768. 10.1080/03639040500216246.
- Allison, K. H., Hammond, M. E. H., Dowsett, M., McKernin, S. E., Carey, L. A., Fitzgibbons, P. L., Hayes, D. F., Lakhani, S. R., et al. (2020). "Estrogen and progesterone receptor testing in breast cancer: American Society of Clinical Oncology/College of American Pathologists Guideline update." *Arch. Pathol. Lab. Med.* 144(5): 545-563. 10.5858/arpa.2019-0904-SA.

- Alluri, P. and Newman, L. A. (2014). "Basal-like and triple-negative breast cancers: searching for positives among many negatives." *Surg. Oncol. Clin. N. Am.* 23(3): 567-577. 10.1016/j.soc.2014.03.003.
- Almeida, T. P., Ferreira, J., Vettorazzi, A., Azqueta, A., Rocha, E. and Ramos, A. A. (2018). "Cytotoxic activity of fucoxanthin, alone and in combination with the cancer drugs imatinib and doxorubicin, in CML cell lines." *Environ. Toxicol. Pharmacol.* 59: 24-33. 10.1016/j.etap.2018.02.006.
- Almeida, T. P., Ramos, A. A., Ferreira, J., Azqueta, A. and Rocha, E. (2020). "Bioactive compounds from seaweed with anti-leukemic activity: A mini-review on carotenoids and phlorotannins." *Mini Rev. Med. Chem.* 20(1): 39-53. 10.2174/1389557519666190311095655.
- Amaral, R. L. F., Miranda, M., Marcato, P. D. and Swiech, K. (2017). "Comparative analysis of 3D bladder tumor spheroids obtained by forced floating and hanging drop methods for drug screening." *Front. Physiol.* 8: 605. 10.3389/fphys.2017.00605.
- Ambati, R. R., Phang, S. M., Ravi, S. and Aswathanarayana, R. G. (2014). "Astaxanthin: sources, extraction, stability, biological activities and its commercial applications--a review." *Mar. Drugs* 12(1): 128-152. 10.3390/md12010128.
- American Cancer Society. (2021). "Survival rates for breast cancer." Retrieved 1<sup>st</sup> November 2021, available from <https://www.cancer.org/cancer/breast-cancer/understanding-a-breast-cancer-diagnosis/breast-cancer-survival-rates.html>.
- Amin, A., Gali-Muhtasib, H., Ocker, M. and Schneider-Stock, R. (2009). "Overview of major classes of plant-derived anticancer drugs." *Int. J. Biomed. Sci.* 5(1): 1-11. PMID: 23675107
- Andersen, A. P., Flinck, M., Oernbo, E. K., Pedersen, N. B., Viuff, B. M. and Pedersen, S. F. (2016). "Roles of acid-extruding ion transporters in regulation of breast cancer cell growth in a 3-dimensional microenvironment." *Mol. Cancer* 15(1): 45. 10.1186/s12943-016-0528-0.
- Andryukov, B. G., Besednova, N. N., Kuznetsova, T. A., Zaporozhets, T. S., Ermakova, S. P., Zvyagintseva, T. N., Chingizova, E. A., Gazha, A. K., et al. (2020). "Sulfated polysaccharides from marine algae as a basis of modern biotechnologies for creating wound dressings: Current achievements and future prospects." *Biomedicines* 8(9): 301. 10.3390/biomedicines8090301.
- Antoni, D., Burckel, H., Josset, E. and Noel, G. (2015). "Three-dimensional cell culture: A breakthrough in vivo." *Int. J. Mol. Sci.* 16(3): 5517-5527. 10.3390/ijms16035517.
- Aonuma, M., Saeki, Y., Akimoto, T., Nakayama, Y., Hattori, C., Yoshitake, Y., Nishikawa, K., Shibuya, M., et al. (1999). "Vascular endothelial growth factor overproduced by tumour cells acts predominantly as a potent angiogenic factor contributing to

- malignant progression." *Int. J. Exp. Pathol.* 80(5): 271-281. 10.1046/j.1365-2613.1999.00122.x.
- Apostolova, E., Lukova, P., Baldzhieva, A., Katsarov, P., Nikolova, M., Iliev, I., Peychev, L., Trica, B., et al. (2020). "Immunomodulatory and anti-inflammatory effects of fucoidan: A review." *Polymers* 12(10): 2338. 10.3390/polym12102338.
- Arcamone, F., Cassinelli, G., Fantini, G., Grein, A., Orezzi, P., Pol, C. and Spalla, C. (1969). "Adriamycin, 14-hydroxydaimomycin, a new antitumor antibiotic from *S. Peuceetius var. caesius*." *Biotechnol. Bioeng.* 11(6): 1101-1110. 10.1002/bit.260110607.
- Armas, P. d., García-Tellado, F., Marrero-Tellado, J. J. and Robles, J. (1998). "Diastereoselective formal synthesis of the antifungal agent, (+)-preussin. A new entry to chiral pyrrolidines." *Tetrahedron Lett.* 39(1): 131-134. 10.1016/S0040-4039(97)10468-3.
- Asai, A., Sugawara, T., Ono, H. and Nagao, A. (2004). "Biotransformation of fucoxanthinol into amarouciaxanthin A in mice and HepG2 cells: formation and cytotoxicity of fucoxanthin metabolites." *Drug. Metab. Dispos.* 32(2): 205-211. 10.1124/dmd.32.2.205.
- Asai, A., Yonekura, L. and Nagao, A. (2008). "Low bioavailability of dietary epoxyxanthophylls in humans." *Br. J. Nutr.* 100(2): 273-277. 10.1017/s0007114507895468.
- Asaoka, M., Gandhi, S., Ishikawa, T. and Takabe, K. (2020). "Neoadjuvant chemotherapy for breast cancer: Past, present, and future." *Breast Cancer* 14: 1178223420980377. 10.1177/1178223420980377.
- Aslam, A., Bahadar, A., Liaquat, R., Saleem, M., Waqas, A. and Zwawi, M. (2021). "Algae as an attractive source for cosmetics to counter environmental stress." *Sci. Total Environ.* 772: 144905. 10.1016/j.scitotenv.2020.144905.
- Atalay, P. B., Kuku, G. and Tuna, B. G. (2019). "Effects of carbendazim and astaxanthin co-treatment on the proliferation of MCF-7 breast cancer cells." *In Vitro Cell Dev. Biol. Anim.* 55(2): 113-119. 10.1007/s11626-018-0312-0.
- Atashrazm, F., Lowenthal, R. M., Dickinson, J. L., Holloway, A. F. and Woods, G. M. (2016). "Fucoidan enhances the therapeutic potential of arsenic trioxide and all-trans retinoic acid in acute promyelocytic leukemia, in vitro and in vivo." *Oncotarget* 7(29): 46028-46041. 10.18632/oncotarget.10016.
- ATCC. (2022). Retrieved 28<sup>th</sup> November 2021, available from <https://www.atcc.org/products/htb-30>.

- Augustine, R., Kalva, S. N., Ahmad, R., Zahid, A. A., Hasan, S., Nayeem, A., McClements, L. and Hasan, A. (2021). "3D bioprinted cancer models: Revolutionizing personalized cancer therapy." *Transl. Oncol.* 14(4): 101015. 10.1016/j.tranon.2021.101015.
- Ayrapetyan, O. N., Obluchinskaya, E. D., Zhurishkina, E. V., Skorik, Y. A., Lebedev, D. V., Kulminskaya, A. A. and Lapina, I. M. (2021). "Antibacterial properties of fucoidans from the brown algae *Fucus vesiculosus* L. of the Barents Sea." *Biology* 10(1): 67. 10.3390/biology10010067.
- Ayyad, S. E., Ezmirly, S. T., Basaif, S. A., Alarif, W. M., Badria, A. F. and Badria, F. A. (2011). "Antioxidant, cytotoxic, antitumor, and protective DNA damage metabolites from the red sea brown alga *Sargassum* sp." *Pharmacognosy Res.* 3(3): 160-165. 10.4103/0974-8490.85000.
- Azadi, S., Aboulkheyr Es, H., Razavi Bazaz, S., Thiery, J. P., Asadnia, M. and Ebrahimi Warkiani, M. (2019). "Upregulation of PD-L1 expression in breast cancer cells through the formation of 3D multicellular cancer aggregates under different chemical and mechanical conditions." *Biochim. Biophys. Acta Mol. Cell Res.* 1866(12): 118526. 10.1016/j.bbamcr.2019.118526.
- Azimi, T., Loizidou, M. and Dwek, M. V. (2020). "Cancer cells grown in 3D under fluid flow exhibit an aggressive phenotype and reduced responsiveness to the anti-cancer treatment doxorubicin." *Sci. Rep.* 10(1): 12020. 10.1038/s41598-020-68999-9.
- Badea, M. A., Balas, M., Hermenean, A., Ciceu, A., Herman, H., Ionita, D. and Dinischiotu, A. (2019). "Influence of matrigel on single- and multiple-spheroid cultures in breast cancer research." *SLAS Discov.* 24(5): 563-578. 10.1177/2472555219834698.
- Bae, H., Lee, J. Y., Song, G. and Lim, W. (2020a). "Fucosterol suppresses the progression of human ovarian cancer by inducing mitochondrial dysfunction and endoplasmic reticulum stress." *Mar. Drugs* 18(5): 261. 10.3390/md18050261.
- Bae, H., Song, G., Lee, J. Y., Hong, T., Chang, M. J. and Lim, W. (2020b). "Laminarin-derived from brown algae suppresses the growth of ovarian cancer cells via mitochondrial dysfunction and ER stress." *Mar. Drugs* 18(3): 152. 10.3390/md18030152.
- Bahaddin, M. M. (2020). "A comparative study between Ki67 positive versus Ki67 negative females with breast cancer: Cross sectional study." *Ann. Med. Surg.* 60: 232-235. 10.1016/j.amsu.2020.10.049.

- Baker, B. M. and Chen, C. S. (2012). "Deconstructing the third dimension: how 3D culture microenvironments alter cellular cues." *J. Cell Sci.* 125(Pt 13): 3015-3024. 10.1242/jcs.079509.
- Balalaeva, I. V., Sokolova, E. A., Puzhikhina, A. D., Brilkina, A. A. and Deyev, S. M. (2017). "Spheroids of HER2-positive breast adenocarcinoma for studying anticancer immunotoxins in vitro." *Acta Naturae* 9(1): 38-43. PMID: 28461972.
- Banafa, A. M., Roshan, S., Liu, Y. Y., Chen, H. J., Chen, M. J., Yang, G. X. and He, G. Y. (2013). "Fucoidan induces G1 phase arrest and apoptosis through caspases-dependent pathway and ROS induction in human breast cancer MCF-7 cells." *J. Huazhong Univ. Sci. Technol. Med. Sci.* 33(5): 717-724. 10.1007/s11596-013-1186-8.
- Bandaranayake, W. M. (1998). "Traditional and medicinal uses of mangroves." *Wetl Ecol. Manag.* 2(3): 133-148. 10.1023/A:1009988607044.
- Bang, M.-H., Kim, H.-H., Lee, D.-Y., Han, M.-W., Baek, Y.-S., Chung, D. K. and Baek, N.-I. (2011). "Anti-osteoporotic activities of fucosterol from sea mustard (*Undaria pinnatifida*)." *Food Sci. Biotechnol.* 20(2): 343. 10.1007/s10068-011-0048-z.
- Barbosa, M. A. G., Xavier, C. P. R., Pereira, R. F., Petrikaitė, V. and Vasconcelos, M. H. (2022). "3D cell culture models as recapitulators of the tumor microenvironment for the screening of anti-cancer drugs." *Cancers (Basel)* 14(1): 190. 10.3390/cancers14010190.
- Baru, A., Mazumder, S., Kundu, P. K., Sharma, S., Das Purkayastha, B. P., Khan, S., Gupta, R. and Mehrotra Arora, N. (2022). "Recapitulating tumor microenvironment using AXTEX-4DTM for accelerating cancer research and drug screening." *Asian Pac. J. Cancer Prev.* 23(2): 561-571. 10.31557/apjcp.2022.23.2.561.
- Baudino, T. A. (2015). "Targeted cancer therapy: The next generation of cancer treatment." *Curr. Drug Discov. Technol.* 12(1): 3-20. 10.2174/1570163812666150602144310.
- Bayat Mokhtari, R., Homayouni, T. S., Baluch, N., Morgatskaya, E., Kumar, S., Das, B. and Yeger, H. (2017). "Combination therapy in combating cancer." *Oncotarget* 8(23): 38022-38043. 10.18632/oncotarget.16723.
- Becker, S. (2015). "A historic and scientific review of breast cancer: The next global healthcare challenge." *Int. J. Gynaecol. Obstet.* 131: S36-S39. 10.1016/j.ijgo.2015.03.015.
- Becker, S., Tebben, J., Coffinet, S., Wiltshire, K., Iversen, M. H., Harder, T., Hinrichs, K.-U. and Hehemann, J.-H. (2020). "Laminarin is a major molecule in the marine carbon cycle." *PNAS* 117(12): 6599-6607. 10.1073/pnas.1917001117.

- Belfiore, L., Aghaei, B., Law, A. M. K., Dobrowolski, J. C., Raftery, L. J., Tjandra, A. D., Yee, C., Piloni, A., et al. (2021). "Generation and analysis of 3D cell culture models for drug discovery." *Eur J Pharm Sci* 163: 105876. 10.1016/j.ejps.2021.105876.
- Benton, G., DeGray, G., Kleinman, H. K., George, J. and Arnaoutova, I. (2015). "In vitro microtumors provide a physiologically predictive tool for breast cancer therapeutic screening." *PLoS One* 10(4): e0123312. 10.1371/journal.pone.0123312.
- Beppu, F., Hosokawa, M., Niwano, Y. and Miyashita, K. (2012). "Effects of dietary fucoxanthin on cholesterol metabolism in diabetic/obese KK-Aymice." *Lipids Health Dis.* 11(1): 112. 10.1186/1476-511X-11-112.
- Beppu, F., Niwano, Y., Sato, E., Kohno, M., Tsukui, T., Hosokawa, M. and Miyashita, K. (2009). "In vitro and in vivo evaluation of mutagenicity of fucoxanthin (Fx) and its metabolite fucoxanthinol (FxoI)." *J. Toxicol. Sci.* 34(6): 693-698. 10.2131/jts.34.693.
- Bhushan, A., Gonsalves, A. and Menon, J. U. (2021). "Current state of breast cancer diagnosis, treatment, and theranostics." *Pharmaceutics* 13(5):723. 10.3390/pharmaceutics13050723.
- Bi, J., Cui, R., Li, Z., Liu, C. and Zhang, J. (2017). "Astaxanthin alleviated acute lung injury by inhibiting oxidative/nitrative stress and the inflammatory response in mice." *Biomed. Pharmacother.* 95: 974-982. 10.1016/j.biopha.2017.09.012.
- Bilal, M. and Iqbal, H. M. N. (2019). "Marine seaweed polysaccharides-based engineered cues for the modern biomedical sector." *Mar. Drugs* 18(1): 7. 10.3390/md18010007.
- Bilan, M. I., Grachev, A. A., Ustuzhanina, N. E., Shashkov, A. S., Nifantiev, N. E. and Usov, A. I. (2002). "Structure of a fucoidan from the brown seaweed *Fucus evanescens* C. Ag." *Carbohydr. Res.* 337(8): 719-730. 10.1016/s0008-6215(02)00053-8.
- Bills, G. F. and Gloer, J. B. (2016). "Biologically active secondary metabolites from the Fungi." *Microbiol. Spectr.* 4(6). 10.1128/microbiolspec.FUNK-0009-2016.
- Bistoni, G. and Farhadi, J. (2015). Anatomy and physiology of the breast. In *Plastic and reconstructive surgery* (eds R.D. Farhadieh, N.W. Bulstrode and S. Cugno). 477-485. 10.1002/9781118655412.ch37
- Blank, C. (2018). "The rise of seaweed." Retrieved 10<sup>th</sup> April 2022 available from <https://www.seafoodsource.com/features/the-rise-of-seaweed>.
- Blau, M., Hazani, R. and Hekmat, D. (2016). "Anatomy of the gynecomastia tissue and its clinical significance." *Plast. Reconstr. Surg. Glob. Open* 4(8): e854-e854. 10.1097/GOX.0000000000000844.
- Bocanegra, A., Bastida, S., Benedí, J., Ródenas, S. and Sánchez-Muniz, F. J. (2009). "Characteristics and nutritional and cardiovascular-health properties of seaweeds." *J. Med. Food* 12(2): 236-258. 10.1089/jmf.2008.0151.

- Bock, C., Rack, B., Kuhn, C., Hofmann, S., Finkenzeller, C., Jäger, B., Jeschke, U. and Doisneau-Sixou, S. F. (2012). "Heterogeneity of ER $\alpha$  and ErbB2 status in cell lines and circulating tumor cells of metastatic breast cancer patients." *Transl. Oncol.* 5(6): 475-485. 10.1593/tlo.12310.
- Bogdanowicz, D. R. and Lu, H. H. (2014). "Multifunction co-culture model for evaluating cell-cell interactions." *Methods Mol. Biol.* 1202: 29-36. 10.1007/7651\_2013\_62.
- Bonacho, T., Rodrigues, F. and Liberal, J. (2020). "Immunohistochemistry for diagnosis and prognosis of breast cancer: a review." *Biotech. Histochem.* 95(2): 71-91. 10.1080/10520295.2019.1651901.
- Bouquet de Jolinière, J., Major, A., Khomsi, F., Ben Ali, N., Guillou, L. and Feki, A. (2018). "The sentinel lymph node in breast cancer: Problems posed by examination during surgery. A review of current literature and management." *Front. Surg.* 5: 56.10.3389/fsurg.2018.00056.
- Bowers, H. J., Fannin, E. E., Thomas, A. and Weis, J. A. (2020). "Characterization of multicellular breast tumor spheroids using image data-driven biophysical mathematical modeling." *Sci. Rep.* 10(1): 11583. 10.1038/s41598-020-68324-4.
- Boyer, J. Z., Phillips, G. D. L., Nitta, H., Garsha, K., Admire, B., Kraft, R., Dennis, E., Vela, E., et al. (2021). "Activity of trastuzumab emtansine (T-DM1) in 3D cell culture." *Breast Cancer Res. Treat.* 188(1): 65-75. 10.1007/s10549-021-06272-x.
- Brancato, V., Gioiella, F., Imperato, G., Guarnieri, D., Urciuolo, F. and Netti, P. A. (2018). "3D breast cancer microtissue reveals the role of tumor microenvironment on the transport and efficacy of free-doxorubicin in vitro." *Acta Biomater.* 75: 200-212. 10.1016/j.actbio.2018.05.055.
- Bresciani, G., Hofland, L. J., Dogan, F., Giamas, G., Gagliano, T. and Zatelli, M. C. (2019). "Evaluation of spheroid 3D culture methods to study a pancreatic neuroendocrine neoplasm cell line." *Front. Endocrinol.* 10: 682.10.3389/fendo.2019.00682.
- Breslin, S. and O'Driscoll, L. (2013). "Three-dimensional cell culture: the missing link in drug discovery "Drug Discov. Today" 18(5-6): 240-249. 10.1016/j.drudis.2012.10.003
- Brown, E. S., Allsopp, P. J., Magee, P. J., Gill, C. I., Nitecki, S., Strain, C. R. and McSorley, E. M. (2014). "Seaweed and human health." *Nutr. Rev.* 72(3): 205-216. 10.1111/nure.12091.
- Buettner, C., Kroenke, C. H., Phillips, R. S., Davis, R. B., Eisenberg, D. M. and Holmes, M. D. (2006). "Correlates of use of different types of complementary and alternative medicine by breast cancer survivors in the nurses' health study." *Breast Cancer Res. Treat.* 100(2): 219-227. 10.1007/s10549-006-9239-3.

- Bugni, T. S. and Ireland, C. M. (2004). "Marine-derived fungi: a chemically and biologically diverse group of microorganisms." *Nat. Prod. Rep.* 21(1): 143-163. 10.1039/b301926h.
- Burguin, A., Diorio, C. and Durocher, F. (2021). "Breast cancer treatments: Updates and new challenges." *J. Pers. Med.* 11(8): 808. 10.3390/jpm11080808.
- Burney, M., Mathew, L., Gaikwad, A., Nugent, E. K., Gonzalez, A. O. and Smith, J. A. (2017). "Evaluation fucoïdan extracts from *Undaria pinnatifida* and *Fucus vesiculosus* in combination with anticancer drugs in human cancer orthotopic mouse models." *Integr. Cancer Ther.* 17(3): 755-761. 10.1177/1534735417740631.
- Buttachon, S., Ramos, A. A., Inacio, A., Dethoup, T., Gales, L., Lee, M., Costa, P. M., Silva, A. M. S., et al. (2018). "Bis-Indolyl benzenoids, hydroxypyrrolidine derivatives and other constituents from cultures of the marine sponge-associated Fungus *Aspergillus candidus* KUFA0062." *Mar. Drugs* 16(4): 119. 10.3390/md16040119.
- Butti, R., Gunasekaran, V. P., Kumar, T. V. S., Banerjee, P. and Kundu, G. C. (2019). "Breast cancer stem cells: Biology and therapeutic implications." *Int. J. Biochem. Cell Biol.* 107: 38-52. 10.1016/j.biocel.2018.12.001.
- Caamal-Fuentes, E., Moo-Puc, R., Freile-Pelegrin, Y. and Robledo, D. (2014). "Cytotoxic and antiproliferative constituents from *Dictyota ciliolata*, *Padina sanctae-crucis* and *Turbinaria tricostata*." *Pharm. Biol.* 52(10): 1244-1248. 10.3109/13880209.2014.886273.
- Caciolla, J., Bisi, A., Belluti, F., Rampa, A. and Gobbi, S. (2020). "Reconsidering aromatase for breast cancer treatment: New roles for an old target." *Molecules* 25(22): 5351. 10.3390/molecules25225351.
- Cappello, E. and Nieri, P. (2021). "From life in the sea to the clinic: The marine drugs approved and under clinical trial." *Life* 11(12): 1390. 10.3390/life11121390.
- Capula, M., Corno, C., El Hassouni, B., Li Petri, G. and Arandelović, S. (2019). "A brief guide to performing pharmacological studies in vitro: Reflections from the EORTC-PAMM course "Preclinical and early-phase clinical pharmacology"." *Anticancer Res.* 39(7): 3413-3418. 10.21873/anticancer.13485.
- Carbonell-Capella, J. M., Buniowska, M., Barba, F. J., Esteve, M. J. and Frígola, A. (2014). "Analytical methods for determining bioavailability and bioaccessibility of bioactive compounds from fruits and vegetables: A review." *Compr. Rev. Food Sci. Food Saf.* 13(2): 155-171. 10.1111/1541-4337.12049.
- Cardoso, M. J., Costa, R. R. and Mano, J. F. (2016). "Marine origin polysaccharides in drug delivery systems." *Mar. Drugs* 14(2):34. 10.3390/md14020034.



- Carvalho, C., Santos, R. X., Cardoso, S., Correia, S., Oliveira, P. J., Santos, M. S. and Moreira, P. I. (2009). "Doxorubicin: the good, the bad and the ugly effect." *Curr. Med. Chem.* 16(25): 3267-3285. 10.2174/092986709788803312.
- Casey, R. C., Burleson, K. M., Skubitz, K. M., Pambuccian, S. E., Oegema, T. R., Jr., Ruff, L. E. and Skubitz, A. P. (2001). "Beta 1-integrins regulate the formation and adhesion of ovarian carcinoma multicellular spheroids." *Am. J. Pathol.* 159(6): 2071-2080. 10.1016/s0002-9440(10)63058-1.
- Cassileth, B. R., Gubili, J. and Simon Yeung, K. (2009). "Integrative medicine: complementary therapies and supplements." *Nat. Rev. Urol.* 6(4): 228-233. 10.1038/nrurol.2009.41.
- Castaneda, S. A. and Strasser, J. (2017). "Updates in the treatment of breast cancer with radiotherapy." *Surg. Oncol. Clin. N. Am.* 26(3): 371-382. 10.1016/j.soc.2017.01.013.
- Castanheira, E. J., Correia, T. R., Rodrigues, J. M. M. and Mano, J. F. (2020). "Novel biodegradable laminarin microparticles for biomedical applications." *Bull. Chem. Soc. Jpn.* 93(6): 713-719. 10.1246/bcsj.20200034.
- Catanzaro, E., Bishayee, A. and Fimognari, C. (2020). "On a beam of light: photoprotective activities of the marine carotenoids Astaxanthin and Fucoxanthin in suppression of inflammation and cancer." *Mar. Drugs* 18(11): 544. 10.3390/md18110544.
- Catarino, M. D., Fernandes, I., Oliveira, H., Carrascal, M., Ferreira, R., Silva, A. M. S., Cruz, M. T., Mateus, N., et al. (2021a). "Antitumor activity of *Fucus vesiculosus*-derived phlorotannins through activation of apoptotic signals in gastric and colorectal tumor cell lines." *Int. J. Mol. Sci.* 22(14): 7604. 10.3390/ijms22147604.
- Catarino, M. D., Marçal, C., Bonifácio-Lopes, T., Campos, D., Mateus, N., Silva, A. M. S., Pintado, M. M. and Cardoso, S. M. (2021b). "Impact of phlorotannin extracts from *Fucus vesiculosus* on human gut microbiota." *Mar. Drugs* 19(7): 375. 10.3390/md19070375.
- Catarino, M. D., Silva, A. M. S. and Cardoso, S. M. (2017). "Fucaceae: A source of bioactive phlorotannins." *Int. J. Mol. Sci.* 18(6): 1327. 10.3390/ijms18061327.
- Cazarin, C. B. B., Bicas, J. L., Pastore, G. M. and Marostica Junior, M. R. (2022). *Bioactive food components activity in mechanistic approach.* Marostica Junior Academic Press. 10.1016/C2019-0-05482-9
- Chaicharoenaudomrung, N., Kunhorm, P. and Noisa, P. (2019). "Three-dimensional cell culture systems as an in vitro platform for cancer and stem cell modeling." *World J. Stem Cells* 11(12): 1065-1083. 10.4252/wjsc.v11.i12.1065.

- Chan, H. F., Zhang, Y., Ho, Y.-P., Chiu, Y.-L., Jung, Y. and Leong, K. W. (2013). "Rapid formation of multicellular spheroids in double-emulsion droplets with controllable microenvironment." *Sci. Rep.* 3(1): 3462. 10.1038/srep03462.
- Chandwani, K. D., Ryan, J. L., Peppone, L. J., Janelins, M. M., Sprod, L. K., Devine, K., Trevino, L., Gewandter, J., et al. (2012). "Cancer-related stress and complementary and alternative medicine: a review." *Evid. Based Complement. Alternat. Med.* 2012: 979213. 10.1155/2012/979213.
- Chang, P.-M., Li, K.-L. and Lin, Y.-C. (2019). "Fucoxanthin ameliorated cardiac function via IRS1/GRB2/ SOS1, GSK3 $\beta$ /CREB pathways and metabolic pathways in senescent mice." *Mar. Drugs* 17(1): 69. 10.3390/md17010069.
- Chang, Y. H., Chen, Y. L., Huang, W. C. and Liou, C. J. (2018). "Fucoxanthin attenuates fatty acid-induced lipid accumulation in FL83B hepatocytes through regulated Sirt1/AMPK signaling pathway." *Biochem. Biophys. Res. Commun.* 495(1): 197-203. 10.1016/j.bbrc.2017.11.022.
- Chantree, P., Na-Bangchang, K. and Martviset, P. (2021). "Anticancer activity of fucoxanthin via apoptosis and cell cycle arrest on cholangiocarcinoma cell." *Asian Pac. J. Cancer Prev.* 22(1): 209-217. 10.31557/apjcp.2021.22.1.209.
- Chavez, K. J., Garimella, S. V. and Lipkowitz, S. (2010). "Triple negative breast cancer cell lines: one tool in the search for better treatment of triple negative breast cancer." *Breast Dis.* 32(1-2): 35-48. 10.3233/BD-2010-0307.
- Chen, S., Zhao, Y., Zhang, Y. and Zhang, D. (2014). "Fucoxanthin induces cancer cell apoptosis by modulating the endoplasmic reticulum stress cascades." *PLoS One* 9(9): e108157. 10.1371/journal.pone.0108157.
- Chen, X., He, C., Han, D., Zhou, M., Wang, Q., Tian, J., Li, L., Xu, F., et al. (2017). "The predictive value of Ki-67 before neoadjuvant chemotherapy for breast cancer: a systematic review and meta-analysis." *Future Oncol.* 13(9): 843-857. 10.2217/fon-2016-0420.
- Cho, H. J. and Yoon, I. S. (2015). "Pharmacokinetic interactions of herbs with cytochrome p450 and p-glycoprotein." *Evid. Based Complement. Alternat. Med.* 2015: 736431. 10.1155/2015/736431.
- Choi, J. I., Kim, H. J. and Lee, J. W. (2011). "Structural feature and antioxidant activity of low molecular weight laminarin degraded by gamma irradiation." *Food Chem.* 129(2): 520-523. 10.1016/j.foodchem.2011.03.078.
- Choi, J. S., Han, Y. R., Byeon, J. S., Choung, S. Y., Sohn, H. S. and Jung, H. A. (2015). "Protective effect of fucoxanthin isolated from the edible brown algae, *Ecklonia stolonifera* and *Eisenia bicyclis*, on tert-butyl hydroperoxide- and tacrine-induced HepG2 cell injury." *J. Pharm. Pharmacol.* 67(8): 1170-1178. 10.1111/jphp.12404.

- Chou, T.-C. (2006). "Theoretical basis, experimental design, and computerized simulation of synergism and antagonism in drug combination studies." *Pharmacol. Rev.* 58(3): 621. 10.1124/pr.58.3.10.
- Chung, T.-W., Choi, H.-J., Lee, J.-Y., Jeong, H.-S., Kim, C.-H., Joo, M., Choi, J.-Y., Han, C.-W., et al. (2013). "Marine algal fucoxanthin inhibits the metastatic potential of cancer cells." *Biochem. Biophys. Res. Commun.* 439(4): 580-585. 10.1016/j.bbrc.2013.09.019.
- Cioce, M., Gherardi, S., Viglietto, G., Strano, S., Blandino, G., Muti, P. and Ciliberto, G. (2014). "Mammosphere-forming cells from breast cancer cell lines as a tool for the identification of CSC-like- and early progenitor-targeting drugs." *Cell Cycle* 9(14): 2950-2959. 10.4161/cc.9.14.12371.
- Citkowska, A., Szekalska, M. and Winnicka, K. (2019). "Possibilities of fucoidan utilization in the development of pharmaceutical dosage forms." *Mar. Drugs* 17(8): 458. 10.3390/md17080458.
- Close, D. A., Wang, A. X., Kochanek, S. J., Shun, T., Eiseman, J. L. and Johnston, P. A. (2019). "Implementation of the NCI-60 human tumor cell line panel to screen 2260 cancer drug combinations to generate >3 million data points used to populate a large matrix of anti-neoplastic agent combinations (ALMANAC) Database." *SLAS Discov.* 24(3): 242-263. 10.1177/2472555218812429.
- Collaborative Group on Hormonal Factors in Breast Cancer (2019). "Type and timing of menopausal hormone therapy and breast cancer risk: individual participant meta-analysis of the worldwide epidemiological evidence." *The Lancet* 394 (10204): 1159-1168. 10.1016/S0140-6736(19)31709-X.
- Comsa, S., Cimpean, A. M. and Raica, M. (2015). "The story of MCF-7 breast cancer cell line: 40 years of experience in research." *Anticancer Res.* 35(6): 3147-3154. PMID: 26026074.
- Cooper, D. A. (2004). "Carotenoids in health and disease: Recent scientific evaluations, research recommendations and the consumer." *J. Nutr.* 134(1): 221S-224S. 10.1093/jn/134.1.221S.
- Cooper, T. M. (2007). "Role of nelarabine in the treatment of T-cell acute lymphoblastic leukemia and T-cell lymphoblastic lymphoma." *Ther. Clin. Risk Manag.* 3(6): 1135-1141. PMID: 18516261.
- Correia, A. S., Gärtner, F. and Vale, N. (2021). "Drug combination and repurposing for cancer therapy: The example of breast cancer." *Heliyon* 7(1): e05948. 10.1016/j.heliyon.2021.e05948.
- Cosentino, G., Plantamura, I., Tagliabue, E., Iorio, M. V. and Cataldo, A. (2021). "Breast cancer drug resistance: Overcoming the challenge by capitalizing on microRNA and

- tumor microenvironment interplay." *Cancers* (Basel) 13(15). 10.3390/cancers13153691.
- Costa, E. C., Moreira, A. F., de Melo-Diogo, D., Gaspar, V. M., Carvalho, M. P. and Correia, I. J. (2016). "3D tumor spheroids: An overview on the tools and techniques used for their analysis." *Biotechnol. Adv.* 34(8): 1427-1441. 10.1016/j.biotechadv.2016.11.002.
- Costa, M., Cardoso, C., Afonso, C., Bandarra, N. M. and Prates, J. A. M. (2021). "Current knowledge and future perspectives of the use of seaweeds for livestock production and meat quality: a systematic review." *J. Anim. Physiol. Anim. Nutr.* 105(6): 1075-1102. 10.1111/jpn.13509.
- Cotas, J., Leandro, A., Monteiro, P., Pacheco, D., Figueirinha, A., Goncalves, A. M. M., da Silva, G. J. and Pereira, L. (2020). "Seaweed phenolics: From extraction to applications." *Mar. Drugs* 18(8): 384. 10.3390/md18080384.
- Cotas, J., Pacheco, D., Gonçalves, A. M. M., Silva, P., Carvalho, L. G. and Pereira, L. (2021). "Seaweeds' nutraceutical and biomedical potential in cancer therapy: A concise review." *J. Cancer Metastasis Treat.* 7: 13. 10.20517/2394-4722.2020.134.
- Cox, M. C., Reese, L. M., Bickford, L. R. and Verbridge, S. S. (2015). "Toward the broad adoption of 3D tumor models in the cancer drug pipeline." *ACS Biomater. Sci. Eng.* 1(10): 877-894. 10.1021/acsbiomaterials.5b00172.
- Cragg, G. M. and Pezzuto, J. M. (2016). "Natural products as a vital source for the discovery of cancer chemotherapeutic and chemopreventive agents." *Med. Princ. Pract.* 25 (Suppl 2): 41-59. 10.1159/000443404.
- Crocetti, E., Crotti, N., Feltrin, A., Ponton, P., Geddes, M. and Buiatti, E. (1998). "The use of complementary therapies by breast cancer patients attending conventional treatment." *Eur. J. Cancer* 34(3): 324-328. 10.1016/S0959-8049(97)10043-0.
- Crozier, A., Jaganath, I. B. and Clifford, M. N. (2009). "Dietary phenolics: chemistry, bioavailability and effects on health." *Nat. Prod. Rep.* 26(8): 1001-1043. 10.1039/b802662a.
- Cserni, G., Chmielik, E., Cserni, B. and Tot, T. (2018). "The new TNM-based staging of breast cancer." *Virchows Arch.* 472(5): 697-703. 10.1007/s00428-018-2301-9.
- Cumashi, A., Ushakova, N. A., Preobrazhenskaya, M. E., D'Incecco, A., Piccoli, A., Totani, L., Tinari, N., Morozevich, G. E., et al. (2007). "A comparative study of the anti-inflammatory, anticoagulant, antiangiogenic, and antiadhesive activities of nine different fucoidans from brown seaweeds." *Glycobiology* 17(5): 541-552. 10.1093/glycob/cwm014.

- Cunha, L. and Grenha, A. (2016). "Sulfated seaweed polysaccharides as multifunctional materials in drug delivery applications." *Mar. Drugs* 14(3): 42. 10.3390/md14030042.
- D'Andrea, G. M. (2005). "Use of antioxidants during chemotherapy and radiotherapy should be avoided." *CA Cancer J. Clin.* 55(5): 319-321. 10.3322/canjclin.55.5.319.
- D'Anselmi, F., Masiello, M. G., Cucina, A., Proietti, S., Dinicola, S., Pasqualato, A., Ricci, G., Dobrowolny, G., et al. (2013). "Microenvironment promotes tumor cell reprogramming in human breast cancer cell lines." *PLoS One* 8(12): e83770. 10.1371/journal.pone.0083770.
- Dai, J., Jian, J., Bosland, M., Frenkel, K., Bernhardt, G. and Huang, X. (2008). "Roles of hormone replacement therapy and iron in proliferation of breast epithelial cells with different estrogen and progesterone receptor status." *Breast* 17(2): 172-179. 10.1016/j.breast.2007.08.009.
- Dai, X., Cheng, H., Bai, Z. and Li, J. (2017). "Breast cancer cell line classification and its relevance with breast tumor subtyping." *J. Cancer* 8(16): 3131-3141. 10.7150/jca.18457.
- Dall, G. V. and Britt, K. L. (2017). "Estrogen effects on the mammary gland in early and late life and breast cancer risk." *Front. Oncol.* 7: 110-110. 10.3389/fonc.2017.00110.
- Dankó, T., Petővári, G., Raffay, R., Sztankovics, D., Moldvai, D., Vetlényi, E., Krencz, I., Rókusz, A., et al. (2022). "Characterisation of 3D bioprinted human breast cancer model for in vitro drug and metabolic targeting." *Int. J. Mol. Sci.* 23(13): 7444. 10.3390/ijms23137444.
- Das, S. K., Hashimoto, T. and Kanazawa, K. (2008). "Growth inhibition of human hepatic carcinoma HepG2 cells by fucoxanthin is associated with down-regulation of cyclin D." *Biochim. Biophys. Acta* 1780(4): 743-749. 10.1016/j.bbagen.2008.01.003.
- Das, S. K., Hashimoto, T., Shimizu, K., Yoshida, T., Sakai, T., Sowa, Y., Komoto, A. and Kanazawa, K. (2005). "Fucoxanthin induces cell cycle arrest at G0/G1 phase in human colon carcinoma cells through up-regulation of p21WAF1/Cip1." *Biochim. Biophys. Acta* 1726(3): 328-335. 10.1016/j.bbagen.2005.09.007.
- Daster, S., Amatruda, N., Calabrese, D., Ivanek, R., Turrini, E., Droeser, R. A., Zajac, P., Fimognari, C., et al. (2017). "Induction of hypoxia and necrosis in multicellular tumor spheroids is associated with resistance to chemotherapy treatment." *Oncotarget* 8(1): 1725-1736. 10.18632/oncotarget.13857.
- Davinelli, S., Nielsen, M. E. and Scapagnini, G. (2018). "Astaxanthin in skin health, repair, and disease: A comprehensive review." *Nutrients* 10(4): 522. 10.3390/nu10040522.

- de la Cruz-López, K. G., Castro-Muñoz, L. J., Reyes-Hernández, D. O., García-Carrancá, A. and Manzo-Merino, J. (2019). "Lactate in the regulation of tumor microenvironment and therapeutic approaches." *Front. Oncol.* 9: 1143. 10.3389/fonc.2019.01143.
- de la Mare, J. A., Sterrenberg, J. N., Sukhthankar, M. G., Chiwakata, M. T., Beukes, D. R., Blatch, G. L. and Edkins, A. L. (2013). "Assessment of potential anti-cancer stem cell activity of marine algal compounds using an in vitro mammosphere assay." *Cancer Cell Int.* 13(1): 39. 10.1186/1475-2867-13-39.
- de Vries, R. P., Riley, R., Wiebenga, A., Aguilar-Osorio, G., Amillis, S., Uchima, C. A., Anderluh, G., Asadollahi, M., et al. (2017). "Comparative genomics reveals high biological diversity and specific adaptations in the industrially and medically important fungal genus *Aspergillus*." *Genome Biol.* 18(1): 28-28. 10.1186/s13059-017-1151-0.
- Debbab, A., Aly, A. H. and Proksch, P. (2012). "Endophytes and associated marine derived fungi—ecological and chemical perspectives." *Fungal Divers.* 57(1): 45-83. 10.1007/s13225-012-0191-8.
- Deeks, E. D. (2019). "Polatuzumab vedotin: First global approval." *Drugs* 79(13): 1467-1475. 10.1007/s40265-019-01175-0.
- Demuyne, R., Efimova, I., Lin, A., Declercq, H. and Krysko, D. V. (2020). "A 3D cell death assay to quantitatively determine ferroptosis in spheroids." *Cells* 9(3): 703. 10.3390/cells9030703.
- Deng, G. and Cassileth, B. (2014). "Integrative oncology: An overview." *Am. Soc. Clin. Oncol. Educ. Book.* (34) 233-242. 10.14694/EdBook\_AM.2014.34.233.
- Deniaud-Bouët, E., Hardouin, K., Potin, P., Kloareg, B. and Hervé, C. (2017). "A review about brown algal cell walls and fucose-containing sulfated polysaccharides: Cell wall context, biomedical properties and key research challenges." *Carbohydr. Polym.* 175: 395-408. 10.1016/j.carbpol.2017.07.082.
- DeSantis, C. E., Bray, F., Ferlay, J., Lortet-Tieulent, J., Anderson, B. O. and Jemal, A. (2015). "International variation in female breast cancer incidence and mortality rates." *Cancer Epidemiol. Biomark. Prev.* 24(10): 1495-1506. 10.1158/1055-9965.EPI-15-0535.
- Deshmukh, S. K., Prakash, V. and Ranjan, N. (2018). "Marine fungi: A source of potential anticancer compounds." *Front. Microbiol.* 8: 2536. 10.3389/fmicb.2017.02536.
- Dieterich, M., Stubert, J., Reimer, T., Erickson, N. and Berling, A. (2014). "Influence of lifestyle factors on breast cancer risk." *Breast Care (Basel)* 9(6): 407-414. 10.1159/000369571.

- Dittmer, A., Hohlfeld, K., Lutzkendorf, J., Muller, L. P. and Dittmer, J. (2009). "Human mesenchymal stem cells induce E-cadherin degradation in breast carcinoma spheroids by activating ADAM10." *Cell Mol. Life Sci.* 66(18): 3053-3065. 10.1007/s00018-009-0089-0.
- do Amaral, J. B., Rezende-Teixeira, P., Freitas, V. M. and Machado-Santelli, G. M. (2011). "MCF-7 cells as a three-dimensional model for the study of human breast cancer." *Tissue Eng. Part C Methods* 17(11): 1097-1107. 10.1089/ten.tec.2011.0260.
- do Nascimento, R. G. and Otoni, K. M. (2020). "Histological and molecular classification of breast cancer: what do we know?" *Mastology* 30: e20200024. 10.29289/25945394202020200024.
- Domchek, S. M., Postel-Vinay, S., Im, S. A., Park, Y. H., Delord, J. P., Italiano, A., Alexandre, J., You, B., et al. (2020). "Olaparib and durvalumab in patients with germline BRCA-mutated metastatic breast cancer (MEDIOLA): an open-label, multicentre, phase 1/2, basket study." *Lancet Oncol.* 21(9): 1155-1164. 10.1016/s1470-2045(20)30324-7.
- Dose, J., Matsugo, S., Yokokawa, H., Koshida, Y., Okazaki, S., Seidel, U., Eggersdorfer, M., Rimbach, G., et al. (2016). "Free radical scavenging and cellular antioxidant properties of astaxanthin." *Int. J. Mol. Sci.* 17(1): 103. 10.3390/ijms17010103.
- Dursun, B., He, Z., Somers, H., Oh, D. J., Faubel, S. and Edelstein, C. L. (2006). "Caspases and calpain are independent mediators of cisplatin-induced endothelial cell necrosis." *Am. J. Physiol. Renal Physiol.* 291(3): F578-587. 10.1152/ajprenal.00455.2005.
- Dybdal-Hargreaves, N. F., Risinger, A. L. and Mooberry, S. L. (2015). "Eribulin mesylate: Mechanism of action of a unique microtubule-targeting agent." *Clin. Cancer Res.* 21(11): 2445-2452. 10.1158/1078-0432.CCR-14-3252.
- Dyshlovoy, S. A. (2021). "Recent updates on marine cancer-preventive compounds." *Mar. Drugs* 19(10): 558. 10.3390/md19100558.
- Edwards, V., Benkendorff, K. and Young, F. (2012). "Marine compounds selectively induce apoptosis in female reproductive cancer cells but not in primary-derived human reproductive granulosa cells." *Mar. Drugs* 10(1): 64-83. 10.3390/md10010064.
- Eid, S. Y., Althubiti, M. A., Abdallah, M. E., Wink, M. and El-Readi, M. Z. (2020). "The carotenoid fucoxanthin can sensitize multidrug resistant cancer cells to doxorubicin via induction of apoptosis, inhibition of multidrug resistance proteins and metabolic enzymes." *Phytomedicine* 77: 153280. 10.1016/j.phymed.2020.153280.

- Eid, S. Y., El-Readi, M. Z. and Wink, M. (2012). "Carotenoids reverse multidrug resistance in cancer cells by interfering with ABC-transporters." *Phytomedicine* 19(11): 977-987. 10.1016/j.phymed.2012.05.010.
- Eilenberger, C., Kratz, S. R. A., Rothbauer, M., Ehmoser, E. K., Ertl, P. and Küpcü, S. (2018). "Optimized alamarBlue assay protocol for drug dose-response determination of 3D tumor spheroids." *MethodsX* 5: 781-787. 10.1016/j.mex.2018.07.011.
- El-Demerdash, A., Atanasov, A. G., Horbanczuk, O. K., Tammam, M. A., Abdel-Mogib, M., Hooper, J. N. A., Sekeroglu, N., Al-Mourabit, A., et al. (2019). "Chemical diversity and biological activities of marine sponges of the genus suberea: A systematic review." *Mar. Drugs* 17(2): 115. 10.3390/md17020115.
- El Hassouni, B., Franczak, M., Capula, M., Vonk, C. M., Gomez, V. M., Smolenski, R. T., Granchi, C., Peters, G. J., et al. (2020). "Lactate dehydrogenase A inhibition by small molecular entities: steps in the right direction." *Oncoscience* 7(9-10): 76-80. 10.18632/oncoscience.519.
- Engel, A., Frenzel, F., Niemann, B., Braeuning, A., Lampen, A. and Buhrke, T. (2019). "The use of 3D cultures of MCF-10A and MCF-12A cells by high content screening for effect-based analysis of non-genotoxic carcinogens." *Toxicol. In Vitro* 59: 55-63. 10.1016/j.tiv.2019.04.008.
- Ercolano, G., De Cicco, P. and Ianaro, A. (2019). "New drugs from the sea: Pro-apoptotic activity of sponges and algae derived compounds." *Mar. Drugs* 17(1): 31. 10.3390/md17010031.
- Ermakova, S., Sokolova, R., Kim, S. M., Um, B. H., Isakov, V. and Zvyagintseva, T. (2011). "Fucoïdians from brown seaweeds *Sargassum hornery*, *Eclonia cava*, *Costaria costata*: structural characteristics and anticancer activity." *Appl. Biochem. Biotechnol.* 164(6): 841-850. 10.1007/s12010-011-9178-2.
- Escriva-de-Romani, S., Arumi, M., Bellet, M. and Saura, C. (2018). "HER2-positive breast cancer: Current and new therapeutic strategies." *Breast* 39: 80-88. 10.1016/j.breast.2018.03.006.
- Esteva, F. J., Hubbard-Lucey, V. M., Tang, J. and Puzstai, L. (2019). "Immunotherapy and targeted therapy combinations in metastatic breast cancer." *Lancet Oncol.* 20(3): e175-e186. 10.1016/s1470-2045(19)30026-9.
- Fang, Y. and Eglen, R. M. (2017). "Three-dimensional cell cultures in drug discovery and development." *SLAS Discov.* 22(5): 456-472. 10.1177/1087057117696795.
- Farruggia, C., Kim, M. B., Bae, M., Lee, Y., Pham, T. X., Yang, Y., Han, M. J., Park, Y. K., et al. (2018). "Astaxanthin exerts anti-inflammatory and antioxidant effects in



- macrophages in NRF2-dependent and independent manners." *J. Nutr. Biochem.* 62: 202-209. 10.1016/j.jnutbio.2018.09.005.
- Fentiman, I. S., Fourquet, A. and Hortobagyi, G. N. (2006). "Male breast cancer." *Lancet* 367(9510): 595-604. 10.1016/s0140-6736(06)68226-3.
- Fernando, I. N., Bowden, S. J., Herring, K., Brookes, C. L., Ahmed, I., Marshall, A., Grieve, R., Churn, M., et al. (2020). "Synchronous versus sequential chemoradiotherapy in patients with early stage breast cancer (SECRAB): A randomised, phase III, trial." *Radiother. Oncol.* 142: 52-61. 10.1016/j.radonc.2019.10.014.
- Fernando, I. P. S., Jayawardena, T. U., Kim, H. S., Lee, W. W., Vaas, A., De Silva, H. I. C., Abayaweera, G. S., Nanayakkara, C. M., et al. (2019). "Beijing urban particulate matter-induced injury and inflammation in human lung epithelial cells and the protective effects of fucosterol from *Sargassum binderi* (Sonder ex J. Agardh)." *Environ. Res.* 172: 150-158. 10.1016/j.envres.2019.02.016.
- Ferreira, L. P., Gaspar, V. M. and Mano, J. F. (2018). "Design of spherically structured 3D in vitro tumor models -Advances and prospects." *Acta Biomater.* 75: 11-34. 10.1016/j.actbio.2018.05.034.
- Fitton, J. H., Stringer, D. N. and Karpiniec, S. S. (2015). "Therapies from fucoidan: An update." *Mar. Drugs* 13(9): 5920-5946. 10.3390/md13095920.
- Fitzpatrick, P. A., Akrap, N., Söderberg, E. M. V., Harrison, H., Thomson, G. J. and Landberg, G. (2017). "Robotic mammosphere assay for high-throughput screening in triple-negative breast cancer." *SLAS Discov.* 22(7): 827-836. 10.1177/2472555217692321.
- Fong, E. L. S., Toh, T. B., Yu, H. and Chow, E. K. (2017). "3D culture as a clinically relevant model for personalized medicine." *SLAS Technol.* 22(3): 245-253. 10.1177/2472630317697251.
- Fouad, M. A., Sayed-Ahmed, M. M., Huwait, E. A., Hafez, H. F. and Osman, A.-M. M. (2021). "Epigenetic immunomodulatory effect of eugenol and astaxanthin on doxorubicin cytotoxicity in hormonal positive breast cancer cells." *BMC Pharmacol. Toxicol.* 22(1): 8. 10.1186/s40360-021-00473-2.
- Foucquier, J. and Guedj, M. (2015). "Analysis of drug combinations: current methodological landscape." *Pharmacol. Res. Perspect.* 3(3): e00149. 10.1002/prp2.149.
- Fougner, C., Bergholtz, H., Norum, J. H. and Sørli, T. (2020). "Re-definition of claudin-low as a breast cancer phenotype." *Nat. Commun.* 11(1): 1787. 10.1038/s41467-020-15574-5.

- Fragomeni, S. M., Sciallis, A. and Jeruss, J. S. (2018). "Molecular subtypes and local-regional control of breast cancer." *Surg. Oncol. Clin. N. Am.* 27(1): 95-120. 10.1016/j.soc.2017.08.005.
- Frearson, J. and Wyatt, P. (2010). "Drug discovery in Academia- the third way?" *Expert Opin. Drug Discov.* 5(10): 909-919. 10.1517/17460441.2010.506508.
- Freshney, R. I. (2010). *Culture of animal cells: A Manual of Basic Technique and Specialized Applications*, 6<sup>th</sup> Edition, Wiley-Blackwell.
- Friedrich, J., Ebner, R. and Kunz-Schughart, L. A. (2007). "Experimental anti-tumor therapy in 3-D: spheroids-old hat or new challenge?" *Int. J. Radiat. Biol.* 83(11-12): 849-871. 10.1080/09553000701727531.
- Friedrich, J., Seidel, C., Ebner, R. and Kunz-Schughart, L. A. (2009). "Spheroid-based drug screen: considerations and practical approach." *Nat. Protoc.* 4(3): 309-324. 10.1038/nprot.2008.226.
- Froehlich, K., Haeger, J. D., Heger, J., Pastuschek, J., Photini, S. M., Yan, Y., Lupp, A., Pfarrer, C., et al. (2016). "Generation of multicellular breast cancer tumor spheroids: Comparison of different protocols." *J. Mammary Gland Biol. Neoplasia* 21(3-4): 89-98. 10.1007/s10911-016-9359-2.
- Funahashi, H., Imai, T., Mase, T., Sekiya, M., Yokoi, K., Hayashi, H., Shibata, A., Hayashi, T., et al. (2001). "Seaweed prevents breast cancer?" *J. Cancer Res.* 92(5): 483-487. 10.1111/j.1349-7006.2001.tb01119.x.
- Gaillard, S., Oaknin, A., Ray-Coquard, I., Vergote, I., Scambia, G., Colombo, N., Fernandez, C., Alfaro, V., et al. (2021). "Lurbinectedin versus pegylated liposomal doxorubicin or topotecan in patients with platinum-resistant ovarian cancer: A multicenter, randomized, controlled, open-label phase 3 study (CORAIL)." *Gynecol. Oncol.* 163(2): 237-245. 10.1016/j.ygyno.2021.08.032.
- Galasso, C., Corinaldesi, C. and Sansone, C. (2017). "Carotenoids from marine organisms: Biological functions and industrial applications." *Antioxidants* 6(4): 96. 10.3390/antiox6040096.
- Gamal-Eldeen, A. M., Ahmed, E. F. and Abo-Zeid, M. A. (2009). "In vitro cancer chemopreventive properties of polysaccharide extract from the brown alga, *Sargassum latifolium*." *Food Chem. Toxicol.* 47(6): 1378-1384. 10.1016/j.fct.2009.03.016.
- Gammone, M. A. and D'Orazio, N. (2015). "Anti-obesity activity of the marine carotenoid fucoxanthin." *Mar. Drugs* 13(4): 2196-2214. 10.3390/md13042196.
- Ganesan, A. R., Tiwari, U. and Rajauria, G. (2019). "Seaweed nutraceuticals and their therapeutic role in disease prevention." *Food Sci. Hum. Wellness.* 8(3): 252-263. 10.1016/j.fshw.2019.08.001.

- Gao, W., Wu, D., Wang, Y., Wang, Z., Zou, C., Dai, Y., Ng, C.-F., Teoh, J. Y.-C., et al. (2018). "Development of a novel and economical agar-based non-adherent three-dimensional culture method for enrichment of cancer stem-like cells." *Stem Cell Res. Ther.* 9(1): 243. 10.1186/s13287-018-0987-x.
- Garg, S., Afzal, S., Elwakeel, A., Sharma, D., Radhakrishnan, N., Dhanjal, J. K., Sundar, D., Kaul, S. C., et al. (2019). "Marine carotenoid fucoxanthin possesses anti-metastasis activity: molecular evidence." *Mar. Drugs* 17(6): 338. 10.3390/md17060338.
- Gelfand, R., Vernet, D., Bruhn, K., Vadgama, J. and Gonzalez-Cadavid, N. F. (2016). "Long-term exposure of MCF-12A normal human breast epithelial cells to ethanol induces epithelial mesenchymal transition and oncogenic features." *Int. J. Oncol.* 48(6): 2399-2414. 10.3892/ijo.2016.3461.
- Gencoglu, M. F., Barney, L. E., Hall, C. L., Brooks, E. A., Schwartz, A. D., Corbett, D. C., Stevens, K. R. and Peyton, S. R. (2018). "Comparative study of multicellular tumor spheroid formation methods and implications for drug screening." *ACS Biomater. Sci. Eng.* 4(2): 410-420. 10.1021/acsbiomaterials.7b00069.
- Gerratana, L., Fanotto, V., Pelizzari, G., Agostinetto, E. and Puglisi, F. (2016). "Do platinum salts fit all triple negative breast cancers?" *Cancer Treat. Rev.* 48: 34-41. 10.1016/j.ctrv.2016.06.004.
- Gest, C., Joimel, U., Huang, L., Pritchard, L. L., Petit, A., Dulong, C., Buquet, C., Hu, C. Q., et al. (2013). "Rac3 induces a molecular pathway triggering breast cancer cell aggressiveness: differences in MDA-MB-231 and MCF-7 breast cancer cell lines." *BMC Cancer* 13: 63. 10.1186/1471-2407-13-63.
- Gille, A., Stojnic, B., Derwenskus, F., Trautmann, A., Schmid-Staiger, U., Posten, C., Briviba, K., Palou, A., et al. (2019). "A lipophilic fucoxanthin-rich *Phaeodactylum tricornutum* extract ameliorates effects of diet-induced obesity in C57BL/6J mice." *Nutrients* 11(4): 796. 10.3390/nu11040796.
- Ginsburg, O., Yip, C.-H., Brooks, A., Cabanes, A., Caleffi, M., Dunstan Yataco, J. A., Gyawali, B., McCormack, V., et al. (2020). "Breast cancer early detection: A phased approach to implementation." *Cancer* 126(S10): 2379-2393. 10.1002/cncr.32887.
- Godoy-Ortiz, A., Sanchez-Munoz, A., Chica Parrado, M. R., Alvarez, M., Ribelles, N., Rueda Dominguez, A. and Alba, E. (2019). "Deciphering HER2 breast cancer disease: Biological and clinical implications." *Front. Oncol.* 9: 1124. 10.3389/fonc.2019.01124.
- Gomes, N. G. M., Madureira-Carvalho, Á., Dias-da-Silva, D., Valentão, P. and Andrade, P. B. (2021). "Biosynthetic versatility of marine-derived fungi on the delivery of novel

- antibacterial agents against priority pathogens." *Biomed. Pharmacother.* 140: 111756. 10.1016/j.biopha.2021.111756.
- Gomes, N. G. M., Valentão, P., Andrade, P. B. and Pereira, R. B. (2020). "Plitidepsin to treat multiple myeloma." *Drugs Today* 56(5): 337-347. 10.1358/dot.2020.56.5.3135886.
- Gordon, E. M., Sankhala, K. K., Chawla, N. and Chawla, S. P. (2016). "Trabectedin for soft tissue sarcoma: Current status and future perspectives." *Adv. Ther.* 33(7): 1055-1071. 10.1007/s12325-016-0344-3.
- Goss Kinzy, T., Harger, J. W., Carr-Schmid, A., Kwon, J., Shastry, M., Justice, M. and Dinman, J. D. (2002). "New targets for antivirals: the ribosomal A-site and the factors that interact with it." *Virology* 300(1): 60-70. 10.1006/viro.2002.1567.
- Gote, V., Nookala, A. R., Bolla, P. K. and Pal, D. (2021). "Drug resistance in metastatic breast cancer: Tumor targeted nanomedicine to the rescue." *Int. J. Mol. Sci.* 22(9): 4673. 10.3390/ijms22094673.
- Greenlee, H., Kwan, M. L., Kushi, L. H., Song, J., Castillo, A., Weltzien, E., Quesenberry, C. P., Jr. and Caan, B. J. (2012). "Antioxidant supplement use after breast cancer diagnosis and mortality in the Life After Cancer Epidemiology (LACE) cohort." *Cancer* 118(8): 2048-2058. 10.1002/cncr.26526.
- Grimaldi, A. M., Conte, F., Pane, K., Fiscon, G., Mirabelli, P., Baselice, S., Giannatiempo, R., Messina, F., et al. (2020). "The new paradigm of network medicine to analyze breast cancer phenotypes." *Int. J. Mol. Sci.* 21(18): 6690. 10.3390/ijms21186690.
- Grimmig, B., Kim, S. H., Nash, K., Bickford, P. C. and Douglas Shytle, R. (2017). "Neuroprotective mechanisms of astaxanthin: a potential therapeutic role in preserving cognitive function in age and neurodegeneration." *Geroscience* 39(1): 19-32. 10.1007/s11357-017-9958-x.
- Griñan-Lison, C., Blaya-Cánovas, J. L., López-Tejada, A., Ávalos-Moreno, M., Navarro-Ocón, A., Cara, F. E., González-González, A., Lorente, J. A., et al. (2021). "Antioxidants for the treatment of breast cancer: Are we there yet?" *Antioxidants* 10(2): 205. 10.3390/antiox10020205.
- Gu, B. B., Jiao, F. R., Wu, W., Jiao, W. H., Li, L., Sun, F., Wang, S. P., Yang, F., et al. (2018). "Preussins with inhibition of IL-6 expression from *Aspergillus flocculosus* 16D-1, a fungus isolated from the marine sponge *Phakellia fusca*." *J. Nat. Prod.* 81(10): 2275-2281. 10.1021/acs.jnatprod.8b00662.
- Gucalp, A., Traina, T. A., Eisner, J. R., Parker, J. S., Selitsky, S. R., Park, B. H., Elias, A. D., Baskin-Bey, E. S., et al. (2019). "Male breast cancer: a disease distinct from female breast cancer." *Breast Cancer Res. Treat.* 173(1): 37-48. 10.1007/s10549-018-4921-9.

- Guzmán, E. A., Pitts, T. P., Winder, P. L. and Wright, A. E. (2021). "The marine natural product furospinulosin 1 induces apoptosis in MDA-MB-231 triple negative breast cancer cell spheroids, but not in cells grown traditionally with longer treatment." *Mar. Drugs* 19(5): 249. 10.3390/md19050249.
- Halfter, K., Hoffmann, O., Ditsch, N., Ahne, M., Arnold, F., Paepke, S., Grab, D., Bauerfeind, I., et al. (2016). "Testing chemotherapy efficacy in HER2 negative breast cancer using patient-derived spheroids." *J. Transl. Med.* 14(1): 112. 10.1186/s12967-016-0855-3.
- Han, H., Lim, J. W. and Kim, H. (2020). "Astaxanthin inhibits Helicobacter pylori-induced inflammatory and oncogenic responses in gastric mucosal tissues of mice." *J. Cancer Prev.* 25(4): 244-251. 10.15430/jcp.2020.25.4.244.
- Han, M. H., Lee, D. S., Jeong, J. W., Hong, S. H., Choi, I. W., Cha, H. J., Kim, S., Kim, H. S., et al. (2017). "Fucoidan induces ROS-dependent apoptosis in 5637 human bladder cancer cells by downregulating telomerase activity via inactivation of the PI3K/Akt signaling pathway." *Drug Dev. Res.* 78(1): 37-48. 10.1002/ddr.21367.
- Han, Y. and Shi, S. (2016). "Protective effects of laminarin on cisplatin-induced ototoxicity in HEIOC1 auditory cells." *J. Nutr. Food Sci.* 6(4): 1-5. 10.4172/2155-9600.1000537.
- Han, Y. S., Lee, J. H. and Lee, S. H. (2015). "Fucoidan inhibits the migration and proliferation of HT-29 human colon cancer cells via the phosphoinositide-3 kinase/Akt/mechanistic target of rapamycin pathways." *Mol. Med. Rep.* 12(3): 3446-3452. 10.3892/mmr.2015.3804.
- Hannan, M. A., Dash, R., Sohag, A. A. M. and Moon, I. S. (2019). "Deciphering molecular mechanism of the neuropharmacological action of fucosterol through integrated system pharmacology and in silico analysis." *Mar. Drugs* 17(11): 0. 10.3390/md17110639.
- Harbeck, N., Penault-Llorca, F., Cortes, J., Gnant, M., Houssami, N., Poortmans, P., Ruddy, K., Tsang, J., et al. (2019). "Breast cancer." *Nat. Rev. Dis. Primers* 5(1): 66. 10.1038/s41572-019-0111-2.
- Hardin, C., Shum, E., Singh, A. P., Perez-Soler, R. and Cheng, H. (2017). "Emerging treatment using tubulin inhibitors in advanced non-small cell lung cancer." *Expert Opin. Pharmacother.* 18(7): 701-716. 10.1080/14656566.2017.1316374.
- Harma, V., Schukov, H. P., Happonen, A., Ahonen, I., Virtanen, J., Siitari, H., Akerfelt, M., Lotjonen, J., et al. (2014). "Quantification of dynamic morphological drug responses in 3D organotypic cell cultures by automated image analysis." *PLoS One* 9(5): e96426. 10.1371/journal.pone.0096426.

- Haroun-Bouhedja, F., Lindenmeyer, F., Lu, H., Soria, C., Jozefonvicz, J. and Boisson-Vidal, C. (2002). "In vitro effects of fucans on MDA-MB-231 tumor cell adhesion and invasion." *Anticancer Res.* 22(4): 2285-2292. PMID: 12174916.
- Hasanov, M., Rieth, M. J., Kendra, K., Hernandez-Aya, L., Joseph, R. W., Williamson, S., Chandra, S., Shirai, K., et al. (2020). "A Phase II study of Glembatumumab vedotin for metastatic uveal melanoma." *Cancers* 12(8): 2270. 10.3390/cancers12082270.
- Hashemi, S. H. B., Karimi, S. and Mahboobi, H. (2014). "Lifestyle changes for prevention of breast cancer." *Electron. Physician* 6(3): 894-905. 10.14661/2014.894-905.
- Hashimoto, T., Ozaki, Y., Mizuno, M., Yoshida, M., Nishitani, Y., Azuma, T., Komoto, A., Maoka, T., et al. (2012). "Pharmacokinetics of fucoxanthinol in human plasma after the oral administration of kombu extract." *Br. J. Nutr.* 107(11): 1566-1569. 10.1017/s0007114511004879.
- Hatem, E., Azzi, S., El Banna, N., He, T., Heneman-Masurel, A., Vernis, L., Baïlle, D., Masson, V., et al. (2018). "Auranofin/Vitamin C: A novel drug combination targeting triple-negative breast cancer." *J. Natl. Cancer. Inst.* 111(6): 597-608. 10.1093/jnci/djy149.
- Hay, M., Thomas, D. W., Craighead, J. L., Economides, C. and Rosenthal, J. (2014). "Clinical development success rates for investigational drugs." *Nat. Biotechnol.* 32(1): 40-51. 10.1038/nbt.2786.
- Hazlehurst, L. A. and Dalton, W. S. (2006). *De novo and acquired resistance to antitumor alkylating agents. Cancer Drug Resistance. B. A. Teicher.* Totowa, NJ Humana Press. 10.1007/978-1-59745-035-5\_20.
- He, X., Xue, M., Jiang, S., Li, W., Yu, J. and Xiang, S. (2019). "Fucoidan promotes apoptosis and inhibits EMT of breast cancer cells." *Biol. Pharm. Bull.* 42(3): 442-447. 10.1248/bpb.b18-00777.
- Heffernan, N., Brunton, N. P., FitzGerald, R. J. and Smyth, T. J. (2015). "Profiling of the molecular weight and structural isomer abundance of macroalgae-derived phlorotannins." *Mar. Drugs* 13(1): 509-528. 10.3390/md13010509.
- Heo, S. J. and Jeon, Y. J. (2009). "Protective effect of fucoxanthin isolated from *Sargassum siliquastrum* on UV-B induced cell damage." *J. Photochem. Photobiol. B* 95(2): 101-107. 10.1016/j.jphotobiol.2008.11.011.
- Hernando, C., Ortega-Morillo, B., Tapia, M., Moragón, S., Martínez, M. T., Eroles, P., Garrido-Cano, I., Adam-Artigues, A., et al. (2021). "Oral selective estrogen receptor degraders (SERDs) as a novel breast cancer therapy: Present and future from a clinical perspective." *Int. J. Mol. Sci.* 22(15): 7812. 10.3390/ijms22157812.

- Hero, T., Buhler, H., Kouam, P. N., Priesch-Grzeszowiak, B., Lateit, T. and Adamietz, I. A. (2019). "The triple-negative breast cancer cell line MDA-MB 231 is specifically inhibited by the Ionophore Salinomycin." *Anticancer Res.* 39(6): 2821. 10.21873/anticancer.13410.
- Herschkowitz, J. I., Simin, K., Weigman, V. J., Mikaelian, I., Usary, J., Hu, Z., Rasmussen, K. E., Jones, L. P., et al. (2007). "Identification of conserved gene expression features between murine mammary carcinoma models and human breast tumors." *Genome Biol.* 8(5): R76. 10.1186/gb-2007-8-5-r76.
- Hickey, B. E., Francis, D. P. and Lehman, M. (2013). "Sequencing of chemotherapy and radiotherapy for early breast cancer." *Cochrane Database Syst. Rev.* 30;(4):CD005212. 10.1002/14651858.CD005212.pub3.
- Hickman, J. A., Graeser, R., de Hoogt, R., Vidic, S., Brito, C., Gutekunst, M. and van der Kuip, H. (2014). "Three-dimensional models of cancer for pharmacology and cancer cell biology: capturing tumor complexity in vitro/ex vivo." *Biotechnol. J.* 9(9): 1115-1128. 10.1002/biot.201300492.
- Hira, V. V. V., Breznik, B., Van Noorden, C. J. F., Lah, T. and Molenaar, R. J. (2020). "2D and 3D in vitro assays to quantify the invasive behavior of glioblastoma stem cells in response to SDF-1 $\alpha$ ." *BioTechniques* 69(5): 339-346. 10.2144/btn-2020-0046.
- Hirschhaeuser, F., Menne, H., Dittfeld, C., West, J., Mueller-Klieser, W. and Kunz-Schughart, L. A. (2010). "Multicellular tumor spheroids: An underestimated tool is catching up again." *J. Biotechnol.* 148(1): 3-15. 10.1016/j.jbiotec.2010.01.012.
- Ho, W. Y., Yeap, S. K., Ho, C. L., Rahim, R. A. and Alitheen, N. B. (2012). "Development of multicellular tumor spheroid (MCTS) culture from breast cancer cell and a high throughput screening method using the MTT assay." *PLoS One* 7(9): e44640. 10.1371/journal.pone.0044640.
- Hoffman, R., Paper, D. H., Donaldson, J. and Vogl, H. (1996). "Inhibition of angiogenesis and murine tumour growth by laminarin sulphate." *Br. J. Cancer* 73(10): 1183-1186. 10.1038/bjc.1996.228.
- Holbrook, A. M., Pereira, J. A., Labiris, R., McDonald, H., Douketis, J. D., Crowther, M. and Wells, P. S. (2005). "Systematic overview of warfarin and its drug and food interactions." *Arch. Intern. Med.* 165(10): 1095-1106. 10.1001/archinte.165.10.1095.
- Holliday, D. L. and Speirs, V. (2011). "Choosing the right cell line for breast cancer research." *Breast Cancer Res.* 13(4): 215. 10.1186/bcr2889.
- Hosokawa, M., Kudo, M., Maeda, H., Kohno, H., Tanaka, T. and Miyashita, K. (2004). "Fucoxanthin induces apoptosis and enhances the antiproliferative effect of the

- PPARgamma ligand, troglitazone, on colon cancer cells." *Biochim. Biophys. Acta* 1675(1-3): 113-119. 10.1016/j.bbagen.2004.08.012.
- Howes, A. L., Richardson, R. D., Finlay, D. and Vuori, K. (2014). "3-Dimensional culture systems for anti-cancer compound profiling and high-throughput screening reveal increases in EGFR inhibitor-mediated cytotoxicity compared to monolayer culture systems." *PLoS One* 9(9): e108283. 10.1371/journal.pone.0108283.
- Hsu, H. Y., Lin, T. Y., Hu, C. H., Shu, D. T. F. and Lu, M. K. (2018). "Fucoidan upregulates TLR4/CHOP-mediated caspase-3 and PARP activation to enhance cisplatin-induced cytotoxicity in human lung cancer cells." *Cancer Lett.* 432: 112-120. 10.1016/j.canlet.2018.05.006.
- Hsu, H. Y., Lin, T. Y., Hwang, P. A., Tseng, L. M., Chen, R. H., Tsao, S. M. and Hsu, J. (2013). "Fucoidan induces changes in the epithelial to mesenchymal transition and decreases metastasis by enhancing ubiquitin-dependent TGFbeta receptor degradation in breast cancer." *Carcinogenesis* 34(4): 874-884. 10.1093/carcin/bgs396.
- Hsu, W.-J., Lin, M.-H., Kuo, T.-C., Chou, C.-M., Mi, F.-L., Cheng, C.-H. and Lin, C.-W. (2020). "Fucoidan from *Laminaria japonica* exerts antitumor effects on angiogenesis and micrometastasis in triple-negative breast cancer cells." *Int. J. Biol. Macromol.* 149: 600-608. 10.1016/j.ijbiomac.2020.01.256.
- Hu, X., Tao, N., Wang, X., Xiao, J. and Wang, M. (2016). "Marine-derived bioactive compounds with anti-obesity effect: A review." *J. Funct. Foods* 21: 372-387. 10.1016/j.jff.2015.12.006.
- Huang, L., Wen, K., Gao, X. and Liu, Y. (2010). "Hypolipidemic effect of fucoidan from *Laminaria japonica* in hyperlipidemic rats." *Pharm. Biol.* 48(4): 422-426. 10.3109/13880200903150435.
- Huang, P.-Q., Geng, H., Tian, Y.-S., Peng, Q.-R. and Xiao, K.-J. (2015). "The first enantioselective total synthesis of (+)-preussin B and an improved synthesis of (+)-preussin by step-economical methods." *Sci. China Chem.* 58(3): 478-482. 10.1007/s11426-014-5270-0.
- Huang, Z., Yu, P. and Tang, J. (2020). "Characterization of triple-negative breast cancer MDA-MB-231 cell spheroid model." *OncoTargets Ther.* 13: 5395-5405. 10.2147/OTT.S249756.
- Hughes, J. P., Rees, S., Kalindjian, S. B. and Philpott, K. L. (2011). "Principles of early drug discovery." *Br. J. Pharmacol.* 162(6): 1239-1249. 10.1111/j.1476-5381.2010.01127.x.
- Huo, X., Li, J., Zhao, F., Ren, D., Ahmad, R., Yuan, X., Du, F. and Zhao, J. (2021). "The role of capecitabine-based neoadjuvant and adjuvant chemotherapy in early-stage



- triple-negative breast cancer: a systematic review and meta-analysis." *BMC Cancer* 21(1): 78. 10.1186/s12885-021-07791-y.
- Hussein, G., Sankawa, U., Goto, H., Matsumoto, K. and Watanabe, H. (2006). "Astaxanthin, a carotenoid with potential in human health and nutrition." *J. Nat. Prod.* 69(3): 443-449. 10.1021/np050354+.
- IARC. Retrieved 4<sup>th</sup> October 2021, available from [https://gco.iarc.fr/today/online-analysispie?v=2020&mode=cancer&mode\\_population=continents&population=900&populations=900&key=total&sex=2&cancer=39&type=0&statistic=5&prevalence=0&population\\_group=0&ages\\_group%5B%5D=0&ages\\_group%5B%5D=17&nb\\_items=7&group\\_cancer=1&include\\_nmsc=1&include\\_nmsc\\_other=1&half\\_pie=0&donut=0](https://gco.iarc.fr/today/online-analysispie?v=2020&mode=cancer&mode_population=continents&population=900&populations=900&key=total&sex=2&cancer=39&type=0&statistic=5&prevalence=0&population_group=0&ages_group%5B%5D=0&ages_group%5B%5D=17&nb_items=7&group_cancer=1&include_nmsc=1&include_nmsc_other=1&half_pie=0&donut=0).
- Iglesias, J. M., Beloqui, I., Garcia-Garcia, F., Leis, O., Vazquez-Martin, A., Eguiara, A., Cufi, S., Pavon, A., et al. (2013). "Mammosphere formation in breast carcinoma cell lines depends upon expression of E-cadherin." *PLoS One* 8(10): e77281. 10.1371/journal.pone.0077281.
- Iino, K., Okada, Y. and Ishikura, M. (2011). "Single and 13-week oral toxicity study of fucoxanthin oil from microalgae in rats." *Shokuhin Eiseigaku Zasshi* 52(3): 183-189. 10.3358/shokueishi.52.183.
- Ikeguchi, M., Yamamoto, M., Arai, Y., Maeta, Y., Ashida, K., Katano, K., Miki, Y. and Kimura, T. (2011). "Fucoidan reduces the toxicities of chemotherapy for patients with unresectable advanced or recurrent colorectal cancer." *Oncol. Lett.* 2(2): 319-322. 10.3892/ol.2011.254.
- Imamura, Y., Mukohara, T., Shimono, Y., Funakoshi, Y., Chayahara, N., Toyoda, M., Kiyota, N., Takao, S., et al. (2015). "Comparison of 2D- and 3D-culture models as drug-testing platforms in breast cancer." *Oncol. Rep.* 33(4): 1837-1843. 10.3892/or.2015.3767.
- Insua-Rodríguez, J. and Oskarsson, T. (2016). "The extracellular matrix in breast cancer." *Adv. Drug Deliv. Rev.* 97: 41-55. 10.1016/j.addr.2015.12.017.
- Ishikawa, C., Tafuku, S., Kadekaru, T., Sawada, S., Tomita, M., Okudaira, T., Nakazato, T., Toda, T., et al. (2008). "Anti-adult T-cell leukemia effects of brown algae fucoxanthin and its deacetylated product, fucoxanthinol." *Int. J. Cancer* 123(11): 2702-2712. 10.1002/ijc.23860.
- Ivascu, A. and Kubbies, M. (2006). "Rapid generation of single-tumor spheroids for high-throughput cell function and toxicity analysis." *J. Biomol. Screen.* 11(8): 922-932. 10.1177/1087057106292763.
- Ivascu, A. and Kubbies, M. (2007). "Diversity of cell-mediated adhesions in breast cancer spheroids." *Int. J. Oncol.* 31(6): 1403-1413. PMID: 17982667

- Jang, H., Choi, J., Park, J. K., Won, G. and Seol, J. W. (2021). "Fucoxanthin exerts anti-tumor activity on canine mammary tumor cells via tumor cell apoptosis induction and angiogenesis inhibition." *Animals* 11(6): 1512. 10.3390/ani11061512.
- Jayawardena, T. U., Sanjeewa, K. K. A., Lee, H.-G., Nagahawatta, D. P., Yang, H.-W., Kang, M.-C. and Jeon, Y.-J. (2020). "Particulate matter-induced inflammation/oxidative stress in macrophages: Fucosterol from *Padina boryana* as a potent protector, activated via NF- $\kappa$ B/MAPK pathways and Nrf2/HO-1 involvement." *Mar. Drugs* 18(12): 628. 10.3390/md18120628.
- Jensen, C. and Teng, Y. (2020). "Is it time to start transitioning from 2D to 3D cell culture?" *Front. Mol. Biosci.* 7: 33. 10.3389/fmolb.2020.00033.
- Jesumani, V., Du, H., Aslam, M., Pei, P. and Huang, N. (2019). "Potential use of seaweed bioactive compounds in skincare - A review." *Mar. Drugs* 17(12): 688. 10.3390/md17120688.
- Jeukendrup, A. E. and Randell, R. (2011). "Fat burners: nutrition supplements that increase fat metabolism." *Obes. Rev.* 12(10): 841-851. 10.1111/j.1467-789X.2011.00908.x.
- Jha, R. K. and Zi-rong, X. (2004). "Biomedical compounds from marine organisms." *Mar. Drugs* 2(3): 123-146. PMID: PMC3783866.
- Ji, C. F. and Ji, Y. B. (2014). "Laminarin-induced apoptosis in human colon cancer LoVo cells." *Oncol. Lett.* 7(5): 1728-1732. 10.3892/ol.2014.1952.
- Ji, C. F., Ji, Y. B. and Meng, D. Y. (2013). "Sulfated modification and anti-tumor activity of laminarin." *Exp. Ther. Med.* 6(5): 1259-1264. 10.3892/etm.2013.1277.
- Ji, X., Lu, Y., Tian, H., Meng, X., Wei, M. and Cho, W. C. (2019). "Chemoresistance mechanisms of breast cancer and their countermeasures." *Biomed. Pharmacother.* 114: 108800. 10.1016/j.biopha.2019.108800.
- Ji, Y., Bi, J.-N., Yan, B. and Zhu, X.-D. (2006). "Taxol-producing fungi: A new approach to industrial production of taxol." *Chin. J. Biotechnol.* 22(1): 1-6. 10.1016/S1872-2075(06)60001-0.
- Ji, Y. B., Ji, C. F. and Yue, L. (2014). "Study on human promyelocytic leukemia HL-60 cells apoptosis induced by fucosterol." *Biomed. Mater. Eng.* 24(1): 845-851. 10.3233/BME-130876.
- Jiang, H., Li, J., Chen, A., Li, Y., Xia, M., Guo, P., Yao, S. and Chen, S. (2018). "Fucosterol exhibits selective antitumor anticancer activity against HeLa human cervical cell line by inducing mitochondrial mediated apoptosis, cell cycle migration inhibition and downregulation of m-TOR/PI3K/Akt signalling pathway." *Oncol. Lett* 15(3): 3458-3463. 10.3892/ol.2018.7769.

- Jiang, Y., Xie, Q. and Chen, R. (2021). "Breast cancer incidence and mortality in relation to hormone replacement therapy use among postmenopausal women: Results from a prospective cohort study." *Clin. Breast Cancer* 26: S1526-8209(1521)00171-00173. 10.1016/j.clbc.2021.06.010.
- Jimenez, P. C., Wilke, D. V., Branco, P. C., Bauermeister, A., Rezende-Teixeira, P., Gaudêncio, S. P. and Costa-Lotufu, L. V. (2020). "Enriching cancer pharmacology with drugs of marine origin." *Br. J. Pharmacol.* 177(1): 3-27. 10.1111/bph.14876.
- Jimenez, P. C., Wilke, D. V. and Costa-Lotufu, L. V. (2018). "Marine drugs for cancer: Surfacing biotechnological innovations from the oceans." *Clinics* 73(suppl 1): e482s. 10.6061/clinics/2018/e482s.
- Jin, J. O., Song, M. G., Kim, Y. N., Park, J. I. and Kwak, J. Y. (2010). "The mechanism of fucoidan-induced apoptosis in leukemic cells: involvement of ERK1/2, JNK, glutathione, and nitric oxide." *Mol. Carcinog.* 49(8): 771-782. 10.1002/mc.20654.
- Jin, J. O., Zhang, W., Du, J. Y., Wong, K. W., Oda, T. and Yu, Q. (2014). "Fucoidan can function as an adjuvant in vivo to enhance dendritic cell maturation and function and promote antigen-specific T cell immune responses." *PLoS One* 9(6): e99396. 10.1371/journal.pone.0099396.
- Jin, L., Quan, C., Hou, X. and Fan, S. (2016). "Potential pharmacological resources: Natural bioactive compounds from marine-derived fungi." *Mar. Drugs* 14(4): 76.10.3390/md14040076.
- John Hopkins Medicine Pathology (2021). "Staging & Grade Breast Cancer. Retrieved 28<sup>th</sup>.October 2022, available from <https://pathology.jhu.edu/breast/staging-grade>.
- Johnson, J. H., Phillipson, D. W. and Kahle, A. D. (1989). "The relative and absolute stereochemistry of the antifungal agent preussin." *J. Antibiot. (Tokyo)* 42(7): 1184-1185. 10.7164/antibiotics.42.1184.
- Jordan, M. A. and Wilson, L. (2004). "Microtubules as a target for anticancer drugs." *Nat. Rev. Cancer* 4(4): 253-265. 10.1038/nrc1317.
- Jung, A. Y., Cai, X., Thoene, K., Obi, N., Jaskulski, S., Behrens, S., Flesch-Janys, D. and Chang-Claude, J. (2019). "Antioxidant supplementation and breast cancer prognosis in postmenopausal women undergoing chemotherapy and radiation therapy." *Am. J. Clin. Nutr.* 109(1): 69-78. 10.1093/ajcn/nqy223.
- Jung, H. A., Jin, S. E., Ahn, B. R., Lee, C. M. and Choi, J. S. (2013). "Anti-inflammatory activity of edible brown alga *Eisenia bicyclis* and its constituents fucosterol and phlorotannins in LPS-stimulated RAW264.7 macrophages." *Food Chem. Toxicol.* 59: 199-206. 10.1016/j.fct.2013.05.061.
- Jung, H. A., Jung, H. J., Jeong, H. Y., Kwon, H. J., Ali, M. Y. and Choi, J. S. (2014a). "Phlorotannins isolated from the edible brown alga *Ecklonia stolonifera* exert anti-

- adipogenic activity on 3T3-L1 adipocytes by downregulating C/EBP $\alpha$  and PPAR $\gamma$ ." *Fitoterapia* 92: 260-269. 10.1016/j.fitote.2013.12.003.
- Jung, H. A., Kim, J. I., Choung, S. Y. and Choi, J. S. (2014b). "Protective effect of the edible brown alga *Ecklonia stolonifera* on doxorubicin-induced hepatotoxicity in primary rat hepatocytes." *J. Pharm. Pharmacol.* 66(8): 1180-1188. 10.1111/jphp.12241.
- Jyonouchi, H., Sun, S., Iijima, K. and Gross, M. D. (2000). "Antitumor activity of astaxanthin and its mode of action." *Nutr. Cancer* 36(1): 59-65. 10.1207/S15327914NC3601\_9.
- Kadam, S. U., O'Donnell, C. P., Rai, D. K., Hossain, M. B., Burgess, C. M., Walsh, D. and Tiwari, B. K. (2015a). "Laminarin from Irish brown seaweeds *Ascophyllum nodosum* and *Laminaria hyperborea*: Ultrasound assisted extraction, characterization and bioactivity." *Mar. Drugs* 13(7): 4270-4280. 10.3390/md13074270.
- Kadam, S. U., Tiwari, B. K. and O'Donnell, C. P. (2015b). "Extraction, structure and biofunctional activities of laminarin from brown algae." *J. Food Sci. Technol.* 50(1): 24-31. 10.1111/ijfs.12692.
- Kallioniemi, O. P., Kallioniemi, A., Kurisu, W., Thor, A., Chen, L. C., Smith, H. S., Waldman, F. M., Pinkel, D., et al. (1992). "ERBB2 amplification in breast cancer analyzed by fluorescence in situ hybridization." *Proc. Natl. Acad. Sci. USA* 89(12): 5321-5325. 10.1073/pnas.89.12.5321.
- Kang, C. and Syed, Y. Y. (2020). "Atezolizumab (in combination with nab-paclitaxel): A review in advanced triple-negative breast cancer." *Drugs* 80(6): 601-607. 10.1007/s40265-020-01295-y.
- Kang, K. A., Lee, K. H., Chae, S., Zhang, R., Jung, M. S., Ham, Y. M., Baik, J. S., Lee, N. H., et al. (2006). "Cytoprotective effect of phloroglucinol on oxidative stress induced cell damage via catalase activation." *J. Cell Biochem.* 97(3): 609-620. 10.1002/jcb.20668.
- Kang, M.-C., Ahn, G., Yang, X., Kim, K.-N., Kang, S.-M., Lee, S.-H., Ko, S.-C., Ko, J.-Y., et al. (2012a). "Hepatoprotective effects of dieckol-rich phlorotannins from *Ecklonia cava*, a brown seaweed, against ethanol induced liver damage in BALB/c mice." *Food Chem. Toxicol.* 50(6): 1986-1991. 10.1016/j.fct.2012.03.078.
- Kang, M. H., Kim, I. H. and Nam, T. J. (2014). "Phloroglucinol induces apoptosis via apoptotic signaling pathways in HT-29 colon cancer cells." *Oncol. Rep.* 32(4): 1341-1346. 10.3892/or.2014.3355.
- Kang, S. M., Cha, S. H., Ko, J. Y., Kang, M. C., Kim, D., Heo, S. J., Kim, J. S., Heu, M. S., et al. (2012b). "Neuroprotective effects of phlorotannins isolated from a brown

- alga, *Ecklonia cava*, against H<sub>2</sub>O<sub>2</sub>-induced oxidative stress in murine hippocampal HT22 cells." *Environ. Toxicol. Pharmacol.* 34(1): 96-105. 10.1016/j.etap.2012.03.006.
- Kao, J., Salari, K., Bocanegra, M., Choi, Y. L., Girard, L., Gandhi, J., Kwei, K. A., Hernandez-Boussard, T., et al. (2009). "Molecular profiling of breast cancer cell lines defines relevant tumor models and provides a resource for cancer gene discovery." *PLoS One* 4(7): e6146. 10.1371/journal.pone.0006146.
- Kapadia, G. J., Rao, G. S., Ramachandran, C., Iida, A., Suzuki, N. and Tokuda, H. (2013). "Synergistic cytotoxicity of red beetroot (*Beta vulgaris* L.) extract with doxorubicin in human pancreatic, breast and prostate cancer cell lines." *J. Complement. Integr. Med.* 10 :/j/jcim.2013.10.issue-1/jcim-2013-0007/jcim-2013-0007.xml. 10.1515/jcim-2013-0007.
- Kapalczyńska, M., Kolenda, T., Przybyła, W., Zajaczkowska, M., Teresiak, A., Filas, V., Ibbes, M., Blizniak, R., et al. (2018). "2D and 3D cell cultures - a comparison of different types of cancer cell cultures." *Arch. Med. Sci.* 14(4): 910-919. 10.5114/aoms.2016.63743.
- Karadeniz, F., Ahn, B.-N., Kim, J.-A., Seo, Y., Jang, M.-S., Nam, K.-H., Kim, M., Lee, S.-H., et al. (2015). "Phlorotannins suppress adipogenesis in pre-adipocytes while enhancing osteoblastogenesis in pre-osteoblasts." *Arch. Pharm. Res.* 38(12): 2172-2182. 10.1007/s12272-015-0637-0.
- Karimian, A., Mir Mohammadrezaei, F., Hajizadeh Moghadam, A., Bahadori, M. H., Ghorbani-Anarkooli, M., Asadi, A. and Abdolmaleki, A. (2022). "Effect of astaxanthin and melatonin on cell viability and DNA damage in human breast cancer cell lines." *Acta Histochem.* 124(1): 151832. 10.1016/j.acthis.2021.151832.
- Karpiński, T. M. and Adamczak, A. (2019). "Fucoxanthin-An antibacterial carotenoid." *Antioxidants* 24;8(8):239. 10.3390/antiox8080239.
- Kasahara, K., Yoshida, M., Eishima, J., Takesako, K., Beppu, T. and Horinouchi, S. (1997). "Identification of preussin as a selective inhibitor for cell growth of the fission yeast ts mutants defective in Cdc2-regulatory genes." *J. Antibiot.* 50(3): 267-269. PMID: 9127201
- Katt, M. E., Placone, A. L., Wong, A. D., Xu, Z. S. and Searson, P. C. (2016). "In vitro tumor models: Advantages, disadvantages, variables, and selecting the right platform." *Front. Bioeng. Biotechnol.* 4: 12. 10.3389/fbioe.2016.00012.
- Kaur, V., Kumar, M., Kumar, A., Kaur, K., Dhillon, V. S. and Kaur, S. (2018). "Pharmacotherapeutic potential of phytochemicals: Implications in cancer chemoprevention and future perspectives." *Biomed. Pharmacother.* 97: 564-586. 10.1016/j.biopha.2017.10.124.

- Keelan, S., Flanagan, M. and Hill, A. D. K. (2021). "Evolving trends in surgical management of breast cancer: An analysis of 30 years of practice changing papers." *Front. Oncol.* 11(1608): 622621. 10.3389/fonc.2021.622621.
- Kelm, J. M., Timmins, N. E., Brown, C. J., Fussenegger, M. and Nielsen, L. K. (2003). "Method for generation of homogeneous multicellular tumor spheroids applicable to a wide variety of cell types." *Biotechnol. Bioeng.* 83(2): 173-180. 10.1002/bit.10655.
- Kenny, P. A., Lee, G. Y., Myers, C. A., Neve, R. M., Semeiks, J. R., Spellman, P. T., Lorenz, K., Lee, E. H., et al. (2007). "The morphologies of breast cancer cell lines in three-dimensional assays correlate with their profiles of gene expression." *Mol. Oncol.* 1(1): 84-96. 10.1016/j.molonc.2007.02.004.
- Kepp, O., Zitvogel, L. and Kroemer, G. (2020). "Lurbinectedin: an FDA-approved inducer of immunogenic cell death for the treatment of small-cell lung cancer." *Oncoimmunology* 9(1): 1795995-1795995. 10.1080/2162402X.2020.1795995.
- Keyvani, S., Karimi, N., Orafa, Z., Bouzari, S. and Oloomi, M. (2016). "Assessment of cytokeratin-19 gene expression in peripheral blood of breast cancer patients and breast cancer cell lines." *Biomark Cancer.* 8: 57-63. 10.4137/BIC.S38229.
- Khaitan, D., Chandna, S., Arya, M. B. and Dwarakanath, B. S. (2006). "Establishment and characterization of multicellular spheroids from a human glioma cell line; Implications for tumor therapy." *J. Transl. Med.* 4: 12. 10.1186/1479-5876-4-12.
- Khan, F., Tabassum, N., Bamunuarachchi, N. I. and Kim, Y.-M. (2022). "Phloroglucinol and its derivatives: Antimicrobial properties toward microbial pathogens." *J. Agric. Food Chem.* 70(16): 4817-4838. 10.1021/acs.jafc.2c00532.
- Khan, T., Date, A., Chawda, H. and Patel, K. (2019). "Polysaccharides as potential anticancer agents - A review of their progress." *Carbohydr. Polym.* 210: 412-428. 10.1016/j.carbpol.2019.01.064.
- Khanavi, M., Gheidarloo, R., Sadati, N., Ardekani, M. R., Nabavi, S. M., Tavajohi, S. and Ostad, S. N. (2012). "Cytotoxicity of fucosterol containing fraction of marine algae against breast and colon carcinoma cell line." *Pharmacogn. Mag.* 8(29): 60-64. 10.4103/0973-1296.93327.
- Khaw, Y. S., Yusoff, F. M., Tan, H. T., Noor Mazli, N. A. I., Nazarudin, M. F., Shaharuddin, N. A. and Omar, A. R. (2021). "The critical studies of fucoxanthin research trends from 1928 to June 2021: A bibliometric review." *Mar. Drugs* 19(11): 606. 10.3390/md19110606.
- Khdair, A., Di, C., Patil, Y., Ma, L., Dou, Q. P., Shekhar, M. P. V. and Panyam, J. (2010). "Nanoparticle-mediated combination chemotherapy and photodynamic therapy overcomes tumor drug resistance." *J. Control Release* 141(2): 137-144. 10.1016/j.jconrel.2009.09.004.

- Khurana, R. K., Jain, A., Jain, A., Sharma, T., Singh, B. and Kesharwani, P. (2018). "Administration of antioxidants in cancer: debate of the decade." *Drug Discov Today* 23(4): 763-770. 10.1016/j.drudis.2018.01.021.
- Kim, E. J., Park, S. Y., Lee, J. Y. and Park, J. H. (2010a). "Fucoidan present in brown algae induces apoptosis of human colon cancer cells." *BMC Gastroenterol.* 10: 96. 10.1186/1471-230x-10-96.
- Kim, J. H., Lee, J. O., Moon, J. W., Kang, M. J., Byun, W. S., Han, J. A., Kim, S. J., Park, S. H., et al. (2020a). "Laminarin from *Salicornia herbacea* stimulates glucose uptake through AMPK-p38 MAPK pathways in L6 muscle Cells." *Nat. Prod. Commun.* 15(3). 10.1177/1934578x20901409.
- Kim, K. H., Kim, Y. W., Kim, H. B., Lee, B. J. and Lee, D. S. (2006). "Anti-apoptotic activity of laminarin polysaccharides and their enzymatically hydrolyzed oligosaccharides from *Laminaria japonica*." *Biotechnol. Lett.* 28(6): 439-446. 10.1007/s10529-005-6177-9.
- Kim, K. I., Lee, K. H., Kim, T. R., Chun, Y. S., Lee, T. H. and Park, H. K. (2014). "Ki-67 as a predictor of response to neoadjuvant chemotherapy in breast cancer patients." *J. Breast Cancer* 17(1): 40-46. 10.4048/jbc.2014.17.1.40.
- Kim, K. N., Heo, S. J., Yoon, W. J., Kang, S. M., Ahn, G., Yi, T. H. and Jeon, Y. J. (2010b). "Fucoxanthin inhibits the inflammatory response by suppressing the activation of NF- $\kappa$ B and MAPKs in lipopolysaccharide-induced RAW 264.7 macrophages." *Eur. J. Pharmacol.* 649(1-3): 369-375. 10.1016/j.ejphar.2010.09.032.
- Kim, M.-S., Oh, G.-H., Kim, M.-J. and Hwang, J.-K. (2013). "Fucosterol inhibits matrix metalloproteinase expression and promotes type-1 procollagen production in UVB-induced HaCaT cells." *Photochem. Photobiol.* 89(4): 911-918. 10.1111/php.12061.
- Kim, M. M. and Kim, S. K. (2010). "Effect of phloroglucinol on oxidative stress and inflammation." *Food Chem. Toxicol.* 48(10): 2925-2933. 10.1016/j.fct.2010.07.029.
- Kim, M. S., Ahn, Y. T., Lee, C. W., Kim, H. and An, W. G. (2020b). "Astaxanthin modulates apoptotic molecules to induce death of SKBR3 breast cancer cells." *Mar. Drugs* 18(5): 266. 10.3390/md18050266.
- Kim, R. K., Suh, Y., Yoo, K. C., Cui, Y. H., Hwang, E., Kim, H. J., Kang, J. S., Kim, M. J., et al. (2015a). "Phloroglucinol suppresses metastatic ability of breast cancer cells by inhibition of epithelial-mesenchymal cell transition." *Cancer Sci.* 106(1): 94-101. 10.1111/cas.12562.
- Kim, R. K., Uddin, N., Hyun, J. W., Kim, C., Suh, Y. and Lee, S. J. (2015b). "Novel anticancer activity of phloroglucinol against breast cancer stem-like cells." *Toxicol. Appl. Pharmacol.* 286(3): 143-150. 10.1016/j.taap.2015.03.026.

- Kimlin, L. C., Casagrande, G. and Virador, V. M. (2013). "In vitro three-dimensional (3D) models in cancer research: an update." *Mol. Carcinog.* 52(3): 167-182. 10.1002/mc.21844.
- Kirschbrown, W. P., Kågedal, M., Wang, B., Lindbom, L., Knott, A., Mack, R., Monemi, S., Nijem, I., et al. (2019). "Pharmacokinetic and exploratory exposure-response analysis of pertuzumab in patients with operable HER2-positive early breast cancer in the APHINITY study." *Cancer Chemother. Pharmacol.* 83(6): 1147-1158. 10.1007/s00280-019-03826-1.
- Kitaeva, K. V., Rutland, C. S., Rizvanov, A. A. and Solovyeva, V. V. (2020). "Cell culture based in vitro test systems for anticancer drug screening." *Front. Bioeng. Biotechnol.* 8: 322. 10.3389/fbioe.2020.00322.
- Kochanek, S. J., Close, D. A., Camarco, D. P. and Johnston, P. A. (2020). "Maximizing the value of cancer drug screening in multicellular tumor spheroid cultures: A case study in five head and neck squamous cell carcinoma cell lines." *SLAS Discov.* 25(4): 329-349. 10.1177/2472555219896999.
- Kong, C. S., Kim, J. A., Yoon, N. Y. and Kim, S. K. (2009). "Induction of apoptosis by phloroglucinol derivative from *Ecklonia cava* in MCF-7 human breast cancer cells." *Food Chem. Toxicol.* 47(7): 1653-1658. 10.1016/j.fct.2009.04.013.
- Kong, D., Hughes, C. J. and Ford, H. L. (2020). "Cellular plasticity in breast cancer progression and therapy." *Front. Mol. Biosci.* 7: 72. 10.3389/fmolb.2020.00072.
- Konishi, I., Hosokawa, M., Sashima, T., Kobayashi, H. and Miyashita, K. (2006). "Halocynthiaxanthin and fucoxanthinol isolated from *Halocynthia roretzi* induce apoptosis in human leukemia, breast and colon cancer cells." *Comp Biochem. Physiol. C Toxicol. Pharmacol.* 142(1-2): 53-59. 10.1016/j.cbpc.2005.10.005.
- Kopp, S., Sahana, J., Islam, T., Petersen, A. G., Bauer, J., Corydon, T. J., Schulz, H., Saar, K., et al. (2018). "The role of NFκB in spheroid formation of human breast cancer cells cultured on the Random Positioning Machine." *Sci. Rep.* 8(1): 921. 10.1038/s41598-017-18556-8.
- Kornienko, A., Evidente, A., Vurro, M., Mathieu, V., Cimmino, A., Evidente, M., van Otterlo, W. A. L., Dasari, R., et al. (2015). "Toward a cancer drug of fungal origin." *Med. Res. Rev.* 35(5): 937-967. 10.1002/med.21348.
- Kotake-Nara, E., Kushiro, M., Zhang, H., Sugawara, T., Miyashita, K. and Nagao, A. (2001). "Carotenoids affect proliferation of human prostate cancer cells." *J. Nutr.* 131(12): 3303-3306. 10.1093/jn/131.12.3303.
- Kotake-Nara, E., Terasaki, M. and Nagao, A. (2005). "Characterization of apoptosis induced by fucoxanthin in human promyelocytic leukemia cells." *Biosci. Biotechnol. Biochem.* 69(1): 224-227. 10.1271/bbb.69.224.



- Koyanagi, S., Tanigawa, N., Nakagawa, H., Soeda, S. and Shimeno, H. (2003). "Oversulfation of fucoidan enhances its anti-angiogenic and antitumor activities." *Biochem. Pharmacol.* 65(2): 173-179. 10.1016/s0006-2952(02)01478-8.
- Kozuki, Y., Miura, Y. and Yagasaki, K. (2000). "Inhibitory effects of carotenoids on the invasion of rat ascites hepatoma cells in culture." *Cancer Lett.* 151(1): 111-115. 10.1016/s0304-3835(99)00418-8.
- Krause, S., Maffini, M. V., Soto, A. M. and Sonnenschein, C. (2010). "The microenvironment determines the breast cancer cells' phenotype: organization of MCF7 cells in 3D cultures." *BMC Cancer* 10(1): 263. 10.1186/1471-2407-10-263.
- Krushkal, J., Negi, S., Yee, L. M., Evans, J. R., Grkovic, T., Palmisano, A., Fang, J., Sankaran, H., et al. (2021). "Molecular genomic features associated with in vitro response of the NCI-60 cancer cell line panel to natural products." *Mol. Oncol.* 15(2): 381-406. 10.1002/1878-0261.12849.
- Kumar, A., Casulo, C., Advani, R. H., Budde, E., Barr, P. M., Batlevi, C. L., Caron, P., Constine, L. S., et al. (2021). "Brentuximab vedotin combined with chemotherapy in patients with newly diagnosed early-stage, unfavorable-risk Hodgkin lymphoma." *Am. J. Clin. Oncol.* 39(20): 2257-2265. 10.1200/JCO.21.00108.
- Kumar, L. R. G., Paul, P. T., Anas, K. K., Tejpal, C. S., Chatterjee, N. S., Anupama, T. K., Mathew, S. and Ravishankar, C. N. (2022). "Phlorotannins–bioactivity and extraction perspectives." *J. Appl. Phycol.* 34(4): 2173-2185. 10.1007/s10811-022-02749-4.
- Kumar, M. S. and Sharma, S. A. (2021). "Toxicological effects of marine seaweeds: a cautious insight for human consumption." *Crit. Rev. Food Sci. Nutr.* 61(3): 500-521. 10.1080/10408398.2020.1738334.
- Kumar, P., Senthamilselvi, S., Govindaraju, M. and Sankar, R. (2014). "Unraveling the caspase-mediated mechanism for phloroglucinol-encapsulated starch biopolymer against the breast cancer cell line MDA-MB-231." *RSC Adv.* 4(86): 46157-46163. 10.1039/c4ra06664b.
- Kumar, P., Yuvakkumar, R., Vijayakumar, S. and Vaseeharan, B. (2018). "Cytotoxicity of phloroglucinol engineered silver (Ag) nanoparticles against MCF-7 breast cancer cell lines." *Mater. Chem. Phys.* 220: 402-408. 10.1016/j.matchemphys.2018.08.074.
- Kumar, S. R., Hosokawa, M. and Miyashita, K. (2013). "Fucoxanthin: a marine carotenoid exerting anti-cancer effects by affecting multiple mechanisms." *Mar. Drugs.* 11(12): 5130-5147. 10.3390/md11125130.
- Kumar, S. S., Kumar, Y., Khan, M. S. and Gupta, V. (2010). "New antifungal steroids from *Turbinaria conoides* (J. Agardh) Kützinger." *Nat. Prod. Res.* 24(15): 1481-1487. 10.1080/14786410903245233.

- Landry, I., Sumbly, V. and Vest, M. (2022). "Advancements in the treatment of triple-negative breast cancer: A narrative review of the literature." *Cureus* 14(2): e21970. 10.7759/cureus.21970.
- Langhans, S. A. (2018). "Three-dimensional in vitro cell culture models in drug discovery and drug repositioning." *Front. Pharmacol.* 9: 6. 10.3389/fphar.2018.00006.
- Lanz, H. L., Saleh, A., Kramer, B., Cairns, J., Ng, C. P., Yu, J., Trietsch, S. J., Hankemeier, T., et al. (2017). "Therapy response testing of breast cancer in a 3D high-throughput perfused microfluidic platform." *BMC Cancer* 17(1): 709. 10.1186/s12885-017-3709-3.
- Lassiter, G., Bergeron, C., Guedry, R., Cucarola, J., Kaye, A. M., Cornett, E. M., Kaye, A. D., Varrassi, G., et al. (2021). "Belantamab mafodotin to treat multiple myeloma: A comprehensive review of disease, drug efficacy and side effects." *Curr. Oncol.* 28(1): 640-660. 10.3390/curroncol28010063.
- Latte-Naor, S. and Mao, J. J. (2019). "Putting integrative oncology into practice: Concepts and approaches." *J. Oncol. Pract.* 15(1): 7-14. 10.1200/JOP.18.00554.
- Lee, A., Moon, B. I. and Kim, T. H. (2020a). "BRCA1/BRCA2 pathogenic variant breast cancer: Treatment and prevention strategies." *Ann. Lab. Med.* 40(2): 114-121. 10.3343/alm.2020.40.2.114.
- Lee, A. V., Oesterreich, S. and Davidson, N. E. (2015). "MCF-7 cells—Changing the course of breast cancer research and care for 45 years." *J. Natl. Cancer Inst.* 107(7): 1 djv073. 10.1093/jnci/djv073.
- Lee, D. G., Park, S. Y., Chung, W. S., Park, J. H., Shin, H. S., Hwang, E., Kim, I. H. and Yi, T. H. (2014). "The bone regenerative effects of fucosterol in in vitro and in vivo models of postmenopausal osteoporosis." *Mol. Nutr. Food Res.* 58(6): 1249-1257. 10.1002/mnfr.201300319.
- Lee, G. Y., Kenny, P. A., Lee, E. H. and Bissell, M. J. (2007). "Three-dimensional culture models of normal and malignant breast epithelial cells." *Nat. Methods* 4(4): 359-365. 10.1038/nmeth1015.
- Lee, J.-H., Jung, H. A., Kang, M. J., Choi, J. S. and Kim, G.-D. (2017). "Fucosterol, isolated from *Ecklonia stolonifera*, inhibits adipogenesis through modulation of FoxO1 pathway in 3T3-L1 adipocytes." *J. Pharm. Pharmacol.* 69(3): 325-333. 10.1111/jphp.12684.
- Lee, J. B., Hayashi, K., Hashimoto, M., Nakano, T. and Hayashi, T. (2004a). "Novel antiviral fucoidan from sporophyll of *Undaria pinnatifida* (Mekabu)." *Chem. Pharm. Bull.* 52(9): 1091-1094. 10.1248/cpb.52.1091.

- Lee, J. C., Hou, M. F., Huang, H. W., Chang, F. R., Yeh, C. C., Tang, J. Y. and Chang, H. W. (2013). "Marine algal natural products with anti-oxidative, anti-inflammatory, and anti-cancer properties." *Cancer Cell Int.* 13(1): 55. 10.1186/1475-2867-13-55.
- Lee, K. J., Kang, E. H., Yoon, M., Jo, M. R., Yu, H., Son, K. T., Jeong, S. H. and Kim, J. H. (2022). "Comparison of heavy metals and arsenic species in seaweeds collected from different regions in Korea." *Appl. Sci.* 12(14): 7000. 10.3390/app12147000.
- Lee, S., Lee, Y. S., Jung, S. H., Kang, S. S. and Shin, K. H. (2003). "Anti-oxidant activities of fucosterol from the marine algae *Pelvetia siliquosa*." *Arch. Pharm. Res.* 26(9): 719-722. 10.1007/BF02976680.
- Lee, S. H. and Jeon, Y. J. (2013). "Anti-diabetic effects of brown algae derived phlorotannins, marine polyphenols through diverse mechanisms." *Fitoterapia* 86: 129-136. 10.1016/j.fitote.2013.02.013.
- Lee, Y.-M., Oh, M. H., Go, J.-H., Han, K. and Choi, S.-Y. (2020b). "Molecular subtypes of triple-negative breast cancer: understanding of subtype categories and clinical implication." *Genes Genomics* 42(12): 1381-1387. 10.1007/s13258-020-01014-7.
- Lee, Y. S., Shin, K. H., Kim, B. K. and Lee, S. (2004b). "Anti-diabetic activities of fucosterol from *Pelvetia siliquosa*." *Arch. Pharm. Res.* 27(11): 1120-1122. 10.1007/bf02975115.
- Leung, E. Y., Kim, J. E., Askarian-Amiri, M., Joseph, W. R., McKeage, M. J. and Baguley, B. C. (2014). "Hormone resistance in two MCF-7 breast cancer cell lines is associated with reduced mTOR signaling, decreased glycolysis, and increased sensitivity to cytotoxic drugs." *Front. Oncol.* 4: 221. 10.3389/fonc.2014.00221.
- Lewis, N. S., Lewis, E. E., Mullin, M., Wheadon, H., Dalby, M. J. and Berry, C. C. (2017). "Magnetically levitated mesenchymal stem cell spheroids cultured with a collagen gel maintain phenotype and quiescence." *J. Tissue Eng.* 8: 2041731417704428. 10.1177/2041731417704428.
- Li, J., Chen, X., Qi, M. and Li, Y. (2018a). "Sentinel lymph node biopsy mapped with methylene blue dye alone in patients with breast cancer: A systematic review and meta-analysis." *PLoS One* 13(9): e0204364-e0204364. 10.1371/journal.pone.0204364.
- Li, J., Dai, W., Xia, Y., Chen, K., Li, S., Liu, T., Zhang, R., Wang, J., et al. (2015). "Astaxanthin inhibits proliferation and induces apoptosis of human hepatocellular carcinoma cells via Inhibition of Nf-Kappab P65 and Wnt/Beta-catenin in vitro." *Mar. Drugs* 13(10): 6064-6081. 10.3390/md13106064.
- Li, J., Fang, K., Choppavarapu, L., Yang, K., Yang, Y., Wang, J., Cao, R., Jatoi, I., et al. (2021a). "Hi-C profiling of cancer spheroids identifies 3D-growth-specific chromatin

- interactions in breast cancer endocrine resistance." *Clin. Epigenetics* 13(1): 175. 10.1186/s13148-021-01167-6.
- Li, N., Khan, S. I., Qiu, S. and Li, X.-C. (2018b). "Synthesis and anti-inflammatory activities of phloroglucinol-based derivatives." *Molecules* 23(12): 3232. 10.3390/molecules23123232.
- Li, Q., Chen, C., Kapadia, A., Zhou, Q., Harper, M. K., Schaack, J. and LaBarbera, D. V. (2011). "3D models of epithelial-mesenchymal transition in breast cancer metastasis: high-throughput screening assay development, validation, and pilot screen." *J. Biomol. Screen.* 16(2): 141-154. 10.1177/10870571110392995.
- Li, W., Xue, D., Xue, M., Zhao, J., Liang, H., Liu, Y. and Sun, T. (2019). "Fucoidan inhibits epithelial-to-mesenchymal transition via regulation of the HIF-1 $\alpha$  pathway in mammary cancer cells under hypoxia." *Oncol. Lett.* 18(1): 330-338. 10.3892/ol.2019.10283.
- Li, X., Lin, B., Lin, Z., Ma, Y., Wang, Q., Zheng, Y., Cui, L., Luo, H., et al. (2021b). "Exploration in the mechanism of fucosterol for the treatment of non-small cell lung cancer based on network pharmacology and molecular docking." *Sci. Rep.* 11(1): 4901. 10.1038/s41598-021-84380-w.
- Li, Y., Hu, J., Song, H. and Wu, T. (2018c). "Antibiotic anisomycin selectively targets leukemia cell lines and patient samples through suppressing Wnt/ $\beta$ -catenin signaling." *Biochem. Biophys. Res. Commun.* 505(3): 858-864. 10.1016/j.bbrc.2018.09.183.
- Li, Y., Zheng, Y., Zhang, Y., Yang, Y., Wang, P., Imre, B., Wong, A. C. Y., Hsieh, Y. S. Y., et al. (2021c). "Brown algae carbohydrates: Structures, pharmaceutical properties, and research challenges." *Mar. Drugs* 19(11): 620. 10.3390/md19110620.
- Li, Y. F., Chang, L., Li, W. H., Xiao, M. Y., Wang, Y., He, W. J., Xia, Y. X., Wang, L., et al. (2016). "Radiotherapy concurrent versus sequential with endocrine therapy in breast cancer: A meta-analysis." *Breast* 27: 93-98. 10.1016/j.breast.2015.09.005.
- Liao, G. S., Apaya, M. K. and Shyur, L. F. (2013). "Herbal medicine and acupuncture for breast cancer palliative care and adjuvant therapy." *Evid. Based Complement. Alternat. Med.* 2013: 437948. 10.1155/2013/437948.
- Lichota, A. and Gwozdziński, K. (2018). "Anticancer activity of natural compounds from plant and marine environment." *Int. J. Mol. Sci.* 19(11): 3533. 10.3390/ijms19113533.
- Lien, Y. H. and Scott, K. (2000). "Long-term cyclophosphamide treatment for recurrent type I membranoproliferative glomerulonephritis after transplantation." *Am. J. Kidney Dis.* 35(3): 539-543. 10.1016/s0272-6386(00)70211-3.

- Lin, H. V., Tsou, Y. C., Chen, Y. T., Lu, W. J. and Hwang, P. A. (2017). "Effects of low-molecular-weight fucoidan and high stability fucoxanthin on glucose homeostasis, lipid metabolism, and liver function in a mouse model of type II diabetes." *Mar. Drugs* 15(4):113. 10.3390/md15040113.
- Lin, S. R., Chang, C. H., Hsu, C. F., Tsai, M. J., Cheng, H., Leong, M. K., Sung, P. J., Chen, J. C., et al. (2020a). "Natural compounds as potential adjuvants to cancer therapy: Preclinical evidence." *Br. J. Pharmacol.* 177(6): 1409-1423. 10.1111/bph.14816.
- Lin, Y., Qi, X., Liu, H., Xue, K., Xu, S. and Tian, Z. (2020b). "The anti-cancer effects of fucoidan: a review of both in vivo and in vitro investigations." *Cancer Cell Int.* 20(1): 154. 10.1186/s12935-020-01233-8.
- Linnewiel-Hermoni, K., Khanin, M., Danilenko, M., Zango, G., Amosi, Y., Levy, J. and Sharoni, Y. (2015). "The anti-cancer effects of carotenoids and other phytonutrients resides in their combined activity." *Arch. Biochem. Biophys* 572: 28-35. 10.1016/j.abb.2015.02.018.
- Liu, B., Ezeogu, L., Zellmer, L., Yu, B., Xu, N. and Joshua Liao, D. (2015). "Protecting the normal in order to better kill the cancer." *Cancer Med.* 4(9): 1394-1403. 10.1002/cam4.488.
- Liu, C. L., Lim, Y. P. and Hu, M. L. (2013). "Fucoxanthin enhances cisplatin-induced cytotoxicity via NFkappaB-mediated pathway and downregulates DNA repair gene expression in human hepatoma HepG2 cells." *Mar. Drugs* 11(1): 50-66. 10.3390/md11010050.
- Liu, M., Li, W., Chen, Y., Wan, X. and Wang, J. (2020). "Fucoxanthin: A promising compound for human inflammation-related diseases." *Life Sci.* 255: 117850. 10.1016/j.lfs.2020.117850.
- Lomartire, S., Marques, J. C. and Gonçalves, A. M. M. (2021). "An overview to the health benefits of seaweeds consumption." *Mar. Drugs* 19(6): 341. 10.3390/md19060341.
- Lombaerts, M., van Wezel, T., Philippo, K., Dierssen, J. W., Zimmerman, R. M., Oosting, J., van Eijk, R., Eilers, P. H., et al. (2006). "E-cadherin transcriptional downregulation by promoter methylation but not mutation is related to epithelial-to-mesenchymal transition in breast cancer cell lines." *Br. J. Cancer* 94(5): 661-671. 10.1038/sj.bjc.6602996.
- Lombardi, A., Lazzeroni, R., Bersigotti, L., Vitale, V. and Amanti, C. (2021). "The proper Ki-67 cut-off in hormone responsive breast cancer: A monoinstitutional analysis with long-term follow-up." *Breast Cancer (Dove Med Press)* 13: 213-217. 10.2147/bctt.S305440.

- Lombardo, Y., de Giorgio, A., Coombes, C. R., Stebbing, J. and Castellano, L. (2015). "Mammosphere formation assay from human breast cancer tissues and cell lines." *J. Vis. Exp.* (97): 52671. 10.3791/52671.
- Longley, D. B., Harkin, D. P. and Johnston, P. G. (2003). "5-Fluorouracil: mechanisms of action and clinical strategies." *Nat. Rev. Cancer* 3(5): 330-338. 10.1038/nrc1074.
- Lopes-Costa, E., Abreu, M., Gargiulo, D., Rocha, E. and Ramos, A. A. (2017). "Anticancer effects of seaweed compounds fucoxanthin and phloroglucinol, alone and in combination with 5-fluorouracil in colon cells." *J. Toxicol. Environ. Health A* 80(13-15): 776-787. 10.1080/15287394.2017.1357297.
- Lopes, G., Sousa, C., Valentão, P. and Andrade, P. B. (2014). Sterols in algae and health. Bioactive compounds from marine foods: Plant and animal sources. *Compounds from Marine Foods* (eds B. Hernández-Ledesma and M. Herrero). L. John Wiley & Sons. 10.1002/9781118412893.ch9.
- Lourenço-Lopes, C., Fraga-Corral, M., Jimenez-Lopez, C., Carpena, M., Pereira, A. G., Garcia-Oliveira, P., Prieto, M. A. and Simal-Gandara, J. (2021). "Biological action mechanisms of fucoxanthin extracted from algae for application in food and cosmetic industries." *Trends Food Sci. Technol.* 117: 163-181. 10.1016/j.tifs.2021.03.01210.
- Lu, J., Shi, K. K., Chen, S., Wang, J., Hassouna, A., White, L. N., Merien, F., Xie, M., et al. (2018). "Fucoidan extracted from the New Zealand *Undaria pinnatifida*- Physicochemical comparison against five other fucoidans: Unique low molecular weight fraction bioactivity in breast cancer cell lines." *Mar. Drugs* 16(12): 461. 10.3390/md16120461.
- Ly, D., Forman, D., Ferlay, J., Brinton, L. A. and Cook, M. B. (2013). "An international comparison of male and female breast cancer incidence rates." *Int. J. Cancer* 132(8): 1918-1926. 10.1002/ijc.27841.
- Ma, W.-P., Yin, S.-N., Chen, J.-P., Geng, X.-C., Liu, M.-F., Li, H.-H., Liu, M. and Liu, H.-B. (2022). "Stimulating the hematopoietic effect of simulated digestive product of fucoidan from *Sargassum fusiforme* on cyclophosphamide-induced hematopoietic damage in mice and its protective mechanisms based on serum lipidomics." *Mar. Drugs* 20(3):201.10.3390/md20030201.
- Maadi, H., Soheilifar, M. H., Choi, W. S., Moshtaghian, A. and Wang, Z. (2021). "Trastuzumab mechanism of action; 20 Years of research to unravel a dilemma." *Cancers (Basel)* 13(14): 3540. 10.3390/cancers13143540.
- Mabate, B., Daub, C. D., Malgas, S., Edkins, A. L. and Pletschke, B. I. (2021). "Fucoidan structure and its impact on glucose metabolism: implications for diabetes and cancer therapy." *Mar. Drugs* 19(1):30. 10.3390/md19010030.

- Macias, H. and Hinck, L. (2012). "Mammary gland development." *WIREs Dev. Biol.* 1, 533-557. 10.1002/wdev.35.
- Madhavi, D., Kagan, D. and Seshadri, S. (2018). "A study on the bioavailability of a proprietary, sustained-release formulation of astaxanthin." *Integr. Med.* 17(3): 38-42. PMID: 30962794
- Maeda, H. (2015). "Nutraceutical effects of fucoxanthin for obesity and diabetes therapy: A review." *J. Oleo Sci.* 64(2): 125-132. 10.5650/jos.ess14226.
- Mahdavi, M., Nassiri, M., Kooshyar, M. M., Vakili-Azghandi, M., Avan, A., Sandry, R., Pillai, S., Lam, A. K., et al. (2019). "Hereditary breast cancer; Genetic penetrance and current status with BRCA." *J. Cell. Physiol.* 234(5): 5741-5750. 10.1002/jcp.27464.
- Maisonneuve, P. (2017). *Epidemiology, Lifestyle, and Environmental Factors*. In: Veronesi, U., Goldhirsch, A., Veronesi, P., Gentilini, O., Leonardi, M. (eds) *Breast Cancer*. Springer, Cham. 10.1007/978-3-319-48848-6\_7
- Makki, J. (2015). "Diversity of breast carcinoma: Histological subtypes and clinical relevance." *Clin. Med. Insights Pathol.* 8: 23-31. 10.4137/CPath.S31563.
- Malhão, F., Ramos, A. A., Buttachon, S., Dethoup, T., Kijjoa, A. and Rocha, E. (2019). "Cytotoxic and antiproliferative effects of preussin, a hydroxypyrrolidine derivative from the marine sponge-associated fungus *Aspergillus candidus* KUFA 0062, in a panel of breast cancer cell lines and using 2D and 3D cultures." *Mar. Drugs* 17(8): 448. 10.3390/md17080448.
- Maloney, S. M., Hoover, C. A., Morejon-Lasso, L. V. and Prospero, J. R. (2020). "Mechanisms of taxane resistance." *Cancers (Basel)* 12(11): 233. 10.3390/cancers12113323.
- Malter, W., Hellmich, M., Badian, M., Kirn, V., Mallmann, P. and Krämer, S. (2018). "Factors predictive of sentinel lymph node involvement in primary breast cancer." *Anticancer Res.* 38(6): 3657-3662. 10.21873/anticancer.12642.
- Malve, H. (2016). "Exploring the ocean for new drug developments: Marine pharmacology." *J. Pharm. Bioallied Sci.* 8(2): 83-91. 10.4103/0975-7406.171700.
- Malyarenko, O. S. and Ermakova, S. P. (2017). Chapter 10 - Fucoïdans: Anticancer activity and molecular mechanisms of action. *Seaweed Polysaccharides. Isolation, Biological and Biomedical Applications* J. Venkatesan, S. Anil and S.-K. Kim Elsevier. 10.1016/B978-0-12-809816-5.00010-4.
- Malyarenko, O. S., Malyarenko, T. V., Usoltseva, R. V., Silchenko, A. S., Kicha, A. A., Ivanchina, N. V. and Ermakova, S. P. (2021a). "Fucoïdan from brown algae *Fucus evanescens* potentiates the anti-proliferative efficacy of asterosaponins from starfish

- Asteropsis carinifera* in 2D and 3D models of melanoma cells." *Int. J. Biol. Macromol.* 185: 31-39. 10.1016/j.ijbiomac.2021.06.080.
- Malyarenko, O. S., Malyarenko, T. V., Usoltseva, R. V., Surits, V. V., Kicha, A. A., Ivanchina, N. V. and Ermakova, S. P. (2021b). "Combined anticancer effect of sulfated laminaran from the brown alga *Alaria angusta* and polyhydroxysteroid glycosides from the starfish *Protoreaster lincki* on 3D colorectal carcinoma HCT 116 cell line." *Mar. Drugs* 19(10): 540. 10.3390/md19100540.
- Malyarenko, O. S., Usoltseva, R. V., Shevchenko, N. M., Isakov, V. V., Zvyagintseva, T. N. and Ermakova, S. P. (2016). "In vitro anticancer activity of the laminarans from Far Eastern brown seaweeds and their sulfated derivatives." *J. Appl. Phycol.* 29(1): 543-553. 10.1007/s10811-016-0915-3.
- Malyarenko, O. S., Usoltseva, R. V., Silchenko, A. S. and Ermakova, S. P. (2020). "Aminated laminaran from brown alga *Saccharina cichorioides*: Synthesis, structure, anticancer, and radiosensitizing potential in vitro." *Carbohydr. Polym.* 250: 117007. 10.1016/j.carbpol.2020.117007.
- Manmuan, S. and Manmuan, P. (2019). "Fucoxanthin enhances 5-FU chemotherapeutic efficacy in colorectal cancer cells by affecting MMP-9 invasive proteins." *J. App. Pharm. Sci.* 9(12): 7-14. 10.7324/JAPS.2019.91202.
- Mann, J. (2002). "Natural products in cancer chemotherapy: past, present and future." *Nat. Rev. Cancer* 2(2): 143-148. 10.1038/nrc723.
- Mansoori, B., Mohammadi, A., Davudian, S., Shirjang, S. and Baradaran, B. (2017). "The different mechanisms of cancer drug resistance: A brief review." *Adv. Pharm. Bull.* 7(3): 339-348. 10.15171/apb.2017.041.
- Mao, Z., Shen, X., Dong, P., Liu, G., Pan, S., Sun, X., Hu, H., Pan, L., et al. (2019). "Fucosterol exerts antiproliferative effects on human lung cancer cells by inducing apoptosis, cell cycle arrest and targeting of Raf/MEK/ERK signalling pathway." *Phytomedicine* 61: 152809. 10.1016/j.phymed.2018.12.032.
- Maoka, T. (2020). "Carotenoids as natural functional pigments." *J. Nat. Med.* 74(1): 1-16. 10.1007/s11418-019-01364-x.
- Marchese, S. and Silva, E. (2012). "Disruption of 3D MCF-12A breast cell cultures by estrogens-an in vitro model for ER-mediated changes indicative of hormonal carcinogenesis." *PLoS One* 7(10): e45767. 10.1371/journal.pone.0045767.
- Maritan, S. M., Lian, E. Y. and Mulligan, L. M. (2017). "An efficient and flexible cell aggregation method for 3D spheroid production." *J. Vis. Exp.* (121):55544: 10.3791/55544
- Martin, L. J. (2015). "Fucoxanthin and its metabolite fucoxanthinol in cancer prevention and treatment." *Mar. Drugs* 13(8): 4784-4798. 10.3390/md13084784.



- Martín, M. (2001). "Platinum compounds in the treatment of advanced breast cancer." *Clin. Breast Cancer* 2(3): 190-208; discussion 209. 10.3816/CBC.2001.n.022.
- Martinez-Pacheco, S. and O'Driscoll, L. (2021). "Pre-Clinical in vitro models used in cancer research: Results of a worldwide survey." *Cancers (Basel)* 13(23): 6033. 10.3390/cancers13236033.
- Martins, A., Vieira, H., Gaspar, H. and Santos, S. (2014). "Marketed marine natural products in the pharmaceutical and cosmeceutical industries: Tips for success." *Mar. Drugs* 12(2): 1066-101. 10.3390/md12021066.
- Masood, S. (2016). "Neoadjuvant chemotherapy in breast cancers." *Women's health (London, England)* 12(5): 480-491. 10.1177/1745505716677139.
- Masoud, V. and Pagès, G. (2017). "Targeted therapies in breast cancer: New challenges to fight against resistance." *World J. Clin. Oncol.* 8(2): 120-134. 10.5306/wjco.v8.i2.120.
- Matsubara, K., Xue, C., Zhao, X., Mori, M., Sugawara, T. and Hirata, T. (2005). "Effects of middle molecular weight fucoidans on in vitro and ex vivo angiogenesis of endothelial cells." *Int. J. Mol. Med.* 15(4): 695-699. 10.3892/ijmm.15.4.695.
- Matsumoto, M., Hosokawa, M., Matsukawa, N., Hagio, M., Shinoki, A., Nishimukai, M., Miyashita, K., Yajima, T., et al. (2010). "Suppressive effects of the marine carotenoids, fucoxanthin and fucoxanthinol on triglyceride absorption in lymph duct-cannulated rats." *Eur. J. Nutr.* 49(4): 243-249. 10.1007/s00394-009-0078-y.
- Maximiano, S., Magalhães, P., Guerreiro, M. P. and Morgado, M. (2016). "Trastuzumab in the treatment of breast cancer." *BioDrugs* 30(2): 75-86. 10.1007/s40259-016-0162-9.
- Mayakrishnan, V., Kannappan, P., Abdullah, N. and Ahmed, A. B. A. (2013). "Cardioprotective activity of polysaccharides derived from marine algae: An overview." *Trends Food Sci. Technol.* 30(2): 98-104. 10.1016/j.tifs.2013.01.007.
- Mayer, A. M., Glaser, K. B., Cuevas, C., Jacobs, R. S., Kem, W., Little, R. D., McIntosh, J. M., Newman, D. J., et al. (2010). "The odyssey of marine pharmaceuticals: a current pipeline perspective." *Trends Pharmacol. Sci.* 31(6): 255-265. 10.1016/j.tips.2010.02.005.
- Mazzarella, L., Pelicci, P.G. (2017). *Fundamental Pathways in Breast Cancer 4: Signaling to Chromatin in Breast Development*. In: Veronesi, U., Goldhirsch, A., Veronesi, P., Gentilini, O., Leonardi, M. (eds) *Breast Cancer*. Springer, Cham.10.1007/978-3-319-48848-6\_4.
- McCall, B., McPartland, C. K., Moore, R., Frank-Kamenetskii, A. and Booth, B. W. (2018). "Effects of astaxanthin on the proliferation and migration of breast cancer cells in vitro." *Antioxidants* 7(10): 135. 10.3390/antiox7100135.

- Mehta, G., Hsiao, A. Y., Ingram, M., Luker, G. D. and Takayama, S. (2012). "Opportunities and challenges for use of tumor spheroids as models to test drug delivery and efficacy." *J. Control. Release* 164(2): 192-204. 10.1016/j.jconrel.2012.04.045.
- Meinita, M. D. N., Harwanto, D., Tirtawijaya, G., Negara, B., Sohn, J. H., Kim, J. S. and Choi, J. S. (2021). "Fucosterol of marine macroalgae: Bioactivity, safety and toxicity on organism." *Mar. Drugs* 19(10): 545. 10.3390/md19100545.
- Meisel, J. L., Venur, V. A., Gnant, M. and Carey, L. (2018). "Evolution of targeted therapy in breast cancer: Where precision medicine began." *Am Soc Clin Oncol Educ Book*. 38:78-86. 10.1200/EDBK\_201037.
- Melissaridou, S., Wiechec, E., Magan, M., Jain, M. V., Chung, M. K., Farnebo, L. and Roberg, K. (2019). "The effect of 2D and 3D cell cultures on treatment response, EMT profile and stem cell features in head and neck cancer." *Cancer Cell Int*. 19(1): 16. 10.1186/s12935-019-0733-1.
- Melo, F. H. M. d. O., Salles, J., Sartorelli, V. O. B. and Montor, W. R. (2018). "Cancer chemoprevention: Classic and epigenetic mechanisms inhibiting tumorigenesis. What have we learned so far?" *Front. Oncol*. 8: 644. 10.3389/fonc.2018.00644.
- Menshova, R. V., Ermakova, S. P., Anastyyuk, S. D., Isakov, V. V., Dubrovskaya, Y. V., Kusaykin, M. I., Um, B. H. and Zvyagintseva, T. N. (2014). "Structure, enzymatic transformation and anticancer activity of branched high molecular weight laminaran from brown alga *Eisenia bicyclis*." *Carbohydr. Polym*. 99: 101-109. 10.1016/j.carbpol.2013.08.037.
- Mescher, A. L. (2018). *The female reproductive system. Junqueira's Basic Histology: Text and Atlas, 15e.* New York, NY McGraw-Hill Education.
- Miao, H. Q., Ishai-Michaeli, R., Peretz, T. and Vlodavsky, I. (1995). "Laminarin sulfate mimics the effects of heparin on smooth muscle cell proliferation and basic fibroblast growth factor-receptor binding and mitogenic activity." *J. Cell Physiol*. 164(3): 482-490. 10.1002/jcp.1041640306.
- Milovanovic, M., Banjac, N. and Vucelic-Radovic, B. (2009). "Functional Food: Rare herbs, seeds and vegetable oils as sources of flavors and Phytosterols." *J. Agric. Sci*. 54: 81-94. 10.2298/jas0901081m
- Milshteyn, A., Schneider, J. S. and Brady, S. F. (2014). "Mining the metabiome: identifying novel natural products from microbial communities." *Chem. Biol*. 21(9): 1211-1223. 10.1016/j.chembiol.2014.08.006.
- Min, K. W., Kim, D. H., Do, S. I., Pyo, J. S., Chae, S. W., Sohn, J. H., Kim, K., Lee, H. J., et al. (2016). "High Ki67/BCL2 index is associated with worse outcome in early stage

- breast cancer." *Postgrad. Med. J.* 92(1094): 707-714. 10.1136/postgradmedj-2015-133531.
- Minchinton, A. I. and Tannock, I. F. (2006). "Drug penetration in solid tumours." *Nat. Rev. Cancer* 6(8): 583-592. 10.1038/nrc1893.
- Ming, J. X., Wang, Z. C., Huang, Y., Ohishi, H., Wu, R. J., Shao, Y., Wang, H., Qin, M. Y., et al. (2021). "Fucoxanthin extracted from *Laminaria japonica* inhibits metastasis and enhances the sensitivity of lung cancer to Gefitinib." *J. Ethnopharmacol.* 265: 113302. 10.1016/j.jep.2020.113302.
- Mittler, F., Obeid, P., Rulina, A. V., Haguët, V., Gidrol, X. and Balakirev, M. Y. (2017). "High-content monitoring of drug effects in a 3D spheroid model." *Front. Oncol.* 7: 293. 10.3389/fonc.2017.00293.
- Mohamed, A., Krajewski, K., Cakar, B. and Ma, C. X. (2013). "Targeted therapy for breast cancer." *Am. J. Clin. Pathol.* 183(4): 1096-1112. 10.1016/j.ajpath.2013.07.005.
- Moitinho-Silva, L., Díez-Vives, C., Batani, G., Esteves, A. I., Jahn, M. T. and Thomas, T. (2017). "Integrated metabolism in sponge-microbe symbiosis revealed by genome-centered metatranscriptomics." *Isme J.* 11(7): 1651-1666. 10.1038/ismej.2017.25.
- More, G. S., Thomas, A. B., Chitlange, S. S., Nanda, R. K. and Gajbhiye, R. L. (2019). "Nitrogen mustards as alkylating agents: A review on chemistry, mechanism of action and current USFDA status of drugs." *Anticancer Agents Med. Chem.* 19(9): 1080-1102. 10.2174/1871520619666190305141458.
- Mosca, L., Vitiello, F., Coppola, A., Borzacchiello, L., Ilisso, C. P., Pagano, M., Caraglia, M., Cacciapuoti, G., et al. (2020). "Therapeutic potential of the natural compound S-adenosylmethionine as a chemoprotective synergistic agent in breast, and head and neck cancer treatment: Current status of research." *Int. J. Mol. Sci.* 21(22): 8547. 10.3390/ijms21228547.
- Mouritsen, O. G., Bagatolli, L. A., Duelund, L., Garvik, O., Ipsen, J. H. and Simonsen, A. C. (2017). "Effects of seaweed sterols fucosterol and desmosterol on lipid membranes." *Chem. Phys. Lipids* 205: 1-10. 10.1016/j.chemphyslip.2017.03.010.
- Moussavou, G., Kwak, D. H., Obiang-Obonou, B. W., Maranguy, C. A., Dinzouna-Boutamba, S. D., Lee, D. H., Pissibanganga, O. G., Ko, K., et al. (2014). "Anticancer effects of different seaweeds on human colon and breast cancers." *Mar. Drugs* 12(9): 4898-4911. 10.3390/md12094898.
- Muftah, A. A., Aleskandarany, M. A., Al-Kaabi, M. M., Sonbul, S. N., Díez-Rodríguez, M., Nolan, C. C., Caldas, C., Ellis, I. O., et al. (2017). "Ki67 expression in invasive breast cancer: the use of tissue microarrays compared with whole tissue sections." *Breast Cancer Res. Treat.* 164(2): 341-348. 10.1007/s10549-017-4270-0.

- Munro, M. H., Blunt, J. W., Dumdei, E. J., Hickford, S. J., Lill, R. E., Li, S., Battershill, C. N. and Duckworth, A. R. (1999). "The discovery and development of marine compounds with pharmaceutical potential." *J. Biotechnol.* 70(1-3): 15-25. 10.1016/s0168-1656(99)00052-8.
- Murali, V. S., Chang, B.-J., Fiolka, R., Danuser, G., Cobanoglu, M. C. and Welf, E. S. (2019). "An image-based assay to quantify changes in proliferation and viability upon drug treatment in 3D microenvironments." *BMC Cancer* 19(1): 502. 10.1186/s12885-019-5694-1.
- Murase, W., Kamakura, Y., Kawakami, S., Yasuda, A., Wagatsuma, M., Kubota, A., Kojima, H., Ohta, T., et al. (2021). "Fucoxanthin prevents pancreatic tumorigenesis in C57BL/6J mice that received allogenic and orthotopic transplants of cancer cells." *Int. J. Mol. Sci.* 22(24): 13620. 10.3390/ijms222413620.
- Murawa, P., Murawa, D., Adamczyk, B. and Połom, K. (2014). "Breast cancer: Actual methods of treatment and future trends." *Rep. Pract. Oncol. Radiother.* 19(3): 165-172. 10.1016/j.rpor.2013.12.003.
- Murphy, T. and Yee, K. W. L. (2017). "Cytarabine and daunorubicin for the treatment of acute myeloid leukemia." *Expert Opin. Pharmacother.* 18(16): 1765-1780. 10.1080/14656566.2017.1391216.
- Mut-Salud, N., Álvarez, P. J., Garrido, J. M., Carrasco, E., Aránega, A. and Rodríguez-Serrano, F. (2016). "Antioxidant intake and antitumor therapy: Toward nutritional recommendations for optimal results." *Oxid. Med. Cell. Longev.* 2016: 6719534-6719534. 10.1155/2016/6719534.
- Nabholtz, J. M. and Gligorov, J. (2005). "The role of taxanes in the treatment of breast cancer." *Expert Opin. Pharmacother.* 6(7): 1073-1094. 10.1517/14656566.6.7.1073.
- Nagamine, T., Kadena, K., Tomori, M., Nakajima, K. and Iha, M. (2020). "Activation of NK cells in male cancer survivors by fucoidan extracted from *Cladosiphon okamuranus*." *Mol. Clin. Oncol.* 12(1): 81-88. 10.3892/mco.2019.1943.
- Nagelkerke, A., Bussink, J., Sweep, F. C. and Span, P. N. (2013). "Generation of multicellular tumor spheroids of breast cancer cells: how to go three-dimensional." *Anal Biochem.* 437(1): 17-19. 10.1016/j.ab.2013.02.004.
- Namvar, F., Mohamad, R., Baharara, J., Zafar-Balanejad, S., Fargahi, F. and Rahman, H. S. (2013a). "Antioxidant, antiproliferative, and antiangiogenesis effects of polyphenol-rich seaweed (*Sargassum muticum*)." *Biomed. Res. Int.* 2013: 604787. 10.1155/2013/604787.
- Namvar, F., Tahir, P. M., Mohamad, R., Mahdavi, M., Abedi, P., Najafi, T. F., Rahmanand, H. S. and Jawaid, M. (2013b). "Biomedical properties of edible

- seaweed in cancer therapy and chemoprevention trials: a review." *Nat. Prod. Commun.* 8(12): 1811-1820. PMID: 24555303.
- Nanou, A., Lorenzo-Moldero, I., Gazouleas, K. D., Cortese, B. and Moroni, L. (2022). "3D culture modeling of metastatic breast cancer cells in additive manufactured scaffolds." *CS Appl. Mater. Interfaces.* 14(24): 28389-28402. 10.1021/acsami.2c07492.
- Navarrete, M. A. H., Maier, C. M., Falzoni, R., Quadros, L. G. d. A., Lima, G. R., Baracat, E. C. and Nazário, A. C. P. (2005). "Assessment of the proliferative, apoptotic and cellular renovation indices of the human mammary epithelium during the follicular and luteal phases of the menstrual cycle." *Breast Cancer Res.* 7(3): R306. 10.1186/bcr994.
- Nechuta, S., Lu, W., Chen, Z., Zheng, Y., Gu, K., Cai, H., Zheng, W. and Shu, X. O. (2011). "Vitamin supplement use during breast cancer treatment and survival: a prospective cohort study." *Cancer Epidemiol. Biomark. Prev.* 20(2): 262-271. 10.1158/1055-9965.Epi-10-1072.
- Negara, B. F. S. P., Sohn, J. H., Kim, J.-S. and Choi, J.-S. (2021). "Effects of phlorotannins on organisms: Focus on the safety, toxicity, and availability of phlorotannins." *Foods* 10(2): 452. 10.3390/foods10020452.
- Neve, R. M., Chin, K., Fridlyand, J., Yeh, J., Baehner, F. L., Fevr, T., Clark, L., Bayani, N., et al. (2006). "A collection of breast cancer cell lines for the study of functionally distinct cancer subtypes." *Cancer Cell* 10(6): 515-527. 10.1016/j.ccr.2006.10.008.
- Newman, D. J. and Cragg, G. M. (2020). "Natural products as sources of new drugs over the nearly four decades from 01/1981 to 09/2019." *J. Nat. Prod.* 83(3): 770-803. 10.1021/acs.jnatprod.9b01285.
- Neyrinck, A. M., Mouson, A. and Delzenne, N. M. (2007). "Dietary supplementation with laminarin, a fermentable marine beta (1-3) glucan, protects against hepatotoxicity induced by LPS in rat by modulating immune response in the hepatic tissue." *Int. Immunopharmacol.* 7(12): 1497-1506. 10.1016/j.intimp.2007.06.011.
- Nigam, M., Suleria, H. A. R., Farzaei, M. H. and Mishra, A. P. (2019). "Marine anticancer drugs and their relevant targets: a treasure from the ocean." *Daru* 27(1): 491-515. 10.1007/s40199-019-00273-4.
- Nishino, H., Murakoshi, M., Ii, T., Takemura, M., Kuchide, M., Kanazawa, M., Mou, X. Y., Wada, S., et al. (2002). "Carotenoids in cancer chemoprevention." *Cancer Metastasis Rev.* 21(3-4): 257-264. 10.1023/a:1021206826750.
- Noordhoek, I., de Groot, A. F., Cohen, D., Liefers, G. J., Portielje, J. E. A. and Kroep, J. R. (2019). "Higher ER load is not associated with better outcome in stage 1-3 breast

- cancer: a descriptive overview of quantitative HR analysis in operable breast cancer." *Breast Cancer Res. Treat.* 176(1): 27-36. 10.1007/s10549-019-05233-9.
- Ntie-Kang, F. and Svozil, D. (2020). "An enumeration of natural products from microbial, marine and terrestrial sources." *Phys. Sci. Rev.* 5(8): 20180121. 10.1515/psr-2018-0121.
- Nunes, A. S., Barros, A. S., Costa, E. C., Moreira, A. F. and Correia, I. J. (2019). "3D tumor spheroids as in vitro models to mimic in vivo human solid tumors resistance to therapeutic drugs." *Biotechnol. Bioeng.* 116(1): 206-226. 10.1002/bit.26845.
- Núñez, C., Capelo, J. L., Igrejas, G., Alfonso, A., Botana, L. M. and Lodeiro, C. (2016). "An overview of the effective combination therapies for the treatment of breast cancer." *Biomaterials* 97(Suppl C): 34-50. 10.1016/j.biomaterials.2016.04.027.
- Oakes, S. R., Hilton, H. N. and Ormandy, C. J. (2006). "The alveolar switch: coordinating the proliferative cues and cell fate decisions that drive the formation of lobuloalveoli from ductal epithelium." *Breast Cancer Res.* 8(2): 207-207. 10.1186/bcr1411.
- Ojulari, O. V., Lee, S. G. and Nam, J. O. (2020). "Therapeutic effect of seaweed derived xanthophyl carotenoid on obesity management; Overview of the last decade." *Int. J. Mol. Sci.* 21(7): 2502. 10.3390/ijms21072502.
- Okeke, E. S., Nweze, E. J., Chibuogwu, C. C., Anaduaka, E. G., Chukwudozie, K. I. and Ezeorba, T. P. C. (2021). "Aquatic phlorotannins and human health: Bioavailability, toxicity, and future prospects." *Nat. Prod. Commun.* 16(12): 1934578X211056144. 10.1177/1934578x211056144.
- Okue, M., Watanabe, H. and Kitahara, T. (2001). "A concise synthesis of (+)-preussin." *Tetrahedron* 57(19): 4107-4110. 10.1016/S0040-4020(01)00292-7.
- Oliyai, N., Moosavi-Nasab, M., Tamaddon, A. M. and Tanideh, N. (2021). "Antidiabetic effect of fucoxanthin extracted from *Sargassum angustifolium* on streptozotocin-nicotinamide-induced type 2 diabetic mice." *Food Sci. Nutr.* 9(7): 3521-3529. 10.1002/fsn3.2301.
- Ott, P. A., Pavlick, A. C., Johnson, D. B., Hart, L. L., Infante, J. R., Luke, J. J., Lutzky, J., Rothschild, N. E., et al. (2019). "A phase 2 study of glembatumumab vedotin, an antibody-drug conjugate targeting glycoprotein NMB, in patients with advanced melanoma." *Cancer* 125(7): 1113-1123. 10.1002/cncr.31892.
- Pacheco, B. S., Dos Santos, M. A. Z., Schultze, E., Martins, R. M., Lund, R. G., Seixas, F. K., Colepicolo, P., Collares, T., et al. (2018). "Cytotoxic activity of fatty acids from Antarctic macroalgae on the growth of human breast cancer cells." *Front. Bioeng. Biotechnol.* 6: 185-185. 10.3389/fbioe.2018.00185.
- Palozza, P., Torelli, C., Boninsegna, A., Simone, R., Catalano, A., Mele, M. C. and Picci, N. (2009). "Growth-inhibitory effects of the astaxanthin-rich alga *Haematococcus*

- pluvialis* in human colon cancer cells." *Cancer Lett.* 283(1): 108-117. 10.1016/j.canlet.2009.03.031.
- Pan, S. Y., Zhou, J., Gibbons, L., Morrison, H., Wen, S. W. and Canadian Cancer Registries Epidemiology Research, G. (2011). "Antioxidants and breast cancer risk- a population-based case-control study in Canada." *BMC cancer* 11: 372-372. 10.1186/1471-2407-11-372.
- Papoutsis, Z., Zhao, C., Putnik, M., Gustafsson, J. A. and Dahlman-Wright, K. (2009). "Binding of estrogen receptor alpha/beta heterodimers to chromatin in MCF-7 cells." *J. Mol. Endocrinol.* 43(2): 65-72. 10.1677/jme-08-0177.
- Parihar, S. P., Guler, R. and Brombacher, F. (2019). "Statins: a viable candidate for host-directed therapy against infectious diseases." *Nat. Rev. Immunol.* 19(2): 104-117. 10.1038/s41577-018-0094-3.
- Park, C., Cha, H.-J., Hong, S. H., Kim, G.-Y., Kim, S., Kim, H.-S., Kim, B. W., Jeon, Y.-J., et al. (2019). "Protective effect of phloroglucinol on oxidative stress-induced DNA damage and apoptosis through activation of the Nrf2/HO-1 signaling pathway in HaCaT human keratinocytes." *Mar. Drugs* 17(4): 225. 10.3390/md17040225.
- Park, E.-J. and Pezzuto, J. M. (2013a). "Antioxidant marine products in cancer chemoprevention." *Antioxid. Redox Signal.* 19(2): 115-138. 10.1089/ars.2013.5235.
- Park, E. J. and Pezzuto, J. M. (2013b). "Antioxidant marine products in cancer chemoprevention." *Antioxid. Redox Signal* 19(2): 115-138. 10.1089/ars.2013.5235.
- Park, H.-K., Kim, I.-H., Kim, J. and Nam, T.-J. (2012). "Induction of apoptosis by laminarin, regulating the insulin-like growth factor-IR signaling pathways in HT-29 human colon cells." *Int. J. Mol. Med.* 30(4): 734-738. 10.3892/ijmm.2012.1084.
- Park, H.-K., Kim, I.-H., Kim, J. and Nam, T.-J. (2013). "Induction of apoptosis and the regulation of ErbB signaling by laminarin in HT-29 human colon cancer cells." *Int. J. Mol. Med.* 32(2): 291-295. 10.3892/ijmm.2013.1409.
- Park, J. S., Chyun, J. H., Kim, Y. K., Line, L. L. and Chew, B. P. (2010). "Astaxanthin decreased oxidative stress and inflammation and enhanced immune response in humans." *Nutr. Metab* 7: 18. 10.1186/1743-7075-7-18.
- Parsons, H. A. and Burstein, H. J. (2021). "Adjuvant capecitabine in triple-negative breast cancer: New strategies for tailoring treatment recommendations." *JAMA* 325(1): 36-38. 10.1001/jama.2020.23371.
- Patel, H. K. and Bihani, T. (2018). "Selective estrogen receptor modulators (SERMs) and selective estrogen receptor degraders (SERDs) in cancer treatment." *Pharmacol. Ther.* 186: 1-24. 10.1016/j.pharmthera.2017.12.012.

- Patra, B., Peng, C.-C., Liao, W.-H., Lee, C.-H. and Tung, Y.-C. (2016). "Drug testing and flow cytometry analysis on a large number of uniform sized tumor spheroids using a microfluidic device." *Sci. Rep.* 6(1): 21061. 10.1038/srep21061.
- Pavlopoulou, A., Oktay, Y., Vougas, K., Louka, M., Vorgias, C. E. and Georgakilas, A. G. (2016). "Determinants of resistance to chemotherapy and ionizing radiation in breast cancer stem cells." *Cancer Lett.* 380(2): 485-493. 10.1016/j.canlet.2016.07.018.
- Pawar, V. K., Singh, Y., Sharma, K., Shrivastav, A., Sharma, A., Singh, A., Meher, J. G., Singh, P., et al. (2019). "Improved chemotherapy against breast cancer through immunotherapeutic activity of fucoidan decorated electrostatically assembled nanoparticles bearing doxorubicin." *Int. J. Biol. Macromol.* 122: 1100-1114. 10.1016/j.ijbiomac.2018.09.059.
- Peñalver, R., Lorenzo, J. M., Ros, G., Amarowicz, R., Pateiro, M. and Nieto, G. (2020). "Seaweeds as a functional ingredient for a healthy diet." *Mar. Drugs* 18(6): 301. 10.3390/md18060301.
- Peng, J., Yuan, J.-P., Wu, C.-F. and Wang, J.-H. (2011). "Fucoxanthin, a marine carotenoid present in brown seaweeds and diatoms: metabolism and bioactivities relevant to human health." *Mar. Drugs* 9(10): 1806-1828. 10.3390/md9101806.
- Perche, F. and Torchilin, V. P. (2012). "Cancer cell spheroids as a model to evaluate chemotherapy protocols." *Cancer Biol. Ther.* 13(12): 1205-1213. 10.4161/cbt.21353.
- Pereira, A. G., Otero, P., Echave, J., Carreira-Casais, A., Chamorro, F., Collazo, N., Jaboui, A., Lourenço-Lopes, C., et al. (2021a). "Xanthophylls from the sea: Algae as source of bioactive carotenoids." *Mar. Drugs* 19(4): 188. 10.3390/md19040188.
- Pereira, C. P. M., Souza, A. C. R., Vasconcelos, A. R., Prado, P. S. and Name, J. J. (2021b). "Antioxidant and anti-inflammatory mechanisms of action of astaxanthin in cardiovascular diseases (Review)." *Int. J. Mol. Med.* 47(1): 37-48. 10.3892/ijmm.2020.4783.
- Perou, C. M., Sørlie, T., Eisen, M. B., van de Rijn, M., Jeffrey, S. S., Rees, C. A., Pollack, J. R., Ross, D. T., et al. (2000). "Molecular portraits of human breast tumours." *Nature* 406(6797): 747-752. 10.1038/35021093.
- Pesapane, F., Suter, M. B., Rotili, A., Penco, S., Nigro, O., Cremonesi, M., Bellomi, M., Jereczek-Fossa, B. A., et al. (2020). "Will traditional biopsy be substituted by radiomics and liquid biopsy for breast cancer diagnosis and characterisation?" *Med. Oncol.* 37(4): 29. 10.1007/s12032-020-01353-1.
- Peshkin, B. N., Alabek, M. L. and Isaacs, C. (2010). "BRCA1/2 mutations and triple negative breast cancers." *Breast Dis.* 32(1-2): 25-33. 10.3233/BD-2010-0306.



- Petrelli, F., Barni, S., Bregni, G., de Braud, F. and Di Cosimo, S. (2016). "Platinum salts in advanced breast cancer: a systematic review and meta-analysis of randomized clinical trials." *Breast Cancer Res. Treat.* 160(3): 425-437. 10.1007/s10549-016-4025-3.
- Petrova, R. D., Reznick, A. Z., Wasser, S. P., Denchev, C. M., Nevo, E. and Mahajna, J. (2008). "Fungal metabolites modulating NF-kappaB activity: an approach to cancer therapy and chemoprevention (review)." *Oncol. Rep.* 19(2): 299-308. PMID: 18202775.
- Petty, R., Anthoney, A., Metges, J. P., Alsina, M., Gonçalves, A., Brown, J., Montagut, C., Gunzer, K., et al. (2016). "Phase Ib/II study of elisidepsin in metastatic or advanced gastroesophageal cancer (IMAGE trial)." *Cancer Chemother. Pharmacol.* 77(4): 819-827. 10.1007/s00280-016-2991-0.
- Phull, A. R. and Kim, S. J. (2017). "Fucoidan as bio-functional molecule: Insights into the anti-inflammatory potential and associated molecular mechanisms." *J. Funct. Foods* 38: 415-426. 10.1016/j.jff.2017.09.051.
- Piccinini, F. (2015). "AnaSP: a software suite for automatic image analysis of multicellular spheroids." *Comput. Methods Programs Biomed.* 119(1): 43-52. 10.1016/j.cmpb.2015.02.006.
- Pięt, M., Zając, A., Paduch, R., Jaszek, M., Frant, M., Stefaniuk, D., Matuszewska, A. and Grzywnowicz, K. (2021). "Chemopreventive activity of bioactive fungal fractions isolated from milk-supplemented cultures of *Cerrena unicolor* and *Pycnoporus sanguineus* on colon cancer cells." *3 Biotech.* 11(1): 5. 10.1007/s13205-020-02591-w.
- Piggott, L., Omidvar, N., Marti Perez, S., French, R., Eberl, M. and Clarkson, R. W. (2011). "Suppression of apoptosis inhibitor c-FLIP selectively eliminates breast cancer stem cell activity in response to the anti-cancer agent, TRAIL." *Breast Cancer Res.* 13(5): R88. 10.1186/bcr2945.
- Pinnarò, P., Rambone, R., Giordano, C., Giannarelli, D., Strigari, L. and Arcangeli, G. (2011). "Long-term results of a randomized trial on the sequencing of radiotherapy and chemotherapy in breast cancer." *Am. J. Clin. Oncol.* 34(3): 238-244. 10.1097/COC.0b013e3181dea9b8.
- Poggio, F., Bruzzone, M., Ceppi, M., Pondé, N. F., La Valle, G., Del Mastro, L., de Azambuja, E. and Lambertini, M. (2018). "Platinum-based neoadjuvant chemotherapy in triple-negative breast cancer: a systematic review and meta-analysis." *Ann. Oncol.* 29(7): 1497-1508. 10.1093/annonc/mdy127.
- Poloz, Y., Dowling, R. J. and Stambolic, V. (2017). Fundamental pathways in breast cancer 1: signaling from the membrane. *Breast Cancer. U. Veronesi, A. Goldhirsch,*

- P. Veronesi, O. Gentilini and L. M. Springer, Cham. 10.1007/978-3-319-48848-6\_1: 3-12.10.1007/978-3-319-48848-6\_1
- Powles, T., Rosenberg, J. E., Sonpavde, G. P., Loriot, Y., Durán, I., Lee, J.-L., Matsubara, N., Vulsteke, C., et al. (2021). "Enfortumab vedotin in previously treated advanced urothelial carcinoma." *N. Engl. J. Med.* 384(12): 1125-1135. 10.1056/NEJMoa2035807.
- Prior, H., Baldrick, P., de Haan, L., Downes, N., Jones, K., Mortimer-Cassen, E. and Kimber, I. (2018). "Reviewing the utility of two species in general toxicology related to drug development." *Int. J. Toxicol.* 37(2): 121-124. 10.1177/1091581818760564.
- Qi, Y., Wang, L., You, Y., Sun, X., Wen, C., Fu, Y. and Song, S. (2022). "Preparation of low-molecular-weight fucoidan with anticoagulant activity by photocatalytic degradation method." *Foods* 11(6):822. 10.3390/foods11060822.
- Qiu, W.-L., Tseng, A.-J., Hsu, H.-Y., Hsu, W.-H., Lin, Z.-H., Hua, W.-J. and Lin, T.-Y. (2020). "Fucoidan increased the sensitivity to gefitinib in lung cancer cells correlates with reduction of TGF $\beta$ -mediated Slug expression." *Int. J. Biol. Macromol.* 153: 796-805. 10.1016/j.ijbiomac.2020.03.066.
- Queguineur, B., Goya, L., Ramos, S., Martin, M. A., Mateos, R. and Bravo, L. (2012). "Phloroglucinol: antioxidant properties and effects on cellular oxidative markers in human HepG2 cell line." *Food Chem. Toxicol.* 50(8): 2886-2893. 10.1016/j.fct.2012.05.026.
- Rädler, P. D., Wehde, B. L., Triplett, A. A., Shrestha, H., Shepherd, J. H., Pfefferle, A. D., Rui, H., Cardiff, R. D., et al. (2021). "Highly metastatic claudin-low mammary cancers can originate from luminal epithelial cells." *Nat. Commun.* 12(1): 3742. 10.1038/s41467-021-23957-5.
- Raghavan, S., Mehta, P., Horst, E. N., Ward, M. R., Rowley, K. R. and Mehta, G. (2016). "Comparative analysis of tumor spheroid generation techniques for differential in vitro drug toxicity." *Oncotarget* 7(13): 16948-16961. 10.18632/oncotarget.7659.
- Ramos, A. A., Almeida, T., Lima, B. and Rocha, E. (2019). "Cytotoxic activity of the seaweed compound fucosterol, alone and in combination with 5-fluorouracil, in colon cells using 2D and 3D culturing." *J. Toxicol. Environ. Health A* 82(9): 537-549. 10.1080/15287394.2019.1634378.
- Rateb, M. E. and Ebel, R. (2011). "Secondary metabolites of fungi from marine habitats." *Nat. Prod. Rep.* 28(2): 290-344. 10.1039/C0NP00061B.
- Ravichandran, A., Clegg, J., Adams, M. N., Hampson, M., Fielding, A. and Bray, L. J. (2021). "3D breast tumor models for radiobiology applications." *Cancers (Basel)* 13(22): 5714. 10.3390/cancers13225714.

- Rejhová, A., Opattová, A., Čumová, A., Slíva, D. and Vodička, P. (2018). "Natural compounds and combination therapy in colorectal cancer treatment." *Eur. J. Med. Chem.* 144: 582-594. 10.1016/j.ejmech.2017.12.039.
- Reyes, M. E., Riquelme, I., Salvo, T., Zanella, L., Letelier, P. and Brebi, P. (2020). "Brown seaweed fucoidan in cancer: implications in metastasis and drug resistance." *Mar. Drugs* 18(5): 232. 10.3390/md18050232.
- Reynolds, D. S., Tevis, K. M., Blessing, W. A., Colson, Y. L., Zaman, M. H. and Grinstaff, M. W. (2017). "Breast cancer spheroids reveal a differential cancer stem cell response to chemotherapeutic treatment." *Sci. Rep.* 7(1): 10382. 10.1038/s41598-017-10863-4.
- Rezai, M., Kraemer, S. (2017). *Breast-Conserving Surgery After Neoadjuvant Therapy*. In: Veronesi, U., Goldhirsch, A., Veronesi, P., Gentilini, O., Leonardi, M. (eds) *Breast Cancer*. Springer, Cham. 10.1007/978-3-319-48848-6\_28
- Rezayatmand, H., Razmkhah, M. and Razeghian-Jahromi, I. (2022). "Drug resistance in cancer therapy: the Pandora's Box of cancer stem cells." *Stem Cell Res. Ther.* 13(1): 181. 10.1186/s13287-022-02856-6.
- Rhein-Knudsen, N., Ale, M. T. and Meyer, A. S. (2015). "Seaweed hydrocolloid production: An update on enzyme assisted extraction and modification technologies." *Mar. Drugs* 13(6): 3340-59. 10.3390/md13063340.
- Ribeiro-Filho, A. C., Levy, D., Ruiz, J. L. M., Mantovani, M. D. C. and Bydlowski, S. P. (2019). "Traditional and advanced cell cultures in hematopoietic stem cell studies." *Cells* 8(12):1628. 10.3390/cells8121628.
- Ricci, F., Tedeschi, A., Morra, E. and Montillo, M. (2009). "Fludarabine in the treatment of chronic lymphocytic leukemia: a review." *Ther. Clin. Risk Manag.* 5(1): 187-207. 10.2147/tcrm.s3688.
- Rich, J. N. (2016). "Cancer stem cells: understanding tumor hierarchy and heterogeneity." *Medicine* 95(1 Suppl 1): S2-S7. 10.1097/MD.0000000000004764.
- Roarty, K. and Echeverria, G. V. (2021). "Laboratory models for investigating breast cancer therapy resistance and metastasis." *Front. Oncol.* 11: 645698. 10.3389/fonc.2021.645698.
- Roper, S. J. and Coyle, B. (2022). "Establishing an in vitro 3D spheroid model to study medulloblastoma drug response and tumor dissemination." *Curr. Protoc.* 2(1): e357. 10.1002/cpz1.357.
- Rosen, R. D. and Sapra, A. (2021). "TNM Classification." In: *StatPearls* [Internet]. Treasure Island (FL): StatPearls. Retrieved 2<sup>nd</sup>.December 2021. Available from: <https://www.ncbi.nlm.nih.gov/books/NBK553187/>.

- Rosenberg, J. E., Ballman, K. A., Halabi, S., Atherton, P. J., Mortazavi, A., Sweeney, C., Stadler, W. M., Teply, B. A., et al. (2021). "Randomized phase III Trial of Gemcitabine and Cisplatin with Bevacizumab or placebo in patients with advanced urothelial carcinoma: Results of CALGB 90601 (Alliance)." *Am. J. Clin. Oncol.* 39(22): 2486-2496. 10.1200/JCO.21.00286.
- Roskoski, R. (2014). "The ErbB/HER family of protein-tyrosine kinases and cancer." *Pharmacol. Res. Commun.* 79: 34-74. 10.1016/j.phrs.2013.11.002.
- Rotem, A., Janzer, A., Izar, B., Ji, Z., Doench, J. G., Garraway, L. A. and Struhl, K. (2015). "Alternative to the soft-agar assay that permits high-throughput drug and genetic screens for cellular transformation." *Proc. Natl. Acad. Sci.* 112(18): 5708-5713. 10.1073/pnas.1505979112.
- Ruiz-Torres, V., Encinar, J. A., Herranz-López, M., Pérez-Sánchez, A., Galiano, V., Barrajón-Catalán, E. and Micol, V. (2017). "An updated review on marine anticancer compounds: The use of virtual screening for the discovery of small-molecule cancer drugs." *Molecules* 22(7): 1037. 10.3390/molecules22071037.
- Russo, E., Scicchitano, F., Whalley, B. J., Mazzitello, C., Ciriaco, M., Esposito, S., Patanè, M., Upton, R., et al. (2014). "*Hypericum perforatum*: pharmacokinetic, mechanism of action, tolerability, and clinical drug-drug interactions." *Phytother. Res.* 28(5): 643-655. 10.1002/ptr.5050.
- Ruud, K. F., Hiscox, W. C., Yu, I., Chen, R. K. and Li, W. (2020). "Distinct phenotypes of cancer cells on tissue matrix gel." *Breast Cancer Res.* 22(1): 82. 10.1186/s13058-020-01321-7.
- Rwigemera, A., Mamelona, J. and Martin, L. J. (2014). "Inhibitory effects of fucoxanthinol on the viability of human breast cancer cell lines MCF-7 and MDA-MB-231 are correlated with modulation of the NF-kappaB pathway." *Cell. Biol. Toxicol.* 30(3): 157-167. 10.1007/s10565-014-9277-2.
- Rwigemera, A., Mamelona, J. and Martin, L. J. (2015). "Comparative effects between fucoxanthinol and its precursor fucoxanthin on viability and apoptosis of breast cancer cell lines MCF-7 and MDA-MB-231." *Anticancer Res.* 35(1): 207-219. PMID: 25550553
- Sachindra, N. M., Sato, E., Maeda, H., Hosokawa, M., Niwano, Y., Kohno, M. and Miyashita, K. (2007). "Radical scavenging and singlet oxygen quenching activity of marine carotenoid fucoxanthin and its metabolites." *J. Agric. Food Chem.* 55(21): 8516-8522. 10.1021/jf071848a.
- Sanjeeva, K. K. A. and Jeon, Y.-J. (2021). "Fucoidans as scientifically and commercially important algal polysaccharides." *Mar. Drugs* 19(6): 284. 10.3390/md19060284.

- Sanjeeva, K. K. A., Kang, N., Ahn, G., Jee, Y., Kim, Y.-T. and Jeon, Y.-J. (2018). "Bioactive potentials of sulfated polysaccharides isolated from brown seaweed *Sargassum* spp in related to human health applications: A review." *Food Hydrocoll.* 81: 200-208. 10.1016/j.foodhyd.2018.02.040.
- Sanniyasi, E., Venkatasubramanian, G., Anbalagan, M. M., Raj, P. P. and Gopal, R. K. (2019). "In vitro anti-HIV-1 activity of the bioactive compound extracted and purified from two different marine macroalgae (seaweeds) (*Dictyota bartayesiana* J.V.Lamouroux and *Turbinaria decurrens* Bory)." *Sci. Rep.* 9(1): 12185. 10.1038/s41598-019-47917-8.
- Sant, S. and Johnston, P. A. (2017). "The production of 3D tumor spheroids for cancer drug discovery." *Drug Discov. Today Technol.* 23: 27-36. 10.1016/j.ddtec.2017.03.002.
- Satomi, Y. (2012). "Fucoxanthin induces GADD45A expression and G1 arrest with SAPK/JNK activation in LNCap human prostate cancer cells." *Anticancer Res.* 32(3): 807-813. PMID: 22399598
- Satomi, Y. (2017). "Antitumor and cancer-preventative function of fucoxanthin: a marine carotenoid." *Anticancer Res.* 37(4): 1557-1562. 10.21873/anticancer.11484.
- Satomi, Y. and Nishino, H. (2013). "Inhibition of the enzyme activity of cytochrome P450 1A1, 1A2 and 3A4 by fucoxanthin, a marine carotenoid." *Oncol. Lett.* 6(3): 860-864. 10.3892/ol.2013.1457.
- Sauter, E. R. (2020). "Cancer prevention and treatment using combination therapy with natural compounds." *Expert Rev. Clin. Pharmacol.* 13(3): 265-285. 10.1080/17512433.2020.1738218.
- Schröder, L., Koch, J., Mahner, S., Kost, B. P., Hofmann, S., Jeschke, U., Haumann, J., Schmedt, J., et al. (2017). "The effects of *Petroselinum crispum* on estrogen receptor-positive benign and malignant mammary cells (MCF12A/MCF7)." *Anticancer Res.* 37(1): 95-102. 10.21873/anticancer.11294.
- Schwartz, R. E., Liesch, J., Hensens, O., Zitano, L., Honeycutt, S., Garrity, G., Fromtling, R. A., Onishi, J., et al. (1988). "L-657,398, a novel antifungal agent: fermentation, isolation, structural elucidation and biological properties." *J. Antibiot. (Tokyo)* 41(12): 1774-1779. 10.7164/antibiotics.41.1774.
- Scott, L. J. (2017). "Brentuximab vedotin: A review in CD30-positive Hodgkin lymphoma." *Drugs* 77(4): 435-445. 10.1007/s40265-017-0705-5.
- Selby, M., Delosh, R., Laudeman, J., Ogle, C., Reinhart, R., Silvers, T., Lawrence, S., Kinders, R., et al. (2017). "3D models of the NCI60 cell lines for screening oncology compounds." *SLAS Discov.* 22(5): 473-483. 10.1177/2472555217697434.

- Senkus, E. (2018). "Principles of radiation therapy." *Breast* 41: S7. 10.1016/j.breast.2018.08.024.
- Senthilkumar, K. and Kim, S. K. (2014). "Anticancer effects of fucoidan." *Adv. Food Nutr. Res.* 72: 195-213. 10.1016/B978-0-12-800269-8.00011-7.
- Serrano, M. J., Ortega, F. G., Alvarez-Cubero, M. J., Nadal, R., Sanchez-Rovira, P., Salido, M., Rodríguez, M., García-Puche, J. L., et al. (2014). "EMT and EGFR in CTCs cytokeratin negative non-metastatic breast cancer." *Oncotarget* 5(17): 7486-7497. 10.18632/oncotarget.2217.
- Shah, A. N. and Gradishar, W. J. (2018). "Adjuvant anthracyclines in breast cancer: What is their role?" *Oncologist* 23(10): 1153-1161. 10.1634/theoncologist.2017-0672.
- Shannon, E. and Abu-Ghannam, N. (2019). "Seaweeds as nutraceuticals for health and nutrition." *Phycologia* 58(5): 563-577. 10.1080/00318884.2019.1640533.
- Shiratori, K., Ohgami, K., Ilieva, I., Jin, X. H., Koyama, Y., Miyashita, K., Yoshida, K., Kase, S., et al. (2005). "Effects of fucoxanthin on lipopolysaccharide-induced inflammation in vitro and in vivo." *Exp. Eye Res.* 81(4): 422-428. 10.1016/j.exer.2005.03.002.
- Shoemaker, R. H. (2006). "The NCI60 human tumour cell line anticancer drug screen." *Nat Rev Cancer* 6(10): 813-823. 10.1038/nrc1951.
- Siddik, Z. H. (2003). "Cisplatin: mode of cytotoxic action and molecular basis of resistance." *Oncogene* 22(47): 7265-7279. 10.1038/sj.onc.1206933.
- Silva, J., Alves, C., Freitas, R., Martins, A., Pinteus, S., Ribeiro, J., Gaspar, H., Alfonso, A., et al. (2019). "Antioxidant and neuroprotective potential of the brown seaweed *Bifurcaria bifurcata* in an in vitro Parkinson's disease model." *Mar. Drugs* 17(2):85.10.3390/md17020085.
- Singh, I. P., Sidana, J., Bharate, S. B. and Foley, W. J. (2010). "Phloroglucinol compounds of natural origin: synthetic aspects." *Nat. Prod. Rep.* 27(3): 393-416. 10.1039/b914364p.
- Singh, K., Bhorl, M., Kasu, Y. A., Bhat, G. and Marar, T. (2018). "Antioxidants as precision weapons in war against cancer chemotherapy induced toxicity - Exploring the armoury of obscurity." *Saudi Pharm J.* 26(2): 177-190. 10.1016/j.jsps.2017.12.013.
- Singh, V. K. and Seed, T. M. (2021). "How necessary are animal models for modern drug discovery?" *Expert Opin. Drug Discov.* 16(12): 1391-1397. 10.1080/17460441.2021.1972255.
- Sleightholm, R., Neilsen, B. K., Elkhatib, S., Flores, L., Dukkupati, S., Zhao, R., Choudhury, S., Gardner, B., et al. (2021). "Percentage of hormone receptor positivity

- in breast cancer provides prognostic value: A Single-institute study." *J. Clin. Med. Res* 13(1): 9-19. 10.14740/jocmr4398.
- Slepicka, P. F., Somasundara, A. V. H. and dos Santos, C. O. (2021). "The molecular basis of mammary gland development and epithelial differentiation." *Semin. Cell Dev. Biol.* 114: 93-112. 10.1016/j.semcdb.2020.09.014.
- Sommers, C. L., Walker-Jones, D., Heckford, S. E., Worland, P., Valverius, E., Clark, R., McCormick, F., Stampfer, M., et al. (1989). "Vimentin rather than keratin expression in some hormone-independent breast cancer cell lines and in oncogene-transformed mammary epithelial cells." *Cancer Res.* 49(15): 4258-4263. PMID: 2472876
- Song, K. and Farzaneh, M. (2021). "Signaling pathways governing breast cancer stem cells behavior." *Stem Cell Res.* 12(1): 245. 10.1186/s13287-021-02321-w.
- Song, K., Xu, L., Zhang, W., Cai, Y., Jang, B., Oh, J. and Jin, J. O. (2017a). "Laminarin promotes anti-cancer immunity by the maturation of dendritic cells." *Oncotarget* 8(24): 38554-38567. 10.18632/oncotarget.16170.
- Song, X. D., Zhang, J. J., Wang, M. R., Liu, W. B., Gu, X. B. and Lv, C. J. (2011). "Astaxanthin induces mitochondria-mediated apoptosis in rat hepatocellular carcinoma CBRH-7919 cells." *Biol. Pharm. Bull* 34(6): 839-844. 10.1248/bpb.34.839.
- Song, Y., Oh, G. H., Kim, M.-B. and Hwang, J.-K. (2017b). "Fucosterol inhibits adipogenesis through the activation of AMPK and Wnt/ $\beta$ -catenin signaling pathways." *Food Sci. Biotechnol.* 26(2): 489-494. 10.1007/s10068-017-0067-5.
- Sorlie, T., Tibshirani, R., Parker, J., Hastie, T., Marron, J. S., Nobel, A., Deng, S., Johnsen, H., et al. (2003). "Repeated observation of breast tumor subtypes in independent gene expression data sets." *PNAS* 100(14): 8418-8423. 10.1073/pnas.0932692100.
- Sousa, C., Cruz, M., Neto, A., Pereira, K., Peixoto, M., Bastos, J., Henriques, M., Roda, D., et al. (2020). "Neoadjuvant radiotherapy in the approach of locally advanced breast cancer." *ESMO open* 4(Suppl 2): e000640. 10.1136/esmoopen-2019-000640.
- Souza, A. G., Silva, I. B. B., Campos-Fernandez, E., Barcelos, L. S., Souza, J. B., Marangoni, K., Goulart, L. R. and Alonso-Goulart, V. (2018). "Comparative assay of 2D and 3D cell culture models: Proliferation, gene Expression and anticancer drug response." *Curr. Pharm. Des.* 24(15): 1689-1694. 10.2174/1381612824666180404152304.
- Sowmya, P. R.-R., Arathi, B. P., Vijay, K., Baskaran, V. and Lakshminarayana, R. (2017). "Astaxanthin from shrimp efficiently modulates oxidative stress and allied cell death

- progression in MCF-7 cells treated synergistically with  $\beta$ -carotene and lutein from greens." *Food Chem. Toxicol.* 106: 58-69. 10.1016/j.fct.2017.05.024.
- Sporn, M. B., Dunlop, N. M., Newton, D. L. and Smith, J. M. (1976). "Prevention of chemical carcinogenesis by vitamin A and its synthetic analogs (retinoids)." *Fed. Proc.* 35(6): 1332-1338.
- Sporn, M. B. and Suh, N. (2000). "Chemoprevention of cancer." *Carcinogenesis* 21(3): 525-530. 10.1093/carcin/21.3.525.
- Stock, K., Estrada, M. F., Vidic, S., Gjerde, K., Rudisch, A., Santo, V. E., Barbier, M., Blom, S., et al. (2016). "Capturing tumor complexity in vitro: Comparative analysis of 2D and 3D tumor models for drug discovery." *Sci. Rep.* 6(1): 28951. 10.1038/srep28951.
- Stonik, V. A. and Fedorov, S. N. (2014). "Marine low molecular weight natural products as potential cancer preventive compounds." *Mar. Drugs* 12(2): 636-671. 10.3390/md12020636.
- Subaraja, M., Anantha Krishnan, D., Edwin Hillary, V., William Raja, T. R., Mathew, P., Ravikumar, S., Gabriel Paulraj, M. and Ignacimuthu, S. (2020). "Fucoidan serves a neuroprotective effect in an Alzheimer's disease model." *Front. Biosci. (Elite Ed)* 12(1): 1-34. 10.2741/e855.
- Subik, K., Lee, J.-F., Baxter, L., Strzepek, T., Costello, D., Crowley, P., Xing, L., Hung, M.-C., et al. (2010). "The expression patterns of ER, PR, HER2, CK5/6, EGFR, Ki-67 and AR by immunohistochemical analysis in breast cancer cell lines." *Breast Cancer* 4: 35-41. 10.1177/1178223418806626.
- Sugawara, T., Matsubara, K., Akagi, R., Mori, M. and Hirata, T. (2006). "Antiangiogenic activity of brown algae fucoxanthin and its deacetylated product, fucoxanthinol." *J. Agric. Food Chem.* 54(26): 9805-9810. 10.1021/jf062204q.
- Suleria, H. A., Osborne, S., Masci, P. and Gobe, G. (2015). "Marine-based nutraceuticals: An innovative trend in the food and supplement industries." *Mar. Drugs* 13(10): 6336-6351. 10.3390/md13106336.
- Sun, S. Q., Zhao, Y. X., Li, S. Y., Qiang, J. W. and Ji, Y. Z. (2020). "Anti-tumor effects of astaxanthin by inhibition of the expression of STAT3 in prostate cancer." *Mar. Drugs* 18(8): 415. 10.3390/md18080415.
- Sun, Y.-S., Zhao, Z., Yang, Z.-N., Xu, F., Lu, H.-J., Zhu, Z.-Y., Shi, W., Jiang, J., et al. (2017). "Risk factors and preventions of breast cancer." *Int. J. Biol. Sci.* 13(11): 1387-1397. 10.7150/ijbs.21635.
- Sung, H., Ferlay, J., Siegel, R. L., Laversanne, M., Soerjomataram, I., Jemal, A. and Bray, F. (2021). "Global cancer statistics 2020: GLOBOCAN estimates of incidence



- and mortality worldwide for 36 cancers in 185 countries." *CA Cancer J. Clin.* 71(3): 209-249. 10.3322/caac.21660.
- Sutherland, R. M., Sordat, B., Bamat, J., Gabbert, H., Bourrat, B. and Mueller-Klieser, W. (1986). "Oxygenation and differentiation in multicellular spheroids of human colon carcinoma." *Cancer Res.* 46(10): 5320-5329. PMID: 3756881
- Swaby, R. F., Sharma, C. G. N. and Jordan, V. C. (2007). "SERMs for the treatment and prevention of breast cancer." *Rev. Endocr. Metab. Disord.* 8(3): 229-239. 10.1007/s11154-007-9034-4.
- Swami, U., Shah, U. and Goel, S. (2015). "Eribulin in cancer treatment." *Mar. Drugs* 13(8): 5016-5058. 10.3390/md13085016.
- Swaminathan, S., Hamid, Q., Sun, W. and Clyne, A. M. (2019). "Bioprinting of 3D breast epithelial spheroids for human cancer models." *Biofabrication* 11(2): 025003. 10.1088/1758-5090/aafc49.
- Sweeney, M. F., Sonnenschein, C. and Soto, A. M. (2018). "Characterization of MCF-12A cell phenotype, response to estrogens, and growth in 3D." *Cancer Cell Int.* 18: 43-43. 10.1186/s12935-018-0534-y.
- Sy, C., Gleize, B., Dangles, O., Landrier, J. F., Veyrat, C. C. and Borel, P. (2012). "Effects of physicochemical properties of carotenoids on their bioaccessibility, intestinal cell uptake, and blood and tissue concentrations." *Mol. Nutr. Food Res.* 56(9): 1385-1397. 10.1002/mnfr.201200041.
- Sznarkowska, A., Kostecka, A., Meller, K. and Bielawski, K. P. (2017). "Inhibition of cancer antioxidant defense by natural compounds." *Oncotarget* 8(9): 15996-16016. 10.18632/oncotarget.13723.
- Sztretye, M., Dienes, B., Gönczi, M., Czirják, T., Csernoch, L., Dux, L., Szentesi, P. and Keller-Pintér, A. (2019). "Astaxanthin: A potential mitochondrial-targeted antioxidant treatment in diseases and with aging." *Oxid. Med. Cell. Longev.* 2019: 3849692-3849692. 10.1155/2019/3849692.
- Tachjian, A., Maria, V. and Jahangir, A. (2010). "Use of herbal products and potential interactions in patients with cardiovascular diseases." *J. Am. Coll. Cardiol.* 55(6): 515-525. 10.1016/j.jacc.2009.07.074.
- Tafuku, S., Ishikawa, C., Yasumoto, T. and Mori, N. (2012). "Anti-neoplastic effects of fucoxanthin and its deacetylated product, fucoxanthinol, on Burkitt's and Hodgkin's lymphoma cells." *Oncol. Rep.* 28(4): 1512-1518. 10.3892/or.2012.1947.
- Takahashi, H., Kawaguchi, M., Kitamura, K., Narumiya, S., Kawamura, M., Tengan, I., Nishimoto, S., Hanamura, Y., et al. (2017). "An exploratory study on the anti-inflammatory effects of fucoidan in relation to quality of life in advanced cancer patients." *Integr. Cancer Ther.* 17(2): 282-291. 10.1177/1534735417692097.

- Takaichi, S. (2011). "Carotenoids in algae: distributions, biosyntheses and functions." *Mar. Drugs* 9(6): 1101-1118. 10.3390/md9061101.
- Tamura, S., Narita, T., Fujii, G., Miyamoto, S., Hamoya, T., Kurokawa, Y., Takahashi, M., Miki, K., et al. (2019). "Inhibition of NF-kappaB transcriptional activity enhances fucoxanthinol-induced apoptosis in colorectal cancer cells." *Genes Environ.* 41: 1. 10.1186/s41021-018-0116-1.
- Tan, C. P. and Hou, Y. H. (2014). "First evidence for the anti-inflammatory activity of fucoxanthin in high-fat-diet-induced obesity in mice and the antioxidant functions in PC12 cells." *Inflammation* 37(2): 443-450. 10.1007/s10753-013-9757-1.
- Tanaka, K., Tokunaga, E., Inoue, Y., Yamashita, N., Saeki, H., Okano, S., Kitao, H., Oki, E., et al. (2016). "Impact of expression of vimentin and axl in breast cancer." *Clin. Breast Cancer* 16(6): 520-526.e522. 10.1016/j.clbc.2016.06.015.
- Tanaka, T., Kawamori, T., Ohnishi, M., Makita, H., Mori, H., Satoh, K. and Hara, A. (1995a). "Suppression of azoxymethane-induced rat colon carcinogenesis by dietary administration of naturally occurring xanthophylls astaxanthin and canthaxanthin during the postinitiation phase." *Carcinogenesis* 16(12): 2957-2963. 10.1093/carcin/16.12.2957.
- Tanaka, T., Makita, H., Ohnishi, M., Mori, H., Satoh, K. and Hara, A. (1995b). "Chemoprevention of rat oral carcinogenesis by naturally occurring xanthophylls, astaxanthin and canthaxanthin." *Cancer Res.* 55(18): 4059-4064. PMID: 7664280
- Tanaka, T., Morishita, Y., Suzui, M., Kojima, T., Okumura, A. and Mori, H. (1994). "Chemoprevention of mouse urinary bladder carcinogenesis by the naturally occurring carotenoid astaxanthin." *Carcinogenesis* 15(1): 15-19. 10.1093/carcin/15.1.15.
- Tanaka, T., Shnimizu, M. and Moriwaki, H. (2012). "Cancer chemoprevention by carotenoids." *Molecules* 17(3): 3202-3242. 10.3390/molecules17033202.
- Tao, J. J., Visvanathan, K. and Wolff, A. C. (2015). "Long term side effects of adjuvant chemotherapy in patients with early breast cancer." *Breast* 24: S149-S153. 10.1016/j.breast.2015.07.035.
- Taylor, A. P., Leon, E. and Goldenberg, D. M. (2010). "Placental growth factor (PIGF) enhances breast cancer cell motility by mobilising ERK1/2 phosphorylation and cytoskeletal rearrangement." *Br. J. Cancer* 103(1): 82-89. 10.1038/sj.bjc.6605746.
- Taylor, M. W., Radax, R., Steger, D. and Wagner, M. (2007). "Sponge-associated microorganisms: evolution, ecology, and biotechnological potential." *Microbiol. Mol. Biol. Rev.* 71(2): 295-347. 10.1128/mnbr.00040-06.

- Teas, J., Vena, S., Cone, D. L. and Irhimeh, M. (2013). "The consumption of seaweed as a protective factor in the etiology of breast cancer: proof of principle." *J. Appl. Phycol.* 25(3): 771-779. 10.1007/s10811-012-9931-0.
- Tengdelius, M., Gurav, D., Konradsson, P., Pålsson, P., Griffith, M. and Oommen, O. P. (2015). "Synthesis and anticancer properties of fucoidan-mimetic glycopolymer coated gold nanoparticles." *Chem. Commun.* 51(40): 8532-8535. 10.1039/c5cc02387d.
- Terasaki, M., Iida, T., Kikuchi, F., Tamura, K., Endo, T., Kuramitsu, Y., Tanaka, T., Maeda, H., et al. (2019a). "Fucoxanthin potentiates anoikis in colon mucosa and prevents carcinogenesis in AOM/DSS model mice." *J. Nutr. Biochem.* 64: 198-205. 10.1016/j.jnutbio.2018.10.007.
- Terasaki, M., Maeda, H., Miyashita, K. and Mutoh, M. (2017). "Induction of anoikis in human colorectal cancer cells by fucoxanthinol." *Nutr. Cancer* 69(7): 1-10. 10.1080/01635581.2017.1339814.
- Terasaki, M., Matsumoto, N., Hashimoto, R., Endo, T., Maeda, H., Hamada, J., Osada, K., Miyashita, K., et al. (2019b). "Fucoxanthin administration delays occurrence of tumors in xenograft mice by colonospheres, with an anti-tumor predictor of glycine." *J. Clin. Biochem. Nutr.* 64(1): 52-58. 10.3164/jcbn.18-45.
- Terasaki, M., Murase, W., Kamakura, Y., Kawakami, S., Kubota, A., Kojima, H., Ohta, T., Tanaka, T., et al. (2022). "A Biscuit containing fucoxanthin prevents colorectal carcinogenesis in mice." *Nutr. Cancer.* 74(10):3651-366. 10.1080/01635581.2022.2086703
- Thakur, V., Lu, J., Roscilli, G., Aurisicchio, L., Cappelletti, M., Pavoni, E., White, W. L. and Bedogni, B. (2017). "The natural compound fucoidan from New Zealand *Undaria pinnatifida* synergizes with the ERBB inhibitor lapatinib enhancing melanoma growth inhibition." *Oncotarget* 8(11): 17887-17896. 10.18632/oncotarget.14437.
- Thakuri, P. S., Liu, C., Luker, G. D. and Tavana, H. (2018). "Biomaterials-based approaches to tumor spheroid and organoid modeling." *Adv. Healthc. Mater.* 7(6): e1700980. 10.1002/adhm.201700980.
- Thorn, C. F., Oshiro, C., Marsh, S., Hernandez-Boussard, T., McLeod, H., Klein, T. E. and Altman, R. B. (2011). "Doxorubicin pathways: pharmacodynamics and adverse effects." *Pharmacogenet. Genomics* 21(7): 440-446. 10.1097/FPC.0b013e32833ffb56.
- Thuy, T. T., Ly, B. M., Van, T. T., Quang, N. V., Tu, H. C., Zheng, Y., Seguin-Devaux, C., Mi, B., et al. (2015). "Anti-HIV activity of fucoidans from three brown seaweed species." *Carbohydr. Polym.* 115: 122-128. 10.1016/j.carbpol.2014.08.068.

- Tian, L., Li, C.-M., Li, Y.-F., Huang, T.-M., Chao, N.-X., Luo, G.-R. and Mo, F.-R. (2020a). "Laminarin from seaweed (*Laminaria japonica*) inhibits hepatocellular carcinoma through upregulating senescence marker protein-30." *Cancer Biother Radiopharm.* 35(4): 277-283. 10.1089/cbr.2019.3179.
- Tian, L., Li, C. M., Li, Y. F., Huang, T. M., Chao, N. X., Luo, G. R. and Mo, F. R. (2020b). "Laminarin from seaweed (*Laminaria japonica*) inhibits hepatocellular carcinoma through upregulating senescence marker protein-30." *Cancer Biother. Radiopharm.* 35(4): 277-283. 10.1089/cbr.2019.3179.
- Tocaciu, S., Oliver, L. J., Lowenthal, R. M., Peterson, G. M., Patel, R., Shastri, M., McGuinness, G., Olesen, I., et al. (2016). "The effect of *Undaria pinnatifida* fucoidan on the pharmacokinetics of letrozole and tamoxifen in patients with breast cancer." *Integr. Cancer Ther.* 17(1): 99-105. 10.1177/1534735416684014.
- Trail, P. A., Dubowchik, G. M. and Lowinger, T. B. (2018). "Antibody drug conjugates for treatment of breast cancer: Novel targets and diverse approaches in ADC design." *Pharmacol. Ther.* 181: 126-142. 10.1016/j.pharmthera.2017.07.013.
- Tsai, H. L., Tai, C. J., Huang, C. W., Chang, F. R. and Wang, J. Y. (2017). "Efficacy of low-molecular-weight fucoidan as a supplemental therapy in metastatic colorectal cancer patients: A double-blind randomized controlled trial." *Mar. Drugs* 15(4): 122. 10.3390/md15040122.
- Uawisetwathana, U., Rodpai, E. and Moongkarndi, P. (2016). "Gene expression of cytokeratin 19 and its molecular detection in human breast cancer cell lines." *J. Pharm. Biomed. Anal.* 120: 25-31. 10.1016/j.jpba.2015.11.034.
- Urruticoechea, A., Smith, I. E. and Dowsett, M. (2005). "Proliferation marker Ki-67 in early breast cancer." *J. Clin. Oncol.* 23(28): 7212-7220. 10.1200/jco.2005.07.501.
- Uzma, F., Mohan, C. D., Hashem, A., Konappa, N. M., Rangappa, S., Kamath, P. V., Singh, B. P., Mudili, V., et al. (2018). "Endophytic fungi-alternative sources of cytotoxic compounds: a review." *Front. Pharmacol.* 9: 309. 10.3389/fphar.2018.00309.
- Vahdat, L. T., Schmid, P., Forero-Torres, A., Blackwell, K., Telli, M. L., Melisko, M., Möbus, V., Cortes, J., et al. (2021). "Glembatumumab vedotin for patients with metastatic, gpNMB overexpressing, triple-negative breast cancer ("METRIC"): a randomized multicenter study." *NPJ Breast Cancer* 7(1): 57-57. 10.1038/s41523-021-00244-6.
- Valdoz, J. C., Johnson, B. C., Jacobs, D. J., Franks, N. A., Dodson, E. L., Sanders, C., Cribbs, C. G. and Van Ry, P. M. (2021). "The ECM: To scaffold, or not to scaffold, that is the question." *Int. J. Mol. Sci.* 22(23): 12690. 10.3390/ijms222312690.

- Vamvakidou, A. P., Mondrinos, M. J., Petushi, S. P., Garcia, F. U., Lelkes, P. I. and Tozeren, A. (2007). "Heterogeneous breast tumoroids: An in vitro assay for investigating cellular heterogeneity and drug delivery." *J. Biomol. Screen.* 12(1): 13-20. 10.1177/1087057106296482.
- Vantangoli, M. M., Madnick, S. J., Huse, S. M., Weston, P. and Boekelheide, K. (2015). "MCF-7 human breast cancer cells form differentiated microtissues in scaffold-free hydrogels." *PLoS One* 10(8): e0135426. 10.1371/journal.pone.0135426.
- Vasir, J. K. and Labhasetwar, V. (2005). "Targeted drug delivery in cancer therapy." *Technol. Cancer Res. Treat.* 4(4): 363-374. 10.1177/153303460500400405.
- Venkatesan, J., Keekan, K. K., Anil, S., Bhatnagar, I. and Kim, S.-K. (2019). Phlorotannins. *Encyclopedia of Food Chemistry.* 10.1016/B978-0-08-100596-5.22360-3.
- Vergés, A. and Campbell, A. H. (2020). "Kelp forests." *Curr. Biol.* 30(16): R919-r920. 10.1016/j.cub.2020.06.053.
- Verjans, E. T., Doijen, J., Luyten, W., Landuyt, B. and Schoofs, L. (2018). "Three-dimensional cell culture models for anticancer drug screening: Worth the effort?" *J. Cell. Physiol.* 233(4): 2993-3003. 10.1002/jcp.26052.
- Vetvicka, V. and Vetvickova, J. (2017). "Fucoidans stimulate immune reaction and suppress cancer growth." *Anticancer Res.* 37(11): 6041-6046. 10.21873/anticancer.12051.
- Vidi, P. A., Bissell, M. J. and Lelievre, S. A. (2013). "Three-dimensional culture of human breast epithelial cells: the how and the why." *Methods Mol. Biol.* 945: 193-219. 10.1007/978-1-62703-125-7\_13.
- Viedma-Rodríguez, R., Baiza-Gutman, L., Salamanca-Gómez, F., Diaz-Zaragoza, M., Martínez-Hernández, G., Ruiz Esparza-Garrido, R., Velázquez-Flores, M. A. and Arenas-Aranda, D. (2014). "Mechanisms associated with resistance to tamoxifen in estrogen receptor-positive breast cancer (Review)." *Oncol. Rep.* 32(1): 3-15. 10.3892/or.2014.3190.
- Vijay, K., Sowmya, P. R., Arathi, B. P., Shilpa, S., Shwetha, H. J., Raju, M., Baskaran, V. and Lakshminarayana, R. (2018). "Low-dose doxorubicin with carotenoids selectively alters redox status and upregulates oxidative stress-mediated apoptosis in breast cancer cells." *Food Chem. Toxicol.* 118: 675-690. 10.1016/j.fct.2018.06.027.
- Vinci, M., Box, C. and Eccles, S. A. (2015). "Three-dimensional (3D) tumor spheroid invasion assay." *J. Vis. Exp.* 10.3791/52686(99): e52686. 10.3791/52686.
- Vinci, M., Gowan, S., Boxall, F., Patterson, L., Zimmermann, M., Court, W., Lomas, C., Mendiola, M., et al. (2012). "Advances in establishment and analysis of three-

- dimensional tumor spheroid-based functional assays for target validation and drug evaluation." *BMC Biol.* 10: 29. 10.1186/1741-7007-10-29.
- Vishchuk, O. S., Ermakova, S. P. and Zvyagintseva, T. N. (2011). "Sulfated polysaccharides from brown seaweeds *Saccharina japonica* and *Undaria pinnatifida*: isolation, structural characteristics, and antitumor activity." *Carbohydr. Res.* 346(17): 2769-2776. 10.1016/j.carres.2011.09.034.
- Vishchuk, O. S., Sun, H., Wang, Z., Ermakova, S. P., Xiao, J., Lu, T., Xue, P., Zvyagintseva, T. N., et al. (2016). "PDZ-binding kinase/T-LAK cell-originated protein kinase is a target of the fucoidan from brown alga *Fucus evanescens* in the prevention of EGF-induced neoplastic cell transformation and colon cancer growth." *Oncotarget* 7(14): 18763-18773. 10.18632/oncotarget.7708.
- Visioli, F. and Artaria, C. (2017). "Astaxanthin in cardiovascular health and disease: mechanisms of action, therapeutic merits, and knowledge gaps." *Food Funct.* 8(1): 39-63. 10.1039/c6fo01721e.
- Wahba, H. A. and El-Hadaad, H. A. (2015). "Current approaches in treatment of triple-negative breast cancer." *Cancer Biol. Med.* 12(2): 106-116. 10.7497/j.issn.2095-3941.2015.0030.
- Wahl, M., Goecke, F., Labes, A., Dobretsov, S. and Weinberger, F. (2012). "The second skin: ecological role of epibiotic biofilms on marine organisms." *Front. Microbiol.* 3: 292. 10.3389/fmicb.2012.00292.
- Waks, A. G. and Winer, E. P. (2019). "Breast cancer treatment: A review." *Jama* 321(3): 288-300. 10.1001/jama.2018.19323.
- Walko, C. M. and Lindley, C. (2005). "Capecitabine: a review." *Clin. Ther.* 27(1): 23-44. 10.1016/j.clinthera.2005.01.005.
- Walzl, A., Unger, C., Kramer, N., Unterleuthner, D., Scherzer, M., Hengstschläger, M., Schwanzer-Pfeiffer, D. and Dolznig, H. (2014). "The resazurin reduction assay can distinguish cytotoxic from cytostatic compounds in spheroid screening assays." *J. Biomol. Screen.* 19(7): 1047-1059. 10.1177/1087057114532352.
- Wang, E., Sorolla, M. A., Krishnan, P. D. G. and Sorolla, A. (2020). "From seabed to bedside: A review on promising marine anticancer compounds." *Biomolecules* 10(2): 248. 10.3390/biom10020248.
- Wang, H., Brown, P. C., Chow, E. C. Y., Ewart, L., Ferguson, S. S., Fitzpatrick, S., Freedman, B. S., Guo, G. L., et al. (2021). "3D cell culture models: Drug pharmacokinetics, safety assessment, and regulatory consideration." *Clin. Transl. Sci.* 14(5): 1659-1680. 10.1111/cts.13066.

- Wang, J., Ma, Y., Yang, J., Jin, L., Gao, Z., Xue, L., Hou, L., Sui, L., et al. (2019a). "Fucoxanthin inhibits tumour-related lymphangiogenesis and growth of breast cancer." *J. Cell Mol. Med.* 23(3): 2219-2229. 10.1111/jcmm.14151.
- Wang, J. and Xu, B. (2019). "Targeted therapeutic options and future perspectives for HER2-positive breast cancer." *Signal Transduct. Target. Ther.* 4(1): 34. 10.1038/s41392-019-0069-2.
- Wang, L., Zeng, Y., Liu, Y., Hu, X., Li, S., Wang, Y., Li, L., Lei, Z., et al. (2014). "Fucoxanthin induces growth arrest and apoptosis in human bladder cancer T24 cells by up-regulation of p21 and down-regulation of mortalin." *Acta Biochim. Biophys. Sin.* 46(10): 877-884. 10.1093/abbs/gmu080.
- Wang, M., Zhao, J., Zhang, L., Wei, F., Lian, Y., Wu, Y., Gong, Z., Zhang, S., et al. (2017a). "Role of tumor microenvironment in tumorigenesis." *J Cancer* 8(5): 761-773. 10.7150/jca.17648.
- Wang, P., Zhang, J., Zhan, N., Yang, S., Yu, M. and Liu, H. (2022). "The pharmacokinetic characteristics and excretion studies of fucosterol from *Sargassum fusiforme* in rats." *Biomed. Chromatogr.* 36(4): e5309. 10.1002/bmc.5309.
- Wang, X., Li, H., Wang, F., Xia, G., Liu, H., Cheng, X., Kong, M., Liu, Y., et al. (2017b). "Isolation of fucoxanthin from *Sargassum thunbergii* and preparation of microcapsules based on palm stearin solid lipid core." *Front. Mater. Sci.* 11(1): 66-74. 10.1007/s11706-017-0372-1.
- Wang, X., Zhang, H. and Chen, X. (2019b). "Drug resistance and combating drug resistance in cancer." *Cancer Drug Resist.* 2(2): 141-160. 10.20517/cdr.2019.10.
- Wang, X., Zhang, J. and Xu, T. (2007). "Cyclophosphamide as a potent inhibitor of tumor thioredoxin reductase in vivo." *Toxicol. Appl. Pharmacol.* 218(1): 88-95. 10.1016/j.taap.2006.10.029.
- Watson, C. J. (2006). "Key stages in mammary gland development - Involution: apoptosis and tissue remodelling that convert the mammary gland from milk factory to a quiescent organ." *Breast Cancer Res.* 8(2): 203. 10.1186/bcr1401.
- Weber-Ouellette, A., Busby, M. and Plante, I. (2018). "Luminal MCF-12A & myoepithelial-like Hs 578Bst cells form bilayered acini similar to human breast." *Future Sci. OA* 4(7): FSO315-FSO315. 10.4155/fsoa-2018-0010.
- Weigelt, B., Ghajar, C. M. and Bissell, M. J. (2014). "The need for complex 3D culture models to unravel novel pathways and identify accurate biomarkers in breast cancer." *Adv. Drug Deliv. Rev.* 69-70: 42-51. 10.1016/j.addr.2014.01.001.
- Weinberg, S. E. and Chandel, N. S. (2015). "Targeting mitochondria metabolism for cancer therapy." *Nat. Chem. Biol.* 11(1): 9-15. 10.1038/nchembio.1712.

- Weiss, R. B., Woolf, S. H., Demakos, E., Holland, J. F., Berry, D. A., Falkson, G., Cirrincione, C. T., Robbins, A., et al. (2003). "Natural history of more than 20 years of node-positive primary breast carcinoma treated with cyclophosphamide, methotrexate, and fluorouracil-based adjuvant chemotherapy: a study by the Cancer and Leukemia Group B." *J. Clin. Oncol.* 21(9): 1825-1835. 10.1200/jco.2003.09.006.
- Weiswald, L. B., Bellet, D. and Dangles-Marie, V. (2015). "Spherical cancer models in tumor biology." *Neoplasia* 17(1): 1-15. 10.1016/j.neo.2014.12.004.
- Wen, Y., Gao, L., Zhou, H., Ai, C., Huang, X., Wang, M., Zhang, Y. and Zhao, C. (2021). "Opportunities and challenges of algal fucoidan for diabetes management." *Trends Food Sci. Technol.* 111: 628-641. 10.1016/j.tifs.2021.03.028.
- Wibowo, J. T., Ahmadi, P., Rahmawati, S. I., Bayu, A., Putra, M. Y. and Kijjoa, A. (2022). "Marine-derived indole alkaloids and their biological and pharmacological activities." *Mar. Drugs* 20(1): 3. 10.3390/md20010003.
- Widmer, N., Bardin, C., Chatelut, E., Paci, A., Beijnen, J., Levêque, D., Veal, G. and Astier, A. (2014). "Review of therapeutic drug monitoring of anticancer drugs part two--targeted therapies." *Eur. J. Cancer* 50(12): 2020-2036. 10.1016/j.ejca.2014.04.015.
- Wojtkowiak, J. W., Verduzco, D., Schramm, K. J. and Gillies, R. J. (2011). "Drug resistance and cellular adaptation to tumor acidic pH microenvironment." *Mol. Pharm.* 8(6): 2032-2038. 10.1021/mp200292c.
- Woo, M. N., Jeon, S. M., Kim, H. J., Lee, M. K., Shin, S. K., Shin, Y. C., Park, Y. B. and Choi, M. S. (2010). "Fucoxanthin supplementation improves plasma and hepatic lipid metabolism and blood glucose concentration in high-fat fed C57BL/6N mice." *Chem. Biol. Interact.* 186(3): 316-322. 10.1016/j.cbi.2010.05.006.
- World Health Organization (2019). *Breast Tumors*, 5<sup>th</sup> Edition, IARC., Retrieved 21<sup>st</sup> November, 2021, available from <https://www.iarc.who.int/news-events/who-classification-of-tumours-5th-edition-volume-2-breast-tumours/>.
- Wu, Q., Ma, G., Deng, Y., Luo, W., Zhao, Y., Li, W. and Zhou, Q. (2019). "Prognostic value of Ki-67 in patients with resected triple-negative breast cancer: A meta-analysis." *Front. Oncol.* 9:1068.10.3389/fonc.2019.01068.
- Wu, S.-Y., Yan, M.-D., Wu, A. T. H., Yuan, K. S.-P. and Liu, S. H. (2016a). "Brown seaweed fucoidan inhibits cancer progression by dual regulation of mir-29c/ADAM12 and miR-17-5p/PTEN axes in human breast cancer cells." *J. Cancer* 7(15): 2408-2419. 10.7150/jca.15703.
- Wu, S. Y., Wu, A. T., Yuan, K. S. and Liu, S. H. (2016b). "Brown seaweed fucoidan inhibits cancer progression by dual regulation of mir-29c/ADAM12 and miR-17-



- 5p/PTEN Axes in human breast cancer cells." *J. Cancer* 7(15): 2408-2419. 10.7150/jca.15703.
- Xia, S., Wang, K., Wan, L., Li, A., Hu, Q. and Zhang, C. (2013). "Production, characterization, and antioxidant activity of fucoxanthin from the marine diatom *Odontella aurita*." *Mar. Drugs* 11(7): 2667-2681. 10.3390/md11072667.
- Xu, Y., Shi, T., Xu, A. and Zhang, L. (2016). "3D spheroid culture enhances survival and therapeutic capacities of MSCs injected into ischemic kidney." *J. Cell Mol. Med.* 20(7): 1203-1213. 10.1111/jcmm.12651.
- Yakavets, I., Francois, A., Benoit, A., Merlin, J.-L., Bezdetnaya, L. and Vogin, G. (2020). "Advanced co-culture 3D breast cancer model for investigation of fibrosis induced by external stimuli: optimization study." *Sci. Rep.* 10(1): 21273. 10.1038/s41598-020-78087-7.
- Yalaza, M., Inan, A. and Bozer, M. (2016). "Male breast cancer." *J. Breast Health* 12(1): 1-8. 10.5152/tjbh.2015.2711.
- Yamada, K. M., Doyle, A. D. and Lu, J. (2022). "Cell–3D matrix interactions: recent advances and opportunities." *Trends Cell Biol.* 32(10):883-895. 10.1016/j.tcb.2022.03.00210.1016/j.tcb.2022.03.002.
- Yamamoto, K., Ishikawa, C., Katano, H., Yasumoto, T. and Mori, N. (2011). "Fucoxanthin and its deacetylated product, fucoxanthinol, induce apoptosis of primary effusion lymphomas." *Cancer Lett.* 300(2): 225-234. 10.1016/j.canlet.2010.10.016.
- Yamasaki-Miyamoto, Y., Yamasaki, M., Tachibana, H. and Yamada, K. (2009). "Fucoidan induces apoptosis through activation of caspase-8 on human breast cancer MCF-7 cells." *J. Agric. Food Chem.* 57(18): 8677-8682. 10.1021/jf9010406.
- Yang, L., Wang, P., Wang, H., Li, Q., Teng, H., Liu, Z., Yang, W., Hou, L., et al. (2013a). "Fucoidan derived from *Undaria pinnatifida* induces apoptosis in human hepatocellular carcinoma SMMC-7721 cells via the ROS-mediated mitochondrial pathway." *Mar. Drugs* 11(6): 1961-1976. 10.3390/md11061961.
- Yang, T. J. and Ho, A. Y. (2013). "Radiation therapy in the management of breast cancer." *Surg. Clin. North Am.* 93(2): 455-471. 10.1016/j.suc.2013.01.002.
- Yang, Y., Kim, B. and Lee, J. (2013b). "Astaxanthin structure, metabolism, and health benefits." *J. Hum. Nutr. Food Sci.* 1: 1003.
- Yang, Y. I., Ahn, J. H., Choi, Y. S. and Choi, J. H. (2015). "Brown algae phlorotannins enhance the tumoricidal effect of cisplatin and ameliorate cisplatin nephrotoxicity." *Gynecol. Oncol.* 136(2): 355-364. 10.1016/j.ygyno.2014.11.015.
- Yang, Y. J., Nam, S.-J., Kong, G. and Kim, M. K. (2010). "A case–control study on seaweed consumption and the risk of breast cancer." *Br. J. Nutr.* 103(9): 1345-1353. 10.1017/S0007114509993242.

- Yasui, Y., Hosokawa, M., Mikami, N., Miyashita, K. and Tanaka, T. (2011). "Dietary astaxanthin inhibits colitis and colitis-associated colon carcinogenesis in mice via modulation of the inflammatory cytokines." *Chem. Biol. Interact.* 193(1): 79-87. 10.1016/j.cbi.2011.05.006.
- Yatiwella, L. N. S. B., Chathurangi, D. U. and Kothalawala, S. G. (2018). "Brief overview of bioactive compounds in seaweeds, their properties and practical applications in functional foods." *Int. J. Sci. Res.* 8(8): 594-602. 10.29322/IJSRP.8.8.2018.p8077.
- Ye, G., Wang, L., Yang, K. and Wang, C. (2020). "Fucoxanthin may inhibit cervical cancer cell proliferation via downregulation of HIST1H3D." *J. Int. Med. Res.* 48(10): 300060520964011. 10.1177/0300060520964011.
- Yersal, O. and Barutca, S. (2014). "Biological subtypes of breast cancer: Prognostic and therapeutic implications." *World J. Clin. Oncol.* 5(3): 412-424. 10.5306/wjco.v5.i3.412.
- Yi, J., Chen, S., Yi, P., Luo, J., Fang, M., Du, Y., Zou, L. and Fan, P. (2020). "Pyrotinib sensitizes 5-fluorouracil-resistant HER2(+) breast cancer cells to 5-fluorouracil." *Oncol. Res.* 28(5): 519-531. 10.3727/096504020X15960154585410.
- Yilancioglu, K., Weinstein, Z. B., Meydan, C., Akhmetov, A., Toprak, I., Durmaz, A., Iossifov, I., Kazan, H., et al. (2014). "Target-independent prediction of drug synergies using only drug lipophilicity." *J. Chem. Inf. Model.* 54(8): 2286-2293. 10.1021/ci500276x.
- Yilmazer, A. (2018). "Evaluation of cancer stemness in breast cancer and glioblastoma spheroids in vitro." *3 Biotech* 8(9): 390-390. 10.1007/s13205-018-1412-y.
- Yoon, J. Y., Choi, H. and Jun, H. S. (2017). "The effect of phloroglucinol, a component of *Ecklonia cava* extract, on hepatic glucose production." *Mar. Drugs* 15(4):106. 10.3390/md15040106.
- Yoon, S., Park, S. J., Han, J. H., Kang, J. H., Kim, J. h., Lee, J., Park, S., Shin, H. J., et al. (2014). "Caspase-dependent cell death-associated release of nucleosome and damage-associated molecular patterns." *Cell Death Dis.* 5(10): e1494-e1494. 10.1038/cddis.2014.450.
- Young-Ju, L. (2020). "Dieckol or phlorofuocufuroeckol extracted from *Ecklonia cava* suppresses lipopolysaccharide-mediated human breast cancer cell migration and invasion." *J. Appl. Phycol.* v. 32(no. 1): 631-640. 10.1007/s10811-019-01899-2.
- Yu, R. X., Hu, X. M., Xu, S. Q., Jiang, Z. J. and Yang, W. (2011). "Effects of fucoxanthin on proliferation and apoptosis in human gastric adenocarcinoma MGC-803 cells via JAK/STAT signal pathway." *Eur. J. Pharmacol.* 657(1-3): 10-19. 10.1016/j.ejphar.2010.12.006.

- Zaha, D. C. (2014). "Significance of immunohistochemistry in breast cancer." *World J. Clin. Oncol.* 5(3): 382-392. 10.5306/wjco.v5.i3.382.
- Zaheed, M., Wilcken, N., Willson, M. L., O'Connell, D. L. and Goodwin, A. (2019). "Sequencing of anthracyclines and taxanes in neoadjuvant and adjuvant therapy for early breast cancer." *Cochrane Database Syst. Rev.* 2(2): Cd012873. 10.1002/14651858.CD012873.pub2.
- Zanoni, M., Piccinini, F., Arienti, C., Zamagni, A., Santi, S., Polico, R., Bevilacqua, A. and Tesei, A. (2016). "3D tumor spheroid models for in vitro therapeutic screening: A systematic approach to enhance the biological relevance of data obtained." *Sci. Rep.* 6: 19103. 10.1038/srep19103.
- Zanoni, M., Pignatta, S., Arienti, C., Bonafè, M. and Tesei, A. (2019). "Anticancer drug discovery using multicellular tumor spheroid models." *Expert Opin. Drug Discov.* 14(3): 289-301. 10.1080/17460441.2019.1570129.
- Zargarzadeh, M., Amaral, A. J. R., Custódio, C. A. and Mano, J. F. (2020). "Biomedical applications of laminarin." *Carbohydr. Polym.* 232: 115774. 10.1016/j.carbpol.2019.115774.
- Zava, T. T. and Zava, D. T. (2011). "Assessment of Japanese iodine intake based on seaweed consumption in Japan: A literature-based analysis." *Thyroid Res.* 4: 14-14. 10.1186/1756-6614-4-14.
- Zeillinger, R., Tantscher, E., Schneeberger, C., Tschugguel, W., Eder, S., Sliutz, G. and Huber, J. C. (1996). "Simultaneous expression of nitric oxide synthase and estrogen receptor in human breast cancer cell lines." *Breast Cancer Res. Treat.* 40(2): 205-207. 10.1007/bf01806216.
- Zhang, C., Yang, Z., Dong, D. L., Jang, T. S., Knowles, J. C., Kim, H. W., Jin, G. Z. and Xuan, Y. (2020a). "3D culture technologies of cancer stem cells: promising ex vivo tumor models." *J. Tissue Eng.* 11: 2041731420933407. 10.1177/2041731420933407.
- Zhang, J., Riby, J. E., Conde, L., Grizzle, W. E., Cui, X. and Skibola, C. F. (2016). "A *Fucus vesiculosus* extract inhibits estrogen receptor activation and induces cell death in female cancer cell lines." *BMC Complement. Altern. Med.* 16: 151. 10.1186/s12906-016-1129-6.
- Zhang, J., Sun, Z., Lin, N., Lu, W., Huang, X., Weng, J., Sun, S., Zhang, C., et al. (2020b). "Fucoidan from *Fucus vesiculosus* attenuates doxorubicin-induced acute cardiotoxicity by regulating JAK2/STAT3-mediated apoptosis and autophagy." *Biomed. Pharmacother.* 130: 110534. 10.1016/j.biopha.2020.110534.
- Zhang, L., Hao, J., Zheng, Y., Su, R., Liao, Y., Gong, X., Liu, L. and Wang, X. (2018). "Fucoidan protects dopaminergic neurons by enhancing the mitochondrial function

- in a rotenone-induced rat model of Parkinson's disease." *Aging Dis.* 9(4): 590-604. 10.14336/ad.2017.0831.
- Zhang, N., Xue, M., Wang, Q., Liang, H., Yang, J., Pei, Z. and Qin, K. (2021). "Inhibition of fucoidan on breast cancer cells and potential enhancement of their sensitivity to chemotherapy by regulating autophagy." *Phytother. Res.* 35(12): 6904-6917 10.1002/ptr.730310.1002/ptr.7303.
- Zhang, Q., Fan, H., Shen, J., Hoffman, R. M. and Xing, H. R. (2010). "Human breast cancer cell lines co-express neuronal, epithelial, and melanocytic differentiation markers in vitro and in vivo." *PLoS One* 5(3): e9712-e9712. 10.1371/journal.pone.0009712.
- Zhang, T., Rao, J., Li, W., Wang, K. and Qiu, F. (2020c). "Mechanism-based inactivation of cytochrome P450 enzymes by natural products based on metabolic activation." *Drug Metab. Rev.* 52(4): 501-530. 10.1080/03602532.2020.1828910.
- Zhang, Z., Teruya, K., Eto, H. and Shirahata, S. (2011). "Fucoidan extract induces apoptosis in MCF-7 cells via a mechanism involving the ROS-dependent JNK Activation and mitochondria-mediated pathways." *PLoS One* 6(11): e27441. 10.1371/journal.pone.0027441.
- Zhang, Z., Teruya, K., Eto, H. and Shirahata, S. (2013a). "Induction of apoptosis by low-molecular-weight fucoidan through calcium- and caspase-dependent mitochondrial pathways in MDA-MB-231 breast cancer cells." *Biosci. Biotechnol. Biochem.* 77(2): 235-242. 10.1271/bbb.120631.
- Zhang, Z., Teruya, K., Yoshida, T., Eto, H. and Shirahata, S. (2013b). "Fucoidan extract enhances the anti-cancer activity of chemotherapeutic agents in MDA-MB-231 and MCF-7 breast cancer cells." *Mar. Drugs* 11(1): 81-98. 10.3390/md11010081.
- Zhao, Y.-Q., Zhang, L., Zhao, G.-X., Chen, Y., Sun, K.-L. and Wang, B. (2019). "Fucoxanthin attenuates doxorubicin-induced cardiotoxicity via anti-oxidant and anti-apoptotic mechanisms associated with p38, JNK and p53 pathways." *J. Funct. Foods* 62: 103542. 10.1016/j.jff.2019.103542.
- Zheng, J., Tian, X., Zhang, W., Zheng, P., Huang, F., Ding, G. and Yang, Z. (2019). "Protective effects of fucoxanthin against alcoholic liver injury by activation of Nrf2-mediated antioxidant defense and inhibition of TLR4-mediated inflammation." *Mar. Drugs* 17(10): 552. 10.3390/md17100552.
- Zhou, Q.-R., Wei, X.-Y., Li, Y.-Q., Huang, D. and Wei, B.-G. (2014). "An efficient method for the preparation of 3-hydroxyl-5-substituted 2-pyrrolidones and application in the divergent synthesis of (-)-preussin and its analogues." *Tetrahedron* 70(32): 4799-4808. 10.1016/j.tet.2014.05.037.

- Zhou, S., Gao, Y., Jiang, W., Huang, M., Xu, A. and Paxton, J. W. (2003). "Interactions of herbs with cytochrome P450." *Drug Metab. Rev.* 35(1): 35-98. 10.1081/dmr-120018248.
- Zhu, X., Zhu, R., Jian, Z. and Yu, H. (2019). "Laminarin enhances the activity of natural killer cells in immunosuppressed mice." *Cent. Eur. J. Immunol.* 44(4): 357-363. 10.5114/ceji.2019.92784.
- Zimmermann, G. R., Lehár, J. and Keith, C. T. (2007). "Multi-target therapeutics: when the whole is greater than the sum of the parts." *Drug Discov. Today* 12(1-2): 34-42. 10.1016/j.drudis.2006.11.008.
- Zou, Y., Qian, Z. J., Li, Y., Kim, M. M., Lee, S. H. and Kim, S. K. (2008). "Antioxidant effects of phlorotannins isolated from *Ishige okamurae* in free radical mediated oxidative systems." *J. Agric. Food Chem.* 56(16): 7001-7009. 10.1021/jf801133h.
- Zurina, I. M., Gorkun, A. A., Dzhussoeva, E. V., Kolokoltsova, T. D., Markov, D. D., Kosheleva, N. V., Morozov, S. G. and Saburina, I. N. (2020). "Human melanocyte-derived spheroids: A precise test system for drug screening and a multicellular unit for tissue engineering." *Front. Bioeng. Biotechnol.* 8: 540-540. 10.3389/fbioe.2020.00540.
- Zvyagintseva, T. N., Shevchenko, N. M., Chizhov, A. O., Krupnova, T. N., Sundukova, E. V. and Isakov, V. V. (2003). "Water-soluble polysaccharides of some far-eastern brown seaweeds. Distribution, structure, and their dependence on the developmental conditions." *J. Exp. Mar. Biol. Ecol.* 294(1): 1-13. 10.1016/S0022-0981(03)00244-2.

# **Chapter 2** - Morphometrical, Morphological and Immunocytochemical Characterization of a Tool for Cytotoxicity Research: 3D Cultures of Breast Cell Lines Grown in Ultra-low Attachment Plates

---



## Article

# Morphometrical, Morphological, and Immunocytochemical Characterization of a Tool for Cytotoxicity Research: 3D Cultures of Breast Cell Lines Grown in Ultra-Low Attachment Plates

Fernanda Malhão <sup>1,2</sup> , Ana Catarina Macedo <sup>1,2</sup> , Alice Abreu Ramos <sup>1,2</sup>  and Eduardo Rocha <sup>1,2,\*</sup> 

<sup>1</sup> Laboratory of Histology and Embryology, Department of Microscopy, ICBAS–School of Medicine and Biomedical Sciences, University of Porto (U.Porto), Rua de Jorge Viterbo Ferreira n° 228, 4050-313 Porto, Portugal; fcmalhao@icbas.up.pt (F.M.); acfpmacedo@gmail.com (A.C.M.); ramosalic@gmail.com (A.A.R.)

<sup>2</sup> Histomorphology, Physiopathology, and Applied Toxicology Team, Interdisciplinary Center for Marine and Environmental Research (CIIMAR/CIMAR), University of Porto (U.Porto), Avenida General Norton de Matos s/n, 4450-208 Matosinhos, Portugal

\* Correspondence: erocha@icbas.up.pt

**Abstract:** Three-dimensional cell cultures may better mimic avascular tumors. Yet, they still lack characterization and standardization. Therefore, this study aimed to (a) generate multicellular aggregates (MCAs) of four breast cell lines: MCF7, MDA-MB-231, and SKBR3 (tumoral) and MCF12A (non-tumoral) using ultra-low attachment (ULA) plates, (b) detail the methodology used for their formation and analysis, providing technical tips, and (c) characterize the MCAs using morphometry, qualitative cytology (at light and electron microscopy), and quantitative immunocytochemistry (ICC) analysis. Each cell line generated uniform MCAs with structural differences among cell lines: MCF7 and MDA-MB-231 MCAs showed an ellipsoid/discoid shape and compact structure, while MCF12A and SKBR3 MCAs were loose, more flattened, and presented bigger areas. MCF7 MCAs revealed glandular breast differentiation features. ICC showed a random distribution of the proliferating and apoptotic cells throughout the MCAs, not fitting in the traditional spheroid model. ICC for cytokeratin, vimentin, and E-cadherin showed different results according to the cell lines. Estrogen (ER) and progesterone (PR) receptors were positive only in MCF7 and human epidermal growth factor receptor 2 (HER-2) in SKBR3. The presented characterization of the MCAs in non-exposed conditions provided a good baseline to evaluate the cytotoxic effects of potential anticancer compounds.

**Keywords:** 3D cell culture; breast cancer; model characterization; light and electron microscopy



**Citation:** Malhão, F.; Macedo, A.C.; Ramos, A.A.; Rocha, E. Morphometrical, Morphological, and Immunocytochemical Characterization of a Tool for Cytotoxicity Research: 3D Cultures of Breast Cell Lines Grown in Ultra-Low Attachment Plates. *Toxics* **2022**, *10*, 415. <https://doi.org/10.3390/toxics10080415>

Academic Editor: Teresa D. Tetley

Received: 23 June 2022

Accepted: 20 July 2022

Published: 24 July 2022

**Publisher's Note:** MDPI stays neutral with regard to jurisdictional claims in published maps and institutional affiliations.



**Copyright:** © 2022 by the authors. Licensee MDPI, Basel, Switzerland. This article is an open access article distributed under the terms and conditions of the Creative Commons Attribution (CC BY) license (<https://creativecommons.org/licenses/by/4.0/>).

## 1. Introduction

Human cancer cell lines are largely used to study the disease mechanisms and in vitro drug screening. Most of these studies are based on two-dimensional (2D) cell cultures in which cells grow in a monolayer adhered to a flat plastic surface [1,2]. This structural geometry is associated with fewer cellular interactions leading to a restricted cellular microenvironment that is translated into more restricted biochemistry, gene expression, and drug metabolism [3–5]. The strategy provides a model with limited predictive capacity, especially in drug discovery [3,6,7]. Therefore, there has been a growing interest in upgrading the 2D culture models to approach them to the in vivo solid tumors. Three-dimensional (3D) culture techniques have emerged as an attempt to mimic the physiological conditions of tumors and therefore bridge the gap between 2D and in vivo studies [2,3].

Traditionally, 3D cell cultures are described as an agglomerate of cells with a spherical shape, characterized by a decreasing gradient of nutrients, growth factors, oxygen, and pH values from the surface to the core [8,9]. This cell line culture configuration encompasses



three zones: (1) an outer proliferative zone (where cells have direct access to the oxygen and nutrients); (2) an intermediate zone with quiescent cells; (3) an inner necrotic center due to the lack of nutrients and oxygen [2,10–12].

The arrangement of cells into 3D aggregates favors their functionality [4,13–15]. While morphological differentiation can be restored, cell multilayers promote diffusion gradients with heterogeneous populations of dividing, quiescent and dead cells, thus mimicking well nonvascular tumors [3,11,16]. These multilayers also constitute a barrier to the penetration of compounds [11], offering better predictions of the *in vivo* drug efficacy and toxicity [17]. Additionally, more cell-to-cell interactions promote higher intercellular networks and stimulate the production of extracellular matrix (ECM) proteins [6]. All the mentioned differences between 2D and 3D cultures explain why the former provides insufficient or inappropriate information and may sometimes overestimate the efficacy of some potential antineoplastic drugs [8,15,18].

There are several techniques for generating 3D cell cultures, but they overall fall into two main approaches: (a) scaffold-based, where cells are cultivated in synthetic or biological matrices; (b) scaffold-free, where cells are cultivated only in a culture medium, using, e.g., hanging drop or low attachment plates [19,20]. Different methodologies can generate different 3D cell aggregates that vary in size, shape, density, compactness, surface features, and internal structure [21,22].

One of the simplest methods for obtaining 3D cultures is the forced floating method [23]. This technique uses non-adhesive surfaces, such as the ultra-low attachment (ULA) plates with U-shaped bottomed wells or other surfaces coated with hydrophilic substances (e.g., agar or poly-Hema), to minimize cell–substrate adhesion, and forcing cells to remain suspended. A centrifugation step is commonly included to help cells aggregate and form spheroids (one per well) [24,25]. These plates are described to generate reproducible spheroids with uniform size and shape, suitable for high-throughput drug screening [1].

Breast cancer (BC) is the most commonly diagnosed cancer among women in western countries [26,27] and a leading cause of cancer death [28]. Male BC is rare (1% of all cancer in men), but the prognosis is much worse than in women [29]. BC comprises different biological subtypes with distinct histological and molecular characteristics, implying different therapeutic approaches and clinical outcomes [30,31]. The main differences in the molecular subtypes rely on the presence or absence of estrogen (ER) and progesterone receptors (PR), and the overexpression of the oncogene human epidermal growth factor receptor 2 (HER-2) [31]. Given the needs, new drugs continue to be investigated (particularly for the most lethal triple-negative BC) and translated from the laboratory to patients [32].

Considering the presented scenario, the use of 3D cell cultures of breast cell lines can be a very useful tool in the screening of anticancer compounds. Some authors have already reported the formation of 3D cultures from different cell lines, including BC ones, using ULA 96-well plates [22,33–35]. However, there are quite different results reported in the literature, especially about their morphology. These differences can be related to the characteristics of the cell line, and to the applied culture methodologies that many times are not described in detail hampering the investigators to reproduce them. Furthermore, we agree with other researchers who call for the need for a detailed morphofunctional and phenotypic characterization of the 3D models to better understand the results and properly compare studies [3,22,36,37].

For this study, three human BC cell lines were selected to represent the main BC subtypes: (1) MCF7: ER<sup>+</sup>, PR<sup>+</sup>, and HER-2<sup>-</sup>, corresponding to the most common BC type-Luminal A, (2) SKBR3: ER<sup>-</sup>, PR<sup>-</sup>, and HER-2<sup>+</sup> representing the HER-2 BC subtype [38,39], and (3) MDA-MB-231, a “triple-negative cell line” (ER<sup>-</sup>, PR<sup>-</sup>, HER-2<sup>-</sup>), corresponding to the basal type breast carcinoma cell [38,40]. Additionally, we included a non-tumoral breast cell line (4) MCF12A [38,40], as some studies also include non-tumoral cells when screening new drugs or studying the toxicity of known compounds [41].

Given the above, the objectives of this study were: (1) to describe in detail the protocols and give some technical tips for the formation and analysis of MCAs from the four men-

tioned human breast cell lines using the ULA plates, and (2) to characterize the MCAs using morphometry, descriptive morphology (at light and electron microscopy) and quantitative immunocytochemistry (% labeled cells). This baseline characterization under no exposure conditions may offer a good starting point to evaluate the possible cytotoxic effects of compounds including potential anticancer ones.

## 2. Materials and Methods

### 2.1. Cell Lines and Culture Conditions

The MCF7 cell line was purchased from the European Collection of Authenticated Cell Cultures (ECACC, London, UK). MCF12A, MDA-MB-231, and SKBR3 cell lines were acquired from American Tissue Culture Collection (ATCC, Massanas, VA, USA). Cell lines were cultivated in T75 cm<sup>2</sup> culture flasks in an MCO 19AIC (Sanyo, Osaka, Japan) incubator with 5% CO<sub>2</sub> at 37 °C and subcultured at 80–90% confluence. MCF7, MDA-MB-231, and SKBR3 cells were cultivated with Dulbecco's modified Eagle's medium-high glucose (DMEM) without glutamine and phenol red, supplemented with 10% fetal bovine serum (FBS) (*v/v*) and 1% penicillin/streptomycin (100 U/mL/100 µg/mL, respectively). MCF12A cells were cultivated in Dulbecco's modified Eagle's medium/Ham's nutrient mixture F12 (DMEM/F12) medium supplemented with 20 ng/mL human epidermal growth factor (EGFR), 100 ng/mL cholera toxin, 0.01 mg/mL insulin and 500 ng/mL hydrocortisone, 10% FBS and 1% penicillin/streptomycin.

### 2.2. Cell Culture Reagents and Wares

Cholera toxin, insulin, human epidermal growth factor, and hydrocortisone (Sigma Aldrich, St. Louis, MO, USA). DMEM without glutamine and phenol red, Trypsin/EDTA, penicillin/streptomycin, and FBS (Biochrom KG, Berlin, Germany). DMEM/F12 medium without phenol red (GE Healthcare, Chicago, IL, USA). All other used reagents and chemicals were analytical grade. T75 cm<sup>2</sup> flasks were from (Orange Scientific, Braine-l'Alleud, Belgium) and ULA plates (Corning, New York, MA, USA).

### 2.3. 3D Cell Culture Procedure

Cell suspensions were obtained by trypsinization of confluent T75 cm<sup>2</sup> flasks using 0.25% trypsin/0.02% EDTA, at 37 °C until cell detachment. Trypsin was inactivated by adding twice the volume of the complete fresh medium. Cell suspensions were counted using a Neubauer chamber and then cells were seeded in 96-well ULA plates (200 µL per well). In a preliminary test, cells were seeded at different cell densities: MCF7 and SKBR3-10, 20, and 40 × 10<sup>4</sup> cells/mL; MDA-MB-231-20, 40 and 50 × 10<sup>4</sup> cells/mL and MCF12A 5, 10 and 20 × 10<sup>4</sup> cells/mL. The plates were centrifuged with a Rotina 380 R (Hettich, Tuttlingen, Germany), at 200 × *g* for 10 min, at room temperature, and then placed in an incubation chamber with 5% CO<sub>2</sub> at 37 °C. A 7-day experiment was made, using 3 days (72 h) for MCA formation [24,42], then the medium was replaced by a culture medium with 0.1% DMSO [24], simulating a potential drug/compound exposure for more 4 days (96 h). On day 3, we collected MCAs of 2 independent replicas to compare their morphology with MCAs collected on day 7.

### 2.4. Study Design

Nine independent replicas were performed, each one corresponding to one 96-well microplate. The same MCAs were measured and paired at the two time points (days 3 and 7 in culture). The number of MCAs per replica was dependent on the studied parameter: (a) 12 MCAs of each cell line per replica were used for morphometry (108 MCAs measured per cell line); (b) 3 MCAs of each cell line per replica were harvested for cytological and immunocytochemical analysis at light microscopy; (c) 2 MCAs of each cell line per replica were harvested for transmission electron microscopy (TEM).

## 2.5. Morphological Analysis

### 2.5.1. MCA Area Measurements

Each MCA (one per well) was photographed with an SZX10 stereomicroscope (Olympus, Tokyo, Japan) linked to a DP21 digital camera (Olympus, Tokyo, Japan), at two time points: day 3 (before removing medium for exposure simulation) and day 7 (after the simulation of 96 h of exposure)—immediately before sampling. The images were submitted to the AnaSP freeware [43] for area measurements.

Data were statistically analyzed using PAST 3.1 [44] and GraphPad Prism 6 (GraphPad Software, San Diego, CA, USA). Data obtained from MCAs areas and corresponding to nine independent replicates were presented as mean  $\pm$  standard deviation (SD). Data sets were tested for normality (Shapiro–Wilk test) and homogeneity of variances (Levene test) and then paired Student *t*-tests were applied to compare the area variation of the same MCAs between days 3 and 7. The significance level was set at 5%.

### 2.5.2. Cytological Analysis at Light Microscopy

#### Processing for Paraffin Embedding

First, the culture medium was removed from the wells containing the MCAs, and then 200  $\mu$ L/well of 10% buffered formalin (Bioptica, Milan, Italy) was gently added and left for 20 min. This brief first fixation step into the wells helped to prevent the disintegration of the MCAs during their collection. Then, the MCAs were transferred to Eppendorf microtubes containing the same fixative, using a P1000 micropipette with a sectioned tip to augment the diameter of the tip to prevent damaging the MCAs. After 24 h fixation, MCAs were embedded in histogel (Thermo Scientific, Waltham, MA, USA), according to the manufacturer's instructions, to avoid the loss of MCAs during processing for paraffin embedding. Next, histogel containing MCAs was placed into tissue cassettes and processed using an automatic tissue processor Leica TP120 (Leica, Nussloch, Germany). The processing protocol consisted of 1 h in each of the following sequence of reagents: ethanol (70%, 90%, 95%, and 100% (twice); xylene: ethanol (1:1); xylene (twice); liquid paraffin (twice)). Paraffin blocks were performed in an embedding station EG 1140H (Leica, Nussloch Germany). Three-micrometer thickness sections were obtained in a Leica 2255 microtome (Leica, Nussloch Germany) and placed onto silane-treated KP-frost slides (Klinipath, Duiven, Nederland). For paraffin melting, slides were placed for 20 min at 60 °C and then kept overnight at 37 °C. They were used either for standard hematoxylin-eosin (HE) staining or immunocytochemistry (ICC).

#### HE Staining

MCA sections were deparaffinized in xylene (2  $\times$  10 min) and hydrated following a descendent sequence of ethanol (100%, 95%, 70%) and running tap water, 5 min each. Nuclei were stained with Mayer's hematoxylin (Merck, Darmstadt, Germany) for 3 min, and then slides were washed in running tap water for 5 min to remove the excess dye. Next, slides were immersed in aqueous 1% eosin Y for 5 min (Merck, Darmstadt, Germany), followed by quick dips into distilled water. Lastly, slides were dehydrated in an ascending series of ethanol (95%, 100%, 100%), 5 min each, cleared in xylene (2  $\times$  5 min), and coverslipped using Coverquik 2000 medium (VWR Chemicals, Briari, France).

### 2.5.3. Immunocytochemistry (ICC)

For ICC, MCA sections were deparaffinized and hydrated as described for HE staining. Heat antigen retrieval was performed in a pressure cooker, where slides were immersed in boiling citrate buffer 0.01 M, pH 6.0. The cooker was then closed, and slides were left 3 min after reaching maximum pressure. After slowly cooling, endogenous peroxidase blocking was made with 3% hydrogen peroxide in methanol (10 min). The excess hydrogen peroxide was removed by washing twice (5 min each) in Tris-buffer saline pH 7.6 (TBS). Slides were dried around the sections (without leaving them to dry or damage), and the sections were circled with a hydrophobic pen (Leica Biosystems, Milton Keynes, UK). In

sequence, unspecific reactions were blocked using the protein block-specific reagent for that of the Novolink™ Polymer detection kit (Leica Biosystems, Milton Keynes, UK) (5 min), followed by two washes in TBST (TBS with 0.05% of Tween 20). Primary antibodies were diluted in phosphate buffer saline (PBS) with 5% of bovine serum albumin and incubated overnight at 4 °C (corresponding to 16 h of incubation), using a humidified chamber (details of antibodies and used dilutions in Table 1).

**Table 1.** Antibodies used in ICC characterization.

Antibody, Brand, City, Country	Host	Type, Clone	Dilution
Ki67, Biocare Medical, Pacheco, CA, USA	Rabbit	Monoclonal, SP6	1/200
Caspase-3 ab 13847, Abcam, Cambridge, UK	Rabbit	Polyclonal	1/5000
E-cadherin, Dako, Santa Clara, CA, USA	Mouse	Monoclonal, NCH-38	1/200
Cytokeratin, Cell Marque, Rocklin, CA, USA	Mouse	Monoclonal, AE1/AE3	1/1000
Vimentin, Novocastra, Milton Keynes, UK	Mouse	Monoclonal, V9	1/1600
Estrogen receptor (ER), Biocare Medical, Pacheco, CA, USA	Rabbit	Monoclonal, SP1	1/200
Progesterone receptor (PR), Biocare Medical, Pacheco, CA, USA	Rabbit	Monoclonal, 16	1/200
HER-2, Biocare Medical, Pacheco, CA, USA	Rabbit	Monoclonal, EP3	1/400

For negative control, the primary antibody was substituted by antibody diluent only. According to antibody datasheet recommendations, the positive controls used corresponded to human tissues where the target antigens are expressed.

The mentioned Novolink™ Polymer detection system was used for signal amplification, according to the manufacturer's instructions, using the chromogen 3,3'-Diaminobenzidine (DAB). After the primary antibody incubation and after each step of the detection system, slides were washed twice (5 min each) in TBST. For nuclear counterstain, cells were immersed in Mayer's hematoxylin (1 min), washed, then slides were dehydrated with an ascendant sequence of ethanol (90%, 95%, absolute ethanol (twice)), cleared in xylene, and mounted. Lastly, slides were observed with a light microscope BX50 (Olympus, Tokyo, Japan) and photographed with a DP21 digital camera (Olympus, Tokyo, Japan).

We selected a panel of antibodies targeting different outputs for the MCAs' ICC characterization. First, we investigated the proliferating and death status of the cells within the MCAs using Ki67 and caspase-3 antibodies as markers of proliferation [45,46] and apoptosis [47,48], respectively.

Additionally, we evaluated the expression of the cell surface E-cadherin, a protein related to cell adhesion [49] and cell polarity [50]. Additionally, the epithelial-mesenchymal transition was evaluated by using the epithelial marker AE1/AE3 [51] and the mesenchymal marker vimentin [52].

Finally, we investigated the expression of the ER and PR and the overexpression of HER-2, both described as discriminative characteristics of the used breast cell lines [38,39,53].

#### 2.5.4. Immunocytochemistry Quantitative Analysis

For each tested antibody, three representative images corresponding to the central part (equator) of three random MCAs were analyzed. Estimation of the percentage of immunomarked cells was made by superimposing to the section a sampling grid with forbidden lines to prevent edge effects [54]. Only cells with a sectioned nucleus were counted. A minimum of 150 cells was counted per MCA, and a total of 500 cells were counted per cell line. Data were statistically analyzed using PAST 3.1 [44] and GraphPad Prism 6 (GraphPad Software, San Diego, CA, USA). Normality and homogeneity of variances were tested using the Shapiro–Wilk and Levene tests, respectively. Significant differences ( $p < 0.05$ ) were assessed by one-way ANOVA, followed by the post hoc Holm–Šidák multiple comparison test.

#### 2.5.5. Transmission Electron Microscopy (TEM)

MCAs were collected as described for the analysis by light microscopy. After harvesting to Eppendorf microtubes, MCAs were fixed for 2 h in 2.5% glutaraldehyde in 0.15 M

sodium cacodylate-HCl buffer, pH 7.2, 4 °C, and then washed ( $2 \times 10$  min) in the same buffer. Post fixation was carried out using a 1% osmium tetroxide solution in the mentioned buffer for 2 h at 4 °C, followed by two washes of 10 min. MCAs were then sequentially dehydrated (30 min in each reagent) in: 50%; 70%; 95%, 100% ethanol (twice); propylene oxide (30 min, twice). For epoxy resin embedding, we used consecutive mixtures consisting of different parts of propylene oxide and epoxy resin, respectively, (3:1); (1:1); (1:3), and ultimately only resin (1 h each), to allow an optimal and gradual resin penetration in the MCAs. After embedding in rubber molds, they were placed in the oven at 60 °C for 48 h for resin polymerization. Semithin (1.25  $\mu$ m thick) and ultrathin (90 nm thick) were obtained in an ultramicrotome EM UC7 (Leica, Nussloch, Germany). Semithin sections were collected onto silane-coated slides (Klinipath, Duiven, The Netherlands) and stained with a mixture of aqueous azure II and methylene blue (1:1), observed in a BX50 light microscope (Olympus, Tokyo, Japan) and photographed with a DP21 digital camera (Olympus, Tokyo, Japan). Ultrathin sections were obtained with a diamond knife (Diatome, Nidau, Switzerland), placed onto 200 mesh copper grids (Agar Scientific, Stansted, UK), and contrasted with 3% aqueous uranyl acetate (20 min) and Reynold's lead citrate (10 min). TEM observations used a 100CXII microscope (Jeol, Tokyo, Japan), operated at 60 kV, equipped with an Orius SC1000 CCD digital camera (Gatan, Pleasanton, CA, USA), controlled by the Digital Micrograph software (Gatan, Pleasanton, CA, USA).

### 3. Results

#### 3.1. MCA Area Measurements

After the preliminary test with different cell densities, the densities that corresponded to better formation of MCAs were selected for each cell line (see representative images of the MCAs in Figure S1). The selected cell densities were:  $40 \times 10^4$  cells/mL (MCF7, MDA-MB-231, and SKBR3) and  $20 \times 10^4$  cells/mL (MCF12A). The MCAs were observed daily, and images were captured on days 3 and 7 of culture. Figure 1 summarizes the key aspects of MCAs from all cell lines, showing their morphology using comparative images of the same MCAs on the two sampling days. It includes graphs of their areas, highlighting the variance among replicates, making it easier to compare morphology with size changes.

During the first days of culture, cells aggregated progressively, and on day 3 all the cell lines formed MCAs (see Figure 1). On day 3, stereomicroscopic observation showed that the MCAs were spherical (Figure 1), the MDA-MB-231 aggregates being the ones that most resembled a perfect sphere (Figure 1C). However, when the MCAs were manipulated to change the culture medium (at day 3), it became clear that the actual shape of the 3D structures was more of an ellipsoid (an oblate spheroid) than of a sphere, especially in the SKBR3 and MCF12A cell lines.

Irrespective of the number of days in culture, SKBR3 MCAs were the largest ones, followed, in decreasing order, by the MCF12A, MCF7, and MDA-MB-231 MCAs. The size of the MCAs was related to the degree of compactness, as the larger MCAs were also the looser ones, where cells were not so closely attached (SKBR3 and MCF12A, Figure 1B and D), while the smaller MCAs were more compact, containing cells that were more tightly packed (MCF7 and MDA-MB-231, Figure 1A,C). Additionally, MDA-MB-231 displayed well-defined borders, contrary to other cell lines where the limits were more irregular; as it is noticeable comparing Figure 1C with Figure 1A,B,D.

When comparing MCAs from days 3 and 7, it was possible to observe some changes in size and morphological appearance. In MDA-MB-231 MCAs, there was clear compaction, resulting in a statistically significant area reduction (Figure 1C). Although not as visually evident, a statistically significant decrease in areas of MCAs was also noted in SKBR3 MCAs (Figure 1B).

The most variable MCAs were the ones from the MCF12A cell line, on both 3 and 7 days, because the areas would either increase or decrease, as noted by the large amplitude of the standard deviations and morpho-phenotype (Figure 1D).



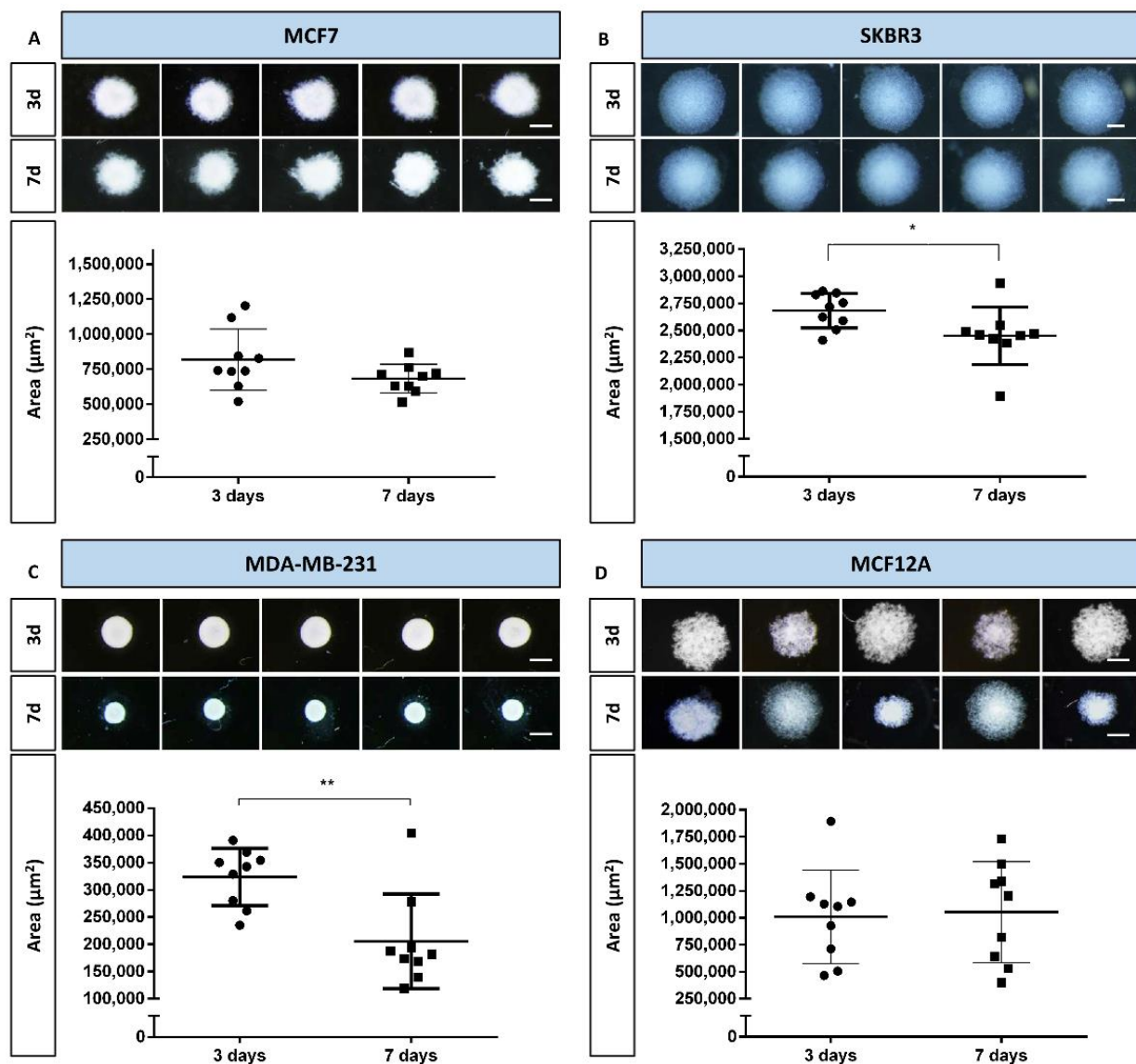


**Figure 1.** Representative stereomicroscopic images and areas (measured by AnaSP software) of multicellular aggregates (MCAs) of the four cell lines, on days 3 and 7: (A) MCF7, (B) SKBR3, (C) MDA-MB-231, and (D) MCF12A. Areas are expressed as mean  $\pm$  standard deviation of nine independent experiments. Each dot in the graphs corresponds to the mean area of one replicate. Significant differences: \*  $p < 0.05$ , \*\*  $p < 0.01$ . Scale bar: 500  $\mu\text{m}$ .

### 3.2. Histological Analysis

Figure 2 presents the typical morphology of the MCAs cultured for 3 and 7 days, at the light microscopic level. In line with the stereomicroscopic analysis, cell compactness in the MCAs varied among cell lines. MCF7 and MDA-MB-231 were more compact, while SKBR3 and MCF12A were not tightly packed. There was a notable space among SKBR3 cells, contrasting with the more cell-tightened MCAs. Besides the loose structure, SKBR3 MCAs were quite resistant to manipulation. The same was not true for MCF12A MCAs, since they tend to partially or totally disintegrate when manipulated. Regarding these MCAs, the inner core stayed more attached, while the outer part tended to disaggregate, showing dispersed cells around the central region.

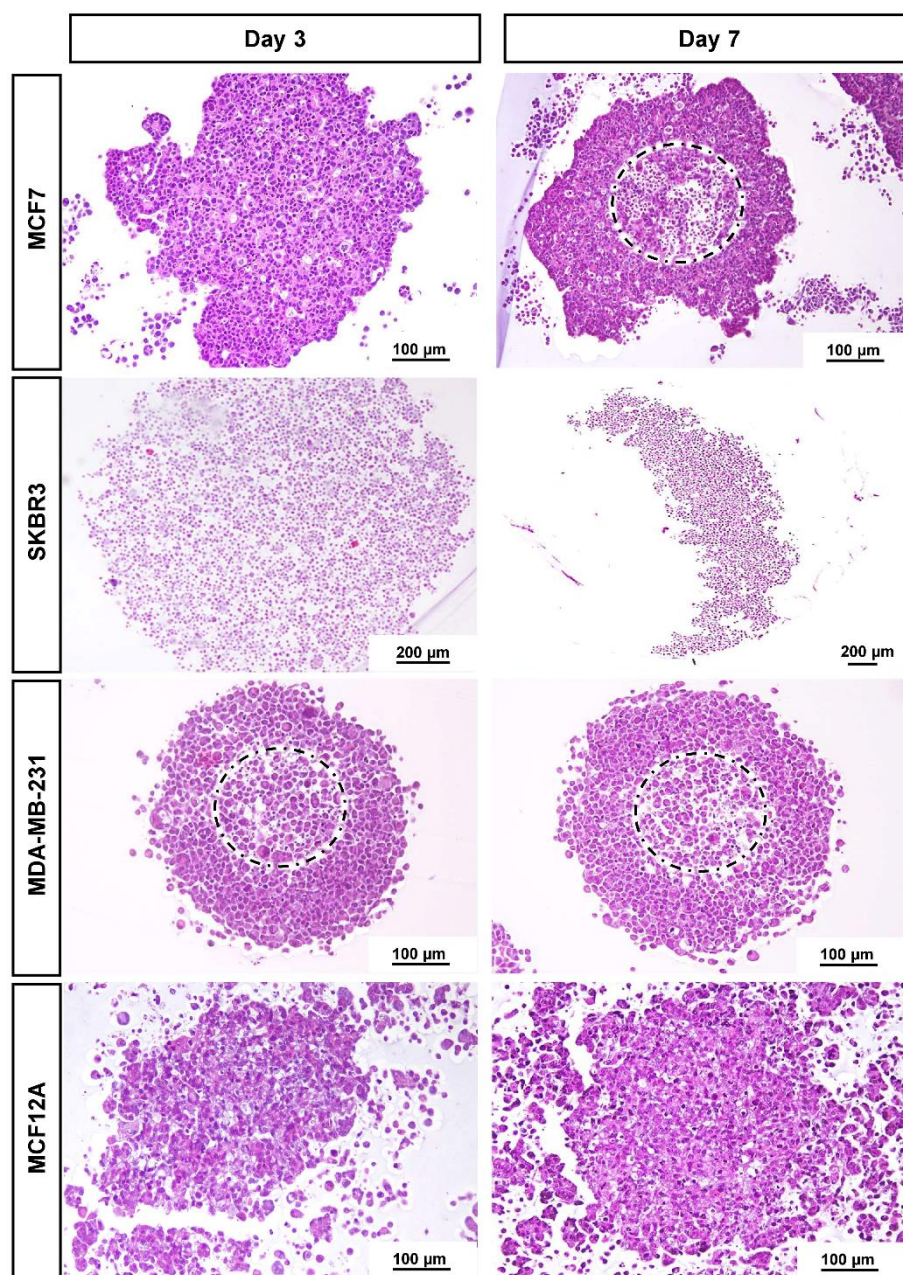


**Figure 2.** Representative histological images of MCAs of the four cell lines: MCF7, SKBR3, MDA-MB-231, and MCF12A stained with HE on days 3 and 7 in culture. MCF7 and MDA-MB-231 formed compact MCAs, while SKBR3 and MCF12A formed loose MCAs. The dashed circles limit the apoptotic/necrotic core in compact MCAs.

When sections reached nearly the core of the compact MCAs harvested on both days 3 or 7, it was observed in some MCAs the presence of an apoptotic/necrotic zone of different sizes (dashed circles in Figure 2). The central core had “empty” spaces and a higher number of cells with hyperchromatic and pycnotic nuclei, hyper eosinophilic cytoplasm, and apoptotic bodies. In parallel, some cells presented nuclear swelling and pale cytoplasm. In contrast, the looser MCAs did not present apoptotic/necrotic cores.

The general morphology of the MCAs from each cell line, observed with light microscopy, was similar on the two sampled days (days 3 and 7). As we wanted to evaluate the MCAs in the context of an experimental setting of exposure to a compound of interest (3 days for MCAs formation plus 4 days of exposure), further characterization data are only



given after 7 days in culture. The MCF7 MCAs presented some unique features that are described along with the ICC and TEM results.

### 3.3. Immunocytochemical Characterization

The distribution of the immunostaining was easily seen in low magnification images (Figure 3).

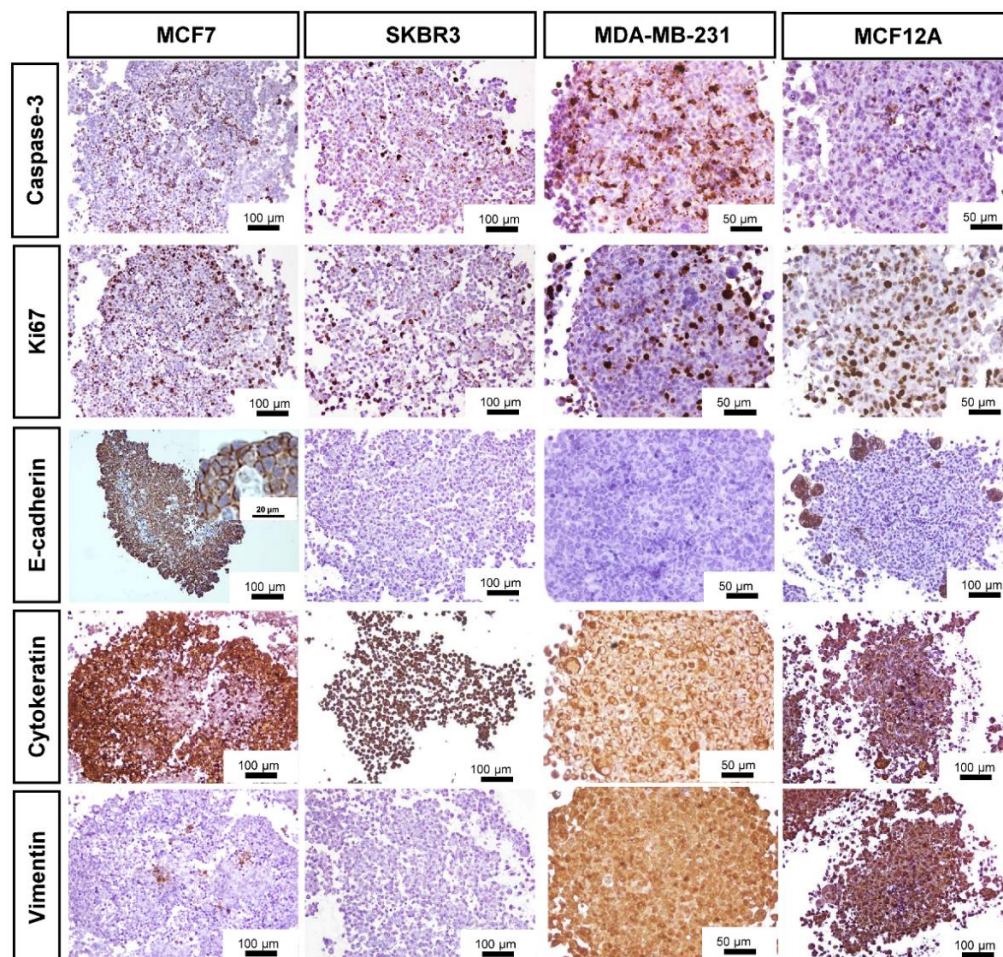


**Figure 3.** Representative images of ICC characterization of MCAs from MCF7, SKBR3, MDA-MB-231, and MCF12A after 7 days in culture. Brown staining with diaminobenzidine (DAB) indicates positive staining at different cellular parts according to the antigen localization: Caspase-3: nucleus and cytoplasm; Ki67: nucleus; E-cadherin: cell membrane; Cytokeratin AE1/AE3: cytoplasm; Vimentin: cytoplasm.

All MCAs displayed cells immunostained for caspase-3, varying on average from 15 to 30%. The positively stained caspase-3 cells were randomly distributed throughout the whole MCAs from all cell lines. However, when an apoptotic/necrotic core was present in MCF7 and MDA-MB-231 MCAs, a high number of caspase-3 positive cells existed in the central region; despite the immunostaining reaching the outer cell layers. In MCF7 MCAs there were additional caspase-3 positive cells inside the lumen of acinar-like structures.

The pattern of Ki67 immunostaining was similar to that of caspase-3. All MCAs showed scattered proliferating cells (at the periphery, middle part, and core). Even when an apoptotic/necrotic core was present, there were some proliferating cells inside it.

Other MCAs immunophenotypes were assessed, such as the expression of the tumor suppressor protein E-cadherin. MCF7 MCAs highly expressed E-cadherin (ca. 70%), except in the central region when an apoptotic/necrotic core was present. In this case, cells



changed their morphology and acquired characteristics of death, losing the E-cadherin immunomarking. MCF12A MCAs expressed E-cadherin in small groups of peripheral cells (ca. 11%). The SKBR3 and MDA-MB-231 were negative for E-cadherin.

Regarding the cytokeratin AE1/AE3 (epithelial marker), most cells in MCF7 MCAs were positive (ca. 76%). However, in the presence of an apoptotic/necrotic core, the cells lost the positivity for that marker, similarly to what was described for E-cadherin tagging in MCF7. Differently, in SKBR3, MCF12A, and MDA-MB-231 MCAs, all cells were positive for AE1/AE3.

As to the intermediate filament protein vimentin, all cells were positive in MDA-MB-231 and MCF12A MCAs. In contrast, in MCF7 MCAs just a few cells stained positive (ca. 5%), and in SKBR3 MCAs no cells were tagged (Figure 3).

Additionally, we checked the ER/PR expression in the MCF7 and MCF12A MCAs, as well as the expression of the growth-promoting protein HER-2 in SKBR3 (Figure 4). Revealed by the nuclear brown staining, MCF7 MCAs had an average of 53% of their cells positively tagged for ER while 49% were stained for PR. The labeled cells were preferentially located in the outer part of the MCAs, where the intensity of the immunostaining was also stronger. In MCF12A MCAs, there were no positive cells for any of the hormone receptors. In SKBR3 MCAs, 82% of cells had the membrane totally stained for HER-2.

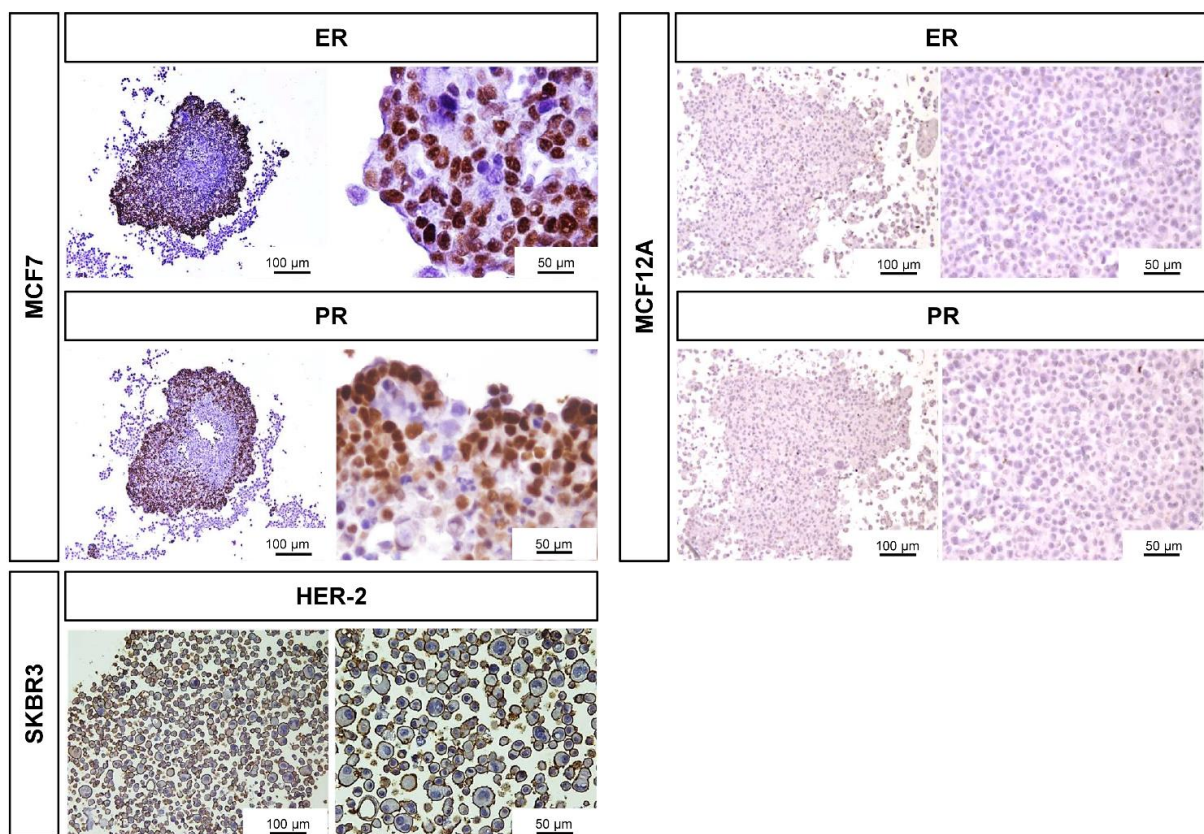


**Figure 4.** Representative images of ICC characterization of MCAs relative to the expression of ER, PR in MCF7 and MCF12A MCAs, and HER-2 staining in SKBR3 MCAs, after 7 days in culture. The brown DAB staining corresponds to the immunolocalization of the tested antibodies according to the antigen localization: ER/PR: nucleus; HER-2: membrane.

Table 2 summarizes the ICC quantification. For caspase-3 and Ki67 markers, we performed ANOVA statistical analysis to compare the different cell lines. There were no observed statistically significant differences in relation to caspase-3 positive cells. Concerning the percentage of proliferating cells stained with Ki67, the only statistical difference

was observed between MCF7 and MCF12A ( $p < 0.05$ ), MCF7 being more proliferative than MCF12A MCAs.

**Table 2.** Summary of the quantitative ICC analysis of the MCAs. Data (% of cells tagged) are given as mean  $\pm$  standard deviation (3 independent replicates).

Markers	Cell Lines			
	MCF7	SKBR3	MDA-MB-231	MCF12A
Caspase-3	15 $\pm$ 5	26 $\pm$ 3	30 $\pm$ 11	21 $\pm$ 2
Ki67	38 $\pm$ 10 *	21 $\pm$ 5	26 $\pm$ 4	14 $\pm$ 10 *
AE1/AE3	76 $\pm$ 15	100	100	100
Vimentin	5 $\pm$ 2	0	100	100
E-cadherin	70 $\pm$ 4	0	0	11 $\pm$ 3
ER	53 $\pm$ 13	n.a.	n.a.	0
PR	49 $\pm$ 10	n.a.	n.a.	0
HER-2	n.a.	82 $\pm$ 1	n.a.	n.a.

\*  $p < 0.05$  (MCF7 vs. MCF12A); n.a.: not applicable; no standard variation applies to 0 or 100%.

### 3.4. Specific Structural Features of MCF7 MCAs

In all MCF7 MCAs, from days 3 and 7, it was noted many acinar-like structures were well visualized in HE staining (Figure 5A,B). In their lumina, they commonly had cells with structural features compatible with apoptosis, such as condensed hyperchromatic nuclei, nuclear fragmentation, and hypereosinophilic cytoplasm [55]. Additionally, there were cells with morphology compatible with necrotic cells presenting pale eosinophilic cytoplasm with a ghost cell aspect that at TEM corresponded to decreased electron density in the cytoplasm, loss of cell membrane integrity with leakage of cytoplasmic content, organelle disruption, and nucleus dissolution morphology [55,56] (Figure 5B–D). The presence of apoptotic cells was confirmed by ICC against caspase-3 (Figure 5C,D). The cells of acinar-like structures revealed polarity, with microvilli in the apical pole (Figure 5E,F). The apical basophilic line (arrowheads in Figure 5B), that at TEM corresponded to long rows of secretory vesicles aligned towards the lumen (Figure 5E,F), reinforcing the presence of cell polarity.

### 3.5. General Ultrastructure of MCAs

The four cell lines formed MCAs with different ultrastructural characteristics. MCF7 MCAs presented irregularly shaped nuclei with prominent nucleoli and round to elongated mitochondria. Rough endoplasmic reticulum and Golgi apparatus were rarely seen. The cytoplasm could show glycogen or lipids. Nevertheless, while some cells had neither glycogen nor lipids, others had moderate to high amounts of these substances (Figure 6A,B). There was no simultaneous presence of glycogen and lipid droplets within the same cell.

Concomitantly with the recovery of cell polarity described above (Figure 5), small canaliculi, formed by the apposition of cells presenting features similar to acinar-like structures, were seen between some cells, also with microvilli and an accumulation of secretory vesicles towards the lumen (Figure 6C,D). MCF7 MCAs cells were closely attached, with many tight junctions, desmosomes, and interdigitations (Figure 6E,F).

SKBR3 MCAs were cell-loose structures, and this characteristic was evident in both HE and TEM sections. Cells with microvilli presented large intercellular spaces (white arrows) (Figure 7A–D). Nonetheless, some cells were attached, and among them, it was regularly observed small intercellular canaliculi bordered by the microvilli of adjacent cells (Figure 7B,C). The presence of secretory vesicles near these canaliculi was not so evident as in MCF7 MCAs, but in some canaliculi, they were present, although to a lesser extent (Figure 7C). Cells in the MCAs commonly had very irregularly shaped nuclei, prominent nucleoli, presented rare rough endoplasmic reticulum cisternae, and were rich in mitochondria. The most common storage substance was lipid droplets (Figure 7C,D). Desmosomes were rarely observed (Figure 7D).



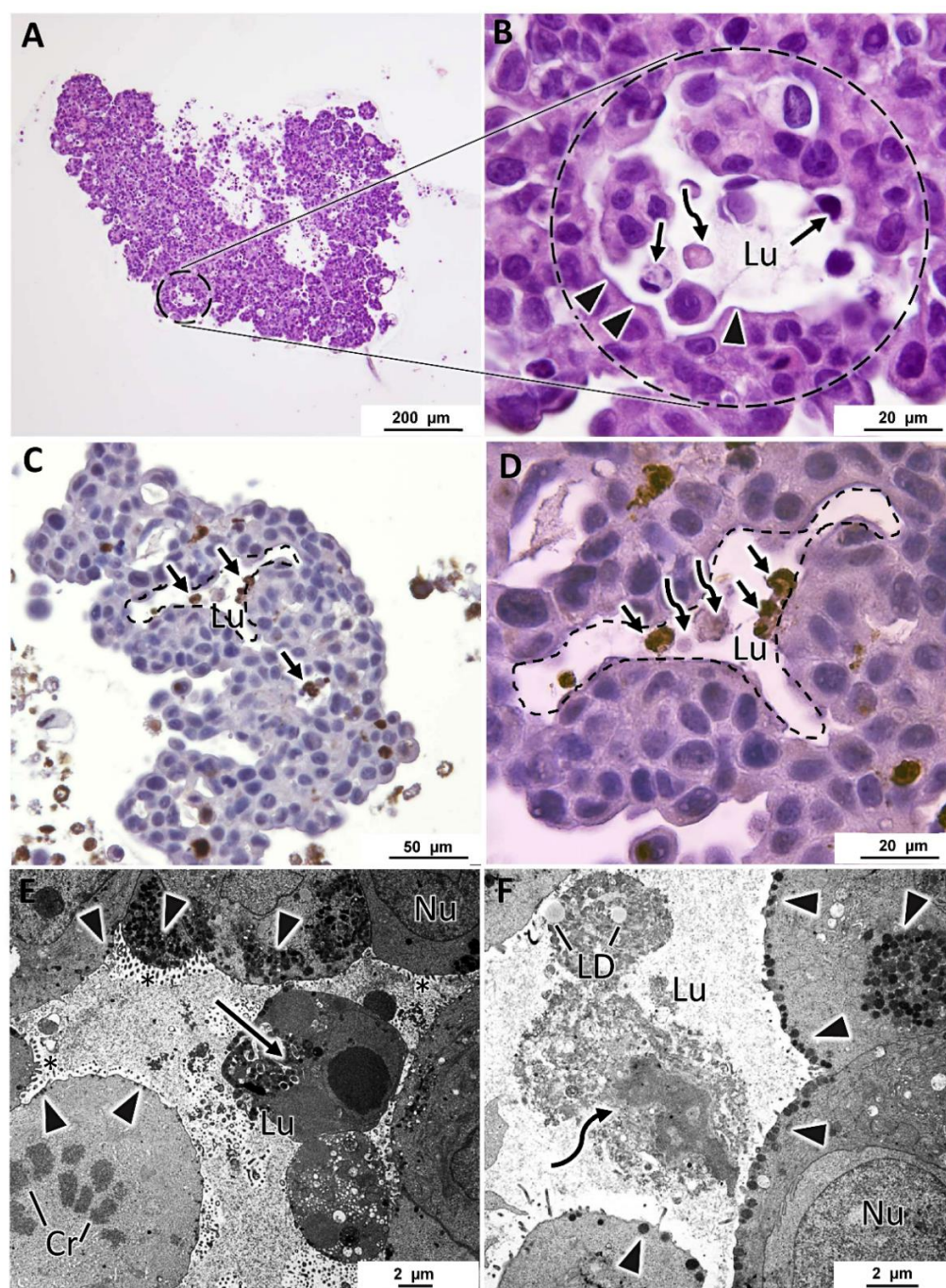


**Figure 5.** Representative aspects of acinar-like structures in MCF7 MCAs. (A,B) correspond to HE staining highlighting one acinar-like structure surrounded by a dashed circle. (B) is a higher magnification of (A) and shows apoptotic (arrows) and necrotic (curved arrows) cells within the lumen (Lu). Arrowheads evidence a basophilic line limiting the lumen. (C,D) ((D) is a higher magnification of (C)) correspond to ICC anti-caspase-3, acinar-like structures delimited with a dashed line; within the lumen, there are caspase-3 positive cells, stained in brown (arrows) and necrotic cells that do not stain with caspase-3 (curved arrows). (E,F) are TEM images showing acinar-like structures with a central lumen, containing apoptotic cells (arrow) in (E) and lipid droplets (LD) and necrotic cells (curved arrow) in (F). Cells show polarity, having microvilli towards the lumen (asterisks) and subplasmalemma alignment of secretory vesicles (arrowheads). Cr: chromosomes in a mitotic cell; Nu: nucleus.



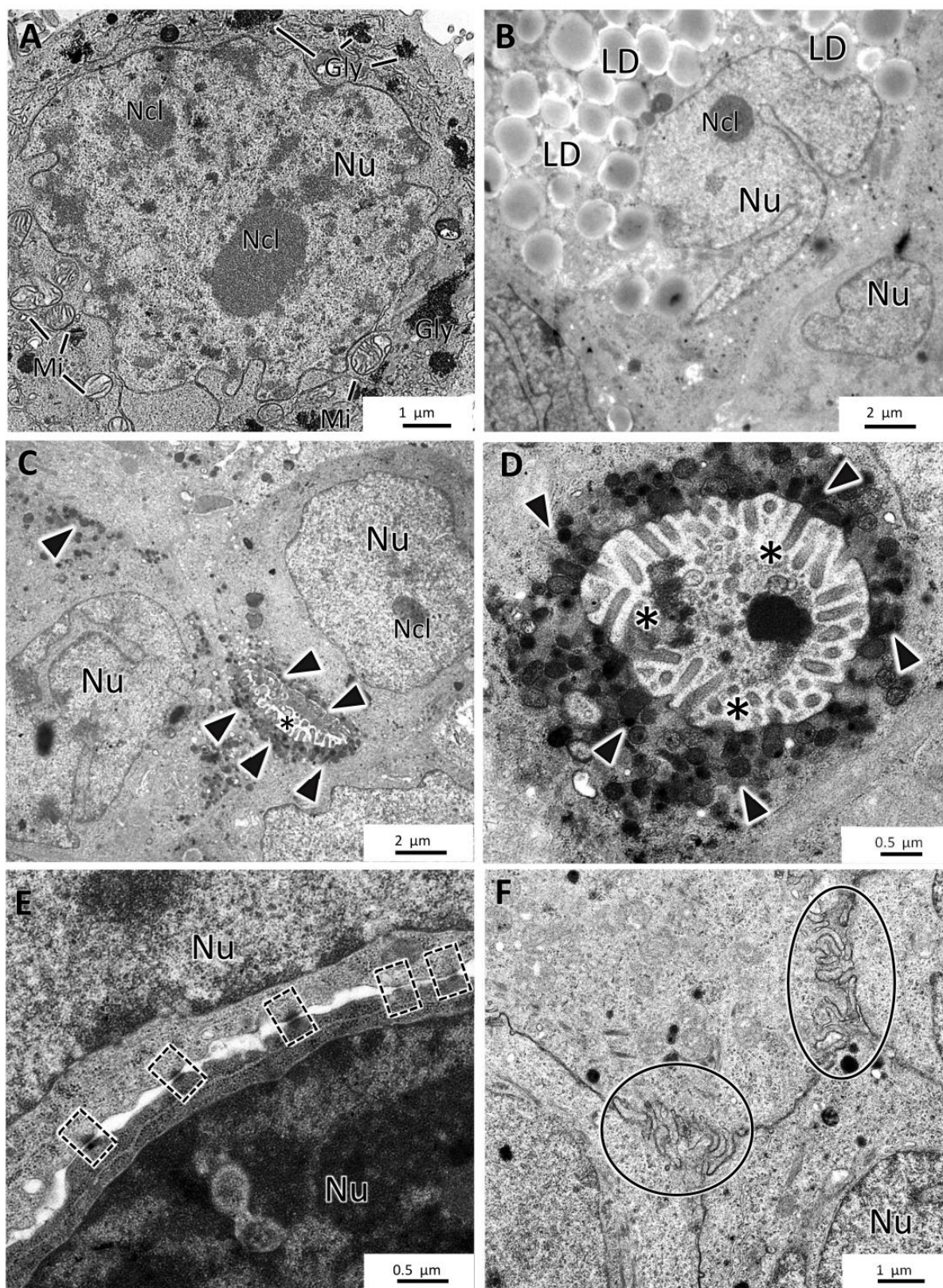


**Figure 6.** TEM representative images of MCF7 MCAs. (A,B) show storage of glycogen (Gly) and lipid droplets (LD), respectively. (C,D) display small intercellular canaliculi with microvilli (asterisks) and secretory vesicles (arrowheads). (E,F) highlight the presence of desmosomes (dashed-lined rectangles) and interdigitations (circles). Mi: mitochondria; Ncl: nucleoli; Nu: nucleus.



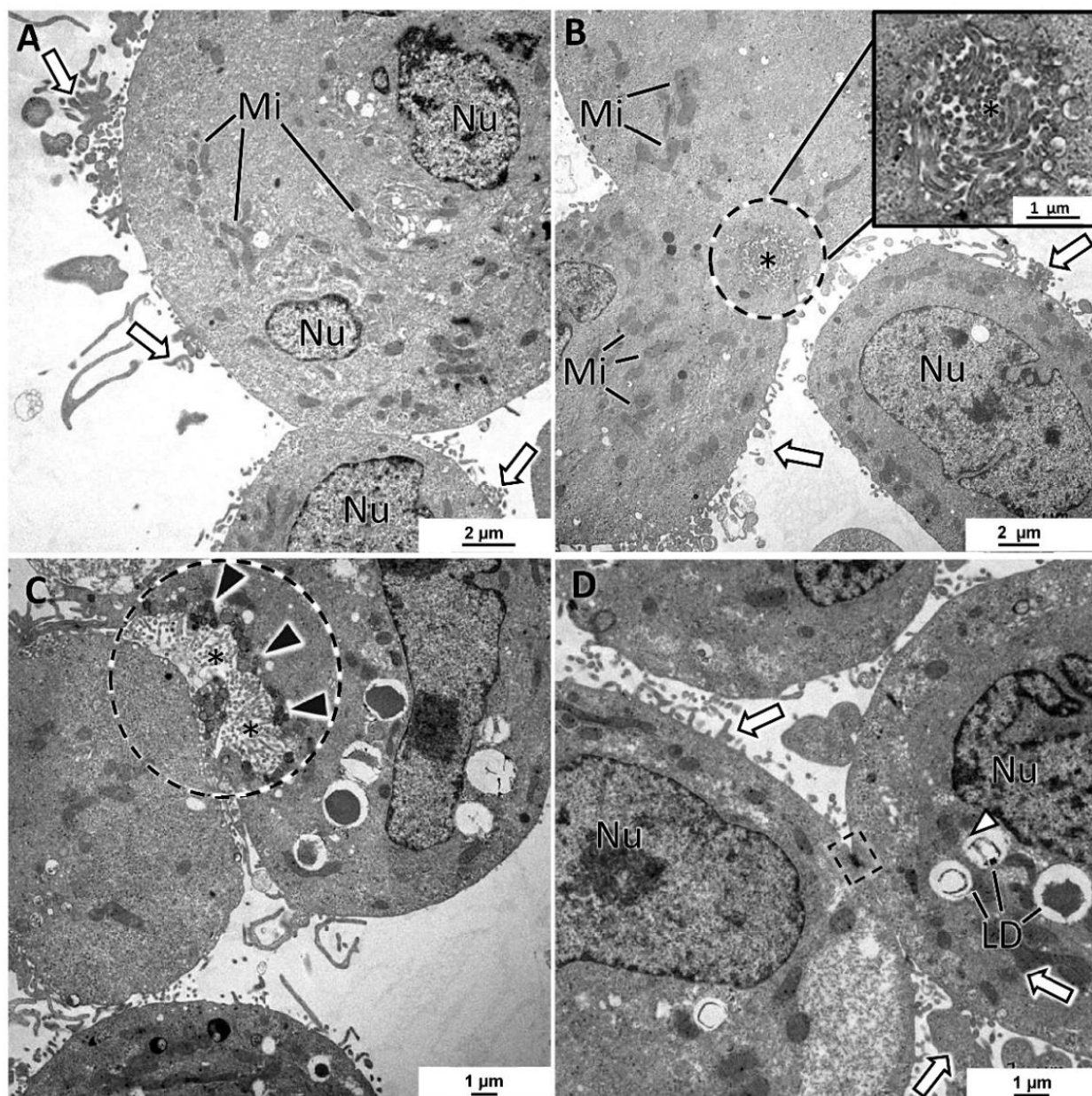


**Figure 7.** TEM representative images of SKBR3 MCAs. (A–D) show intercellular spaces with microvilli (white arrows). (B,C) evidence in the dashed-lined circles of the intercellular canaliculi formed by microvilli (asterisks) of adjacent cells. (C) depicts a canaliculus with some secretory vesicles nearby the lumen direction (black arrowheads). Cells presented different amounts of lipid droplets (LD) and were rich in mitochondria (Mi). Dashed-lined rectangles: desmosome; Ncl: nucleoli; Nu: nucleus.

The MDA-MB-231 MCAs revealed cells with irregular nuclei, many dense bodies, and lipid droplets (Figure 8A–D). The remaining cytoplasmic contents were scarce, with the Golgi cisternae and mitochondria being rarely seen. In some aleatory areas, cells showed tight cell-to-cell adhesions, while in other areas, cells were not so closely attached. At their surface, cells possessed a high number of membrane projections, forming areas of tangled microvilli projected to the intercellular spaces. A few cells presented an elongated spindle morphology (Figure 8D), contrasting with the usual roundish-to-ellipsoidal structure.



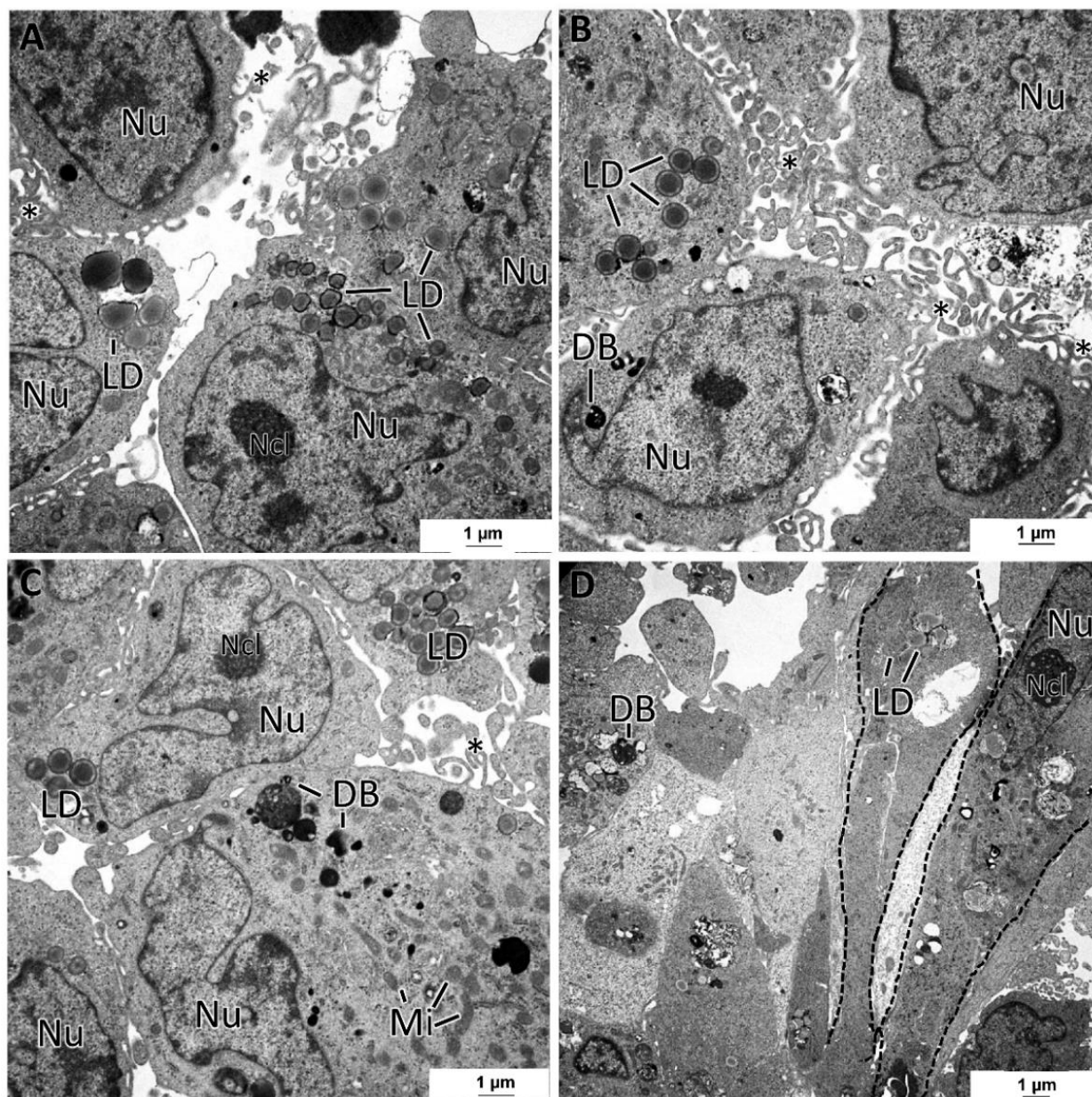


**Figure 8.** TEM representative images of MDA-MB-231 MCAs. (A–D) pictures illustrate cells displaying variable amounts of lipid droplets (LD) and dense bodies (DB). Intercellular spaces are circumscribed by cells displaying microvilli (asterisks). (D) shows some spindle cells (dashed lines). mitochondria: Mi; nucleus: Nu; nucleoli: Ncl.

The MCF12A MCAs were characterized as having the lowest degree of intercellular adhesion. At TEM observation, cells almost did not adhere to each other and presented microvilli and larger cytoplasmic projections on their surfaces directed to the intercellular spaces (Figure 9A). Despite the loose structure of the MCAs, desmosomes were present but were rarely observed (Figure 9B). Additionally, some cells were joined by a net of tangled membrane projections (Figure 9D). The MCF12A cells had the most irregular nuclei of all the studied MCAs and were the richest in organelle content. They had a profuse number of mitochondria and rough endoplasmic reticulum cisternae (Figure 9C). Additionally, it was common to see lipid droplets, small glycogen deposits (Figure 9C), and bundles of cytoplasmic microfilaments around the nucleus (Figure 9D) or dispersed in the cytoplasm.



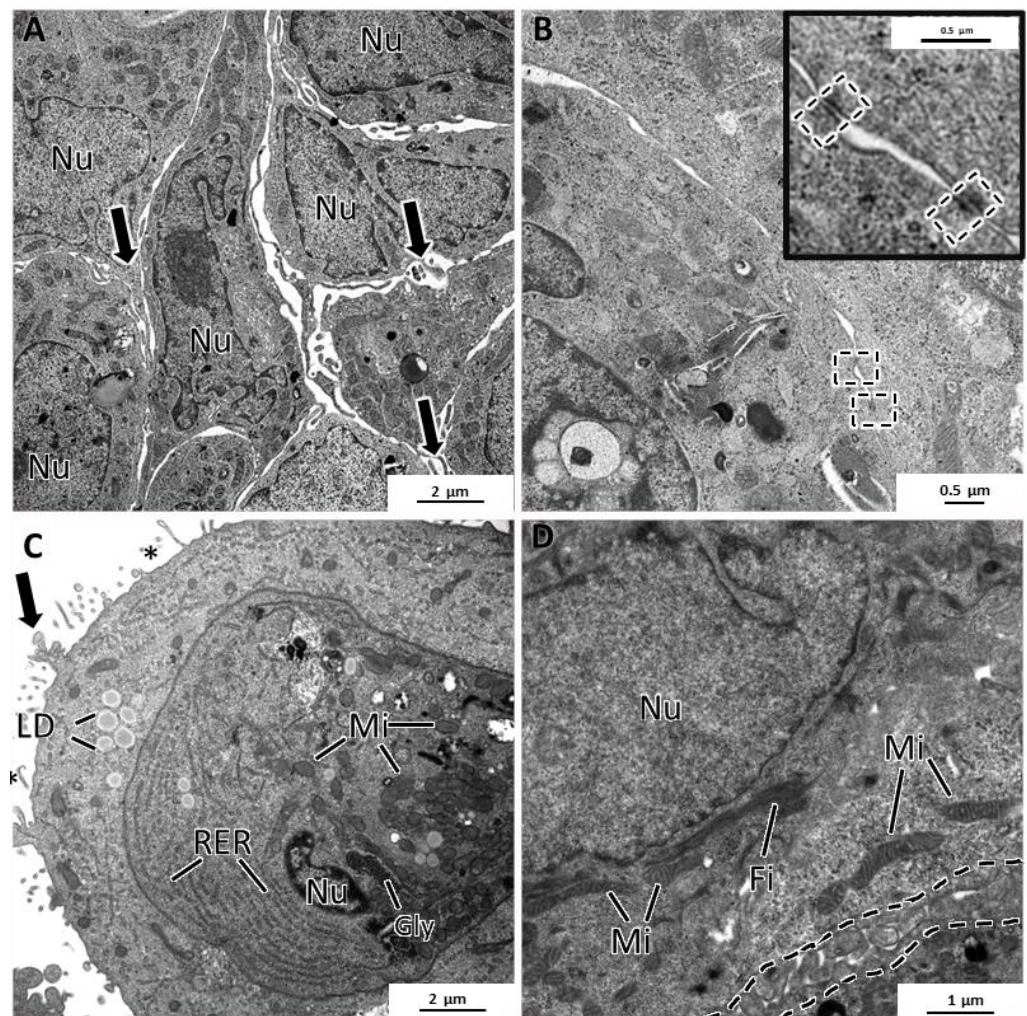


**Figure 9.** TEM representative images of MCF12A MCAs. (A) highlights intercellular spaces occupied by the cytoplasmic projections on the cell's surface (arrows). (B) shows some rare desmosomes (dashed rectangle). (C) depicts the cytoplasm content, rich in organelles such as mitochondria (Mi), rough endoplasmic reticulum (RER), storage substances, lipid droplets (LD), glycogen (Gly), microvilli (asterisks), and larger cytoplasmic projections (arrow). (D) shows cytoplasmic filaments (Fi) arranged in bundles and the net of tangled short cytoplasmic projections (dashed line).

#### 4. Discussion

This study detailed a single procedure to obtain MCAs of three BC cell lines from different molecular subtypes and one non-tumoral cell line using ULA plates. Furthermore, and to our best knowledge, we characterized for the first time those MCAs using morphometry, cytology (light and electron microscopy), and immunocytochemistry. We recorded some practical experiences from this study, which we have organized here as a set of “tips and tricks” to assist readers in effectively obtaining and analyzing MCAs using ULA plates (Table S1).

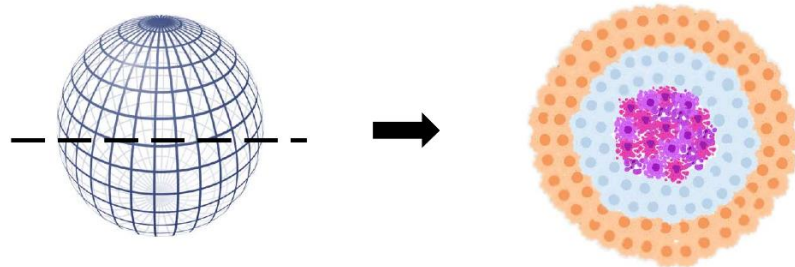
##### 4.1. MCAs' Formation in ULA Plates

This methodology enabled the generation of uniform MCAs (a single MCA per well) from all the cell lines within 3 days of culture, which accords with other authors that used the same methodology [11,22,57]. Another report described spheroids formation in 1 to 2 days [18], but although this time would be enough for the MDA-MB-231 cell line, it would not allow the spheroid formation for the other cell lines. Thus, to uniformize and perform the experiment in all cell lines at the same time, we used 3 days. Indeed, the adopted total of

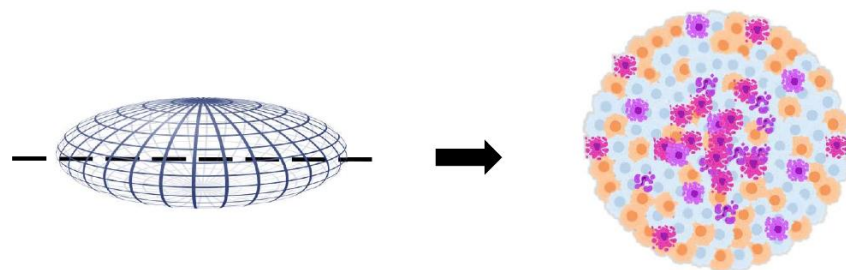
7 days in culture (3 days of MCA formation plus simulation of 4 days of exposure) was similar to some studies [34,58]. However, others have extended this time until 12–14 days [59,60].

According to the authors that used similar methodologies, the 3D cultures were reported to be spherical or nearly spherical [14,61,62]. Contrarily, here the formed MCAs were ellipsoids or flattened discoid aggregates, as schematically represented in Figure 10. However, it is important to mention that the referred studies did not include histological analysis and only relied on observations with stereomicroscopy. At this level, our images are similar to previous findings [14,61,62]. Only when processing the MCAs for light and electron microscopy their real shape was observed, which varied according to the cell line, as well as their size and cellular compactness.

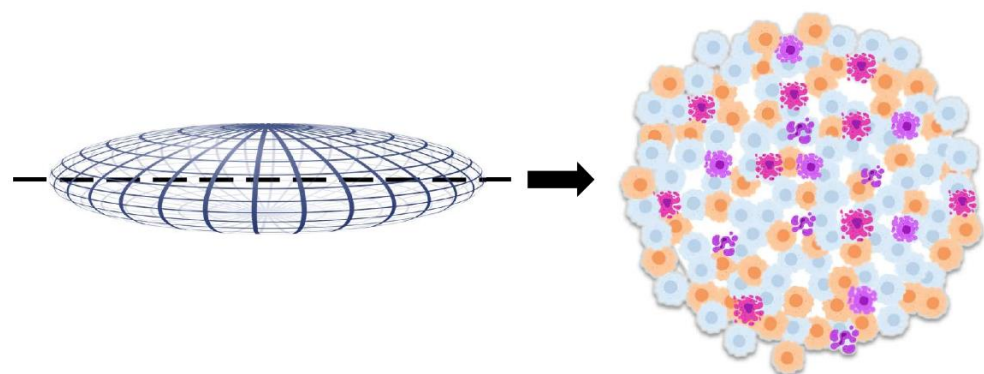
### (A) Traditional View of 3D Breast Cancer Cell Spheroids



### (B) Proposed Model of the 3D MCAs of Breast Cells using ULA plates



MCF7, MDA-MB-231



MCF12A, SKBR3

**Legend:**  Apoptotic/Necrotic cells  Proliferating cells  Quiescent cells

**Figure 10.** Schematic comparison of the traditional idealized three-layered distribution of dying, quiescent, and proliferating cells in spheroids, and the observed pattern in MCF7, MDA-MB-231, MCF12A, and SKBR3 MCAs obtained using ULA plates.



#### 4.2. MCAs' Compactness and Size

MCF7 and MDA-MB-231 formed compact MCAs, while SKBR3 and MCF12A formed loose MCAs. Previous studies with MCF7, MDA-MB-231 and SKBR3 also obtained 3D cultures with different compactness [22,49,63]. The more compact MCAs had a lower degree of flatness and smaller areas, while in loose MCAs the flatness was more pronounced and the areas were bigger (Figure 10).

The observation of HE-stained sections validated the degree of compactness, showing cells tightly packed in compact MCAs. TEM also confirmed the status of intercellular adhesion, with desmosomes, tight junctions, and interdigitations being more developed and numerous in MCF7 MCAs, following prior studies [64,65]. Moreover, most MCF7 cells were positive for the E-cadherin cell adhesion protein, as in previous descriptions [66–68], agreeing well with the compactness of their 3D cultures [61]. The cell compaction in MDA-MB-231 was also explained by intercellular adhesions, but according to previous descriptions, it is not mediated by E-cadherin, otherwise by collagen I/integrin  $\beta$ 1 interactions [61].

Most studies referred that MCF7 spontaneously formed compact spheroids [58,61,69,70], while one group described it as forming loose spheroids [15]. However, some authors report the addition of Matrigel or other viscosity raiser compound to the medium as a requirement for obtaining compact spheroids of MCF7 [22] and MDA-MB-231 [22,61,63]. This study produced similar results with the ULA plates without adding those compounds. Concerning the MDA-MB-231 cell line, our results are similar to some authors that obtained compact spheroids [69,71,72] but differ from others reporting loose aggregates [15,70]. These divergent results could be related to different methodologies to generate the 3D cultures, including different plate coatings, culture mediums with respective supplementations, and cell densities since all these factors can influence the formation of these models.

In the case of MCF12A, due to its shorter population doubling time (PDT) (19 h) compared to the other cell lines (MCF7, SKBR3, MDA-MB-231 (29, 30, and 38 h, respectively), half of the cell seeding density was used (40.000 cells/well) [73]; even so, the MCAs areas were bigger when compared to compact MCAs. This was probably due to the low compactness of its MCAs, confirmed in HE and TEM analysis, and not to its shorter PDT that, in theory, could contribute to a higher number of cells. Additionally, it is crucial to keep in mind that the available data about the PDT is relative to 2D cell cultures, and the behavior in 3D cell culture may not be the same, precisely due to the 3D nature of the cell-to-cell interactions.

#### 4.3. Inner MCAs' Structure

Many compact MCAs presented an apoptotic/necrotic core. The choice of this nomenclature "apoptotic/necrotic core" is associated with the fact that in HE and TEM there were cells with morphologies compatible with both apoptotic and necrotic cells. Here we confirmed apoptosis by ICC using an apoptotic marker (caspase-3 antibody), but according to the morphology observed in HE and electron microscopy, necrosis also occurs.

Spheroids with diameters over 500  $\mu$ m have been described as presenting a central necrotic area resultant from the depletion of oxygen, nutrients, and decreased pH [3,25]. Our MCAs were larger than 500  $\mu$ m (except for MDA-MB-231), and only some compact MCAs presented apoptotic/necrotic cores.

Generally, our MCAs were larger than those reported before [15,57,62]. We opted to use high cell densities for obtaining large MCAs, which could better represent a model for microvascular tumors or micrometastasis [3,74]. Furthermore, the large size of the MCAs facilitated their visualization and manipulation for morphological analysis.

Compared to the existing literature, the cell densities used in this study were, depending on the cell line, similar to or greater (up to about 60 times) than the ones used in other studies [15,58,62,70,71]. Nonetheless, the time for 3D formation and morphology was very similar. For example, Selby et al. (2017) plated only 5000 MCF7 cells/well using the same plates and equal time formation and obtained spheroids with diameters around 500  $\mu$ m. Despite using 16 times more cells/well for the same cell line, the average diameters

of the MCAs were only 1.4 times higher, around 700  $\mu\text{m}$ . This leads us to hypothesize that cell density is not the most determinant factor for the MCAs size, contrarily it seems more relevant to the inner characteristics of the cell lines that lead to different degrees of aggregation.

Whatever the aggregate size, dying cells existed in the core. Smaller MCF7 spheroids have shown necrotic cores after 5 days in culture [22], and MDA-MB-231 also presented necrotic cores within 6 and 7 days in culture [75,76]; the diameters of these MCAs were in one case half the size of the ones in our study, showing that the size of the MCAs is not the only factor responsible for the apoptotic/necrotic core. Similarly, compact MCAs have been described as having a higher percentage of dead cells [61]. However, no differences in the % of caspase-3 positive cells were found in this study between the compact and loose MCAs. This was probably because the larger MCAs also presented low compactness allowing better diffusion of oxygen and nutrients.

Following the MCAs' characterization, both light and electron microscopy disclosed some peculiar characteristics, especially in MCF7 MCAs, where it was detected the presence of acinar-like structures of different sizes that resemble the glandular acini of the mammary gland. The morphogenesis of this kind of acinar-like structure is said to involve the clearance of inner cells by apoptosis to allow lumen formation [67,77]. This is in line with our observations of cells with an apoptotic morphology and with the positive immunomarking for caspase-3 inside the lumen, equally reported by other authors [78]. Therefore, our results support the previous study of Amaral et al. [67], defending that the lumen formation was not due to the presence of substances that mimic the extracellular matrix (ECM). Nevertheless, the latter authors described that the luminal differentiation in spheroids only occurred after 50 days in culture. Herein, the acinar structures were detected on days 3 and 7 in culture, meaning that their differentiation, in the tested conditions, does not need so much time to occur.

TEM observation revealed that the acinar-like structures presented cellular polarization with periluminal microvilli [65,66,79] and secretory vesicles [66], features that have been described earlier. Secretory vesicles (with  $\beta$ -casein, a protein of human milk) were attributed to the presence of egg white in unfertilized chicken eggs in the culture medium [66]. Differently, in our culture medium, there was no egg white. There is another major difference between our study and that of D'Anselmi et al. (2013), as they worked in monolayer cultures while we used 3D cultures, which are described as being more prone to promote cellular differentiation [16,80] and tissue recapitulation [81,82]. Still, regarding TEM observations, high amounts of glycogen existed in MCAs of MCF7, similar to previous descriptions [83]. The same applies to lipid droplets in MCAs of MCF7 and MDA-MB-231 [84]. Lastly, the presence of many dense bodies was characteristic in MCAs of MDA-MB-231, also following a previous observation in a 3D culture with the same cell line [85].

Regarding the formation of MCAs from the SKBR3 cell line, other researchers had already described the unsuccessful formation of 3D structures using ULA plates [69]. This might have happened because Piggott et al. [69] used a serum-free medium, and serum contains growth factors necessary to maintain cell proliferation; therefore, their withdrawal can cause cell arrest and apoptosis [86]. SKBR3 cells observed in scanning electron microscopy also revealed poor aggregation in 3D arrangements [87]. Nevertheless, SKBR3 could successfully form 3D cultures when a viscosity raiser was added to the medium [22,61]. The poor cell adhesion is correlated with the noted lack of expression of E-cadherin in SKBR3 MCAs, corroborating previous descriptions [49,68]. The low compactness can also be explained by the low expression of other adhesion molecules such as integrin  $\beta$ 1 in this cell line [88].

MCF12A MCAs were the least compact aggregates in our study, which made them very difficult to manipulate without causing disaggregation. This study seems to be the first report describing the formation of MCF12A MCAs using ULA plates since the literature only reports MCF12A 3D cultures, using other techniques that include Matrigel [89,90].

In opposition to compact MCAs, the looser ones presented bigger areas, reflecting the intercellular spaces observed in HE staining and the decreased number of cellular adhesions in TEM analysis.

In MCF12A, just a small number of cells stained positive for E-cadherin, forming clusters that appeared in the outer part of the MCAs. The literature relative to the expression of this protein is divergent since one study did not detect E-cadherin protein by Western blot [91], while another described this cell line as positive to E-cadherin using ICC [92]. However, the presented immunostaining was not in the membrane as expected for this marker and as we obtained in MCF12A (and MCF7) MCAs.

In contrast to compact MCAs, there were no observed apoptotic/necrotic cores in loose MCAs. We hypothesize that the low compactness and the flattened shape increase the surface area and reduce the distance from the long axis to the MCAs center of mass, promoting better access to the nutrients and oxygen and, as a consequence, preventing the formation of a hypoxic central region [93].

The proportion of apoptotic and proliferating cells in the MCAs was evaluated using anti-caspase-3 and anti-Ki67 antibodies, respectively. In both compact and loose MCAs, there were proliferating cells throughout all the MCAs without preferential localization (see the schematic diagram in Figure 10). Even when an apoptotic/necrotic core was present, there were some Ki67 positive cells among the apoptotic cells, differing from the reported traditional diagrams of 3D cultures composed of three zones [2,13,16,25], in which proliferating cells were located solely in the outer part of the spheroids. The distribution of caspase-3 positive cells was overall similar to the one relative to Ki67, but there was a higher number of apoptotic cells in the apoptotic/necrotic core (whenever present).

Compared to the typical schematic portrayal of 3D cultures, these changes in the distribution of caspase-3 and Ki67 positive cells may be attributed to the ellipsoid form of the MCAs. However, a similar random distribution of Ki67 positive cells was observed in MCF7 [22] ( $\approx 300\text{--}400\ \mu\text{m}$  of diameter) and MDA-MB-231 spheroids ( $\approx 500\text{--}600\ \mu\text{m}$ ) [94], and other small spheroids from breast cell lines ( $\approx 300\ \mu\text{m}$ ) [95]. Thus, according to our results, the classical three-layered spheroid structure is too simplistic and does not represent the real structure of all the 3D cell cultures. Thus, at least for the four cell lines and used culture conditions studied here, we propose a new schematic model integrating the MCAs' morphology, compactness, and distribution of proliferating and dead cells (Figure 10).

The MCAs were also analyzed for the expression of epithelial (AE1/AE3) and mesenchymal (vimentin) antigens, both important when studying the epithelial–mesenchymal transition (EMT), where epithelial cells lose their polarity, change their shape, acquire motility, and start to express mesenchymal markers [96]. There has been a growing interest in developing drugs that target EMT [97,98], reinforcing the importance of studying epithelial and mesenchymal markers within the MCAs.

All MCAs stained positive for AE1/AE3. Our results are in accordance with the literature concerning MCF7 [99,100], SKBR3 [99,100], and MCF12A [92]. For MDA-MB-231, there is conflicting information in the published data, with some authors, like us, describing this cell line as being positive for CK19 [101], one of the various cytokeratins recognized by AE1/AE3 [102]. However, others reported that CK19 was not detected in this cell line by semi-quantitative RT-PCR and Western blot analyses [100] or that epithelial markers were weakly expressed in MDA-MB-231 [66].

Concerning vimentin, we have found strong positive immunomarking in MDA-MB-231 and MCF12A MCAs, and a few positive cells in MCF7. In general, our results corroborated the literature: MCF7 [66,99] and SKBR3 [99,103] had been described as negative for vimentin, while MDA-MB-231 [66,99] and MCF12A are reported as being positive for this marker [92,104]. However, we found a low number of vimentin-positive cells in MCF7 MCAs, suggesting that these cells have undergone EMT, a hypothesis supported by one study indicating that only around 5% of cells undergo EMT in 3D arrangement [105].

Another important characteristic of the breast cell lines is the expression of ER and PR hormonal receptors and the growth factor receptor HER-2, especially when studying

the response or interaction of drugs with these receptors [106]. For MCF7, there is a broad consensus about its positivity to ER and PR [38,107,108], which is in perfect agreement with our results. Additionally, we unveiled for the first time that the positive cells are preferentially located in the outer part of the MCAs. For MCF12A, the literature presents contradictory data. Our results corroborate studies reporting that this cell line is negative for ER [39]. Other authors stated that it weakly expressed ER [109] or was non-responsive to estrogen [92]. Contrarily, some authors affirmed that MCF12A is ER/PR positive [40,110] and that it even highly expresses ER $\alpha$  and ER $\beta$  [89]. SKBR3 presented overexpression of HER-2 as it was supposed [38], with more than 80% of the cells in the MCAs showing a thick, circumferential uniform membrane staining [111].

## 5. Conclusions

The use of ULA plates was revealed to be a simple, fast, reproducible, and cost-effective technical option for generating and analyzing the MCAs of MCF7, MDA-MB-231, SKBR3, and MCF12A cell lines. The MCAs had an ellipsoid to discoid shape, either compact (MCF7 and MDA-MB-231) or loose and more flattened (MCF12A and SKBR3). Compact MCAs presented smaller areas with more cellular adhesions and apoptotic/necrotic cores. In looser MCAs, proliferating and apoptotic cells were more randomly distributed. MCF7 MCAs presented glandular breast differentiation features with the formation of acinar-like structures, with apical microvilli and adluminal accumulation of secretory vesicles. Given the conflicting data found in the literature, we recommend characterizing 3D models using different outputs. The presented cytological and ICC characterizations of MCAs from MCF7, SKBR3, MDA-MB-231, and MCF12A cell lines using ULA plates help to understand the strengths and weaknesses of this model but also give a baseline to the interpretation of experimental results, namely from cytotoxic assays and drug screening. The very inconsistent data in the literature concerning the characterization of 3D models of breast cell lines also reinforces the need to detail the used protocols and promote the use of standardized culture conditions, aiming for better replication.

**Supplementary Materials:** The following supporting information can be downloaded at: <https://www.mdpi.com/article/10.3390/toxics10080415/s1>, Table S1: Tips and tricks for successful MCAs analysis from our experience. Figure S1. Representative images of the morphology (after 3 days in culture) of the 3D MCAs of MCF7, SKBR3, MDA-MB-231, and MCF12A cell lines seeded at three different cell densities.

**Author Contributions:** Conceptualization, F.M., A.C.M., A.A.R. and E.R.; methodology, F.M., A.A.R. and E.R.; formal analysis, F.M.; investigation, F.M. and A.C.M.; resources, E.R.; writing—original draft preparation, F.M.; writing—review and editing, A.A.R., A.C.M. and E.R.; visualization, F.M., A.A.R., A.C.M. and E.R.; supervision, A.A.R. and E.R.; project administration, E.R.; funding acquisition, E.R. All authors have read and agreed to the published version of the manuscript.

**Funding:** The Strategic Funding UIDB/04423/2020 and UIDP/04423/2020 partially supported this research, through national funds provided by FCT and ERDF to CIIMAR/CIMAR, in the framework of the program PT2020. The Doctoral Program in Biomedical Sciences, of the ICBAS—School of Medicine and Biomedical Sciences, U.Porto, offered additional funds.

**Institutional Review Board Statement:** Not applicable.

**Informed Consent Statement:** Not applicable.

**Data Availability Statement:** The data presented in this study are available on request from the corresponding author on reasonable request.

**Conflicts of Interest:** The authors declare no conflict of interest.



## References

1. Breslin, S.; O'Driscoll, L. Three-dimensional cell culture: The missing link in drug discovery. *Drug Discov. Today* **2013**, *18*, 240–249. [[CrossRef](#)] [[PubMed](#)]
2. Costa, E.C.; Moreira, A.F.; De Melo-Diogo, D.M.; Gaspar, V.M.; Carvalho, M.P.; Correia, I.J. 3D tumor spheroids: An overview on the tools and techniques used for their analysis. *Biotechnol. Adv.* **2016**, *34*, 1427–1441. [[CrossRef](#)] [[PubMed](#)]
3. Verjans, E.-T.; Doijen, J.; Luyten, W.; Landuyt, B.; Schoofs, L. Three-dimensional cell culture models for anticancer drug screening: Worth the effort? *J. Cell. Physiol.* **2018**, *233*, 2993–3003. [[CrossRef](#)]
4. Antoni, D.; Burckel, H.; Josset, E.; Noel, G. Three-Dimensional Cell Culture: A Breakthrough in Vivo. *Int. J. Mol. Sci.* **2015**, *16*, 5517–5527. [[CrossRef](#)] [[PubMed](#)]
5. L'Espérance, S.; Bachvarova, M.; Tetu, B.; Mes-Masson, A.-M.; Bachvarov, D. Global gene expression analysis of early response to chemotherapy treatment in ovarian cancer spheroids. *BMC Genom.* **2008**, *9*, 99. [[CrossRef](#)] [[PubMed](#)]
6. Lovitt, C.J.; Shelper, T.B.; Avery, V.M. Advanced Cell Culture Techniques for Cancer Drug Discovery. *Biology* **2014**, *3*, 345–367. [[CrossRef](#)] [[PubMed](#)]
7. Gomez-Roman, N.; Stevenson, K.; Gilmour, L.; Hamilton, G.; Chalmers, A.J. A novel 3D human glioblastoma cell culture system for modeling drug and radiation responses. *Neuro-Oncol.* **2017**, *19*, 229–241. [[CrossRef](#)]
8. Friedrich, J.; Ebner, R.; Kunz-Schughart, L. Experimental anti-tumor therapy in 3-D: Spheroids-old hat or new challenge? *Int. J. Radiat. Biol.* **2007**, *83*, 849–871. [[CrossRef](#)]
9. Sutherland, R.M.; Sordat, B.; Bamat, J.; Gabbert, H.; Bourrat, B.; Mueller-Klieser, W. Oxygenation and differentiation in multicellular spheroids of human colon carcinoma. *Cancer Res.* **1986**, *46*, 5320–5329.
10. Reynolds, D.S.; Tevis, K.M.; Blessing, W.A.; Colson, Y.L.; Zaman, M.H.; Grinstaff, M.W. Breast Cancer Spheroids Reveal a Differential Cancer Stem Cell Response to Chemotherapeutic Treatment. *Sci. Rep.* **2017**, *7*, 10382. [[CrossRef](#)]
11. Sant, S.; Johnston, P.A. The production of 3D tumor spheroids for cancer drug discovery. *Drug Discov. Today Technol.* **2017**, *23*, 27–36. [[CrossRef](#)] [[PubMed](#)]
12. Mehta, G.; Hsiao, A.Y.; Ingram, M.; Luker, G.D.; Takayama, S. Opportunities and challenges for use of tumor spheroids as models to test drug delivery and efficacy. *J. Control. Release* **2012**, *164*, 192–204. [[CrossRef](#)] [[PubMed](#)]
13. Hirschhaeuser, F.; Menne, H.; Dittfeld, C.; West, J.; Mueller-Klieser, W.; Kunz-Schughart, L.A. Multicellular tumor spheroids: An underestimated tool is catching up again. *J. Biotechnol.* **2010**, *148*, 3–15. [[CrossRef](#)] [[PubMed](#)]
14. Friedrich, J.; Seidel, C.; Ebner, R.; Kunz-Schughart, L.A. Spheroid-based drug screen: Considerations and practical approach. *Nat. Protoc.* **2009**, *4*, 309–324. [[CrossRef](#)]
15. Imamura, Y.; Mukohara, T.; Shimono, Y.; Funakoshi, Y.; Chayahara, N.; Toyoda, M.; Kiyota, N.; Takao, S.; Kono, S.; Nakatsura, T.; et al. Comparison of 2D- and 3D-culture models as drug-testing platforms in breast cancer. *Oncol. Rep.* **2015**, *33*, 1837–1843. [[CrossRef](#)]
16. Edmondson, R.; Broglie, J.J.; Adcock, A.F.; Yang, L. Three-Dimensional Cell Culture Systems and Their Applications in Drug Discovery and Cell-Based Biosensors. *ASSAY Drug Dev. Technol.* **2014**, *12*, 207–218. [[CrossRef](#)]
17. Minchinton, A.I.; Tannock, I.F. Drug penetration in solid tumours. *Nat. Rev. Cancer* **2006**, *6*, 583–592. [[CrossRef](#)]
18. Vinci, M.; Gowan, S.; Boxall, F.; Patterson, L.; Zimmermann, M.; Court, W.; Lomas, C.; Mendiola, M.; Hardisson, D.; Eccles, S.A. Advances in establishment and analysis of three-dimensional tumor spheroid-based functional assays for target validation and drug evaluation. *BMC Biol.* **2012**, *10*, 29. [[CrossRef](#)]
19. Langhans, S.A. Three-Dimensional in Vitro Cell Culture Models in Drug Discovery and Drug Repositioning. *Front. Pharmacol.* **2018**, *9*, 6. [[CrossRef](#)]
20. Nunes, A.S.; Barros, A.S.; Costa, E.C.; Moreira, A.F.; Correia, I.J. 3D tumor spheroids as in vitro models to mimic in vivo human solid tumors resistance to therapeutic drugs. *Biotechnol. Bioeng.* **2019**, *116*, 206–226. [[CrossRef](#)]
21. Härmä, V.; Schukov, H.-P.; Happonen, A.; Ahonen, I.; Virtanen, J.; Siitari, H.; Åkerfelt, M.; Lötjönen, J.; Nees, M. Quantification of Dynamic Morphological Drug Responses in 3D Organotypic Cell Cultures by Automated Image Analysis. *PLoS ONE* **2014**, *9*, e96426. [[CrossRef](#)] [[PubMed](#)]
22. Froehlich, K.; Haeger, J.-D.; Heger, J.; Pastuschek, J.; Photini, S.M.; Yan, Y.; Lupp, A.; Pfarrer, C.; Mrowka, R.; Schleußner, E.; et al. Generation of Multicellular Breast Cancer Tumor Spheroids: Comparison of Different Protocols. *J. Mammary Gland Biol. Neoplasia* **2016**, *21*, 89–98. [[CrossRef](#)] [[PubMed](#)]
23. Costa, E.C.; de Melo-Diogo, D.; Moreira, A.F.; Carvalho, M.P.; Correia, I.J. Spheroids Formation on Non-Adhesive Surfaces by Liquid Overlay Technique: Considerations and Practical Approaches. *Biotechnol. J.* **2018**, *13*, 1700417. [[CrossRef](#)] [[PubMed](#)]
24. Malhão, F.; Ramos, A.A.; Buttachon, S.; Dethoup, T.; Kijjoa, A.; Rocha, E. Cytotoxic and Antiproliferative Effects of Preussin, a Hydroxypyrrrolidine Derivative from the Marine Sponge-Associated Fungus *Aspergillus candidus* KUFA 0062, in a Panel of Breast Cancer Cell Lines and Using 2D and 3D Cultures. *Mar. Drugs* **2019**, *17*, 448. [[CrossRef](#)] [[PubMed](#)]
25. Zanoni, M.; Piccinini, F.; Arienti, C.; Zamagni, A.; Santi, S.; Polico, R.; Bevilacqua, A.; Tesi, A. 3D tumor spheroid models for in vitro therapeutic screening: A systematic approach to enhance the biological relevance of data obtained. *Sci. Rep.* **2016**, *6*, 19103. [[CrossRef](#)]
26. Dai, X.; Li, T.; Bai, Z.; Yang, Y.; Liu, X.; Zhan, J.; Shi, B. Breast cancer intrinsic subtype classification, clinical use and future trends. *Am. J. Cancer Res.* **2015**, *5*, 2029–2943.

27. Bray, F.; Ferlay, J.; Soerjomataram, I.; Siegel, R.L.; Torre, L.A.; Jemal, A. Global cancer statistics 2018: GLOBOCAN estimates of incidence and mortality worldwide for 36 cancers in 185 countries. *CA Cancer J. Clin.* **2018**, *68*, 394–424. [[CrossRef](#)]
28. DeSantis, C.E.; Bray, F.; Ferlay, J.; Lortet-Tieulent, J.; Anderson, B.O.; Jemal, A. International Variation in Female Breast Cancer Incidence and Mortality Rates. *Cancer Epidemiol. Biomark. Prev.* **2015**, *24*, 1495–1506. [[CrossRef](#)]
29. Sanguinetti, A.; Polistena, A.; Lucchini, R.; Monacelli, M.; Galasse, S.; Avenia, S.; Triola, R.; Bugiantella, W.; Ciocchi, R.; Rondelli, F.; et al. Male breast cancer, clinical presentation, diagnosis and treatment: Twenty years of experience in our Breast Unit. *Int. J. Surg. Case Rep.* **2016**, *20*, 8–11. [[CrossRef](#)]
30. Polyak, K. Heterogeneity in breast cancer. *J. Clin. Investig.* **2011**, *121*, 3786–3788. [[CrossRef](#)]
31. Hoon Tan, P.; Ellis, I.; Allison, K.; Brogi, E.; Fox, S.B.; Lakhani, S.; Lazar, A.J.; Morris, E.A.; Sahin, A.; Salgado, R.; et al. The 2019 World Health Organization classification of tumours of the breast. *Histopathology* **2020**, *77*, 181–185. [[CrossRef](#)] [[PubMed](#)]
32. Adams, E.; Wildiers, H.; Neven, P.; Punie, K. Sacituzumab govitecan and trastuzumab deruxtecan: Two new antibody–drug conjugates in the breast cancer treatment landscape. *ESMO Open* **2021**, *6*, 100204. [[CrossRef](#)] [[PubMed](#)]
33. de la Mare, J.-A.; Sterrenberg, J.N.; Sukhthankar, M.G.; Chiwakata, M.T.; Beukes, D.R.; Blatch, G.L.; Ekins, A.L. Assessment of potential anti-cancer stem cell activity of marine algal compounds using an in vitro mammosphere assay. *Cancer Cell Int.* **2013**, *13*, 39. [[CrossRef](#)] [[PubMed](#)]
34. Raghavan, S.; Mehta, P.; Horst, E.N.; Ward, M.R.; Rowley, K.R.; Mehta, G. Comparative analysis of tumor spheroid generation techniques for differential in vitro drug toxicity. *Oncotarget* **2016**, *7*, 16948–16961. [[CrossRef](#)] [[PubMed](#)]
35. Howes, A.L.; Richardson, R.D.; Finlay, D.; Vuori, K. 3-Dimensional Culture Systems for Anti-Cancer Compound Profiling and High-Throughput Screening Reveal Increases in EGFR Inhibitor-Mediated Cytotoxicity Compared to Monolayer Culture Systems. *PLoS ONE* **2014**, *9*, e108283. [[CrossRef](#)]
36. Katt, M.E.; Placone, A.L.; Wong, A.D.; Xu, Z.S.; Searson, P.C. In Vitro Tumor Models: Advantages, Disadvantages, Variables, and Selecting the Right Platform. *Front. Bioeng. Biotechnol.* **2016**, *4*, 12. [[CrossRef](#)]
37. Huang, Z.; Yu, P.; Tang, J. Characterization of Triple-Negative Breast Cancer MDA-MB-231 Cell Spheroid Model. *OncoTargets Ther.* **2020**, *13*, 5395–5405. [[CrossRef](#)]
38. Holliday, D.L.; Speirs, V. Choosing the right cell line for breast cancer research. *Breast Cancer Res.* **2011**, *13*, 215. [[CrossRef](#)]
39. Subik, K.; Lee, J.-F.; Baxter, L.; Strzepak, T.; Costello, D.; Crowley, P.; Xing, L.; Hung, M.-C.; Bonfiglio, T.; Hicks, D.G.; et al. The expression patterns of ER, PR, HER2, CK5/6, EGFR, Ki-67 and AR by immunohistochemical analysis in breast cancer cell lines. *Breast Cancer* **2010**, *4*, 35–41. [[CrossRef](#)]
40. Dai, J.; Jian, J.; Bosland, M.; Frenkel, K.; Bernhardt, G.; Huang, X. Roles of hormone replacement therapy and iron in proliferation of breast epithelial cells with different estrogen and progesterone receptor status. *Breast* **2008**, *17*, 172–179. [[CrossRef](#)]
41. Gomes, N.G.M.; Lefranc, F.; Kijjoa, A.; Kiss, R. Can Some Marine-Derived Fungal Metabolites Become Actual Anticancer Agents? *Mar. Drugs* **2015**, *13*, 3950–3991. [[CrossRef](#)] [[PubMed](#)]
42. Malhão, F.; Ramos, A.A.; Macedo, A.C.; Rocha, E. Cytotoxicity of Seaweed Compounds, Alone or Combined to Reference Drugs, against Breast Cell Lines Cultured in 2D and 3D. *Toxics* **2021**, *9*, 24. [[CrossRef](#)] [[PubMed](#)]
43. Piccinini, F. AnaSP: A software suite for automatic image analysis of multicellular spheroids. *Comput. Methods Programs Biomed.* **2015**, *119*, 43–52. [[CrossRef](#)]
44. Hammer, O.; Harper, D.; Ryan, P. PAST: Paleontological statistics software package for education and data analysis. *Palaeontol. Electron.* **2001**, *4*, 1–9.
45. Gil, R.S.; Vagnarelli, P. Ki-67: More Hidden behind a ‘Classic Proliferation Marker’. *Trends Biochem. Sci.* **2018**, *43*, 747–748. [[CrossRef](#)]
46. Inwald, E.C.; Klinkhammer-Schalke, M.; Hofstädter, F.; Zeman, F.; Koller, M.; Gerstenhauer, M.; Ortmann, O. Ki-67 is a prognostic parameter in breast cancer patients: Results of a large population-based cohort of a cancer registry. *Breast Cancer Res. Treat.* **2013**, *139*, 539–552. [[CrossRef](#)] [[PubMed](#)]
47. Bressenot, A.; Marchal, S.; Bezdetnaya, L.; Garrier, J.; Guillemin, F.; Plénat, F. Assessment of Apoptosis by Immunohistochemistry to Active Caspase-3, Active Caspase-7, or Cleaved PARP in Monolayer Cells and Spheroid and Subcutaneous Xenografts of Human Carcinoma. *J. Histochem. Cytochem.* **2009**, *57*, 289–300. [[CrossRef](#)]
48. Riss, T.L.; Moravec, R.A. Use of Multiple Assay Endpoints to Investigate the Effects of Incubation Time, Dose of Toxin, and Plating Density in Cell-Based Cytotoxicity Assays. *ASSAY Drug Dev. Technol.* **2004**, *2*, 51–62. [[CrossRef](#)]
49. Iglesias, J.M.; Belouqui, I.; Garcia-Garcia, F.; Leis, O.; Vazquez-Martin, A.; Eguiara, A.; Cufi, S.; Pavon, A.; Menendez, J.A.; Dopazo, J.; et al. Mammosphere Formation in Breast Carcinoma Cell Lines Depends upon Expression of E-cadherin. *PLoS ONE* **2013**, *8*, e77281. [[CrossRef](#)]
50. Carvalho, S.; Reis, C.; Pinho, S.S. Cadherins Glycans in Cancer: Sweet Players in a Bitter Process. *Trends Cancer* **2016**, *2*, 519–531. [[CrossRef](#)]
51. Pai, V.C.; Glasgow, B.J. MUC16 as a Sensitive and Specific Marker for Epithelial Downgrowth. *Arch. Ophthalmol.* **2010**, *128*, 1407–1412. [[CrossRef](#)] [[PubMed](#)]
52. Liu, C.Y.; Lin, H.H.; Tang, M.J.; Wang, Y.K. Vimentin contributes to epithelial-mesenchymal transition cancer cell mechanics by mediating cytoskeletal organization and focal adhesion maturation. *Oncotarget* **2015**, *6*, 15966–15983. [[CrossRef](#)] [[PubMed](#)]
53. Dai, X.; Cheng, H.; Bai, Z.; Li, J. Breast Cancer Cell Line Classification and Its Relevance with Breast Tumor Subtyping. *J. Cancer* **2017**, *8*, 3131–3141. [[CrossRef](#)] [[PubMed](#)]

54. Gundersen, H.J.G. Notes on the estimation of the numerical density of arbitrary profiles: The edge effect. *J. Microsc.* **1977**, *111*, 219–223. [CrossRef]
55. Elmore, S.A.; Dixon, D.; Hailey, J.R.; Harada, T.; Herbert, R.A.; Maronpot, R.R.; Nolte, T.; Rehg, J.E.; Rittinghausen, S.; Rosol, T.J.; et al. Recommendations from the INHAND Apoptosis/Necrosis Working Group. *Toxicol. Pathol.* **2016**, *44*, 173–188. [CrossRef]
56. Sachet, M.; Liang, Y.Y.; Oehler, R. The immune response to secondary necrotic cells. *Apoptosis* **2017**, *22*, 1189–1204. [CrossRef]
57. Benton, G.; DeGray, G.; Kleinman, H.K.; George, J.; Arnaoutova, I. In Vitro Microtumors Provide a Physiologically Predictive Tool for Breast Cancer Therapeutic Screening. *PLoS ONE* **2015**, *10*, e0123312. [CrossRef]
58. Ho, W.Y.; Yeap, S.K.; Ho, C.L.; Rahim, R.A.; Alitheen, N.B. Development of Multicellular Tumor Spheroid (MCTS) Culture from Breast Cancer Cell and a High Throughput Screening Method Using the MTT Assay. *PLoS ONE* **2012**, *7*, e44640. [CrossRef]
59. Cavo, M.; Cave, D.D.; D'Amone, E.; Gigli, G.; Lonardo, E.; Del Mercato, L.L. A synergic approach to enhance long-term culture and manipulation of MiaPaCa-2 pancreatic cancer spheroids. *Sci. Rep.* **2020**, *10*, 10192. [CrossRef]
60. Hagemann, J.; Jacobi, C.; Hahn, M.; Schmid, V.; Welz, C.; Schwenk-Zieger, S.; Stauber, R.; Baumeister, P.; Becker, S. Spheroid-based 3D Cell Cultures Enable Personalized Therapy Testing and Drug Discovery in Head and Neck Cancer. *Anticancer Res.* **2017**, *37*, 2201–2210. [CrossRef]
61. Ivascu, A.; Kubbies, M. Diversity of cell-mediated adhesions in breast cancer spheroids. *Int. J. Oncol.* **2007**, *31*, 1403–1413. [CrossRef] [PubMed]
62. Pereira, P.; Berisha, N.; Bhupathiraju, N.V.S.D.K.; Fernandes, R.; Tomé, J.P.C.; Drain, C.M. Cancer cell spheroids are a better screen for the photodynamic efficiency of glycosylated photosensitizers. *PLoS ONE* **2017**, *12*, e0177737. [CrossRef] [PubMed]
63. Ivascu, A.; Kubbies, M. Rapid Generation of Single-Tumor Spheroids for High-Throughput Cell Function and Toxicity Analysis. *J. Biomol. Screen.* **2006**, *11*, 922–932. [CrossRef]
64. Faute, M.A.D.; Laurent, L.; Ploton, D.; Poupon, M.-F.; Jardillier, J.-C.; Bobichon, H. Distinctive alterations of invasiveness, drug resistance and cell–cell organization in 3D-cultures of MCF-7, a human breast cancer cell line, and its multidrug resistant variant. *Clin. Exp. Metastasis* **2002**, *19*, 161–168. [CrossRef]
65. Vantangoli, M.M.; Madnick, S.J.; Huse, S.M.; Weston, P.; Boekelheide, K. MCF-7 Human Breast Cancer Cells Form Differentiated Microtissues in Scaffold-Free Hydrogels. *PLoS ONE* **2015**, *10*, e0135426. [CrossRef]
66. D'Anselmi, F.; Masiello, M.G.; Cucina, A.; Proietti, S.; Dinicola, S.; Pasqualato, A.; Ricci, G.; Dobrowolny, G.; Catizone, A.; Palombo, A.; et al. Microenvironment Promotes Tumor Cell Reprogramming in Human Breast Cancer Cell Lines. *PLoS ONE* **2013**, *8*, e83770. [CrossRef] [PubMed]
67. Amaral, J.B.D.; Rezende-Teixeira, P.; Freitas, V.; Machado-Santelli, G.M. MCF-7 Cells as a Three-Dimensional Model for the Study of Human Breast Cancer. *Tissue Eng. Part C: Methods* **2011**, *17*, 1097–1107. [CrossRef]
68. Vamvakidou, A.P.; Mondrinos, M.J.; Petushi, S.P.; Garcia, F.U.; Lelkes, P.I.; Tozeren, A. Heterogeneous Breast Tumoroids: An In Vitro Assay for Investigating Cellular Heterogeneity and Drug Delivery. *J. Biomol. Screen.* **2007**, *12*, 13–20. [CrossRef]
69. Piggott, L.; Omidvar, N.; Pérez, S.M.; Eberl, M.; Clarkson, R.W.E. Suppression of apoptosis inhibitor c-FLIP selectively eliminates breast cancer stem cell activity in response to the anti-cancer agent, TRAIL. *Breast Cancer Res.* **2011**, *13*, R88. [CrossRef]
70. Selby, M.; Delosh, R.; Laudeman, J.; Ogle, C.; Reinhart, R.; Silvers, T.; Lawrence, S.; Kinders, R.; Parchment, R.; Teicher, B.A.; et al. 3D Models of the NCI60 Cell Lines for Screening Oncology Compounds. *SLAS Discov.* **2017**, *22*, 473–483. [CrossRef]
71. Dubois, C.; Dufour, R.; Daumar, P.; Aubel, C.; Szczepaniak, C.; Blavignac, C.; Mounetou, E.; Penault-Llorca, F.; Bamdad, M. Development and cytotoxic response of two proliferative MDA-MB-231 and non-proliferative SUM1315 three-dimensional cell culture models of triple-negative basal-like breast cancer cell lines. *Oncotarget* **2017**, *8*, 95316–95331. [CrossRef] [PubMed]
72. Scolamiero, G.; Pazzini, C.; Bonafè, F.; Guarnieri, C.; Muscari, C. Effects of  $\alpha$ -Mangostin on Viability, Growth and Cohesion of Multicellular Spheroids Derived from Human Breast Cancer Cell Lines. *Int. J. Med. Sci.* **2018**, *15*, 23–30. [CrossRef] [PubMed]
73. ATCC. Available online: [https://www.lgcstandards-atcc.org/products/all/HTB-22.aspx?geo\\_country=ro#specifications](https://www.lgcstandards-atcc.org/products/all/HTB-22.aspx?geo_country=ro#specifications) (accessed on 31 March 2020).
74. Carver, K.; Ming, X.; Juliano, R.L. Multicellular Tumor Spheroids as a Model for Assessing Delivery of Oligonucleotides in Three Dimensions. *Mol. Ther. Nucleic Acids* **2014**, *3*, e153. [CrossRef] [PubMed]
75. Badea, M.A.; Balas, M.; Hermenean, A.; Ciceu, A.; Herman, H.; Ionita, D.; Dinischiotu, A. Influence of Matrigel on Single- and Multiple-Spheroid Cultures in Breast Cancer Research. *SLAS Discov.* **2019**, *24*, 563–578. [CrossRef]
76. Dubois, C.; Daumar, P.; Aubel, C.; Gauthier, J.; Vidalinc, B.; Mounetou, E.; Penault-Llorca, F.; Bamdad, M. The New Synthetic Serum-Free Medium OptiPASS Promotes High Proliferation and Drug Efficacy Prediction on Spheroids from MDA-MB-231 and SUM1315 Triple-Negative Breast Cancer Cell Lines. *J. Clin. Med.* **2019**, *8*, 397. [CrossRef]
77. Maillieux, A.A.; Overholtzer, M.; Brugge, J.S. Lumen formation during mammary epithelial morphogenesis: Insights from in vitro and in vivo models. *Cell Cycle* **2008**, *7*, 57–62. [CrossRef]
78. Kirshner, J.; Chen, C.-J.; Liu, P.; Huang, J.; Shively, J.E. CEACAM1-4S, a cell–cell adhesion molecule, mediates apoptosis and reverts mammary carcinoma cells to a normal morphogenic phenotype in a 3D culture. *Proc. Natl. Acad. Sci. USA* **2003**, *100*, 521–526. [CrossRef]
79. Morales, J.; Alpaugh, M.L. Gain in cellular organization of inflammatory breast cancer: A 3D in vitro model that mimics the in vivo metastasis. *BMC Cancer* **2009**, *9*, 462. [CrossRef]
80. Bin Kim, J.; Stein, R.; O'Hare, M.J. Three-dimensional in vitro tissue culture models of breast cancer—A review. *Breast Cancer Res. Treat.* **2004**, *85*, 281–291. [CrossRef]



81. Yamada, K.M.; Cukierman, E. Modeling Tissue Morphogenesis and Cancer in 3D. *Cell* **2007**, *130*, 601–610. [[CrossRef](#)]
82. Weigelt, B.; Ghajar, C.M.; Bissell, M.J. The need for complex 3D culture models to unravel novel pathways and identify accurate biomarkers in breast cancer. *Adv. Drug Deliv. Rev.* **2014**, *69–70*, 42–51. [[CrossRef](#)] [[PubMed](#)]
83. Pelletier, J.; Bellot, G.; Gounon, P.; Lacas-Gervais, S.; Pouyssegur, J.; Mazure, N.M. Glycogen Synthesis is Induced in Hypoxia by the Hypoxia-Inducible Factor and Promotes Cancer Cell Survival. *Front. Oncol.* **2012**, *2*, 18. [[CrossRef](#)]
84. Abramczyk, H.; Surmacki, J.; Kopeć, M.; Olejnik, A.K.; Lubecka-Pietruszewska, K.; Fabianowska-Majewska, K. The role of lipid droplets and adipocytes in cancer. Raman imaging of cell cultures: MCF10A, MCF7, and MDA-MB-231 compared to adipocytes in cancerous human breast tissue. *Analyst* **2015**, *140*, 2224–2235. [[CrossRef](#)] [[PubMed](#)]
85. Ivers, L.P.; Cummings, B.; Owolabi, F.; Welzel, K.; Klinger, R.; Saitoh, S.; O'Connor, D.; Fujita, Y.; Scholz, D.; Itasaki, N. Dynamic and influential interaction of cancer cells with normal epithelial cells in 3D culture. *Cancer Cell Int.* **2014**, *14*, 108. [[CrossRef](#)] [[PubMed](#)]
86. Letai, A. Growth Factor Withdrawal and Apoptosis: The Middle Game. *Mol. Cell* **2006**, *21*, 728–730. [[CrossRef](#)] [[PubMed](#)]
87. Colone, M.; Kaliappan, S.; Calcabrini, A.; Tortora, M.; Cavalieri, F.; Stringaro, A. Redox-active Microcapsules as Drug Delivery System in Breast Cancer Cells and Spheroids. *J. Mol. Genet. Med.* **2016**, *10*, 1. [[CrossRef](#)]
88. Meyer, T.; Marshall, J.F.; Hart, I.R. Expression of  $\alpha v$  integrins and vitronectin receptor identity in breast cancer cells. *Br. J. Cancer* **1998**, *77*, 530–536. [[CrossRef](#)]
89. Marchese, S.; Silva, E. Disruption of 3D MCF-12A Breast Cell Cultures by Estrogens—An In Vitro Model for ER-Mediated Changes Indicative of Hormonal Carcinogenesis. *PLoS ONE* **2012**, *7*, e45767. [[CrossRef](#)]
90. Weber-Ouellette, A.; Busby, M.; Plante, I. Luminal MCF-12A & myoepithelial-like Hs 578Bst cells form bilayered acini similar to human breast. *Future Sci. OA* **2018**, *4*, FSO315. [[CrossRef](#)]
91. Lombaerts, M.; Van Wezel, T.; Philippo, K.; Dierssen, J.W.F.; Zimmerman, R.M.E.; Oosting, J.; Van Eijk, R.; Eilers, P.H.; Van De Water, B.; Cornelisse, C.J.; et al. E-cadherin transcriptional downregulation by promoter methylation but not mutation is related to epithelial-to-mesenchymal transition in breast cancer cell lines. *Br. J. Cancer* **2006**, *94*, 661–671. [[CrossRef](#)]
92. Sweeney, M.F.; Sonnenschein, C.; Soto, A.M. Characterization of MCF-12A cell phenotype, response to estrogens, and growth in 3D. *Cancer Cell Int.* **2018**, *18*, 43. [[CrossRef](#)] [[PubMed](#)]
93. Leung, B.M.; Leshner-Perez, S.C.; Matsuoka, T.; Moraes, C.; Takayama, S. Media additives to promote spheroid circularity and compactness in hanging drop platform. *Biomater. Sci.* **2015**, *3*, 336–344. [[CrossRef](#)] [[PubMed](#)]
94. Da Motta, L.L.; Ledaki, I.; Purshouse, K.; Haider, S.; De Bastiani, M.A.; Baban, D.; Morotti, M.; Steers, G.; Wigfield, S.; Bridges, E.; et al. The BET inhibitor JQ1 selectively impairs tumour response to hypoxia and downregulates CA9 and angiogenesis in triple negative breast cancer. *Oncogene* **2017**, *36*, 122–132. [[CrossRef](#)] [[PubMed](#)]
95. Roberts, G.C.; Morris, P.G.; Moss, M.A.; Maltby, S.L.; Palmer, C.A.; Nash, C.E.; Smart, E.; Holliday, D.L.; Speirs, V. An Evaluation of Matrix-Containing and Humanised Matrix-Free 3-Dimensional Cell Culture Systems for Studying Breast Cancer. *PLoS ONE* **2016**, *11*, e0157004. [[CrossRef](#)]
96. Mendez, M.G.; Kojima, S.; Goldman, R.D. Vimentin induces changes in cell shape, motility, and adhesion during the epithelial to mesenchymal transition. *FASEB J.* **2010**, *24*, 1838–1851. [[CrossRef](#)]
97. Jonckheere, S.; Adams, J.; De Groote, D.; Campbell, K.; Bex, G.; Goossens, S. Epithelial-Mesenchymal Transition (EMT) as a Therapeutic Target. *Cells Tissues Organs* **2021**, *211*, 157–182. [[CrossRef](#)]
98. Cho, E.S.; Kang, H.E.; Kim, N.H.; Yook, J.I. Therapeutic implications of cancer epithelial-mesenchymal transition (EMT). *Arch. Pharmacol. Res.* **2019**, *42*, 14–24. [[CrossRef](#)]
99. Sommers, C.L.; Walker-Jones, D.; Heckford, S.E.; Worland, P.; Valverius, E.; Clark, R.; McCormick, F.; Stampfer, M.; Abularach, S.; Gelmann, E.P. Vimentin rather than keratin expression in some hormone-independent breast cancer cell lines and in oncogene-transformed mammary epithelial cells. *Cancer Res.* **1989**, *49*, 4258–4263.
100. Keyvani, S.; Karimi, N.; Orafa, Z.; Bouzari, S.; Oloomi, M. Assessment of Cytokeratin-19 Gene Expression in Peripheral Blood of Breast Cancer Patients and Breast Cancer Cell Lines. *Biomark. Cancer* **2016**, *8*, 57–63. [[CrossRef](#)]
101. Nerlich, A.G.; Bachmeier, B.E. Density-dependent lineage instability of MDA-MB-435 breast cancer cells. *Oncol. Lett.* **2013**, *5*, 1370–1374. [[CrossRef](#)]
102. Wahba, O.M. The diagnostic utility of pan-cytokeratin, CK19, CEA, CD10, and p63 in differentiating clear cell odontogenic carcinoma from hyalinizing clear cell carcinoma. *Tanta Dent. J.* **2016**, *13*, 73–82. [[CrossRef](#)]
103. Serrano, M.J.; Ortega, F.G.; Alvarez-Cubero, M.J.; Nadal, R.; Sanchez-Rovira, P.; Salido, M.; Rodriguez, M.; García-Puche, J.L.; Delgado-Rodriguez, M.; Solé, F.; et al. EMT and EGFR in CTCs cytokeratin negative non-metastatic breast cancer. *Oncotarget* **2014**, *5*, 7486–7497. [[CrossRef](#)]
104. Alsuliman, A.; Colak, D.; Al-Harazi, O.; Fitwi, H.; Tulbah, A.; Al-Tweigeri, T.; Al-Alwan, M.; Ghebeh, H. Bidirectional crosstalk between PD-L1 expression and epithelial to mesenchymal transition: Significance in claudin-low breast cancer cells. *Mol. Cancer* **2015**, *14*, 149. [[CrossRef](#)] [[PubMed](#)]
105. Herheliuk, T.; Peregelytsina, O.; Yurchenko, N.; Sydorenko, M.; Osapchenko, L. Expression of tumor associated and epithelial-mesenchymal transition download citation markers in 2d and 3d cell cultures of MCF-7. *EUREKA Health Sci.* **2016**, *6*, 37–44. [[CrossRef](#)]
106. Azimi, T.; Loizidou, M.; Dwek, M.V. Cancer cells grown in 3D under fluid flow exhibit an aggressive phenotype and reduced responsiveness to the anti-cancer treatment doxorubicin. *Sci. Rep.* **2020**, *10*, 12020. [[CrossRef](#)]



107. Metsiou, D.N.; Siatis, K.E.; Giannopoulou, E.; Papachristou, D.J.; Kalofonos, H.P.; Koutras, A.; Athanassiou, G. The Impact of Anti-tumor Agents on ER-Positive MCF-7 and HER2-Positive SKBR-3 Breast Cancer Cells Biomechanics. *Ann. Biomed. Eng.* **2019**, *47*, 1711–1724. [[CrossRef](#)]
108. Visagie, M.; Mqoco, T.; Joubert, A.M. Sulphamoylated estradiol analogue induces antiproliferative activity and apoptosis in breast cell lines. *Cell. Mol. Biol. Lett.* **2012**, *17*, 549–558. [[CrossRef](#)]
109. Zeillinger, R.; Tantscher, E.; Schneeberger, C.; Tschugguel, W.; Eder, S.; Sliutz, G.; Huber, J.C. Simultaneous expression of nitric oxide synthase and estrogen receptor in human breast cancer cell lines. *Breast Cancer Res. Treat.* **1996**, *40*, 205–207. [[CrossRef](#)]
110. Schröder, L.; Koch, J.; Mahner, S.; Kost, B.P.; Hofmann, S.; Jeschke, U.; Haumann, J.; Schmedt, J.; Richter, D.U. The Effects of Petroselinum Crispum on Estrogen Receptor-positive Benign and Malignant Mammary Cells (MCF12A/MCF7). *Anticancer Res.* **2017**, *37*, 95–102. [[CrossRef](#)]
111. Hicks, D.G.; Schiffhauer, L. Standardized Assessment of the HER2 Status in Breast Cancer by Immunohistochemistry. *Lab. Med.* **2011**, *42*, 459–467. [[CrossRef](#)]

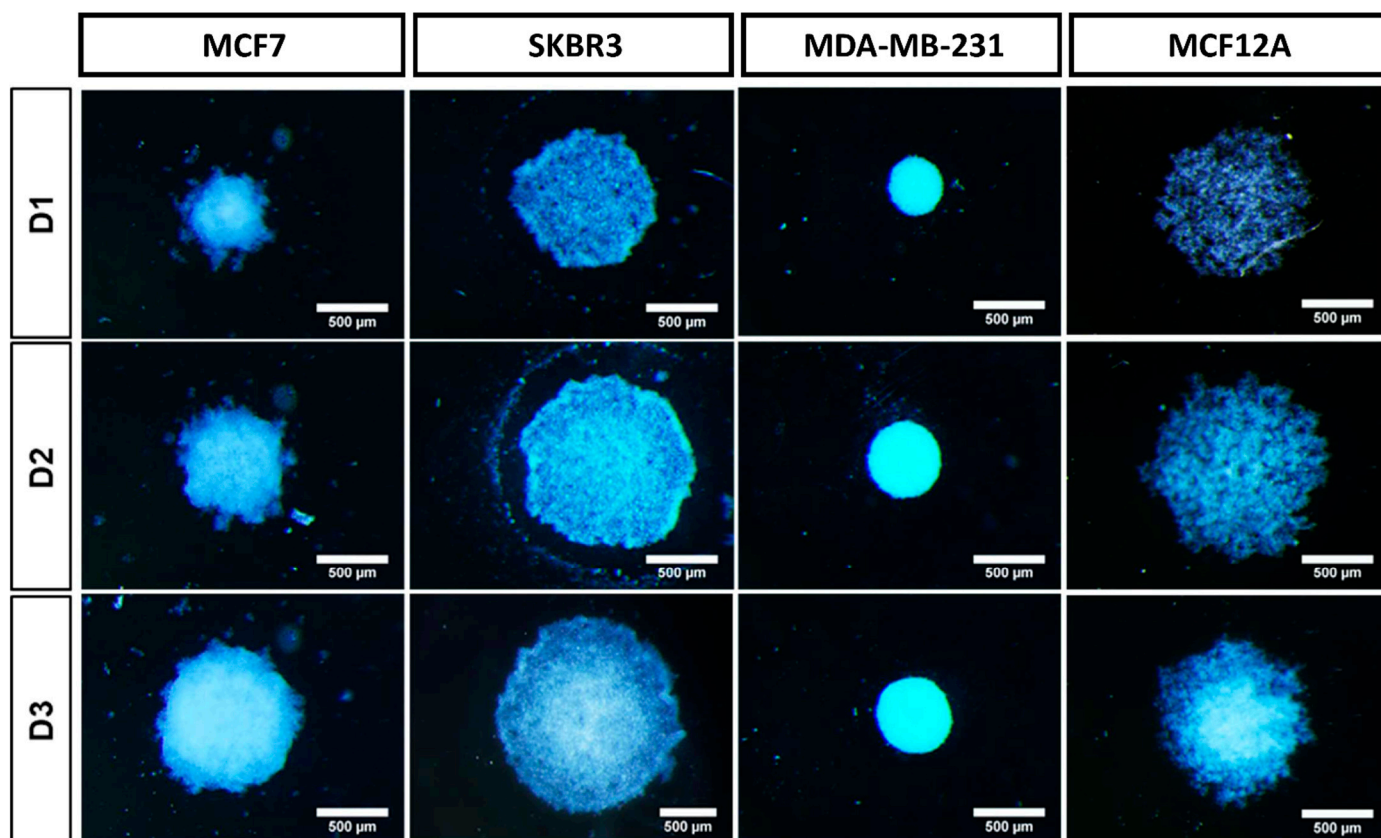


**Figure S1.** Representative images of the morphology (after 3 days in culture) of the 3D MCAs of MCF7, SKBR3, MDA-MB-231 and MCF12A cell lines seeded at three different cell densities. MCF-7 and SKBR3 cells were seeded at  $10 \times 10^4$  cells/mL (D1),  $20 \times 10^4$  cells/mL (D2) and  $40 \times 10^4$  cells/mL (D3). MDA-MB-231 cells were seeded at  $20 \times 10^4$  cells/mL (D1),  $40 \times 10^4$  cells/mL (D2) and  $50 \times 10^4$  cells/mL (D3). MCF-12A cells were seeded at  $5 \times 10^4$  cells/mL (D1),  $10 \times 10^4$  cells/mL (D2), and  $20 \times 10^4$  cells/mL (D3).

## Supplementary Materials

**Table S1:** Tips and tricks of successful MCAs analysis by our experience.

Problem	Recommendations
Cells do not form MCAs	<ul style="list-style-type: none"> <li>- Increase cell density.</li> <li>- Centrifugation step is crucial to gather the cells.</li> </ul>
MCAs are too small, easily lost during their manipulation	<ul style="list-style-type: none"> <li>- Increase cell density.</li> </ul>
Irregular MCAs formation due to the presence of fibres into the wells	<ul style="list-style-type: none"> <li>- Use a laminar hood with good filters.</li> <li>- Use synthetic lab coats.</li> <li>- Keep the plate uncovered the least time possible.</li> <li>- Plate the cells using multichannel pipettes to be faster.</li> </ul>
MCAs lost or damaged during medium change	<ul style="list-style-type: none"> <li>- Use a 100 <math>\mu</math>l micropipette and place the tip against the wall of the well to aspirate and replace the medium.</li> <li>- Both aspiration and medium replacement should be done very slowly and carefully, as too much pressure can cause MCAs' damage.</li> <li>- Lean the plate around 30°, since this helps seeing the MCAs and prevent their aspiration.</li> </ul>
MCAs lost or damaged during harvesting for optical and electron microscopy	<ul style="list-style-type: none"> <li>- Carefully remove the medium and replace it with the proper fixative, in the well. Incubate for 10 min before harvesting. Be careful not to leak the fixative</li> </ul>

	<p>into other wells destined for other types of proxies. In this step leave the lid open because fixatives release vapours than can interfere with other techniques.</p> <ul style="list-style-type: none"> <li>- For harvesting use a 1000 µl micropipette with a sectioned tip that offers a larger circumference and prevents the MCAs' damage.</li> <li>- The harvesting procedure should be performed slowly and carefully.</li> <li>- Transfer to an Eppendorf tube containing the appropriate fixative.</li> </ul>
<p>MCAs lost or damaged during processing for optical and electron microscopy</p>	<ul style="list-style-type: none"> <li>- After the fixation step, embed the MCAs in histogel according to the supplier's instructions.</li> </ul>
<p>Difficult in finding MCAs during paraffin block sectioning</p>	<ul style="list-style-type: none"> <li>- Histogel containing the MCAs should be oriented during the embedding procedure. Sometimes it is necessary to remove the excess of histogel to facilitate the sectioning step.</li> <li>- When sectioning, it is extremely important not to remove a large thickness of paraffin, as MCAs are not easy to see and therefore can be easily lost.</li> <li>- Sections should be checked under the microscope to assess the presence of the MCA. Its observation is easier if the sections have been recently collected from the water.</li> </ul> <p>Note: It is important to mention that to check the presence of an apoptotic core, it is necessary to section nearly all the MCA to assure that we have passed through the core</p>







# **Chapter 3** - Cytotoxic and Antiproliferative Effects of Preussin, a Hydroxypyrrolidine Derivative from the Marine Sponge-Associated Fungus *Aspergillus candidus* KUFA 0062, in a Panel of Breast Cancer Cell Lines and Using 2D and 3D Culture

---



Article

# Cytotoxic and Antiproliferative Effects of Preussin, a Hydroxypyrrolidine Derivative from the Marine Sponge-Associated Fungus *Aspergillus candidus* KUFA 0062, in a Panel of Breast Cancer Cell Lines and Using 2D and 3D Cultures

Fernanda Malhão <sup>1,2</sup> , Alice A. Ramos <sup>1,2</sup>, Suradet Buttachon <sup>1,2</sup> , Tida Dethoup <sup>3</sup>, Anake Kijjoa <sup>1,2</sup>  and Eduardo Rocha <sup>1,2,\*</sup> 

<sup>1</sup> Institute of Biomedical Sciences Abel Salazar (ICBAS), Universidade do Porto (U.Porto), Rua de Jorge Viterbo Ferreira n 228, 4050-313 Porto, Portugal

<sup>2</sup> Interdisciplinary Center for Marine and Environmental Research (CIIMAR), Universidade do Porto (U.Porto), Avenida General Norton de Matos s/n, 4450-208 Matosinhos, Portugal

<sup>3</sup> Department of Plant Pathology, Faculty of Agriculture, Kasetsart University, Bangkok 10240, Thailand

\* Correspondence: [erocha@icbas.up.pt](mailto:erocha@icbas.up.pt); Tel.: +351-220-428-245

Received: 16 July 2019; Accepted: 27 July 2019; Published: 30 July 2019



**Abstract:** Preussin, a hydroxyl pyrrolidine derivative isolated from the marine sponge-associated fungus *Aspergillus candidus* KUFA 0062, displayed anticancer effects in some cancer cell lines, including MCF7. Preussin was investigated for its cytotoxic and antiproliferative effects in breast cancer cell lines (MCF7, SKBR3, and MDA-MB-231), representatives of major breast cancers subtypes, and in a non-tumor cell line (MCF12A). Preussin was first tested in 2D (monolayer), and then in 3D (multicellular aggregates), cultures, using a multi-endpoint approach for cytotoxicity (3-(4,5-dimethylthiazol-2-yl)-2,5-diphenyltetrazolium bromide (MTT), resazurin and lactate dehydrogenase (LDH)) and proliferative (5-bromo-2'-deoxyuridine (BrdU)) assays, as well as the analysis of cell morphology by optical/electron microscopy and immunocytochemistry for caspase-3 and ki67. Preussin affected cell viability and proliferation in 2D and 3D cultures in all cell lines tested. The results in the 3D culture showed the same tendency as in the 2D culture, however, cells in the 3D culture were less responsive. The effects were observed at different concentrations of preussin, depending on the cell line and assay method. Morphological study of preussin-exposed cells revealed cell death, which was confirmed by caspase-3 immunostaining. In view of the data, we recommend a multi-endpoint approach, including histological evaluation, in future assays with the tested 3D models. Our data showed cytotoxic and antiproliferative activities of preussin in breast cancer cell lines in 2D and 3D cultures, warranting further studies for its anticancer potential.

**Keywords:** 3D cell culture; antiproliferative activity; breast cancer; cytotoxic activity; preussin

## 1. Introduction

Since cancer incidence keeps rising each year [1,2], the scientific community and pharmaceutical industry have focused their attention on the discovery of new drugs or drug adjuvants to improve the fight against this disease [3]. Consequently, one hotspot of interest for drug discovery is anticancer drugs, whose rising costs have been applied to drug research and development [3,4].

On the other hand, oceans not only cover 70% of the Earth's surface, but also represent a variety of environmental niches, due to different salinities, pressures, light and oxygen levels, nutrient availability, and temperatures, which result in a great diversity of marine fauna and flora. Moreover, oceans are



still an under-investigated source of bioactive compounds with medicinal benefits for human health and/or disease treatment. For this endeavor, marine-derived compounds have gained much attention in the past decades [5–8]. An example of this is the discovery of a large number of novel marine bioactive compounds with anticancer properties, leading to an increasing number of screening studies covering compounds derived from macro- and microorganisms, such as bacteria, fungi, microalgae, and seaweeds [9–13]. To the best of our knowledge, there are seven marine-derived drugs in clinical use for cancer treatment, e.g., cytarabine (Cytosar-U<sup>®</sup>) and trabectedin (Yodelis<sup>®</sup>), and more than twenty-three others under clinical trials, between phase II and phase III [14].

Among naturally occurring marine-derived compounds with anticancer activity, those from marine-derived fungi have been in the spotlight. Marine-derived fungi possess unique features not encountered in their terrestrial counterparts [15], and have been considered as a rich source of secondary metabolites with promising anticancer effects [12,13,16,17], representing unprecedented scaffolds for further drug design for specific modes of action [12]. Marine-derived fungi commonly exist in association with other organisms, mostly sessile invertebrates [16,18], acting as endophytes [19]. This type of association, together with the need to adapt to adverse conditions in the marine environment, contributes to a great diversity of secondary metabolites produced by marine-derived fungi [20].

Recently, Buttachon et al. [21] have described the isolation and structure elucidation of—in addition to several *bis*-indolyl benzenoids—two hydroxypyrrolidine derivatives, preussin (1) and preussin C (2) (Figure 1), from the ethyl acetate extract of the culture of the marine sponge-associated fungus *Aspergillus candidus* KUFA 0062. Furthermore, all the isolated compounds were screened for their cytotoxic effect, using 3-(4,5-dimethylthiazol-2-yl)-2,5-diphenyltetrazolium bromide (MTT) assay, against eight human cancer cell lines derived from different types of tissues. Interestingly, only preussin (1) exhibited a significant decrease in cell viability in all the cancer cell lines tested. Consequently, we decided to explore the more in-depth effects of preussin (1) in breast cancer (BC) cell lines.

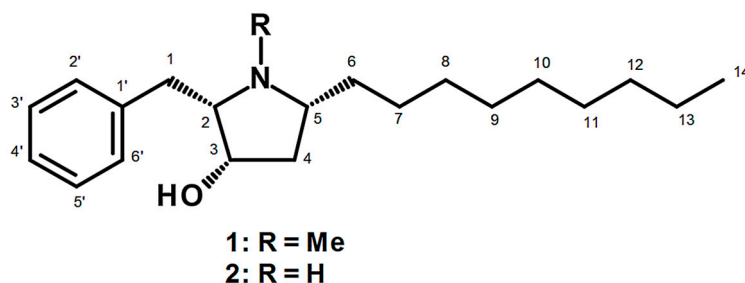


**Figure 1.** Chemical structure of preussin (1) and preussin C (2).

Breast cancer (BC) is the most commonly diagnosed cancer among women in Western countries [22,23], and a leading cause of cancer death among females [24]. Treatment of BC involves surgery, radiotherapy, and the use of anticancer drugs. However, one major problem of cancer treatments, which also applies to BC, is the multidrug resistance coupled with the toxicity of some chemotherapeutics [25,26]. The emergence of drug resistance triggers the search for new drugs or drug adjuvants and, simultaneously, the need for a better understanding of the molecular mechanisms involved in drug resistance [27,28]. Accordingly, a search for compounds that are aimed at different therapeutic targets and/or that potentiate the existing established drugs with minimal, or at least decreased, toxicity towards normal cells has become a priority [29].

Cell lines have greatly contributed to a better understanding of BC molecular mechanisms. Nonetheless, some authors have stressed the importance of choosing an appropriate cell line panel as an experimental model with specific sub-characteristics that could influence the responses to different compounds of potential therapeutic interest [30,31]. Breast cancer is very heterogeneous in terms of histological types and clinical outcomes, namely having different patterns of positivity for estrogen and progesterone receptors, as well as for the expression of the oncogene human epidermal growth

factor receptor 2 (HER-2). These different characteristics are fundamental in determining therapeutic approach [32].

Accordingly, for this study, we selected four human breast cancer cell lines with some characteristics corresponding to BC subtypes: (i) MCF7, which has positive estrogen and progesterone receptors and is negative for HER-2 overexpression (ER+, PR+, HER-2-), corresponding to the most common BC type—Luminal A [30,33]; (ii) SKBR3, a negative for estrogen and progesterone receptors and positive for HER-2 overexpression (ER-, PR-, HER-2+), representing the HER-2 subtype [30,33]; (iii) MDA-MB-231, a ‘triple negative cell line’ (ER-, PR, HER2-), corresponding to the basal-type breast carcinoma cell [30,33]; and (iv) MCF12A, which is a non-tumor breast cell line [30,34].

Nowadays, it is well established that cell culture research performed in monolayer (2D) has a low predictive capacity, especially in the field of drug discovery where great investments have been made each year [35]. The lack of three-dimensional (3D) geometry is associated with less intercellular interactions, and different microenvironments which result in different biochemistry, gene expression, and drug metabolism [36,37]. All these differences partially explain why many drugs tested in 2D cultures fail when tested in *in vivo* models or in clinical trials [38,39]. Three-dimensional (3D) breast cell cultures recapitulate some of the physiological and architectural aspects of breast epithelium [40], which may represent a model closer to the *in vivo* than the 2D cultures.

Based on the promising data of our recent research [21], the aim of this study was to specifically assess the *in vitro* anticancer activity of preussin (**1**), namely cytotoxic and antiproliferative effects, in a panel of three breast cancer cell lines and one non-tumor breast cell line, cultured in 2D and 3D culture models.

## 2. Results

### 2.1. Cells Exposure in 2D

#### 2.1.1. Analysis of Cell Viability—MTT Assay

Cells were exposed for 72 h either to preussin (**1**) at different concentrations (10, 25, 50, and 100  $\mu$ M), or to staurosporine (STS) (1  $\mu$ M), a positive control, for apoptosis induction [41,42]. Culture medium containing only solvent (SC) (medium with 0.1% DMSO, *v/v*) was used as a negative control. Cells exposed to preussin (**1**) at 50 and 100  $\mu$ M showed significant decrease in cell viability in the three cancer cell lines (MCF7, MDA-MB-231, and SKBR3) and in the non-tumor cell line (MCF12A). STS decreased cell viability to less than 50%, in relation to the control, in all cell lines tested (Figure 2).

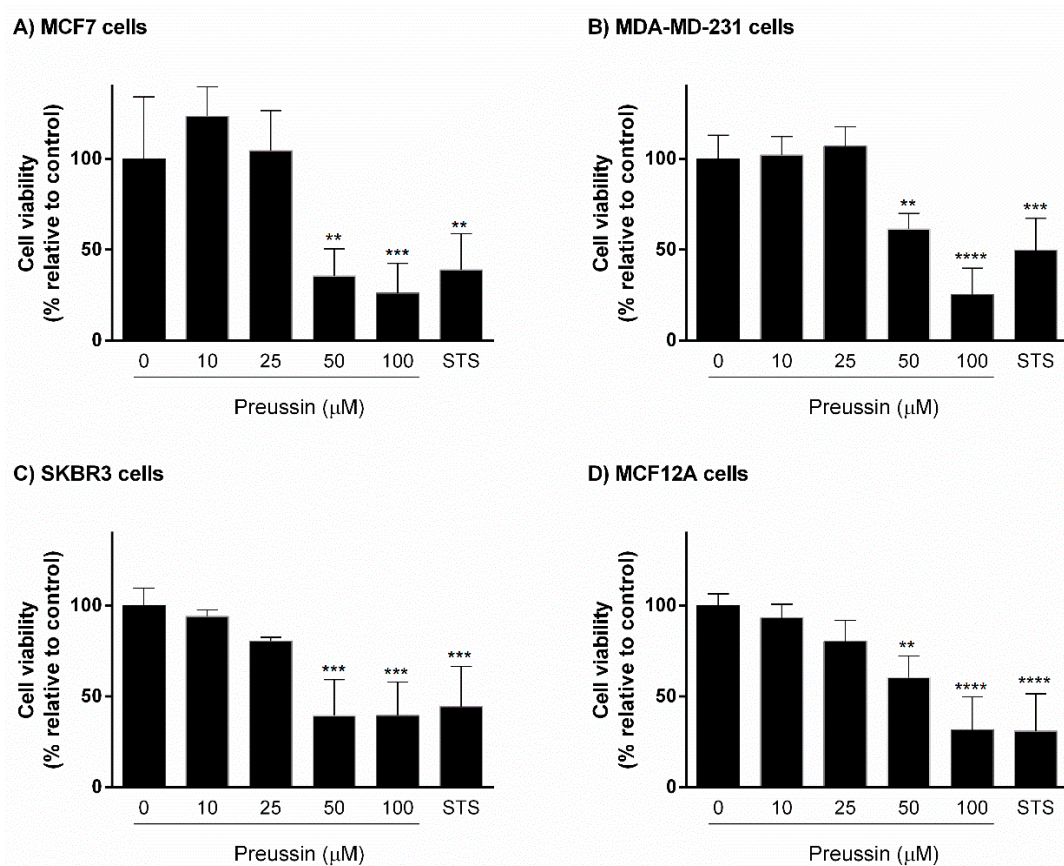


**Figure 2.** Effect of preussin (**1**), at 10, 25, 50, and 100 μM, on cell viability in 2D culture. (A) MCF7, (B) MDA-MB-231, (C) SKBR3, and (D) MCF12A cells after 72 h of incubation, assessed by 3-(4,5-dimethylthiazol-2-yl)-2,5-diphenyltetrazolium bromide (MTT) assay. Cells treated with 0.1% DMSO (solvent; SC) and staurosporine (STS; 1 μM) were included as negative and positive controls, respectively. The results were expressed as the percentage of cell viability, relative to negative control, and are presented as mean ± standard deviation (SD) of four independent experiments (two duplicates per replica). (\*\* $p < 0.01$ ; \*\* $p < 0.001$ ; \*\*\*\* $p < 0.0001$ ).

### 2.1.2. Analysis of Cell Proliferation—5-bromo-2'-deoxyuridine (BrdU) Assay

Cells were exposed for 72 h either to preussin (**1**) at different concentrations (10, 25, 50, and 100 μM) or to STS (1 μM). Preussin (**1**) induced a decrease of cell proliferation in all cell lines. In MCF7 and SKBR3 cells, as well as in MCF12A, preussin (**1**) at 25 μM was able to significantly reduce cell proliferation. In contrast, in MDA-MB-231, preussin (**1**) only at 50 μM significantly inhibited cell proliferation. At 50 μM, preussin (**1**) led to a decrease of cell proliferation below 50%, in relation to the control, in all cell lines. STS inhibited cell proliferation in all cell lines, with less potency toward SKBR3 (Figure 3).

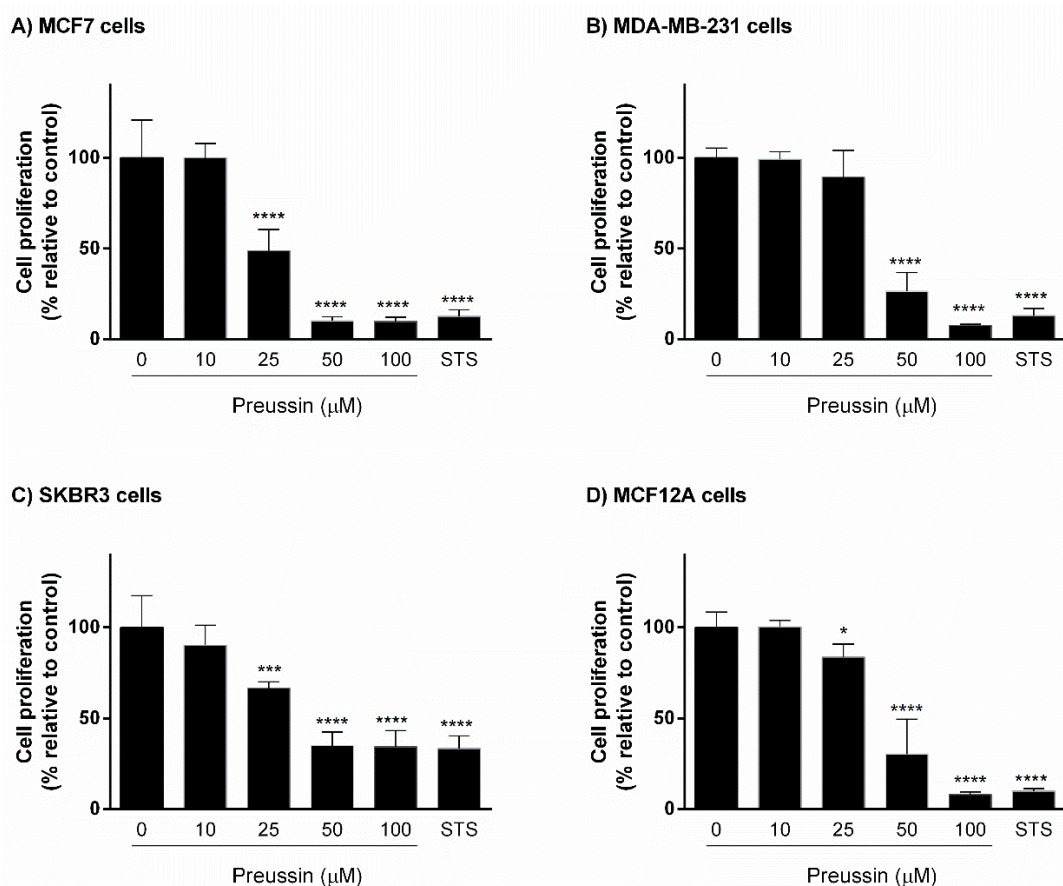


**Figure 3.** Effect of preussin (**1**), at 10, 25, 50, and 100 μM, on cell proliferation in 2D culture. (A) MCF7, (B) MDA-MB-231, (C) SKBR3, and (D) MCF12A cells after 72 h of incubation, assessed by 5-bromo-2'-deoxyuridine (BrdU) assay. Cells treated with 0.1% DMSO (SC) and STS (1 μM) were included as negative and positive controls, respectively. The results were expressed as the percentage of cell proliferation, relative to negative control, and are presented as mean ± SD of four independent experiments (two duplicates per experiment). (\*  $p < 0.05$ ; \*\*\*  $p < 0.001$ ; \*\*\*\*  $p < 0.0001$ ).

### 2.1.3. Cell Morphology

When observed in the phase contrast microscopy, SC groups showed nearly 90% of confluence. Cells exposed to STS and preussin (**1**) at 50 and 100 μM revealed morphological alterations, with vacuolization of the cytoplasm, loss of cell adhesion leading to cell detachment, and, consequently, lower density (data not shown).

## 2.2. Cells Exposure in 3D

### 2.2.1. Analysis of Cell Viability

From the results obtained in 2D culture, we selected the concentrations of preussin (**1**) that exhibited more pronounced effect on cell viability and proliferation (50 and 100 μM). The assessment of the cytotoxic effect of preussin (**1**) in 3D culture was performed using three cell viability assays: MTT, resazurin, and lactate dehydrogenase (LDH).

#### MTT Assay

Cells were exposed for 96 h to preussin (**1**) at two concentrations (50 and 100 μM) or STS (1 μM). Preussin (**1**) at 50 μM revealed significant effect on cell viability only in MCF7 and MCF12A cell lines, decreasing cell viability, while at 100 μM, it decreased cell viability in all cell lines. Similar to preussin

(1) at 50  $\mu\text{M}$ , STS caused a significant decrease in cell viability only in MCF7 and MCF12A cell lines, with no statistically significant effect on cell viability in MDA-MB-231 or SKBR3 cell lines (Figure 4).

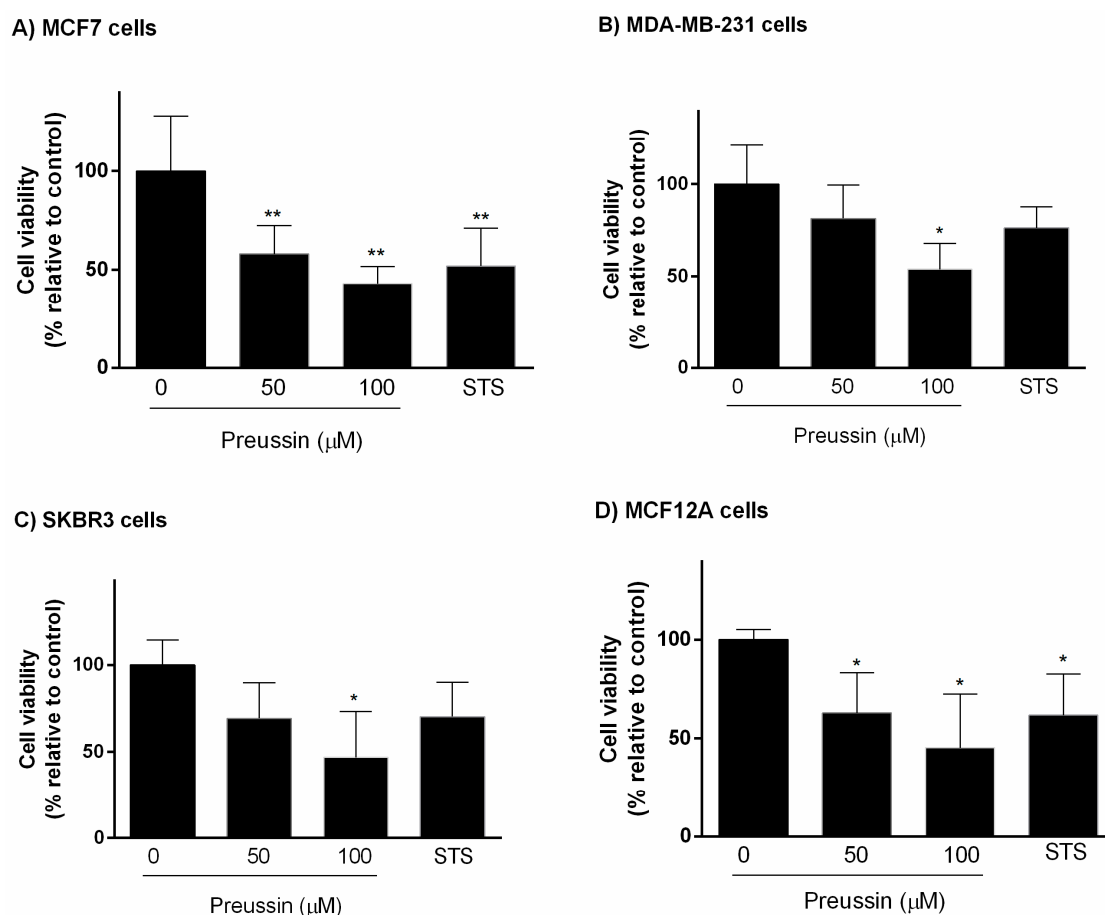


**Figure 4.** Effect of preussin (1), at 50 and 100  $\mu\text{M}$ , on cell viability in 3D culture. (A) MCF7, (B) MDA-MB-231, (C) SKBR3, and (D) MCF12A cells after 96 h of incubation, assessed by MTT assay. Cells treated with 0.1% DMSO (SC) and STS (1  $\mu\text{M}$ ) were included as negative and positive controls, respectively. The results were expressed as the percentage of cell viability, relative to negative control, and are presented as mean  $\pm$  SD of four independent experiments (two duplicates per experiment). (\*  $p < 0.05$ ; \*\*  $p < 0.01$ ).

#### Resazurin Assay

Cell viability was also investigated using the resazurin reduction assay. Figure 5 shows the effect of preussin (1) on cell viability in 3D culture. After 96 h of exposure to preussin (1), either at 50 or 100  $\mu\text{M}$ , significant decreases in cell viability were detected at 100  $\mu\text{M}$  in MCF7, SKBR3, and MCF12A cell lines. As for MDA-MB-231 cells, no differences were observed under preussin (1) influence. STS did not cause any significant impact on MCF7 or MDA-MB-231 cells, but decreased viability of SKBR3 and MCF12A cells.

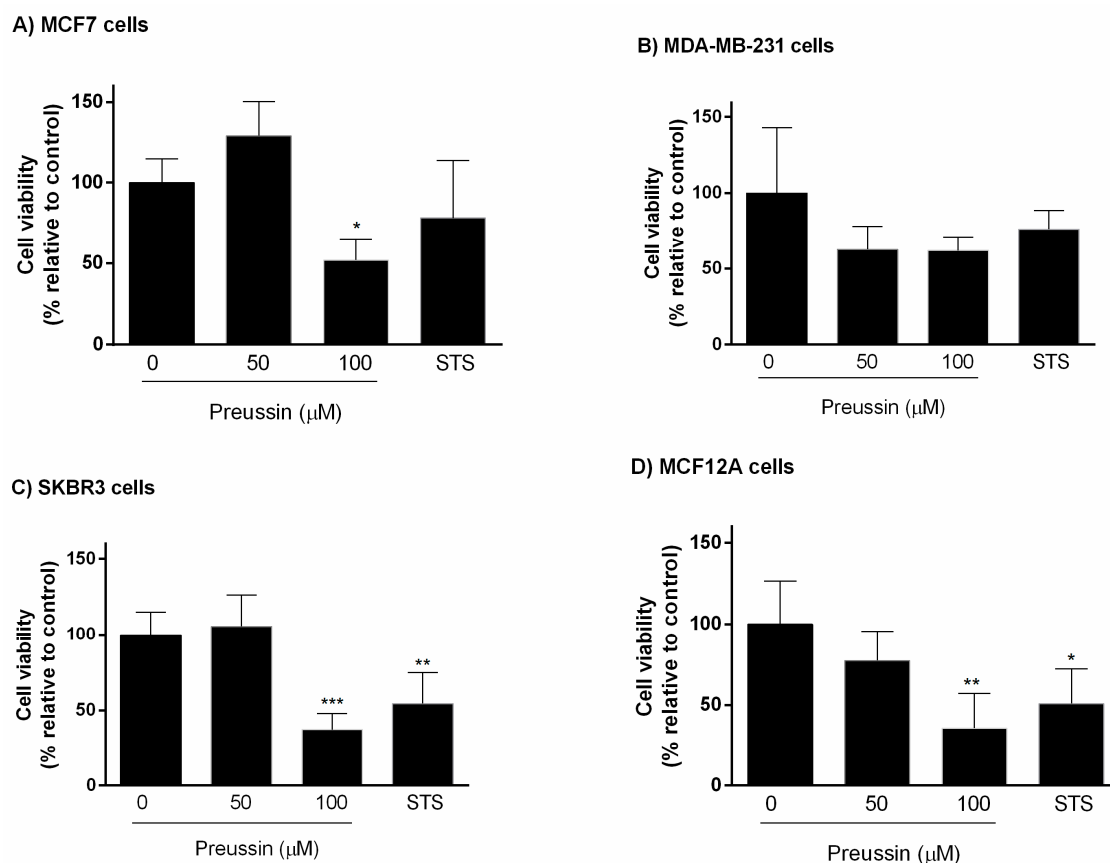


**Figure 5.** Effect of preussin (**1**), at 50 and 100 μM, on cell viability in 3D culture. (A) MCF7, (B) MDA-MB-231, (C) SKBR3, and (D) MCF12A cells after 96 h of incubation, assessed by resazurin assay. Cells treated with 0.1% DMSO (SC) and STS (1 μM) were included as negative and positive control, respectively. The results were expressed as the percentage of cell viability, relative to negative control, and are presented as mean ± SD of four independent experiments (two duplicates per experiment). \*  $p < 0.05$ ; \*\*  $p < 0.01$ ; \*\*\*  $p < 0.001$ .

## LDH

The third endpoint used for evaluating cytotoxic effect of preussin (**1**) in 3D culture was the LDH assay. Preussin (**1**), at 50 and 100 μM, induced an increase in LDH release in relation to negative controls, corresponding to a decrease in cell viability in all cell lines. In the case of SKBR3 and MCF12A cells, preussin (**1**) led to nearly 100% increase in LDH release in comparison to controls. The effects of STS and preussin (**1**) on LDH release were very similar in MCF7, SKBR3, and MCF12A cell lines. However, in MDA-MB-231, STS did not demonstrate a significant effect on LDH release (Figure 6).



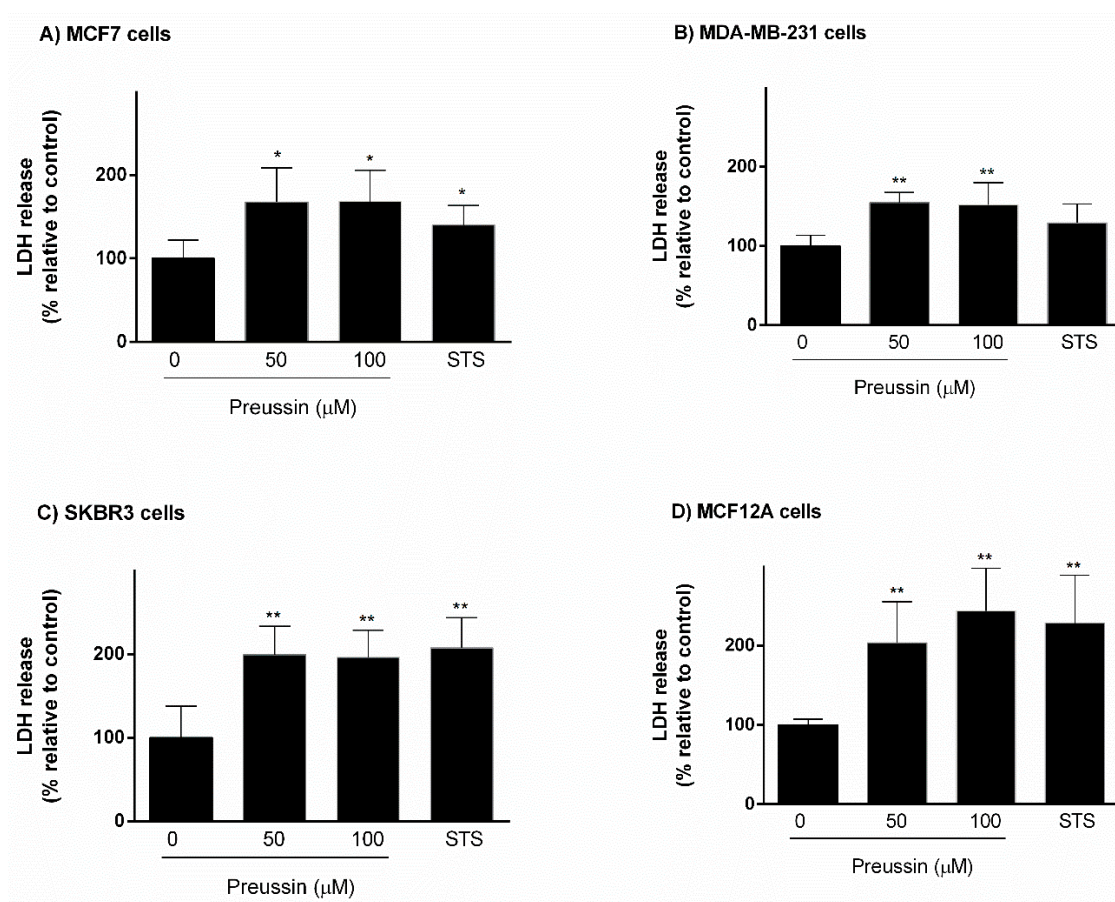


**Figure 6.** Effect of preussin (**1**), at 50 and 100  $\mu\text{M}$ , on cell viability in 3D culture. (A) MCF7, (B) MDA-MB-231, (C) SKBR3, and (D) MCF12A cells after 96 h of incubation, assessed by lactate dehydrogenase (LDH) assay. Cells treated with 0.1% DMSO (SC) and STS (1  $\mu\text{M}$ ) were included as negative and positive controls, respectively. The results were expressed as the percentage of LDH release, relative to negative controls, and are presented as mean  $\pm$  SD of four independent experiments (two duplicates per experiment). (\*  $p < 0.05$ ; \*\*  $p < 0.01$ ).

### 2.2.2. BrdU Proliferation Assay

When compared to controls, preussin (**1**) at 50 and 100  $\mu\text{M}$  inhibited cell proliferation at approximately 50% in all cell lines cultured in 3D (Figure 7). STS promoted similar results in magnitudes comparable to those of preussin (**1**).

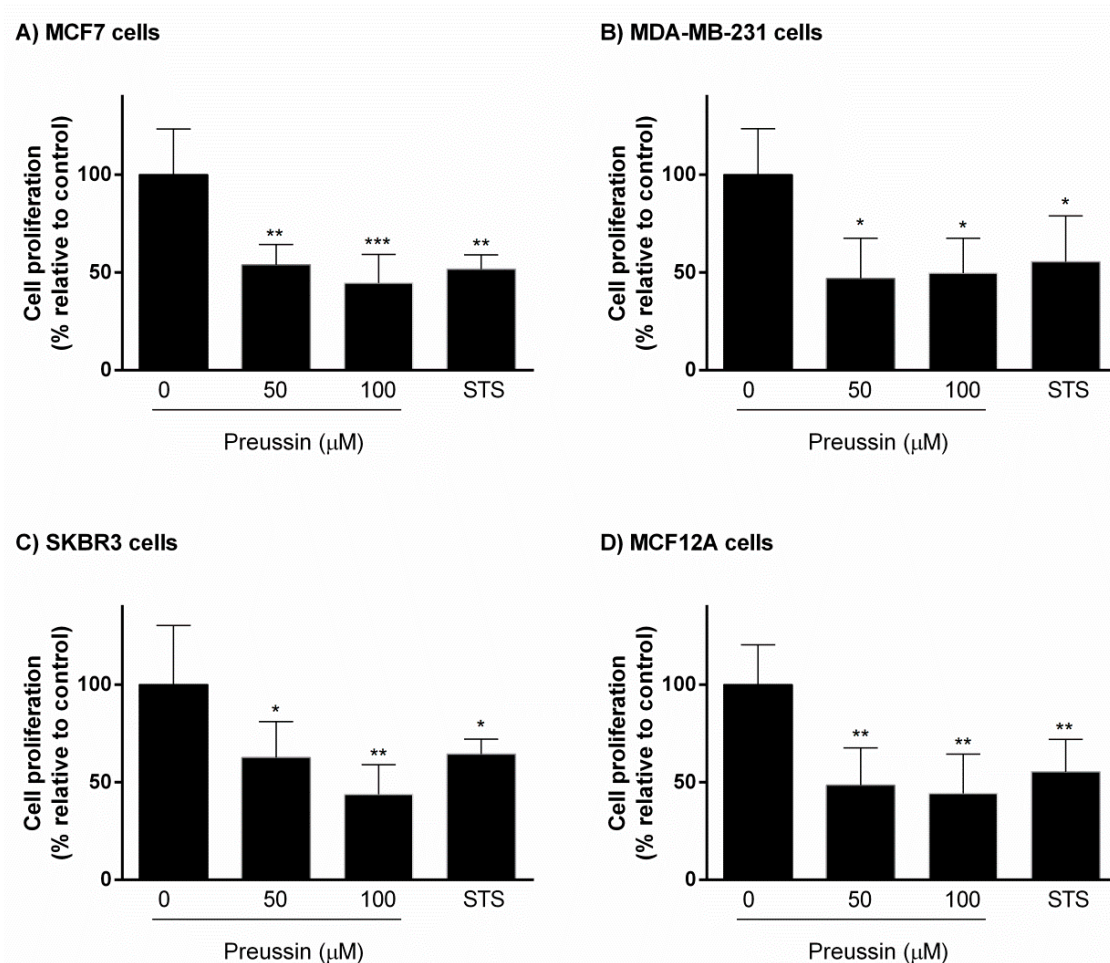


**Figure 7.** Effect of preussin (**1**), at 50 and 100  $\mu\text{M}$ , on cell proliferation in 3D culture. (A) MCF7, (B) MDA-MB-231, (C) SKBR3, and (D) MCF12A cells after 96 h of incubation, assessed by BrdU assay. Cells treated with 0.1% DMSO (SC) and STS (1  $\mu\text{M}$ ) were included as negative and positive controls, respectively. The results were expressed as the percentage of cell proliferation, relative to negative control, and are presented as mean  $\pm$  SD of four independent experiments (two duplicates per experiment). (\*  $p < 0.05$ ; \*\*  $p < 0.01$ ; \*\*\*  $p < 0.001$ ).

### 2.2.3. Analysis of Multicellular Aggregates (MCAs) Morphology in 3D Culture

#### Stereomicroscopy Analysis

Plates containing MCAs were observed daily in a stereomicroscope with dark field. During the formation time, it was possible to observe cell aggregation to form the MCAs. The type of MCA was dependent on the cell line, but the MCAs of the same cell line were quite similar.

Figure 8 shows a typical morphology of MCAs from the four cell lines in the solvent control and exposed conditions after 72 h of formation, plus 96 h of exposure. After MCA formation (before the exposure—data not shown), MCF7 and MDA-MB-231 cells formed MCAs with round shapes, the MDA-MB-231's MCAs being more compact than those of the MCF7. As for MCF12A and SKBR3 cell lines, cells did not aggregate so obviously, even after seven days in culture, ultimately forming loose MCAs. There were no obvious differences in MCAs before and after the exposure. As can be observed in Figure 8, after 96 h of exposure, either to preussin (**1**) or to STS, the shape and size of the MCAs were similar to those of the negative control (SC).



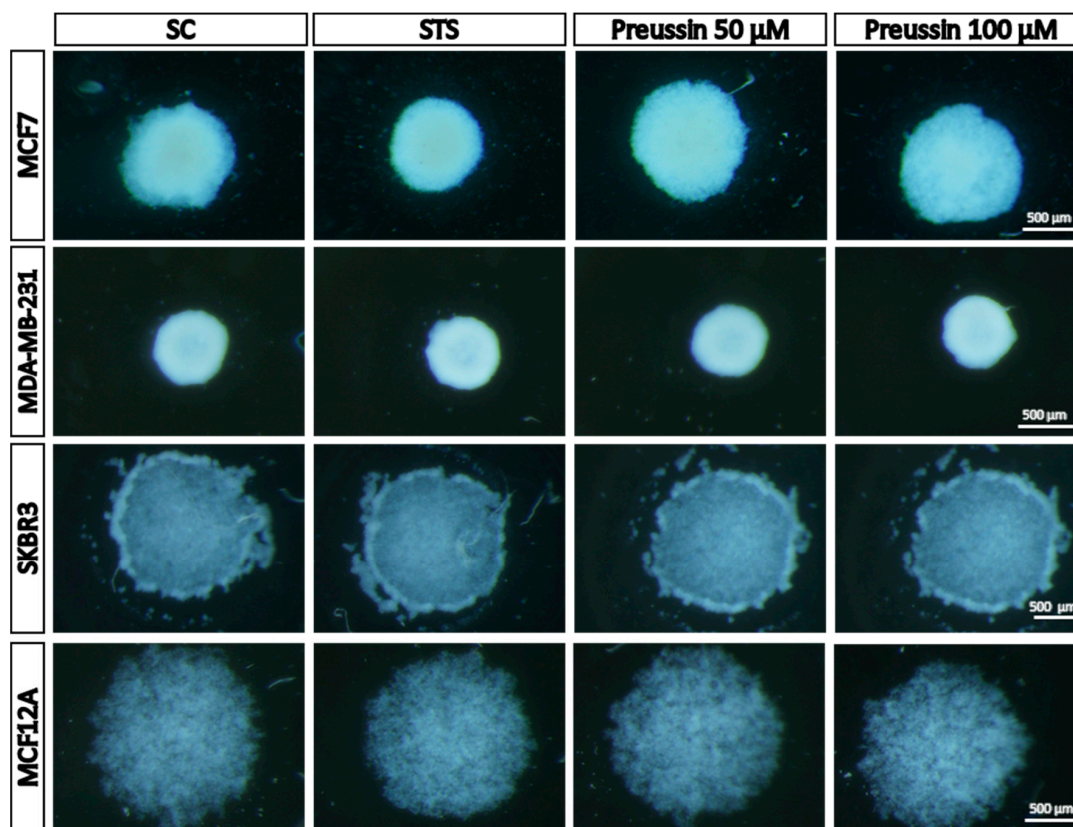


**Figure 8.** Representative morphology of multicellular aggregates (MCAs) in 3D culture, photographed in a stereomicroscope. The MCAs of MCF7, MDA-MB-231, SKBR3, and MCF12A after 96 h of incubation with preussin (1) (50 and 100  $\mu$ M). Cells treated with 0.1% DMSO (SC) and STS (1  $\mu$ M) were included as negative and positive controls, respectively.

#### Multicellular Aggregate Measurements

For their measurements, MCAs were photographed at two different times: (1) After 72 h of spheroids formation (before the exposure); and (2) after 96 h of exposure (total of seven days in culture). Using these pictures, the software performed the segmentation, creating binary images for further data extrapolation. The areas obtained with the AnaSP software [43] are presented in Figure 9. Data from the sphericity and solidity of the MCAs are given in Figure S1.

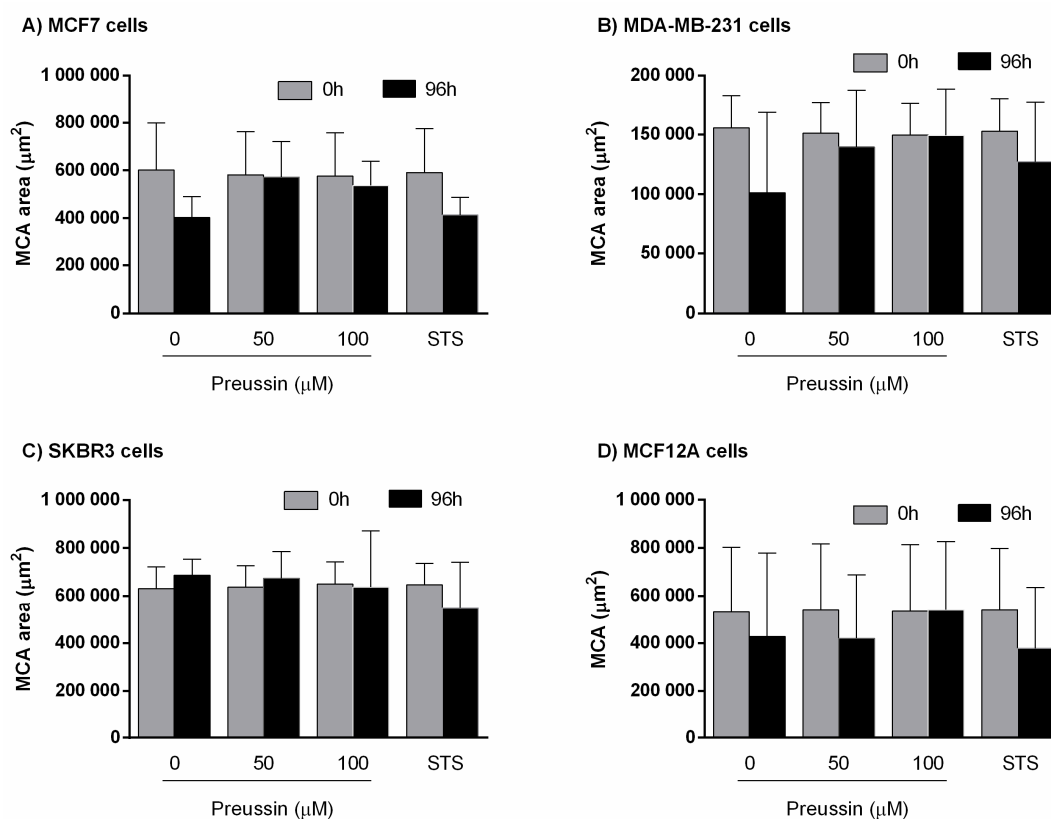


**Figure 9.** Multicellular aggregates (MCAs) areas ( $\mu\text{m}^2$ ) in 3D culture. (A) MCF7, (B) MDA-MB-231, (C) SKBR3, and (D) MCF12A before exposure ( $t_1$ ) (gray bars) and after 96 h of exposure ( $t_2$ ) (black bars). Cells were exposed for 96 h to preussin (1) (50 and 100  $\mu\text{M}$ ). Treated cells with 0.1% DMSO (SC) and STS (1  $\mu\text{M}$ ) were included as negative and positive controls, respectively. Results are presented as mean  $\pm$  SD of four independent experiments (12 duplicates per replica).

There were no significant differences between MCAs' areas of  $t_1 = 0$  h (before exposure), corresponding to 72 h of MCA formation, and  $t_2 = 96$  h, corresponding to after 96 h of exposure.

In the same manner, there were no differences between SC and any of the other conditions (Figure 9).

### Morphology

After 96 h of exposure, MCAs were fixed, processed for paraffin embedding, and sectioned for hematoxylin-eosin (HE) staining and immunocytochemistry analysis (ICC).

Through the observation of MCAs stained with HE, at the microscopic level, it was possible to note that different cell lines (SC groups) displayed different levels of cell compaction, similar to those observed by stereomicroscopy (compare Figure 8 with Figure 10). Also, MCAs from SC groups revealed a more intact structure than those exposed to preussin (1). This is explained by the fact that when MCAs from preussin-treated cells were transferred either to a flat-bottom plate for the viability assays or to a tube for fixation, they tended to easily disintegrate, forming a cell suspension (see preussin 50  $\mu\text{M}$  exposed cells in Figure 10).

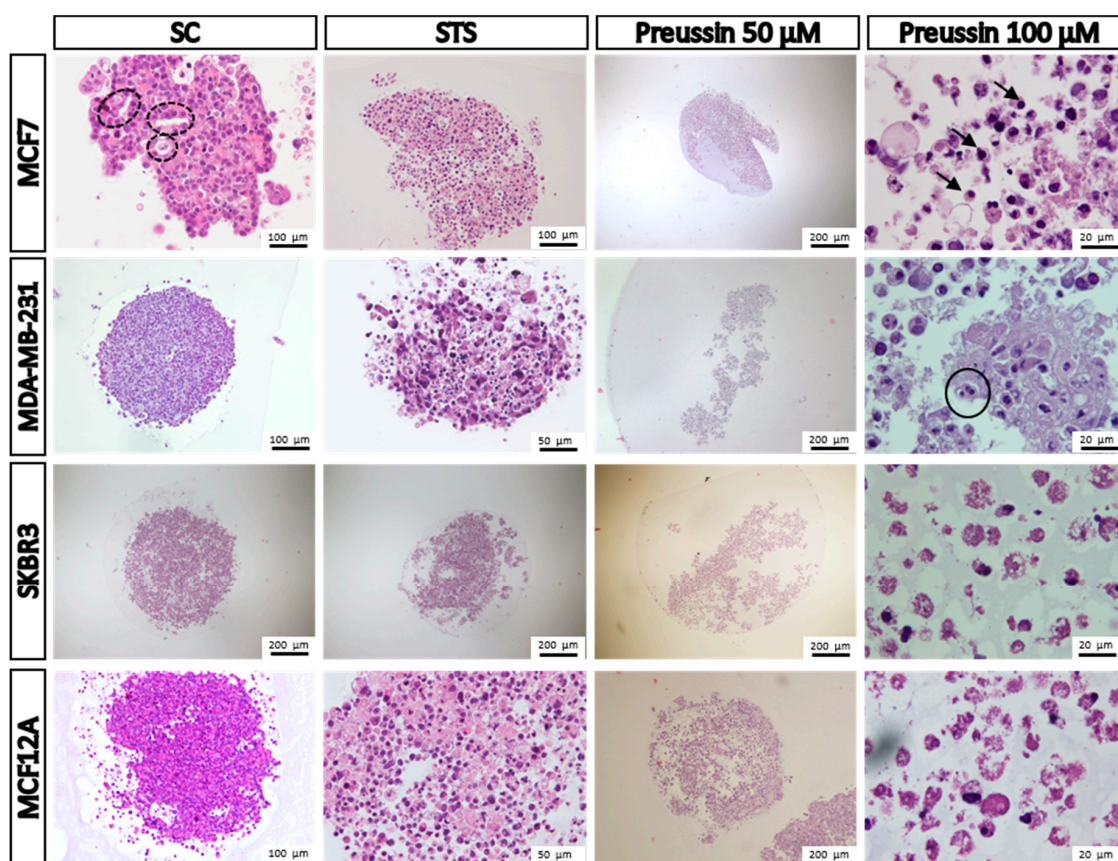


**Figure 10.** Representative morphology of the multicellular aggregates (MCAs) of MCF7, MDA-MB-231, SKBR3 and MCF12A after 96h of incubation with preussin (1) at 50 and 100  $\mu\text{M}$ . Cells treated with 0.1% DMSO (SC) and STS (1  $\mu\text{M}$ ) were included as negative and positive controls, respectively. Hematoxylin-eosin (HE) staining. Arrowhead: Dense chromatic and nuclear shrinkage; dashed line circle: Acinar-like structures; straight line circle: Nuclear fragmentation.

In all sectioned MCAs (eight per condition and per cell line), there was only one (from a SC group of MCF7 cells) that showed a central necrotic core. In the case of the groups exposed to STS or preussin (1), most MCAs cells showed damaged morphology, indicating cell death. The degree of damage was more severe after exposure to preussin (1) than to STS; however, there were no differences between the two tested concentrations of preussin (1). Cells from MCAs exposed to STS and preussin (1) in the four cell lines revealed some of the typical features of apoptotic cells: Cell shrinkage, nuclear condensation, chromatin margination, karyorrhexis, cell detachment, and apoptotic bodies [44,45]. From a histological point of view, the number of cells with a morphology compatible with cell death is evidently higher in the preussin (1)-exposed groups. In MCAs of MCF7 cells (SC group), it was quite common to find acinar-like structures with lumina that resemble those of the normal mammary gland. Indeed, in those cases, groups of cells within the MCAs were organized so that they formed irregular shaped lumina, sometimes containing apoptotic cells [46] (Figure 10).

#### MCA Immunocytochemical Analysis

In order to support the basic morphological information, the immunocytochemistry (ICC) technique was performed using two different antibodies: Anti-caspase-3 and ki67. Caspase-3 is considered a biochemical marker of cell apoptosis [47,48] while ki67 is a classical marker for cell proliferation [49,50]. The results showed that there were some positive cells for caspase-3 in all the MCAs of the SC groups. These positive cells were randomly distributed for all the MCAs, without any specific localization (Figure 11), except for the lumen of acinar-like structures found in MCF7, where it



was quite common to find apoptotic cells (Figure 11). However, when the number of caspase-3-stained cells in the SC group was compared to those in the drug-exposed groups, it was found that the number of apoptotic cells in the drug-exposed group was clearly higher. The immunostaining for ki67 was also distributed all along the MCAs, without having any preferential area (Figure 12).

Immunostaining for caspase-3 showed a pattern of increasing immunostained cell number (SC < STS < preussin (1)) which was inversely proportional to that of ki67, where a higher number of positive cells was found in the SC group (SC > STS > preussin (1)) (Figures 12 and 13, respectively). Moreover, morphological observations did not reveal any differences between the two tested concentrations of preussin (1). Both preussin-exposed conditions showed a great number of cells marked with caspase-3 (more than 80% of all cells) and some cells revealed ki67 immunostaining (Figures 11 and 12, respectively). Judging by the proportion of cells positive for ki67, MCF7 seems to be the most proliferative of the four cell lines, where approximately 50% of their cells, in MCA form, were positive for ki67 (See Figure 12).

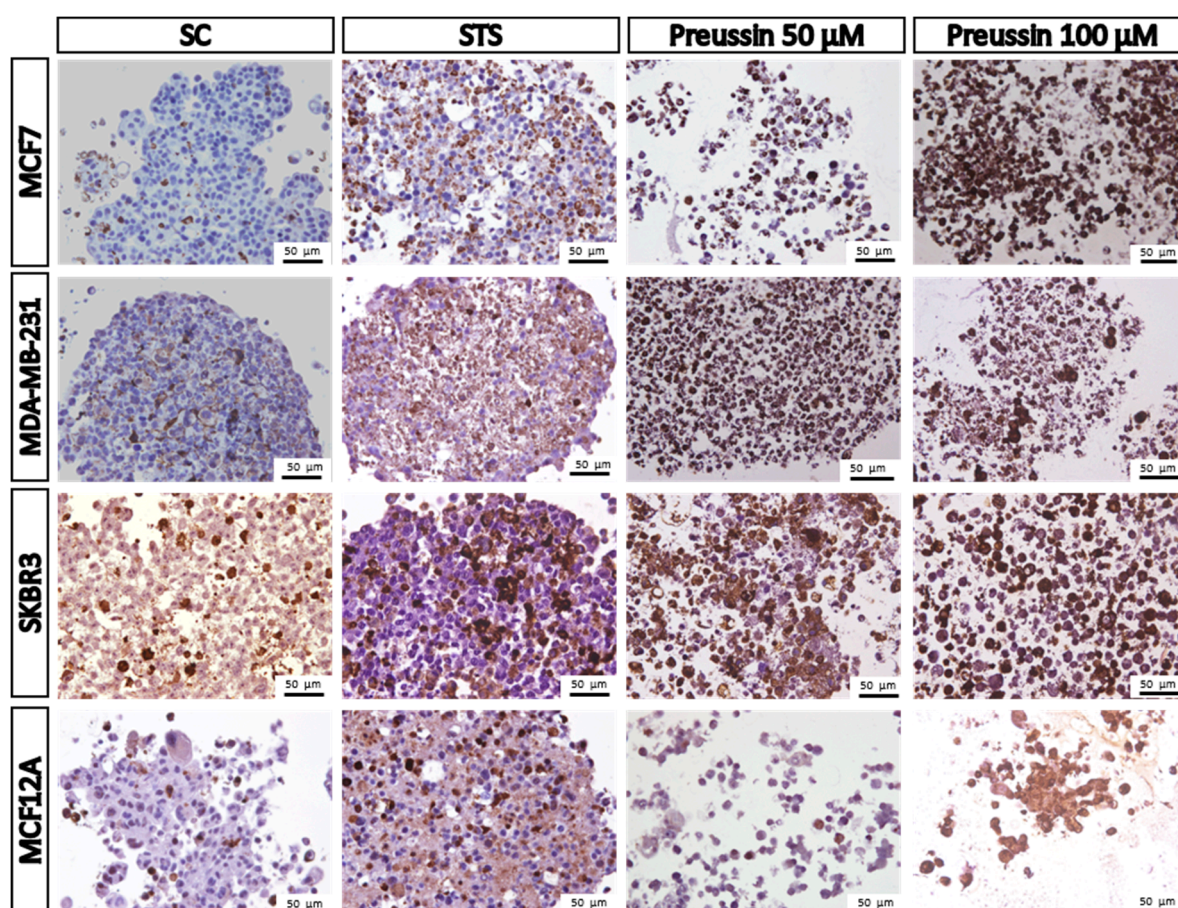


**Figure 11.** Representative images of immunostaining against caspase-3 in multicellular aggregates (MCAs) cells. MCF7, MDA-MB-231, SKBR3, and MCF12A MCAs after 96 h of incubation with preussin (1) at 50 and 100  $\mu$ M. Cells treated with 0.1% DMSO (SC) and STS (1  $\mu$ M) were included as negative and positive controls, respectively. The brown staining in the cytoplasm corresponds to the immunolocalization of caspase-3 protein, as revealed by the diaminobenzidine chromogen.

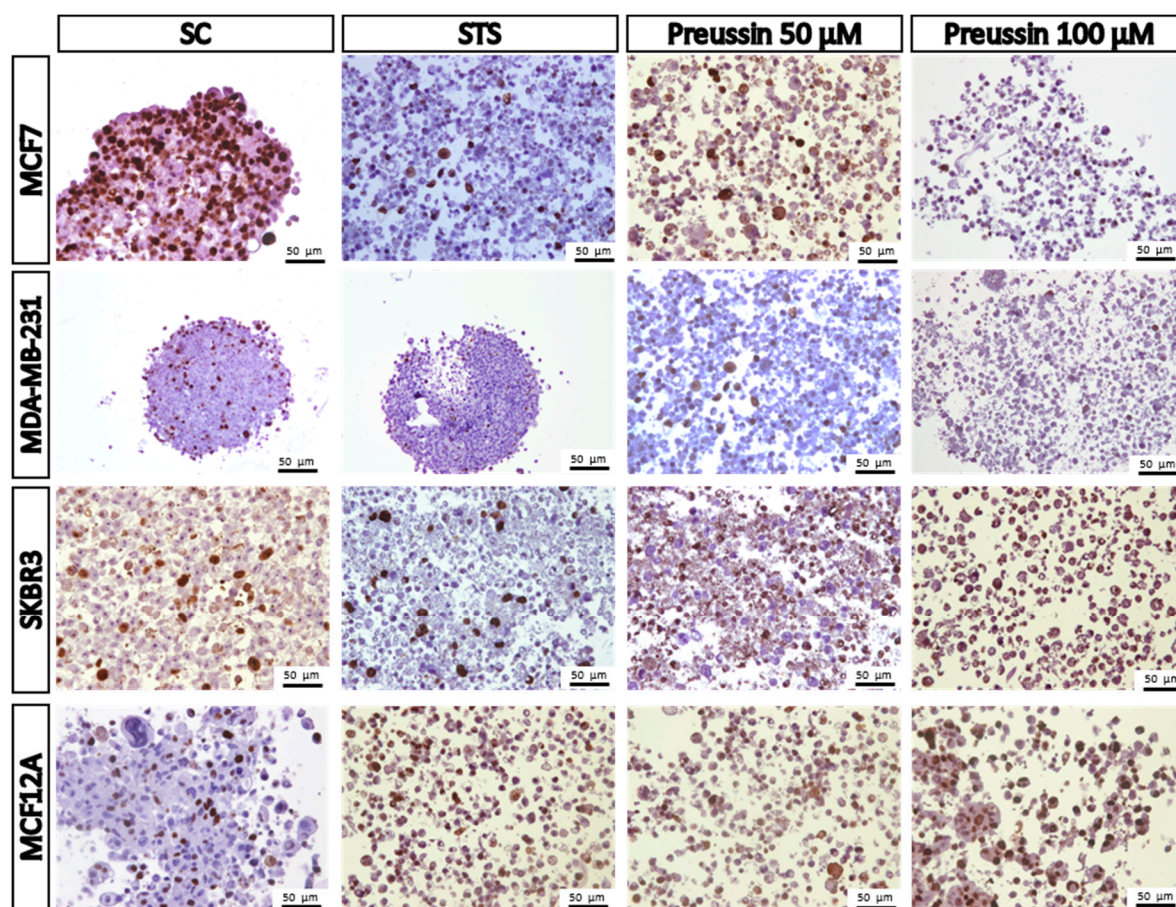


**Figure 12.** Representative images of immunostaining against ki67 of multicellular aggregates (MCAs). MCF7, MDA-MB-231, SKBR3, and MCF12A MCAs after 96 h of incubation with preussin (**1**) at 50 and 100  $\mu\text{M}$ . Cells treated with 0.1% DMSO (SC) and STS (1  $\mu\text{M}$ ) were included as negative and positive controls, respectively. The brown staining in the nuclei corresponds to the immunolocalization of ki67 protein, as revealed by the diaminobenzidine chromogen.

#### MCA Electron Microscopy

The ultrastructural morphology of MCAs revealed that all cell lines in the SC groups displayed some common features, such as euchromatic, irregular shape nuclei with prominent nucleoli, and an abundant presence of mitochondria, in contrast with rare rough endoplasmic reticulum (RER) and Golgi apparatus profiles. In MCF7, MCF12A, and SKBR3, many cells showed glycogen deposits (not seen in all images) and lipid droplets (Figure 13).

All cell lines treated with STS and preussin (**1**) (at both concentrations) showed an increased number of enlarged pleomorphic vacuoles (some with concentric degenerative appearance) and dense bodies in the cytoplasm. In the same manner, a great number of nuclei with peripheral coarse chromatin condensation and karyorrhexis was observed. Lipid droplets and vesicles were also increased in drug-treated cells (Figure 13).



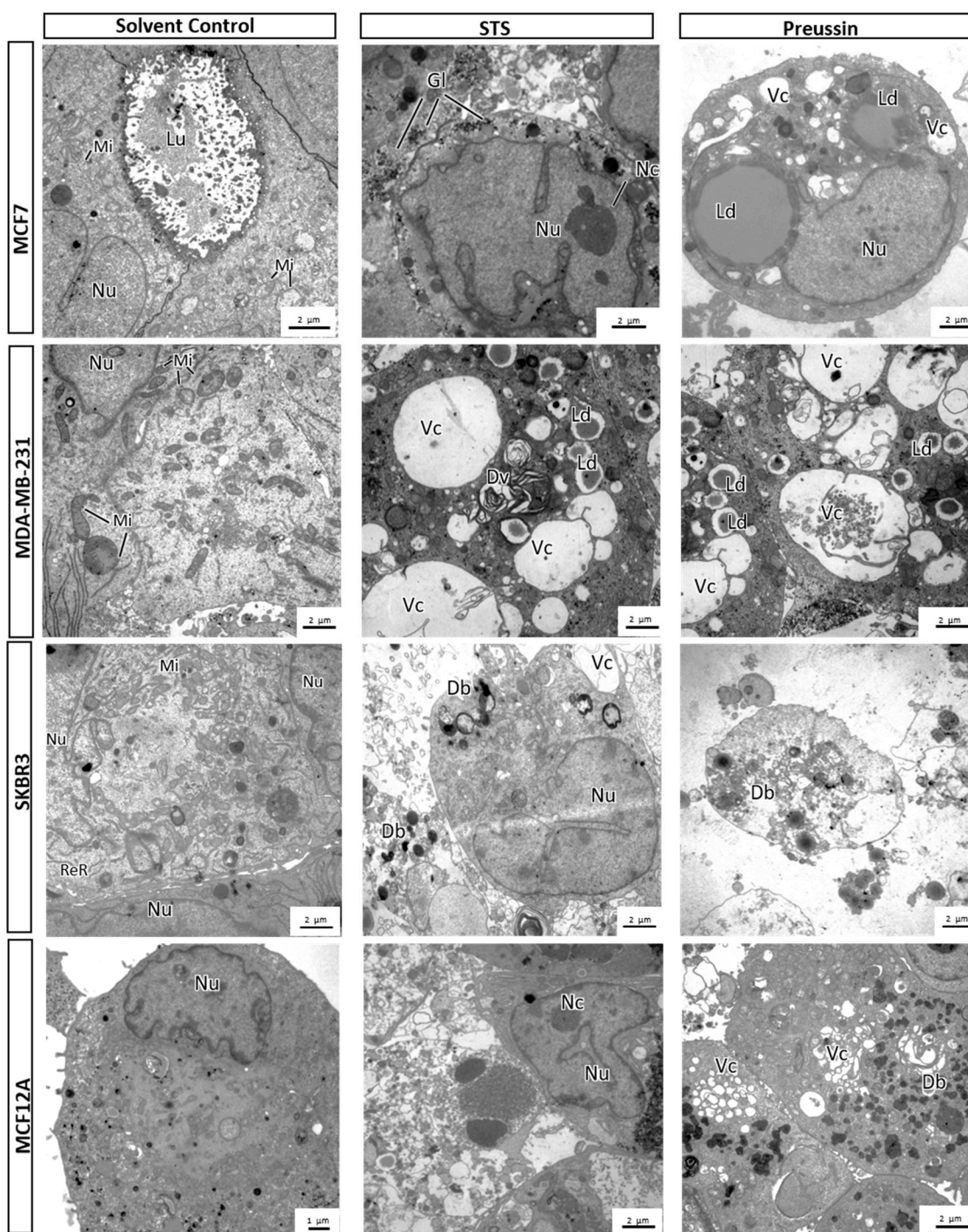


**Figure 13.** Representative pictures of electron microscopy analysis of multicellular aggregates (MCAs). MCF7, MDA-MB-231, SKBR3, and MCF12A MCAs after 96 h of incubation with preussin (1) (50 and 100  $\mu\text{M}$ ). Cells treated with 0.1% DMSO (SC) and STS (1  $\mu\text{M}$ ) were included as negative and positive controls, respectively. Db: Dense bodies; Dv: Degenerative vesicles; Gl: Glycogen; Ld: Lipid droplets; Lm: Lumen; Mi: Mitochondria; Nc: Nucleoli; Nu: Nucleus; ReR: Rough endoplasmic reticulum; Vc: Vacuole.

### 3. Discussion

To the best of our knowledge, this is the first study on cytotoxicity and antiproliferative effects of preussin (1), a hydroxypyrrolidine derivative, isolated from the marine-derived *A. candidus* KUFA 0062,

in a panel of three BC cell lines (MCF7, SKBR3, and MDA-MB-231) which correspond to three biological and immunophenotypic distinct types of BC, and one non-tumor breast cell line (MCF12A), with a comparison of its effects in 2D and 3D cultures. The 2D culture approach was used initially to obtain the results, which allowed us to proceed to the 3D model, a more sophisticated and physiologically relevant type of culture, which generates more predictive data than monolayer cultures [38,51].

The screening of the cytotoxic and antiproliferative effects of preussin (1) was performed in 2D culture, using MTT and BrdU assays, respectively. STS, an apoptosis inducer [42], was used as a positive control. Preussin (1) at 50  $\mu$ M, and STS, decreased cell viability in all cell lines. In relation to the effects on cell proliferation, preussin (1) at 25  $\mu$ M was enough to inhibit cell proliferation in MCF7, MCF12A, and SKBR3, but not in MDA-MB-231, where inhibition only occurred at 50  $\mu$ M. Regarding STS, it had negative effects in all cell lines.

After confirming that preussin (1) could elicit cytotoxic and antiproliferative effects in 2D culture, our next goal was to verify if such effects were maintained when cells are in a 3D culture model. For this, we selected concentrations that showed significant effects in 2D (50 and 100  $\mu$ M). Several studies have shown that cancer cell lines, including BC cell lines, are less sensitive to anticancer agents in 3D cultures [39,52]. Accordingly, it is known that there is a refractory effect towards drugs when tested in 3D cultures, where cells are less susceptible to the impact, so that the concentrations that cause similar effects in 3D cultures are higher than in 2D cultures [53]. Despite being closer to the *in vivo* setting, 3D models are far from routine use, and studies continue to be mainly conducted in 2D cultures.

Concerning 3D culture of cell lines, a variety of methodologies has been developed [34,54,55]. However, the simple and effective method of seeding the cells in ultra-low attachment plates with conical shape was opted in this study. This method produced uniform sized 3D aggregates within the same cell line, as can be verified by morphometric measurements, and in accordance with what was described in the literature [56]. This uniformity is quite important when screening compounds for cytotoxicity [57].

The 3D multicellular structures can differ according to the cell line, methodology used, cell density, and time in culture [58]. Also, they have been named differently: Spheroids [53,56,59]; tumor spheroids [58,60] (even per organ: Breast/mammary cancer spheroids [61,62] or mammospheres [63,64]); microtissues [65]; multicellular tumor spheroids [55,66,67]; and mixed terminology to 3D aggregates/spheroids [53]. Herein, according to the observed morphology, the term 'multicellular aggregates (MCAs)' is used for the 3D multicellular structures, since they are 3D aggregates without a true spheroid shape, being a bit flattened and resembling a 'pancake'.

In this study, after 72 h of seeding, MCF7 and MDA-MB-231 formed tight MCAs, while MCF12A and SKBR3 produced looser MCAs. These observations were in agreement with those reported in previous studies [58,68]. These morphological characteristics were maintained during the exposure to preussin (1) and STS or in the SC. At 72 h (before exposure) ( $t = 0$ ), and after 96 h of exposure ( $t = 96$ ), MCAs were measured using AnaSP software, which allowed the assessment of different parameters in a very limited amount of time without resorting to further instrumentation [35,43]. Spheroid area has been considered as the most informative parameter [69], and changes in MCAs' morphology and size (together with other endpoints) have been reported as a consequence of the drug's effect [69,70]. As there was no difference between MCAs of the SC at the two studied times ( $t = 0$  and  $t = 96$  h), it was concluded that MCAs' areas were stable along the exposure time in solvent control conditions. With regard to preussin (1) exposure, there were no significant differences when compared with SC. This means that, in our study, the area parameter did not reflect any drug effects. At the end of the exposure time, MCAs can be harvested and then analyzed by colorimetric, and fluorescence assays using a plate reader [36]. Accordingly, we studied the cytotoxic and antiproliferative effect of preussin (1) by the same assays used in 2D culture (MTT and BrdU), together with two more assays for cytotoxicity (LDH and resazurin).

The MTT assay in 3D culture showed that MDA-MB-231 and SKBR3 were more resistant to the effects of preussin (1) and STS. Concerning cytotoxicity in MCAs, the LDH assay showed that preussin

(1) at 50  $\mu\text{M}$  caused an increase in LDH release into the extracellular medium (in relation to the control) in all cell lines. When comparing MTT and LDH results, the decrease in cell viability in MTT assay correlates well with an increase in LDH release. It is noteworthy to point out that a concentration of 50  $\mu\text{M}$  of preussin (1) was enough to cause significant differences in the LDH assay; however, in the MTT assay, especially in the MDA-MB-231 and SKBR3 cells, a concentration of 100  $\mu\text{M}$  of preussin (1) was necessary to cause the same effect. In relation to the resazurin reduction assay, differences were detected only after exposure to 100  $\mu\text{M}$  of preussin (1) in MCF7, MCF12A, and SKBR3 cells; however, no differences were detected in MDA-MB-231 cells at this concentration.

Globally, in the comparison of all the endpoints of cell cytotoxicity in 3D culture, all assays pointed to a cytotoxic effect of preussin (1), varying only in the concentration for which the effect was significantly detected. The effect of STS varied according to the assay method. It has also been reported that STS can be used up to 10  $\mu\text{M}$ ; however, in this case a complete dissociation of the spheroid occurred at this concentration [71]. In future studies with MCAs, we suggest using a concentration between 1 and 10  $\mu\text{M}$ .

Considering the characteristics of the cell lines used in this study, different results are logically explainable. MCF7 is a cell line with positive estrogen receptors, which is more responsive to therapeutics [29], while the MCF12A cell line has been described as non-tumorigenic. Both cell lines were more susceptible to the tested compounds. The use of normal cell lines from the same organ/tissue in screening studies of new drugs have been considered important, by some authors, to offer hints about the toxicity of these compounds in non-tumor cells [17]. However, this importance has also been questioned by others, who defend that a compound should not be rejected for further testing just because of its toxicity in “normal cell lines” [72]. This concept is justified by the fact that the clinical relevance of the toxicity is not towards cells of the same tissue, but, conversely, towards other type of tissues, namely fast-proliferating cells—i.e., those that cannot regenerate (like cardiomyocytes and neurons)—and cells from metabolic organs where drugs are metabolized or excreted [72]. SKBR3 cells that have HER-2 overexpression, and BC, with this characteristic, normally progress more aggressively than those with normal expression [73]. In accordance with this concept, the SKBR3 cell line viability was affected more with preussin (1) at the highest concentration (100  $\mu\text{M}$ ). The cell line which was less responsive to exposure was the triple-negative MDA-MB-231, a representative of the most aggressive BC subtype, which is harder to treat and more likely to metastasize [74].

Taking into account the results from BrdU proliferation assay, preussin (1) (at respective tested conditions) inhibited cell proliferation in all cell lines, cultured in 2D or in 3D, with lower concentrations in 2D.

All the above findings were corroborated by morphological analysis (optical and electron microscopy). The cytotoxic effects of preussin (1), revealed by histology and electron microscopy observation, were very clear and showed a higher extent of damage than that revealed by the data obtained from cytotoxicity assays. The MCAs exposed to preussin (1) had a normal appearance with intact structure when photographed in the plates, before the collection for optical and electron microscopy. However, when manipulated, they tended to disrupt upon pipette mechanical manipulation. This was not observed in MCAs of the SC. When observing the cells under the microscope, it was understandable why these MCAs disaggregate, as the cells' morphology was severely altered by exposure to compounds, STS and especially preussin (1). In MCAs stained with HE, all typical aspects of apoptosis—i.e., cytoplasmic and nuclear condensation, nuclear fragmentation, and hyper eosinophilic cytoplasm—were observed [75]. In addition to a simple morphological study, the ICC technique against caspase-3 (apoptosis marker) [47,76] and ki67 (proliferation marker) [77] was also performed. Curiously, the more commonly described phenotype for spheroids, with a proliferative outer layer, a quiescent zone, and a necrotic core [38,78], was not found in the MCAs. MCAs of MCF7 in the SC group revealed acinar-like structures with lumina [65,79], inside which caspase-3 positive cells were detected. This is in line with the lumen formation process of acini, where apoptotic clearance of the inner cells occurs [59,80].



The ICC technique provided useful information in relation to cell death and cell proliferation. For the drug-exposed groups, especially for preussin (1) at both concentrations, most cells stained for caspase-3. In accordance with the cells' morphological characteristics, this data is compatible with ongoing cell death. In this scenario, it would be normal to find just a few or no cells under cell division. In fact, besides a huge number of cells stained with caspase-3, ki67 positive cells were not that insignificant. The number of ki67-positive cells was clearly decreased in preussin (1)-exposed MCAs in relation to the control. However, we found more ki67-positive cells in preussin (1)-exposed MCAs than expected. The results obtained from the ICC against ki67 can be compared with those obtained with the BrdU proliferation assay. Ki67 is a protein expressed in almost all phases in the cell cycle: S, G1, G2, and M phases, but not in G0 [77]. On the other hand, BrdU proliferation assay is a technique in which BrdU is incorporated into the DNA in the S phase of the cell cycle [81]. In this circumstance, the number of cells immunostained with ki67 was much lower in the drug-exposed groups than in the SC groups, which were similar to the data obtained from the BrdU proliferation assay.

Our opinion is that the anticancer effects should be assessed using multiple endpoints, as we verified that the results obtained from different assays can be quite different. Morphology can also contribute to a better understanding of the degree of damage affecting the exposed cells.

Overall, the toxicity and antiproliferative data unveiled by this study, using cancer cell lines representative of biologically distinct BC, suggest that preussin (1) can represent a potential scaffold for the development of a future anticancer drug. The data obtained from this study clearly illustrates the importance of conducting comparative studies using 2D and 3D culture models, with the effects observed in the latter reinforcing the potential of preussin (1), warranting more research to explore the *in vitro* cytotoxicity and mechanisms of action. As a next research step, molecular biology tools should help to unveil the possible signaling pathways involved in the cytotoxic and antiproliferative effects of preussin (1).

## 4. Materials and Methods

### 4.1. Cell Lines Cultivation

MCF12A and MDA-MB-231 cell lines were purchased from the American Tissue Culture Collection (ATCC). MCF7 was acquired from the European Collection of Authenticated Cell Cultures (ECACC). The SKBR3 cell line was kindly provided by Professor Carmen Jerónimo of the Portuguese Oncology Institute - Porto. MCF7, MDA-MB-231, and SKBR3 were cultivated in Dulbecco's Modified Eagle's Medium high glucose (DMEM) without glutamine and without phenol red, supplemented with 10% Fetal Bovine Serum (FBS) and 1% penicillin/streptomycin. MCF12A was cultivated in a mixture of DMEM/F12 medium without phenol red, and supplemented with 20 ng/mL human epidermal growth factor, 100 ng/mL cholera toxin, 0.01 mg/mL insulin, and 500 ng/mL hydrocortisone, 10% FBS, and 1% penicillin/streptomycin. All cell lines were cultivated in T75 cm<sup>3</sup> culture flasks (Orange Scientific, Belgium) and maintained in the incubation chamber MCO 19AIC (Sanyo, Japan), with 5% CO<sub>2</sub>, at 37 °C.

### 4.2. Chemicals and Cell Culture Reagents

Staurosporin (STS) (Santa Cruz, Dallas, TX, USA). Dimethyl sulphoxide (DMSO), MTT, cholera toxin, insulin, and hydrocortisone (Sigma Aldrich, St. Louis, MO, USA). Resazurin (Cayman, Ann Arbor, MI, USA). DMEM without glutamine and without phenol red, Trypsin/EDTA, and FBS (Biochrom KG, Berlin, Germany). DMEM/F12 medium without phenol red (GE Healthcare, Chicago, IL, USA). All other reagents and chemicals used were analytical grade.

Stock solutions of STS and preussin (1) were prepared in DMSO, MTT was prepared in Phosphate buffer saline (PBS) at a final concentration of 5 mg/mL, and resazurin in PBS at 1 mM. All the stock solutions (except resazurin) were kept at -20 °C before use.

#### 4.3. Preussin (1)

Preussin (1) was isolated from a marine derived fungus: *A. candidus* KUFA 0062, associated with the marine sponge *Epipolasis* sp. from the coral reef at the Similan Island National Park in Phang-Nga province, Southern Thailand. Isolation, purification, and characterization of preussin (1) have been recently reported by Buttachon et al. [21].

#### 4.4. Cell Exposures

Cell suspensions were obtained by trypsinization of confluent flasks using 0.25% Trypsin/0.02% EDTA at 37 °C until cell detachment. After trypsin stopping action, cell suspensions were counted using a Neubauer chamber. Subsequently, cells were plated in different culture plates with different densities according to the type of the culture: 2D or 3D cultures. For all experiments, the final concentration of DMSO in the medium was 0.1% (*v/v*) and the controls received only 0.1% DMSO. All assays were performed in four independent experiments, in duplicate for each exposure condition.

##### 4.4.1. Exposure in 2D Culture

Cells were plated in 96-multiwell culture plates (Orange Scientific, Belgium) at a density of  $1.0 \times 10^5$  cells/mL, 100  $\mu$ L/well, and kept in the incubator at 37 °C and 5% CO<sub>2</sub> for 24 h for adhesion. Cells were then exposed 72 h to preussin (1) at different concentrations (10, 25, 50, and 100  $\mu$ M), or STS (1  $\mu$ M) as a positive control for apoptosis induction.

##### 4.4.2. Exposure in 3D Culture

Cells were seeded in 96-well ultra-low attachment spheroid plates (Corning, New York, NY USA, at the following densities: MCF7, MDA-MB-231 and SKBR3  $40 \times 10^4$  cells/mL, and MCF12A  $20 \times 10^4$  cells/mL, 200  $\mu$ L/well. Plates were centrifuged in a centrifuge Rotina 380 R (Hettich, Germany) 200 g for 10 min and placed in the incubator at 37 °C and 5% CO<sub>2</sub> for 72 h for the MCA formation. MCAs were exposed 96 h to preussin (1) (50 and 100  $\mu$ M) or STS (1  $\mu$ M).

#### 4.5. Analysis of Cell Viability

##### 4.5.1. 2D Culture

###### MTT Assay

The cytotoxic effect of preussin(1) in breast cell lines was assessed by MTT reduction assay as described previously [82], based on reduction reaction of tetrazolium salt, pale yellow salt, forming formazan dark blue product which are dissolved and read by absorbance. This absorbance is proportional to the number of live cells, as only live cells are able to cleave MTT [83].

Briefly, after 72 h of treatment, MTT solution was added at a final concentration of 0.5 mg/mL (10 times the dilution of the stock solution) and incubated for 2 h in 5% CO<sub>2</sub> at 37 °C. Exposure medium was then aspirated and the formazan crystals were dissolved by adding 150  $\mu$ L of DMSO: ethanol solution (1:1) (*v/v*), followed by 15 min with mild agitation. Absorbance (A) was measured at 570 nm in a microplate reader Multiskan GO (Thermo Fisher Scientific, Waltman, MA, USA) [74]. Results are expressed as a percentage of cell viability relative to the solvent control (cells incubated with culture medium with 0.1% of DMSO), and calculated in accordance with the following equation:

$$\text{Cell viability (\%)} = [(A \text{ sample at } 570 \text{ nm} / A \text{ control at } 570 \text{ nm})] \times 100$$

##### 4.5.2. 3D Culture

MTT and resazurin are metabolic assays based on reduction reactions. MTT has already been described in 2D culture. Resazurin is a blue compound, which acquires fluorescence when reduced into resorufin, which can be read by a fluorimeter. The fluorescence measurement correlates to the

number of viable cells [84]. On the contrary, LDH (lactate dehydrogenase) assay is related to the cell membrane integrity. If the membrane is damaged, it permits the leak of LDH from the cytoplasm to the extracellular medium [48].

#### MTT Assay

MTT in 3D culture was performed according to the method previously described for 2D culture [82], with minor adaptations as MCAs must be transferred from the conical plate (where their formation and exposure occurred) to a new flat bottom 96-well plate, and with a longer incubation time. After removing the medium, formazan crystals were dissolved with DMSO (only). Absorbance measurements and the calculations were carried out in exactly the same manner as in the 2D culture.

#### Resazurin Reduction Assay

In the same way as performed for MTT, before starting the protocol, MCAs were transferred to a flat-bottom 96-well plate. Subsequently, resazurin was added to each well to a final concentration of 10  $\mu\text{M}$  (100 times dilution of the stock solution). Plates were incubated for 4 h, with 5%  $\text{CO}_2$  and at 37  $^\circ\text{C}$ . Fluorescence (F) was read using excitation wavelength at 560 nm and emission wavelength at 590 nm, in a plate reader Synergy H1 (Biotek, Winooski, VT, USA) [48]. Results are expressed as the percentage of cell viability relative to the solvent control (medium culture with 0.11% DMSO), calculated in accordance with the following equation:

$$\text{Cell viability (\%)} = [(F \text{ sample})/F \text{ control}] \times 100$$

#### Lactate Dehydrogenase (LDH) Assay

LDH release from damaged cells in MCAs was evaluated as a biomarker for cellular cytotoxicity and cytolysis. Cell culture medium was transferred to a flat-bottom 96-well plate, and then the LDH release was detected following the manufacturer's instructions of the Pierce™ LDH Cytotoxicity Assay Kit (Thermo Fisher Scientific, Waltham, MA, USA). The lactate produced was detected by measuring the absorbance (A) at 490 nm and 680 nm. Results are expressed as the percentage of LDH release relative to the control, calculated in accordance with the following equation:

$$\text{LDH Release (\%)} = [(A \text{ sample at } 490 \text{ nm} - 680 \text{ nm})/(A \text{ control at } 490 \text{ nm} - 680 \text{ nm})] \times 100$$

### 4.6. Analysis of Cell Proliferation

#### 4.6.1. 2D Culture

##### BrdU Assay

Effects on cell proliferation were evaluated by BrdU assay using the Cell Proliferation ELISA, BrdU (colorimetric) (Roche, Switzerland), according to manufacturer's instructions as described previously [85]. Briefly, BrdU was incorporated in the place of thymidine into the DNA of cell under division. This BrdU was detected by an antibody anti-BrdU conjugated with peroxidase, the reaction product of the enzyme with the given substrate was quantified by measuring its absorbance [86,87]. The absorbance (A) was measured at 370 nm and 492 nm in the microplate reader Multiskan GO (Thermo Fisher Scientific, Waltham, MA, USA). Results are expressed as a percentage of cell proliferation relative to the control, calculated in accordance with the following equation:

$$\text{Cell proliferation (\%)} = [(A \text{ sample at } 370 \text{ nm} - 492 \text{ nm})/(A \text{ control at } 370 \text{ nm} - 492 \text{ nm})] \times 100$$

#### 4.6.2. 3D Culture

The BrdU assays of spheroids in 3D were performed in the same manner as that performed in 2D, with minor modification.

#### 4.7. Analysis of Cell Morphology in 3D Culture

##### 4.7.1. MCA Measurements

Each MCA (one/well) was observed and photographed with an Olympus SZX10 stereomicroscope, equipped with a digital camera DP21 (Olympus, Tokyo, Japan), in two different moments: (1) Before exposure (at 72 h of formation); and (2) immediately before being sampled (after 96 h of exposure). Images were analyzed using free download AnaSP software [43]. For this, binary images were generated to measure three parameters: Area, sphericity, and solidity. For these measurements, all multicellular cell aggregates were considered, even if afterwards they were used for cell viability or other assays, accounting for a total of 12 spheroids/condition/experiment.

##### 4.7.2. Histological Analysis

MCAs were fixed in Eppendorf tubes with 10% buffered formalin (Bioptica, Milan, Italy) for 24 h, then embedded in Histogel (Thermo Scientific, Waltham, MA, USA), according to manufacturer's instructions, and processed for paraffin embedding in tissue cassettes using an automatic tissue processor Leica TP120 (Leica, Nussloch, Germany). The routine processing protocol consisted of the following sequence of reagents (1 h each): 70% ethanol; 90% ethanol; 96% ethanol; absolute ethanol; absolute ethanol; absolute ethanol:xylene (1:1); xylene; xylene; liquid paraffin; and liquid paraffin. Embedding was performed in an embedding station EG 1140H (Leica, Germany). Sections (3  $\mu$ m) were obtained in a Leica 2255 microtome (Leica, Germany), placed onto KP-frost slides (Klinipath, Duiven, The Netherlands), and left for 20 min in a 60 °C oven. Obtained slides were divided for standard HE staining or ICC. For HE, slides were deparaffinized for 10 min (twice) in xylene, hydrated in a decreasing series of ethanol, 5 min each step (100%, 95%, 70%), and finally running tap water, stained with Mayer's hematoxylin (Merck, Darmstadt, Germany) for 3 min, washed with tap water for 5 min, stained with 1% aqueous eosin Y (Merck, Darmstadt, Germany), followed by quick dips in distilled water. In order to obtain definitive preparations, slides were dehydrated in an ascending series of ethanol, 5 min each (95%, 100%, 100%), cleared in xylene, and mounted using the resinous mounting medium Entellan (Merck, Darmstadt, Germany).

##### 4.7.3. Electron Microscopy

MCAs were fixed in Eppendorf tubes with 2.5% glutaraldehyde in sodium cacodylate-HCl buffer (0.15 M, pH 7.2), for 2 h at 4 °C, then washed twice with the same buffer, 10 min each. Post-fixation was performed in 1% osmium tetroxide in the same buffer as glutaraldehyde, for 2 h at 4 °C. Following the routine cell processing for electron microscopy, cells were dehydrated (30 min each step): 50%; ethanol; 70%, ethanol; 95% ethanol; absolute ethanol; absolute ethanol; propylene oxide; and propylene oxide. For epoxy resin embedding (1 h each): Successive mixture of propylene oxide and epoxy resin (respectively, 3 parts:1 part; 1 parts:1 part; 1 part:3 parts) and only resin, for the resin to penetrate gradually in MCAs. Then, embedding was performed in rubber molds, placed in a 60 °C oven for 48 h for resin polymerization. Semi-thin and ultra-thin sections were obtained in an ultramicrotome EM UC7 (Leica, Nussloch, Germany). Ultra-thin sections ( $\approx$ 90 nm thick) were obtained with a diamond knife (Diatome, Nidau, Switzerland), placed onto 200 mesh copper grids (Agar Scientific, Stansted, UK), and contrasted with 3% aqueous uranyl acetate (20 min) and Reynold's [88] lead citrate (10 min). Grids were observed in the transmission electron microscope JEOL 100CXII (JEOL, Tokyo, Japan), operated at 60 kV, and photographed with the Orius SC1000 CCD digital camera (Gatan, Pleasanton, CA, USA).

#### 4.8. Immunocytochemistry in 3D Culture

Sections were deparaffinized and hydrated following the sequence of HE staining. The next step consisted of heat antigen retrieval that was performed in a pressure cooker, using citrate buffer (0.01 M, pH 6.0) for 2 min after reaching the maximum pressure. Later, the slides slowly cooled, and endogenous peroxidases were blocked with 3% hydrogen peroxide in methanol (10 min). The excess of hydrogen peroxide was removed by washing in tris-buffered saline (TBS), pH 7.6 (5 min).

In order to save reagents, water was removed around the sections (without letting them dry) so that a hydrophobic pen could be applied (Leica, Germany). In the sequence, unspecific reactions were blocked using the blocking reagent from the Novolink™ Polymer Detection System kit (Leica Biosystems, Nussloch, Germany) (5 min), followed by two washes in TBST (5 min); that is, in the above-mentioned TBS we added 0.05% of Tween 20 (Sigma, St. Louis, MO, USA). The incubation with primary antibodies was overnight (16 h), using a humidified chamber at 4 °C. Primary antibodies applied were diluted in PBS with 5% bovine serum albumin (BSA) (Nzytech, Lisbon, Portugal). We applied two primary antibodies: Rabbit monoclonal anti-Ki67, clone SP6 (Biocare Medical, Pacheco, CA, USA), dilution of 1:200, for assessing cell proliferation; and rabbit polyclonal anti-caspase-3, ab 13847 (Abcam, Cambridge, United Kingdom), diluted 1:5000, for assessing caspase dependent apoptosis.

The signal amplification and revelation were performed with the Novolink™ Polymer Detection System (Leica Biosystems, Nussloch, Germany) according to the manufacturer's instructions. Slides were counterstained with Mayer's hematoxylin for one min, washed in tap water, dehydrated, and mounted. Observations using an Olympus BX50 light microscope (Olympus, Tokyo, Japan), and photographs were obtained with a digital camera DP21 (Olympus, Tokyo, Japan).

#### 4.9. Statistical Analysis

Descriptive and inferential statistics were performed using GraphPad Prism 6.0 software (GraphPad Software, La Jolla, CA, USA). The results are expressed as mean  $\pm$  standard deviation (SD) of four independent experiments. Significant differences ( $p \leq 0.05$ ) were assessed by one-way ANOVAs, followed by the post-hoc Holm-Šidák multiple comparison test whenever the ANOVA disclosed significant results for the tested effects. The normality and homogeneity of variance were confirmed by the Shapiro-Wilk test and the Levene test, respectively.

### 5. Conclusions

The results obtained in this study are very interesting, since preussin (1)-induced cytotoxic and antiproliferative effects on a panel of human breast cancer cell lines when cultured in 2D and 3D were observed. The effects varied according to the cell line molecular characteristics. The results obtained in the 3D model followed the same tendency as those found in the 2D model; however, cells in the 3D model showed more resistance to the impact of preussin (1). In this regard, the use of a multi-endpoint approach, which included histological evaluations, was important. The cytotoxic activity of preussin (1) in non-tumor cells was also an important point, since, in future studies, strategies to decrease the side effects of preussin (1) in non-target cells should be evaluated. Overall, the data support the potential of preussin (1) as a scaffold for the development of an anticancer drug candidate and call for further fundamental studies in vitro to clarify the molecular targets and the signaling pathways involved in the anticancer activity demonstrated by preussin (1).

**Supplementary Materials:** The following are available online at <http://www.mdpi.com/1660-3397/17/8/448/s1>, Figure S1: Effect of preussin (1) (50 and 100  $\mu$ M) in the MCA sphericity (left side) and solidity (right side) 3D culture. (A, B) MCF7, (C, D) MDA-MB-231, (E, F) SKBR3 and (G, H) MCF12A cells after 96 h of incubation. Cells treated with 0.1% DMSO (SC) and STS at 1  $\mu$ M were included as negative and positive control, respectively. The results were expressed as the percentage of cell viability relative to negative control and are presented as mean  $\pm$  standard deviation (SD) of four independent experiments (twelve duplicates per replica).

**Author Contributions:** F.M., A.A.R., E.R., and A.K. contributed to the conception and design of the work. F.M. did most of the acquisition, analysis and interpretation of data, and drafted the manuscript. F.M., A.A.R., E.R., and



A.K. also contributed to the analysis and interpretation of data, and critically revised the work. S.B. performed the isolation and purification of the preussin (1) used in the experiments, and critically revised the work. T.D. collected, isolated, identified, and cultured the fungus, and critically revised the work. All authors approved the final version of this work.

**Funding:** This research was partially supported by the Strategic Funding UID/Multi/04423/2019 through national funds provided by FCT—Foundation for Science and Technology and European Regional Development Fund (ERDF), under the framework of the PT2020 program.

**Acknowledgments:** We thank Rui Henriques for the professional English proofreading of the manuscript.

**Conflicts of Interest:** The authors declare no conflict of interest.

## References

1. Bray, F.; Ferlay, J.; Soerjomataram, I.; Siegel, R.L.; Torre, L.A.; Jemal, A. Global cancer statistics 2018: GLOBOCAN estimates of incidence and mortality worldwide for 36 cancers in 185 countries. *CA Cancer J. Clin.* **2018**, *68*, 394–424. [[CrossRef](#)] [[PubMed](#)]
2. Ferlay, J.; Colombet, M.; Soerjomataram, I.; Dyba, T.; Randi, G.; Bettio, M.; Gavin, A.; Visser, O.; Bray, F. Cancer incidence and mortality patterns in Europe: Estimates for 40 countries and 25 major cancers in 2018. *Eur. J. Cancer* **2018**, *103*, 356–387. [[CrossRef](#)] [[PubMed](#)]
3. Magalhaes, L.G.; Ferreira, L.L.G.; Andricopulo, A.D. Recent advances and perspectives in cancer drug design. *An. Acad. Bras. Cienc.* **2018**, *90* (Suppl. 2), 1233–1250. [[CrossRef](#)] [[PubMed](#)]
4. Zhang, Z.; Guan, N.; Li, T.; Mais, D.E.; Wang, M. Quality control of cell-based high-throughput drug screening. *Acta Pharm. Sin.* **2012**, *2*, 429–438. [[CrossRef](#)]
5. Sawadogo, W.R.; Schumacher, M.; Teiten, M.H.; Cerella, C.; Dicato, M.; Diederich, M. A survey of marine natural compounds and their derivatives with anti-cancer activity reported in 2011. *Molecules* **2013**, *18*, 3641–3673. [[CrossRef](#)] [[PubMed](#)]
6. Katz, L.; Baltz, R.H. Natural product discovery: Past, present, and future. *J. Ind. Microbiol. Biotechnol.* **2016**, *43*, 155–176. [[CrossRef](#)]
7. Newman, D.J.; Cragg, G.M. Marine-Sourced anti-cancer and cancer pain control agents in clinical and late preclinical development (†). *Mar. Drugs* **2014**, *12*, 255–278. [[CrossRef](#)]
8. Newman, D.J.; Cragg, G.M. Natural products as sources of new drugs from 1981 to 2014. *J. Nat. Prod.* **2016**, *79*, 629–661. [[CrossRef](#)]
9. Talero, E.; García-Mauriño, S.; Ávila-Román, J.; Rodríguez-Luna, A.; Alcaide, A.; Motilva, V. Bioactive compounds isolated from microalgae in chronic inflammation and cancer. *Mar. Drugs* **2015**, *13*, 6152–6209. [[CrossRef](#)]
10. Sithranga Boopathy, N.; Kathiresan, K. Anticancer drugs from marine flora: An overview. *J. Oncol.* **2010**, *2010*, 214186. [[CrossRef](#)]
11. Namvar, F.; Tahir, P.M.; Mohamad, R.; Mahdavi, M.; Abedi, P.; Najafi, T.F.; Rahmanand, H.S.; Jawaid, M. Biomedical properties of edible seaweed in cancer therapy and chemoprevention trials: A review. *Nat. Prod. Commun.* **2013**, *8*, 1811–1820. [[CrossRef](#)] [[PubMed](#)]
12. Deshmukh, S.K.; Prakash, V.; Ranjan, N. Marine Fungi: A Source of Potential Anticancer Compounds. *Front. Microbiol.* **2017**, *8*, 2536. [[CrossRef](#)] [[PubMed](#)]
13. Uzma, F.; Mohan, C.D.; Hashem, A.; Konappa, N.M.; Rangappa, S.; Kamath, P.V.; Singh, B.P.; Mudili, V.; Gupta, V.K.; Siddaiah, C.N.; et al. Endophytic Fungi-Alternative Sources of Cytotoxic Compounds: A Review. *Front. Pharmacol.* **2018**, *9*, 309. [[CrossRef](#)] [[PubMed](#)]
14. Jimenez, P.C.; Wilke, D.V.; Costa-Lotufo, L.V. Marine drugs for cancer: Surfacing biotechnological innovations from the oceans. *Clinics (Sao Paulo)* **2018**, *73* (Suppl. 1), e482s. [[CrossRef](#)] [[PubMed](#)]
15. Bugni, T.S.; Ireland, C.M. Marine-derived fungi: A chemically and biologically diverse group of microorganisms. *Nat. Prod. Rep.* **2004**, *21*, 143–163. [[CrossRef](#)]
16. Rateb, M.E.; Ebel, R. Secondary metabolites of fungi from marine habitats. *Nat. Prod. Rep.* **2011**, *28*, 290–344. [[CrossRef](#)] [[PubMed](#)]
17. Gomes, N.G.; Lefranc, F.; Kijjoo, A.; Kiss, R. Can some marine-derived fungal metabolites become actual anticancer agents? *Mar. Drugs* **2015**, *13*, 3950–3991. [[CrossRef](#)]
18. Yarden, O. Fungal association with sessile marine invertebrates. *Front. Microbiol.* **2014**, *5*, 228. [[CrossRef](#)]

19. Debbab, A.; Aly, A.H.; Proksch, P. Endophytes and associated marine derived fungi—Ecological and chemical perspectives. *Fungal Divers.* **2012**, *57*, 45–83. [[CrossRef](#)]
20. Simmons, T.L.; Andrianasolo, E.; McPhail, K.; Flatt, P.; Gerwick, W.H. Marine natural products as anticancer drugs. *Mol. Cancer Ther.* **2005**, *4*, 333.
21. Buttachon, S.; Ramos, A.A.; Inacio, A.; Dethoup, T.; Gales, L.; Lee, M.; Costa, P.M.; Silva, A.M.S.; Sekeroglu, N.; Rocha, E.; et al. Bis-Indolyl Benzenoids, Hydroxypyrrrolidine Derivatives and Other Constituents from Cultures of the Marine Sponge-Associated Fungus *Aspergillus candidus* KUFA0062. *Mar. Drugs* **2018**, *16*, 119. [[CrossRef](#)] [[PubMed](#)]
22. Gu, Y.H.; Leonard, J. In vitro effects on proliferation, apoptosis and colony inhibition in ER-dependent and ER-independent human breast cancer cells by selected mushroom species. *Oncol. Rep.* **2006**, *15*, 417–423. [[CrossRef](#)] [[PubMed](#)]
23. Dai, X.; Li, T.; Bai, Z.; Yang, Y.; Liu, X.; Zhan, J.; Sho, B. Breast cancer intrinsic subtype classification, clinical use and future trends. *Am. J. Cancer Res.* **2015**, *10*, 2029–2943.
24. Torre, L.A.; Bray, F.; Siegel, R.L.; Ferlay, J.; Lortet-Tieulent, J.; Jemal, A. Global cancer statistics, 2012. *CA Cancer J. Clin.* **2015**, *65*, 87–108. [[CrossRef](#)] [[PubMed](#)]
25. Gonzalez-Angulo, A.M.; Morales-Vasquez, F.; Hortobagyi, G.N. Overview of resistance to systemic therapy in patients with breast cancer. *Adv. Exp. Med. Biol.* **2007**, *608*, 1–22. [[CrossRef](#)] [[PubMed](#)]
26. Housman, G.; Byler, S.; Heerboth, S.; Lapinska, K.; Longacre, M.; Snyder, N.; Sarkar, S. Drug resistance in cancer: An overview. *Cancers* **2014**, *6*, 1769–1792. [[CrossRef](#)] [[PubMed](#)]
27. Elshimali, Y.I.; Wu, Y.; Khaddour, H.; Wu, Y.; Gradinaru, D.; Sukhija, H.; Chung, S.S.; Vadgama, J.V. Optimization OF Cancer Treatment Through Overcoming Drug Resistance. *J. Cancer. Res. Oncobiol.* **2018**, *1*, 107. [[CrossRef](#)] [[PubMed](#)]
28. Nikolaou, M.; Pavlopoulou, A.; Georgakilas, A.G.; Kyrodimos, E. The challenge of drug resistance in cancer treatment: A current overview. *Clin. Exp. Metastasis* **2018**, *35*, 309–318. [[CrossRef](#)]
29. Darzynkiewicz, Z. Novel strategies of protecting non-cancer cells during chemotherapy: Are they ready for clinical testing? *Oncotarget* **2011**, *2*, 107–108. [[CrossRef](#)]
30. Holliday, D.L.; Speirs, V. Choosing the right cell line for breast cancer research. *Breast Cancer Res. BCR* **2011**, *13*, 215. [[CrossRef](#)]
31. Neve, R.M.; Chin, K.; Fridlyand, J.; Yeh, J.; Baehner, F.L.; Fevr, T.; Clark, L.; Bayani, N.; Coppe, J.P.; Tong, F.; et al. A collection of breast cancer cell lines for the study of functionally distinct cancer subtypes. *Cancer cell* **2006**, *10*, 515–527. [[CrossRef](#)] [[PubMed](#)]
32. Polyak, K. Heterogeneity in breast cancer. *J. Clin. Investig.* **2011**, *121*, 3786–3788. [[CrossRef](#)] [[PubMed](#)]
33. Subik, K.; Lee, J.-F.; Baxter, L.; Strzepak, T.; Costello, D.; Crowley, P.; Xing, L.; Hung, M.-C.; Bonfiglio, T.; Hicks, D.G.; et al. The Expression Patterns of ER, PR, HER2, CK5/6, EGFR, Ki-67 and AR by immunohistochemical analysis in breast cancer cell lines. *Breast Cancer (Auckl)* **2010**, *4*, 35–41. [[CrossRef](#)] [[PubMed](#)]
34. Dai, J.; Jian, J.; Bosland, M.; Frenkel, K.; Bernhardt, G.; Huang, X. Roles of hormone replacement therapy and iron in proliferation of breast epithelial cells with different estrogen and progesterone receptor status. *Breast (Edinburgh, Scotland)* **2008**, *17*, 172–179. [[CrossRef](#)] [[PubMed](#)]
35. Breslin, S.; O'Driscoll, L. Three-dimensional cell culture: The missing link in drug discovery. *Drug Discov. Today* **2013**, *18*, 240–249. [[CrossRef](#)] [[PubMed](#)]
36. Verjans, E.T.; Doijen, J.; Luyten, W.; Landuyt, B.; Schoofs, L. Three-dimensional cell culture models for anticancer drug screening: Worth the effort? *J. Cell Physiol.* **2018**, *233*, 2993–3003. [[CrossRef](#)] [[PubMed](#)]
37. Antoni, D.; Burckel, H.; Josset, E.; Noel, G. Three-dimensional cell culture: A breakthrough in vivo. *Int. J. Mol. Sci.* **2015**, *16*, 5517–5527. [[CrossRef](#)]
38. Carvalho, M.R.; Lima, D.; Reis, R.L.; Oliveira, J.M.; Correlo, V.M. Anti-cancer drug validation: The contribution of tissue engineered models. *Stem Cell Rev.* **2017**, *13*, 347–363. [[CrossRef](#)] [[PubMed](#)]
39. Edmondson, R.; Broglie, J.J.; Adcock, A.F.; Yang, L. Three-dimensional cell culture systems and their applications in drug discovery and cell-based biosensors. *Assay Drug Dev. Technol.* **2014**, *12*, 207–218. [[CrossRef](#)] [[PubMed](#)]
40. Vidi, P.A.; Bissell, M.J.; Lelievre, S.A. Three-dimensional culture of human breast epithelial cells: The how and the why. *Methods Mol. Biol.* **2013**, *945*, 193–219. [[CrossRef](#)]

41. Ding, Y.; Wang, B.; Chen, X.; Zhou, Y.; Ge, J. Staurosporine suppresses survival of HepG2 cancer cells through Omi/HtrA2-mediated inhibition of PI3K/Akt signaling pathway. *Tumour Biol.* **2017**, *39*. [[CrossRef](#)] [[PubMed](#)]
42. Xue, L.-y.; Chiu, S.-m.; Oleinick, N.L. Staurosporine-induced death of MCF-7 human breast cancer cells: A distinction between caspase-3-dependent steps of apoptosis and the critical lethal lesions. *Exp. Cell Res.* **2003**, *283*, 135–145. [[CrossRef](#)]
43. Piccinini, F. AnaSP: A software suite for automatic image analysis of multicellular spheroids. *Comput. Methods Progr. Biomed.* **2015**, *119*, 43–52. [[CrossRef](#)] [[PubMed](#)]
44. Ziegler, U.; Groscurth, P. Morphological Features of Cell Death. *Physiology* **2004**, *19*, 124–128. [[CrossRef](#)]
45. Saraste, A.; Pulkki, K. Morphologic and biochemical hallmarks of apoptosis. *Cardiovasc. Res.* **2000**, *45*, 528–537. [[CrossRef](#)]
46. Watson, C.J. Key stages in mammary gland development - Involution: Apoptosis and tissue remodelling that convert the mammary gland from milk factory to a quiescent organ. *Breast Cancer Res.* **2006**, *8*, 203. [[CrossRef](#)] [[PubMed](#)]
47. Bressenot, A.; Marchal, S.; Bezdetnaya, L.; Garrier, J.; Guillemin, F.; Plénat, F. Assessment of apoptosis by immunohistochemistry to active caspase-3, active caspase-7, or cleaved PARP in monolayer cells and spheroid and subcutaneous xenografts of human carcinoma. *J. Histochem. Cytochem.* **2009**, *57*, 289–300. [[CrossRef](#)] [[PubMed](#)]
48. Riss, T.L.; Moravec, R.A. Use of multiple assay endpoints to investigate the effects of incubation time, dose of toxin, and plating density in cell-based cytotoxicity assays. *Assay Drug Dev. Technol.* **2004**, *2*, 51–62. [[CrossRef](#)]
49. Sales Gil, R.; Vagnarelli, P. Ki-67: More Hidden behind a 'Classic Proliferation Marker'. *Trends Biochem. Sci.* **2018**, *43*, 747–748. [[CrossRef](#)]
50. Urruticoechea, A.; Smith, I.E.; Dowsett, M. Proliferation marker Ki-67 in early breast cancer. *J Clin. Oncol.* **2005**, *23*, 7212–7220. [[CrossRef](#)]
51. Mazzoleni, G.; Di Lorenzo, D.; Steimberg, N. Modelling tissues in 3D: The next future of pharmaco-toxicology and food research? *Genes Nutr.* **2009**, *4*, 13–22. [[CrossRef](#)] [[PubMed](#)]
52. Lovitt, C.J.; Shelper, T.B.; Avery, V.M. Advanced cell culture techniques for cancer drug discovery. *Biology* **2014**, *3*, 345–367. [[CrossRef](#)] [[PubMed](#)]
53. Herrmann, R.; Fayad, W.; Schwarz, S.; Berndtsson, M.; Linder, S. Screening for compounds that induce apoptosis of cancer cells grown as multicellular spheroids. *J. Biomol. Screen.* **2008**, *13*, 1–8. [[CrossRef](#)] [[PubMed](#)]
54. Nath, S.; Devi, G.R. Three-dimensional culture systems in cancer research: Focus on tumor spheroid model. *Pharmacol. Ther.* **2016**, *163*, 94–108. [[CrossRef](#)] [[PubMed](#)]
55. Zanoni, M.; Pignatta, S.; Arienti, C.; Bonafè, M.; Tesei, A. Anticancer drug discovery using multicellular tumor spheroid models. *Expert Opin. Drug Discov.* **2019**, *14*, 289–301. [[CrossRef](#)] [[PubMed](#)]
56. Sant, S.; Johnston, P.A. The production of 3D tumor spheroids for cancer drug discovery. *Drug Discov. Today Technol.* **2017**, *23*, 27–36. [[CrossRef](#)] [[PubMed](#)]
57. Ho, W.Y.; Yeap, S.K.; Ho, C.L.; Rahim, R.A.; Alitheen, N.B. Development of multicellular tumor spheroid (MCTS) culture from breast cancer cell and a high throughput screening method using the MTT assay. *PLoS ONE* **2012**, *7*, e44640. [[CrossRef](#)]
58. Froehlich, K.; Haeger, J.D.; Heger, J.; Pastuschek, J.; Photini, S.M.; Yan, Y.; Lupp, A.; Pfarrer, C.; Mrowka, R.; Schleussner, E.; et al. Generation of multicellular breast cancer tumor spheroids: Comparison of different protocols. *J. Mammary Gland. Biol. Neoplasia* **2016**, *21*, 89–98. [[CrossRef](#)]
59. Do Amaral, J.B.; Urabayashi, M.S.; Machado-Santelli, G.M. Cell death and lumen formation in spheroids of MCF-7 cells. *Cell Biol. Int.* **2010**, *34*, 267–274. [[CrossRef](#)]
60. Ivascu, A.; Kubbies, M. Rapid generation of single-tumor spheroids for high-throughput cell function and toxicity analysis. *J. Biomol. Screen.* **2006**, *11*, 922–932. [[CrossRef](#)]
61. Reynolds, D.S.; Tevis, K.M.; Blessing, W.A.; Colson, Y.L.; Zaman, M.H.; Grinstaff, M.W. Breast cancer spheroids reveal a differential cancer stem cell response to chemotherapeutic treatment. *Sci. Rep.* **2017**, *7*, 10382. [[CrossRef](#)] [[PubMed](#)]
62. Ramanujan, V.K. Quantitative imaging of morphometric and metabolic signatures reveals heterogeneity in drug response of three-dimensional mammary tumor spheroids. *Mol. Imaging Biol.* **2019**, *21*, 436–446. [[CrossRef](#)] [[PubMed](#)]



63. Lombardo, Y.; de Giorgio, A.; Coombes, C.R.; Stebbing, J.; Castellano, L. Mammosphere formation assay from human breast cancer tissues and cell lines. *J. Vis. Exp.* **2015**. [[CrossRef](#)] [[PubMed](#)]
64. Guttilla, I.K.; Phoenix, K.N.; Hong, X.; Tirnauer, J.S.; Claffey, K.P.; White, B.A. Prolonged mammosphere culture of MCF-7 cells induces an EMT and repression of the estrogen receptor by microRNAs. *Breast Cancer Res. Treat.* **2012**, *132*, 75–85. [[CrossRef](#)] [[PubMed](#)]
65. Vantangoli, M.M.; Madnick, S.J.; Huse, S.M.; Weston, P.; Boekelheide, K. MCF-7 human breast cancer cells form differentiated microtissues in scaffold-free hydrogels. *PLoS one* **2015**, *10*, e0135426. [[CrossRef](#)] [[PubMed](#)]
66. Hirschhaeuser, F.; Menne, H.; Dittfeld, C.; West, J.; Mueller-Klieser, W.; Kunz-Schughart, L.A. Multicellular tumor spheroids: An underestimated tool is catching up again. *J. Biotechnol.* **2010**, *148*, 3–15. [[CrossRef](#)] [[PubMed](#)]
67. Gencoglu, M.F.; Barney, L.E.; Hall, C.L.; Brooks, E.A.; Schwartz, A.D.; Corbett, D.C.; Stevens, K.R.; Peyton, S.R. Comparative study of multicellular tumor spheroid formation methods and implications for drug screening. *ACS Biomater. Sci. Eng.* **2018**, *4*, 410–420. [[CrossRef](#)] [[PubMed](#)]
68. Krause, S.; Maffini, M.V.; Soto, A.M.; Sonnenschein, C. The microenvironment determines the breast cancer cells' phenotype: Organization of MCF7 cells in 3D cultures. *BMC Cancer* **2010**, *10*, 263. [[CrossRef](#)]
69. Mittler, F.; Obeid, P.; Rulina, A.V.; Haguët, V.; Gidrol, X.; Balakirev, M.Y. High-content monitoring of drug effects in a 3D spheroid Model. *Front. Oncol.* **2017**, *7*, 293. [[CrossRef](#)]
70. Ivanov, D.P.; Parker, T.L.; Walker, D.A.; Alexander, C.; Ashford, M.B.; Gellert, P.R.; Garnett, M.C. Multiplexing spheroid volume, resazurin and acid phosphatase viability assays for high-throughput screening of tumour spheroids and stem cell neurospheres. *PLoS ONE* **2014**, *9*, e103817. [[CrossRef](#)]
71. Wenzel, C.; Riefke, B.; Gründemann, S.; Krebs, A.; Christian, S.; Prinz, F.; Osterland, M.; Golfier, S.; Råse, S.; Ansari, N.; et al. 3D high-content screening for the identification of compounds that target cells in dormant tumor spheroid regions. *Exp. Cell Res.* **2014**, *323*, 131–143. [[CrossRef](#)] [[PubMed](#)]
72. Liu, B.; Ezeogu, L.; Zellmer, L.; Yu, B.; Xu, N.; Joshua Liao, D. Protecting the normal in order to better kill the cancer. *Cancer Med.* **2015**, *4*, 1394–1403. [[CrossRef](#)] [[PubMed](#)]
73. Chung, I.; Reichelt, M.; Shao, L.; Akita, R.W.; Koeppen, H.; Rangell, L.; Schaefer, G.; Mellman, I.; Sliwkowski, M.X. High cell-surface density of HER2 deforms cell membranes. *Nat. Commun.* **2016**, *7*, 12742. [[CrossRef](#)] [[PubMed](#)]
74. Razak, N.A.; Abu, N.; Ho, W.Y.; Zamberi, N.R.; Tan, S.W.; Alitheen, N.B.; Long, K.; Yeap, S.K. Cytotoxicity of eupatorin in MCF-7 and MDA-MB-231 human breast cancer cells via cell cycle arrest, anti-angiogenesis and induction of apoptosis. *Sci. Rep.* **2019**, *9*. [[CrossRef](#)] [[PubMed](#)]
75. Elmore, S.A.; Dixon, D.; Hailey, J.R.; Harada, T.; Herbert, R.A.; Maronpot, R.R.; Nolte, T.; Rehg, J.E.; Rittinghausen, S.; Rosol, T.J.; et al. Recommendations from the INHAND Apoptosis/Necrosis Working Group. *Toxicol. Pathol.* **2016**, *44*, 173–188. [[CrossRef](#)] [[PubMed](#)]
76. Chen, D.L.; Engle, J.T.; Griffin, E.A.; Miller, J.P.; Chu, W.; Zhou, D.; Mach, R.H. Imaging caspase-3 activation as a marker of apoptosis-targeted treatment response in cancer. *Mol. Imaging Biol.* **2015**, *17*, 384–393. [[CrossRef](#)]
77. Inwald, E.C.; Klinkhammer-Schalke, M.; Hofstädter, F.; Zeman, F.; Koller, M.; Gerstenhauer, M.; Ortman, O. Ki-67 is a prognostic parameter in breast cancer patients: Results of a large population-based cohort of a cancer registry. *Breast Cancer Res. Treat.* **2013**, *139*, 539–552. [[CrossRef](#)] [[PubMed](#)]
78. Costa, E.C.; Moreira, A.F.; de Melo-Diogo, D.; Gaspar, V.M.; Carvalho, M.P.; Correia, I.J. 3D tumor spheroids: An overview on the tools and techniques used for their analysis. *Biotechnol. Adv.* **2016**, *34*, 1427–1441. [[CrossRef](#)]
79. Do Amaral, J.B.; Rezende-Teixeira, P.; Freitas, V.M.; Machado-Santelli, G.M. MCF-7 cells as a three-dimensional model for the study of human breast cancer. *Tissue Eng. Part C Methods* **2011**, *17*, 1097–1107. [[CrossRef](#)]
80. Maillieux, A.A.; Overholtzer, M.; Brugge, J.S. Lumen formation during mammary epithelial morphogenesis: Insights from in vitro and in vivo models. *Cell Cycle* **2008**, *7*, 57–62. [[CrossRef](#)]
81. Menyhárt, O.; Harami-Papp, H.; Sukumar, S.; Schäfer, R.; Magnani, L.; de Barrios, O.; Gyórfy, B. Guidelines for the selection of functional assays to evaluate the hallmarks of cancer. *Biochim. Biophys. Acta Rev. Cancer* **2016**, *1866*, 300–319. [[CrossRef](#)] [[PubMed](#)]
82. Prata-Sena, M.; Ramos, A.A.; Buttachon, S.; Castro-Carvalho, B.; Marques, P.; Dethoup, T.; Kijjoa, A.; Rocha, E. Cytotoxic activity of secondary metabolites from marine-derived fungus *Neosartorya siamensis* in Human Cancer Cells. *Phytother. Res.* **2016**, *30*, 1862–1871. [[CrossRef](#)]

83. Mosmann, T. Rapid colorimetric assay for cellular growth and survival: Application to proliferation and cytotoxicity assays. *J. Immunol. Methods* **1983**, *65*, 55–63. [[CrossRef](#)]
84. O'Brien, J.; Wilson, I.; Orton, T.; Pognan, F. Investigation of the Alamar Blue (resazurin) fluorescent dye for the assessment of mammalian cell cytotoxicity. *Eur. J. Biochem.* **2000**, *267*, 5421–5426. [[CrossRef](#)] [[PubMed](#)]
85. Ramos, A.A.; Almeida, T.; Lima, B.; Rocha, E. Cytotoxic activity of the seaweed compound fucosterol, alone and in combination with 5-fluorouracil, in colon cells using 2D and 3D culturing. *J. Toxicol. Environ. Health A* **2019**, 1–13. [[CrossRef](#)] [[PubMed](#)]
86. Cecchini, M.J.; Amiri, M.; Dick, F.A. Analysis of cell cycle position in mammalian cells. *J. Vis. Exp.* **2012**. [[CrossRef](#)] [[PubMed](#)]
87. Padet, L.; St-Amour, I.; Aubin, E.; Proulx, D.P.; Bazin, R.; Lemieux, R. Dose-Dependent Inhibition of BrdU Detection in the Cell proliferation ELISA by culture medium proteins. *J. Immunoass. Immunochem.* **2009**, *30*, 348–357. [[CrossRef](#)] [[PubMed](#)]
88. Reynolds, E.S. The use of lead citrate at high pH as an electron-opaque stain in electron microscopy. *J. Cell. Biol.* **1963**, *17*, 208–212. [[CrossRef](#)] [[PubMed](#)]



© 2019 by the authors. Licensee MDPI, Basel, Switzerland. This article is an open access article distributed under the terms and conditions of the Creative Commons Attribution (CC BY) license (<http://creativecommons.org/licenses/by/4.0/>).

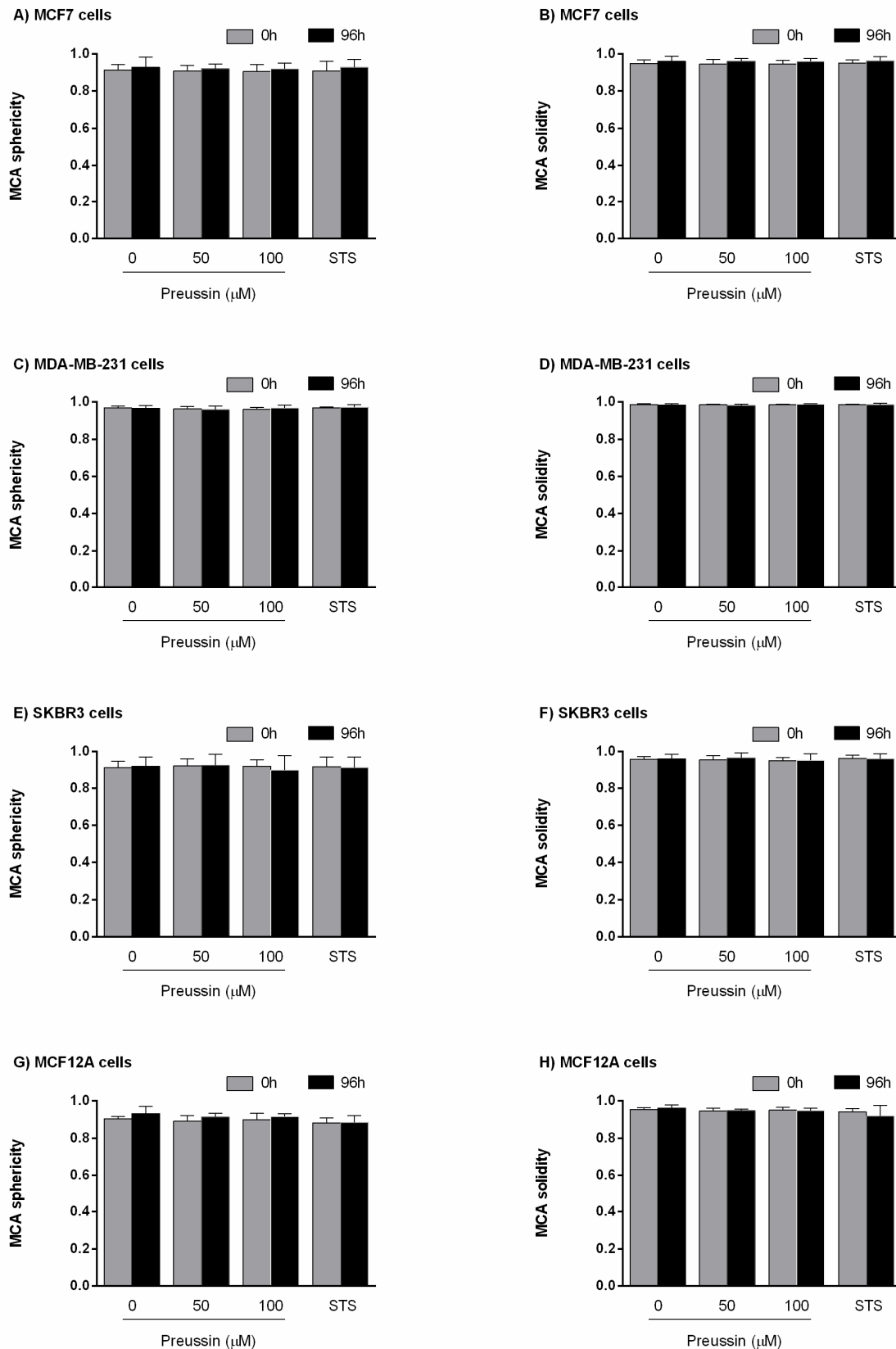


**Figure S1.** Effect of preussin (50 and 100  $\mu\text{M}$ ) in the MCA sphericity (left side) and solidity (right side) 3D culture. (A, B) MCF7, (C, D) MDA-MB-231, (E, F) SKBR3 and (G, H) MCF12A cells after 96 h of incubation, Cells treated with 0.1% DMSO (SC) and STS at 1  $\mu\text{M}$  were included as negative and positive control, respectively. The results were expressed as the percentage of cell viability relative to negative control and are presented as mean  $\pm$  standard deviation (SD) of four independent experiments (twelve duplicates per replica).

# **Chapter 4** - Cytotoxicity of Seaweed Compounds, Alone or Combined to Reference Drugs, against Breast Cell Lines Cultured in 2D and 3D

---



## Article

# Cytotoxicity of Seaweed Compounds, Alone or Combined to Reference Drugs, against Breast Cell Lines Cultured in 2D and 3D

Fernanda Malhão <sup>1,2</sup>, Alice Abreu Ramos <sup>1,2</sup>, Ana Catarina Macedo <sup>1,2</sup> and Eduardo Rocha <sup>1,2,\*</sup>

<sup>1</sup> Institute of Biomedical Sciences Abel Salazar (ICBAS), University of Porto (U.Porto), Rua de Jorge Viterbo Ferreira 228, 4050-313 Porto, Portugal; fmalhao@icbas.up.pt (F.M.); ramosalic@gmail.com (A.A.R.); acfpmacedo@gmail.com (A.C.M.)

<sup>2</sup> Interdisciplinary Center for Marine and Environmental Research (CIIMAR), University of Porto (U.Porto), Avenida General Norton de Matos, 4450-208 Matosinhos, Portugal

\* Correspondence: erocha@icbas.up.pt

**Abstract:** Seaweed bioactive compounds have shown anticancer activities in in vitro and in vivo studies. However, tests remain limited, with conflicting results, and effects in combination with anticancer drugs are even scarcer. Here, the cytotoxic effects of five seaweed compounds (astaxanthin, fucoidan, fucosterol, laminarin, and phloroglucinol) were tested alone and in combination with anticancer drugs (cisplatin—Cis; and doxorubicin—Dox), in breast cell lines (three breast cancer (BC) subtypes and one non-tumoral). The combinations revealed situations where seaweed compounds presented potentiation or inhibition of the drugs' cytotoxicity, without a specific pattern, varying according to the cell line, concentration used for the combination, and drug. Fucosterol was the most promising compound, since: (i) it alone had the highest cytotoxicity at low concentrations against the BC lines without affecting the non-tumoral line; and (ii) in combination (at non-cytotoxic concentration), it potentiated Dox cytotoxicity in the triple-negative BC cell line. Using a comparative approach, monolayer versus 3D cultures, further investigation assessed effects on cell viability and proliferation, morphology, and immunocytochemistry targets. The cytotoxic and antiproliferative effects in monolayer were not observed in 3D, corroborating that cells in 3D culture are more resistant to treatments, and reinforcing the use of more complex models for drug screening and a multi-approach that should include histological and ICC analysis.

**Keywords:** breast cancer; combinatory therapy; drug screening; in vitro; multicellular aggregates



**Citation:** Malhão, F.; Ramos, A.A.; Macedo, A.C.; Rocha, E. Cytotoxicity of Seaweed Compounds, Alone or Combined to Reference Drugs, against Breast Cell Lines Cultured in 2D and 3D. *Toxics* **2021**, *9*, 24. <https://doi.org/10.3390/toxics9020024>

Academic Editor: Matthew J. Winter

Received: 30 December 2020

Accepted: 26 January 2021

Published: 31 January 2021

**Publisher's Note:** MDPI stays neutral with regard to jurisdictional claims in published maps and institutional affiliations.



**Copyright:** © 2021 by the authors. Licensee MDPI, Basel, Switzerland. This article is an open access article distributed under the terms and conditions of the Creative Commons Attribution (CC BY) license (<https://creativecommons.org/licenses/by/4.0/>).

## 1. Introduction

Breast cancer (BC) is the most diagnosed cancer among women in high human development index countries and a leading cause of cancer death among females [1,2]. BC treatment involves different therapeutic approaches based mainly on the extent of the disease and the tumor characteristics [3]. It is a very heterogeneous cancer type, presenting different molecular subtypes which are associated with different prognostics. The determination of the molecular subtype is commonly performed by immunohistochemistry and/or genetic analyses and its classification is related to the positivity or negativity for estrogen and progesterone receptors (ER and PR), as well as for eventual (over)expression of the oncogene human epidermal growth factor receptor 2 (HER-2). The main molecular subtypes are: (a) luminal (ER and PR positive); (b) HER-2 enriched (ER, PR negative, and HER-2 overexpression), and (c) triple-negative breast cancer (TNBC) (ER, PR, and HER-2 negative) [4–6]. For luminal and HER-2 subtypes, there are effective therapeutic drugs [7], such as the well-established ER antagonist tamoxifen for hormone-positive tumors [8] and the antibody trastuzumab, to HER2 subtype [9]. Patients with TNBC are generally considered as high-risk patients, presenting the poorest prognosis as they cannot benefit

from target therapies and therefore, the recommended treatment approach for this type of patients is usually systemic chemotherapy [3].

Transversal to all cancer types is the problematic of drug resistance (innate or acquired) [10] and the high cumulative drug toxicity of some chemotherapeutics on non-cancer cells [11]. Therefore, there has been a great struggle for finding new drugs or drug adjuvants to overcome both drug resistance and toxicity. This topic is a hotspot in the pharmaceutical industry and in the scientific community. In this vein, one therapeutic approach that has been applied is the use of multi-drug combinations that target non-overlapping signaling pathways [12], with the intention to improve the coverage of therapeutic responses and reduce the prospect of resistance [13] and toxicity [14]. This approach has been applied in many cancer types including BC, especially in TNBC or in metastatic BC [15]. The combination therapy revealed efficacy in lowering drugs' doses or acting in a synergistic way, potentiating drugs' effects, or even reducing toxicity against normal cells [16–18].

Although it is almost unknown by the community in general, 50–60% of the drugs approved for cancer treatment are natural compounds and their derivatives [19,20]. The marine environment is an immense reservoir of natural compounds with a huge chemical and biological diversity. Among the rich marine flora, there has been a growing interest in the pharmacological activities of marine macroalgae (seaweeds), especially in their bioactive metabolites that can modulate the mechanisms involved in cancer. Anticancer activities of these compounds have been associated with inhibition of cell proliferation, proapoptotic, antiangiogenic, and anti-metastasis effects [21–25]. Interestingly, seaweeds have been used for centuries in Traditional Chinese and Japanese Folk Medicines in attempts to treat BC [26,27]. Data from several epidemiological and experimental studies confirmed the potential effects of seaweed dietary consumption in BC prevention [28–30]. Various studies reported the use of natural products in combination therapy with anticancer drugs [31–35]. When referring to seaweed compounds, the knowledge of interactions with drugs is limited to a few *in vitro* [36–38] and *in vivo* studies [39,40]. Furthermore, when considering the exploitation of the antioxidant properties of seaweed compounds, it should be remembered that the intake of antioxidants during chemotherapy is controversial, specifically in relation to BC. Evidences suggest that the effects, beneficial or not, are related to the dose intake and type of antioxidant [41]. While some authors advised against the intake of antioxidants during BC treatment [42], others showed that the administration of antioxidants in the first six months after BC diagnosis could reduce the risk of mortality and tumor recurrence [43].

Screening for new anticancer drugs is often performed using *in vitro* studies, and typically with cancer cell lines cultivated in monolayer [44]. Nowadays, there is a consensus in the literature that the use of more complex *in vitro* models, such as three-dimensional (3D) cell cultures, better simulates the *in vivo* tumor microenvironment [45,46]. The arrangement of cells into 3D cell multicellular aggregates (MCAs) is associated with a more functional state and promotes different gradients of nutrients and oxygen supply [47,48]. Additionally, cells cultured in 3D are supposed to be more resistant to drug treatments [49–51].

When referring to the screening of effects of seaweed bioactive compounds in BC cell lines, there are no systematic studies using a panel of cancer cell lines with distinct biological characteristics while comparatively testing normal breast cell lines. Also, in what concerns combinations with drugs, it is poorly explored if the cell line characteristics can influence the type of response.

In concord with the current state of the art, it is worth exploring the anticancer properties of selected seaweed compounds alone and in combination with reference drugs in a panel of breast cancer cell lines. For that, we selected three BC cell lines representative of the main BC subtypes: (i) MCF7 (ER+, PR+, HER-2-), corresponding to the most common BC type—Luminal A; (ii) SKBR3 (ER-, PR-, HER-2+), representing the HER-2

subtype; and (iii) MDA-MB-231, a triple-negative cell line (ER-, PR-, HER-2-), equivalent to TNBC [52,53]. We also included a non-tumor breast cell line (iv) MCF12A [52].

For this combinatory panel screening, we selected five brown seaweed bioactive compounds belonging to different chemical groups: (i) carotenoids: astaxanthin (Asta); (ii) polysaccharides: fucoïdan (Fc) and laminarin (Lm); (iii) sterols: fucosterol (Fct); and (iv) phlorotannins: phloroglucinol (Phg).

### 1.1. Carotenoids—Astaxanthin (Asta)

Carotenoids are fat-soluble organic pigments, naturally occurring in phototrophic organisms [54]. Asta is a xanthophyll carotenoid without vitamin A [55] present in diverse marine organisms, including brown seaweeds [56]. Compared with other carotenoids, its chemical structure possesses a special feature: two keto groups on each ring structure, which enhances its antioxidant properties. That is why it is called the “super antioxidant” [57]. Some anticancer activities of Asta have been reported, such as inhibition of cell proliferation [58,59] and apoptosis induction [58,60,61]. In BC cell lines, Asta significantly reduced proliferation rates and inhibited cell migration compared to control normal breast epithelial cells [62]. Asta was described as having a potent effect in inhibiting tumor growth due to its anti-inflammatory properties [63].

### 1.2. Polysaccharides—Fucoïdan (Fc) and Laminarin (Lm)

Sulphated polysaccharides are a major constituent of seaweeds' cell walls that have attracted much attention as functional additives in the pharmaceutical, food and cosmetic industries [64]. Fc is a complex sulphated polysaccharide, with many biological activities: antioxidant, anticoagulant, antiviral, immunomodulatory, antiproliferative, antilipidemic, anti-inflammatory, and anti-metastasis [22,65–67]. Accumulating data show the anticancer effects of Fc in several cancer cell lines [68–70]. In BC cell lines, Fc induced the apoptosis pathway in MCF7 [71–73] and MDA-MB-231 cells [73,74], inhibiting cell growth in both cell lines [73]. Also, colony formation was inhibited by this compound in the BC cell line T47D [73,75]. Fc was also pointed out as having a regulatory role in migration and invasion in MDA-MB-231 [76]. In vitro co-exposure using Fc with cisplatin, tamoxifen, or paclitaxel, potentiated the effect of the drug in MCF7 and MDA-MB-231 [73]. Moreover, case studies have shown that the use of Fc as alternative medicine in mouse models and human clinical trials seems to alleviate the side effects of anticancer chemotherapy [70].

Lm is a water-soluble polysaccharide, corresponding to a storage glucan. Glucans are Food and Drug Administration approved compounds for lowering cholesterol levels [77] and they have been described to promote anticancer immunity [78]. Evidence have shown that Lm has anticancer activity in HT 29 human colon cells by inducing apoptosis in a dose-dependent way [77,79], and also lead to apoptosis through mitochondrial pathway in human colon cancer cell line LoVo [80]. Laminarins and their sulphated derivatives inhibited proliferation [81], colony formation, and migration in several human cell lines including BC ones [82].

### 1.3. Sterols—Fucosterol (Fct)

Phytosterols represent a class of cholesterol-like molecules that integrate the cellular membranes of plants and algae, having a role in the regulation of membrane permeability [83]. Fct has been mentioned as anti-inflammatory, antibacterial, antifungal, antidiabetic, antidepressant, anticancer, antioxidant, and protective against a wide range of diseases [84,85]. Fct had a cytotoxic effect in T47D breast cell line [86], induced mitochondrial-mediated apoptosis, migration, inhibition, and downregulation of m-TOR/PI3K/Akt signalling pathway in MCF7 [87]. Fct containing fractions presented cytotoxicity against human colon and BC cell line (T47D), without inducing cytotoxic effects on the normal cell line [86], and also reduced cell proliferation and induced apoptosis in MCF7 and MDA-MB-231 cell lines but these effects were not so evident in the non-tumoral cell line CHO [88].



#### 1.4. Phlorotannins–Phloroglucinol (Phg)

Phg is a polyphenolic compound whose chemical structure includes an aromatic phenyl ring with three hydroxyl groups. Its biological activities include antioxidant and anti-inflammatory actions [89,90]. The former seems to be related to free radical-scavenging and metal chelation properties. Phg induced cytotoxicity through caspases activation in MDA-MB-231 BC cell line [91] and suppressed metastasis in invasion assays with the same cell line [92]. Additionally, in assays with BC cell lines, Phg suppressed sphere formation, anchorage-independent colony formation and *in vivo* tumorigenicity, and decreased the cancer stem cell population [92].

As reference anticancer drugs, we chose two drugs used for treating many cancer types, including BC [93,94]: (i) cisplatin (Cis), an alkylating agent that damage the structure of DNA through the crosslinking forming platinum-DNA adducts that interfere with DNA transcription and replication, resulting in cell death; and (ii) doxorubicin (Dox), an anthracycline antibiotic with no completely clear mechanisms of action, but it has been reported to cause oxidative stress and block RNA transcription by intercalation into DNA bases [95]. Both are highly effective drugs, but with associated side effects and drug resistance [96–98]. Cis can cause nephrotoxicity, neurotoxicity and hearing impairments [96]. Dox is vastly used in BC adjuvant and neoadjuvant chemotherapy [99], but it also elicits cardiotoxicity, secondary leukaemia, myelosuppression, intestinal epithelium lesions, and chemotherapy-related infertility [100].

In view of the above, this study aimed to evaluate the cytotoxic activity of the seaweed bioactive compounds Asta, Fc, Fct, Lm, and Phg, alone or combined with Cis and Dox, in three BC cell lines and one non-tumorous breast line, in monolayer culture (2D). The most promising combination of seaweed compound plus drug in monolayer was chosen to be investigated as to viability and proliferation, using a comparative approach with two *in vitro* systems (2D-monolayers versus 3D-MCAs).

## 2. Materials and Methods

### 2.1. Cell Lines and Baseline Culture Conditions

MCF7 was acquired from the European Collection of Authenticated Cell Cultures (ECACC). SKBR3 cell line was kindly provided by Professor Carmen Jerónimo (Portuguese Oncology Institute–Porto, Portugal). MCF12A and MDA-MB-231 cell lines were purchased from the American Tissue Culture Collection (ATCC). MCF7, MDA-MB-231, and SKBR3 were cultivated in high glucose Dulbecco's modified Eagle's medium (DMEM), without glutamine and phenol red, supplemented with 10% Fetal Bovine Serum (FBS) and 1% antibiotics solution penicillin/streptomycin (pen/strep) (10,000 U/mL/10,000 µg/mL, respectively). MCF12A was cultivated in DMEM/Ham's Nutrient Mixture F12 (DMEM/F12) medium without phenol red and supplemented with 20 ng/mL human epidermal growth factor (hEGF), 100 ng/mL cholera toxin, 0.01 mg/mL insulin, 500 ng/mL hydrocortisone, 10% FBS, and 1% of the same antibiotic solution. All cell lines were cultivated in T75 cm<sup>2</sup> culture flasks (Orange Scientific, Braine-l'Alleud, Belgium) and maintained in the incubation chamber MCO 19AIC (Sanyo, Tokyo, Japan), with 5% CO<sub>2</sub>, at 37 °C. For cells' growth and maintenance, the culture medium was replaced every two days. Cells were regularly observed using an inverted phase-contrast microscope CKX41 (Olympus, Tokyo, Japan). The experiments were performed with cells under passage number 30. At 80% of cell confluence, monolayer cells were subcultured using trypsin/ethylenediamine tetraacetic acid (EDTA) (trypsin/EDTA) solution (0.25/0.02 in %).

### 2.2. Chemicals and Solutions

Dimethyl sulfoxide (DMSO) was purchased from VWR Chemicals (Solon, OH, USA). 3-(4,5-Dimethyl-2-thiazolyl)-2,5-diphenyl-2H-tetrazolium bromide (MTT), astaxanthin (SML0982, CAS Number: 472-61-7, MW: 596.84), fucoidan (F8190, CAS Number: 9072-19-9, MW: not determined by the supplier); fucosterol (F5379, CAS Number: 17605-67-3, MW: 412.69), laminarin (L9634, CAS Number: 9008-22-4, MW: not determined by the supplier);

phloroglucinol (79,330, CAS Number: 108-73-6, MW:126.11), cisplatin (C2210000, CAS Number: 15663-27-1; MW:300.05), doxorubicin (D1515, CAS Number: 25316-40-9, MW: 579.98); insulin (I2643); cholera toxin (C8052), hydrocortisone (H088), and hEGF (E9644) were obtained from Sigma Aldrich (St.Louis, MO, USA). DMEM (F045), FBS, pen/strep, trypsin/EDTA, were acquired from Biochrom KG (Berlin, Germany). DMEM/F12 was obtained from GE Healthcare (Chicago, IL, USA). Resazurin (14,322) was purchased from Cayman (AnnArbor, MI, USA). Cell Proliferation ELISA and BrdU (5'-bromo-2'-deoxyuridine) kit (colorimetric) were acquired from Roche (Basel, Switzerland). All other reagents and chemicals used were analytical grade.

Stock solutions of astaxanthin (Asta), fucosterol (Fct), phloroglucinol (Pgh), and doxorubicin (Dox) were prepared in DMSO, while those of fucoidan (Fc) and laminarin (Lm) were prepared in supplemented cell culture medium. All those stock solutions were kept at  $-20\text{ }^{\circ}\text{C}$  until used, except for the stock solutions of Fc and Lm that were prepared immediately before use. The stock solution of cisplatin (Cis) was prepared in a 0.9% NaCl solution and kept at  $4\text{ }^{\circ}\text{C}$  up to 1 month. Exposure solutions were prepared immediately before each experiment by diluting the stock solutions into the appropriate volume of respective fresh culture medium ensuring a final concentration of 0.1% DMSO.

### 2.3. Cell Exposures

#### 2.3.1. Study Design

The study was performed in three phases according to a consecutive set of experiments (Figure 1). In Phase 1, it was performed a screening of the cytotoxic effects of five selected bioactive seaweed compounds (Asta, Fc, Fct, Lm, and Pgh) and the two reference drugs (Cis and Dox). Each compound and drug were tested at five concentrations (Table 1). In Phase 2, two concentrations of each compound used in Phase 1 were selected to be tested in combination (seaweed compound + reference drug). The selected combinations are described in Table 2. In Phases 1 and 2, the screenings were performed in the panel of breast cell lines (MCF7, SKBR3, MDA-MB-231, and MCF12A), cultured in monolayer, and the cytotoxic effects were assessed by MTT assay. The most promising combination obtained in Phase 2 moved to Phase 3. That combination corresponded to the mixture that presented not only a statistically significant cytotoxic effect but also the highest % of reduction of cell viability when compared with the respective isolated compounds. Additionally, higher concentrations of the reference drug were introduced in Phase 3 to guarantee there was a positive control with cytotoxic effects in 3D. At Phase 3, other assays besides MTT were performed: resazurin and BrdU assay for assessing cytotoxic and cell proliferation effects, respectively. Also, the same conditions were tested simultaneously in monolayer (2D) and in 3D cultures for comparison purposes, and a morphological analysis of the 3D cultures was performed.

#### 2.3.2. Exposures (Single or Combination) in Monolayer

Cells were seeded at the density of  $0.05 \times 10^6$  cells/mL,  $100\text{ }\mu\text{L}$ /well, and incubated for 24 h for cell attachment. Then the culture medium was removed, and cells were exposed to the tested conditions for 72 h. At the end of the exposure period, respective cell viability or proliferation assays were performed, according to the phase of the study. Tested concentrations of seaweed bioactive compounds and reference drugs used in the screening of Phase 1 are detailed in Table 1.

Prior to the exposures, the different solvent controls (medium; medium with 0.1% DMSO; and medium with 0.0009% NaCl) were tested in the four cell lines, using MTT to evaluate the effects on cell viability. Four independent methodological experiments (with triplicates per each experiment) were performed and no significant differences among solvents were found (data not shown). For this reason, we opted for using the most common one for the set of compounds—medium with 0.1% DMSO—as the solvent control in all experiments.

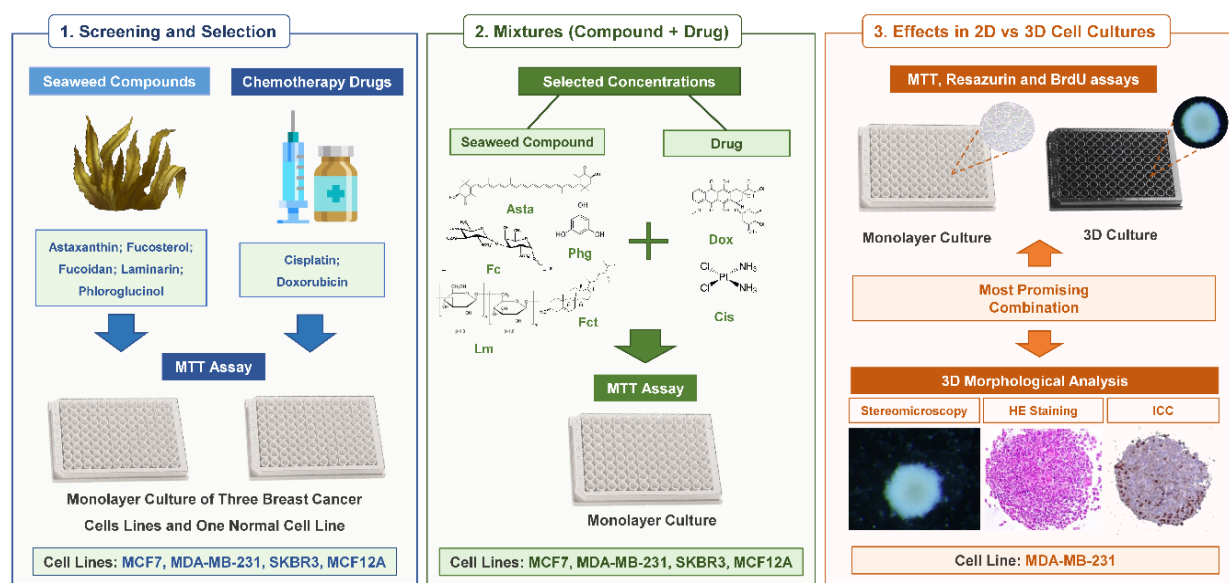


**Figure 1.** Schematic representation of the study design.

**Table 1.** Tested concentrations of bioactive seaweed compounds and reference drugs

Chemicals	Tested Concentrations
Astaxanthin	1; 10; 50; 100 and 200 $\mu\text{M}$
Fucoidan	10; 50; 100; 500 and 1000 $\mu\text{g/mL}$
Fucosterol	1; 2.5; 5; 7.5 and 10 $\mu\text{M}$
Laminarin	10; 50; 100; 500 and 1000 $\mu\text{g/mL}$
Phloroglucinol	10; 50; 100; 500 and 1000 $\mu\text{M}$
Cisplatin	0.1; 1, 10, 20 and 50 $\mu\text{M}$
Doxorubicin	0.001; 0.01; 0.1; 1 and 2 $\mu\text{M}$

Regarding the selection of the concentrations to be tested in combination (Phase 2), we opted to use those that did not have a statistically significant effect on the cell viability of the tested cell lines or, in the case of the reference drugs, concentrations that did not reduce the cell viability below (in mean) 50%. These criteria were considered for each cell line. The selected combinations tested in Phase 2 are presented in Table 2.

**Table 2.** Concentrations of bioactive seaweed compounds and reference drugs used for combinations

Seaweed Compound	Drug	Dox ( $\mu\text{M}$ )			Cis ( $\mu\text{M}$ )		
		0.01	0.1	1	1	10	20
Asta ( $\mu\text{M}$ )	10						
	20						
Fc ( $\mu\text{g/mL}$ )	10						
	50	MCF7 SKBR3	MCF7 SKBR3	MDA-MB-231	MCF12A	MCF7 SKBR3	MCF7 SKBR3
Fct ( $\mu\text{M}$ )	1	MCF12A	MDA-MB-231 MCF12A	MDA-MB-231	MCF12A	MDA-MB-231 MCF12A	MDA-MB-231
	5						
Lm ( $\mu\text{g/mL}$ )	10						
	50						
Phg ( $\mu\text{M}$ )	10						
	50						

Asta: Astaxanthin; Fc: Fucoidan; Fct: Fucosterol; Lm: Laminarin; Phg: Phloroglucinol.

### 2.3.3. Exposures (Single or Combined) in 3D Cultures—Multicellular Aggregates (MCAs)

Cells were seeded in 96-well ultra-low attachment U-shaped spheroid plates (Corning, NY, EUA) at a density of  $40 \times 10^4$  cells/mL, 200  $\mu$ L/well. Plates were then centrifuged in a centrifuge Rotina 380 R (Hettich, Vlotho, Germany) at  $200 \times g$  for 10 min and placed in the incubator at 37 °C and 5% CO<sub>2</sub> for 72 h to promote the MCAs formation. Then MCAs were incubated with the tested conditions for 96 h of exposure. After exposure, cell viability and proliferation assays as well as morphological analysis were performed.

## 2.4. Cell Viability Assessment

### 2.4.1. MTT Assay

Cytotoxic effects of the tested conditions were assessed by MTT reduction assay. In short, 10  $\mu$ L (monolayer) or 20  $\mu$ L (3D) of MTT stock solution was added to each well, and incubated for 2 h (monolayer) and 4 h (3D), at 5% CO<sub>2</sub> at 37 °C. At the end of the incubation period, MCAs must be transferred from the 96-well ULA plates to flat-bottom 96-well plates with the help of a P1000 micropipette with a cut tip. Exposure medium was then aspirated, and formazan crystals were dissolved by adding 100  $\mu$ L of DMSO:ethanol solution (1:1) (*v/v*) (monolayer) or 150  $\mu$ L of DMSO (3D). Plates were left for 15 min under mild agitation to promote total formazan salt dissolution. Absorbance was measured at 570 nm in a microplate reader Multiskan GO (Thermo Fisher Scientific, Waltham, MA, USA). Results are expressed as percentage of cell viability and were calculated based on the absorbance ratio between treated conditions and the untreated control (cells incubated with culture medium with 0.1% (*v/v*) of DMSO). In both situations (tested condition and control), the absorbance of respective mediums without cells was subtracted in each situation to eliminate interferences related to the compounds or drugs.

### 2.4.2. Resazurin Assay

For resazurin assay, 1  $\mu$ L (monolayer) or 2  $\mu$ L (3D) of stock resazurin was added to each well. Plates were incubated for 3 h (monolayer) and 4 h (3D), with 5% CO<sub>2</sub> and at 37 °C. Similarly, to what was performed for the MTT assay, MCAs and respective mediums were transferred to flat-bottom 96-well plates. Fluorescence was then read using excitation wavelength at 560 nm and emission wavelength at 590 nm in the plate reader Synergy H1 (Biotek, Winooski, VT, USA). Results are expressed as a percentage of cell viability in relation to control and were calculated based on the fluorescence ratio between treated conditions and the untreated control (cells incubated with culture medium with 0.1% (*v/v*) of DMSO). In both situations (tested condition and control), the fluorescence of respective mediums without cells was subtracted in each situation to eliminate interferences related to the compounds or drugs.

## 2.5. Cell Proliferation Assessment—BrdU Assay

Effects on cell proliferation were evaluated by BrdU assay (Roche, Basel, Switzerland). For monolayer, the assay was performed according to the manufacturer's instructions. Briefly, cells were labeled with BrdU at a final concentration of 10  $\mu$ M/well and incubated for 4 h at 37 °C, 5% CO<sub>2</sub>. Labeling medium was removed, and cells were stored at 4 °C overnight. Following the protocol, cells were fixed, and DNA denatured by the adding of 100  $\mu$ L of FixDenant reagent (30 min). After removing the FixDenant Reagent, BrdU incorporation into cellular DNA was detected with mouse anti-BrdU conjugated with peroxidase working solution (diluted 1:100) (100  $\mu$ L/well) for 90 min. Wells were rinsed with washing solution and 100  $\mu$ L of substrate solution was added, to perform photometric detection. After 25 min, absorbances were immediately measured at 370 nm in a microplate reader Multiskan GO (Thermo Fisher Scientific, Waltham, MA, USA).

For 3D culture some alterations were implemented. Briefly, after MCAs exposure, 100  $\mu$ L of each well medium was removed, and then MCAs were incubated with 10  $\mu$ L of BrdU labelling solution (final concentration = 10  $\mu$ M BrdU) for 5 h, at 37 °C, 5% CO<sub>2</sub>. Then, MCAs were transferred into a flat-bottom 96-well microplate and following the removal of

the labelling medium, they were kept overnight at 4 °C. The following steps are identical to the monolayer protocol.

Results are expressed as a percentage of cell proliferation in relation to the control and were calculated based on the absorbance ratio between treated conditions and the untreated control (cells incubated with culture medium with 0.1% (*v/v*) of DMSO).

## 2.6. Cell Morphology Assessment

### 2.6.1. Monolayer

The plates containing the monolayer cultures were observed photographed using a phase-contrast inverted microscope CX41 (Olympus, Tokyo, Japan).

### 2.6.2. 3D-MCA Measurements

A total of 16 MCAs per tested condition/independent experiment were photographed at the end of the exposure time, using a stereomicroscope with darkfield SZX10 (Olympus, Tokyo, Japan), equipped with a digital camera DP21 (Olympus, Tokyo, Japan). The MCA areas were analyzed using the freeware AnaSP [101].

### 2.6.3. Histological Analysis

#### MCA Histological Processing

At the end of exposure time, MCAs were collected to Eppendorf tubes with 10% buffered formalin (Bioptica, Milan, Italy) for fixation (24 h). For histological processing, MCAs were embedded in histogel (Thermo Scientific, MA, USA), according to manufacturer's instructions. The following processing protocol consisted in dehydration-1 h in a crescent series of ethanol (70%, 90%, 95%, and two absolute); clearing-1 h in each reagent: xylene: absolute ethanol (1:1); xylene (twice); and infiltrating in liquid paraffin (1 h twice). Paraffin blocks were obtained in an embedding station EG 1140H (Leica, Nussloch Germany). Sections (3 µm) were performed in a microtome RM2255 (Leica, Nussloch Germany) and placed onto silane treated KP-frost slides (Klinipath, Duiven, The Netherlands). Slides were placed at 60 °C for 20 min, and then kept overnight at 37 °C.

#### Hematoxylin-Eosin (HE) Staining

Sections were deparaffinized in xylene and hydrated following the descendent sequence of ethanol (absolute, 95%, 70%), running tap water, 5 min each. Nuclei were stained with Mayer's hematoxylin (Merck, Darmstadt Germany) for 3 min, and then slides were washed to remove dye excess. Following the protocol, sections were stained with 1% eosin Y for 5 min (Merck, Darmstadt, Germany). Lastly, slides were dehydrated in ethanol (95%, 100%, 100%), 5 min each, cleared in xylene (2 × 5 min), and mounted with the medium Q Path® Coverquick 2000 (VWR Chemicals, Briari, France).

#### Immunocytochemistry (ICC)

For ICC, sections were deparaffinized and hydrated as described above. Heat antigen retrieval was made by sections immersion in citrate buffer 0.01 M, pH 6.0, using a pressure cooker (3 min after reaching maximum pressure). Slides were then allowed to cool, and then endogenous peroxidase blocking was performed with 3% hydrogen peroxide in methanol (10 min). After two washes in Tris saline buffer pH 7.6 (TBS) (5 min each), unspecific reactions were blocked using the appropriate reagent of the kit Novolink™ Polymer detection (Leica Biosystems, Milton Keynes, UK) (5 min), followed by two washes in TBST (TBS with 0.05% of Tween 20). Primary antibodies were diluted in phosphate buffer saline with 5% of bovine albumin serum and incubated 2 h at room temperature. For negative control, the primary antibody was substituted by the antibody diluent solvent only. Two primary antibodies were applied: rabbit monoclonal anti-Ki67, clone SP6 (Biocare Medical, USA) as cell proliferation marker [102,103], dilution 1:200, and rabbit polyclonal anti-caspase-3, ab 13,847 (Abcam, UK), diluted 1:5000 for assessing caspase dependent apoptosis [104,105]. Novolink™ Polymer detection system was used for signal amplification and revelation,

according to manufacturer's instructions, using the chromogen 3,3'-Diaminobenzidine (DAB). Nuclear counterstain was obtained using Mayer's hematoxylin (2 min). Lastly, slides were washed, dehydrated, and mounted, then photographed as described before.

### 2.7. Statistical Analysis

Descriptive and inferential statistics were performed using Past3 (version 3.19) free software (<https://folk.universitetetioslo.no/ohammer/past/>) and GraphPad Prism 6.0 software (GraphPad Software, La Jolla, CA, USA). The normality and homogeneity of variance were confirmed by the Shapiro–Wilk and the Levene tests, respectively. The results are expressed as mean + standard deviation, except for the MCAs areas that were presented in median, maximum, minimum, and interquartile range (Q3–Q1), from at least five to six independent experiments (triplicate per each experiment). Significant differences ( $p < 0.05$ ) were assessed by one-way ANOVA, followed by the post-hoc Holm–Šidák multiple comparison test. On selected cases, the significance of the difference between two groups of interest was tested with the Student's *t*-test and using the sequential Holm–Bonferroni correction; the latter was implemented via a freeware spreadsheet calculator [106,107].

## 3. Results

### 3.1. Cytotoxic Effect of Seaweed Bioactive Compounds

Cytotoxic effects of seaweed compounds were assessed by the MTT assay after 72 h of incubation in cultured monolayers. Figure 2 shows the results obtained for tested compounds in cellular viability. Asta was the only compound that had no effects on the cell viability in all used cell lines (Figure 2a). The polysaccharides Fc and Lm promoted a similar result since both only had cytotoxic effects in the non-tumoral cell line MCF-12A at the highest concentration (1000 µg/mL) (Figure 2b,d). Fct was the compound with more cytotoxic effects. It significantly decreased cell viability in SKBR3 (at 2.5 µM), and in SKBR3 and MDA-MB-231 cell lines (at 7.5 µM). At 10 µM it also decreased the cellular viability of the other BC cell line MCF7, however not affecting MCF12A cell line (Figure 2c). Phg decreased cell viability in MCF7 (at 500 µM and 1000 µM) and in MDA-MB-231 cell lines (at 1000 µM) (Figure 2e).

### 3.2. Cytotoxic Effect of the Reference Drugs—Cisplatin and Doxorubicin

Five crescent concentrations were used to assess the cytotoxic effects of Dox and Cis in the panel of breast cell lines, and the effects on cell viability were assessed by the MTT assay.

Considering Cis exposure (Figure 3a), the non-tumoral cell line (MCF12A) was the most susceptible to this drug, being the only cell line that showed a statistically significant reduction on cell viability when cells were exposed to Cis at 1 µM, inducing then a concentration-dependent response. In contrast, MCF7, only showed significant differences in cell viability at Cis (20 µM and 50 µM), while SKBR3 and MDA-MB-231 were still more refractive to Cis action, with a lowering trend at 20 µM that reached significance at 50 µM. At the latter concentration, all cell lines had their cell viability decreased below 50%, in relation to the control.

In relation to Dox cytotoxicity, this drug started to significantly reduce the viability of SKBR3 and MCF12A at 0.1 µM, while for the other two cell lines this effect was only observed at Dox 1 µM and 2 µM. At 1 µM, a reduction in cell viability below 50%, in relation to the control, was observed in all cell lines (Figure 3b).



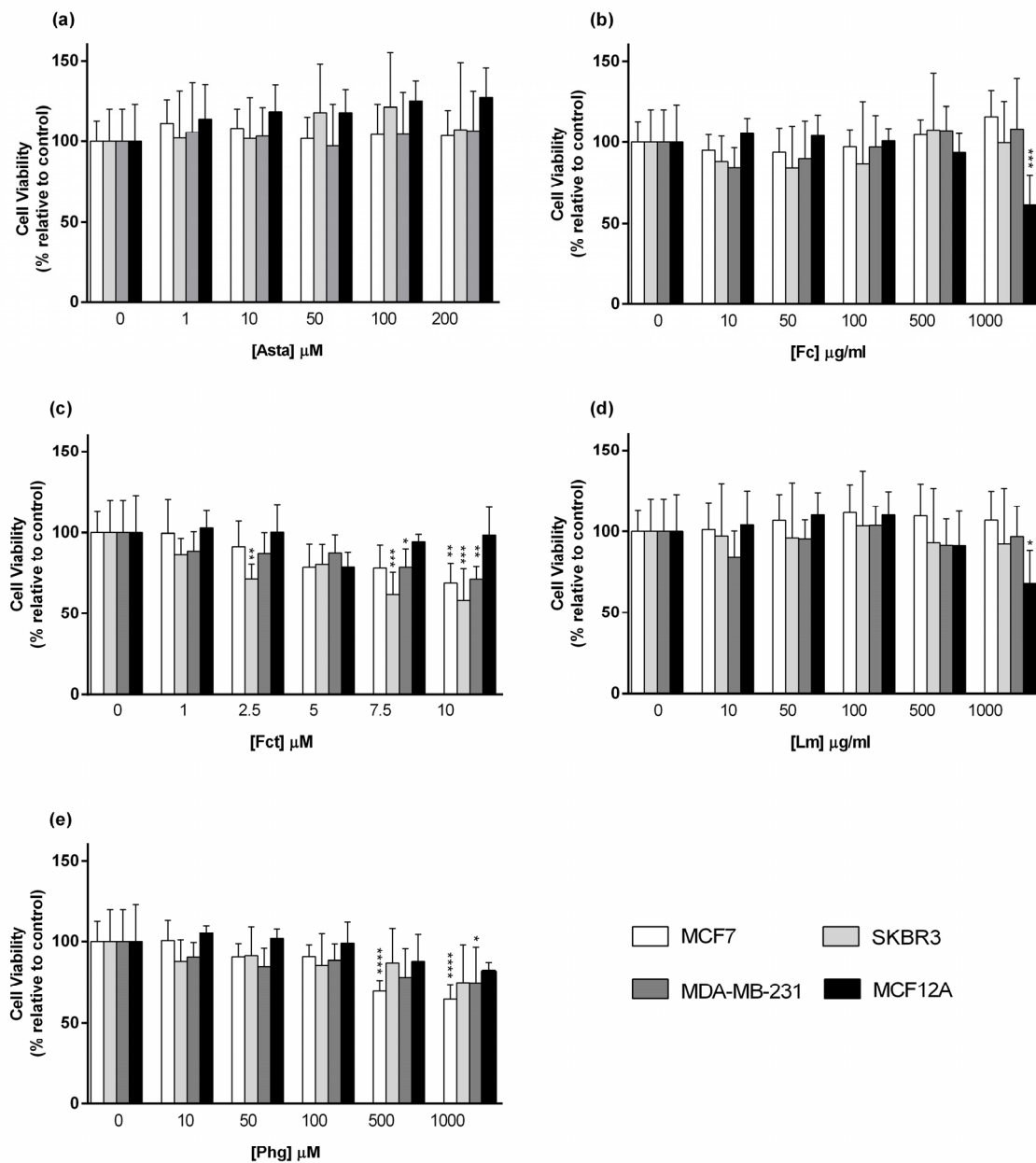


**Figure 2.** Cytotoxic effect of (a) Astaxanthin (Asta), (b) Fucoidan (Fc), (c) Fucosterol (Fct), (d) Laminarin (Lm), and (e) Phloroglucinol (Phg) assessed by MTT assay after 72 h of exposure in the panel of breast cell lines cultured in monolayer. Control corresponds to cells with medium containing 0.1% DMSO. The percentages of cell viability are relative to the controls and presented as mean + standard deviation of six independent experiments (each in triplicate). (\*  $p < 0.05$ , \*\*  $p < 0.01$ , \*\*\*  $p < 0.001$ , \*\*\*\*  $p < 0.0001$ ).

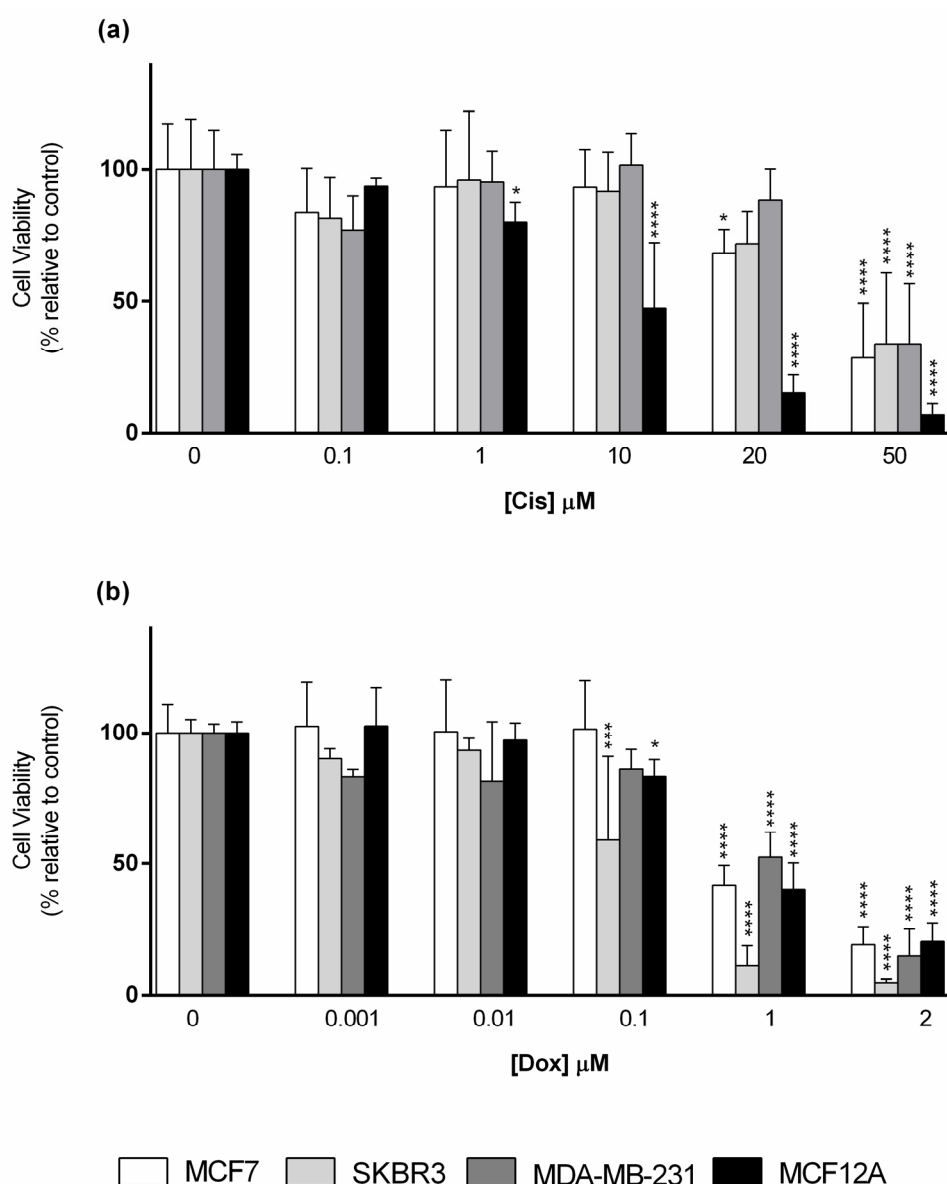


**Figure 3.** Cytotoxic effect of (a) Cisplatin (Cis); (b) Doxorubicin (Dox) assessed by the MTT assay after 72 h of exposure in the panel of breast cell lines cultured in monolayer. Control corresponds to cells incubated with medium containing 0.1% DMSO. The percentages of cell viability are relative to the controls and presented as mean + standard deviation of six independent experiments (each in triplicate). (\*  $p < 0.05$ , \*\*\*  $p < 0.001$ , \*\*\*\*  $p < 0.0001$ ).

### 3.3. Cytotoxic Effect of Selected Combinations of Seaweed Bioactive Compound Plus Reference Drug

In vitro cytotoxic effects of the five seaweed compounds combined with the two reference drugs were assessed by the MTT assay in the panel of BC cell lines. For that, two concentrations of each seaweed compound and two concentrations of each drug were selected for the combination according to the criteria mentioned in Section 2.3.2.

For MCF7 cell line (Figure 4), Cis alone at tested conditions (10 and 20  $\mu\text{M}$ ) decreased cell viability in a concentration-dependent manner. Among the tested seaweed compounds, only Asta was able to reduce the effect of Cis. This happened when cells were exposed to Cis (10  $\mu\text{M}$ ) in combination with Asta (10 and 20  $\mu\text{M}$ ) (Figure 4a).



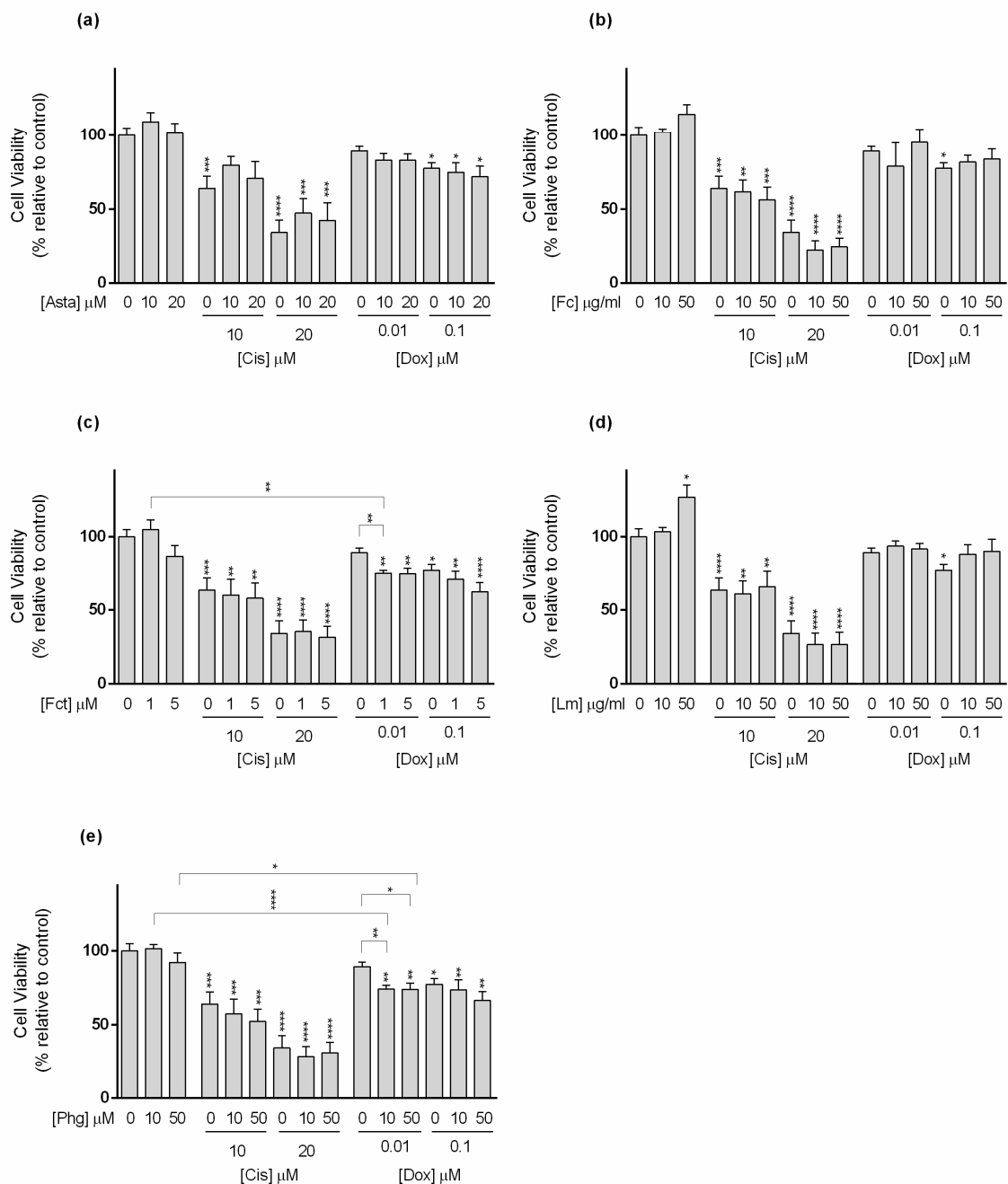


**Figure 4.** Cytotoxic effects of the combination of (a) Astaxanthin (Asta); (b) Fucoidan (Fc); (c) Fucosterol (Fct); (d) Laminarin (Lm); (e) Phloroglucinol (Phg) with the reference drugs cisplatin (Cis) and doxorubicin (Dox) assessed by the MTT the assay after 72 h of exposure in MCF7 cell line cultured in monolayer. Control corresponds to cells incubated with medium containing 0.1% DMSO. The percentages of cell viability are relative to the control and presented as mean + standard deviation of six independent experiments (each in triplicate). Square brackets indicate *t* tests with Sequential Bonferroni corrections. (\*  $p < 0.05$ , \*\*  $p < 0.01$ ; \*\*\*  $p < 0.001$ , \*\*\*\*  $p < 0.0001$ ).

Still in MCF7 cells, only Dox at 0.1 μM significantly decreased cell viability. Nevertheless, Dox (0.01 μM) alone did not show effects on cell viability, but when combined with Fct (1 and 5 μM), and Phg (10 and 50 μM) (Figure 4c,e, respectively), it significantly affected MCF7 cells' viability. Dox (0.01 μM) did not differ from the control, but in combination, cell viability decreased by  $\approx 15\%$  when compared to the drug alone, differing from the control. However, in the case of the combination of Dox (0.01 μM) plus Fct (5 μM), viability did not differ from the Fct alone. In the case of Fc and Lm in combination with Dox (0.1 μM), the

effect was the opposite, and the combination decreased the cytotoxic effect induced by the Dox alone (Figure 4b,d). In line with this result, cells exposed to Lm (50  $\mu\text{M}$ ) presented significantly higher cell viability than the control (Figure 4d).

Regarding the SKBR3 line (Figure 5), Cis alone reduced cell viability at the tested concentrations. As to the combinations, the following conditions: Cis (10  $\mu\text{M}$ ) plus Asta (10 and 20  $\mu\text{M}$ ), Fc (10  $\mu\text{M}$ ), and Lm (10 and 50  $\mu\text{M}$ ), decreased the cytotoxicity of the drug not differing from the control. However, the combination Cis (10  $\mu\text{M}$ ) with Fc (50  $\mu\text{M}$ ) decreased cell viability to a percentage that statistically differed from the drug and Fc alone (Figure 5b). This combination enhanced the cytotoxic effect of Cis in  $\approx 28\%$ . Nonetheless, in the combination of Dox at 0.1  $\mu\text{M}$  with Fct (1 and 5  $\mu\text{M}$ ), and Phg (10 and 50  $\mu\text{M}$ ), the cell viability differed from the control, not differing from the drug nor the compound alone (Figure 5c,e).

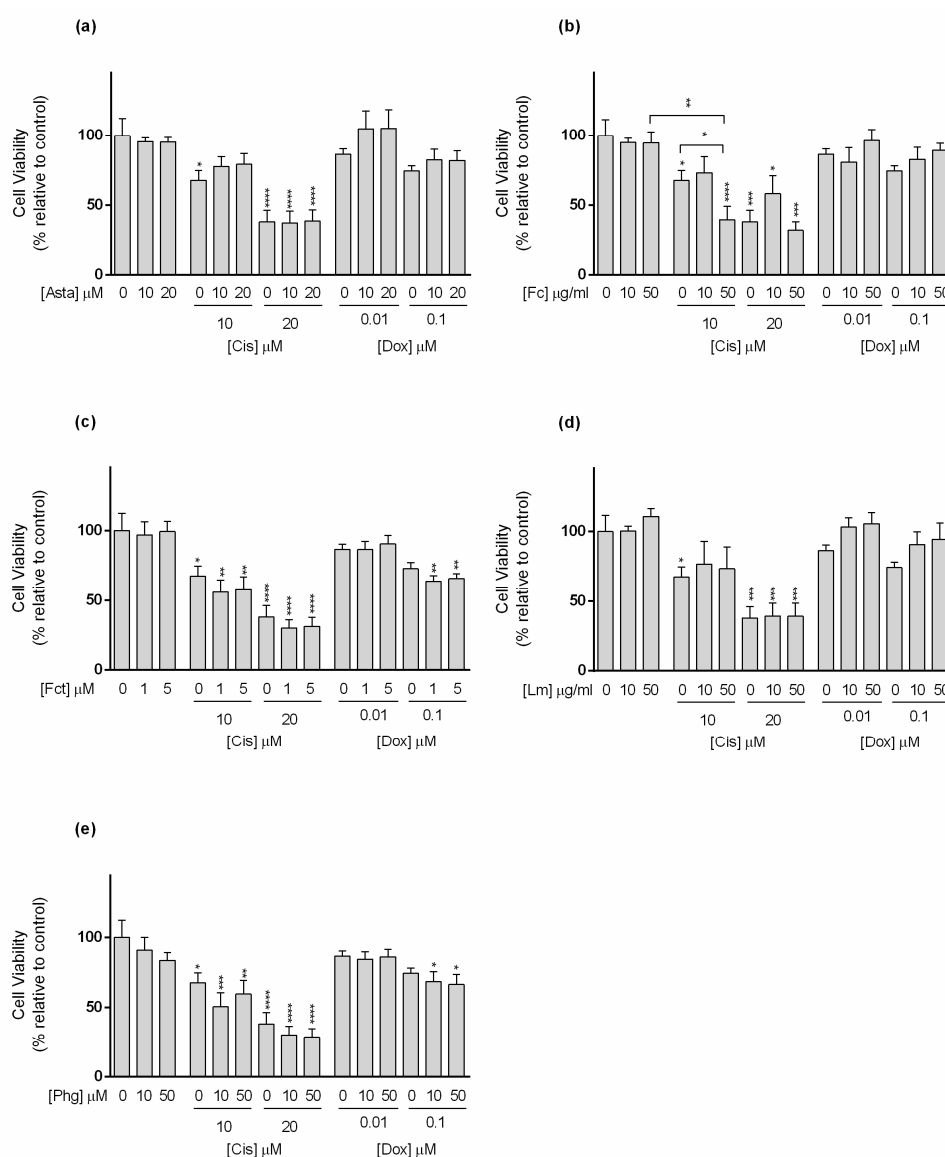


**Figure 5.** Cytotoxic effects of the combination of (a) Astaxanthin (Asta); (b) Fucoidan (Fc); (c) Fucosterol (Fct); (d) Laminarin (Lm); (e) Phloroglucinol (Phg) with the reference drugs cisplatin (Cis) and doxorubicin (Dox) assessed by the MTT assay after 72 h of exposure in SKBR3 cell line cultured in monolayer. Control corresponds to cells incubated with medium containing 0.1% DMSO. The percentages of cell viability are relative to the control and presented as mean + standard deviation of six independent experiments (each in triplicate). Square brackets indicate *t* tests with Sequential Bonferroni corrections. (\*  $p < 0.05$ , \*\*  $p < 0.01$ ; \*\*\*  $p < 0.001$ , \*\*\*\*  $p < 0.0001$ ).

With reference to the TNBC cell line MDA-MB-231 (Figure 6), Cis (10 and 20  $\mu\text{M}$ ) alone did not present significant differences in cell viability in relation to the control. Conversely, when in the following combinations Cis 20  $\mu\text{M}$  plus Fc (10 and 50  $\mu\text{g}/\text{mL}$ ), Lm (10 and 50  $\mu\text{g}/\text{mL}$ ), and Phg (10 and 50  $\mu\text{M}$ ), cell viability significantly decreased relative to control, with a reduction between 13 and 17%, but did not differ statistically from the drug alone (Figure 6b,d,e).

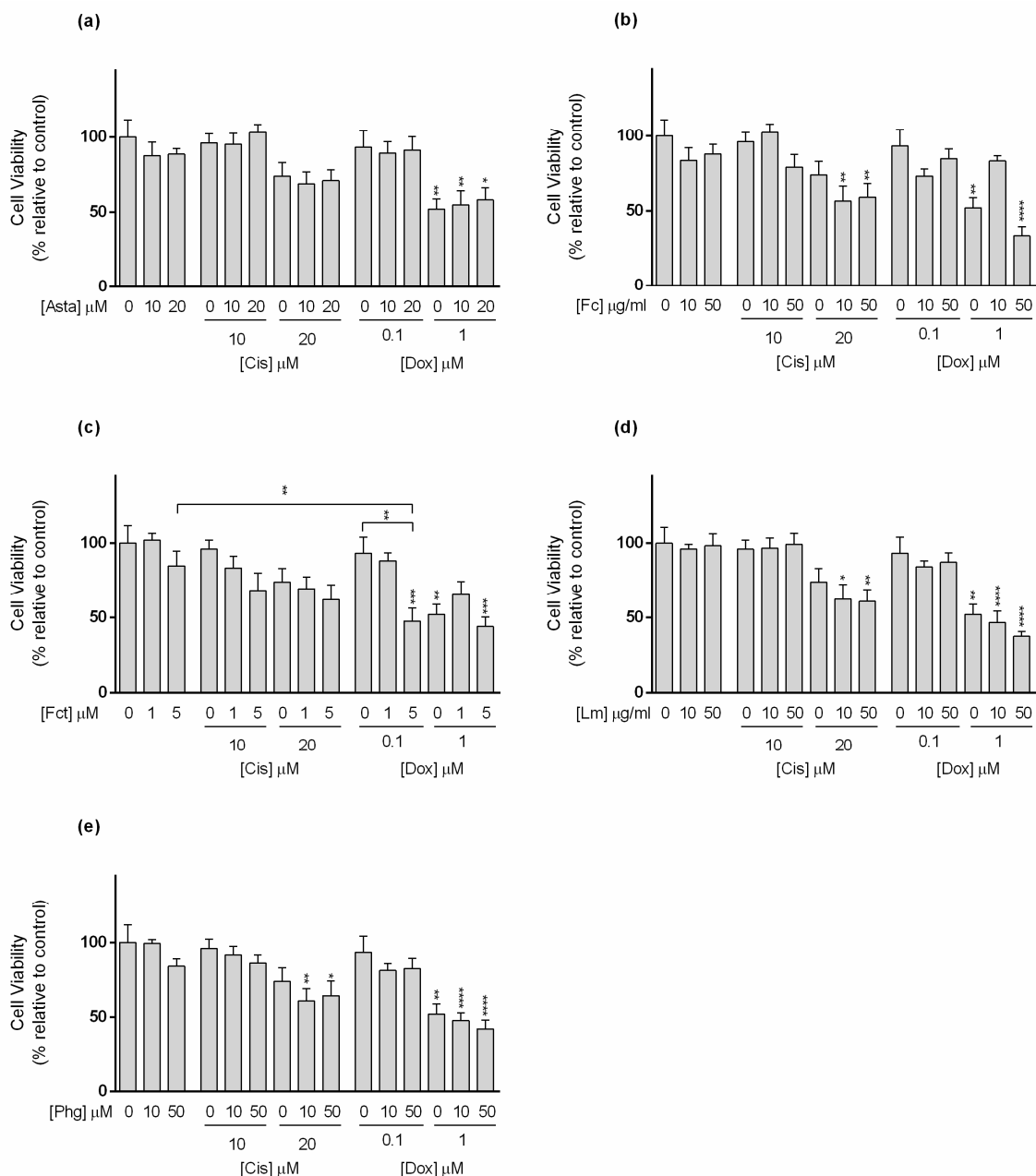


**Figure 6.** Cytotoxic effects of the combination of (a) Astaxanthin (Asta); (b) Fucoidan (Fc); (c) Fucosterol (Fct); (d) Laminarin (Lm); (e) Phloroglucinol (Phg) with the reference drugs cisplatin (Cis) and doxorubicin (Dox) assessed by the MTT assay after 72 h of exposure in MDA-MB-231 cell line cultured in monolayer. Control corresponds to cells incubated with medium containing 0.1% DMSO. The percentages of cell viability are relative to the control and presented as mean + standard deviation of six independent experiments (each in triplicate). Square brackets indicate *t* tests with Sequential Bonferroni corrections. (\*  $p < 0.05$ , \*\*  $p < 0.01$ ; \*\*\*  $p < 0.001$ , \*\*\*\*  $p < 0.0001$ ).

In relation to Dox, alone at 1  $\mu\text{M}$ , it negatively affected cell viability. When combined with Fc (10  $\mu\text{g}/\text{mL}$ ) and Fct (1  $\mu\text{M}$ ), Dox at 1  $\mu\text{M}$  seemed to have lost its action, while in

combination with Fc (50  $\mu\text{g}/\text{mL}$ ) and Fct (5  $\mu\text{M}$ ) its effects were maintained (Figure 6b,c). The combination differing from control and with the most evident impact in cell viability, when compared to either to the compound or to the drug alone, was Dox (0.01  $\mu\text{M}$ ) with Fct (5  $\mu\text{M}$ ), which increased Dox cytotoxicity in  $\approx 46\%$ .

In relation to MCF12A cell line (Figure 7), Cis (1 and 10  $\mu\text{M}$ ) alone decreased cell viability in relation to control. The combination of Cis 1  $\mu\text{M}$  with Asta (10 and 20  $\mu\text{M}$ ), Fct (5  $\mu\text{M}$ ), Lm (50  $\mu\text{g}/\text{mL}$ ), and Phg (10 and 50  $\mu\text{M}$ ), caused the loss of statistical significance found in the drug alone. At 10  $\mu\text{M}$ , Cis alone and all the combinations showed cell viability of less than 50% in relation to the control. Regarding Dox, only the highest tested concentration (0.1  $\mu\text{M}$ ) showed a significant effect on cell viability, however, in this cell line, it occurred the loss of statistical effect in combination with all tested seaweed compounds (Figure 7).

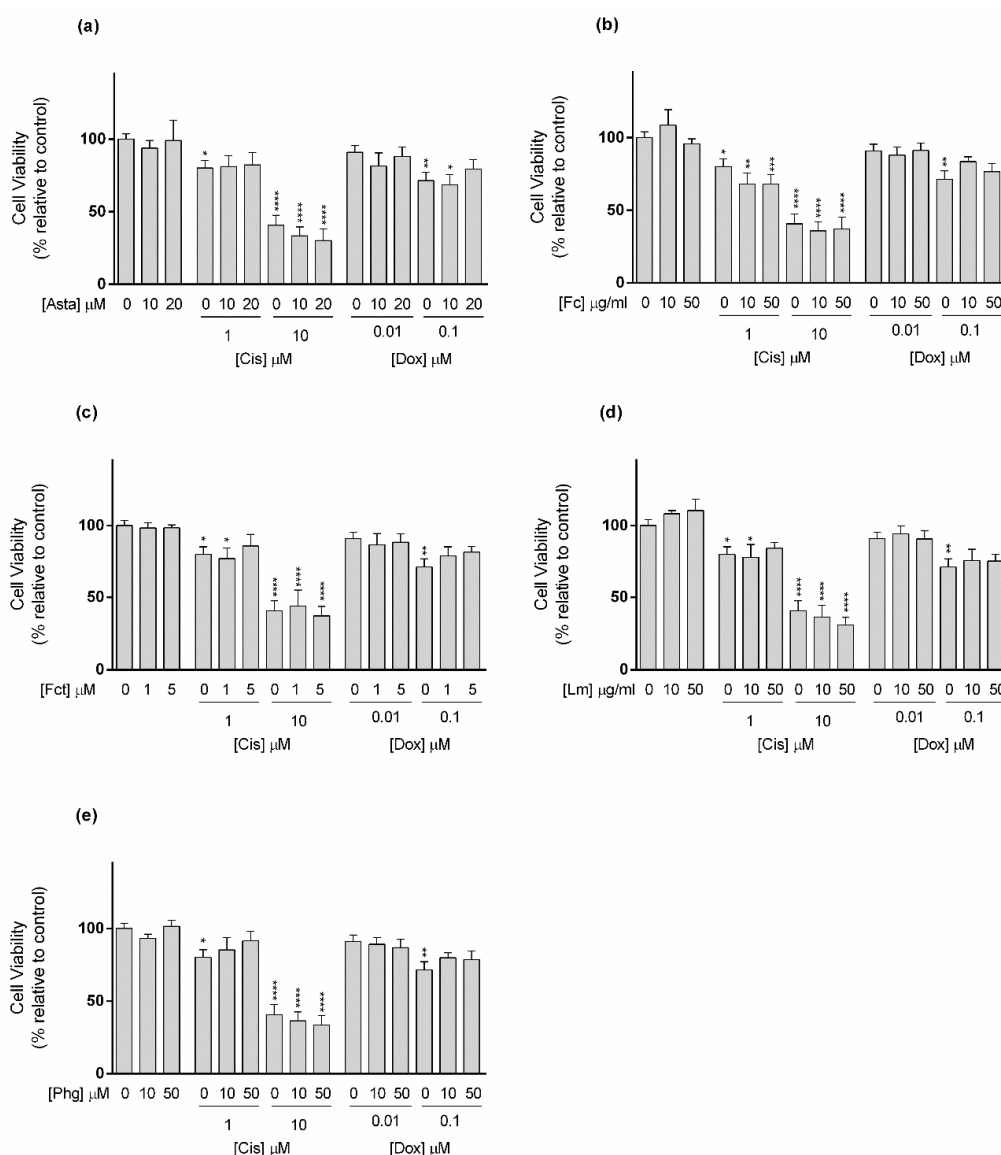


**Figure 7.** Cytotoxic effects of the combination of (a) Astaxanthin (Asta); (b) Fucoidan (Fc); (c) Fucosterol (Fct); (d) Laminarin (Lm); (e) Phloroglucinol (Phg) with the reference drugs cisplatin (Cis) and doxorubicin (Dox) assessed by the MTT assay after 72 h of exposure in MCF12A cell line cultured in monolayer. Control corresponds to cells incubated with medium containing 0.1% DMSO. The percentages of cell viability are relative to the control and presented as mean + standard deviation of six independent experiments (each in triplicate). (\*  $p < 0.05$ , \*\*  $p < 0.01$ , \*\*\*  $p < 0.001$ , \*\*\*\*  $p < 0.0001$ ).

The results of the combinations in the panel of cell lines are summarized in Table 3, using a color code to discriminate the differences in relation to the control.

**Table 3.** Summary of the results on cell viability assessed by MTT of the combination seaweed bioactive compound and reference drugs after 72 h of exposure in monolayer

	Drug ( $\mu\text{M}$ )	Asta ( $\mu\text{M}$ )			Fc ( $\mu\text{g/mL}$ )			Fct ( $\mu\text{M}$ )			Lm ( $\mu\text{g/mL}$ )			Phg ( $\mu\text{M}$ )		
		0	10	20	0	10	50	0	1	5	0	10	50	0	10	50
MCF7	0	Grey	Yellow	Yellow	Grey	Yellow	Yellow	Grey	Yellow	Yellow	Grey	Yellow	Green	Grey	Yellow	Yellow
	Dox 0.01	Yellow	Yellow	Yellow	Yellow	Yellow	Yellow	Yellow	Red	Orange	Yellow	Yellow	Yellow	Yellow	Red	Red
	0.1	Orange	Orange	Orange	Orange	Yellow	Yellow	Orange	Orange	Orange	Orange	Yellow	Yellow	Orange	Orange	Orange
	Cis 0	Grey	Yellow	Yellow	Grey	Yellow	Yellow	Grey	Yellow	Yellow	Grey	Yellow	Yellow	Grey	Yellow	Yellow
	10	Orange	Yellow	Yellow	Orange	Orange	Orange	Orange	Orange	Orange	Orange	Orange	Orange	Orange	Orange	Orange
	20	Orange	Orange	Orange	Orange	Orange	Orange	Orange	Orange	Orange	Orange	Orange	Orange	Orange	Orange	Orange
SKBR3	0	Grey	Yellow	Yellow	Grey	Yellow	Yellow	Grey	Yellow	Yellow	Grey	Yellow	Yellow	Grey	Yellow	Yellow
	Dox 0.01	Yellow	Yellow	Yellow	Yellow	Yellow	Yellow	Yellow	Yellow	Yellow	Yellow	Yellow	Yellow	Yellow	Yellow	Yellow
	0.1	Yellow	Yellow	Yellow	Yellow	Yellow	Yellow	Yellow	Orange	Orange	Yellow	Yellow	Yellow	Yellow	Orange	Orange
	Cis 0	Grey	Yellow	Yellow	Grey	Yellow	Yellow	Grey	Yellow	Yellow	Grey	Yellow	Yellow	Grey	Yellow	Yellow
	10	Orange	Yellow	Yellow	Orange	Yellow	Red	Orange	Orange	Orange	Orange	Yellow	Yellow	Orange	Orange	Orange
	20	Orange	Orange	Orange	Orange	Orange	Orange	Orange	Orange	Orange	Orange	Orange	Orange	Orange	Orange	Orange
MDA-MB-231	0	Grey	Yellow	Yellow	Grey	Yellow	Yellow	Grey	Yellow	Yellow	Grey	Yellow	Yellow	Grey	Yellow	Yellow
	Dox 0.1	Yellow	Yellow	Yellow	Yellow	Yellow	Yellow	Yellow	Red	Orange	Yellow	Yellow	Yellow	Yellow	Yellow	Yellow
	1	Orange	Orange	Orange	Orange	Orange	Orange	Orange	Orange	Orange	Orange	Orange	Orange	Orange	Orange	Orange
	Cis 0	Grey	Yellow	Yellow	Grey	Yellow	Yellow	Grey	Yellow	Yellow	Grey	Yellow	Yellow	Grey	Yellow	Yellow
	10	Yellow	Yellow	Yellow	Yellow	Yellow	Yellow	Yellow	Yellow	Yellow	Yellow	Yellow	Yellow	Yellow	Yellow	Yellow
	20	Yellow	Yellow	Yellow	Orange	Orange	Orange	Yellow	Yellow	Yellow	Orange	Orange	Orange	Yellow	Orange	Orange
MCF12A	0	Grey	Yellow	Yellow	Grey	Yellow	Yellow	Grey	Yellow	Yellow	Grey	Yellow	Yellow	Grey	Yellow	Yellow
	Dox 0.01	Yellow	Yellow	Yellow	Yellow	Yellow	Yellow	Yellow	Yellow	Yellow	Yellow	Yellow	Yellow	Yellow	Yellow	Yellow
	0.1	Orange	Orange	Orange	Orange	Yellow	Yellow	Orange	Orange	Orange	Orange	Yellow	Yellow	Orange	Orange	Orange
	Cis 0	Grey	Yellow	Yellow	Grey	Yellow	Yellow	Grey	Yellow	Yellow	Grey	Yellow	Yellow	Grey	Yellow	Yellow
	1	Orange	Yellow	Yellow	Orange	Orange	Orange	Orange	Orange	Orange	Orange	Orange	Yellow	Orange	Orange	Orange
	10	Orange	Orange	Orange	Orange	Orange	Orange	Orange	Orange	Orange	Orange	Orange	Orange	Orange	Orange	Orange

Control

Cell viability is significantly higher than the control

Cell viability is not significantly different from the control

Cell viability is significantly lower than the control

Cell viability is significantly different from control and from both drug and compound alone

### 3.4. Comparative Study of One Promising Combination—Monolayer vs. 3D Cultures

For comparison purposes, we selected the most promising combination in which the seaweed compound and the drug alone did not have any effect on cell viability in relation to the control, but the combination potentiated the effect of the drug, that is, differing from the control and from the compound and drug alone. The selected combination was Fct 5  $\mu\text{M}$  with Dox 0.1  $\mu\text{M}$  in MDA-MB-231 cell line, as it revealed the most evident effect on cell viability, showing, on average, 46% less cellular viability than the drug alone. This selected combination was tested simultaneously in monolayer and in 3D culture, the latter providing multicellular aggregates (MCAs). Considering that 3D cultures are commonly more resistant to treatments [50,108], we augmented the concentration of Dox (1, 2, and 5  $\mu\text{M}$ ) to allow the visualization of the drug effect and to have a concentration that served as a positive control (in this case Dox 5  $\mu\text{M}$ ). An all-new set of experiments was conducted,

with new replicas, where cell viability was assessed by MTT and resazurin assays, and cell proliferation was evaluated by the BrdU assay. Additionally, MCAs were evaluated by performing area measurement, histological and immunocytochemical analysis.

### 3.4.1. MTT Assay

The results obtained in monolayer by the MTT assay (Figure 8a) were very comparable to those presented before in Section 3.3. Fct alone did not exert effects on cell viability. Dox ( $\geq 1 \mu\text{M}$ ) showed high cytotoxicity, with cell viabilities under 50% in relation to the control. The selected combination of Fct ( $5 \mu\text{M}$ ) with Dox ( $0.1 \mu\text{M}$ ) statistically differed from the control and from drug and seaweed compound alone. As for the combination with higher Dox concentration, there were no statistical differences when compared to drug alone.

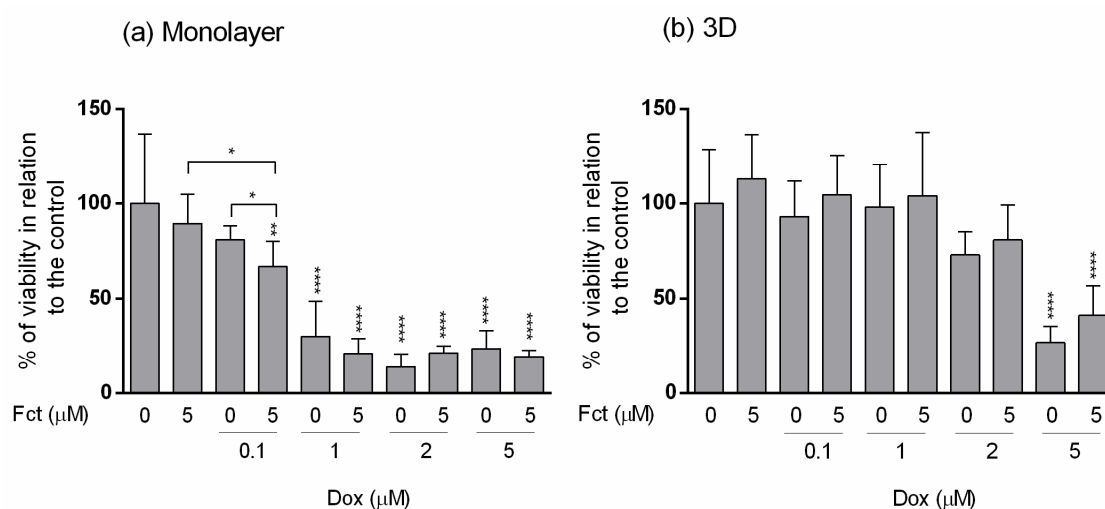


**Figure 8.** Effect of fucosterol (Fct) at  $5 \mu\text{M}$  alone and in combination with doxorubicin (Dox) at  $0.1$ ,  $1$ ,  $2$  and  $5 \mu\text{M}$ , on the viability of MDA-MB-231 cells in monolayer–72 h (a) and 3D–96 h (b) assessed by the MTT assay. Cells treated with 0.1% DMSO and Dox  $5 \mu\text{M}$  were included as negative and positive controls, respectively. The percentages of cell viability are relative to the control and presented as mean + standard deviation of five independent experiments (each in triplicate). (\*  $p < 0.05$ , \*\*  $p < 0.01$  and \*\*\*\*  $p < 0.0001$ ).

In 3D culture (Figure 8b), the results were very different from the ones obtained in monolayer. The cell viability in 3D only differed from the control when cells were exposed to Dox at  $5 \mu\text{M}$ , alone or in combination with Fct ( $5 \mu\text{M}$ ).

### 3.4.2. Resazurin Assay

The resazurin assay performed in monolayer (Figure 9a) reproduced the results obtained in the MTT assay. Fct alone did not impact cell viability, while all Dox ( $\geq 1 \mu\text{M}$ ) conditions significantly differed in cell viability relative to the control. Fct ( $5 \mu\text{M}$ ) and Dox ( $0.1 \mu\text{M}$ ), alone, did not differ from the control, however, the combination Fct ( $5 \mu\text{M}$ ) plus Dox ( $0.1 \mu\text{M}$ ) significantly decreased cell viability relative to control and to the seaweed compound alone.

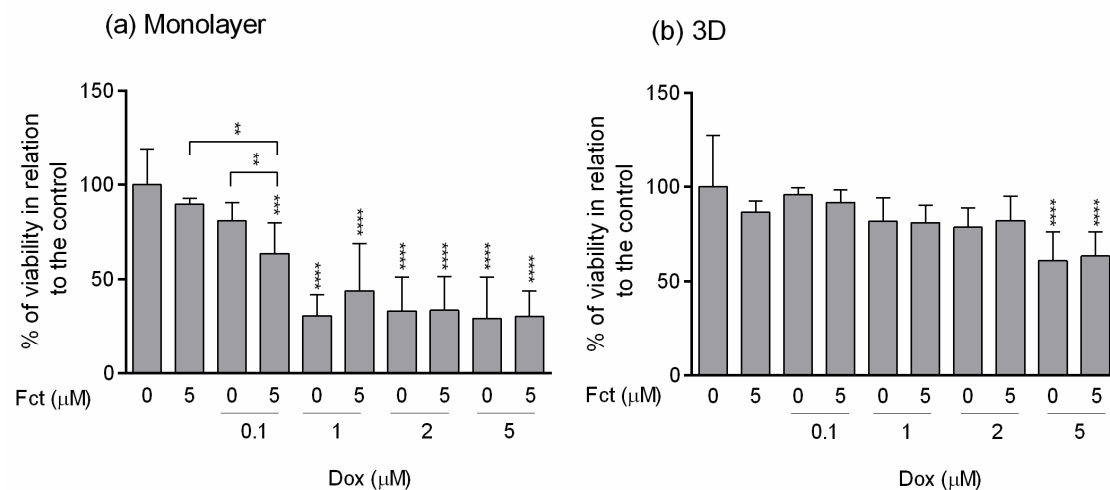


**Figure 9.** Effect of fucosterol (Fct) at 5  $\mu\text{M}$  alone and in combination with doxorubicin (Dox) at 0.1, 1, 2, and 5  $\mu\text{M}$ , on the viability of MDA-MB-231 cells in monolayer–72 h (a) and 3D–96 h (b) assessed by the resazurin assay. Cells treated with 0.1% DMSO and Dox 5  $\mu\text{M}$  were included as negative and positive controls, respectively. The percentages of cell viability are relative to the control and presented as mean + standard deviation of five independent experiments (each in triplicate). Square brackets indicate *t* tests with Sequential Bonferroni corrections (\*\*  $p < 0.01$ , \*\*\*  $p < 0.001$  and \*\*\*\*  $p < 0.0001$ ).

Also, as in the MTT assay, cells in 3D culture (Figure 9b) were more resistant to drug treatment, only revealing significant cytotoxic effect in cells exposed to Dox (5  $\mu\text{M}$ ), alone and in combination with Fct (5  $\mu\text{M}$ ).

### 3.4.3. Assessment of Cell Proliferation

MDA-MB-231 cells cultivated in monolayer (Figure 10a) showed a decrease in cell proliferation comparatively to the control, in all Dox concentrations (from 0.1–5  $\mu\text{M}$ ), and also in all combinations with Fct (5  $\mu\text{M}$ ). The combination Dox (0.1  $\mu\text{M}$ ) with Fct (5  $\mu\text{M}$ ) differed from the control and from the Fct alone, but did not differ from the drug alone. Although no significant statistical differences in cell proliferation were detected, graphically it seems that the combination of Dox (0.1 and 1  $\mu\text{M}$ ) with Fct (5  $\mu\text{M}$ ) had more effect than the drug alone (decreasing the mean of cell proliferation in 22 and 31%, respectively). Fct alone did not have any effect on cell proliferation.

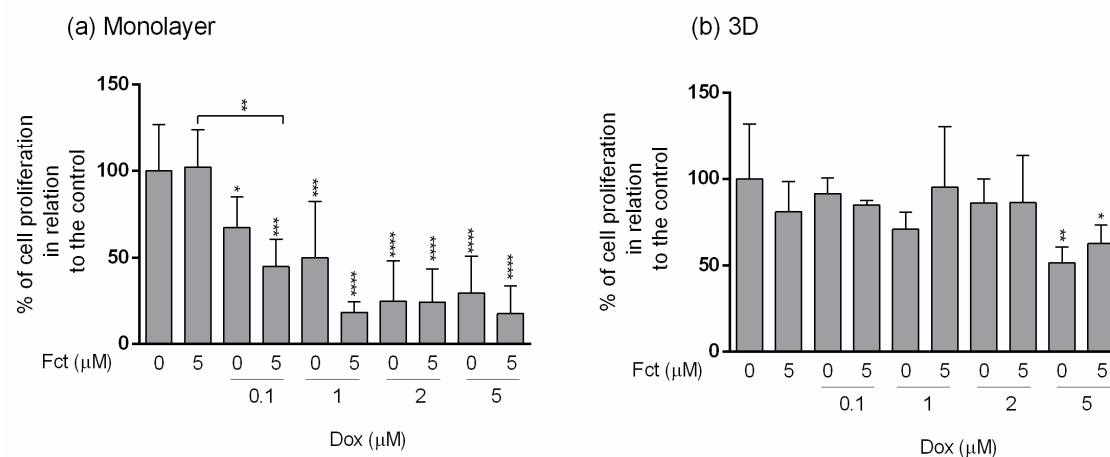


**Figure 10.** Effect of fucosterol (Fct) at 5  $\mu\text{M}$  alone and in combination with doxorubicin (Dox) at 0.1, 1, 2, and 5  $\mu\text{M}$ , on cell proliferation in monolayer–72 h (a) and 3D–96 h (b) assessed by BrdU assay. Cells treated with 0.1% DMSO and Dox 5  $\mu\text{M}$  were included as negative and positive controls, respectively. The percentages of cell proliferation are relative to the control and presented as mean + standard deviation of five independent experiments (each in triplicate). (\*  $p < 0.05$ , \*\*  $p < 0.01$ ; \*\*\*  $p < 0.001$ ; \*\*\*\*  $p < 0.0001$ ).

The effects on cell proliferation in 3D culture (Figure 10b) followed the same tendency as the viability assays, showing more resistance to the treatments. There were significant differences only in cells exposed to Dox (5  $\mu\text{M}$ ) alone (positive control) or in combination with Fct.

#### 3.4.4. Morphological Analysis of 3D Cultures (MCAs) MCAs Measurements

In the stereo microscopic observation of the MCAs (Figure 11a), those exposed to Dox (2 and 5  $\mu\text{M}$ ) (alone and in combination), revealed a loosening effect, which was much more evident in the conditions with Dox (5  $\mu\text{M}$ ). In Figure 11b, representative images of MCAs control (C) and Dox (5  $\mu\text{M}$ ), Fct (5  $\mu\text{M}$ ) and Fct/Dox (both 5  $\mu\text{M}$ ), photographed at the same magnification, were overlapped to highlight this loosening effect. In both situations, there is an evident loosening of the MCAs. There were no differences between the MCAs exposed to the drug alone and its respective combination with Fct (5  $\mu\text{M}$ ). The MCAs photographs were analyzed using AnaSP software. The determined areas are presented in Figure 11c, where it is possible to observe that besides the visual impression from stereomicroscopy, only the conditions with Dox at 5  $\mu\text{M}$  significantly differed from the control.

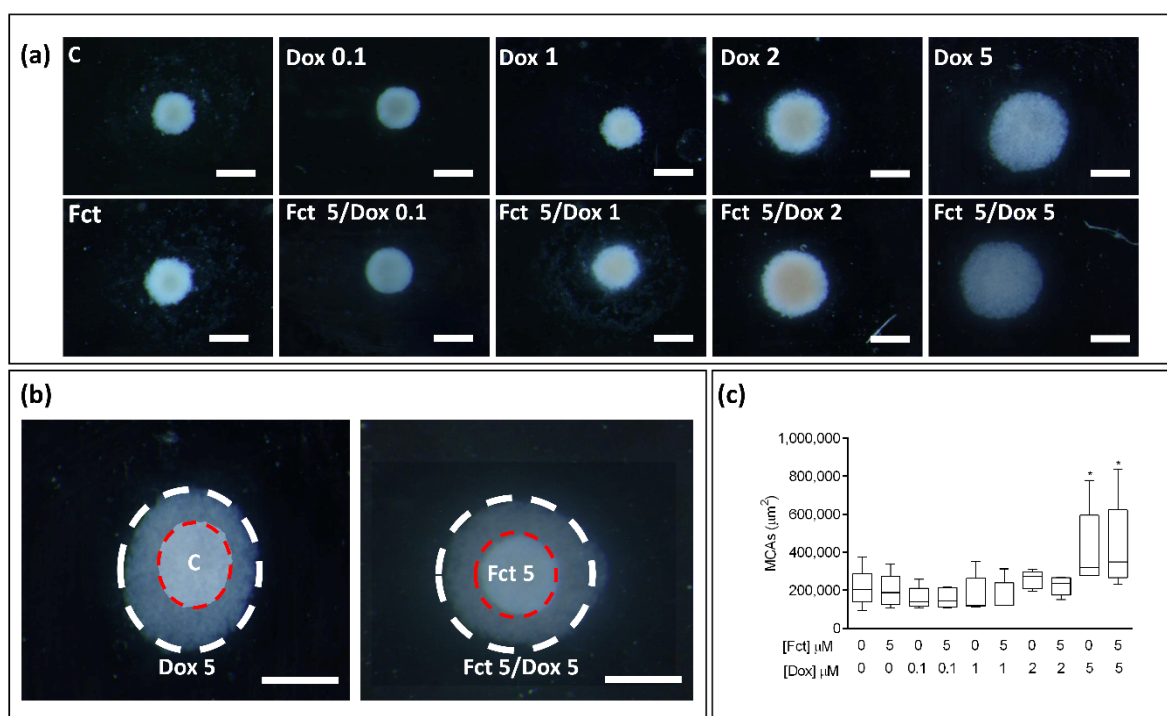


**Figure 11.** Representative stereomicroscopic images of 3D cultures-MCAs in the tested conditions of fucosterol (Fct) at 5  $\mu\text{M}$  alone, and in combination with doxorubicin (Dox) at 0.1, 1, 2, and 5  $\mu\text{M}$ . Cells treated with 0.1% DMSO (C) and Dox (5  $\mu\text{M}$ ) were included as negative and positive controls, respectively (a). Two images of MCAs from C and Fct (5  $\mu\text{M}$ ) (red dashed circle) and Dox (5  $\mu\text{M}$ ) and Fct (5  $\mu\text{M}$ ) + Dox (5  $\mu\text{M}$ ) (white dashed circle) are overlapped to show the difference in cellular aggregation between the two tested conditions (b). Box and whisker graph of Areas of MCAs expressed as median, maximum, minimum, and interquartile range (Q3-Q1) of five independent experiments (16 MCAs/per tested condition/per experiment) (c). Significant differences: \*  $p < 0.05$ . Scale bar: 500  $\mu\text{m}$ .

#### Histological and Immunocytochemical Analysis

After 96 h of exposure, MCAs were fixed, processed for paraffin embedding, and sectioned for hematoxylin-eosin (HE) staining and immunocytochemistry (ICC) analysis. By observing the MCAs stained with HE, the combinations in which morphological alterations were present are given in Figure 12. Under Dox (1  $\mu\text{M}$ ) (alone and combined) the alterations were very subtle, a higher number of cells with hyperchromatic and pyknotic



nuclei were observed, but the MCAs structure was intact. Differently, in the MCAs exposed to Dox (2 and 5  $\mu\text{M}$ ) (alone and in combination with Fct), the structure of the MCAs was concentration-dependent damaged, with looser structure, where cells lost their attachment, and with an increased number of cells with death compatible morphology, as shown in higher magnification in the inserted image of Fct/Dox 5 combination (at the bottom right of Figure 12). MCAs exposed to Dox (5  $\mu\text{M}$ ) tended to disintegrate quickly, forming a cell suspension. Morphologically, there was no difference between the MCAs exposed to Dox alone and the respective combination with the Fct (5  $\mu\text{M}$ ). No necrotic core was observed in the sectioned MCAs.

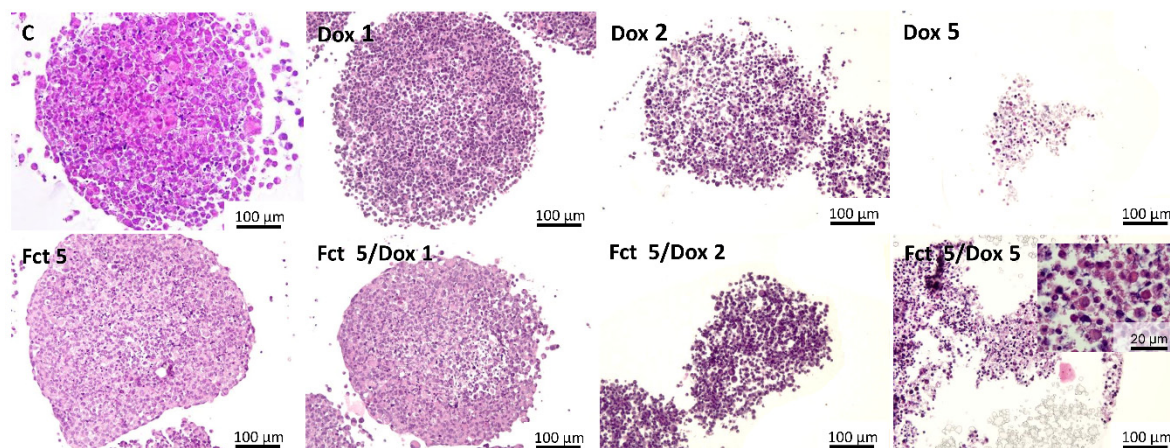


**Figure 12.** Representative histological images of MCAs exposed to the tested conditions: fucosterol (Fct) 5  $\mu\text{M}$  alone and in combination with doxorubicin (Dox) 1, 2, and 5  $\mu\text{M}$ . Cells treated with 0.1% DMSO correspond to the control (C). MCAs sections were stained with hematoxylin-eosin.

Antibodies against caspase-3 and ki67 were used for ICC. Here we show representative images of the control (C) and the combinations of Fct with Dox (1, 2, and 5  $\mu\text{M}$ ), as these were the conditions in which visual alterations of ICC staining existed in relation to the control (Figure 13). Also, in each drug concentration, the results were very similar between the drug alone and its combination with Fct. The outcomes showed that there were caspase-3 positive cells in the MCAs of all tested groups, including in the control, being these positive cells randomly distributed throughout all the MCAs. However, the number of stained cells in the C group is much lower when compared with the positive cellularity in the drug-exposed groups. Positive caspase-3 cells in the groups exposed to Dox (1 and 2  $\mu\text{M}$ ) were similar, but, when using Dox (5  $\mu\text{M}$ ), more than 80% of all cells were positive, indicating a high degree of cell death.

In relation to the immunostainings for ki67, positive cells were also distributed all along the MCAs, with more predominance in their outer region (Figure 13). In Dox (0.1 and 1  $\mu\text{M}$ ) groups, the number of Ki67 positive cells seemed similar to the control. When it comes to MCAs of the Dox groups (2 and 5  $\mu\text{M}$ ), and its combination with Fct, the number of positive cells were visibly lower; less than 10% of the total number of cells (Figure 13).

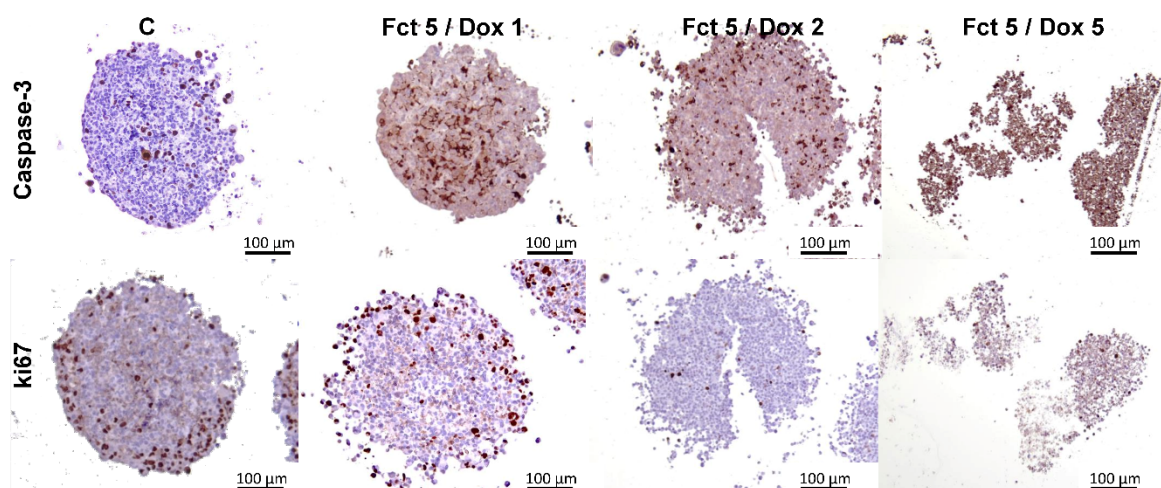


**Figure 13.** Representative histological images of MCAs immunostained against caspase-3 and ki67 after exposure to fucosterol (Fct) at 5  $\mu$ M in combination with doxorubicin (Dox) at 1, 2 and 5  $\mu$ M. Cells treated with 0.1% DMSO correspond to the control (C). Brown color-diaminobenzidine (DAB) indicates positive staining.

#### 4. Discussion

This study explored the cytotoxic effects of five brown seaweed compounds alone and combined with two reference drugs in a panel of breast cell lines, representing three BC subtypes and including a non-tumoral breast cell line. The study is justified considering that seaweed compounds, especially those from brown seaweeds, have been showing anticarcinogenic activities in many *in vitro* and *in vivo* studies related to many types of cancers, including BC [22,24,54,109,110]. The effects of combining seaweed compounds plus chemotherapeutic drugs are also relevant to explore, taking into consideration their implications in clinical scenarios. Despite their importance, the literature about this topic is still scarce [37–39,73,111]. Several studies with natural products, mostly *in vitro*, described beneficial combinatory effects with several anticancer drugs in BC, through diverse action mechanisms, suggesting that these combinations represent a promising strategy to treat BC [95,112]. However, in a clinical scenario, interactions can occur, potentially affecting drug effects [113]. In this vein, many seaweed compounds have antioxidant properties, and the intake of antioxidants during chemotherapy is very controversial, requiring further studies [28,29,114,115]. In connection with this problem, there is nowadays easy access in classical herbalists, or on the internet, to commercially available seaweed products without a medical doctor's prescription and appropriate legislation.

In this study, we started screening five seaweed compounds and two selected drugs in a panel of four breast cell lines, testing five concentrations of each, and then selected two of them for the combinations, according to pre-established criteria. Although there are some data related to the effects of the drugs in the used cell lines, the  $IC_{50}$  values vary from study to study, from 2- to 10-fold of concentration within the same line [116–118]. For this reason, we preferred to screen and select a drug concentration based on our cell culture conditions. In the end, we chose the most interesting result of the combinations in monolayer and tested it in a more complex 3D *in vitro* model [50,119].

Regarding the cytotoxicity of the carotenoid Asta, alone (1–200  $\mu$ M), it had no effects on cell viability. This contrasts with previous studies that reported that Asta (50  $\mu$ M) induced apoptosis in T-47D and MDA-MB-231 cells (both BC cell lines) [120], reduced proliferation rates and inhibited cell migration in MCF7 and MDA-MB-231 cell lines [62]. When in combination with Cis, in MCF7, SKBR3, and MCF12A cell lines, Asta interfered with this drug action, as in the mixture, Cis 10  $\mu$ M lost its effect. Asta has been previously described to confer protection against oxidative stress [121] and, in *in vivo* studies with rats, it had a protective effect against Cis-induced toxicity in the gastrointestinal tract [122],

ear [123], and also retina [124], which could partially explain the loss of effect observed in the present study.

In relation to the polysaccharides, Fc and Lm alone caused significant cytotoxicity in MCF12A cell line at the highest tested concentration (1000 µg/mL). In contrast, other authors reported that Fc from 300 to 1000 µg/mL decreased cellular viability in a dose-dependent manner, induced G1 phase arrest, promoted ROS induction and triggered apoptosis through caspases-dependent pathway [125]. Another work described that Fc at 400 µg/mL inhibited cell proliferation measured by the MTT assay, in MDA-MB-231 and MCF-7 cells [73]. It is unclear why there is such inter-study variability, particularly when using the same cell line, but the facts warn for caution regarding accepting definitive conclusions.

In combination, Fc modelled different effects according to the drug and the cell line tested. In SKBR3, Fc (10 µg/mL) in combination with Cis (10 µM) decreased Cis cytotoxicity, while the combination with Fc (50 µg/mL) statistically increased cell toxicity, differing from both the compound and the drug alone. A similar pattern of Cis enhancement effect with Fc was observed in MCF7, MDA-MB-231, and MCF12A cell lines, even if not with the same statistical significance, suggesting that Fc in higher concentrations may potentiate the effect of Cis in all cell lines. These findings are in line with previous studies where Fc significantly enhanced the cytotoxicity of Cis, Dox, and taxol in MCF7 cells [126]. Fc at 400 µg/mL in co-treatment with Cis at 5 and 10 µM, enhanced intracellular ROS and reduced glutathione (GSH) levels in MCF7 and MDA-MB-231 cells, suggesting that the induction of oxidative stress was an important event in the cell death induced by the combination in those BC cell lines [73].

In some combinations of Fc with Dox—Fc at 10, 50 µg/mL with Dox at 0.1 µM, in MCF7 and MCF12A; Fc at 10 µg/mL with Dox at 1 µM, in MDA-MB-231—Fc seems to decrease Dox effect compared to Dox alone, since in the latter case Dox significantly differed from the control. In contrast, this effect was not verified in the referred combinations. Our results are in contradiction with a previous study describing that Fc enhanced Dox effects [126]. In the opposite view, *in vivo* and *in vitro* studies in rodent models suggest that Fc may play a protective role in Dox-induced acute cardiotoxicity [127]. Therefore, in our research and in some conditions, Fc may have protected the tested breast cell lines from Dox cytotoxicity. These results indicate that we are far from understanding, controlling, and predicting the effects of Fc over cancer cells. In this sense, the anticancer activities of fucoidans continue to be explored, and recently these compounds have been used in clinical trials to evaluate their potential synergy with other anticancer therapies, in several cancer types, including BC [128].

The other tested polysaccharide, Lm, when tested alone, presented significant higher cellular viability than the control in MCF7. Although not statistically significant, the same tendency was observed in SKBR3 and MCF12A cells. Hypothetically, Lm can protect cells from oxidative stress produced by cellular metabolism. Treatment of mouse thymocytes with Lm suppressed apoptotic death around 2- to 3-fold and extended cell culture survival in about 20–30% [129]. Our study in BC cells is well in line with the hypothesis and the given proof of concept with thymocytes. However, a study reported the cytotoxic effects of Lm at 200 µg/mL in MDA-MB-231 cell line [130], and another one described a reduction in cell viability in MCF7 and MDA-MB-231 cell lines exposed to Lm from 12.5 to 400 µg/mL [81].

As to the combinations with Cis, this drug lost its effects in some combinations with Lm (Lm at 10, 50 µg/mL in SKBR3 and Lm at 50 µg/mL in MCF12A). Conversely, in MDA-MB-231, Cis (20 µM) alone did not influence cell viability, but when in combination with Lm it presented lower cell viability, differing from the control. The literature related to the combination of Lm with Cis and Dox is very scarce, but it has been already described a protective effect against Cis-induced toxicity in auditory cells [131]. When combined with Dox, Lm inhibited its effect in MCF7 and MCF12A cells. To the best of our knowledge, no literature was found in relation to the combination of Lm and Dox.



Considering the phlorotannins, Pgh alone had a cytotoxic effect in MCF7 from the concentration of 500  $\mu\text{M}$ , and in MDA-MB-231 at 1000  $\mu\text{M}$ . Our data corroborate a prior study reporting that Pgh at 100  $\mu\text{M}$  was not cytotoxic to MCF7 and SKBR3 cell lines [92]. At the latter concentration, Phg suppressed cell migration and invasion in MDA-MB-231 cell line [132]. At higher concentrations than those described here, Phg induced cytotoxicity through caspases activation in MDA-MB-231 cell line [91].

In combination with Cis, two different effects were observed: in MDA-MB-231, Pgh with Cis (20  $\mu\text{M}$ ) increased Cis cytotoxicity differing from the control, while in MCF12A, the combination with Cis (1  $\mu\text{M}$ ) negatively affected this drug action, rescuing cell viability to the control levels. Therefore, our results point to the possible protective and potentiating effects of Cis, depending on the cell line and the concentration used. The literature is also contradictory. On one hand, Pgh displayed a protective effect against Cis-induced cell death in normal human urothelial and bladder cancer cells [133]. On the other hand, the exposure with Phg before Cis treatment, sensitized the cell to this drug, enhancing its cytotoxic effect in BC cell lines [92]. Phg also enhanced the tumoricidal effect of Cis in ovarian cancer cells in a rodent model [134].

The combinations of Phg with Dox (0.01  $\mu\text{M}$ ) potentiated the effects of the drug in MCF7, where the combination differed from the control and both the compound and drug alone. A similar effect was observed with Dox (0.1  $\mu\text{M}$ ) in SKBR3, but did not differ from the compound and drug alone. However, in MCF12A, the opposite effect was observed. In the literature, we only found reports of the protective effects of Phg: cardioprotective agent against doxorubicin-induced cardiotoxicity [135]. Some new Pgh derivatives reversed multidrug resistance in Dox-induced resistant MCF7/Dox sublines [136]. This finding agrees with ours, that is suggestive of Dox potentiation against MCF7 and calls for more studies to refine what appears to be a promising interaction.

Due to the conflicting information in the literature in relation to the combination of seaweed compounds with anticancer drugs, more studies are necessary to elucidate both methodological aspects and mechanisms beyond these contradictory results. The differences between our study and several others in relation to the cytotoxicity of seaweed compounds can be justified by many possible reasons. First, some concentrations largely differ, and, as we observed, different concentrations can trigger different responses within the same model. Secondly, there are differences in the sources of compounds. We used high purity commercial compounds, but most of the other studies used extracts from different seaweeds species, with diverse extraction processing and certainly different degrees of purity that could interfere with the results. Also, for some compounds, such as Fc, the molecular weight was considered a critical factor for its anticancer activity, and different fucoidans can present different molecular weights [137]. Similarly, the hepatoprotective effects of phlorotannins against Dox-induced cytotoxicity were related to the molecular weight of phlorotannins [138]. Thus, for these cited compounds, and possibly for others, the specific chemical characteristics can determine the biological effect and their bioavailability. Beyond chemistry and experimental procedures, even the statistical analyses follow different options that influence the acceptance/rejection of hypotheses and conclusions.

From the five tested compounds, Fct had the most promising results. Fct alone at 10  $\mu\text{M}$  induced cytotoxicity effects in the three BC cell lines, not affecting the non-tumoral cell line (MCF12A). Such pattern also existed in some other studies. Fct containing fractions of seaweeds were cytotoxic for colon cell lines and T47D BC cell line, without cytotoxic effects on the normal cell line [86]. Fct from lipid extracts of Antarctic seaweeds also reduced cell proliferation and induced apoptosis in MCF7 and MDA-MB-231 cell line, but these effects were not so evident in the non-tumoral cell line CHO [88].

Globally, and according to the present data and literature, Fct seemed to have less (or even no) impact on the non-tumoral cell lines than in cancer ones. This notion goes beyond breast cells. Indeed, besides colon cell lines [87], others reported that Fct exerted minimal cytotoxicity in non-tumoral lung cell lines with  $\text{IC}_{50} > 100 \mu\text{M}$  [139], therefore suggesting

that Fct selectively impacts cancer cells. Conversely, Fct did not show any cytotoxicity in the liver cancer cell line HepG2 at concentrations up to 100  $\mu\text{M}$  [140].

For the Fct combination with drugs, we selected a non-cytotoxic concentration of the former. The combination of Fct with Cis did not differ from the effects of Cis alone. Contrary to our results, one study showed a synergistic anticancer effect of Fct in combination with Cis, related to the expression of apoptotic and angiogenic genes, in ovarian cancer cell lines [141].

Differently, the combination of Fct with Dox enhanced cytotoxicity in MCF7 and MDA-MB-231 cells. In both situations, the lowest Dox concentration did not have cytotoxicity alone. Still, combined with Fct, the cytotoxic effects increased, differing from the control and the compound and drug alone. In MDA-MB-231, the potentiation of Dox effects was more evident, because Dox (0.1  $\mu\text{M}$ ) in combination with Fct (5  $\mu\text{M}$ ) differed from the control, from Fct alone and almost doubled the impact of the drug alone. In SKBR3 the same enhancement trend of Dox toxicity was observed, but without statistical significance. By the opposite, in MCF12A cell line, the combination of Fct with Dox increased cell viability suggesting a protective effect against Dox action.

Notably, the most promising combination involving Fct was noted in the MDA-MB-231 cell line, representative of TNBC. From our data, Fct seems to be a promising drug adjuvant in this type of BC type. Owing to the lack of ER, PR, and HER2 receptors, which are nowadays the available BC target therapies, TNBC presents poor prognosis, being the systemic chemotherapy (often using Dox) the mainstream treatment [142–144]. Despite the advancement of molecular technologies that identified TNBC as a disease with intrinsic molecular and immunological heterogeneity, recognizing the variety of clinical phenotypes and revealing several putative biomarkers in TNBC, some of them already used in clinical approach, there is necessary preclinical and clinical research mainly for resistant population in order to improve the development of new therapeutic strategies [145,146]. Drug resistance is also a major problem in the treatment of TNBC [147]. Thus, the investigation of new drugs or drug adjuvants to boost cytotoxicity, overcome drug resistance or reduce drug toxicity is of utmost importance. Indeed, it has been described that plant-derived compounds in combination with classical chemotherapeutic agents were more efficient in the treatment of TNBCs [112].

The most promising combination determined here was further explored, moving to what we called Phase 3, where another set of experiments was performed, including different types of assays for assessing cell viability (MTT and resazurin assays). Additionally, BrdU assay was included to evaluate the effects on cell proliferation. The new set of experiments was made in monolayer and, simultaneously, in multicellular aggregates (MCAs), which are 3D cell cultures. It is expectable that the other combinations that had no effect in monolayer would also have no effect in 3D culture, however, we cannot ensure this is the case because we did not test it.

In 3D culture models, cells are not attached to a plastic surface. Conversely, they form a three-dimensional cell arrangement. In the case of our study, the MCAs were self-assembled due to the use of low-attachment plates, and they were not grown in any matrix or scaffolds. These MCAs have cells in multilayers, which constitute a barrier to the penetration of chemicals to be tested [148], and therefore MCAs are considered a more realistic representation of an *in vivo* tumor for testing drug efficacy and toxicity [149]. For this reason, we selected higher Dox concentrations to be tested in the MCAs, to guarantee the drug effect.

The results obtained in this set of experiments (Phase 3) relative to monolayer cultures, replicated the results of Phase 2 in terms of cell viability, thus reinforcing the value of the obtained data. Both viability assays were concordant, because Fct alone did not present cytotoxicity while Dox (0.1  $\mu\text{M}$ ) plus Fct continued to cause effect, that significantly differed from the effects of both the compound and drug alone. Thus, Fct seemed to have potentiated Dox's cytotoxicity. We consider these data as impressive in terms of future applications for cancer treatment, especially for TNBC: a low Dox concentration that alone did not have an effect on cell viability, when combined with a non-toxic compound, in this

case, Fct significantly decreased cancer cells' viability. This triad Fct/Dox/TNBC deserves further studies to explore the mechanisms involved in these interactions, namely using a pathway-focused gene expression analysis and additional cell-based assays. As to the latter, and because Fct may change the levels of reactive oxygen species (ROS) [87,141], the fine balance of which is critical for cancer cells to thrive, the determination of ROS would be a particularly relevant target in the future mechanistic assays.

Interestingly, the combination of Dox (0.1  $\mu$ M) with Fct also had effects on cell proliferation, being more effective in inhibiting cell proliferation than the compounds in single exposure. Similar to what was seen in our study, Fct from two brown seaweeds induced antiproliferative effects on the MCF-7 cell line but using much higher concentrations than the ones applied here [150]. As we stressed earlier, factors such as the purity of freshly obtained isolates may as well promote inter-assay variability.

Despite the promising effects that we observed in monolayer cultures, they were not detected in 3D cultures. It was expectable that in 3D the same drug concentrations did not induce the same degree of cytotoxicity than in monolayer, as 3D cultures seem more resistant to drugs cytotoxicity [151,152], including Dox in 3D BC models [153,154]. Our results support this phenomenon. While in monolayer, Dox at 1  $\mu$ M decreased cell viability by more than 50%, in 3D, a similar effect was only observed when the MCAs were exposed to Dox at 5  $\mu$ M. The MCAs exposed to Dox from 0.1 to 2  $\mu$ M did not show significant differences neither in viability nor in proliferation assays. As to the cell morphology, the qualitative stereomicroscopy and the measured areas corroborate the results of the bioassays. Only the MCAs exposed to Dox at 5  $\mu$ M presented loose structures, correspondent to bigger areas. At this level, there were no differences between the drug alone and the combination with Fct, at any concentration.

However, when MCAs were observed after processing for light microscopy analysis and ICC, the drug effects started to be noticed at 1  $\mu$ M, with a discrete but noticeable increase of cells with a morphology that was compatible with apoptosis; presenting cell shrinkage, nuclear condensation, chromatin margination, karyorrhexis, and putative apoptotic bodies [155,156]. These morphological aspects were confirmed by the increase of positive cells for caspase-3, indicating a higher number of apoptotic cells. With Dox at 2  $\mu$ M, the effect was similar to Dox at 1  $\mu$ M, but in the MCAs exposed to Dox at 5  $\mu$ M the number of apoptotic cells greatly increased—over 80% of the cells stained positively for caspase-3. This high number of cells undergoing death caused a disaggregation of the MCAs' structure and subsequent increase in their areas. There were no observed differences between the MCAs exposed to the drug alone and those subjected to its respective combination with Fct. As for cell proliferation, evaluated using Ki67, the control revealed a higher number of Ki67 positive cells, preferentially located in the outer part of the MCAs. In Dox and Dox combinations, there were still observed Ki67 positive cells, located in the inner part of the MCAs and not in the outer zone. There were no observed evident differences between Dox concentrations and even in Dox at 5  $\mu$ M there were ki67 positive cells. In BrdU assay, differences in cell proliferation were only observed in Dox 5  $\mu$ M and its combination with Fct.

From the structural evaluation in 3D culture, we conclude that the qualitative histology complemented with ICC, is an important and useful tool for evaluating the cytotoxicity of the tested drugs, as the effects were observable in more detail, revealing damages that were neither detected by the stereomicroscopic images, and respective measurements of areas, nor by the viability assays. Cell-based assays represent a technically simpler and quick way of assessing drug effects, while histological and ICC analyses are more time-consuming, require more equipment and know-how, and can be more expensive, especially due to the reagents for ICC; yet, they can give information on the localization of the processes through the MCAs. Furthermore, by using paraffin sections a great number of proteins related to different outputs, such as stem cell, epithelial-mesenchymal transition, and senescence markers can be detected. Our data calls for using histological analysis as an output to be included in drug testing.

## 5. Conclusions

This study tested the cytotoxic effects of five seaweed bioactive compounds (Asta, Fc, Fct, Lm, and Phg) alone and in a range of combinations with the reference drugs (Cis, Dox), in a panel of breast cell lines. We described concentrations in which the seaweed compounds alone presented cytotoxic effects against the BC cell lines. Also, conditions existed where a non-toxic concentration of the seaweed compound revealed potentiation or inhibition of the drug's cytotoxicity. The results did not unveil patterns, varying according to the cell line, compound concentration used for the combination, and the drug in the combination. The overall findings showed that seaweed compounds may have anticancer effects against BC cell lines. However, studying and establishing an effective combinatory therapy is complex, with variability between cell lines and the used compounds and concentrations.

Among the tested compounds, Fct was the most promising compound concerning higher anticancer activity. Alone, Fct induced cytotoxicity at low concentrations against the three BC cell lines, without cytotoxic effects in the non-tumoral cell line. Also, in combination with Dox, it enhanced the drug's effect under certain conditions. The data supported the importance of performing cytotoxicity screening in more complex culture models, as the effects found in monolayer were not reproducible in 3D, at least using the same bioassays. Our data stressed the importance of using other techniques, namely histological analysis, and ICC, for better understanding the cytotoxic effects and underlying mechanisms of seaweed bioactive compounds, alone and combined with drugs. Although there were no effects in the 3D model, the mixture of Dox with Fct, especially in TNBC needs further investigation, from increasing the concentration of Fct to recurring to other technologies for delivery of both types of chemicals.

**Author Contributions:** Conceptualization by F.M., A.A.R., and E.R.; Methodology by F.M., A.A.R., and E.R.; Formal analysis by F.M. and A.A.R.; Investigation by F.M. and A.C.M.; Resources by E.R.; Writing—Original Draft Preparation by F.M.; Writing—Review and Editing by A.A.R., A.C.M., and E.R.; Visualization by F.M., A.A.R., A.C.M., and E.R.; Supervision by A.A.R. and E.R.; Project administration by E.R.; Funding acquisition by E.R. All authors have read and agreed to the published version of the manuscript.

**Funding:** The Strategic Funding UIDB/04423/2020 and UIDP/04423/2020 partially supported this research, through national funds provided by FCT and ERDF to CIIMAR/CIMAR, in the framework of the program PT2020. The Doctoral Program in Biomedical Sciences, of the ICBAS—University of Porto, offered additional funds.

**Institutional Review Board Statement:** Not applicable.

**Informed Consent Statement:** Not applicable.

**Data Availability Statement:** The data are available on request from the corresponding author.

**Conflicts of Interest:** The authors declare no conflict of interest.

## References

1. Bray, F.; Ferlay, J.; Soerjomataram, I.; Siegel, R.L.; Torre, L.A.; Jemal, A. Global cancer statistics 2018: GLOBOCAN estimates of incidence and mortality worldwide for 36 cancers in 185 countries. *CA Cancer J. Clin.* **2018**, *68*, 394–424. [[CrossRef](#)] [[PubMed](#)]
2. Akram, M.; Iqbal, M.; Daniyal, M.; Khan, A.U. Awareness and current knowledge of breast cancer. *Biol. Res.* **2017**, *50*, 33. [[CrossRef](#)] [[PubMed](#)]
3. Moo, T.-A.; Sanford, R.; Dang, C.; Morrow, M. Overview of breast cancer therapy. *PET Clin.* **2018**, *13*, 1244–1248. [[CrossRef](#)]
4. Lin, Y.; Zhang, W.; Cao, H.; Li, G.; Du, W. Classifying breast cancer subtypes using deep neural networks based on multi-omics data. *Genes* **2020**, *11*, 888. [[CrossRef](#)] [[PubMed](#)]
5. Fragomeni, S.M.; Sciallis, A.; Jeruss, J.S. Molecular subtypes and local-regional control of breast cancer. *Surg. Oncol. Clin. N. Am.* **2018**, *27*, 95–120. [[CrossRef](#)]
6. Polyak, K. Heterogeneity in breast cancer. *J. Clin. Investig.* **2011**, *121*, 3786–3788. [[CrossRef](#)]
7. Masoud, V.; Pagès, G. Targeted therapies in breast cancer: New challenges to fight against resistance. *World J. Clin. Oncol.* **2017**, *8*, 120–134. [[CrossRef](#)]
8. Tremont, A.; Lu, J.; Cole, J.T. Endocrine therapy for early breast cancer: Updated review. *Ochsner J.* **2017**, *17*, 405–441.



9. Wang, J.; Xu, B. Targeted therapeutic options and future perspectives for HER2-positive breast cancer. *Signal. Transduct. Target. Ther.* **2019**, *4*, 34. [[CrossRef](#)]
10. Alfarouk, K.O.; Stock, C.-M.; Taylor, S.; Walsh, M.; Muddathir, A.K.; Verduzco, D.; Bashir, A.H.H.; Mohammed, O.Y.; Elhassan, G.O.; Harguindey, S.; et al. Resistance to cancer chemotherapy: Failure in drug response from ADME to P-gp. *Cancer Cell Int.* **2015**, *15*, 71. [[CrossRef](#)]
11. Cho, H.; Lee, S.; Sim, S.H.; Park, I.H.; Lee, K.S.; Kwak, M.H.; Kim, H.J. Cumulative incidence of chemotherapy-induced cardiotoxicity during a 2-year follow-up period in breast cancer patients. *Breast Cancer Res. Treat.* **2020**, *182*, 544–553. [[CrossRef](#)] [[PubMed](#)]
12. Zagidullin, B.; Aldahdooh, J.; Zheng, S.; Wang, W.; Wang, Y.; Saad, J.; Malyutina, A.; Jafari, M.; Tanoli, Z.; Pessia, A.; et al. DrugComb: An integrative cancer drug combination data portal. *Nucleic Acids Res.* **2019**, *47*, 43–51. [[CrossRef](#)] [[PubMed](#)]
13. Palmer, A.C.; Sorger, P.K. Combination cancer therapy can confer benefit via patient-to-patient variability without drug additivity or synergy. *Cell* **2017**, *171*, 1678–1691. [[CrossRef](#)] [[PubMed](#)]
14. Jeon, M.; Kim, S.; Park, S.; Lee, H.; Kang, J. In silico drug combination discovery for personalized cancer therapy. *BMC Syst. Biol.* **2018**, *12*, 580–585. [[CrossRef](#)] [[PubMed](#)]
15. Lee, J.H.; Nan, A. Combination drug delivery approaches in metastatic breast cancer. *J. Drug Deliv.* **2012**, *2012*, 915375. [[CrossRef](#)]
16. Saldanha, S.N.; Tollefsbol, T.O. The role of nutraceuticals in chemoprevention and chemotherapy and their clinical outcomes. *J. Oncol.* **2012**, *2012*, 192464. [[CrossRef](#)]
17. Wang, P.; Yang, H.L.; Yang, Y.J.; Wang, L.; Lee, S.C. Overcome cancer cell drug resistance using natural products. *Evid. Based Complement. Alternat. Med.* **2015**, *2015*, 767136. [[CrossRef](#)]
18. Marostica, L.L.; de Barros, A.L.B.; Oliveira, J.; Salgado, B.S.; Cassali, G.D.; Leite, E.A.; Cardoso, V.N.; Lang, K.L.; Caro, M.S.B.; Duran, F.J.; et al. Antitumor effectiveness of a combined therapy with a new cucurbitacin B derivative and paclitaxel on a human lung cancer xenograft model. *Toxicol. Appl. Pharmacol.* **2017**, *329*, 272–281. [[CrossRef](#)]
19. Boopathy, N.S.; Kathiresan, K. Anticancer drugs from marine flora: An overview. *J. Oncol.* **2010**, *2010*, 214186. [[CrossRef](#)]
20. Newman, D.J.; Cragg, G.M. Natural products as sources of new drugs over the 30 years from 1981 to 2010. *J. Nat. Prod.* **2012**, *75*, 255–278. [[CrossRef](#)]
21. Moghadamtousi, S.Z.; Karimian, H.; Khanabdali, R.; Razavi, M.; Firoozinia, M.; Zandi, K.; Abdul Kadir, H. Anticancer and antitumor potential of fucoidan and fucoxanthin, two main metabolites isolated from brown algae. *Sci. World J.* **2014**, *2014*, 768323. [[CrossRef](#)]
22. Pádua, D.; Rocha, E.; Gargiulo, D.; Ramos, A.A. Bioactive compounds from brown seaweeds: Phloroglucinol, fucoxanthin and fucoidan as promising therapeutic agents against breast cancer. *Phytochem. Lett.* **2015**, *14*, 91–98. [[CrossRef](#)]
23. Gutiérrez-Rodríguez, A.G.; Juárez-Portilla, C.; Olivares-Bañuelos, T.; Zepeda, R.C. Anticancer activity of seaweeds. *Drug Discov. Today* **2018**, *23*, 434–447. [[CrossRef](#)] [[PubMed](#)]
24. Rocha, D.H.A.; Seca, A.M.L.; Pinto, D.C.G.A. Seaweed secondary metabolites in vitro and in vivo anticancer activity. *Mar. Drugs* **2018**, *16*, 410. [[CrossRef](#)] [[PubMed](#)]
25. Murphy, C.; Hotchkiss, S.; Worthington, J.; McKeown, S.R. The potential of seaweed as a source of drugs for use in cancer chemotherapy. *J. Appl. Phycol.* **2014**, *26*, 2211–2264. [[CrossRef](#)]
26. Liao, G.S.; Apaya, M.K.; Shyur, L.F. Herbal medicine and acupuncture for breast cancer palliative care and adjuvant therapy. *Evid. Based Complement. Alternat. Med.* **2013**, *2013*, 437948. [[CrossRef](#)]
27. Moussavou, G.; Kwak, D.H.; Obiang-Obonou, B.W.; Maranguy, C.A.; Dinzouna-Boutamba, S.D.; Lee, D.H.; Pissibanganga, O.G.; Ko, K.; Seo, J.I.; Choo, Y.K. Anticancer effects of different seaweeds on human colon and breast cancers. *Mar. Drugs* **2014**, *12*, 4898–4911. [[CrossRef](#)]
28. Yang, Y.J.; Nam, S.-J.; Kong, G.; Kim, M.K. A case-control study on seaweed consumption and the risk of breast cancer. *Br. J. Nutr.* **2010**, *103*, 1345–1353. [[CrossRef](#)]
29. Teas, J.; Vena, S.; Cone, D.L.; Irhimeh, M. The consumption of seaweed as a protective factor in the etiology of breast cancer: Proof of principle. *J. Appl. Phycol.* **2013**, *25*, 771–779. [[CrossRef](#)]
30. Xue, M.; Ge, Y.; Zhang, J.; Liu, Y.; Wang, Q.; Hou, L.; Zheng, Z. Fucoidan inhibited 4T1 mouse breast cancer cell growth in vivo and in vitro via downregulation of Wnt/beta-catenin signaling. *Nutr. Cancer* **2013**, *65*, 898–908. [[CrossRef](#)]
31. Lin, S.-R.; Chang, C.-H.; Hsu, C.-F.; Tsai, M.-J.; Cheng, H.; Leong, M.K.; Sung, P.-J.; Chen, J.-C.; Weng, C.-F. Natural compounds as potential adjuvants to cancer therapy: Preclinical evidence. *Br. J. Pharmacol.* **2020**, *177*, 1409–1423. [[CrossRef](#)] [[PubMed](#)]
32. Lichota, A.; Gwozdziński, K. Anticancer activity of natural compounds from plant and marine environment. *Int. J. Mol. Sci.* **2018**, *19*, 3533. [[CrossRef](#)] [[PubMed](#)]
33. Wang, J.; Jiang, Y.-F. Natural compounds as anticancer agents: Experimental evidence. *World J. Exp. Med.* **2012**, *2*, 45–47. [[CrossRef](#)] [[PubMed](#)]
34. Fujiki, H.; Saganuma, M. Green tea: An effective synergist with anticancer drugs for tertiary cancer prevention. *Cancer Lett.* **2012**, *324*, 119–125. [[CrossRef](#)] [[PubMed](#)]
35. Kapadia, G.J.; Rao, G.S.; Ramachandran, C.; Iida, A.; Suzuki, N.; Tokuda, H. Synergistic cytotoxicity of red beetroot (*Beta vulgaris* L.) extract with doxorubicin in human pancreatic, breast and prostate cancer cell lines. *J. Altern. Complement. Med.* **2013**, *10*. [[CrossRef](#)] [[PubMed](#)]



36. Lopes-Costa, E.; Abreu, M.; Gargiulo, D.; Rocha, E.; Ramos, A.A. Anticancer effects of seaweed compounds fucoxanthin and phloroglucinol, alone and in combination with 5-fluorouracil in colon cells. *J. Toxicol. Environ. Health Part A* **2017**, *80*, 776–787. [[CrossRef](#)]
37. Ramos, A.A.; Almeida, T.; Lima, B.; Rocha, E. Cytotoxic activity of the seaweed compound fucosterol, alone and in combination with 5-fluorouracil, in colon cells using 2D and 3D culturing. *J. Toxicol. Environ. Health Part A* **2019**, *82*, 537–549. [[CrossRef](#)]
38. Eid, S.Y.; Althubiti, M.A.; Abdallah, M.E.; Wink, M.; El-Readi, M.Z. The carotenoid fucoxanthin can sensitize multidrug resistant cancer cells to doxorubicin via induction of apoptosis, inhibition of multidrug resistance proteins and metabolic enzymes. *Phytomedicine* **2020**, *77*, 153280. [[CrossRef](#)]
39. Alekseyenko, T.V.; Zhanayeva, S.Y.; Venediktova, A.A.; Zvyagintseva, T.N.; Kuznetsova, T.A.; Besednova, N.N.; Korolenko, T.A. Antitumor and antimetastatic activity of fucoidan, a sulfated polysaccharide isolated from the Okhotsk Sea *Fucus evanescens* brown alga. *Exp. Biol. Med.* **2007**, *143*, 730–732. [[CrossRef](#)]
40. Cheng, S.H.; Nian, Y.Q.; Ding, M.; Hu, S.B.; He, H.T.; Li, L.; Wang, Y.H. Phloroglucinol combined with parecoxib for cystospasm after transurethral resection of the prostate. *Zhonghua Nan Ke Xue* **2016**, *22*, 641–644.
41. Pan, S.Y.; Zhou, J.; Gibbons, L.; Morrison, H.; Wen, S.W. Antioxidants and breast cancer risk- a population-based case-control study in Canada. *BMC Cancer* **2011**, *11*, 372. [[CrossRef](#)] [[PubMed](#)]
42. Jung, A.Y.; Cai, X.; Thoene, K.; Obi, N.; Jaskulski, S.; Behrens, S.; Flesch-Janys, D.; Chang-Claude, J. Antioxidant supplementation and breast cancer prognosis in postmenopausal women undergoing chemotherapy and radiation therapy. *Am. J. Clin. Nutr.* **2019**, *109*, 69–78. [[CrossRef](#)] [[PubMed](#)]
43. Nechuta, S.; Lu, W.; Chen, Z.; Zheng, Y.; Gu, K.; Cai, H.; Zheng, W.; Shu, X.O. Vitamin supplement use during breast cancer treatment and survival: A prospective cohort study. *Cancer Epidemiol. Biomark. Prev.* **2011**, *20*, 262–271. [[CrossRef](#)] [[PubMed](#)]
44. Kitaeva, K.V.; Rutland, C.S.; Rizvanov, A.A.; Solovyeva, V.V. Cell culture based in vitro test systems for anticancer drug screening. *Front. Bioeng. Biotechnol.* **2020**, *8*, 322. [[CrossRef](#)]
45. Imamura, Y.; Mukohara, T.; Shimono, Y.; Funakoshi, Y.; Chayahara, N.; Toyoda, M.; Kiyota, N.; Takao, S.; Kono, S.; Nakatsura, T.; et al. Comparison of 2D- and 3D-culture models as drug-testing platforms in breast cancer. *Oncol. Rep.* **2015**, *33*, 1837–1843. [[CrossRef](#)]
46. Ravi, M.; Ramesh, A.; Pattabhi, A. Contributions of 3D cell cultures for cancer research. *J. Cell Physiol.* **2017**, *232*, 2679–2697. [[CrossRef](#)]
47. Costa, E.C.; Moreira, A.F.; de Melo-Diogo, D.; Gaspar, V.M.; Carvalho, M.P.; Correia, I.J. 3D tumor spheroids: An overview on the tools and techniques used for their analysis. *Biotechnol. Adv.* **2016**, *34*, 1427–1441. [[CrossRef](#)]
48. Kapałczyńska, M.; Kolenda, T.; Przybyła, W.; Zajączkowska, M.; Teresiak, A.; Filas, V.; Ibbs, M.; Bliźniak, R.; Łuczewski, Ł.; Lamperska, K. 2D and 3D cell cultures—A comparison of different types of cancer cell cultures. *Arch. Med. Sci.* **2018**, *14*, 910–919. [[CrossRef](#)]
49. Mikhail, A.S.; Eetezadi, S.; Allen, C. Multicellular tumor spheroids for evaluation of cytotoxicity and tumor growth inhibitory effects of nanomedicines in vitro: A comparison of docetaxel-loaded block copolymer micelles and Taxotere<sup>®</sup>. *PLoS ONE* **2013**, *8*, e62630. [[CrossRef](#)]
50. Edmondson, R.; Broglie, J.J.; Adcock, A.F.; Yang, L. Three-dimensional cell culture systems and their applications in drug discovery and cell-based biosensors. *Assay Drug Dev. Technol.* **2014**, *12*, 207–218. [[CrossRef](#)]
51. Breslin, S.; O'Driscoll, L. Three-dimensional cell culture: The missing link in drug discovery. *Drug Discov. Today* **2013**, *18*, 240–249. [[CrossRef](#)] [[PubMed](#)]
52. Holliday, D.L.; Speirs, V. Choosing the right cell line for breast cancer research. *Breast Cancer Res. BCR* **2011**, *13*, 215. [[CrossRef](#)] [[PubMed](#)]
53. Subik, K.; Lee, J.-F.; Baxter, L.; Strzepak, T.; Costello, D.; Crowley, P.; Xing, L.; Hung, M.-C.; Bonfiglio, T.; Hicks, D.G.; et al. The expression patterns of ER, PR, HER2, CK5/6, EGFR, Ki-67 and AR by immunohistochemical analysis in breast cancer cell lines. *Breast Cancer Basic Clin. Res.* **2010**, *4*, 35–41. [[CrossRef](#)]
54. Boominathan, M.; Mahesh, A. Seaweed carotenoids for cancer therapeutics. In *Handbook of Anticancer Drugs from Marine Origin*; Kim, S.K., Ed.; Springer: Cham, Switzerland, 2015; pp. 185–203. [[CrossRef](#)]
55. Jyonouchi, H.; Sun, S.; Iijima, K.; Gross, M.D. Antitumor activity of astaxanthin and its mode of action. *Nutr. Cancer* **2000**, *36*, 59–65. [[CrossRef](#)] [[PubMed](#)]
56. Miyashita, K.; Beppu, F.; Hosokawa, M.; Liu, X.; Wang, S. Nutraceutical characteristics of the brown seaweed carotenoid fucoxanthin. *Arch. Biochem. Biophys.* **2020**, *686*, 108364. [[CrossRef](#)] [[PubMed](#)]
57. Tanaka, T.; Shnimizu, M.; Moriwaki, H. Cancer chemoprevention by carotenoids. *Molecules* **2012**, *17*, 3202–3242. [[CrossRef](#)]
58. Song, X.D.; Zhang, J.J.; Wang, M.R.; Liu, W.B.; Gu, X.B.; Lv, C.J. Astaxanthin induces mitochondria-mediated apoptosis in rat hepatocellular carcinoma CBRH-7919 cells. *Biol. Pharm. Bull.* **2011**, *34*, 839–844. [[CrossRef](#)] [[PubMed](#)]
59. Zhang, X.; Zhao, W.E.; Hu, L.; Zhao, L.; Huang, J. Carotenoids inhibit proliferation and regulate expression of peroxisome proliferators-activated receptor gamma (PPAR $\gamma$ ) in K562 cancer cells. *Arch. Biochem. Biophys.* **2011**, *512*, 96–106. [[CrossRef](#)]
60. Kavitha, K.; Kowshik, J.; Kishore, T.K.; Baba, A.B.; Nagini, S. Astaxanthin inhibits NF- $\kappa$ B and Wnt/ $\beta$ -catenin signaling pathways via inactivation of Erk/MAPK and PI3K/Akt to induce intrinsic apoptosis in a hamster model of oral cancer. *Biochim. Biophys. Acta* **2013**, *1830*, 4433–4444. [[CrossRef](#)]

61. Song, X.; Wang, M.; Zhang, L.; Zhang, J.; Wang, X.; Liu, W.; Gu, X.; Lv, C. Changes in cell ultrastructure and inhibition of JAK1/STAT3 signaling pathway in CBRH-7919 cells with astaxanthin. *Toxicol. Mech. Methods* **2012**, *22*, 679–686. [[CrossRef](#)]
62. McCall, B.; McPartland, C.K.; Moore, R.; Frank-Kamenetskii, A.; Booth, B.W. Effects of astaxanthin on the proliferation and migration of breast cancer cells in vitro. *Antioxidants* **2018**, *7*, 135. [[CrossRef](#)] [[PubMed](#)]
63. Yasui, Y.; Hosokawa, M.; Mikami, N.; Miyashita, K.; Tanaka, T. Dietary astaxanthin inhibits colitis and colitis-associated colon carcinogenesis in mice via modulation of the inflammatory cytokines. *Chem. Biol. Interact.* **2011**, *193*, 79–87. [[CrossRef](#)] [[PubMed](#)]
64. Cunha, L.; Grenha, A. Sulfated seaweed polysaccharides as multifunctional materials in drug delivery applications. *Mar. Drugs* **2016**, *14*, 42. [[CrossRef](#)] [[PubMed](#)]
65. Zhuang, C.; Itoh, H.; Mizuno, T.; Ito, H. Antitumor active fucoidan from the brown seaweed, *Umitoranoo* (*Sargassum thunbergii*). *Biosci. Biotechnol. Biochem.* **1995**, *59*, 563–567. [[CrossRef](#)]
66. Cumashi, A.; Ushakova, N.A.; Preobrazhenskaya, M.E.; D’Incecco, A.; Piccoli, A.; Totani, L.; Tinari, N.; Morozovich, G.E.; Berman, A.E.; Bilan, M.I.; et al. A comparative study of the anti-inflammatory, anticoagulant, antiangiogenic, and antiadhesive activities of nine different fucoidans from brown seaweeds. *Glycobiology* **2007**, *17*, 541–552. [[CrossRef](#)]
67. Vetvicka, V.; Vetvickova, J. Fucoidans stimulate immune reaction and suppress cancer growth. *Anticancer Res.* **2017**, *37*, 6041–6046. [[CrossRef](#)]
68. Han, Y.-S.; Lee, J.H.; Lee, S.H. Fucoidan inhibits the migration and proliferation of HT-29 human colon cancer cells via the phosphoinositide-3 kinase/Akt/mechanistic target of rapamycin pathways. *Mol. Med. Rep.* **2015**, *12*, 3446–3452. [[CrossRef](#)]
69. Arumugam, P.; Arunkumar, K.; Sivakumar, L.; Murugan, M.; Murugan, K. Anticancer effect of fucoidan on cell proliferation, cell cycle progression, genetic damage and apoptotic cell death in HepG2 cancer cells. *Toxicol. Rep.* **2019**, *6*, 556–563. [[CrossRef](#)]
70. Hsu, H.Y.; Hwang, P.A. Clinical applications of fucoidan in translational medicine for adjuvant cancer therapy. *Clin. Transl. Med.* **2019**, *8*, 15. [[CrossRef](#)]
71. Yamasaki-Miyamoto, Y.; Yamasaki, M.; Tachibana, H.; Yamada, K. Fucoidan induces apoptosis through activation of caspase-8 on human breast cancer MCF-7 cells. *J. Agric. Food Chem.* **2009**, *57*, 8677–8682. [[CrossRef](#)]
72. Zhang, Z.; Teruya, K.; Eto, H.; Shirahata, S. Fucoidan extract induces apoptosis in MCF-7 cells via a mechanism involving the ROS-dependent JNK Activation and mitochondria-mediated pathways. *PLoS ONE* **2011**, *6*, e27441. [[CrossRef](#)] [[PubMed](#)]
73. Zhang, Z.; Teruya, K.; Yoshida, T.; Eto, H.; Shirahata, S. Fucoidan extract enhances the anti-cancer activity of chemotherapeutic agents in MDA-MB-231 and MCF-7 breast cancer cells. *Mar. Drugs* **2013**, *11*, 81–98. [[CrossRef](#)] [[PubMed](#)]
74. Zhang, Z.; Teruya, K.; Eto, H.; Shirahata, S. Induction of apoptosis by low-molecular-weight fucoidan through calcium- and caspase-dependent mitochondrial pathways in MDA-MB-231 breast cancer cells. *Biosci. Biotechnol. Biochem.* **2013**, *77*, 235–242. [[CrossRef](#)] [[PubMed](#)]
75. Vishchuk, O.S.; Ermakova, S.P.; Zvyagintseva, T.N. Sulfated polysaccharides from brown seaweeds *Saccharina japonica* and *Undaria pinnatifida*: Isolation, structural characteristics, and antitumor activity. *Carbohydr. Res.* **2011**, *346*, 2769–2776. [[CrossRef](#)] [[PubMed](#)]
76. Haroun-Bouhedja, F.; Lindenmeyer, F.; Lu, H.; Soria, C.; Jozefonvicz, J.; Boisson-Vidal, C. In vitro effects of fucans on MDA-MB231 tumor cell adhesion and invasion. *Anticancer Res.* **2002**, *22*, 2285–2292.
77. Park, H.-K.; Kim, I.-H.; Kim, J.; Nam, T.-J. Induction of apoptosis by laminarin, regulating the insulin-like growth factor-IR signaling pathways in HT-29 human colon cells. *Int. J. Mol. Med.* **2012**, *30*, 734–738. [[CrossRef](#)]
78. Song, K.; Xu, L.; Zhang, W.; Cai, Y.; Jang, B.; Oh, J.; Jin, J.O. Laminarin promotes anti-cancer immunity by the maturation of dendritic cells. *Oncotarget* **2017**, *8*, 38554–38567. [[CrossRef](#)]
79. Park, H.-K.; Kim, I.-H.; Kim, J.; Nam, T.-J. Induction of apoptosis and the regulation of ErbB signaling by laminarin in HT-29 human colon cancer cells. *Int. J. Mol. Med.* **2013**, *32*, 291–295. [[CrossRef](#)]
80. Ji, C.F.; Ji, Y.B. Laminarin-induced apoptosis in human colon cancer LoVo cells. *Oncol. Lett.* **2014**, *7*, 1728–1732. [[CrossRef](#)]
81. Xu, H.; Zou, S.; Xu, X. The  $\beta$ -glucan from *Lentinus edodes* suppresses cell proliferation and promotes apoptosis in estrogen receptor positive breast cancers. *Oncotarget* **2017**, *8*, 86693–86709. [[CrossRef](#)]
82. Malyarenko, O.S.; Usoltseva, R.V.; Shevchenko, N.M.; Isakov, V.V.; Zvyagintseva, T.N.; Ermakova, S.P. In vitro anticancer activity of the laminarans from far-eastern brown seaweeds and their sulfated derivatives. *J. Appl. Phycol.* **2017**, *29*, 543–553. [[CrossRef](#)]
83. Mouritsen, O.G.; Bagatolli, L.A.; Duelund, L.; Garvik, O.; Ipsen, J.H.; Simonsen, A.C. Effects of seaweed sterols fucosterol and desmosterol on lipid membranes. *Chem. Phys. Lipids* **2017**, *205*, 1–10. [[CrossRef](#)] [[PubMed](#)]
84. Abdul, Q.A.; Choi, R.J.; Jung, H.A.; Choi, J.S. Health benefit of fucosterol from marine algae: A review. *J. Sci. Food Agric.* **2016**, *96*, 1856–1866. [[CrossRef](#)] [[PubMed](#)]
85. Kim, S.-K.; Van Ta, Q. Potential beneficial effects of marine algal sterols on human health. In *Advances in Food and Nutrition Research*; Kim, S.-K., Ed.; Academic Press: Cambridge, MA, USA, 2011; Volume 64, Chapter 14; pp. 191–198. [[CrossRef](#)]
86. Khanavi, M.; Gheidarloo, R.; Sadati, N.; Ardekani, M.R.; Nabavi, S.; Tavajohi, S.; Ostad, S. Cytotoxicity of fucosterol containing fraction of marine algae against breast and colon carcinoma cell line. *Pharmacogn. Mag.* **2012**, *8*, 60–64. [[CrossRef](#)]
87. Jiang, H.; Li, J.; Chen, A.; Li, Y.; Xia, M.; Guo, P.; Yao, S.; Chen, S. Fucosterol exhibits selective antitumor anticancer activity against HeLa human cervical cell line by inducing mitochondrial mediated apoptosis, cell cycle migration inhibition and downregulation of m-TOR/PI3K/Akt signalling pathway. *Oncol. Lett.* **2018**, *15*, 3458–3463. [[CrossRef](#)]

88. Pacheco, B.S.; Dos Santos, M.A.Z.; Schultze, E.; Martins, R.M.; Lund, R.G.; Seixas, F.K.; Colepiccolo, P.; Collares, T.; Paula, F.R.; De Pereira, C.M.P. Cytotoxic activity of fatty acids from Antarctic macroalgae on the growth of human breast cancer cells. *Front. Bioeng. Biotechnol.* **2018**, *6*, 185. [CrossRef]
89. Kim, M.-M.; Kim, S.-K. Effect of phloroglucinol on oxidative stress and inflammation. *Food Chem. Toxicol.* **2010**, *48*, 2925–2933. [CrossRef]
90. Kang, M.-H.; Kim, I.-H.; Nam, T.-J.N. Phloroglucinol induces apoptosis via apoptotic signaling pathways in HT-29 colon cancer cells. *Oncol. Rep.* **2014**, *32*, 1341–1346. [CrossRef]
91. Kumar, P.; Senthamilselvi, S.; Govindaraju, M.; Sankar, R. Unraveling the caspase-mediated mechanism for phloroglucinol-encapsulated starch biopolymer against the breast cancer cell line MDA-MB-231. *RSC Adv.* **2014**, *4*, 46157–46163. [CrossRef]
92. Kim, R.K.; Uddin, N.; Hyun, J.W.; Kim, C.; Suh, Y.; Lee, S.J. Novel anticancer activity of phloroglucinol against breast cancer stem-like cells. *Toxicol. Appl. Pharmacol.* **2015**, *286*, 143–150. [CrossRef]
93. Prabhakaran, P.; Hassiotou, F.; Blancafort, P.; Filgueira, L. Cisplatin induces differentiation of breast cancer cells. *Front. Oncol.* **2013**, *3*, 134. [CrossRef] [PubMed]
94. Al-malky, H.S.; Osman, A.-M.M.; Damanhour, Z.A.; Alkreathy, H.M.; Al Aama, J.Y.; Ramadan, W.S.; Al Qahtani, A.A.; Al Mahdi, H.B. Modulation of doxorubicin-induced expression of the multidrug resistance gene in breast cancer cells by diltiazem and protection against cardiotoxicity in experimental animals. *Cancer Cell Int.* **2019**, *19*, 191. [CrossRef] [PubMed]
95. Zhang, Y.; Li, H.; Zhang, J.; Zhao, C.; Lu, S.; Qiao, J.; Han, M. The combinatory effects of natural products and chemotherapy drugs and their mechanisms in breast cancer treatment. *Phytochem. Rev.* **2020**, *19*, 1179–1197. [CrossRef]
96. Amable, L. Cisplatin resistance and opportunities for precision medicine. *Pharmacol. Res.* **2016**, *106*, 27–36. [CrossRef] [PubMed]
97. Smith, L.; Welham, K.J.; Watson, M.B.; Drew, P.J.; Lind, M.J.; Cawkwell, L. The proteomic analysis of cisplatin resistance in breast cancer cells. *Oncol. Res.* **2007**, *16*, 497–506. [CrossRef]
98. Verrill, M. Anthracyclines in breast cancer: Therapy and issues of toxicity. *Breast* **2001**, *10*, 8–15. [CrossRef]
99. Shevchuk, O.O.; Posokhova, E.A.; Sakhno, L.A.; Nikolaev, V.G. Theoretical ground for adsorptive therapy of anthracyclines cardiotoxicity. *Exp. Oncol.* **2012**, *34*, 314–322.
100. Lüpertz, R.; Wätjen, W.; Kahl, R.; Chovolou, Y. Dose- and time-dependent effects of doxorubicin on cytotoxicity, cell cycle and apoptotic cell death in human colon cancer cells. *Toxicology* **2010**, *271*, 115–121. [CrossRef]
101. Piccinini, F.; Ana, S.P. A software suite for automatic image analysis of multicellular spheroids. *Comput. Methods Programs Biomed.* **2015**, *119*, 43–52. [CrossRef]
102. Gil, R.S.; Vagnarelli, P. Ki-67: More hidden behind a ‘classic proliferation marker’. *Trends Biochem. Sci.* **2018**, *43*, 747–748. [CrossRef]
103. Urruticochea, A.; Smith, I.E.; Dowsett, M. Proliferation marker Ki-67 in early breast cancer. *J. Clin. Oncol.* **2005**, *23*, 7212–7220. [CrossRef] [PubMed]
104. Bressenot, A.; Marchal, S.; Bezdetsnaya, L.; Garrier, J.; Guillemain, F.; Plénat, F. Assessment of apoptosis by immunohistochemistry to active caspase-3, active caspase-7, or cleaved PARP in monolayer cells and spheroid and subcutaneous xenografts of human carcinoma. *J. Histochem. Cytochem.* **2009**, *57*, 289–300. [CrossRef] [PubMed]
105. Riss, T.L.; Moravec, R.A. Use of multiple assay endpoints to investigate the effects of incubation time, dose of toxin, and plating density in cell-based cytotoxicity assays. *Assay Drug Dev. Technol.* **2004**, *2*, 51–62. [CrossRef] [PubMed]
106. Holm, S. A simple sequentially rejective multiple test procedure. *Scand. J. Stat.* **1979**, *6*, 65–70.
107. Gaetano, J. Holm-Bonferroni Sequential Correction: An Excel Calculator (1.3) [Microsoft Excel Workbook]. Available online: [https://www.researchgate.net/publication/322568540\\_Holm-Bonferroni\\_sequential\\_correction\\_An\\_Excel\\_calculator\\_13](https://www.researchgate.net/publication/322568540_Holm-Bonferroni_sequential_correction_An_Excel_calculator_13) (accessed on 26 December 2020).
108. Lovitt, C.J.; Shelper, T.B.; Avery, V.M. Advanced cell culture techniques for cancer drug discovery. *Biology* **2014**, *3*, 345–367. [CrossRef] [PubMed]
109. Yun, C.W.; Kim, H.J.; Lee, S.H. Therapeutic application of diverse marine-derived natural products in cancer therapy. *Anticancer Res.* **2019**, *39*, 5261–5284. [CrossRef]
110. Rusdi, N.A.; Kue, C.S.; Yu, K.-X.; Lau, B.F.; Chung, L.Y.; Kiew, L.V. Assessment of potential anticancer activity of brown seaweed compounds using zebrafish phenotypic assay. *Nat. Prod. Commun.* **2019**, *14*. [CrossRef]
111. Ferreira, J.; Ramos, A.A.; Almeida, T.; Azqueta, A.; Rocha, E. Drug resistance in glioblastoma and cytotoxicity of seaweed compounds, alone and in combination with anticancer drugs: A mini review. *Phytomedicine* **2018**, *48*, 84–93. [CrossRef]
112. Varghese, E.; Samuel, S.M.; Abotaleb, M.; Cheema, S.; Mamtani, R.; Büsselberg, D. The “Yin and Yang” of natural compounds in anticancer therapy of triple-negative breast cancers. *Cancers* **2018**, *10*, 346. [CrossRef]
113. Roe, A.L.; Paine, M.F.; Gurley, B.J.; Brouwer, K.R.; Jordan, S.; Griffiths, J.C. Assessing natural product–drug interactions: An end-to-end safety framework. *Regul. Toxicol. Pharmacol.* **2016**, *76*, 1–6. [CrossRef]
114. D’Andrea, G.M. Use of antioxidants during chemotherapy and radiotherapy should be avoided. *CA Cancer J. Clin.* **2005**, *55*. [CrossRef]
115. Funahashi, H.; Imai, T.; Mase, T.; Sekiya, M.; Yokoi, K.; Hayashi, H.; Shibata, A.; Hayashi, T.; Nishikawa, M.; Suda, N.; et al. Seaweed prevents breast cancer? *Jpn. J. Cancer Res.* **2001**, *92*, 483–487. [CrossRef] [PubMed]
116. Pilco-Ferreto, N.; Calaf, G.M. Influence of doxorubicin on apoptosis and oxidative stress in breast cancer cell lines. *Int. J. Oncol.* **2016**, *49*, 753–762. [CrossRef] [PubMed]



117. Tassone, P.; Tagliaferri, P.; Perricelli, A.; Blotta, S.; Quaresima, B.; Martelli, M.L.; Goel, A.; Barbieri, V.; Costanzo, F.; Boland, C.R.; et al. BRCA1 expression modulates chemosensitivity of BRCA1-defective HCC1937 human breast cancer cells. *Br. J. Cancer* **2003**, *88*, 1285–1291. [[CrossRef](#)]
118. Altharawi, A.; Rahman, K.M.; Chan, K.L.A. Identifying the responses from the estrogen receptor-expressed MCF7 cells treated in anticancer drugs of different modes of action using live-cell FTIR spectroscopy. *ACS Omega* **2020**, *5*, 12698–12706. [[CrossRef](#)]
119. Thippabhotla, S.; Zhong, C.; He, M. 3D cell culture stimulates the secretion of in vivo like extracellular vesicles. *Sci. Rep.* **2019**, *9*, 13012. [[CrossRef](#)]
120. Karimian, A.; Bahadori, M.H.; Moghaddam, A.H.; Mohammadrezaei, F.M. Effect of astaxanthin on cell viability in T-47D and MDA-MB-231 breast cancer cell lines. *Multidiscip. Cancer Investig.* **2017**, *1*. [[CrossRef](#)]
121. Franceschelli, S.; Pesce, M.; Ferrone, A.; De Lutiis, M.A.; Patruno, A.; Grilli, A.; Felaco, M.; Speranza, L. Astaxanthin treatment confers protection against oxidative stress in U937 cells stimulated with lipopolysaccharide reducing O<sub>2</sub><sup>−</sup> production. *PLoS ONE* **2014**, *9*, e88359. [[CrossRef](#)]
122. Yilmaz, Y.; Tunkaya, L.; Mercantepe, T.; Akyildiz, K. Protective effect of astaxanthin against cisplatin-induced gastrointestinal toxicity in rats. *Eur. Surg.* **2020**. [[CrossRef](#)]
123. Kinal, M.E.; Tatlıpınar, A.; Uzun, S.; Keskin, S.; Tekdemir, E.; Özbeyli, D.; Akakın, D. Investigation of astaxanthin effect on cisplatin ototoxicity in rats by using otoacoustic emission, total antioxidant capacity, and histopathological methods. *Ear Nose Throat J.* **2019**. [[CrossRef](#)]
124. Findik, H.; Tunkaya, L.; Yilmaz, A.; Gökhan Aslan, M.; Okutucu, M.; Akyildiz, K.; Mercantepe, T. The protective effects of astaxanthin against cisplatin-induced retinal toxicity. *Cutan. Ocul. Toxicol.* **2019**, *38*, 59–65. [[CrossRef](#)] [[PubMed](#)]
125. Banafa, A.M.; Roshan, S.; Liu, Y.Y.; Chen, H.J.; Chen, M.J.; Yang, G.X.; He, G.Y. Fucoïdan induces G1 phase arrest and apoptosis through caspases-dependent pathway and ROS induction in human breast cancer MCF-7 cells. *J. Huazhong Univ. Sci. Technolog. Med. Sci.* **2013**, *33*, 717–724. [[CrossRef](#)] [[PubMed](#)]
126. Abudabbus, A.; Badmus, J.A.; Shalaweh, S.; Bauer, R.; Hiss, D. Effects of fucoïdan and chemotherapeutic agent combinations on malignant and non-malignant breast cell lines. *Curr. Pharm. Biotechnol.* **2017**, *18*, 748–757. [[CrossRef](#)] [[PubMed](#)]
127. Zhang, J.; Sun, Z.; Lin, N.; Lu, W.; Huang, X.; Weng, J.; Sun, S.; Zhang, C.; Yang, Q.; Zhou, G.; et al. Fucoïdan from *Fucus vesiculosus* attenuates doxorubicin-induced acute cardiotoxicity by regulating JAK2/STAT3-mediated apoptosis and autophagy. *Biomed. Pharmacother.* **2020**, *130*, 110534. [[CrossRef](#)] [[PubMed](#)]
128. Reyes, M.E.; Riquelme, I.; Salvo, T.; Zanella, L.; Letelier, P.; Brebi, P. Brown seaweed fucoïdan in cancer: Implications in metastasis and drug resistance. *Mar. Drugs* **2020**, *18*, 232. [[CrossRef](#)]
129. Kim, K.H.; Kim, Y.W.; Kim, H.B.; Lee, B.J.; Lee, D.S. Anti-apoptotic activity of laminarin polysaccharides and their enzymatically hydrolyzed oligosaccharides from *Laminaria japonica*. *Biotechnol. Lett.* **2006**, *28*, 439–446. [[CrossRef](#)]
130. Malyarenko, O.S.; Usoltseva, R.V.; Silchenko, A.S.; Ermakova, S.P. Aminated laminaran from brown alga *Saccharina cichorioides*: Synthesis, structure, anticancer, and radiosensitizing potential in vitro. *Carbohydr. Polym.* **2020**, *250*, 117007. [[CrossRef](#)]
131. Han, Y.; Shi, S.; Xu, L.; Han, Y.; Li, J.; Sun, Q.; Zheng, Q.; Bai, X.; Wang, H. Protective effects of laminarin on cisplatin-induced ototoxicity in HEIOC1 auditory cells. *J. Nutr. Food Sci.* **2016**, *6*, 1–5. [[CrossRef](#)]
132. Kim, R.K.; Suh, Y.; Yoo, K.C.; Cui, Y.H.; Hwang, E.; Kim, H.J.; Kang, J.S.; Kim, M.J.; Lee, Y.Y.; Lee, S.J. Phloroglucinol suppresses metastatic ability of breast cancer cells by inhibition of epithelial-mesenchymal cell transition. *Cancer Sci.* **2015**, *106*, 94–101. [[CrossRef](#)]
133. Lin, K.W.; Huang, A.M.; Tu, H.Y.; Weng, J.R.; Hour, T.C.; Wei, B.L.; Yang, S.C.; Wang, J.P.; Pu, Y.S.; Lin, C.N. Phloroglucinols inhibit chemical mediators and xanthine oxidase, and protect cisplatin-induced cell death by reducing reactive oxygen species in normal human urothelial and bladder cancer cells. *J. Agric. Food Chem.* **2009**, *57*, 8782–8787. [[CrossRef](#)]
134. Yang, Y.I.; Ahn, J.H.; Choi, Y.S.; Choi, J.H. Brown algae phlorotannins enhance the tumoricidal effect of cisplatin and ameliorate cisplatin nephrotoxicity. *Gynecol. Oncol.* **2015**, *136*, 355–364. [[CrossRef](#)] [[PubMed](#)]
135. Ahn, H.S.; Lee, D.H.; Kim, T.J.; Shin, H.C.; Jeon, H.K. Cardioprotective effects of a phlorotannin extract against doxorubicin-induced cardiotoxicity in a rat model. *J. Med. Food* **2017**, *20*, 944–950. [[CrossRef](#)] [[PubMed](#)]
136. Li, X.; Li, Y.; Luo, J.; Zhou, Z.; Xue, G.; Kong, L. New phloroglucinol derivatives from the whole plant of *Hypericum uralum*. *Fitoterapia* **2017**, *123*, 59–64. [[CrossRef](#)] [[PubMed](#)]
137. Lu, J.; Shi, K.K.; Chen, S.; Wang, J.; Hassouna, A.; White, L.N.; Merien, F.; Xie, M.; Kong, Q.; Li, J.; et al. Fucoïdan extracted from the New Zealand *Undaria pinnatifida*-physicochemical comparison against five other fucoïdins: Unique low molecular weight fraction bioactivity in breast cancer cell lines. *Mar. Drugs* **2018**, *16*, 461. [[CrossRef](#)] [[PubMed](#)]
138. Jung, H.A.; Kim, J.I.; Choung, S.Y.; Choi, J.S. Protective effect of the edible brown alga *Ecklonia stolonifera* on doxorubicin-induced hepatotoxicity in primary rat hepatocytes. *J. Pharm. Pharmacol.* **2014**, *66*, 1180–1188. [[CrossRef](#)] [[PubMed](#)]
139. Mao, Z.; Shen, X.; Dong, P.; Liu, G.; Pan, S.; Sun, X.; Hu, H.; Pan, L.; Huang, J. Fucosterol exerts antiproliferative effects on human lung cancer cells by inducing apoptosis, cell cycle arrest and targeting of Raf/MEK/ERK signalling pathway. *Phytomedicine* **2019**, *61*, 152809. [[CrossRef](#)]
140. Choi, J.S.; Han, Y.R.; Byeon, J.S.; Choung, S.Y.; Sohn, H.S.; Jung, H.A. Protective effect of fucosterol isolated from the edible brown algae, *Ecklonia stolonifera* and *Eisenia bicyclis*, on tert-butyl hydroperoxide- and tacrine-induced HepG2 cell injury. *J. Pharm. Pharmacol.* **2015**, *67*, 1170–1178. [[CrossRef](#)]

141. Bae, H.; Lee, J.-Y.; Song, G.; Lim, W. Fucosterol suppresses the progression of human ovarian cancer by inducing mitochondrial dysfunction and endoplasmic reticulum stress. *Mar. Drugs* **2020**, *18*, 261. [[CrossRef](#)]
142. Kumar, P.; Aggarwal, R. An overview of triple-negative breast cancer. *Arch. Gynecol. Obstet.* **2016**, *293*, 247–269. [[CrossRef](#)]
143. Dai, X.; Li, T.; Bai, Z.; Yang, Y.; Liu, X.; Zhan, J.; Sho, B. Breast cancer intrinsic subtype classification, clinical use and future trends. *Am. J. Cancer* **2015**, *10*, 2029–2943.
144. Chaudhary, L.N.; Wilkinson, K.H.; Kong, A. Triple-negative breast cancer: Who should receive neoadjuvant chemotherapy? *Surg. Oncol. Clin. N. Am.* **2018**, *27*, 141–153. [[CrossRef](#)] [[PubMed](#)]
145. Cocco, S.; Piezzo, M.; Calabrese, A.; Cianniello, D.; Caputo, R.; Lauro, V.D.; Fusco, G.; Gioia, G.D.; Licenziato, M.; Laurentiis, M.D. Biomarkers in triple-negative breast cancer: State-of-the-art and future perspectives. *Int. J. Mol. Sci.* **2020**, *21*, 4579. [[CrossRef](#)] [[PubMed](#)]
146. da Silva, J.L.; Cardoso Nunes, N.C.; Izetti, P.; de Mesquita, G.G.; de Melo, A.C. Triple negative breast cancer: A thorough review of biomarkers. *Crit Rev. Oncol. Hematol.* **2020**, *145*, 102855. [[CrossRef](#)] [[PubMed](#)]
147. Nedeljković, M.; Damjanović, A. Mechanisms of chemotherapy resistance in triple-negative breast cancer-how we can rise to the challenge. *Cells* **2019**, *8*, 957. [[CrossRef](#)] [[PubMed](#)]
148. Sant, S.; Johnston, P.A. The production of 3D tumor spheroids for cancer drug discovery. *Drug Discov. Today Technol.* **2017**, *23*, 27–36. [[CrossRef](#)] [[PubMed](#)]
149. Minchinton, A.I.; Tannock, I.F. Drug penetration in solid tumours. *Nat. Rev. Cancer* **2006**, *6*, 583–592. [[CrossRef](#)] [[PubMed](#)]
150. Caamal-Fuentes, E.; Moo-Puc, R.; Freile-Pelegrín, Y.; Robledo, D. Cytotoxic and antiproliferative constituents from *Dictyota ciliolata*, *Padina sanctae-crucis* and *Turbinaria tricostrata*. *Pharm. Biol.* **2014**, *52*, 1244–1248. [[CrossRef](#)] [[PubMed](#)]
151. Fontoura, J.C.; Viezzer, C.; dos Santos, F.G.; Ligabue, R.A.; Weinlich, R.; Puga, R.D.; Antonow, D.; Severino, P.; Bonorino, C. Comparison of 2D and 3D cell culture models for cell growth, gene expression and drug resistance. *Mater. Sci. Eng. C* **2020**, *107*, 110264. [[CrossRef](#)]
152. Langhans, S.A. Three-Dimensional in vitro cell culture models in drug discovery and drug repositioning. *Front. Pharmacol.* **2018**, *9*, 6. [[CrossRef](#)]
153. Lovitt, C.J.; Shelper, T.B.; Avery, V.M. Doxorubicin resistance in breast cancer cells is mediated by extracellular matrix proteins. *BMC Cancer* **2018**, *18*, 41. [[CrossRef](#)]
154. Nunes, A.S.; Costa, E.C.; Barros, A.S.; de Melo-Diogo, D.; Correia, I.J. Establishment of 2D cell cultures derived from 3D MCF-7 spheroids displaying a doxorubicin resistant profile. *Biotechnol. J.* **2019**, *14*, e1800268. [[CrossRef](#)] [[PubMed](#)]
155. Ziegler, U.; Groscurth, P. Morphological features of cell death. *Physiology* **2004**, *19*, 124–128. [[CrossRef](#)] [[PubMed](#)]
156. Saraste, A.; Pulkki, K. Morphologic and biochemical hallmarks of apoptosis. *Cardiovasc. Res.* **2000**, *45*, 528–537. [[CrossRef](#)]





# **Chapter 5** - Fucoxanthin Holds Potential to Become a Drug Adjuvant in Breast Cancer Treatment: Evidence from 2D and 3D Cell Cultures

---



## Article

# Fucoxanthin Holds Potential to Become a Drug Adjuvant in Breast Cancer Treatment: Evidence from 2D and 3D Cell Cultures

Fernanda Malhão <sup>1,2,†</sup> , Ana Catarina Macedo <sup>1,2,†</sup> , Carla Costa <sup>3,4</sup>, Eduardo Rocha <sup>1,2,\*</sup>  and Alice Abreu Ramos <sup>1,2</sup> 

- <sup>1</sup> Institute of Biomedical Sciences Abel Salazar (ICBAS), University of Porto (U.Porto), Rua de Jorge Viterbo Ferreira 228, 4050-313 Porto, Portugal; fcmalhao@icbas.up.pt (F.M.); acfpmacedo@gmail.com (A.C.M.); ramosalic@gmail.com (A.A.R.)
- <sup>2</sup> Interdisciplinary Center for Marine and Environmental Research (CIIMAR), University of Porto (U.Porto), Avenida General Norton de Matos, 4450-208 Matosinhos, Portugal
- <sup>3</sup> Environmental Health Department, National Health Institute Dr. Ricardo Jorge, Rua Alexandre Herculano 321, 4000-055 Porto, Portugal; carla.trindade@insa.min-saude.pt
- <sup>4</sup> EPIUnit—Instituto de Saúde Pública, University of Porto (U.Porto), Rua das Taipas 135, 4050-600 Porto, Portugal
- \* Correspondence: erocha@icbas.up.pt
- † Fernanda Malhão and Ana Catarina Macedo contributed equally to this work and are joint first authors.



**Citation:** Malhão, F.; Macedo, A.C.; Costa, C.; Rocha, E.; Ramos, A.A. Fucoxanthin Holds Potential to Become a Drug Adjuvant in Breast Cancer Treatment: Evidence from 2D and 3D Cell Cultures. *Molecules* **2021**, *26*, 4288. <https://doi.org/10.3390/molecules26144288>

Academic Editors: Madalena Pinto and Marta Correia-da-Silva

Received: 14 June 2021

Accepted: 11 July 2021

Published: 15 July 2021

**Publisher's Note:** MDPI stays neutral with regard to jurisdictional claims in published maps and institutional affiliations.



**Copyright:** © 2021 by the authors. Licensee MDPI, Basel, Switzerland. This article is an open access article distributed under the terms and conditions of the Creative Commons Attribution (CC BY) license (<https://creativecommons.org/licenses/by/4.0/>).

**Abstract:** Fucoxanthin (Fx) is a carotenoid derived from marine organisms that exhibits anticancer activities. However, its role as a potential drug adjuvant in breast cancer (BC) treatment is still poorly explored. Firstly, this study investigated the cytotoxic effects of Fx alone and combined with doxorubicin (Dox) and cisplatin (Cis) on a panel of 2D-cultured BC cell lines (MCF7, SKBR3 and MDA-MB-231) and one non-tumoral cell line (MCF12A). Fucoxanthin induced cytotoxicity against all the cell lines and potentiated Dox cytotoxic effects towards the SKBR3 and MDA-MB-231 cells. The combination triggering the highest cytotoxicity (Fx 10  $\mu$ M + Dox 1  $\mu$ M in MDA-MB-231) additionally showed significant induction of cell death and genotoxic effects, relative to control. In sequence, the same combination was tested on 3D cultures using a multi-endpoint approach involving bioactivity assays and microscopy techniques. Similar to 2D cultures, the combination of Fx and Dox showed higher cytotoxic effects on 3D cultures compared to the isolated compounds. Furthermore, this combination increased the number of apoptotic cells, decreased cell proliferation, and caused structural and ultrastructural damages on the 3D models. Overall, our findings suggest Fx has potential to become an adjuvant for Dox chemotherapy regimens in BC treatment.

**Keywords:** cisplatin; combinatorial therapy; doxorubicin; fucoxanthin; seaweed compounds; triple-negative breast cancer

## 1. Introduction

Nature has always been a source of active substances for drug development, and despite the advances in synthetic biology, most of the currently approved medicines are based on natural products [1,2]. In fact, more than 60% of the anticancer drugs used in clinical practice are derived from natural sources, including the well-known chemotherapeutics doxorubicin (Dox), paclitaxel, vincristine and vinblastine [1,3]. In the last few decades, there has been a growing interest in exploring the marine ecosystem for drug discoveries [4,5]. Marine organisms yield a wide variety of bioactive compounds with unique properties and promising potential for developing new anticancer drugs [6,7]. Recent data report that, so far, five marine-derived drugs have been approved for cancer treatment [8], while 24 drug candidates are being tested in clinical trials [9].



Among marine organisms, seaweeds (or macroalgae) bear a high content of phytochemicals (e.g., carotenoids, polyphenolic compounds and polysaccharides) with promising chemopreventive and chemotherapeutic properties towards several types of cancer, namely breast cancer (BC) [10]. Interestingly, in Asiatic folk medicine, seaweeds have been used since ancient times as potential weapons to treat BC [11]. Besides, some studies have also been pointing out the benefits of dietary seaweed consumption on the prevention of BC [12,13].

Fucoxanthin (Fx) is one of the most abundant xanthophyll carotenoids of the marine environment that is mainly found in brown seaweeds such as the popular edible algae Wakame (*Undaria pinnatifida*) [14,15]. This orange-colored pigment is known for having distinct health-promoting activities, such as anti-inflammatory, antioxidant, antidiabetic, anti-obesity and anticancer effects in various types of cancers [16–22], including BC [23]. The anticancer effects comprise proapoptotic, antiproliferative, antimetastatic and antiangiogenic activities [24]. In BC cells, Fx increases apoptosis [14,22,23] and decreases lymphangiogenesis [25].

BC is currently the most prevalent cancer and the leading cause of cancer-related deaths amongst females worldwide [26,27]. In 2020, there were 2.3 million women diagnosed with this disease, accounting for 685,000 deaths globally [28]. BC comprises tumors with high heterogeneity and a wide variety of histological and molecular features, which translate into distinct biological behaviors and treatments [29]. According to the St. Gallen International Breast Cancer Conference 2013, BC is classified into four molecular subtypes: Luminal A, Luminal B, HER-2 overexpression, and triple-negative. These BC subtypes are differentiated by the presence of estrogen receptor (ER), progesterone receptor (PgR) and different expression levels of the human epidermal growth factor receptor 2 (HER-2) and antigen Ki67 [30]. Luminal A (ER+/PgR+/HER-2– with low ki67) and B (ER+/PgR+/HER-2– with high ki67) subtypes present the lowest recurrence rates and the best prognosis [30,31], being typically treated with hormonal therapy or a combination of both chemotherapy and hormonal treatments [32]. The HER-2 overexpression subtype (ER–/PR–/HER-2+) is linked with an aggressive phenotype and worse prognosis, however, it is often successfully treated with HER-2 targeted therapies, such as trastuzumab and pertuzumab [33]. The triple-negative BC (TNBC) subtype (ER–/PR–/HER-2–) accounts for the poorest clinical outcomes due to its aggressive metastatic behavior and the lack of targeted therapies, being chemotherapy the single treatment option currently available [34]. Despite being the most chemotherapy-responsive subtype, TNBCs still present the highest recurrence and metastasis rate compared to other BCs [35].

Current neoadjuvant or adjuvant chemotherapy treatments for BC usually involve the administration of reference anticancer drugs such as Dox, cisplatin (Cis), or paclitaxel isolated or in combination regimens [36]. While commonly used, chemotherapy drugs can cause severe adverse effects, as they induce cytotoxicity in non-target cells (non-tumorigenic cells) [37]. For instance, Dox is normally associated with cardiotoxicity, myelosuppression, intestinal epithelium lesions [36], and Cis can induce nephrotoxicity, neurotoxicity and hearing impairments [38]. Additionally, the onset of multidrug resistance is still one of the major hurdles of chemotherapy, being responsible for the death of many cancer patients [37]. Therefore, strategies to overcome chemotherapy-associated limitations are in need, encouraging the search for new anticancer drugs or adjuvant drugs.

In this vein, recent reports have shown that the combination of established anticancer drugs with natural products, such as marine-derived compounds, can potentiate drug efficacy and reduce the administered doses, causing the mitigation of the associated adverse effects and preventing the onset of drug resistance [39,40].

Although data are scarce, a few studies tested the effects of Fx in combination with conventional anticancer drugs such as 5-Fluorouracil [41], Imatinib [42] and Dox [43]. A recent review on the mechanisms of the anticancer effects of Fx and its combination with chemotherapy drugs reported that generally the combinations were more effective than either Fx or the drugs alone [44]. However, more mechanistic studies are required to investigate the interactions of Fx with anticancer drugs and elucidate the processes

underlying the combinatorial effects. Knowledge on this subject is of utmost importance not only for oncological medicine, but also for the field of nutritional therapy, as seaweeds can be included in diets or be consumed as dietary supplements [45].

Most of the existing data regarding the anticancer effects of Fx were obtained from *in vitro* studies using monolayer cultures. Despite providing valuable information in the scope of oncology drug discovery, 2D cell culture models present several limitations in predicting drug activity and toxicity *in vivo* [46,47]. One of the main disadvantages of these models is the lack of interactions between cell–cell and cell–extracellular environment. These are usually found in solid tumors, affecting cell polarity and other related cellular functions, including proliferation and differentiation, viability, apoptosis, proteins and gene expression, response to stimuli, and drug metabolism [48]. Accumulating evidence confirms that cells grown in a 3D physical shape have a better predictive capacity of *in vivo* cellular responses than cells grown as a monolayer [49,50].

To make up for the current lack of information, this study aimed to: (1) evaluate the cytotoxic effects of Fx alone and in combination with reference drugs—Cis or Dox—on a panel of four 2D-cultured cell lines (three BC cell lines of different molecular subtypes and one non-tumoral breast cell line); (2) select the combination with the most promising cytotoxic effect and further investigate its effects in the respective 3D cell model; and (3) explore some possible underlying anticancer mechanisms of that combination on both cell models, using bioactivity assays and microscopy techniques.

## 2. Results

### 2.1. Phase 1—Cytotoxic Effects of Fx Alone in 2D Cell Cultures

The cytotoxicity of Fx was evaluated by the MTT assay after 72 h of exposure. Fucoxanthin induced dose-dependent cytotoxic effects in all the tested cell lines at concentrations equal to or above 10  $\mu\text{M}$  (Figure 1). At 10 and 20  $\mu\text{M}$ , Fx reduced the viability of MCF7, SKBR3 and MDA-MB-231 cells to approximately 62 and 22%, respectively. For the MCF12A cells treated with the same concentrations, the viability decreased to around 74 and 31%. At the highest tested concentration (50  $\mu\text{M}$ ), Fx induced significant cytotoxic effects on all the cell lines by reducing their viabilities to nearly 10%.

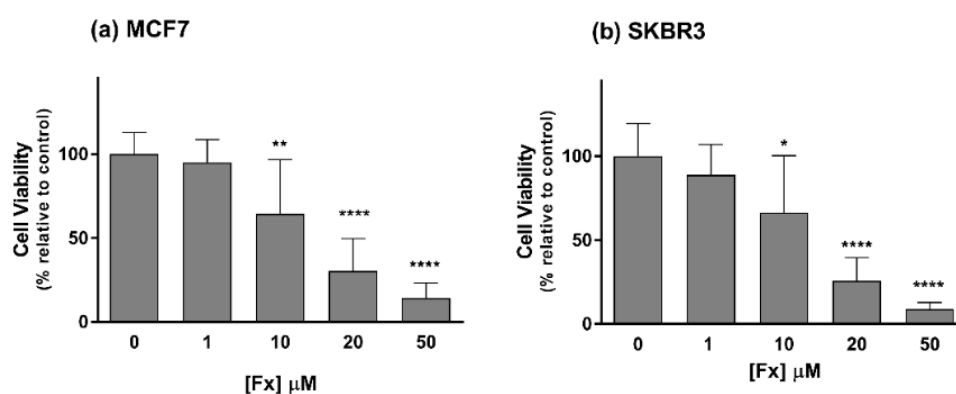
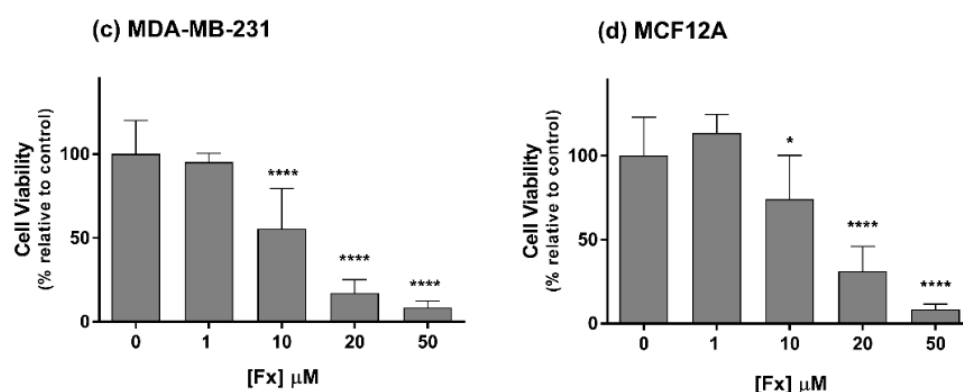


Figure 1. *Conts.*



**Figure 1.** Effects of Fx on the viability of MCF7 (a), SKBR3 (b), MDA-MB-231 (c) and MCF12A (d) cells, assessed by the MTT assay after 72 h of incubation. Results are expressed as mean + standard deviation of six independent experiments. Asterisks indicate significant differences relative to control (\*  $p < 0.05$ ; \*\*  $p < 0.01$ ; \*\*\*\*  $p < 0.0001$ ).

## 2.2. Phase 2—Cytotoxic Effects of Fx Combined with Dox or Cis in 2D Cell Cultures

Considering the cytotoxicity data and the selection criteria defined in Section 4.4, two concentrations of Fx and two concentrations of Dox and Cis were selected to be tested in combination on the panel of BC cell lines. The effects of these mixtures and respective isolated compounds on cell viability were determined by the MTT assay after 72 h.

Regarding the MCF7 and SKBR3 cells (Figure 2a,b), the drug Cis at 10 and 20  $\mu\text{M}$  markedly reduced the viability of both cell lines by 35% and 62%, respectively. Additionally, all the combinations between this drug and Fx induced significant cytotoxic effects on both cell lines in relation to the control group. Still, those effects did not differ from the ones of the single compounds. Fx at 10  $\mu\text{M}$  induced a significant cytotoxic effect on the SKBR3 cell line, either alone or in combination with Dox at 0.1  $\mu\text{M}$ , resulting in a reduction in cell viability of roughly 31% and 43%, compared to the control. Beyond that, the mentioned combination was also found to cause significantly higher cytotoxicity than the compounds alone, resulting in a cell viability loss of 12% in relation to Fx and 18% compared to Dox.

Results from the MDA-MB-231 cell line (Figure 2c) showed that Cis alone did not induce statistically significant cytotoxic effects. However, the combination of Fx (1 or 10  $\mu\text{M}$ ) with Cis 20  $\mu\text{M}$  decreased cell viability in relation to the control. Moreover, cells treated with Dox alone at 1  $\mu\text{M}$  as well as with the combinations Fx 10  $\mu\text{M}$  + Dox 0.1  $\mu\text{M}$  and Fx 1/10  $\mu\text{M}$  + Dox 1  $\mu\text{M}$  also presented a statistically significant decrease in cell viability compared to control cells. Noteworthy, the combination of Dox 1  $\mu\text{M}$  with Fx 10  $\mu\text{M}$  was the only one that remarkably decreased MDA-MB-231 viability to a percentage that statistically differed from both Fx and the drug alone. This combination was able to cause a reduction in cell viability of 73%, in relation to the control, and to increase Dox cytotoxicity by approximately 26%.

In line with the one-way ANOVA analysis detecting differences between groups in the MDA-MB-231 and MCF7 cell lines, the Holm–Bonferroni corrected t-tests comparing only the Fx 10  $\mu\text{M}$  with control ( $p < 0.05$  and  $p < 0.001$ , respectively) indicated that Fx induced statistically significant cytotoxicity in those cells.

Concerning the MCF12A cell line (Figure 2d), Fx at 10  $\mu\text{M}$  exhibited significant cytotoxic effects, reducing cell viability by 37% relative to the control group. Cytotoxicity was also observed in cells exposed to Cis 1  $\mu\text{M}$  combined with Fx 10  $\mu\text{M}$  and to Cis 10  $\mu\text{M}$ , alone and combined with Fx 1 or 10  $\mu\text{M}$ . Furthermore, Dox only significantly increased cytotoxicity in MCF12A cells when combined with Fx 1  $\mu\text{M}$  (Dox 0.1  $\mu\text{M}$ ) or Fx 10  $\mu\text{M}$  (Dox 0.01 and 0.1  $\mu\text{M}$ ).

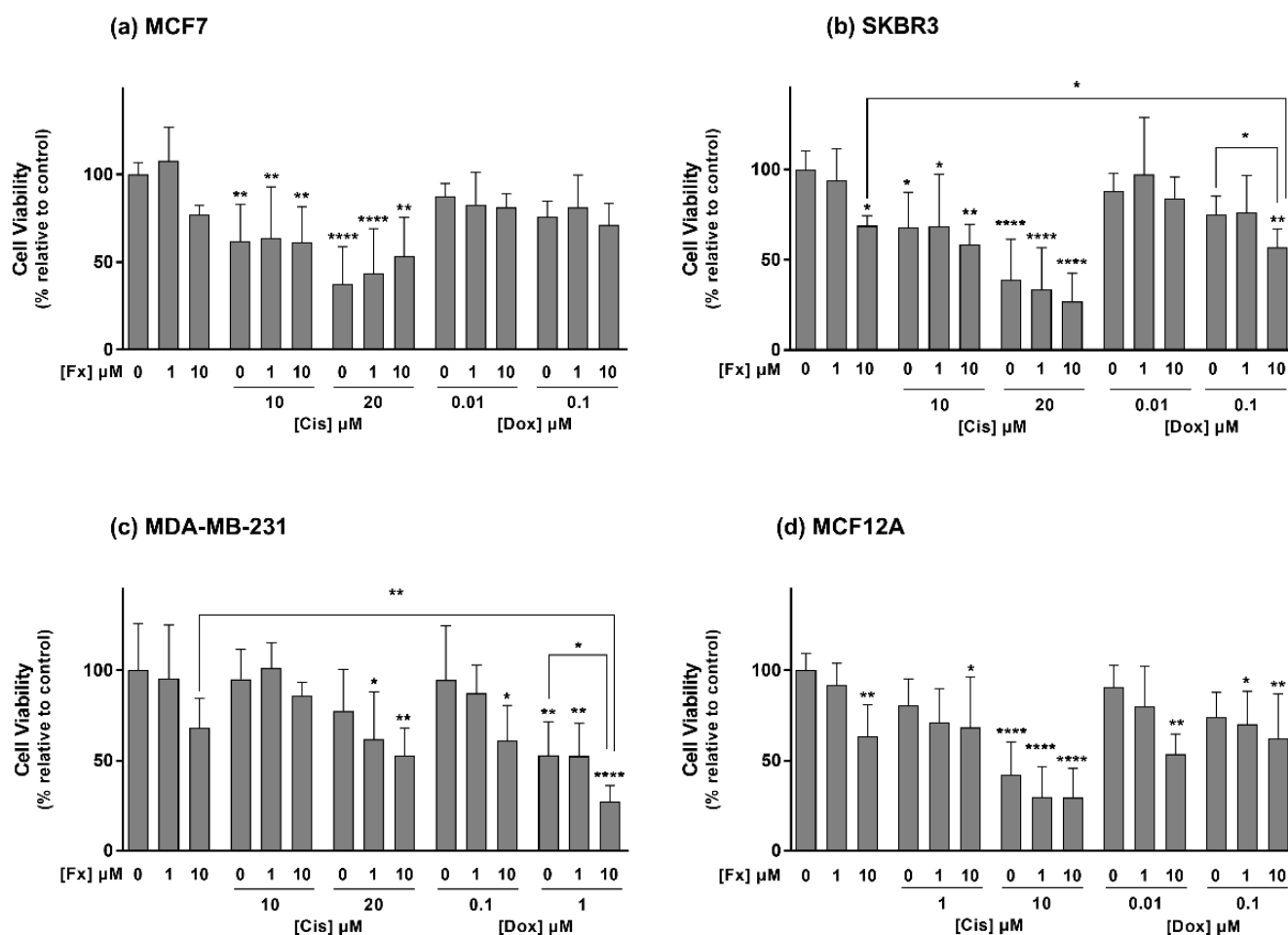


**Figure 2.** Effects of Fx alone and in combination with Dox or Cis on the viability of MCF7 (a), SKBR3 (b), MDA-MB-231 (c) and MCF12A (d) cells, assessed by the MTT assay after 72 h of incubation. Results are expressed as mean + standard deviation of five independent experiments. Asterisks indicate significant differences relative to control (\*  $p < 0.05$ ; \*\*  $p < 0.01$ ; \*\*\*\*  $p < 0.0001$ ). Square brackets indicate differences between conditions using t-tests with sequential Holm–Bonferroni corrections.

Given all the above results, the condition Fx 10  $\mu\text{M}$  + Dox 1  $\mu\text{M}$  tested in MDA-MB-231 cells was elected as the most promising combination since it showed the highest decrease in cell viability, which statistically differed from the control and both the drug and Fx alone. To explore the possible mechanisms of action underlying its cytotoxic activity, the nuclear condensation and comet assays were performed in 2D cultures.

### 2.3. Phase 3—Effects of Fx Combined with Dox on Cell Death and DNA Damage in 2D Cell Cultures

The effect of the selected combination and respective isolated compounds on the induction of cell death in MDA-MB-231 cells was evaluated by the nuclear condensation assay after 72 h of exposure. Statistical results (Figure 3a) showed that Fx alone did not induce effects on cell death. On the other hand, Dox 1  $\mu\text{M}$  and the combination Fx 10  $\mu\text{M}$  + Dox 1  $\mu\text{M}$  markedly increased the number of cells with condensed nuclei (both around 13%), relative to control. Concordantly, when analyzing the images from the nuclear condensation assay (Figure 3c), it was noted that those conditions exhibited a higher number of cells with condensed nuclei, as compared to Fx and the control.

Effects on DNA damage (strand breaks) were determined by the alkaline version of the comet assay following 2 h of exposure. According to the statistical results (Figure 3b), Dox alone and in combination with Fx showed a significant increase in DNA damages compared to the control, accounting for a tail intensity of 26% and 21%, respectively. In

both conditions, it was observed an increase of fluorescence intensity in the comet tail (Figure 3d). In contrast, both the control and Fx-treated groups presented a low level of DNA damages, as the DNA of most cells occurred as a nucleoid with no or a small tail.

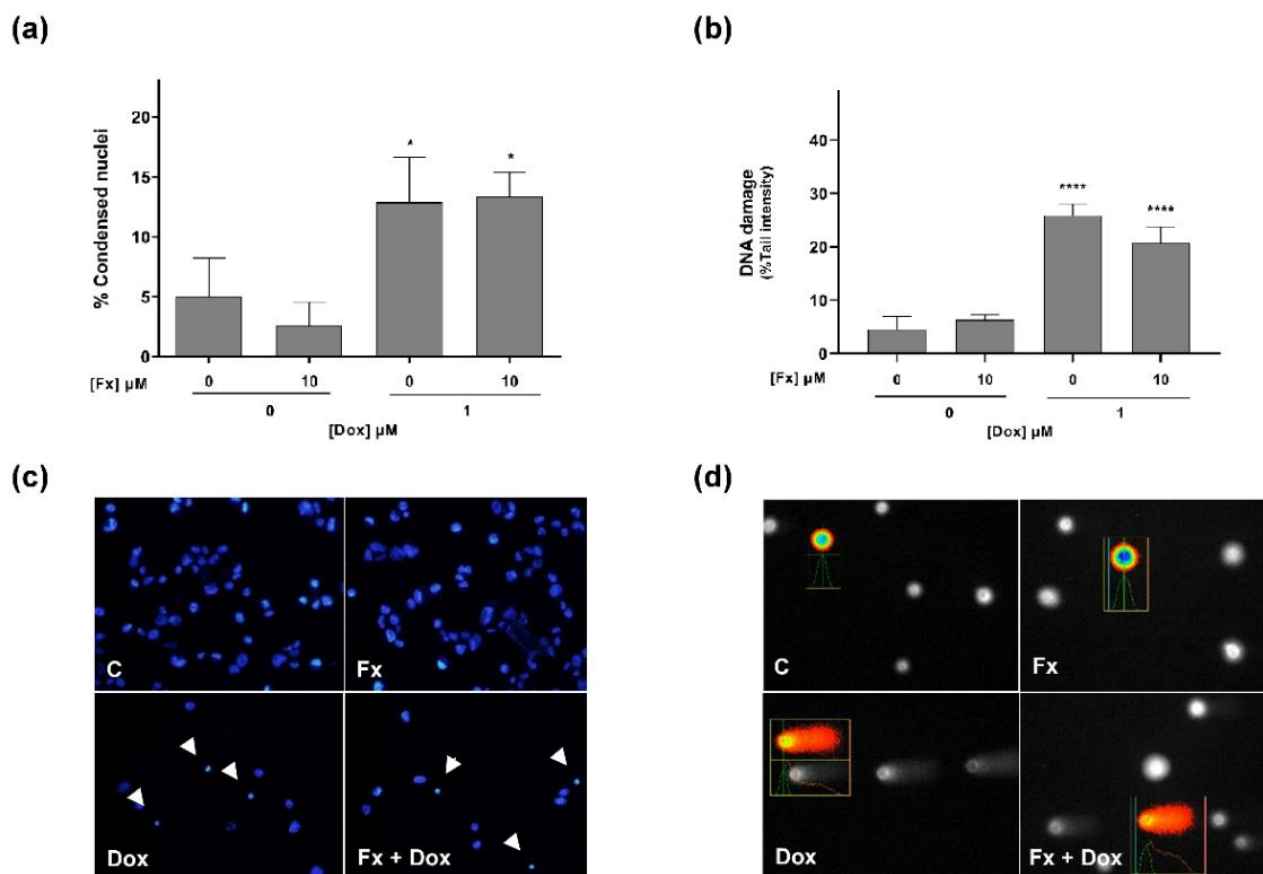


**Figure 3.** Effects of Fx alone and in combination with Dox on the cell death (a,c) and DNA damage (b,d) of the MDA-MB-231 cell line, assessed by the nuclear condensation and comet assays, respectively. Images illustrate the induced cell death (b) and genotoxic effects (d). The white arrowheads indicate the cells with condensed nuclei. Results are expressed as mean + standard deviation of three to five independent experiments. Asterisks indicate significant differences relative to control (\*  $p < 0.05$ ; \*\*\*\*  $p < 0.0001$ ). Scale Bar: 100  $\mu\text{m}$ .

#### 2.4. Phase 4—Effects of Fx Combined with Dox in 3D Cell Cultures (Multicellular Aggregates-MCAs)

##### 2.4.1. Cytotoxic Effects

The most promising combination in the 2D cell culture screening (Fx 10  $\mu\text{M}$  + Dox 1  $\mu\text{M}$ ) was selected to be tested in 3D culture. Additionally, combinations with higher concentrations of Fx (20  $\mu\text{M}$ ) and Dox (2  $\mu\text{M}$ ) were included, as well as a positive control for cytotoxicity (Dox 5  $\mu\text{M}$ ). Effects on cell viability were assessed by two assays: MTT and LDH.

According to the MTT assay (Figure 4a), Fx alone did not present effects on cell viability in MDA-MB-231 MCAs. Doxorubicin ( $\geq 2$   $\mu\text{M}$ ) and respective combinations showed cytotoxicity, with cell viabilities under 55% in relation to the control. At 1  $\mu\text{M}$ , Dox alone did not significantly affect cell viability, but in combination with Fx 10  $\mu\text{M}$ , it statistically differed from the control and the drug, causing a decrease in 22% of cell viability in relation to the drug and 30% in relation to the seaweed compound alone. As for the other combinations with higher Fx and Dox concentrations, they did not statistically differ from Dox alone.

In the LDH assay (Figure 4b), Fx alone did not present cytotoxic effects on the MDA-MB-231 MCAs. The same was observed after exposure to Dox 1  $\mu\text{M}$  (alone and combined) and Dox 2  $\mu\text{M}$  (alone and combined with Fx 10  $\mu\text{M}$ ). The conditions that presented higher

LDH release, differing from the control and indicating high cytotoxicity, were Dox 2  $\mu\text{M}$  combined with Fx 20  $\mu\text{M}$  (56%) and Dox 5  $\mu\text{M}$  (77%).

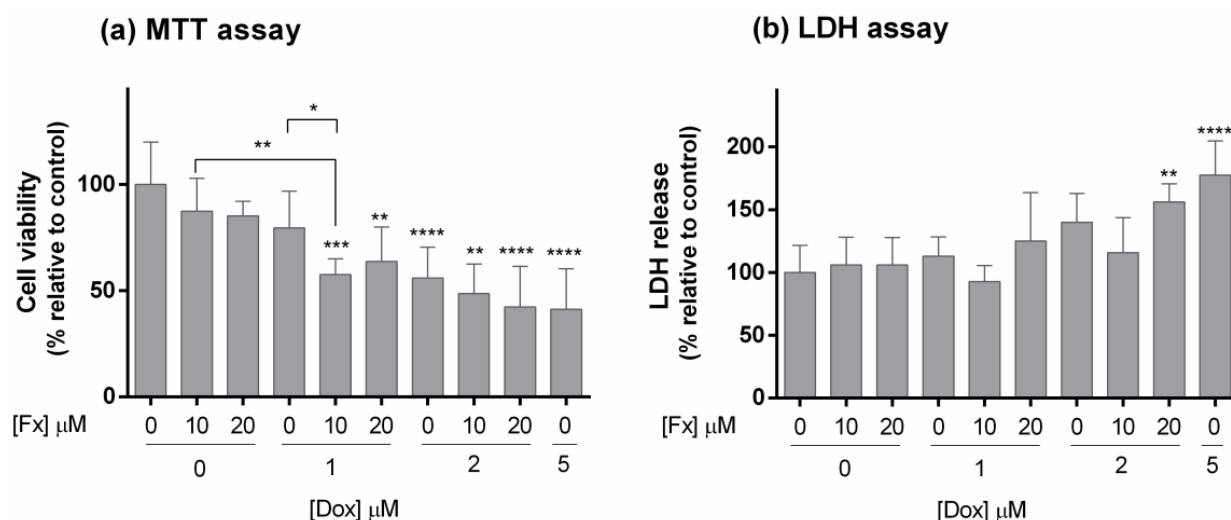


**Figure 4.** Effects of Fx alone and in combination with Dox on the cell viability of MDA-MB-231 MCAs, assessed by the MTT (a) and LDH (b) assays after 96 h of incubation. The percentages of cell viability and LDH release are relative to the control and presented as mean + standard deviation of five independent experiments (each in triplicate). Asterisks indicate significant differences relative to control (\*  $p < 0.05$ ; \*\*  $p < 0.01$ ; \*\*\*  $p < 0.001$ ; \*\*\*\*  $p < 0.0001$ ). Square brackets indicate differences between conditions using  $t$ -tests with sequential Holm–Bonferroni corrections.

#### 2.4.2. Stereomicroscopic Analysis and Area Measurements

MCAs were monitored throughout the exposure by regular observation under a stereomicroscope (Figure 5a), and photographs of each MCA were taken at the end of the exposure period (96 h). To explore the single and combinatory effects of Fx and Dox on the MCAs morphology, the areas of each MCA were measured by the AnaSP software. Results indicated that only the MCAs exposed to Dox 5  $\mu\text{M}$  presented a significant increase in area, compared to control (Figure 5b).

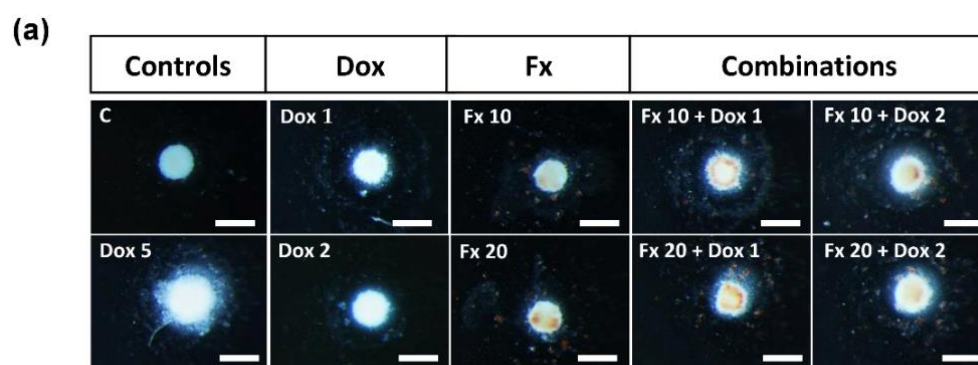


**Figure 5.** *Conts.*



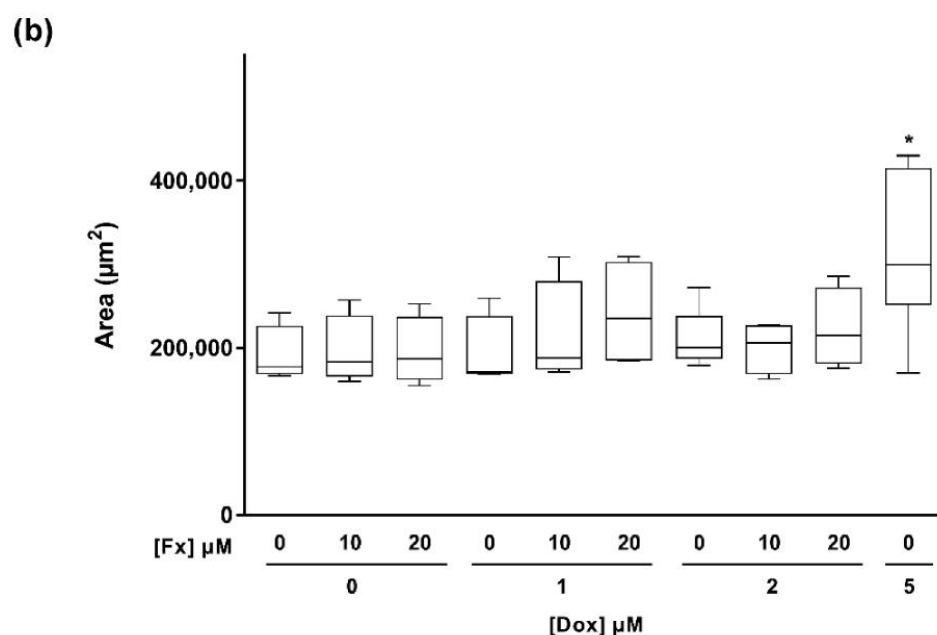


**Figure 5.** Representative stereomicroscopic images of MDA-MB-231 MCAs exposed to Fx (10 and 20  $\mu\text{M}$ ) and Dox (1, 2 and 5  $\mu\text{M}$ ), alone and combined, for 96 h (a). MCAs area measurements are expressed as median, maximum, minimum and interquartile range (Q3–Q1) of four to six independent experiments (b). Asterisks indicate significant differences relative to control (\*  $p < 0.05$ ). Scale bar: 500  $\mu\text{m}$ .

#### 2.4.3. Structural and Ultrastructural Analysis

At the end of the exposure time, MCAs from all tested conditions were fixed, and processed for light and electron microscopy. Paraffin sections were submitted to Hematoxylin-Eosin (HE) staining for assessing the general morphology and for Immunocytochemistry (ICC) analysis to study the apoptotic and proliferative status of the MCAs. Additionally, semithin and ultrathin sections of epoxy-embedded MCAs were obtained to analyze the ultrastructural changes caused by the compounds.

##### HE Staining

Observation of the HE-stained MCAs (Figure 6) revealed that most MCAs presented a compact structure. This compactness was gradually lost in the exposure conditions of Dox 2  $\mu\text{M}$  > Fx 20  $\mu\text{M}$  + Dox 2  $\mu\text{M}$  > Dox 5  $\mu\text{M}$ . There was a total disaggregation of the MCAs exposed to Dox 5  $\mu\text{M}$  when collecting them for fixation and processing. In all MCAs, there were some cells with hyperchromatic or pyknotic nuclei; however, these features were more evident in Dox 2  $\mu\text{M}$  (alone and combined) and Dox 5  $\mu\text{M}$ .

A higher degradation of the MCAs structure was noticed in the aggregates exposed to the combinations of Fx with Dox, when compared to MCAs treated with the drug alone, especially in the mixtures with Dox plus Fx 20  $\mu\text{M}$ . These MCAs revealed an increased number of cells with an apoptotic morphology comprising pyknotic nuclei, and/or nuclear fragmentation. At the combination of Fx 20  $\mu\text{M}$  with Dox 1  $\mu\text{M}$ , it was observed a marked increase in cellular eosinophilia. The same was not so evident in the combination of Fx 20  $\mu\text{M}$  with Dox 2  $\mu\text{M}$ . No necrotic cores were observed in the sectioned MCAs.

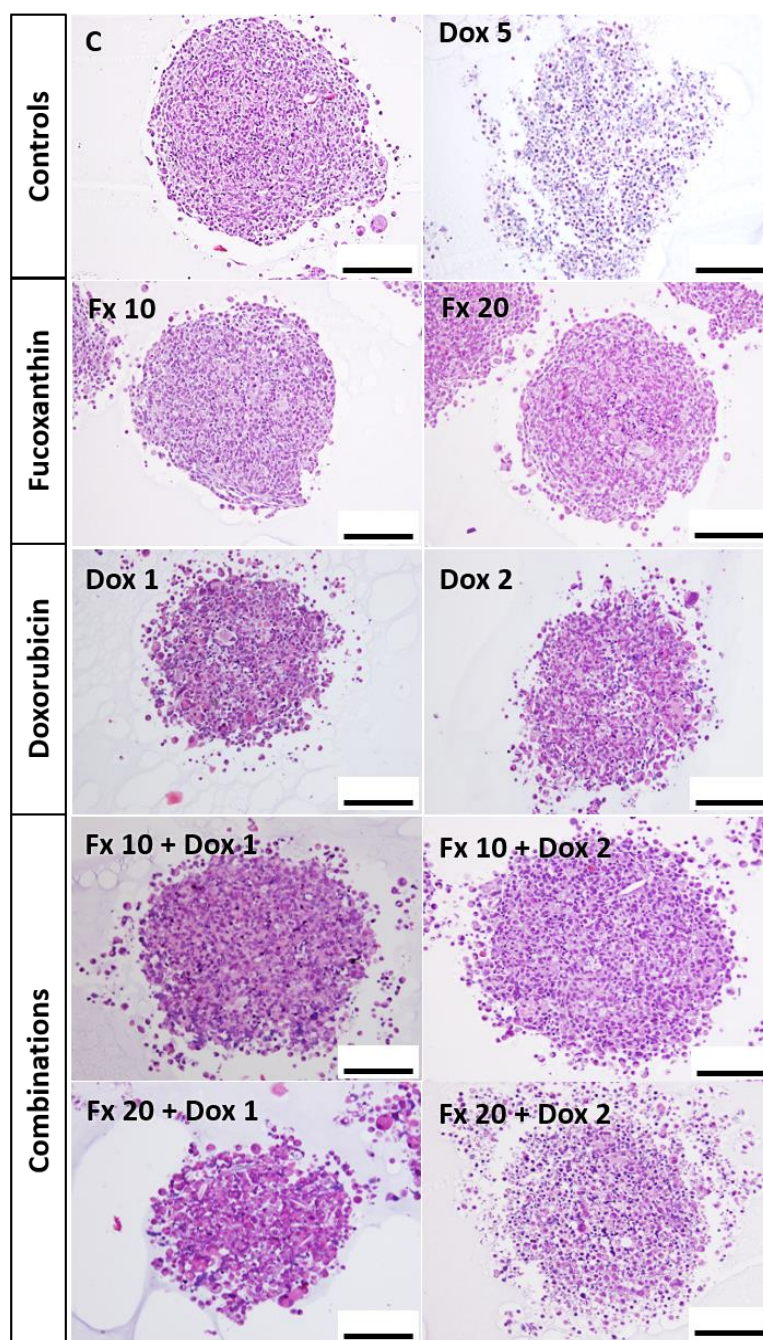


**Figure 6.** Representative histological images of the MDA-MB-231 MCAs exposed to Fx (10 and 20  $\mu\text{M}$ ) and Dox (1 and 2  $\mu\text{M}$ ), alone and combined, for 96 h. Dox 5  $\mu\text{M}$  was included as a positive control. MCAs from at least three independent experiments were sectioned and stained with HE staining. Scale bar: 100  $\mu\text{m}$ .

### ICC

An ICC analysis was performed on the MCAs from all the tested conditions, and the correspondent percentages of positive cells for caspase-3 and ki67 are displayed in Figure 7. About caspase-3 (Figure 7a), the control MCAs presented, on average, 15% of positive cells, revealed by brown staining in the cytoplasm of apoptotic cells (Figure 8). Fucoxanthin and Dox 1  $\mu\text{M}$  alone did not differ from the control. However, when Dox 1  $\mu\text{M}$  is combined with Fx 10 and 20  $\mu\text{M}$ , statistical differences relative to control were found, presenting a significantly higher number of apoptotic cells. Additionally, Dox 2  $\mu\text{M}$  alone and in



combinations with Fx, statistically differed from the control. Still, only the combination of Fx 20  $\mu\text{M}$  + Dox 2  $\mu\text{M}$  differed from the control and both compounds alone, presenting an increase of 23% of positive cells relative to Dox 2  $\mu\text{M}$  alone. Figure 8 shows representative images of these conditions immunomarked with caspase-3. Most cells of the MCAs exposed to Fx 20  $\mu\text{M}$  + Dox 2  $\mu\text{M}$  are brown stained, contrasting with the control where the brown staining is restricted to a small number of cells distributed throughout the MCAs. The conditions Fx 20  $\mu\text{M}$  + Dox 2  $\mu\text{M}$  and Dox 5  $\mu\text{M}$  showed marked apoptotic effects as the percentages of positive cells for caspase-3 were five times higher than the control.

Regarding the ki67 proliferation marker (Figure 7b), there was an opposite trend as the number of positive cells decreased with the compound's concentration increase. The control MCAs showed, on average, 23% of immunomarked cells, corresponding to the brown color in the nucleus (Figure 8). The ki67 positive cells were distributed in the MCAs without any preferential localization. Fx alone did not differ from the control, however, the combination of Fx 20  $\mu\text{M}$  with Dox 1  $\mu\text{M}$  showed a decrease in the number of proliferating cells (8.5% on average) that not only differed from the control but also from both Fx 20  $\mu\text{M}$  (18%) and Dox 1  $\mu\text{M}$  (16%) alone. Representative images of ki67 immunostaining relative to this combination are given in Figure 8. Dox 2  $\mu\text{M}$  (alone and combined) and Dox 5  $\mu\text{M}$  differed from the control, showing fewer ki67-positive cells.

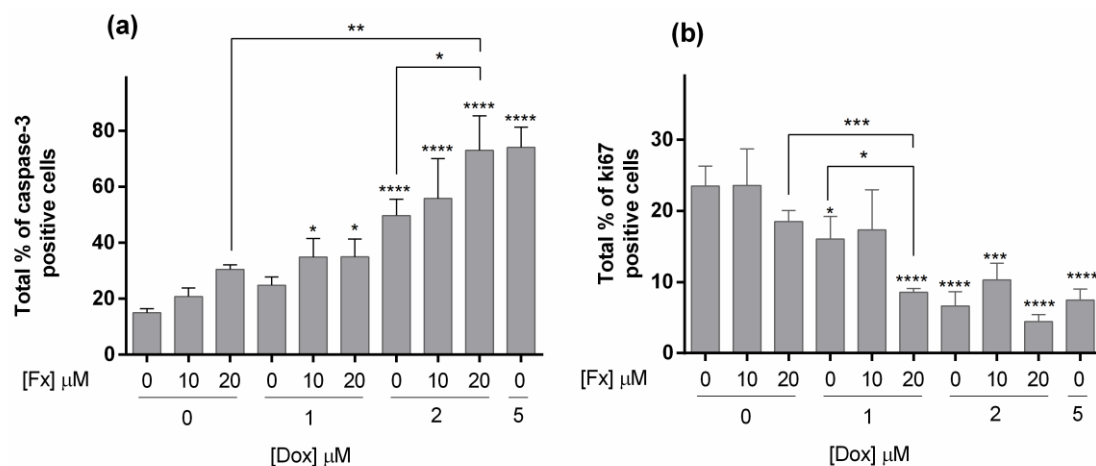


**Figure 7.** ICC against caspase-3 (a) and ki67 (b) in MDA-MB-231 MCAs exposed to Fx alone and in combination with Dox for 96 h. Dox 5  $\mu\text{M}$  was included as a positive control. The results are expressed as absolute percentages and presented as mean + standard deviation of three independent experiments. Asterisks indicate significant differences relative to control (\*  $p < 0.05$ ; \*\*  $p < 0.01$ ; \*\*\*  $p < 0.001$ ; \*\*\*\*  $p < 0.0001$ ). Square brackets indicate differences between conditions using t-tests with sequential Holm–Bonferroni corrections.

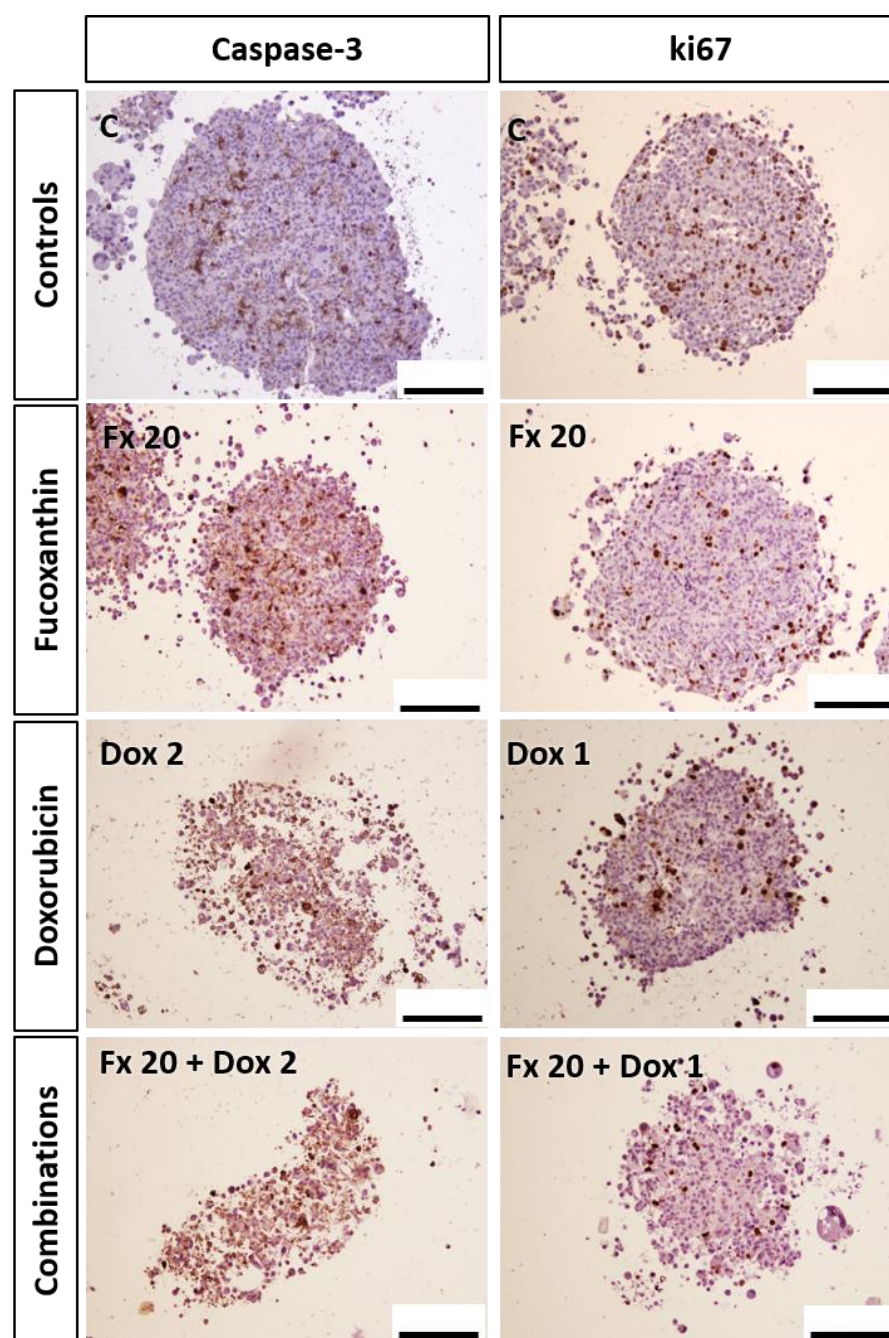


**Figure 8.** Representative images of ICC against caspase-3 and ki67 in the MDA-MB-231 MCAs exposed to Fx (20  $\mu$ M) and Dox (1 and 2  $\mu$ M), alone and combined, for 96 h. Brown staining corresponds to positive immunomarking. Scale bar: 100  $\mu$ m.

#### Transmission Electron Microscopy (TEM)

The observation of the MCAs semithin sections revealed a subset of cells with high cytoplasmic lipid content. These cells were present in all tested conditions, even in the control group (Figure 9a,b). The study of the MCAs ultrathin sections confirmed a high amount of lipid droplets in some cells (Figure 9c). Generally, cells possessed very irregular nuclei, a cytoplasm rich in organelles, constituted mainly by Golgi apparatus, rough endoplasmic reticulum cisternae and irregularly shaped mitochondria (Figure 9c,d).

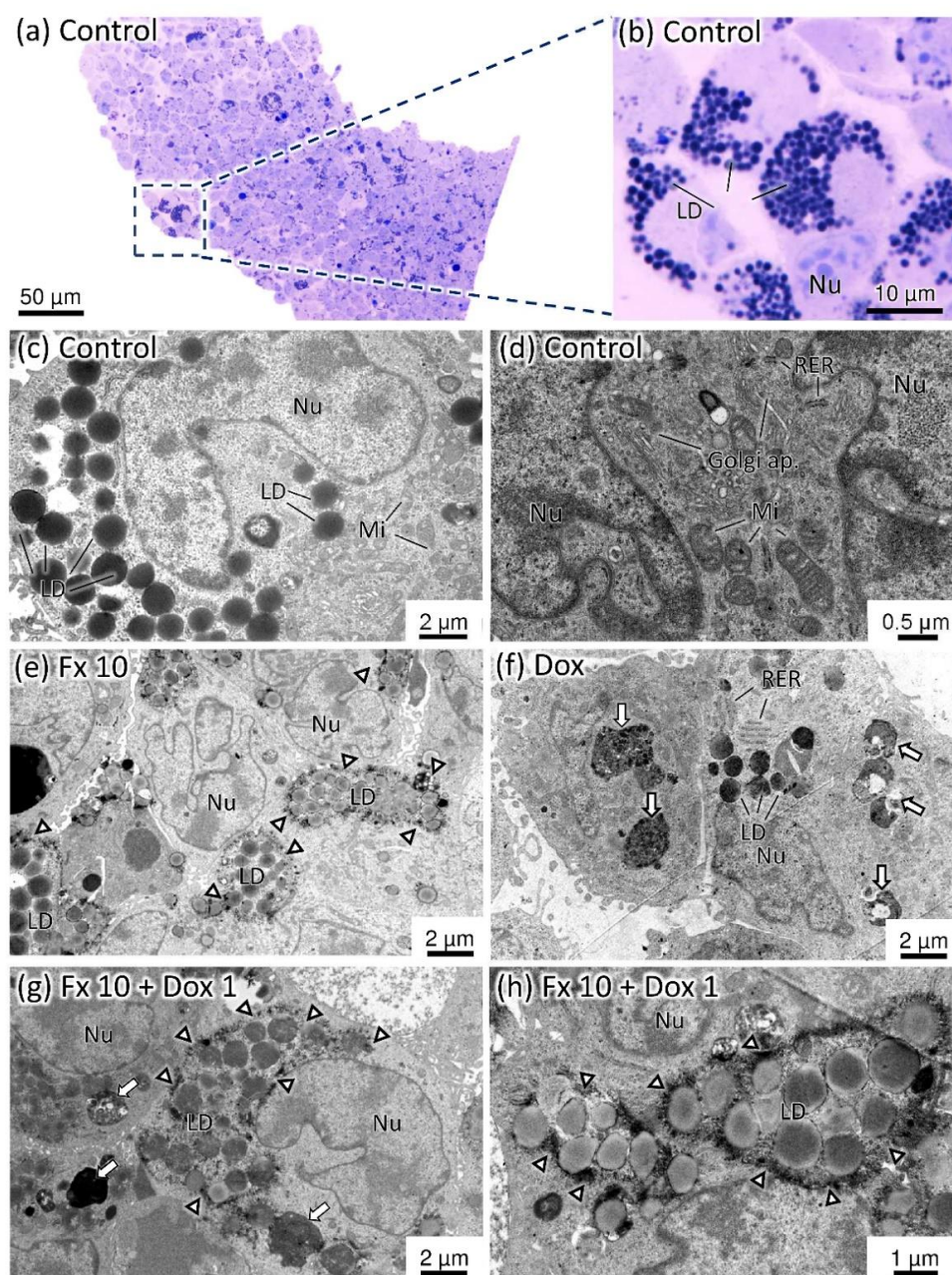


**Figure 9.** Representative images of semithin (a,b) and ultrathin sections (c–h) of MDA-MB-231 MCAs after 96 h of incubation. Golgi ap.—Golgi apparatus; LD—lipid droplets; Mi—mitochondria; Nu—nucleus; RER—rough endoplasmic reticulum. The arrows indicate the autophagic vacuoles and arrowheads point to the electron-dense granular deposits around lipid droplets.

Figure 9e–h illustrate the ultrastructural changes found in the most promising combination (Fx 10  $\mu$ M + Dox 1  $\mu$ M).

The MCAs exposed to Dox alone and Dox combined exhibited cells with dense bodies and pleomorphic autophagic vacuoles (Figure 9f–h), which were more pronounced at the tested conditions that contained Dox 2  $\mu$ M and Dox 5  $\mu$ M.

The MCAs exposed to Fx displayed lipid droplets too, but with a lower electron density when compared to those of the control and Dox alone. In these latter conditions, lipid droplets appeared as denser structures. Additionally, in the Fx exposed cells, there was a deposition of fine granular electron-dense material around the lipid droplets (arrowheads in Figure 9e,g,h). These deposits existed in all tested conditions that involved Fx, being more evident at Fx 20  $\mu$ M.



The MCAs treated with the combinations of Fx and Dox presented the same alterations observed in the MCAS exposed to each compound alone.

### 3. Discussion

Fucoxanthin has been considered as a promising anticancer compound. However, most of the available data regarding its effects derive from *in vitro* studies performed in 2D cultures, and its underlying mechanisms of action are not fully elucidated. Apart from this, there are just a few studies about its combinatory effects with reference anticancer drugs, especially in BC. Thus, our study aimed to bring new insights into the effects of Fx alone and in combination with two reference drugs (Dox and Cis) in a panel of 2D-cultured breast cell lines and investigate the most promising combination (Fx + drug) in a more physiologically relevant *in vitro* model—the 3D cell culture. This study is the first to report the effects of Fx in combination with a chemotherapy drug in a BC 3D model.

Considering 2D cultures, Fx exerted cytotoxicity in all the cell lines (tumoral and non-tumoral) in a dose-dependent manner. Even though we found no studies in the literature for the SKBR3 BC cell line, several authors have reported the cytotoxic activities of Fx towards the MCF7 and MDA-MB-231 cells [14,23,51]. For instance, Rwigemera and colleagues stated that Fx promotes a dose-dependent decrease in the metabolic activity of MCF7 and MDA-MB-231 cells, at similar concentrations to the ones used herein [14]. The cytotoxic effects of Fx in the non-tumoral cells are controversial in the literature, since some authors claim the absence of Fx-induced effects on normal cells [21,52], while others as de La Mare and coworkers, showed that Fx at 10  $\mu$ M reduced the percentage survival of MCF12A cells to around 71% [53]. Our results are in line with the latter one indicating that Fx is not specific to tumor cells since MCF12A cells were also affected.

According to our results, Fx did not induce cell death nor DNA damage detectable by the conducted assays. Nonetheless, some studies suggested that Fx caused apoptotic and genotoxic effects in BC cells [14,23,51]. When analyzing the existing reports, we noted that apart from the differences in the BC cell lines tested, some used different culture conditions, higher concentrations of Fx, different exposure times, and/or distinct experimental methods for analyzing cell death and DNA damage. Besides, the used alkaline version of the comet assay only detects strand-breaks and alkali-labile sites [54], not excluding that other DNA damages might occur. All these factors might explain the divergent outcomes compared to our study.

Regarding the individual effects of the drugs in 2D cultures, Cis reduced the viability of all cell lines except the MDA-MB-231 cells. These results suggest that MDA-MB-231 is more resistant to Cis than other BC cell lines, as Leon-Galicia and colleagues reported [55]. Differently, Dox only showed cytotoxicity in MDA-MB-231 cells at the highest tested concentration. In agreement, other authors also reported cytotoxicity in the MDA-MB-231 cell line at the same Dox concentration [56]. Dox cytotoxicity seems to be correlated to the increase of DNA damages and consequently induction of cell death in MDA-MB-231 cells, concordantly with other reports with the same cell line [57,58]. Dox is known for causing DNA damage through several different mechanisms (e.g., DNA intercalation, topoisomerase II inhibition, ROS induction), which can trigger cell cycle arrest, impairment of mitochondrial function and cell death [59,60].

Drug combinations bring several benefits in cancer treatment as they might, for instance, increase drug efficacy, decrease drug resistance and reduce the adverse effects. In this scenario, the combination of anticancer drugs with natural compounds has been reported in some clinical trials as a promising chemotherapeutic strategy [61]. In this study, the drug concentrations used in the combinatorial experiments were clinically relevant as they were similar to plasmatic concentrations found in oncological patients after intravenous infusion [62]. Besides, they were in line with other studies that used BC lines [63,64].

Our results showed that the combination of Fx with Dox promotes greater cytotoxic effects than each of the compounds separately on the SKBR3 and MDA-MB-231 cell lines. Interestingly, the most promising anticancer effects were noted for the combination Fx

10  $\mu\text{M}$  + Dox 1  $\mu\text{M}$  in the MDA-MB-231 cell line, representative of TNBC, the BC subtype where chemotherapy with drugs like Dox is the unique treatment option.

Recent reports have assessed the effects of Fx combined with conventional drugs in several types of cancer (e.g., leukaemia and colon cancer) [42,44,65]. However, data is almost non-existent in the context of BC, being, as far as we know, restricted to one study performed by Vijay and colleagues [43]. The latter supports our results, showing that the combination of Fx with Dox was more cytotoxic to MDA-MB-231 cells than the individual compounds. Also, in our study, the combination of Dox with Fx promoted genotoxicity and cell death in MDA-MB-231 cells, however, the effects were not different from Dox alone. These findings do not fully explain the increased cytotoxicity registered for this combination. One possible explanation for the observed effect might be the induction of cell cycle arrest since it is one of the mechanisms induced by Fx in different cancer cell lines [66,67]. Some reports also describe that the combination of carotenoids with ROS-inducing anticancer drugs like Dox, can act synergistically, enhancing the toxicity of the drug [68] which probably occur in this case, as Fx can also have a pro-oxidant action, increasing ROS, and consequently triggering cell death pathways [17,69].

Regardless of the inconclusive mechanistic data reported in 2D, the most promising combination was explored in a more complex cell model—3D MCAs. Although many studies reported the effects of Fx in 2D cultures, in 3D cultures, as far as we investigated, the literature is limited to four studies [53,70–72]. Only de la Mare and collaborators reported Fx effects in a BC cell line cultured in 3D [53]. However, they aimed to test the impact of Fx on the formation of mammospheres and not in already formed 3D BC cultures. The scarce data on 3D cultures reinforces the need for more studies exploring the effects of Fx alone and combined with the chemotherapy drugs.

It seems now consensual that 3D cell cultures are more resistant to drug treatments and better translate organism-level realities [73,74]. That is why we prolonged the exposure time in MDA-MB-231 3D cultures and tested not only the most promising combination in 2D, but also higher Fx and Dox concentrations alone and in combination.

In the MTT assay, effects on cell viability were observed at Dox 1  $\mu\text{M}$  only when combined with Fx, and at higher concentrations of Dox, alone and combined. Otherwise, in the LDH assay, cytotoxic effects were only observed in two conditions: Fx 20  $\mu\text{M}$  + Dox 2  $\mu\text{M}$  and Dox 5  $\mu\text{M}$ . The used viability tests (MTT and LDH) are both colorimetric assays, although they are based on two different approaches. The MTT assay relies on mitochondrial metabolic activity [75], while the LDH test evaluates plasmatic membrane integrity through the quantification of the LDH released from damaged cells [76]. MTT assay detected differences in cell viability at lower Dox and Fx concentrations, while in LDH, only higher concentrations differed from the control. Thus, the differences in the detected cytotoxicity can be related to the different targets of these assays. The cytotoxic effect of the combination Fx with Dox obtained by the MTT, in 3D cultures, lined up with the results from 2D cultures.

A previous study from our group showed similar results to Dox's cytotoxicity in MDA-MB-231 cells [77]. Other authors tested Dox's concentrations that were from 10 [53] to 100 [78] times higher than the ones applied in our study, and surprisingly did not induce greater cytotoxicity.

Furthermore, the morphological evaluation by stereomicroscopy only revealed a significant increase in the area of the MCAs treated with the highest cytotoxic condition. Thus, no significant variations were detected for the conditions with a lower cytotoxicity degree, showing that the evaluation of the MCAs areas alone has not enough sensibility to detect cytotoxic effects.

The histological analysis of the HE-stained MCAs supports the results of the MTT assay. It was observed a deterioration in cell morphology of the MCAs treated with the conditions that statistically differed from the control in MTT. Additionally, the MCAs that revealed the highest degree of morphological damage presented cytotoxic effects that statistically differed from the control in both cytotoxic assays.

Apoptosis is widely used to evaluate the cellular response to a chemotherapeutic agent [79], and caspase-3 is frequently employed as a biomarker of apoptosis [80]. The ICC evaluation of caspase-3 expression showed that Fx alone did not differ from the control, similarly to 2D results from the nuclear condensation assay. The combination of Fx with Dox increased the percentage of caspase-3 positive cells in relation to the drug alone, suggesting a possible pro-apoptotic effect of Fx. Previous studies also reported that Fx induces apoptosis in several cell lines [18,23,61], even in 3D models [72]. However, due to the non-existing data on the combined effects of Fx and Dox in 3D BC cultures, it was not possible to compare our results in such situations.

Additionally, the results of ICC for caspase-3 and MTT in 3D were very similar, as both experiments showed that Fx and Dox 1  $\mu\text{M}$  alone did not present differences in relation to the control, while Dox  $\geq 1 \mu\text{M}$  in combination with Fx revealed differences that show cell cytotoxicity and apoptosis induction. Once again, these findings reinforce the promising effects of combining Fx with Dox.

The effects on cell proliferation were evaluated using ki67, a well-known prognostic marker for BC [81], that is expressed in all phases of the cell cycle, except the G0 phase [82]. In 3D culture, Fx alone did not show effects on cellular proliferation, however, the combination of Fx 20  $\mu\text{M}$  with Dox 1  $\mu\text{M}$  augmented the drug effects, lowering cell proliferation to nearly half of the percentage of the compounds alone. These results point to a possible decrease in the cell proliferation caused by the combination of Fx and Dox. Still, further evaluation of the cell cycle will be necessary to elucidate this topic.

The histological analysis complemented with ICC unveiled as a useful tool for evaluating the cytotoxicity of the tested compounds, not only for corroboration of the cytotoxic assays and verifying the proliferation and apoptotic status, but also to give a general view of the morphology of the MCAs, verify the existence of necrotic cores, and correlate the ICC markers with their localization into the MCAs. An additional advantage of processing MCAs for paraffin embedding is the possibility of having the biological samples in a form that can be stored indefinitely and generate sections for different ICC markers or even extract genetic material for further studies.

The ultrastructural analysis revealed that MDA-MB-231 MCAs presented a pool of cells with high lipid droplets content, not noticeable in paraffin sections due to lipid dissolution during the processing. These lipid droplets were previously reported in this cell line, and the authors described that the sub-population of highly enriched lipid cells was related to stemness features [83]. In MCAs exposed to Fx (alone and combined), a lower electron density of the lipid droplets was observed. Knowing that the electron density of lipid droplets reflects fatty acid composition [84], this can indicate that Fx can influence the composition of the lipid droplets. Additionally, it was noted a deposition of a granular electron-dense material around the lipid droplets. The explanation of such changes needs to be investigated, however, it could be related to lipidic trafficking as Fx is described as a regulator of pathways related to fatty acid synthesis, lipolysis, and thermogenesis [85]. Indeed, the presence of lipid droplets is thought to be part of stress response to treatments, regulation of proliferation, migration and survival of cancer cells [86]. The additional presence of a great number of autophagic vacuoles in the cytoplasm indicates that Dox induced autophagy in the MDA-MB-231 cell line, which agrees with a previous report [87].

In summary, our results indicated that Fx alone had cytotoxic effects in all the 2D-cultured breast cell lines. In combination with Dox, Fx suggestively potentiated the drug effect in SKBR3 and MDA-MB-231 cells, being these effects more pronounced in the TNBC cell line. However, the mechanisms behind the enhanced cytotoxicity need further elucidation, since in addition to DNA damage and cell death induction, other mechanisms as cell cycle arrest, ROS induction and alteration of lipid metabolism may occur.

Besides being more resistant to Fx and Dox alone, 3D cultures also presented higher cytotoxic effects in the combination of Dox with Fx, corroborating the 2D results. The cytotoxicity in 3D was supported by the morphological analysis (light and electron microscopy) and ICC. Apart from increasing the number of apoptotic cells and lowering cell prolifera-

tion, the combination of Fx and Dox damaged the MCAs histological structure and caused ultrastructural alterations. These findings reinforce the utility of using a multi-endpoint approach for evaluating the cytotoxic effects of compounds.

Our data from 2D and 3D cultures suggest that Fx has potential as a drug adjuvant in TNBC treatment when Dox is applied for chemotherapy. Notwithstanding, more *in vitro* and *in vivo* studies are necessary to explore the underlying mechanisms of action of Fx and its combination with Dox.

## 4. Materials and Methods

### 4.1. Chemicals

3-(4,5-Dimethyl-2-thiazolyl)-2,5-diphenyl-2H-tetrazolium bromide (MTT), 4',6-diamidino-2-phenylindole (DAPI), cisplatin, cholera toxin, doxorubicin, epidermal growth factor receptor (EGFR), fucoxanthin, hydrocortisone, insulin, low and normal melting agarose and triton X-100 were obtained from Sigma Aldrich (St. Louis, MO, USA). Dimethyl sulfoxide (DMSO) was purchased from VWR Chemicals (Solon, OH, USA). Dulbecco's modified Eagle's medium (DMEM) high glucose without glutamine and phenol red, fetal bovine serum (FBS), streptomycin-penicillin and trypsin-ethylenediaminetetraacetic acid (EDTA) solution were acquired from Biochrom KG (Berlin, Germany). Dulbecco's modified Eagle's medium/Ham's nutrient mixture F12 (DMEM/F12) medium without phenol red was obtained from GE Healthcare (Chicago, IL, USA). All the other reagents and chemicals used were analytical grade.

### 4.2. Stock and Exposure Solutions

Stock solutions of Dox and Fx were prepared in DMSO and the stock solution of Cis was prepared in 0.9% NaCl solution. All stock solutions were kept at  $-20\text{ }^{\circ}\text{C}$  before use, except Cis stock solution that was kept at  $4\text{ }^{\circ}\text{C}$  for up to 1 month. Exposure solutions were always prepared before experiments by diluting the appropriate volume of each compound stock solution into the respective supplemented fresh culture medium (DMEM or DMEM/F12 medium, dependent on the cell line).

### 4.3. Cell Culture

#### 4.3.1. 2D Cell Culture

The MDA-MB-231, SKBR3 and MCF12A cell lines were purchased from the American Tissue Culture Collection (ATCC) and the MCF7 cell line was acquired from the European Collection of Authenticated Cell Cultures (ECACC). MCF12A is a non-tumor breast cell line, while the others are tumor cell lines representative of different BC subtypes: MCF7—Luminal A; SKBR3—HER-2 subtype; MDA-MB-231—TNBC [88,89]. MCF7, SKBR3 and MDA-MB-231 cells were cultured in high glucose DMEM deprived of phenol red and supplemented with 10% of FBS and 1% of the streptomycin-penicillin solution. MCF12A cells were cultured in DMEM/F12 supplemented with 20 ng/mL of EGFR, 100 ng/mL of cholera toxin, 0.01 mg/mL of human insulin and 500 ng/mL hydrocortisone, 10% FBS and 1% of streptomycin-penicillin solution. All the cell lines were maintained as monolayer cultures in T75 cm<sup>2</sup> culture flasks (Orange Scientific, Belgium) and incubated under standard cell culture conditions ( $37\text{ }^{\circ}\text{C}$ , 5% CO<sub>2</sub>). When reaching approximately 80% confluence, cells were subcultured using 0.25% trypsin/EDTA at  $37\text{ }^{\circ}\text{C}$ , counted in a hemocytometer and assessed for their viability using the standard trypan blue staining procedure. All experiments were conducted with cells at passages under 40.

#### 4.3.2. 3D Cell Culture—Multicellular Aggregates (MCAs)

MCAs were formed in ultra-low attachment plates (Corning Inc., Corning, NY, USA) as described in a previous report [90]. Cells were seeded at  $40 \times 10^4$  cells/mL, 200  $\mu\text{L}$  per well, and MCAs were formed after 72 h of incubation at  $37\text{ }^{\circ}\text{C}$ , 5% CO<sub>2</sub>.

#### 4.4. Study Design

Experiments were conducted according to the study design represented in Figure 10. First, in Phase 1, the cytotoxic effects of four concentrations of Fx (1; 10; 20 and 50  $\mu\text{M}$ ) were screened by the MTT assay in the panel of breast cell lines cultured in 2D. Considering the results obtained in Phase 1, two concentrations of Fx were selected to be tested in combination with two reference drugs (Cis and Dox) in Phase 2 (Table 1). For each cell line, one concentration of Fx was selected with no statistical effect on cell viability and another that did not reduce the cell viability below 50% (on average). The drug concentrations were chosen according to the results of a recent report [77]. Only the concentrations with no effects or that did not affect cell viability by more than 50% were selected for our study. As in Phase 1, in Phase 2 the cytotoxic effects of the combinations and respective isolated compounds were also assessed by the MTT assay on the 2D-cultured breast cell lines. According to the results obtained in Phase 2, we selected the most promising combination, that is, the one with the highest cytotoxic effects that statistically differed from the control and both isolated compounds. This combination and constituent compounds were further explored in the respective cell line, during Phases 3 and 4. In Phase 3, the nuclear condensation and comet assays were conducted on 2D cultures to study the potential mechanisms behind the induced cytotoxicity. In Phase 4, the combination and respective individual compounds were tested on 3D cultures at equal and higher concentrations than the ones tested in the 2D cultures. The effects were evaluated using a combination of functional and morphological methodologies, including cytotoxic assays (MTT and LDH assays), stereomicroscopy, hematoxylin and eosin (HE) staining, immunocytochemistry (ICC) and transmission electron microscopy (TEM).

**Table 1.** Tested concentrations of Fx, Cis and Dox in the combinatorial experiments.

Cell Line	Compound	Fucoxanthin (Fx)	Cisplatin (Cis)	Doxorubicin (Dox)
MCF7 SKBR3 MDA-MB-231 MCF12A		1; 10 $\mu\text{M}$	10; 20 $\mu\text{M}$	0.01; 0.1 $\mu\text{M}$ 0.1; 1 $\mu\text{M}$ 0.01; 0.1 $\mu\text{M}$

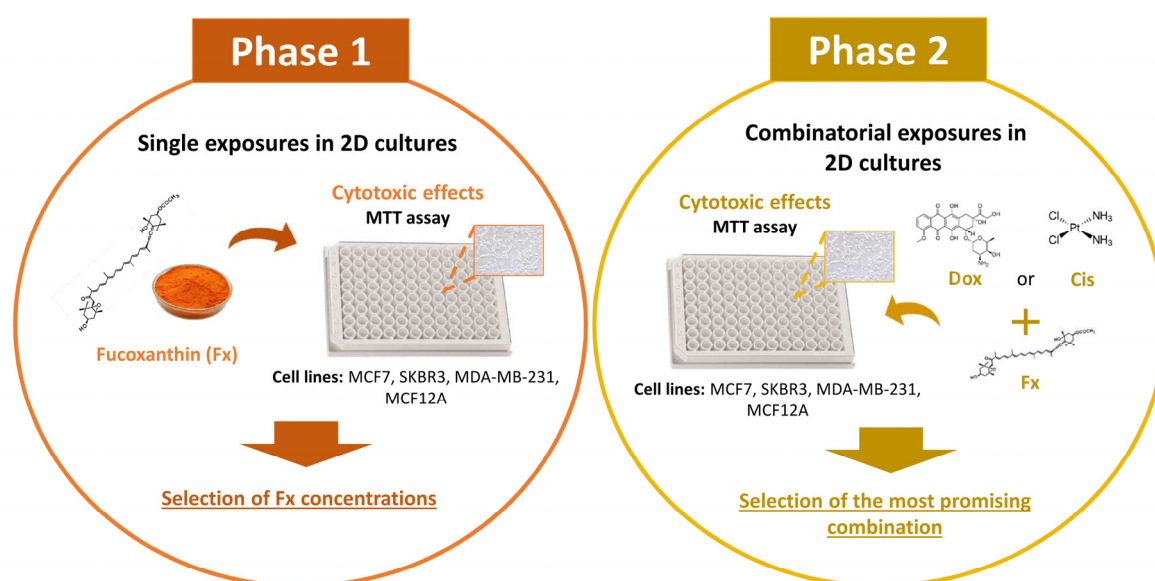


**Figure 10.** *Conts.*



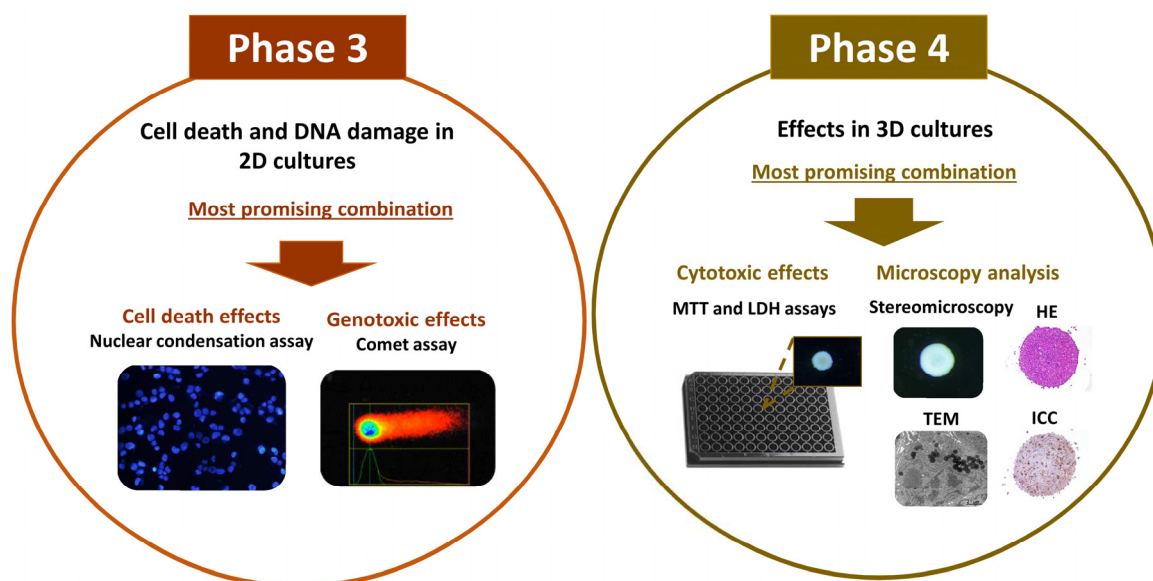


**Figure 10.** Schematic representation of the study design. HE: hematoxylin and eosin; ICC: immunohistochemistry and TEM: transmission electron microscopy.

In all the experiments, control cells (negative control) were incubated in a culture medium with 0.1% DMSO.

#### 4.5. Exposures (Single or Combination) in 2D Cell Cultures

##### 4.5.1. MTT Assay

Cells were seeded in 96-multiwell culture plates (Orange Scientific, Braine-l'Alleud, Belgium) at a density of  $0.5 \times 10^5$  cells/mL (100  $\mu$ L/well) and left to adhere for 24 h. Then, cells were exposed for 72 h to different concentrations of Fx alone (Phase 1) and in combination with Dox or Cis (Phase 2). After the exposure, 10  $\mu$ L (0.5 mg/mL) of MTT stock reagent was added to the wells, and the microplate was incubated for 2 h at 37 °C, 5% CO<sub>2</sub>. The medium was then removed, and the formazan crystals were dissolved in 150  $\mu$ L of DMSO under slight agitation for 30 min in the dark. Absorbance (A) was measured at 570 nm using a microplate reader Multiskan GO (Thermo Fisher Scientific, Waltham, MA, USA). Results were expressed as % of cell viability relative to the control—an average of five to six independent experiments performed in triplicate—and calculated according to the following equation:

$$\text{Cell viability (\%)} = (A_{\text{Sample}} \div A_{\text{Control}}) \times 100$$

##### 4.5.2. Nuclear Condensation Assay

Cells were seeded (1000  $\mu$ L/well) in 24-multiwell culture plates (Orange Scientific, Belgium) at a density of  $0.5 \times 10^5$  cells/mL and incubated for 24 h under standard cell culture conditions. Cells were then exposed for 72 h to the most promising combination selected in Phase 2 and respective isolated compounds. Briefly, both adherent and non-adherent cells were collected, washed, centrifuged and fixated with 4% (*w/v*) paraformaldehyde (Sigma Aldrich, St. Louis, MO, USA) in PBS. Then, cells were placed onto silane adhesive microscope slides (VWR International B.V, Amsterdam, The Netherlands) by cytocentrifugation using Shandon Cytospin 3 cytocentrifuge (Thermo Fisher Scientific, Waltham, MA, USA) at  $28 \times g$  for 5 min. Slides were incubated with DAPI staining solution (1  $\mu$ g/mL) for 10 min in the dark and after incubation, at least 300 cells per sample were counted under a fluorescence microscope (Olympus IX71, Tokyo, Japan) using the total magnification of  $200 \times$  ( $20 \times$  objective lens plus  $10 \times$  eyepiece lens). The results were expressed as percent-

age of condensed nuclei—an average of three to five independent experiments, with one replicate per condition—and calculated according to the following equation:

$$\% \text{ Condensed nuclei} = (\text{No. cells with nuclear condensation} \div \text{No. total cells}) \times 100$$

#### 4.5.3. Comet Assay

Cells were seeded at  $0.5 \times 10^5$  cells/mL (1000  $\mu$ L/well) in 24-multiwell culture plates and allowed to adhere for 24 h, under standard conditions. Subsequently, cells were treated for 2 h with the test conditions and by the end of the treatments they were washed with PBS, trypsinized with 0.25% Trypsin/EDTA solution, collected and centrifuged at  $1700 \times g$  for 1 min using the Micro Star 12 microcentrifuge (VWR International, Pennsylvania, USA). After centrifugation and removal of the supernatant, the cells were mixed with 0.5% (*w/v*) Low Melting Point Agarose and transferred to microscope slides previously coated with 1% (*w/v*) Normal Melting Point Agarose. Slides were immediately covered with glass coverslips (Thermo Fisher Scientific, Waltham, MA, USA) and maintained at 4 °C for 10 min. Then, the coverslips were removed, and slides were incubated in a lysis solution [2.5 M NaCl, 100 mM Na<sub>2</sub>EDTA, 10 mM Tris Base, pH 10 plus 1% (*v/v*) Triton X-100, pH 10] for 1 h, at 4 °C, to lyse the cells and release the DNA. Subsequently, slides were washed with distilled water, transferred into a horizontal electrophoresis tank, and immersed in electrophoresis buffer (300 mM NaOH and 1 mM Na<sub>2</sub>EDTA, pH  $\geq$  13) for 40 min at 4 °C for DNA unwinding. Electrophoresis ran for 20 min at 4 °C under a voltage gradient of 1 V per cm (20 V). Following electrophoresis, slides were rinsed in distilled water, dehydrated with absolute ethanol, and lastly air-dried. Before analysis, slides were rehydrated in 25 mL of Tris-EDTA (TE) Buffer (Tris-HCl 10 mM and EDTA 1 mM) for 15 min under slight agitation, and then 20  $\mu$ L of SYBR Gold (Thermo Fisher Scientific, Waltham, MA, USA) was added to the TE buffer for DNA staining. Slides were incubated for 30 min in the dark under slight agitation. After staining, slides were analyzed with a Nikon Eclipse E400 microscope (Nikon, Tokyo, Japan) connected to an epi-fluorescence illuminator Nikon C-SHG1 power supply for HG 100 W with 250 $\times$  magnification (Semrock SYBRGold-A-NQF filter, Rochester, NY, USA). Samples were analyzed by the Comet Assay IV<sup>TM</sup> software (Perceptive Instruments, Haverhill, UK) and the parameter “tail intensity” (percentage of DNA in the comet tail) was used to evaluate the DNA damages. A hundred randomly selected nucleoids were analyzed per sample. Results were expressed as the mean of three independent experiments, with one replicate per condition.

#### 4.6. Exposures (Single or Combination) in 3D Cell Cultures

MCAs were exposed to Fx alone and combined with Dox for 96 h under standard cell culture conditions. Cells treated with 0.1% DMSO and Dox 5  $\mu$ M were included as a negative and positive control, respectively.

##### 4.6.1. MTT Assay

The MTT assay was performed as previously described for monolayer cultures, with slight modifications. MCAs were incubated in the dark at 37 °C in a 5% CO<sub>2</sub> atmosphere with 20  $\mu$ L of the MTT stock solution per well for 4 h. After incubation, the MCAs were transferred from the ULA 96-well microplates into 96-well flat-bottomed microplates and the medium was removed. Formazan crystals were dissolved in 150  $\mu$ L of DMSO and after 30 min under slight agitation in the dark, absorbance measurements were performed. The cell viability percentages were calculated according to the formula mentioned above. The results were expressed as the mean of five independent experiments performed in triplicate.

##### 4.6.2. Lactate Dehydrogenase (LDH) Assay

LDH assay was performed using the LDH Cytotoxicity Assay Kit (Enzo Life Sciences, Lausen, Switzerland) according to the manufacturer’s instructions. The medium from the treated conditions, high control (maximum LDH release by applying the lysis buffer) and negative control wells were transferred to a flat-bottom 96-well microplate. Then, the working

solution from the LDH kit was added and after the incubation period, the reaction was terminated by the stop solution. Absorbance (A) was measured at 490 nm in a microplate reader Multiskan GO (Thermo Fisher Scientific, Waltman, MA, USA). The results were expressed as percentage of cytotoxicity based on the LDH release—mean of five independent experiments performed in triplicate—and calculated using the following equation:

$$\text{Cytotoxicity (\%)} = (A_{\text{test substance}} - A_{\text{negative control}}) \div (A_{\text{high control}} - A_{\text{negative control}}) \times 100$$

#### 4.6.3. Stereomicroscopic Analysis and Area Measurements

MCAs were photographed at the end of the exposure (96 h) using an Olympus SZX10 stereomicroscope, equipped with a digital camera DP21 (Olympus, Tokyo, Japan). Stereomicroscope images were analyzed by the free download AnaSP software [91] that measured the MCAs areas. Results were expressed as the mean of four independent experiments performed in triplicate.

#### 4.6.4. Hematoxylin and Eosin (HE) Staining

MCAs were fixed, harvested, processed, embedded in paraffin blocks and ultimately sectioned as previously described [77]. The obtained slides were selected and divided for standard HE staining and immunocytochemistry (ICC). For HE, sections were deparaffinized in xylene (twice, 10 min each), rehydrated in descending alcoholic concentration solutions (absolute ethanol, ethanol 95% and ethanol 70%, 5 min each) and rinsed in running tap water. Then, sections were stained with Mayer's hematoxylin (Merck, Darmstadt, Germany) for 2 min, rinsed in tap water, stained with eosin Y 1% aqueous solution (Merck, Darmstadt, Germany) for 5 min and newly washed in tap water. Following the HE staining, sections were dehydrated in absolute ethanol (thrice, 5 min each) and diaphanized in xylene (twice, 3 min each). Finally, slides were mounted using Coverquick 2000 mounting medium (VWR International, France). Representative images of MCAs sections were taken using a DP21 camera (Olympus, Tokyo, Japan) linked to an Olympus BX50 microscope (Olympus, Tokyo, Japan).

#### 4.6.5. Immunocytochemical Analysis

ICC was performed using ki67 and caspase-3 as proliferation [92] and apoptosis [93] markers, respectively. Sections of the paraffin-embedded MCAs were deparaffinized and hydrated as described for the HE staining protocol. The heat antigen retrieval step was performed in a pressure cooker by placing the slides in boiling citrate buffer (0.01 M, pH 6.0) for 2 min after reaching the maximum pressure. After cooling and rinsing with distilled water, slides were immersed for 10 min in a solution of 3% hydrogen peroxide in methanol to block endogenous peroxidase activity and rinsed in tris-buffered saline (TBS, pH 7.6). Briefly, unspecific antibody binding was blocked for 5 min using the Protein block reagent from the NovoLink™ Max Polymer Detection System Kit (Leica Biosystems, Nussloch, Germany) and the sections were rinsed with TBS (twice, 5 min each). Thereafter, the sections were incubated for 2 h in a humidified chamber at room temperature with the following primary antibodies: Rabbit monoclonal anti-Ki67, clone SP6 (Biocare Medical, Pacheco, CA, USA), dilution of 1:200; rabbit polyclonal anti-caspase-3, ab 13847 (Abcam, Cambridge, UK), dilution 1:5000. All the primary antibodies were diluted in PBS with 5% bovine serum albumin (BSA) (Nzytech, Lisbon, Portugal). As a negative control, sections were incubated in PBS with 5% BSA solution under the same conditions. After incubation, sections were rinsed (twice, 5 min each) in TBST (TBS with 0.05% Tween 20) (Sigma Aldrich, St. Louis, MO, USA), incubated for 30 min with the Post Primary solution from the kit and again washed with TBST. Slides were incubated with the NovoLink™ Polymer reagent (30 min), washed in TBST (twice, 5 min each) incubated with DAB (3,3'-diaminobenzidine) working solution from the kit for signal revelation (2 min) and rinsed in tap water. Lastly, slides were counterstained with Mayer's hematoxylin (Merck, Darmstadt, Germany) for 1 min, washed in tap water, dehydrated in ethanol, cleared in xylene and coverslipped with Coverquick 2000 mounting medium (VWR International, Fontenay sous Bois, France).

In every independent experiment, one representative image of a single MCA per test condition was captured using an Olympus BX50 microscope (Olympus, Tokyo, Japan) attached to a DP21 camera (Olympus, Tokyo, Japan). From those images, a quantification of the percentage of positive immunomarked cells was calculated by superimposing a grid for preventing the edging effects. A total of 200–800 cells were counted per condition (fewer cells were counted in high cytotoxicity treatments due to cell loss).

#### 4.6.6. Transmission Electron Microscopy (TEM)

MCAs were processed for TEM to assess their ultrastructural morphology. Fixation was conducted with 2.5% Glutaraldehyde in Cacodylate buffer (0.15 M, pH 7.2) for 2 h, and then the MCAs were washed twice in Cacodylate buffer (30 min each). Post-fixation was performed with 1% osmium tetroxide (Agar Scientific, Stansted, UK) in Cacodylate buffer for 2 h. MCAs were then washed with the same buffer and dehydrated in graded ethanol series up to 100% (50% ethanol; 70% ethanol; 95% ethanol; absolute ethanol; absolute ethanol—30 min each). Until this step, all procedures were conducted at 4°C. Then, MCAs were placed at room temperature and the dehydrating agent was replaced for propylene oxide (Merck, Darmstadt, Germany) (two baths of 30 min each). Following the resin impregnation, MCAs were subjected to three mixtures of propylene oxide and epoxy resin with increasing resin concentration (propylene oxide + epon 3:1; 1:1; 1:3—1 h each mixture) and ultimately embedded in only resin (epon—1 h; epon—10 min at 60°C). After, TEM blocks were obtained by placing the MCAs in rubber molds and then transferring them to the oven where they stayed for 48 h at 60 °C for resin polymerization. Semithin (1.25 µm) and ultrathin (90 nm) sections were obtained with a diamond knife (Diatome, Nidau, Switzerland) on an ultramicrotome EM UC7 (Leica, Nussloch, Germany). Ultrathin sections were placed on 200 mesh hexagonal copper grids (Agar Scientific, Stansted, UK) and contrasted with 3% aqueous uranyl acetate (20 min) (Merck, Darmstadt, Germany) and Reynolds' lead citrate (10 min) (Merck, Darmstadt, Germany). Grids were analyzed under an electron microscope JEOL 100CXII (JEOL, Tokyo, Japan), operated at 60 kV, and photographs of representative ultrastructural features were taken with the Orius SC1000 CCD digital camera (Gatan, Pleasanton, CA, USA).

#### 4.7. Statistical Analysis

The descriptive and analytical statistics were performed with Past3 (version 3.19) freeware [94] and GraphPad Prism 6.0 software (GraphPad Software, La Jolla, CA, USA). The normality and homogeneity of variance were tested by the Shapiro–Wilk and the Levene tests, respectively. All the results were obtained from at least three independent experiments and expressed as mean + standard deviation (SD), except for the MCAs areas that were presented in median, maximum, minimum, and interquartile range (Q3–Q1). Significant differences ( $p < 0.05$ ) were assessed by one-way ANOVA, followed by the post hoc Holm–Šidák multiple comparison test. In selected cases, the significance of the difference between two groups of interest was tested using the Student's *t*-test together with the sequential Holm–Bonferroni correction. The latter was applied via a free spreadsheet calculator [95,96].

**Author Contributions:** Conceptualization by F.M., A.C.M., A.A.R. and E.R.; methodology by A.C.M., F.M., C.C., A.A.R. and E.R.; formal analysis by A.C.M., F.M. and A.A.R.; investigation by A.C.M. and F.M.; resources by C.C. and E.R.; writing—original draft preparation by A.C.M. and F.M.; writing—review and editing by A.C.M., F.M., C.C., A.A.R. and E.R.; visualization by A.C.M., F.M., C.C., A.A.R. and E.R.; supervision by A.A.R. and E.R.; project administration by E.R.; funding acquisition by E.R. All authors have read and agreed to the published version of the manuscript.

**Funding:** The Strategic Funding UIDB/04423/2020 and UIDP/04423/2020 partially supported this research, through national funds provided by FCT and ERDF to CIIMAR/CIMAR, in the framework of the program PT2020. The Doctoral Program in Biomedical Sciences, of the ICBAS-University of Porto, offered additional funds.

**Informed Consent Statement:** Not applicable.

**Data Availability Statement:** The data presented in this study are available on request from the corresponding author.

**Conflicts of Interest:** The authors declare no conflict of interest.

**Sample Availability:** Not available.

## References

- Newman, D.J.; Cragg, G.M. Natural products as sources of new drugs from 1981 to 2014. *J. Nat. Prod.* **2016**, *79*, 629–661. [[CrossRef](#)]
- Wright, G.D. Unlocking the potential of natural products in drug discovery. *Microb. Biotechnol.* **2019**, *12*, 55–57. [[CrossRef](#)] [[PubMed](#)]
- Sharifi-Rad, J.; Ozleyen, A.; Boyunegmez Tumer, T.; Oluwaseun Adetunji, C.; El Omari, N.; Balahbib, A.; Taheri, Y.; Bouyahya, A.; Martorell, M.; Martins, N.; et al. Natural products and synthetic analogs as a source of antitumor drugs. *Biomolecules* **2019**, *9*, 679. [[CrossRef](#)]
- Ruan, B.F.; Ge, W.W.; Lin, M.X.; Li, Q.S. A review of the components of seaweeds as potential candidates in cancer therapy. *Curr. Med. Chem. Anticancer Agents* **2018**, *18*, 354–366. [[CrossRef](#)]
- Schumacher, M.; Kelkel, M.; Dicato, M.; Diederich, M. Gold from the sea: Marine compounds as inhibitors of the hallmarks of cancer. *Biotechnol. Adv.* **2011**, *29*, 531–547. [[CrossRef](#)]
- Proksch, P.; Edrada-Ebel, R.; Ebel, R. Drugs from the sea—Opportunities and obstacles. *Mar. Drugs* **2003**, *1*, 5–17. [[CrossRef](#)]
- Khalifa, S.A.M.; Elias, N.; Farag, M.A.; Chen, L.; Saeed, A.; Hegazy, M.F.; Moustafa, M.S.; Abd El-Wahed, A.; Al-Mousawi, S.M.; Musharraf, S.G.; et al. Marine natural products: A source of novel anticancer drugs. *Mar. Drugs* **2019**, *17*, 491. [[CrossRef](#)]
- Jimenez, P.C.; Wilke, D.V.; Branco, P.C.; Bauermeister, A.; Rezende-Teixeira, P.; Gaudêncio, S.P.; Costa-Lotufo, L.V. Enriching cancer pharmacology with drugs of marine origin. *Br. J. Pharmacol.* **2020**, *177*, 3–27. [[CrossRef](#)]
- Dyshlovoy, S.A.; Honecker, F. Marine compounds and cancer: The first two decades of XXI century. *Mar. Drugs* **2019**, *18*, 20. [[CrossRef](#)] [[PubMed](#)]
- Khalid, S.; Abbas, M.; Saeed, F.; Bader-Ul-Ain, H.; Ansar Rasul Suleria, H. Therapeutic potential of seaweed bioactive compounds. In *Seaweed Biomaterials*; Maiti, S., Ed.; IntechOpen: London, UK, 2018; pp. 8–25. [[CrossRef](#)]
- Teas, J.; Vena, S.; Cone, D.L.; Irhimeh, M. The consumption of seaweed as a protective factor in the etiology of breast cancer: Proof of principle. *J. Appl. Phycol.* **2013**, *25*, 771–779. [[CrossRef](#)] [[PubMed](#)]
- Yang, Y.J.; Nam, S.-J.; Kong, G.; Kim, M.K. A case–control study on seaweed consumption and the risk of breast cancer. *Br. J. Nutr.* **2010**, *103*, 1345–1353. [[CrossRef](#)]
- Funahashi, H.; Imai, T.; Mase, T.; Sekiya, M.; Yokoi, K.; Hayashi, H.; Shibata, A.; Hayashi, T.; Nishikawa, M.; Suda, N.; et al. Seaweed prevents breast cancer? *Jpn. J. Cancer Res.* **2001**, *92*, 483–487. [[CrossRef](#)]
- Rwigemera, A.; Mamelona, J.; Martin, L.J. Inhibitory effects of fucoxanthinol on the viability of human breast cancer cell lines MCF-7 and MDA-MB-231 are correlated with modulation of the NF-kappaB pathway. *Cell Biol. Toxicol.* **2014**, *30*, 157–167. [[CrossRef](#)]
- Bae, M.; Kim, M.B.; Park, Y.K.; Lee, J.Y. Health benefits of fucoxanthin in the prevention of chronic diseases. *Biochim. Biophys. Acta Mol. Cell Biol. Lipids* **2020**, *1865*, 158618. [[CrossRef](#)]
- Martin, L.J. Fucoxanthin and its metabolite fucoxanthinol in cancer prevention and treatment. *Mar. Drugs* **2015**, *13*, 4784–4798. [[CrossRef](#)]
- Kumar, S.R.; Hosokawa, M.; Miyashita, K. Fucoxanthin: A marine carotenoid exerting anti-cancer effects by affecting multiple mechanisms. *Mar. Drugs* **2013**, *11*, 5130–5147. [[CrossRef](#)]
- Meresse, S.; Fodil, M.; Fleury, F.; Chenais, B. Fucoxanthin, a marine-derived carotenoid from brown seaweeds and microalgae: A promising bioactive compound for cancer therapy. *Int. J. Mol. Sci.* **2020**, *21*, 9273. [[CrossRef](#)]
- Garg, S.; Afzal, S.; Elwakeel, A.; Sharma, D.; Radhakrishnan, N.; Dhanjal, J.K.; Sundar, D.; Kaul, S.C.; Wadhwa, R. Marine carotenoid fucoxanthin possesses anti-metastasis activity: Molecular evidence. *Mar. Drugs* **2019**, *17*, 338. [[CrossRef](#)]
- Zhang, H.; Tang, Y.; Zhang, Y.; Zhang, S.; Qu, J.; Wang, X.; Kong, R.; Han, C.; Liu, Z. Fucoxanthin: A promising medicinal and nutritional ingredient. *Evid. Based Complement. Alternat. Med.* **2015**, *2015*, 723515. [[CrossRef](#)]
- Ishikawa, C.; Tafuku, S.; Kadekaru, T.; Sawada, S.; Tomita, M.; Okudaira, T.; Nakazato, T.; Toda, T.; Uchihara, J.N.; Taira, N.; et al. Anti-adult T-cell leukemia effects of brown algae fucoxanthin and its deacetylated product, fucoxanthinol. *Int. J. Cancer* **2008**, *123*, 2702–2712. [[CrossRef](#)]
- Satomi, Y. Antitumor and cancer-preventative function of fucoxanthin: A marine carotenoid. *Anticancer Res.* **2017**, *37*, 1557–1562. [[CrossRef](#)]
- Rwigemera, A.; Mamelona, J.; Martin, L.J. Comparative effects between fucoxanthinol and its precursor fucoxanthin on viability and apoptosis of breast cancer cell lines MCF-7 and MDA-MB-231. *Anticancer Res.* **2015**, *35*, 207–219. [[PubMed](#)]
- Wang, J.; Jiang, Y.-F. Natural compounds as anticancer agents: Experimental evidence. *World J. Exp. Med.* **2012**, *2*, 45–57. [[CrossRef](#)] [[PubMed](#)]
- Wang, J.; Ma, Y.; Yang, J.; Jin, L.; Gao, Z.; Xue, L.; Hou, L.; Sui, L.; Liu, J.; Zou, X. Fucoxanthin inhibits tumour-related lymphangiogenesis and growth of breast cancer. *J. Cell Mol. Med.* **2019**, *23*, 2219–2229. [[CrossRef](#)]
- Sung, H.; Ferlay, J.; Siegel, R.L.; Laversanne, M.; Soerjomataram, I.; Jemal, A.; Bray, F. Global cancer statistics 2020: GLOBOCAN estimates of incidence and mortality worldwide for 36 cancers in 185 countries. *CA Cancer J. Clin.* **2021**. [[CrossRef](#)] [[PubMed](#)]



27. Siegel, R.L.; Miller, K.D.; Jemal, A. Cancer statistics, 2020. *CA Cancer J. Clin.* **2020**, *70*, 7–30. [CrossRef]
28. World Health Organization. Breast Cancer—WHO | World Health Organization. Available online: <https://www.who.int/news-room/fact-sheets/detail/breast-cancer> (accessed on 1 May 2021).
29. Fragomeni, S.M.; Sciallis, A.; Jeruss, J.S. Molecular Subtypes and Local-Regional Control of Breast Cancer. *Surg. Oncol. Clin. N. Am.* **2018**, *27*, 95–120. [CrossRef]
30. Goldhirsch, A.; Winer, E.P.; Coates, A.S.; Gelber, R.D.; Piccart-Gebhart, M.; Thürlimann, B.; Senn, H.J. Personalizing the treatment of women with early breast cancer: Highlights of the St Gallen International Expert Consensus on the primary therapy of early breast cancer 2013. *Ann. Oncol.* **2013**, *24*, 2206–2223. [CrossRef]
31. Yersal, O.; Barutca, S. Biological subtypes of breast cancer: Prognostic and therapeutic implications. *World J. Clin. Oncol.* **2014**, *5*, 412–424. [CrossRef]
32. Dai, J.; Jian, J.; Bosland, M.; Frenkel, K.; Bernhardt, G.; Huang, X. Roles of hormone replacement therapy and iron in proliferation of breast epithelial cells with different estrogen and progesterone receptor status. *Breast* **2008**, *17*, 172–179. [CrossRef] [PubMed]
33. Trendowski, M. Recent advances in the development of antineoplastic agents derived from natural products. *Drugs* **2015**, *75*, 1993–2016. [CrossRef] [PubMed]
34. Garrido-Castro, A.C.; Lin, N.U.; Polyak, K. Insights into molecular classifications of triple-negative breast cancer: Improving patient selection for treatment. *Cancer Discov.* **2019**, *9*, 176–198. [CrossRef]
35. Yin, L.; Duan, J.J.; Bian, X.W.; Yu, S.C. Triple-negative breast cancer molecular subtyping and treatment progress. *Breast Cancer Res.* **2020**, *22*, 61. [CrossRef] [PubMed]
36. Fisusi, F.A.; Akala, E.O. Drug combinations in breast cancer therapy. *Pharm. Nanotechnol.* **2019**, *7*, 3–23. [CrossRef] [PubMed]
37. Masui, K.; Gini, B.; Wykosky, J.; Zanca, C.; Mischel, P.S.; Furnari, F.B.; Cavenee, W.K. A tale of two approaches: Complementary mechanisms of cytotoxic and targeted therapy resistance may inform next-generation cancer treatments. *Carcinogenesis* **2013**, *34*, 725–738. [CrossRef]
38. Amable, L. Cisplatin resistance and opportunities for precision medicine. *Pharmacol. Res.* **2016**, *106*, 27–36. [CrossRef]
39. Pádua, D.; Rocha, E.; Gargiulo, D.; Ramos, A.A. Bioactive compounds from brown seaweeds: Phloroglucinol, fucoxanthin and fucoidan as promising therapeutic agents against breast cancer. *PhytoChem. Lett.* **2015**, *14*, 91–98. [CrossRef]
40. Yun, C.W.; Kim, H.J.; Lee, S.H. Therapeutic application of diverse marine-derived natural products in cancer therapy. *Anti-cancer Res.* **2019**, *39*, 5261–5284. [CrossRef]
41. Lopes-Costa, E.; Abreu, M.; Gargiulo, D.; Rocha, E.; Ramos, A.A. Anticancer effects of seaweed compounds fucoxanthin and phloroglucinol, alone and in combination with 5-fluorouracil in colon cells. *J. Toxicol. Environ. Health A* **2017**, *80*, 776–787. [CrossRef]
42. Almeida, T.P.; Ferreira, J.; Vettorazzi, A.; Azqueta, A.; Rocha, E.; Ramos, A.A. Cytotoxic activity of fucoxanthin, alone and in combination with the cancer drugs imatinib and doxorubicin, in CML cell lines. *Environ. Toxicol. Pharmacol.* **2018**, *59*, 24–33. [CrossRef]
43. Vijay, K.; Sowmya, P.R.; Arathi, B.P.; Shilpa, S.; Shwetha, H.J.; Raju, M.; Baskaran, V.; Lakshminarayana, R. Low-dose doxorubicin with carotenoids selectively alters redox status and upregulates oxidative stress-mediated apoptosis in breast cancer cells. *Food Chem. Toxicol.* **2018**, *118*, 675–690. [CrossRef]
44. Wang, Z.; Li, H.; Dong, M.; Zhu, P.; Cai, Y. The anticancer effects and mechanisms of fucoxanthin combined with other drugs. *J. Cancer Res. Clin. Oncol.* **2019**, *145*, 293–301. [CrossRef] [PubMed]
45. Cherry, P.; O'Hara, C.; Magee, P.J.; McSorley, E.M.; Allsopp, P.J. Risks and benefits of consuming edible seaweeds. *Nutr. Rev.* **2019**, *77*, 307–329. [CrossRef] [PubMed]
46. Kim, J.B.; Stein, R.; O'Hare, M.J. Three-dimensional in vitro tissue culture models of breast cancer—A review. *Breast Cancer Res. Treat.* **2004**, *85*, 281–291. [CrossRef]
47. Verjans, E.T.; Doijen, J.; Luyten, W.; Landuyt, B.; Schoofs, L. Three-dimensional cell culture models for anticancer drug screening: Worth the effort? *J. Cell Physiol.* **2018**, *233*, 2993–3003. [CrossRef] [PubMed]
48. Kapałczyńska, M.; Kolenda, T.; Przybyła, W.; Zajączkowska, M.; Teresiak, A.; Filas, V.; Ibbs, M.; Bliźniak, R.; Łuczewski, Ł.; Lamperska, K. 2D and 3D cell cultures—A comparison of different types of cancer cell cultures. *Arch. Med. Sci.* **2018**, *14*, 910–919. [CrossRef]
49. Santo, V.E.; Rebelo, S.P.; Estrada, M.F.; Alves, P.M.; Boghaert, E.; Brito, C. Drug screening in 3D in vitro tumor models: Overcoming current pitfalls of efficacy read-outs. *Biotechnol. J.* **2017**, *12*. [CrossRef] [PubMed]
50. Imamura, Y.; Mukohara, T.; Shimono, Y.; Funakoshi, Y.; Chayahara, N.; Toyoda, M.; Kiyota, N.; Takao, S.; Kono, S.; Nakatsura, T.; et al. Comparison of 2D- and 3D-culture models as drug-testing platforms in breast cancer. *Oncol. Rep.* **2015**, *33*, 1837–1843. [CrossRef] [PubMed]
51. Konishi, I.; Hosokawa, M.; Sashima, T.; Kobayashi, H.; Miyashita, K. Halocynthiaxanthin and fucoxanthinol isolated from *Halocynthia roretzi* induce apoptosis in human leukemia, breast and colon cancer cells. *Comp. BioChem. Physiol. C Toxicol. Pharmacol.* **2006**, *142*, 53–59. [CrossRef]
52. Yamamoto, K.; Ishikawa, C.; Katano, H.; Yasumoto, T.; Mori, N. Fucoxanthin and its deacetylated product, fucoxanthinol, induce apoptosis of primary effusion lymphomas. *Cancer Lett.* **2011**, *300*, 225–234. [CrossRef]
53. De la Mare, J.A.; Sterrenberg, J.N.; Sukhthankar, M.G.; Chiwakata, M.T.; Beukes, D.R.; Blatch, G.L.; Edkins, A.L. Assessment of potential anti-cancer stem cell activity of marine algal compounds using an in vitro mammosphere assay. *Cancer Cell Int.* **2013**, *13*, 39. [CrossRef]

54. Møller, P. The alkaline comet assay: Towards validation in biomonitoring of DNA damaging exposures. *Basic. Clin. Pharmacol. Toxicol.* **2006**, *98*, 336–345. [[CrossRef](#)]
55. Leon-Galicia, I.; Diaz-Chavez, J.; Albino-Sanchez, M.E.; Garcia-Villa, E.; Bermudez-Cruz, R.; Garcia-Mena, J.; Herrera, L.A.; Garcia-Carrancá, A.; Gariglio, P. Resveratrol decreases Rad51 expression and sensitizes cisplatin-resistant MCF-7 breast cancer cells. *Oncol. Rep.* **2018**, *39*, 3025–3033. [[CrossRef](#)]
56. Lee, K.S.; Lee, M.G.; Kwon, Y.S.; Nam, K.S. Arctigenin enhances the cytotoxic effect of doxorubicin in MDA-MB-231 breast cancer cells. *Int. J. Mol. Sci.* **2020**, *21*, 2997. [[CrossRef](#)]
57. Antberg, L.; Cifani, P.; Levander, F.; James, P. Pathway-centric analysis of the DNA damage response to chemotherapeutic agents in two breast cell lines. *EuPA Open Proteom.* **2015**, *8*, 128–136. [[CrossRef](#)]
58. Pilco-Ferreto, N.; Calaf, G.M. Influence of doxorubicin on apoptosis and oxidative stress in breast cancer cell lines. *Int. J. Oncol.* **2016**, *49*, 753–762. [[CrossRef](#)]
59. Yang, F.; Teves, S.S.; Kemp, C.J.; Henikoff, S. Doxorubicin, DNA torsion, and chromatin dynamics. *Biochim. Biophys. Acta* **2014**, *1845*, 84–89. [[CrossRef](#)]
60. Kim, H.S.; Lee, Y.S.; Kim, D.K. Doxorubicin exerts cytotoxic effects through cell cycle arrest and Fas-mediated cell death. *Pharmacology* **2009**, *84*, 300–309. [[CrossRef](#)]
61. Lin, S.R.; Chang, C.H.; Hsu, C.F.; Tsai, M.J.; Cheng, H.; Leong, M.K.; Sung, P.J.; Chen, J.C.; Weng, C.F. Natural compounds as potential adjuvants to cancer therapy: Preclinical evidence. *Br. J. Pharmacol.* **2020**, *177*, 1409–1423. [[CrossRef](#)] [[PubMed](#)]
62. Liston, D.R.; Davis, M. Clinically relevant concentrations of anticancer drugs: A guide for nonclinical studies. *Clin. Cancer Res.* **2017**, *23*, 3489–3498. [[CrossRef](#)]
63. Menéndez-Menéndez, J.; Hermida-Prado, F.; Granda-Díaz, R.; González, A.; García-Pedrero, J.M.; Del-Río-Ibáñez, N.; González-González, A.; Cos, S.; Alonso-González, C.; Martínez-Campa, C. Deciphering the molecular basis of melatonin protective effects on breast cells treated with doxorubicin: TWIST1 a transcription factor involved in EMT and metastasis, a novel target of melatonin. *Cancers* **2019**, *11*, 1011. [[CrossRef](#)]
64. Prabhakaran, P.; Hassiotou, F.; Blancafort, P.; Filgueira, L. Cisplatin induces differentiation of breast cancer cells. *Front. Oncol.* **2013**, *3*, 134. [[CrossRef](#)] [[PubMed](#)]
65. Hosokawa, M.; Kudo, M.; Maeda, H.; Kohno, H.; Tanaka, T.; Miyashita, K. Fucoxanthin induces apoptosis and enhances the antiproliferative effect of the PPARγ ligand, troglitazone, on colon cancer cells. *Biochim. Biophys. Acta* **2004**, *1675*, 113–119. [[CrossRef](#)] [[PubMed](#)]
66. Wang, L.; Zeng, Y.; Liu, Y.; Hu, X.; Li, S.; Wang, Y.; Li, L.; Lei, Z.; Zhang, Z. Fucoxanthin induces growth arrest and apoptosis in human bladder cancer T24 cells by up-regulation of p21 and down-regulation of mortalin. *Acta Biochim. Biophys. Sin.* **2014**, *46*, 877–884. [[CrossRef](#)] [[PubMed](#)]
67. Wu, H.L.; Fu, X.Y.; Cao, W.Q.; Xiang, W.Z.; Hou, Y.J.; Ma, J.K.; Wang, Y.; Fan, C.D. Induction of apoptosis in human glioma cells by fucoxanthin via triggering of ROS-mediated oxidative damage and regulation of MAPKs and PI3K-AKT pathways. *J. Agric. Food Chem.* **2019**, *67*, 2212–2219. [[CrossRef](#)] [[PubMed](#)]
68. Shin, J.; Song, M.-H.; Oh, J.-W.; Keum, Y.-S.; Saini, R.K. Pro-oxidant actions of carotenoids in triggering apoptosis of cancer cells: A review of emerging evidence. *Antioxidants* **2020**, *9*, 532. [[CrossRef](#)]
69. Liu, C.L.; Chiu, Y.T.; Hu, M.L. Fucoxanthin enhances HO-1 and NQO1 expression in murine hepatic BNL CL2 cells through activation of the Nrf2/ARE system partially by its pro-oxidant activity. *J. Agric. Food Chem.* **2011**, *59*, 11344–11351. [[CrossRef](#)]
70. Zurina, I.M.; Gorkun, A.A.; Dzhussoeva, E.V.; Kolokoltsova, T.D.; Markov, D.D.; Kosheleva, N.V.; Morozov, S.G.; Saburina, I.N. Human melanocyte-derived spheroids: A precise test system for drug screening and a multicellular unit for tissue engineering. *Front. Bioeng. Biotechnol.* **2020**, *8*, 540. [[CrossRef](#)]
71. Terasaki, M.; Maeda, H.; Miyashita, K.; Mutoh, M. Induction of anoikis in human colorectal cancer cells by fucoxanthin. *Nutr. Cancer* **2017**, *69*, 1–10. [[CrossRef](#)]
72. Terasaki, M.; Matsumoto, N.; Hashimoto, R.; Endo, T.; Maeda, H.; Hamada, J.; Osada, K.; Miyashita, K.; Mutoh, M. Fucoxanthin administration delays occurrence of tumors in xenograft mice by colonospheres, with an anti-tumor predictor of glycine. *J. Clin. Biochem. Nutr.* **2019**, *64*, 52–58. [[CrossRef](#)]
73. Hongisto, V.; Jernström, S.; Fey, V.; Mpindi, J.P.; Kleivi Sahlberg, K.; Kallioniemi, O.; Perälä, M. High-throughput 3D screening reveals differences in drug sensitivities between culture models of JIMT1 breast cancer cells. *PLoS ONE* **2013**, *8*, e77232. [[CrossRef](#)] [[PubMed](#)]
74. Lovitt, C.J.; Shelper, T.B.; Avery, V.M. Doxorubicin resistance in breast cancer cells is mediated by extracellular matrix proteins. *BMC Cancer* **2018**, *18*, 41. [[CrossRef](#)]
75. Prabst, K.; Engelhardt, H.; Ringgeler, S.; Hubner, H. Basic. colorimetric proliferation assays: MTT, WST, and Resazurin. *Methods Mol. Biol.* **2017**, *1601*, 1–17. [[CrossRef](#)]
76. Kumar, P.; Nagarajan, A.; Uchil, P.D. Analysis of cell viability by the lactate dehydrogenase assay. *Cold Spring Harb. Protoc.* **2018**, *2018*. [[CrossRef](#)]
77. Malhão, F.; Ramos, A.A.; Macedo, A.C.; Rocha, E. Cytotoxicity of seaweed compounds, alone or combined to reference drugs, against breast cell lines cultured in 2D and 3D. *Toxics* **2021**, *9*, 24. [[CrossRef](#)] [[PubMed](#)]
78. Huang, Z.; Yu, P.; Tang, J. Characterization of triple-negative breast cancer MDA-MB-231 cell spheroid model. *Oncol. Targets Ther.* **2020**, *13*, 5395–5405. [[CrossRef](#)]

79. Fischer, U.; Schulze-Osthoff, K. Apoptosis-based therapies and drug targets. *Cell Death Differ.* **2005**, *12*, 942–961. [[CrossRef](#)]
80. Chen, D.L.; Engle, J.T.; Griffin, E.A.; Miller, J.P.; Chu, W.; Zhou, D.; Mach, R.H. Imaging caspase-3 activation as a marker of apoptosis-targeted treatment response in cancer. *Mol. Imaging Biol.* **2015**, *17*, 384–393. [[CrossRef](#)]
81. Muftah, A.A.; Aleskandarany, M.A.; Al-Kaabi, M.M.; Sonbul, S.N.; Diez-Rodriguez, M.; Nolan, C.C.; Caldas, C.; Ellis, I.O.; Rakha, E.A.; Green, A.R. Ki67 expression in invasive breast cancer: The use of tissue microarrays compared with whole tissue sections. *Breast Cancer Res. Treat.* **2017**, *164*, 341–348. [[CrossRef](#)]
82. Soliman, N.A.; Yussif, S.M. Ki-67 as a prognostic marker according to breast cancer molecular subtype. *Cancer Biol. Med.* **2016**, *13*, 496–504. [[CrossRef](#)] [[PubMed](#)]
83. Hershey, B.J.; Vazzana, R.; Joppi, D.L.; Havas, K.M. Lipid droplets define a sub-population of breast cancer stem cells. *J. Clin. Med.* **2019**, *9*, 87. [[CrossRef](#)]
84. Cheng, J.; Fujita, A.; Ohsaki, Y.; Suzuki, M.; Shinohara, Y.; Fujimoto, T. Quantitative electron microscopy shows uniform incorporation of triglycerides into existing lipid droplets. *HistoChem. Cell Biol.* **2009**, *132*, 281–291. [[CrossRef](#)] [[PubMed](#)]
85. Gammone, M.A.; D’Orazio, N. Anti-obesity activity of the marine carotenoid fucoxanthin. *Mar. Drugs* **2015**, *13*, 2196–2214. [[CrossRef](#)]
86. Shyu, P., Jr.; Wong, X.; Fah, A.; Crasta, K.; Thibault, G. Dropping in on lipid droplets: Insights into cellular stress and cancer. *Biosci. Rep.* **2018**, *38*. [[CrossRef](#)]
87. Bojko, A.; Staniak, K.; Czarnańska-Herok, J.; Sunderland, P.; Dudkowska, M.; Śliwińska, M.A.; Salmina, K.; Sikora, E. Improved autophagic flux in escapers from doxorubicin-induced senescence/polyploidy of breast cancer cells. *Int. J. Mol. Sci.* **2020**, *21*, 6084. [[CrossRef](#)] [[PubMed](#)]
88. Holliday, D.L.; Speirs, V. Choosing the right cell line for breast cancer research. *Breast Cancer Res.* **2011**, *13*, 215. [[CrossRef](#)] [[PubMed](#)]
89. Subik, K.; Lee, J.-F.; Baxter, L.; Strzepek, T.; Costello, D.; Crowley, P.; Xing, L.; Hung, M.-C.; Bonfiglio, T.; Hicks, D.G.; et al. The expression patterns of ER, PR, HER2, CK5/6, EGFR, Ki-67 and AR by immunohistochemical analysis in breast cancer cell lines. *Breast Cancer* **2010**, *4*, 35–41. [[CrossRef](#)]
90. Malhão, F.; Ramos, A.A.; Buttachon, S.; Dethoup, T.; Kijjoa, A.; Rocha, E. Cytotoxic and antiproliferative effects of preussin, a hydroxypyrrolidine derivative from the marine sponge-associated fungus *Aspergillus candidus* KUFA 0062, in a panel of breast cancer cell lines and using 2D and 3D cultures. *Mar. Drugs* **2019**, *17*, 448. [[CrossRef](#)] [[PubMed](#)]
91. Piccinini, F. AnaSP: A software suite for automatic image analysis of multicellular spheroids. *Comput. Methods Programs Biomed.* **2015**, *119*, 43–52. [[CrossRef](#)] [[PubMed](#)]
92. Sales Gil, R.; Vagnarelli, P. Ki-67: More hidden behind a ‘classic proliferation marker’. *Trends BioChem. Sci.* **2018**, *43*, 747–748. [[CrossRef](#)]
93. Bressenot, A.; Marchal, S.; Bezdetnaya, L.; Garrier, J.; Guillemin, F.; Plenat, F. Assessment of apoptosis by immunohistochemistry to active caspase-3, active caspase-7, or cleaved PARP in monolayer cells and spheroid and subcutaneous xenografts of human carcinoma. *J. HistoChem. CytoChem.* **2009**, *57*, 289–300. [[CrossRef](#)] [[PubMed](#)]
94. Hammer, O.; Harper, D.; Ryan, P. PAST: Paleontological Statistics Software Package for education and data analysis. *Palaeontol. Electron.* **2001**, *4*, 1–9.
95. Gaetano, J. Holm-Bonferroni Sequential Correction: An Excel Calculator (v. 1.3) Microsoft Excel Workbook. Available online: [https://www.researchgate.net/publication/322569220\\_Holm-Bonferroni\\_sequential\\_correction\\_An\\_Excel\\_calculator\\_13](https://www.researchgate.net/publication/322569220_Holm-Bonferroni_sequential_correction_An_Excel_calculator_13) (accessed on 1 June 2021).
96. Holm, S. A simple sequentially rejective multiple test procedure. *Scand. Stat. Theory Appl.* **1979**, *6*, 65–70.





# **Chapter 6** - General Discussion





### **6.1. What is this thesis about?**

This thesis was dedicated to studying the bioactive effects of selected marine-derived compounds - preussin, as isolated from a sponge-associated fungus, and six seaweed compounds - alone and combined with chemotherapy drugs on a panel of breast cell lines cultivated in 2D. For this purpose, we selected a panel of BC cell lines corresponding to the main subtypes of BC: MCF7 (luminal A); SKBR3 (HER-2 overexpression), and MDA-MB-231 (TNBC). Additionally, we included a non-tumoral cell line (MCF12A) for comparative purposes. The selection of the seaweed compounds was made to include compounds of different chemical classes: (a) carotenoids: astaxanthin (Asta) and fucoxanthin (Fx); (b) polysaccharides: fucoidan (Fc) and laminarin (Lm); (c) sterols: fucosterol (Fct); and (d) phlorotannins: phloroglucinol (Phg). By including different chemical classes, we could have a broader view of the effects of seaweed compounds on BC cells and evaluate which class could be more interesting in terms of single and combined exposures with chemotherapy drugs. For the chemotherapy drugs, we selected two currently used in clinical practice to treat BC: Doxorubicin (Dox) and Cisplatin (Cis). In addition to the 2D culture studies, the most promising combinations (seaweed compound + drug) were also evaluated in 3D cell cultures. This multitude of combinations gave us a broad scenario of the cytotoxic effects of these compounds on the BC cell lines.

### **6.2. What were the new aspects tested in this thesis?**

As far as we know, this is the first study that reports on a panel of breast cell lines: (a) characterization of the 3D cell culture models using morphometric, morphological, and immunocytochemical approaches; (b) cytotoxic and antiproliferative effects of preussin in 2D and 3D cell culture; (c) cytotoxic effects of seaweeds compounds belonging to different classes (alone and combined with Dox and Cis) in 2D cell culture; and (d) the cytotoxic and antiproliferative effects of Fct and Fx alone and combined with Dox in 3D cell culture.

In the literature, few studies on BC cell lines tested seaweed compounds combined with a chemotherapy drug (Zhang et al., 2013, Vijay et al., 2018, Fouad et al., 2021), and all rely only on 2D cell cultures. Here, we made a step forward by evaluating the most promising combinations selected on monolayer culture (Fct + Dox and Fx + Dox) in 3D cell culture, using a multi-end approach consisting of cell-based assays for exploring the cytotoxic effects (at least two different ones), and other morphological outputs including

area measurement, histology, immunocytochemistry (ICC), and ultrastructural analysis by transmission electron Microscopy (TEM).

### **6.3. How were obtained the 3D cell cultures? What were the advantages and disadvantages of the method used?**

To assess the effects of the selected marine-derived compounds in 3D cell culture, we first obtained and characterized the 3D cell cultures of the breast cell lines, which consisted of the work presented in Chapter 2.

The 3D cell cultures, here called multicellular aggregates (MCAs), were obtained using a scaffold-free stationary method, the ultra-low-attachment (ULA) plates. This technique was revealed to be a reasonably economical and practical solution when compared to other 3D methods. It was simple to perform and enabled the formation of the MCAs of the four used cell lines without adding medium supplements such as extracellular matrix components or viscosity-raiser compounds. As with any other laboratory procedure, it required optimization. This was partially described in the supplementary files of Chapter 2, together with a table of tips and tricks to solve some problems during the obtention and analysis of the MCAs. In the optimization process, different densities and times in culture were tested, and the best conditions for each cell line were selected and used in the exposure experiments described in the following chapters.

The ULA plates also brought some difficulties and disadvantages. First, during the plating of cells in the wells, if any small fiber or dust falls into the wells, the MCAs tend to form differently. The format of the MCAs followed the fibers' extension, not allowing the use of these MCAs in the exposures. Thus, we found it necessary to have extreme care when plating, maintaining the lid covering the areas that are not being used as much as possible. Another disadvantage is that, due to the wells' curvature, when performing techniques that require absorbance or immunofluorescence measurements, it was necessary to transfer the MCAs to flat-bottom plates. Besides being time-consuming, this step can also disrupt or damage some MCAs. Another aspect worth mentioning is that within the same cell line, and within each experiment, the formed MCAs were relatively uniform in shape and area. However, among different days of experiments, there were observed differences, not in the MCAs' shapes but their areas, corresponding to different cell compaction mainly during 3 days of MCAs formation. These variations among experiments can be easily observed in the graphics in Figure 1 of Chapter 2. We propose that factors like the time of trypsinization, the time between the trypsinization

and the seeding, calibration of the plate during centrifugation, and different cell passages among experiments could explain these variations.

Furthermore, we agree with other authors that it may be a low-throughput strategy as it generates a limited number of MCAs when compared to other techniques as is not amenable to automation of medium change without aspirating or damaging the MCAs (Katt et al., 2016, Jensen and Teng, 2020). However, in our experience during this work, it is a good option for laboratories wanting to start screening compounds in 3D. However, more improvements are required in this technology to make it a higher throughput technique.

#### **6.4. What were the main characteristics of the formed MCAs?**

The type of the formed MCAs depended on each cell line's characteristics, which is in line with previous descriptions (Froehlich et al., 2016, Gencoglu et al., 2018). To exemplify this, of the four used cell lines, two formed compact 3D structures (MCF7 and MDA-MB-231), and two formed loose ones (SKBR3 and MCF12A). The same number of cells was seeded for the three BC cell lines, and the SKBR3 formed the MCAs with bigger areas and loose structures. For MCF12A, the double number of cells were seeded, and the MCAs areas were not higher than the SKBR3. None of the formed 3D cultures was spherical. Contrarily, they were more oblate, discoid structures and the loose ones were even more flattened, which is very far from a spherical structure, as confirmed by the manipulation and histological sectioning. Thus, we opted not to call them spheroids and used the nomenclature MCAs, as this terminology embraces all formed 3D cell cultures.

We reinforce here our opinion about the urgent need to uniform the nomenclature of 3D cell cultures through publication guidelines for scientists. If a generical term could be applied to all 3D cell cultures, we would suggest “multicellular aggregates”, as all 3D cell cultures correspond to a group of cells joined together to form an aggregate, independently of whether they are spherical or not, or if they correspond to compact or loose aggregates. We believe “spheroids” should only be used for compact spherical or nearly spherical models and not for other irregular-shaped and loose cell aggregates.

According to the different techniques used in the thesis, our obtained MCAs do not fit in the classical 3-layered model proposed for the general structure of the 3D cell cultures, with a more proliferative outer layer, followed by senescent cells and an inner necrotic core (Edmondson et al., 2014, Costa et al., 2016). We only observed a central core with concentrated dying cells in some compact MCAs. Once again, relatively to the

nomenclature of this central core with dying cells, there is also a high degree of inconsistency, as most studies call it “necrotic core” (Mehta et al., 2012, Costa et al., 2016), without assessing the type of cell death, or only using techniques for apoptosis detection. In the MCAs, we observed immunostaining and morphological aspects of both death processes, so we opted to call them apoptotic/necrotic core instead of just necrotic.

Additionally, with ICC techniques, proliferating and dying cells were observed throughout all the MCAs, without preferential localization. This spreading may be a consequence of two main facts: first, the loose MCAs display more spaces among cells, and second, the oblate discoid shape increases the surface area and reduce the distance from the MCA's center of mass; both aspects facilitate the diffusion of the nutrients and oxygen and, as a consequence, prevent the formation of a hypoxic central region with a higher number of dying cells (Leung et al., 2015).

The reality is that depending on methodology, the used cell lines, the medium used, and other factors, the 3D models can be quite different not only in terms of gross morphology but also in their inner structures and physiological status. For instance, MCAs may not present an apoptotic/necrotic core because cells have more access to nutrients and oxygen. Therefore, and despite their usefulness, we concur that the responses of these models to a different stimulus can be very different among different 3D models (Barbosa et al., 2022).

As for the characterization, besides the described aspects related to the 3D shape, the compactness of the MCAs, and the presence of proliferating and dying cells, the other techniques (optical and electron microscopies, ICC) gave more information about the inner structure of the MCAs as well as the expression of other selected markers (AE1/AE3, Vimentin, E-cad, ER, PR, and HER-2).

In a brief characterization summary of this study, all the cell lines in 3D expressed the epithelial marker AE1/AE3, and the mesenchymal marker vimentin was expressed in SKBR3 and MCF12A cell lines, which are generally in line with previous studies (Sommers et al., 1989, Holliday and Speirs, 2011, Bock et al., 2012, Sweeney et al., 2018). We found in the literature many incongruences relative to the positive staining or absence of the tested markers, some support our results, and others contradict them.

The MCF7 MCAs were the ones where we encountered aspects of cell differentiation, such as the expression of ER/PR (Sommers et al., 1989, Iglesias et al., 2013) and Ecad (Iglesias et al., 2013, Amaral et al., 2017), restoration of cell polarity and tissue

recapitulation features as the formation of acinar-like structures with an accumulation of secretory vesicles into the lumen MCAs, as previously described in other studies (Krause et al., 2010, D'Anselmi et al., 2013). TEM also showed high amounts of glycogen (Pelletier et al., 2012) and some lipid droplets (Abramczyk et al., 2015), as described in the literature.

SKBR3 MCAs showed more than 80% of cells with complete and intense membrane immunostaining for HER-2. However, the published data only refers to the positivity for HER-2 without describing the percentage or the type of immunostaining (Neve et al., 2006b, Iglesias et al., 2013). This cell line is also negative for E-cad (Iglesias et al., 2013).

MDA-MB-231 MCAs were negative for ER, PR, and HER-2 consistently has been a triple negative cell line (Huang et al., 2020). In TEM, there were observed a high number of lipid droplets (Abramczyk et al., 2015) and dense multi-vesicular bodies, which seemed to be very characteristic of this cell line cultivated in 3D cell culture (Ivers et al., 2014).

MCF12A cells were negative for ER and PR, and just a subset in the outer part of the MCAs was positive for E-cad. Both characteristics are controversial in the literature. Some describe MCF12A cells as positive for ER/PR (Dai et al., 2008, Marchese and Silva, 2012) and E-cad (Neve et al., 2006a, Sweeney et al., 2018), while others declare negativity for ER/PR (Neve et al., 2006a, Sweeney et al., 2018) and E-cad (Lombaerts et al., 2006). TEM showed that these MCAs were the richest cells in terms of organelle content while also revealing some cells with lipid droplets, small glycogen deposits, and bundles of microfilaments dispersed around the nucleus or dispersed in the cytoplasm. Other studies that used this cell line for 3D cell culture with added Matrigel (Marchese and Silva, 2012, Weber-Ouellette et al., 2018) observed acini formation in 3D. In our study, with the ULA plates and without adding such compounds, no acini were observed, and there was only some membrane projection into the intercellular spaces.

Knowing the structure of the MCAs, we can select if they are a good model for studying some particular topics. For instance, if the objective is to study cells' response to hypoxic conditions, the loose MCAs or the MCAs that do not have a dead central core may not be a good model. The same can apply to the delivery of the compound. In theory, in loose MCAs the compounds do not encounter the same resistance to diffusion as in compact MCAs. From our experience, we believe it is essential to characterize the model well before using it to screen compounds. Only an excellent model characterization can be a reference to sustain interpretations when analyzing the compound exposure results.



### **6.5. What were the effects of the preussin on the panel of BC cell lines cultivated in 2D and 3D cell cultures? Are they worth exploring further?**

Regarding the effects of preussin in 3D cell cultures, and to the best of our knowledge, the present study is the first to report cytotoxic effects in such *in vitro* model. We revealed high levels of preussin cytotoxicity at both tested concentrations (50 and 100  $\mu\text{M}$ ), in 2D and 3D cell cultures, in all tested cell lines (Chapter 3). Other studies have reported the cytotoxic effects of preussin in 2D cell cultures of different human cell lines with  $\text{IC}_{50}$  varying between 2.3 – 4.5  $\mu\text{M}$  (Achenbach et al., 2000) and 12.3 – 74.1  $\mu\text{M}$  (Buttachon et al., 2018), including in the MCF7. In the latter, the estimated  $\text{IC}_{50}$  has varied from 3.7  $\mu\text{M}$  (Achenbach et al., 2000) to 53.6  $\mu\text{M}$  (Buttachon et al., 2018). However, in the study of Achenbach et al., 2000, they used a different method for estimating the cell viability, by measuring the crystal violet dye retained by the cells after 48 h of exposure to preussin followed by incubation in a drug-free medium for another 48 h. While Buttachon et al., 2018, also used the MTT assay, in similar conditions to the ones used here.

Despite the relatively high concentrations tested, the marine fungal metabolites have demonstrated unique molecular traits that are very attractive as lead structures, so they should be further investigated (Gomes et al., 2015). Therefore, we propose to study further the impacts of preussin in selected cell lines, particularly by exploring 3D models and covering more concentrations. Moreover, other mechanisms of cell delivery could be equated and tested if preussin continues to evidence interesting anticancer activities.

Notwithstanding, the obtention of this compound and others from natural sources is extremely laborious, time-consuming, and needs highly qualified technical skills and knowledge (Malve, 2016). Also, the yield of the purified compound is tiny (typically only a few mg), limiting the number of assays that can be devised, at least in a short period. Nowadays, it is possible to acquire synthetic preussin commercially, but only by custom synthesis, and the delivery times are high (months). In short, the supply prevents fast scientific advances.

### **6.6. What were the effects of the seaweed compounds (alone or combined with Cis and Dox) on the panel of BC cell lines cultivated in 2D cell culture?**

Relatively to the seaweed compounds, we opted to use high-purity commercial ones, easier to obtain and with more quantity available for different experimental studies. Additionally, it is much easier to compare our results with other studies, as the source and purity of the compounds are the same. This cannot be said for seaweed-extracted compounds since the biological activity of a chemical can be altered by extraction

methods, solvent type, pressure and temperature, solvent-to-solid ratio, and dried seaweed particle size (Okeke et al., 2021). Even when comparing our results with other studies that used the same commercial compounds in similar concentrations, it was common to encounter very different results. From our experience and understanding, this finding can be related to a plethora of factors, such as variations related to the cell culture. These include culture medium and their supplementations, state of the cell line (for instance, the number of passages), different preparations of the stock and working solutions, storage of the compounds, times of exposure, and different methods for detecting the effects. All the mentioned factors can influence the differences in the obtained results.

Compared with the literature, there are examples of these differences in the obtained effects among the seaweed compounds tested in this work (Chapters 4 and 5). However, in other cases, our results corroborated previous studies. For instance, Asta has been reported to induce apoptosis in BC cells in a wide range of concentrations, varying from 2 (Vijay et al., 2018) to 100  $\mu\text{M}$  (Karimian et al., 2022). We tested Asta up to 200  $\mu\text{M}$ , and it did not affect the cell viability of any tested cell lines. Yet, others reported no cytotoxicity in other cell types, despite trying the same concentration range we used (Siangcham et al., 2020). Contrary, concerning the other carotenoid Fx, at 10  $\mu\text{M}$ , it decreased the cell viability of all cell lines with a similar magnitude effect. This result matches others that used the same cell lines (Rwigemera et al., 2014, Vijay et al., 2018, Garg et al., 2019).

The polysaccharides Lm and Fc reduced MCF12A cell viability only at the highest tested concentration (1,000  $\mu\text{g}/\text{mL}$ ). We did not find any study for Lm to compare with our data. Regarding Fc, studies that employed the same commercial chemical reported apoptosis induction at concentrations as low as 100  $\mu\text{g}/\text{mL}$  in the MDA-MB-231 cell line (Chen et al., 2014) and reduced cell viability only at doses of 25  $\text{mg}/\text{mL}$  in the same cell line (Li et al., 2019).

Concerning Fct, most studies used Fct isolated from different seaweed species. The only work that used commercial Fct reported higher cytotoxic concentrations than our study, with  $\text{IC}_{50}$  of 125  $\mu\text{M}$  in MCF7 (Jiang et al., 2018). Our findings show that Fct at 10  $\mu\text{M}$  decreased cell viability of the three BC cell lines by about 30% in MCF7 and MDA-MB-231 and 40% in SKBR3 cell lines, without effects in the non-tumoral MCF12A. However, the referred study does not mention the solvent used nor the percentage of solvent in cells. In our study, we could not raise the concentration of the exposure to Fct, more than

10  $\mu\text{M}$  because of the solubility of Fct in DMSO and in a way not to exceed 0.1% of solvent in cells.

Lastly, for Phg, in our study, cytotoxic effects were observed in MCF7 and MDA-MB-231 cell lines at 1000  $\mu\text{M}$ . In the literature, Phg at lower concentrations (such as 100  $\mu\text{M}$ ) showed suppression of metastatic ability without cytotoxic effects (Kim et al., 2015a) and sphere formations (Kim et al., 2015b); and these outputs were not tested in this work.

### **6.7. Which were the most promising combinations of seaweed compounds plus drugs to be studied in 3D cell culture?**

When studying the combinations of a “seaweed compound + drug” in 2D cell culture, we considered them promising when the resulting cytotoxic effect significantly differed from the control and both compounds alone, suggesting an enhancement of the drug effect. In all BC cell lines, promising combinations existed, while none displayed enhanced drug cytotoxic effects in the non-tumoral cell line MCF12A (Chapters 4 and 5).

The relevant combinations are summarized here, and the mean percentage of enhancement in relation to the drug alone is displayed in brackets. In MCF7 cell line: Fct 5  $\mu\text{M}$  + Dox 0.01  $\mu\text{M}$  (15%) and Phg 10  $\mu\text{M}$  + Dox 0.01  $\mu\text{M}$  (15%). In SKBR3: Fc 50  $\mu\text{g/mL}$  + Cis 10  $\mu\text{M}$  (28%) and Fx 10  $\mu\text{M}$  + Dox 0.1  $\mu\text{M}$  (17%). In MDA-MB-231: Fct 5  $\mu\text{M}$  + Dox 0.1  $\mu\text{M}$  (46%) and Fx 10  $\mu\text{M}$  + Dox 1  $\mu\text{M}$  (19%). For each set of experiments in 2D cultures, the two most promising combinations (that were the ones with the highest percentage of drug enhancement) were studied in 3D cell culture were: Fct 5  $\mu\text{M}$  + Dox 0.1  $\mu\text{M}$  (46%) (Chapter 4) and Fx 10  $\mu\text{M}$  + Dox 1  $\mu\text{M}$  (19%) (Chapter 5). Interestingly, both were in the TNBC cell line (MDA-MB-231).

Although both Fct and Fx seemed to enhance the cytotoxic effects of Dox, there were some relevant differences between the two situations. In monolayers, Fct 5  $\mu\text{M}$  alone did not affect the viability of any cell line. Still, in combination with a low dose of Dox, it enhanced the cytotoxic drug effect and diminished cell proliferation. This combination was the one that revealed the highest Dox cytotoxicity enhancement observed in the experiments of this thesis. Another noteworthy finding with Fct alone is that it decreased the viability of the three tested BC cell lines at 10  $\mu\text{M}$  while not affecting the non-tumoral cell line MCF12A. However, this enhancement was not observed in 3D cell culture. More resistance of 3D cell cultures to the tested compounds is well-documented in other drugs (Breslin and O'Driscoll, 2013, Nowacka et al., 2021). However, the opposite can also occur (Breslin and O'Driscoll, 2013). Likely, for Fct displaying in 3D the same

enhancement of Dox observed in 2D cell culture, it would be necessary to use higher concentrations.

This resistance can be related to the difficulty of drug diffusion caused by the multilayers of cells, the different gradients of nutrients, pH, and oxygen, and the presence of cells at various stages of proliferation, which also can affect sensitivity to drugs (Jo et al., 2018). Additionally, in 3D cell culture, an increment of extracellular membrane components can be secreted, and the cell-ECM interactions and spatial positioning of cells relative to the ECM can affect drug sensitivity to drugs (Law et al., 2021).

However, Fx 10  $\mu\text{M}$  enhancement of Dox effects existed in 2D and 3D cultures. In the 3D cell culture, both Fx 10  $\mu\text{M}$  and Dox 1  $\mu\text{M}$  did not have cytotoxic effects, yet their combination significantly differed from the control and both compounds alone. The difference from the previous combination of Dox with Fct may be due to the different characteristics of the Fx compound which has a high polarity, making it rapidly absorbed into cancer cell organelles (Din et al., 2022). The lipid droplets' electron density decreased in the MCAs exposed to Fx (alone or in combination with Dox), and dense granular material was deposited around them, indicating mechanistic interferences in lipidic trafficking.

### **6.8. Screening compounds in 3D – the importance of a multi-end point assay.**

This work compared 2D and 3D culture conditions and the responses to test compounds. In practical terms, the 3D cell culture, even using a relatively simple technique, is much more challenging, time-consuming, and less handy for performing cell-based assays. Furthermore, in the obtained results, 3D cell cultures were more resistant to effects, even to Dox. In Chapter 4, Dox at 1  $\mu\text{M}$  decreased cell viability by more than 50% in 2D, but in 3D a similar effect was observed when the MCAs were exposed to Dox at 5  $\mu\text{M}$ . This phenomenon has been reported before (Lovitt et al., 2018, Nunes et al., 2019). Similarly, one of the most promising combinations (Fct 5  $\mu\text{M}$  + Dox 0.1  $\mu\text{M}$ ) and Fx 10  $\mu\text{M}$ , which displayed a significantly cytotoxic effect in 2D cell culture, did not affect the viability in 3D cell culture. All these findings support the notion that 3D cell arrangements may be more physiologically relevant models (Duval et al., 2017, Langhans, 2018). We believe that testing compounds in 3D, even in simple 3D culture models like the one used in this thesis, is a step forward in the drug discovery process in the sense that they can be useful to decipher some mechanisms of action of a given compound of interest and are easy to perform a screening study for selecting.

Additionally, when performing a screening compound in 3D cultures, we consider a multi-end approach a valuable strategy to confirm and then further explore selected promising conditions. In this study, we did not rely only on viability assays and complemented the information by performing morphological and immunohistochemical studies. Relatively to this topic, after completing this work, we advise using, if possible, more than one viability assay, as they have different theoretical foundations and procedures, like MTT and LDH assay. MTT relies on mitochondrial metabolism (Prabst et al., 2017), while the LDH test evaluates plasmatic membrane integrity by quantifying the LDH released from damaged cells (Kumar et al., 2018). Accordingly, those tests have different sensitivities to detect cytotoxic effects. One advantage of using both tests in parallel is that they can be performed the same well. The reason is that the LDH technique requires only 50  $\mu$ L of the culture medium for the assay, and the remaining medium can be used to dilute the MTT reagent.

Our study draws attention to the relevance of morphology to a multi-end approach. The processing of the MCAs for optical and electron microscopies revealed several aspects. First, it allowed us to check the presence of an apoptotic/necrotic core, revealing aspects compatible with apoptosis and necrosis cell death processes. Secondly, it was possible to perform ICC and visualize the localization of several markers, especially the caspase-3 and ki67 showing the death and proliferating status of the MCAs, and also allowing their quantification. The morphological and ICC results also contributed to the validation of the cell-based assays by showing a degree of cell damage that, in some situations, was not detected by the cell viability assays. One example is the case of preussin at 50  $\mu$ M, that in different cell lines did not differ from the control using the viability assays. At the same time, the morphology revealed a quite considerable level of cell damage. Another important advantage is that the biological material stored in paraffin can be stored indefinitely at room temperature and can be used to further studies using other markers.

Transmission electron microscopy (TEM) gave additional relevant information about the characteristics of the cells in 3D, revealing the content of organelles, dense bodies, and accumulation substances (glycogen and lipid droplets). The TEM also unveiled the inner structures of the MCAs, revealing the type of cell adhesions, the presence of polarity and microvilli projected into the intercellular spaces, and ultimately the acinar-like structures and associated secretion vesicles. Because of the fixatives used for TEM, it was possible to see lipid droplets and ultrastructural modifications resulting from chemical exposures, as in the case of Fx exposure.

Another component of the multi-end approach was MCAs area measurement which was considered the most informative parameter to characterize spheroid assembly and growth and to evaluate a drug effect (Mittler et al., 2017). With what we know today, it does not seem an appropriate parameter to evaluate the extent of cell damage within the MCAs, at least for our tested condition. Areas maintained even in conditions of high cytotoxicity (observed by optical and electron microscopy), however, the MCAs tended to disintegrate when manipulated. It is important to mention that the pictures used for area measurement were taken before performing the other outputs. The only condition in which a reduction of cell viability paralleled the altered area was Dox at 5  $\mu\text{M}$ , which also corresponded to a reduction of more than 50% in MTT and an increase in LDH release of more than 50% compared to the control. The combination of Fx 20  $\mu\text{M}$  + Dox 2  $\mu\text{M}$ , had similar results in the cytotoxic assays without alteration in the areas of MCAs. Similarly, preussin at 100  $\mu\text{M}$  also had cytotoxic effects of the same magnitude as Dox at 5  $\mu\text{M}$ , without area alterations. Nevertheless, it was crucial to measure the areas for model characterization, understand the dynamics of the MCA formation, and monitor their compaction over time in culture. The area's usefulness was well-illustrated in the case of MCAs from SKBR3 and with a higher degree in MDA-MB-231.

### **6.9. What is the importance of using a panel of BC cell lines? Is it worth including a non-tumoral breast cell line?**

Our data support the usefulness of a panel of cell lines of the same tissue or organ to perform a screening of compounds. In this study, cell lines with different characteristics displayed different sensitivities to the tested compounds, and thus a panel of cell lines allows a broad view of the effects in the type of cells under investigation. Apropos, the most promising combinations of chemicals in the used panel were on the MDA-MB-231 cell line, representing the TNBC, where fewer therapeutic options exist (Li et al., 2022).

The use of a non-tumoral cell line from the same tissue or organ of the cancer type of interest paired with the panel of the immortalized cell lines *in vitro* screening studies is a topic of controversy. The rationale is that if a compound is less toxic to normal than to cancer cell lines, it may have a potential therapeutic application (Liu et al., 2015). Some authors are very stringent about the need to test the effects of the tested compound on normal cells (Gomes et al., 2015). They argue that if a compound displays cytotoxic effects against cancer cells, it must also be tested on normal cells to determine its level of selectivity between normal and cancer cells. If the magnitude of the effects is similar in tumoral and non-tumoral cells or are more cytotoxic to normal cells (Zhou et al., 2022), it should not be considered a potential anticancer agent (Gomes et al., 2015). On the

contrary, others view the argument as a fallacy (Liu et al., 2015) because the main cells affected by the chemotherapy drugs are: a) the fast-proliferating cells, as blood cells; b) the cells that do not have the capacity of regeneration as neurons and cardiomyocytes; and c) cells from the most metabolic organs, that is the liver and kidney, responsible respectively for the metabolization and excretion of the drugs. Moreover, non-tumoral cell lines require special supplementation needs, and some studies cultivate these cell lines in the same medium as the other ones, making them more susceptible to the testing compounds. Overall, we believe there are scientifically sound reasons not to discard a compound just because it is toxic on non-tumoral cell lines, as there are other strategies to direct the compounds to cancer cells.

We used here the non-tumoral cell line (MCF12A), and among the tested compounds, the effects were very similar to the other cell lines; exceptions were for Fct, which was not cytotoxic just in this cell line, and Cis, for which the line was more sensitive to the drug's cytotoxic effects. As we characterized the MCF12A cell line, we thought it did not have a phenotype of a normal epithelial breast cell line for several reasons. Indeed, the ICC characterization revealed some features that are not in line with normal epithelial cells: a) it did not express E-cad (or express just in a small subset of cells); b) it expressed simultaneously the epithelial and the mesenchymal markers (AE1/AE3 and Vim, respectively), similarly to the MDA-MB-231 cell line, that is a basal type cell line; c) it does not express ER and PR. Moreover, the 3D cell cultures did not reveal aspects of "tissue recapitulation", such as the formation of acinar-like structures with the restoration of cell polarity, microvilli, and secretion of vesicles as observed in the MCF7 cell line. In view of the reasons presented, we believe that this cell line is a poor proxy for assessing cytotoxic effects on normal mammary cells, at least in drug discovery screening assays.

#### **6.10. Why is it important to study the interactions of seaweed compounds with chemotherapy drugs?**

In this study, we described an enhancement of Dox cytotoxicity in combination with Fct and Fx. As far as we know, there is no prior study on BC cell lines with the combination of Fct and Dox. In other cell lines, Fct has already enhanced the effects of 5-Fu (Ramos et al., 2019) in cancer colon cells and Cis and paclitaxel in ovarian cancer cells (Bae et al., 2020).

Fct is a sterol that belongs to the class of cholesterol-like molecules (Mouritsen et al., 2017), and its chemical structure is very similar to the cholesterol in vertebrates (Lopes et al., 2014). A recent study discovered that Dox encapsulation with polymeric

nanoparticles containing cholesterol is more active against breast cancer cells, especially in the MCF7 cell line, hypothesizing that the high affinity of steroids to cell membranes improves drug uptake by cancer cells (Misiak et al., 2022). This idea may also be applied to Fct due to its similarity to cholesterol.

In the case of Fx, *in vitro* studies using Fx in combination therapy with Dox showed the enhancement of the drug effect in relation to the inhibition of cell growth in MCF7 and MDA-MB-231 cell lines (Vijay et al., 2018). Other studies reported interactive antiproliferative and cytotoxic effects have been described where Dox was combined with other carotenoids, such as lutein in the MCF7 cell line (Shokrzadeh et al., 2021) and astaxanthin in MDA-MB-231 (Vijay et al., 2018). However, it has been argued that the combination of a carotenoid with DOX can have contradictory effects causing cytotoxicity (breast cancer cells under higher oxidative stress) or cytoprotection (non-cancerous cells under oxidative balance status) depending on the carotenoid and their combination with the drug (Vijay et al., 2018).

The literature on combining seaweed compounds with chemotherapy drugs is still scarce. Nevertheless, most seaweed compounds, including the ones tested here, have antioxidant activities which can potentially interfere with the action of some chemotherapy drugs. However, data concerning antioxidant intake during chemotherapy is very controversial (Mut-Salud et al., 2016, Akanji et al., 2020, Ferdous and Yusof, 2021), and due to insufficient data from clinical studies, clinicians should advise their patients against the use of antioxidant dietary supplements during chemotherapy or radiotherapy (D'Andrea, 2005, Khurana et al., 2018). Of course, this is an *in vitro* study, and the effects on a whole organism cannot be extrapolated. However, we believe it is relevant to call attention to this point for those who may read this thesis while lacking general knowledge about the possible interactions of medical drugs with the ingredients of edible items.

Indeed, the studied seaweed compounds can be consumed through dietary intake or by the consumption of supplements that are sold free of medical prescriptions, without strict governmental regulations or verification by competent authorities, under a strong marketing slogan of promoting several health benefits that are often based on insufficient (or completely absent) evidence from human interventional studies (Kumar and Sharma, 2021). Unfortunately, most patients do not communicate the intake of herbs and other supplements to their doctors with the false belief that natural products cannot be harmful to one's health (Phua et al., 2009, Bhadra et al., 2015). Most patients are unaware that besides the possibility of undesired side effects just for their intake, there is a possibility



of interactions with other drugs (Tachjian et al., 2010, Ekor, 2014). Typically, there are no guidelines on the consumption of seaweeds and their derivatives issued by regulatory bodies, including information on specific drug seaweed interactions (Kumar and Sharma, 2021). Thus, the interactions of the combinations of antioxidants with chemotherapy drugs deserve more studies to understand better the mechanisms behind these interactions.

Conversely, the investigation of marine-derived compounds as a source of new drugs or lead compounds (scaffolds for synthesis and modifications to obtain desired activities) is under the spotlight of academics and industries (Montuori et al., 2022). The preclinical screening pipeline continuously supplies drug discovery with new potential anticancer compounds. The drug discovery process is typically long, taking 10 to 15 years (Sun et al., 2022). Additionally, drug resistance is the main problem in cancer treatment. Thus, the search for new compounds or lead compounds that can be used as a drug or drug adjuvants that can act through different fighting fronts, reducing the doses of the drugs, minimizing side effects, or helping to prevent or reverse drug resistance is of extreme importance.

In this vein, marine-derived compounds are thought to present renewed hope in the drug discovery field as they have shown unique structures with some promising results. Moreover, developing more effective drug combinations is essential in the struggle to overcome drug resistance (Groenendijk and Bernards, 2014). Accordingly, Fct and Fx displayed interesting modulation of Dox cytotoxic effects, deserving further investigation.

Additionally, some marine organisms, like seaweeds, have advantages in farming, i.e., they are easy to produce and generate high amounts of compounds (Stedt et al., 2022).

## References

- Abramczyk, H., Surmacki, J., Kopec, M., Olejnik, A. K., Lubecka-Pietruszewska, K. and Fabianowska-Majewska, K. (2015). "The role of lipid droplets and adipocytes in cancer. Raman imaging of cell cultures: MCF10A, MCF7, and MDA-MB-231 compared to adipocytes in cancerous human breast tissue." *Analyst* 140(7): 2224-2235. 10.1039/c4an01875c.
- Achenbach, T. V., Slater, E. P., Brummerhop, H., Bach, T. and Müller, R. (2000). "Inhibition of cyclin-dependent kinase activity and induction of apoptosis by preussin in human tumor cells." *Antimicrob. Agents Chemother.* 44(10): 2794-2801. 10.1128/AAC.44.10.2794-2801.2000.
- Akanji, M. A., Fatinukun, H. D., Rotimi, D. E., Afolabi, B. L. and Adeyemi, O. S. (2020). The two sides of dietary antioxidants in cancer therapy. In (Ed.), *Antioxidants - Benefits, Sources, Mechanisms of Action*. IntechOpen. 10.5772/intechopen.94988.
- Amaral, R. L. F., Miranda, M., Marcato, P. D. and Swiech, K. (2017). "Comparative analysis of 3D bladder tumor spheroids obtained by forced floating and hanging drop methods for drug screening." *Front. Physiol.* 8: 605. 10.3389/fphys.2017.00605.
- Bae, H., Lee, J. Y., Song, G. and Lim, W. (2020). "Fucosterol suppresses the progression of human ovarian cancer by inducing mitochondrial dysfunction and endoplasmic reticulum stress." *Mar Drugs* 18(5): 261. 10.3390/md18050261.
- Bédard, P., Gauvin, S., Ferland, K., Caneparo, C., Pellerin, È., Chabaud, S. and Bolduc, S. (2020). "Innovative human three-dimensional tissue-engineered models as an alternative to animal testing." *Bioengineering* 7(3): 115. 10.3390/bioengineering7030115.
- Bock, C., Rack, B., Kuhn, C., Hofmann, S., Finkenzeller, C., Jäger, B., Jeschke, U. and Doisneau-Sixou, S. F. (2012). "Heterogeneity of ER $\alpha$  and ErbB2 status in cell lines and circulating tumor cells of metastatic breast cancer patients." *Transl. Oncol.* 5(6): 475-485. 10.1593/tlo.12310.
- Breslin, S. and O'Driscoll, L. (2013). "Three-dimensional cell culture: the missing link in drug discovery." *Drug Discov. Today* 18(5-6): 240-249. 10.1016/j.drudis.2012.10.003.
- Buttachon, S., Ramos, A. A., Inacio, A., Dethoup, T., Gales, L., Lee, M., Costa, P. M., Silva, A. M. S., et al. (2018). "Bis-Indolyl benzenoids, hydroxypyrrolidine derivatives and other constituents from cultures of the marine sponge-associated Fungus *Aspergillus candidus* KUFA0062." *Mar. Drugs* 16(4): 119. 10.3390/md16040119.

- Chen, S., Zhao, Y., Zhang, Y. and Zhang, D. (2014). "Fucoidan induces cancer cell apoptosis by modulating the endoplasmic reticulum stress cascades." *PLoS One* 9(9): e108157. 10.1371/journal.pone.0108157.
- Costa, E. C., Moreira, A. F., de Melo-Diogo, D., Gaspar, V. M., Carvalho, M. P. and Correia, I. J. (2016). "3D tumor spheroids: An overview on the tools and techniques used for their analysis." *Biotechnol. Adv.* 34(8): 1427-1441. 10.1016/j.biotechadv.2016.11.002.
- D'Anselmi, F., Masiello, M. G., Cucina, A., Proietti, S., Dinicola, S., Pasqualato, A., Ricci, G., Dobrowolny, G., et al. (2013). "Microenvironment promotes tumor cell reprogramming in human breast cancer cell lines." *PLoS One* 8(12): e83770. 10.1371/journal.pone.0083770.
- Dai, J., Jian, J., Bosland, M., Frenkel, K., Bernhardt, G. and Huang, X. (2008). "Roles of hormone replacement therapy and iron in proliferation of breast epithelial cells with different estrogen and progesterone receptor status." *Breast* 17(2): 172-179. 10.1016/j.breast.2007.08.009.
- Duval, K., Grover, H., Han, L. H., Mou, Y., Pegoraro, A. F., Fredberg, J. and Chen, Z. (2017). "Modeling physiological events in 2D vs. 3D cell culture." *Physiology* 32(4): 266-277. 10.1152/physiol.00036.2016.
- Edmondson, R., Broglie, J. J., Adcock, A. F. and Yang, L. (2014). "Three-dimensional cell culture systems and their applications in drug discovery and cell-based biosensors." *Assay Drug Dev. Technol.* 12(4): 207-218. 10.1089/adt.2014.573.
- Ekor, M. (2014). "The growing use of herbal medicines: issues relating to adverse reactions and challenges in monitoring safety." *Front. Pharmacol.* 4: 177. 10.3389/fphar.2013.00177.
- Ferdous, U. T. and Yusof, Z. N. B. (2021). "Medicinal prospects of antioxidants from algal sources in cancer therapy." *Front. Pharmacol.* 12: 593116. 10.3389/fphar.2021.593116.
- Fouad, M. A., Sayed-Ahmed, M. M., Huwait, E. A., Hafez, H. F. and Osman, A.-M. M. (2021). "Epigenetic immunomodulatory effect of eugenol and astaxanthin on doxorubicin cytotoxicity in hormonal positive breast cancer cells." *BMC Pharmacol. Toxicol.* 22(1): 8. 10.1186/s40360-021-00473-2.
- Froehlich, K., Haeger, J. D., Heger, J., Pastuschek, J., Photini, S. M., Yan, Y., Lupp, A., Pfarrer, C., et al. (2016). "Generation of multicellular breast cancer tumor spheroids: Comparison of different protocols." *J. Mammary Gland Biol. Neoplasia* 21(3-4): 89-98. 10.1007/s10911-016-9359-2.
- Garg, S., Afzal, S., Elwakeel, A., Sharma, D., Radhakrishnan, N., Dhanjal, J. K., Sundar, D., Kaul, S. C., et al. (2019). "Marine carotenoid fucoxanthin possesses anti-

- metastasis activity: molecular evidence." *Mar. Drugs* 17(6): 338. 10.3390/md17060338.
- Gencoglu, M. F., Barney, L. E., Hall, C. L., Brooks, E. A., Schwartz, A. D., Corbett, D. C., Stevens, K. R. and Peyton, S. R. (2018). "Comparative study of multicellular tumor spheroid formation methods and implications for drug screening." *ACS Biomater. Sci. Eng.* 4(2): 410-420. 10.1021/acsbiomaterials.7b00069.
- Gomes, N. G., Lefranc, F., Kijjoa, A. and Kiss, R. (2015). "Can some marine-derived fungal metabolites become actual anticancer agents?" *Mar. Drugs* 13(6): 3950-3991. 10.3390/md13063950.
- Groenendijk, F. H. and Bernards, R. (2014). "Drug resistance to targeted therapies: deja vu all over again." *Mol Oncol* 8(6): 1067-1083. 10.1016/j.molonc.2014.05.004.
- Hasan, M. R., Alsaiani, A. A., Fakhurji, B. Z., Molla, M. H. R., Asseri, A. H., Sumon, M. A. A., Park, M. N., Ahammad, F., et al. (2022). "Application of mathematical modeling and computational tools in the modern drug design and development process." *Molecules* 27(13): 4169. 10.3390/molecules27134169.
- Holliday, D. L. and Speirs, V. (2011). "Choosing the right cell line for breast cancer research." *Breast Cancer Res.* 13(4): 215. 10.1186/bcr2889.
- Huang, Z., Yu, P. and Tang, J. (2020). "Characterization of triple-negative breast cancer MDA-MB-231 cell spheroid model." *OncoTargets Ther.* 13: 5395-5405. 10.2147/OTT.S249756.
- Iglesias, J. M., Beloqui, I., Garcia-Garcia, F., Leis, O., Vazquez-Martin, A., Eguiara, A., Cufi, S., Pavon, A., et al. (2013). "Mammosphere formation in breast carcinoma cell lines depends upon expression of E-cadherin." *PLoS One* 8(10): e77281. 10.1371/journal.pone.0077281.
- Ivers, L. P., Cummings, B., Owolabi, F., Welzel, K., Klinger, R., Saitoh, S., O'Connor, D., Fujita, Y., et al. (2014). "Dynamic and influential interaction of cancer cells with normal epithelial cells in 3D culture." *Cancer Cell Int.* 14(1): 108. 10.1186/s12935-014-0108-6.
- Jensen, C. and Teng, Y. (2020). "Is it time to start transitioning from 2D to 3D cell culture?" *Front. Mol. Biosci.* 7: 33. 10.3389/fmolb.2020.00033.
- Jiang, H., Li, J., Chen, A., Li, Y., Xia, M., Guo, P., Yao, S. and Chen, S. (2018). "Fucosterol exhibits selective antitumor anticancer activity against HeLa human cervical cell line by inducing mitochondrial mediated apoptosis, cell cycle migration inhibition and downregulation of m-TOR/PI3K/Akt signalling pathway." *Oncol. Lett* 15(3): 3458-3463. 10.3892/ol.2018.7769.
- Karimian, A., Mir Mohammadrezaei, F., Hajizadeh Moghadam, A., Bahadori, M. H., Ghorbani-Anarkooli, M., Asadi, A. and Abdolmaleki, A. (2022). "Effect of astaxanthin

- and melatonin on cell viability and DNA damage in human breast cancer cell lines." *Acta Histochem.* 124(1): 151832. 10.1016/j.acthis.2021.151832.
- Katt, M. E., Placone, A. L., Wong, A. D., Xu, Z. S. and Searson, P. C. (2016). "In vitro tumor models: Advantages, disadvantages, variables, and selecting the right platform." *Front. Bioeng. Biotechnol.* 4: 12. 10.3389/fbioe.2016.00012.
- Kim, R. K., Suh, Y., Yoo, K. C., Cui, Y. H., Hwang, E., Kim, H. J., Kang, J. S., Kim, M. J., et al. (2015a). "Phloroglucinol suppresses metastatic ability of breast cancer cells by inhibition of epithelial-mesenchymal cell transition." *Cancer Sci.* 106(1): 94-101. 10.1111/cas.12562.
- Kim, R. K., Uddin, N., Hyun, J. W., Kim, C., Suh, Y. and Lee, S. J. (2015b). "Novel anticancer activity of phloroglucinol against breast cancer stem-like cells." *Toxicol. Appl. Pharmacol.* 286(3): 143-150. 10.1016/j.taap.2015.03.026.
- Kitaeva, K. V., Rutland, C. S., Rizvanov, A. A. and Solovyeva, V. V. (2020). "Cell culture based in vitro test systems for anticancer drug screening." *Front. Bioeng. Biotechnol.* 8: 322. 10.3389/fbioe.2020.00322.
- Kumar, M. S. and Sharma, S. A. (2021). "Toxicological effects of marine seaweeds: a cautious insight for human consumption." *Crit. Rev. Food Sci. Nutr.* 61(3): 500-521. 10.1080/10408398.2020.1738334.
- Kumar, P., Nagarajan, A. and Uchil, P. D. (2018). "Analysis of cell viability by the lactate dehydrogenase assay." *Cold Spring Harb. Protoc.* 2018(6). 10.1101/pdb.prot095497.
- Langhans, S. A. (2018). "Three-dimensional in vitro cell culture models in drug discovery and drug repositioning." *Front. Pharmacol.* 9: 6. 10.3389/fphar.2018.00006.
- Law, A. M. K., Rodriguez de la Fuente, L., Grundy, T. J., Fang, G., Valdes-Mora, F. and Gallego-Ortega, D. (2021). "Advancements in 3D cell culture systems for personalizing anti-cancer therapies." *Front. Oncol.* 11: 782766. 10.3389/fonc.2021.782766.
- Leung, B. M., Leshner-Perez, S. C., Matsuoka, T., Moraes, C. and Takayama, S. (2015). "Media additives to promote spheroid circularity and compactness in hanging drop platform." *Biomater. Sci.* 3(2): 336-344. 10.1039/c4bm00319e.
- Li, W., Xue, D., Xue, M., Zhao, J., Liang, H., Liu, Y. and Sun, T. (2019). "Fucoidan inhibits epithelial-to-mesenchymal transition via regulation of the HIF-1 $\alpha$  pathway in mammary cancer cells under hypoxia." *Oncol. Lett.* 18(1): 330-338. 10.3892/ol.2019.10283.
- Li, Y., Zhang, H., Merkher, Y., Chen, L., Liu, N., Leonov, S. and Chen, Y. (2022). "Recent advances in therapeutic strategies for triple-negative breast cancer." *J. Hematol. Oncol.* 15(1): 121. 10.1186/s13045-022-01341-0.

- Liu, B., Ezeogu, L., Zellmer, L., Yu, B., Xu, N. and Joshua Liao, D. (2015). "Protecting the normal in order to better kill the cancer." *Cancer Med.* 4(9): 1394-1403. 10.1002/cam4.488.
- Lombaerts, M., van Wezel, T., Philippo, K., Dierssen, J. W., Zimmerman, R. M., Oosting, J., van Eijk, R., Eilers, P. H., et al. (2006). "E-cadherin transcriptional downregulation by promoter methylation but not mutation is related to epithelial-to-mesenchymal transition in breast cancer cell lines." *Br. J. Cancer* 94(5): 661-671. 10.1038/sj.bjc.6602996.
- Lopes, G., Sousa, C., Valentão, P. and Andrade, P. B. (2014). Sterols in algae and health. Bioactive compounds from marine foods: Plant and animal sources. *Compounds from Marine Foods* (eds B. Hernández-Ledesma and M. Herrero). L. John Wiley & Sons. 10.1002/9781118412893.ch9
- Lovitt, C. J., Shelper, T. B. and Avery, V. M. (2018). "Doxorubicin resistance in breast cancer cells is mediated by extracellular matrix proteins." *BMC Cancer* 18(1): 41. 10.1186/s12885-017-3953-6.
- Malve, H. (2016). "Exploring the ocean for new drug developments: Marine pharmacology." *J. Pharm. Bioallied Sci.* 8(2): 83-91. 10.4103/0975-7406.171700.
- Marchese, S. and Silva, E. (2012). "Disruption of 3D MCF-12A breast cell cultures by estrogens-an in vitro model for ER-mediated changes indicative of hormonal carcinogenesis." *PLoS One* 7(10): e45767. 10.1371/journal.pone.0045767.
- Mehta, G., Hsiao, A. Y., Ingram, M., Luker, G. D. and Takayama, S. (2012). "Opportunities and challenges for use of tumor spheroids as models to test drug delivery and efficacy." *J. Control. Release* 164(2): 192-204. 10.1016/j.jconrel.2012.04.045.
- Misiak, P., Niemirowicz-Laskowska, K., Misztalewska-Turkowicz, I., Markiewicz, K. H., Wielgat, P., Car, H. and Wilczewska, A. Z. (2022). "Doxorubicin delivery systems with an acetylacetone-based block in cholesterol-terminated copolymers: Diverse activity against estrogen-dependent and estrogen-independent breast cancer cells." *Chem. Phys. Lipids* 245: 105194. 10.1016/j.chemphyslip.2022.105194.
- Mittler, F., Obeid, P., Rulina, A. V., Haguet, V., Gidrol, X. and Balakirev, M. Y. (2017). "High-content monitoring of drug effects in a 3D spheroid model." *Front. Oncol.* 7: 293. 10.3389/fonc.2017.00293.
- Montuori, E., de Pascale, D. and Lauritano, C. (2022). "Recent discoveries on marine organism immunomodulatory activities." *Mar. Drugs* 20(7): 422. 10.3390/md20070422.

- Mouritsen, O. G., Bagatoli, L. A., Duelund, L., Garvik, O., Ipsen, J. H. and Simonsen, A. C. (2017). "Effects of seaweed sterols fucosterol and desmosterol on lipid membranes." *Chem. Phys. Lipids* 205: 1-10. 10.1016/j.chemphyslip.2017.03.010.
- Mut-Salud, N., Álvarez, P. J., Garrido, J. M., Carrasco, E., Aránega, A. and Rodríguez-Serrano, F. (2016). "Antioxidant intake and antitumor therapy: Toward nutritional recommendations for optimal results." *Oxid. Med. Cell. Longev.* 2016: 6719534-6719534. 10.1155/2016/6719534.
- Neve, R. M., Chin, K., Fridlyand, J., Yeh, J., Baehner, F. L., Fevr, T., Clark, L., Bayani, N., et al. (2006a). "A collection of breast cancer cell lines for the study of functionally distinct cancer subtypes." *Cancer Cell* 10(6): 515-527. 10.1016/j.ccr.2006.10.008.
- Neve, R. M., Chin, K., Fridlyand, J., Yeh, J., Baehner, F. L., Fevr, T., Clark, L., Bayani, N., et al. (2006b). "A collection of breast cancer cell lines for the study of functionally distinct cancer subtypes." *Cancer Cell* 10(6): 515-527. 10.1016/j.ccr.2006.10.008.
- Nowacka, M., Sterzynska, K., Andrzejewska, M., Nowicki, M. and Januchowski, R. (2021). "Drug resistance evaluation in novel 3D in vitro model." *Biomed. Pharmacother.* 138: 111536. 10.1016/j.biopha.2021.111536.
- Nunes, A. S., Barros, A. S., Costa, E. C., Moreira, A. F. and Correia, I. J. (2019). "3D tumor spheroids as in vitro models to mimic in vivo human solid tumors resistance to therapeutic drugs." *Biotechnol. Bioeng.* 116(1): 206-226. 10.1002/bit.26845.
- Pelletier, J., Bellot, G., Gounon, P., Lacas-Gervais, S., Pouysségur, J. and Mazure, N. M. (2012). "Glycogen synthesis is induced in hypoxia by the hypoxia-inducible factor and promotes cancer cell survival." *Front. Oncol.* 2: 18. 10.3389/fonc.2012.00018.
- Prabst, K., Engelhardt, H., Ringgeler, S. and Hubner, H. (2017). "Basic colorimetric proliferation assays: MTT, WST, and Resazurin." *Methods Mol. Biol.* 1601: 1-17. 10.1007/978-1-4939-6960-9\_1.
- Ramos, A. A., Almeida, T., Lima, B. and Rocha, E. (2019). "Cytotoxic activity of the seaweed compound fucosterol, alone and in combination with 5-fluorouracil, in colon cells using 2D and 3D culturing." *J. Toxicol. Environ. Health A* 82(9): 537-549. 10.1080/15287394.2019.1634378.
- Rwigemera, A., Mamelona, J. and Martin, L. J. (2014). "Inhibitory effects of fucoxanthinol on the viability of human breast cancer cell lines MCF-7 and MDA-MB-231 are correlated with modulation of the NF-kappaB pathway." *Cell. Biol. Toxicol.* 30(3): 157-167. 10.1007/s10565-014-9277-2.
- Shokrzadeh, M., Mortazavi, P., Moghadami, A., Khayambashi, B. and Motafeghi, F. (2021). "Synergistic antiproliferative and anticancer activity of carotenoid lutein or coenzyme Q10 in combination with doxorubicin on the MCF7 cell line." *Appl. Vitro Toxicol.* 7(4): 167-174. 10.1089/aivt.2021.0008.

- Siangcham, T., Vivithanaporn, P. and Sangpairoj, K. (2020). "Anti-migration and invasion effects of astaxanthin against A172 human glioblastoma cell line." *Asian Pac. J. Cancer Prev.* 21(7): 2029-2033. 10.31557/apjcp.2020.21.7.2029.
- Sommers, C. L., Walker-Jones, D., Heckford, S. E., Worland, P., Valverius, E., Clark, R., McCormick, F., Stampfer, M., et al. (1989). "Vimentin rather than keratin expression in some hormone-independent breast cancer cell lines and in oncogene-transformed mammary epithelial cells." *Cancer Res.* 49(15): 4258-4263. PMID: 2472876
- Stedt, K., Trigo, J. P., Steinhagen, S., Nylund, G. M., Forghani, B., Pavia, H. and Undeland, I. (2022). "Cultivation of seaweeds in food production process waters: Evaluation of growth and crude protein content." *Algal Res.* 63: 102647. 10.1016/j.algal.2022.102647.
- Sun, D., Gao, W., Hu, H. and Zhou, S. (2022). "Why 90% of clinical drug development fails and how to improve it?" *Acta Pharm. Sin. B* 12(7): 3049-3062. 10.1016/j.apsb.2022.02.002.
- Sweeney, M. F., Sonnenschein, C. and Soto, A. M. (2018). "Characterization of MCF-12A cell phenotype, response to estrogens, and growth in 3D." *Cancer Cell Int.* 18: 43-43. 10.1186/s12935-018-0534-y.
- Tachjian, A., Maria, V. and Jahangir, A. (2010). "Use of herbal products and potential interactions in patients with cardiovascular diseases." *J. Am. Coll. Cardiol.* 55(6): 515-525. 10.1016/j.jacc.2009.07.074.
- Verjans, E. T., Doijen, J., Luyten, W., Landuyt, B. and Schoofs, L. (2018). "Three-dimensional cell culture models for anticancer drug screening: Worth the effort?" *J. Cell. Physiol.* 233(4): 2993-3003. 10.1002/jcp.26052.
- Vijay, K., Sowmya, P. R., Arathi, B. P., Shilpa, S., Shwetha, H. J., Raju, M., Baskaran, V. and Lakshminarayana, R. (2018). "Low-dose doxorubicin with carotenoids selectively alters redox status and upregulates oxidative stress-mediated apoptosis in breast cancer cells." *Food Chem. Toxicol.* 118: 675-690. 10.1016/j.fct.2018.06.027.
- Weber-Ouellette, A., Busby, M. and Plante, I. (2018). "Luminal MCF-12A & myoepithelial-like Hs 578Bst cells form bilayered acini similar to human breast." *Future Sci. OA* 4(7): FSO315-FSO315. 10.4155/fsoa-2018-0010.
- Zhang, Z., Teruya, K., Yoshida, T., Eto, H. and Shirahata, S. (2013). "Fucoidan extract enhances the anti-cancer activity of chemotherapeutic agents in MDA-MB-231 and MCF-7 breast cancer cells." *Mar. Drugs* 11(1): 81-98. 10.3390/md11010081.





# **Chapter 7** - Concluding Remarks





## 7. Concluding Remarks

This study evaluated the cytotoxic effects of marine-derived bioactive compounds (one fungus and six seaweed-derived compounds) on a panel of BC cell lines. The lines MCF7, SKBR3, and MDA-MB-231 were representatives of the three main BC subtypes, while the non-tumoral breast cell line was the MCF12A. We cultured cells as monolayers (2D) and aggregates (3D). The main conclusions were:

1) From the 3D model characterization, we concluded that at the tested conditions, MCF7 and MDA-MB-231 formed compact MCAs, while SKBR3 and MCF12A formed loose MCAs; all MCAs were oblate discoid structures, being the looser ones also flatter and with greater areas. The MCAs do not fit the idealized classical 3D spheroids, as both proliferating and apoptotic cells were randomly distributed throughout all the MCAs, and not concentrated in one specific area. The MCF7 MCAs showed signs of tissue recapitulation, forming acinar-like structures with the presence of microvilli and secretion vesicles projected to the lumen.

2) At 50  $\mu\text{M}$ , the marine-fungi-derived compound preussin showed high cytotoxic and anti-proliferative effects against all cell lines in 2D and 3D cell cultures.

3) In 2D cell culture, the seaweed compounds that exerted cytotoxic effects in lower concentrations were a) Fct, at 10  $\mu\text{M}$ , negatively impacting cell viability in the three BC cell lines and not affecting the non-tumoral; b) Fx, at 10  $\mu\text{M}$ , that affected all cell lines.

4) Fct and Fx, in combination with Dox, enhanced Dox cytotoxicity in 2D. Fct combined with Dox showed enhanced Dox cytotoxic effects in MCF7 and MDA-MB-231 cell lines, while Fx demonstrated similar effects in SKBR3 and MDA-MB-231 cell lines. In both situations, the magnitude of the effects was higher in the triple-negative breast cancer cell line MDA-MB-231. This discovery is especially interesting because chemotherapy is the only treatment option for TNBC patients, and drug resistance is a significant issue.

5) The cytotoxic effects of the combination of Fct + Dox in 2D were not reproduced in 3D cell culture. On the contrary, the mixture of Fx + Dox enhanced Dox's cytotoxic and antiproliferative effects in 2D and 3D. This study's data support that 3D models are a promising tool for screening marine-derived compounds as candidates for anticancer effects in BC.

6) Relatively to the modeling effects of the bioactive compounds with Dox in MDA-MB-231 cells, we observed that in 2D cell culture Fct + Dox increased Dox effects by

induction of apoptosis, corroborated by caspase-3 positive and morphological analysis, and decreased cell proliferation.

As for the combination of Fx + Dox, the enhanced Dox cytotoxic effects in 2D and 3D cell cultures, through induction of apoptosis, displayed by a higher number of caspase-3 positive cells and cells with compatible apoptotic morphology, however, without differences in the DNA damage caused by Dox alone. There was also observed a lower number of ki67-positive cells, indicating inhibition of cell proliferation.

# **Chapter 8** - Future Perspectives





## 8. Future perspectives

This work raised further research questions that we plan to address in the near future.

The characterization of the model we presented here can be helpful as a baseline for other investigators. Nonetheless, there are much more characterization procedures that could be performed. Besides the techniques used in this thesis for assessing the effects of the compounds, other techniques could be applied according to the investigation's interests, such as different immunocytochemical markers, for instance, for stem cells or different types of death, different microscopies such as fluorescence, flow cytometry, Western blot, quantitative real-time reverse transcription polymerase chain reaction (qRT-PCR) of specific target-pathways and other colorimetric assays.

Concerning preussin, more studies are being performed in our laboratory to check other effects, for instance, inhibition of migration and possible mechanisms of action such as cell cycle arrest, cell death, and DNA damage. Besides the promising effects of preussin, one of the main challenges of its application on a larger scale is the obtention of high amounts of the compound, preferably from the same source at this stage of knowledge.

Regarding what we consider promising results, we would like to test Fct and Fx in the same model but under different experimental conditions, such as increasing Fct concentration, as this may be required to maintain its effects of Dox enhancement in 3D. Moreover, we would like to test decreasing Fx concentration (to a non-cytotoxic one) to see if it could maintain the same influence on Dox effects. The ideal situation would be to find a non-toxic compound that could enhance its effects combined with Dox.

Further studies are required to elucidate the mechanisms behind the cytotoxicity and inhibition of cell proliferation of the compounds and the interactions of Fct and Fx with Dox. Given the potential complexity of those effects, little was disclosed in this thesis. Besides the cell damage detected by cell-based assays, the morphological changes and apoptosis induction revealed by caspase-3 immunostaining, we also detected inhibition of cell proliferation by ki67 immunostaining and BrdU assays. For Fx, we further looked into the effects of DNA damage and nuclear condensation. However, none was found. Thus, more research on the involved mechanisms is essential through other techniques. Furthermore, because both Fct and Fx have antioxidant properties and may alter reactive oxygen species (ROS), ROS and mitochondrial functional studies could be informative.



Finally, after better understanding the mechanisms underlying the enhancement of Dox effects and eventually improving the compound's delivery to cancer cells, we could try more sophisticated 3D cell culture models (co-cultures, microfluid) before *in vivo* studies.